University of Zagreb

Faculty of Science, Department of Biology

Sara Šariri

ASSESSMENT OF EXPOSURE, ACCUMULATION, AND TOXICITY OF POLLUTANTS IN FISH INTESTINE AND IN THEIR INTESTINAL PARASITES ACANTHOCEPHALANS (ACANTHOCEPHALA)

DOCTORAL THESIS

Supervisors: Vlatka Filipović Marijić, PhD, Scientific advisor
Irena Vardić Smrzlić, PhD, Senior research associate

Zagreb, 2026.

Sveučilište u Zagrebu

Prirodoslovno-matematički fakultet, Biološki odsjek

Sara Šariri

PROCJENA IZLOŽENOSTI, AKUMULACIJE I TOKSIČNOSTI ZAGAĐIVALA UNESENIH U PROBAVILO RIBA I U NJIHOVE CRIJEVNE NAMETNIKE KUKAŠE (ACANTHOCEPHALA)

DOKTORSKI RAD

Mentori: dr. sc. Vlatka Filipović Marijić, znanstvena savjetnica
dr. sc. Irena Vardić Smrzlić, viša znanstvena suradnica

Zagreb, 2026.

Table of Contents

Zahvale

Izrada ove doktorske disertacije bila je dug i zahtjevan proces, ali istovremeno i razdoblje osobnog i profesionalnog rasta koje ne bi bilo moguće bez podrške mnogih ljudi.

Prije svega, zahvaljujem se svojoj mentorici dr. sc. Vlatki Filipović Marijić na pruženoj prilici za izradu doktorskog rada, uključivanju u projekte i kongrese te kontinuiranoj podršci, savjetima i pomoći tijekom mog rada na Institutu Ruđer Bošković.

Veliko hvala mentorici dr. sc. Ireni Vardić Smrzlić na pristupačnosti, razumijevanju i podršci, kao i na nesebičnom dijeljenju znanja tijekom zajedničkog rada na molekularnim analizama.

Zahvaljujem svim bivšim i sadašnjim članovima Laboratorija za biološke učinke metala na pomoći u terenskom i laboratorijskom radu, dijeljenju znanja i iskustva te na podršci i ugodnoj radnoj atmosferi. Posebno hvala kolegicama iz ureda – Ivani Karamatić, dipl. ing. preh. bioteh., dr. sc. Zrinki Dragun i dr. sc. Tatjani Mijošek Pavin. Moja Mijošek et al., neizmjerno ti hvala na podršci, savjetima, razumijevanju, prijateljstvu i ogromnoj pomoći u svakom koraku. Svojim primjerom i pristupom radu uvijek si me motivirala da budem bolja.

Hvala svim suradnicima na projektu BIOTOXMET na doprinosu laboratorijskim analizama i znanstvenim radovima koji su bili temelj ove disertacije.

Također zahvaljujem članovima povjerenstva na korisnim ispravcima i konstruktivnim komentarima.

Posebno hvala mojoj prijateljici dr. sc. (:P) Ani Ramljak koja je sa mnom dijelila svakodnevicu ovog razdoblja, kroz sve uspone i padove, od prijave za posao do danas. Naši razgovori, pauze i međusobna podrška obilježili su ovo iskustvo i učinili ga lakšim i ljepšim.

Hvala i svim ostalim prijateljima koji su bili uz mene i u najtežim trenutcima i nisu mi dali da odustanem. Lea, Lovro, Ana, Zorko i Anja, ne bih bila tu bez vas.

Od srca hvala mojim roditeljima i sestri Dori na bezuvjetnoj ljubavi, podršci i vjeri u mene kroz sve ove godine. Hvala vam što ste uvijek bili uz mene i omogućili mi da slijedim svoj put.

Na kraju, najveće hvala mom Juri. Hvala ti što si bio moj oslonac u svakom trenutku, pružao mi radost, mir i sigurnost te vjerovao u mene čak i onda kada ja sama nisam.

Information about the supervisors

Vlatka Filipović Marijić, PhD, Scientific Advisor

Dr. Vlatka Filipović Marijić was born on 3 November 1975 in Sisak, Croatia. She is employed at the Laboratory for Biological Effects of Metals, Division for Marine and Environmental Research, at the Ruđer Bošković Institute in Zagreb. She graduated in 2000 from the Department of Biology at the Faculty of Science, University of Zagreb, earning the degree in Ecology, and subsequently completed her master's studies in Oceanology and her doctoral studies in Biology. She currently works as a Scientific Advisor, and her scientific research is focused on the application of various bioindicator organisms for environmental quality assessment, using biological changes as indicators of exposure to different pollutants, particularly metals and microplastics. She leads numerous scientific and commercial projects in the field of ecotoxicology, biomonitoring, and environmental parasitology, which have resulted in multiple publications, conference presentations, lectures, international collaborations, and awards at both national and international levels. In addition to her research, she has been actively involved in the popularization of science for many years, receiving several annual awards from the Ruđer Bošković Institute and the Croatian State Award for Science in the field of popularization of science in 2019.

Irena Vardić Smrzlić, PhD, Senior Research Associate

Dr. Irena Vardić Smrzlić was born on 27 February 1978 in Banja Luka, Bosnia and Herzegovina. She is employed at the Laboratory for Aquaculture and Pathology of Aquatic Organisms, Division for Marine and Environmental Research, at the Ruđer Bošković Institute in Zagreb. She graduated in 2002 from the Department of Biology at the Faculty of Science, University of Zagreb, earning the degree in Molecular Biology, and subsequently completed her master's and doctoral studies in Biology and Oceanology, respectively. She currently works as a Senior Research Associate, with her scientific research focused on the diagnosis of diseases in aquatic organisms and the characterization of their causative agents (viruses, parasites, and bacteria), with a particular emphasis on their role in the environment. She has participated in numerous research and commercial projects in the fields of aquatic animal health, environmental microbiology, and parasitology. She is the author or co-author of several scientific and professional publications and has presented her work at numerous international and national conferences. Under her mentorship, four graduate theses have been completed.

University of Zagreb
Faculty of Science
Department of Biology

Doctoral thesis

ASSESSMENT OF EXPOSURE, ACCUMULATION, AND TOXICITY OF POLLUTANTS IN FISH INTESTINE AND IN THEIR INTESTINAL PARASITES ACANTHOCEPHALANS (ACANTHOCEPHALA)

Sara Šariri

Thesis research was performed at Laboratory for Biological Effects of Metals, Division for Marine and Environmental Research, Ruđer Bošković Institute

Supervisors: Vlatka Filipović Marijić, PhD, Scientific Advisor and Irena Vardić Smrzlić, PhD, Senior Research Associate

Short abstract: This dissertation investigated the exposure, accumulation, and biological effects of pollutants in the intestine of brown trouts (*Salmo trutta*) and their intestinal parasites, acanthocephalans (*Dentitruncus truttae*), from the Krka River. It presents the first results on microplastic occurrence in the upper part of Krka and confirms wastewaters as a source of metal(loid) pollution in water and sediments. Differences in environmental pollutant exposure and dietary uptake were reflected in metal accumulation as well as in transcriptomic and biochemical responses in fish intestine, with subcellular metal distribution indicating regulated detoxification, while no effects were recorded at the organismal level. In acanthocephalans, efficient metal accumulation, metal-specific association with cytosolic biomolecules of various sizes, and host-independent biomarker responses were observed. Their first transcriptomic data revealed proteins involved in metal handling. Overall, the results highlight fish intestine and acanthocephalans as sensitive bioindicators for assessing pollution in freshwater ecosystems.

(261 pages, 60 figures, 21 tables, 564 references, original in English)

Keywords: environmental exposure, metal(loid)s, microplastics, fish, parasites, transcriptomics, subcellular distribution, biological responses, accumulation

Reviewers: Maria Špoljar, PhD, Full Professor with tenure
Dario Omanović, PhD, Scientific advisor with tenure
Ivana Babić, PhD, Senior research associate

Sveučilište u Zagrebu
Prirodoslovno-matematički fakultet
Biološki odsjek

Doktorski rad

PROCJENA IZLOŽENOSTI, AKUMULACIJE I TOKSIČNOSTI ZAGAĐIVALA UNESENIH U PROBAVILO RIBA I U NJIHOVE CRIJEVNE NAMETNIKE KUKAŠE (ACANTHOCEPHALA)

Sara Šariri

Rad je izrađen u Laboratoriju za biološke učinke metala, Zavoda za istraživanje mora i okoliša, Instituta Ruđer Bošković

Mentori: dr. sc. Vlatka Filipović Marijić, znanstvena savjetnica i dr. sc. Irena Vardić Smrzlić, viša znanstvena suradnica

Sažetak: U ovom doktorskom radu istraženi su izloženost, akumulacija i biološki učinci zagađivala u probavilu potočnih pastrva (*Salmo trutta*) i njihovim crijevnim nametnicima, kukašima (*Dentitruncus truttae*), iz rijeke Krke. Prikazani su prvi rezultati o prisutnosti mikroplastike u gornjem toku Krke te je potvrđeno da otpadne vode predstavljaju izvor zagađenja metalima u vodi i sedimentu. Razlike u okolišnoj izloženosti zagađivalima i njihovom unosu probavnim putem očitovale su se u akumulaciji metala te u transkriptomskim i biokemijskim odgovorima u probavilu riba, a unutarstanična raspodjela metala je ukazala na procese detoksifikacije, dok učinci na razini organizma nisu zabilježeni. U kukašima su uočeni efikasna akumulacija metala, specifično vezanje metala s citosolskim biomolekulama različitih veličina te biomarkerski odgovori neovisni o domadaru. Njihovi prvi transkriptomski podaci otkrili su proteine uključene u homeostazu metala. Rezultati ističu probavilo riba i kukaše kao osjetljive bioindikatore za procjenu zagađenja u slatkovodnim ekosustavima.

(261 stranica, 60 slika, 21 tablica, 564 literaturnih navoda, jezik izvornika engleski)

Ključne riječi: metal(oid)i, mikroplastika, ribe, nametnici, transkriptomika, unutarstanična raspodjela, biološki odgovori, akumulacija

Ocjenjivači: prof. dr. sc. Maria Špoljar, redoviti profesor u trajnom izboru
dr. sc. Dario Omanović, znanstveni savjetnik u trajnom izboru
dr. sc. Ivana Babić, viši znanstveni suradnik

Introduction

1. Pollution of freshwater ecosystems

Worldwide, freshwater ecosystems are increasingly exposed to multiple stressors, including climate change, invasive species, exploitation, habitat degradation and complex mixture of chemical pollutants. In recent decades, human activities such as industry, agriculture, mining, transport, inadequate waste management, urbanization, and rapid technological development have posed serious threats to freshwater environments (Amoatey and Baawain 2019).

Pollutants enter freshwater ecosystems through diffuse sources such as land runoff, as well as through direct discharges of wastewater. In many regions, wastewater is inadequately treated before release, resulting in the continuous input of organic and inorganic pollutants into rivers and other freshwater bodies (Jan et al. 2022, Zait et al. 2022). Consequently, rivers are exposed to a wide range of micropollutants, including metals, microplastics, pesticides and other organic pollutants, solvents, and other industrial chemicals, with municipal and industrial wastewaters representing one of the most significant sources of pollution in the aquatic environment (Zait et al. 2022).

Wastewater can be broadly classified as municipal, industrial, agricultural, or sewage effluent, all of which may degrade water quality and render freshwater habitats unsuitable for natural communities of microorganisms and macroorganisms (Galib et al. 2018). In particular, industrial wastewater may contain high concentrations of toxic and persistent substances, such as metals, polymers, petroleum products, oils, acids, and synthetic chemical compounds, posing a substantial risk to freshwater ecosystems (Jan et al. 2022).

1.1. Karst freshwater ecosystems

Karst freshwater ecosystems develop in landscapes formed on soluble rocks such as limestone, dolomite, and gypsum, and are characterized by complex surface–subsurface hydrological connectivity, including caves, conduits, sinkholes, and underground drainage networks (Ford and Williams 2007). These systems represent some of the most diverse and valuable freshwater environments globally, supporting a high number of endemic species and specialized habitats, therefore being considered as a biodiversity hotspot. Owing to their

ecological and hydrological importance, many karst areas have been declared protected regions (Goldscheider 2019, Goldscheider et al. 2020).

Hydrological processes are the defining feature of karst systems and play a central role in regulating water quality and pollutant behavior. Karst aquifers and rivers serve as critical water resources for drinking water supply, agriculture, and ecosystem functioning, yet their distinctive hydrology renders them highly vulnerable to pollution (Goldscheider 2019, Hillebrand et al. 2012). Diffuse agricultural inputs and point-source pollution from landfills, urban areas, and insufficiently treated municipal and industrial wastewater represent the main pressures on karst waters (Ford and Williams 2007, Hillebrand et al. 2012, Malá et al. 2022). As a consequence of specific hydrological characteristics, karst freshwater systems frequently exhibit pronounced spatial and temporal variability in water quality. Pollutants can move rapidly and unfiltered from the surface to groundwater through sinkholes and fracture networks in the bedrock (Ford and Williams 2007, Yue et al. 2019). Pollutants may then be transported quickly over long distances or temporarily stored within the conduit network and remobilized during changes in hydrological conditions, such as high-flow events following intense precipitation, resulting in episodic contamination and legacy pollution effects (Hillebrand et al. 2012, Yue et al. 2019, Vesper et al. 2001). This dynamic behavior complicates the assessment of water quality in karst rivers and necessitates site-specific and temporally resolved approaches to monitoring and interpretation.

Although Europe is the continent with the highest percentage of karst areas, most research on karst waters is conducted in Asia and America, while data on the quality of European karst rivers are scarce (Goldscheider et al. 2020). The majority of studies investigating karst waters in Europe focus on hydrogeology and hydrodynamics (Bonacci et al. 2013, Eftimi 2020, Palacsu et al. 2021), and numerical modelling of water flow (Bailly-Comte et al. 2008, Eris and Wittenberg 2015, Hartmann et al. 2017), probably reflecting the importance of karst aquifers for drinking water supply. In research on pollution and water quality parameters of karst systems in Europe, most studies focuse on springs and groundwater (Bondu et al. 2023, Campanale et al. 2022, Fernández-Ortega et al. 2024, Hoaghia et al. 2021, Reberski et al. 2023, Valentić et al. 2022) and lake systems (Sertić-Petić et al. 2011, Sironić et al. 2017, Vurnek et al. 2021), while water pollution and parameters in surface karst rivers are less frequently included (Balestra et al. 2023, Oppeltová et al. 2024, Selak et al. 2024). Given the ecological significance of surface karst rivers, improved and complete understanding of

pollutant presence and behavior in these systems under different anthropogenic influence, is essential for effective management and long-term protection.

1.2. Metal pollution

Among the diverse pollutants present in freshwater ecosystems, metals are of particular concern due to their persistence, toxicity, and potential for accumulation. Metals occur naturally in aquatic environments as a result of geogenic processes such as chemical and mechanical weathering of rocks, volcanic activity, soil erosion, and atmospheric deposition. However, anthropogenic activities, including municipal and industrial wastewater discharge, mining, agriculture, traffic, and the use of fertilizers, have substantially increased metal inputs to freshwater systems, often leading to concentrations that exceed natural background levels (Gaillardet et al. 2013). Therefore, they are among the priority pollutants whose levels are regularly measured when assessing the quality of freshwater systems (Directive 2008/105/EC).

Elements naturally present at relatively high concentrations in the environment and organisms are classified as macroelements (Ca, K, Mg, Na), whereas elements occurring at low natural concentrations are referred to as trace elements (microelements). Because even small anthropogenic inputs of trace elements can disrupt their natural equilibrium, they are considered sensitive indicators of human impact from local to global scales. Consequently, reliable assessments of metal pollution require knowledge of both natural background concentrations and the environmental behavior of metals within aquatic systems (Gaillardet et al. 2013).

Unlike organic pollutants, metals are not biodegradable and, once introduced into freshwater environments, remain involved in biogeochemical cycling between water, suspended particles, biota and sediments. Their distribution and mobility are strongly influenced by physicochemical conditions such as pH, conductivity, temperature, water hardness, dissolved oxygen, and hydrological dynamics. Processes such as redox cycling and exchange between dissolved and particulate phases can influence behavior of certain metals, leading to pronounced spatial and temporal variability in riverine metal concentrations (Gaillardet et al. 2013).

Element speciation, defined as the chemical forms in which an element occurs, plays a central role in controlling metal(loid) mobility, bioavailability, and toxicity. Seasonal changes in precipitation, river discharge, and groundwater inputs further affect metal concentrations and transport, highlighting the importance of assessing both spatial and temporal patterns of metal(loid)s for accurate ecological characterization and water quality evaluation (Chen et al. 2020). Gaillardet et al. (2013) observed that literature on trace elements in rivers is lacking, especially in Europe, where fewer data are available in the scientific literature and the majority of river systems are heavily impacted by pollution. Despite increasing research efforts over past 13 years, comprehensive field studies addressing multi-element dynamics, long-term trends, and seasonal variability across entire catchments remain limited, particularly in complex and vulnerable systems such as karst rivers. Moreover, metal pollution typically occurs as complex mixtures and in combination with other pollutants, especially emerging pollutants, yet most studies continue to assess metals individually, underscoring the need for integrative approaches under realistic environmental conditions (Gaillardet et al. 2013, Yuan and Zhao 2022).

Research on metals in freshwater ecosystems of the Dinaric karst has so far encompassed a range of environmental compartments, including karst soils (Miko et al. 2003), groundwater from karst springs (Matić et al. 2012, 2016), lake and river water and sediments (Cukrov et al. 2008, Mikac et al. 2011, Vukosav et al. 2014, Maldini et al. 2023), as well as travertines (Boev et al. 2025). In addition, studies have addressed metal mobilization from anthropogenic sources to karst groundwater, particularly in relation to abandoned industrial landfills (Kapelj et al. 2025). Despite these efforts, metal research in the Dinaric karst remains limited in terms of spatial coverage and system integration, with many freshwater habitats still insufficiently investigated.

1.3. Microplastic pollution

Microplastics (MPs) represent another persistent and increasingly widespread pollutant in freshwater ecosystems. Although they are not yet routinely included in standard monitoring programs, MPs have been recognized as an emerging environmental concern, repeatedly highlighted by the United Nations Environment Programme as a priority issue (Blettler et al. 2018). Microplastics are commonly defined as plastic particles ranging between 1 μm and 5 mm, encompassing a heterogeneous group of materials that vary in polymer composition,

shape, size, color, and chemical additives. The most common shapes include filaments, fragments, films, foams and spheres (Cera et al. 2020).

Based on their origin, MPs are generally classified as primary or secondary. Primary MPs are intentionally manufactured at small sizes for use in products such as cosmetics, textiles, and industrial applications, whereas secondary MPs result from the fragmentation and weathering of larger plastic items. Secondary MPs constitute the majority of MP pollution in the environment, generated through mechanical abrasion, UV exposure, and other degradation processes acting on plastic products (Bala et al. 2025, Bhardwaj et al. 2024, Cera et al. 2020). Use of synthetic polymer microparticles has been restricted in European Union since 2023 by Commission Regulation (EU) 2023/2055. In freshwater systems, major sources of MPs include urban areas, inadequate waste disposal, industrial and agricultural activities, wastewater discharge, and stormwater runoff, which collectively facilitate the continuous input of plastic particles into rivers and lakes (Blettler et al. 2018).

Wastewater has been identified as a particularly important pathway for MPs into freshwater environments. Domestic sources such as synthetic textiles, packaging materials, and personal care products often release MPs into municipal wastewaters. Industrial effluents, especially from textile and other manufacturing industries, also contribute substantially to MP loads in receiving waters. Once released, MPs are transported and redistributed among water, biota, sediments, and surrounding environments, with sediments acting as important sinks for MP accumulation. Their environmental behavior is further influenced by biofilm formation, which can affect their transport, residence time, and potential to act as vectors for other pollutants and microorganisms (Bala et al. 2025, Bhardwaj et al. 2024, Yao et al. 2020).

Rivers play a key role in the global transport of plastics, serving as major conduits between terrestrial environments and marine ecosystems. Despite this, freshwater systems remain considerably understudied compared to marine environments, and in 2018 made only 13% of all plastic pollution studies (Blettler et al. 2018, Cera et al. 2020). Although literature on plastics in freshwater is increasing, it is still scarce. Available evidence suggests that MP pollution levels in freshwater ecosystems are comparable to those observed in marine systems, but field data remain spatially fragmented and biased toward developed countries (Blettler et al. 2018, Cera et al. 2020, Yao et al. 2020). Furthermore, methodological inconsistencies in sampling, identification, and reporting units limit comparability among studies and hinder the development of a comprehensive understanding of MP sources,

distribution, and fate in freshwater environments (Blettler et al. 2018, Gao et al. 2024). Due to these numerous research gaps, more research on wastewater and freshwater MPs is required to elucidate the sources, pathways and fate of MPs in freshwater ecosystems, with a focus on understanding how different environments influence their transport and distribution (Bhardwaj et al. 2024, Gao et al. 2024, Yao et al. 2020).

The presence of freshwater MPs in the Dinaric karst has been investigated in various freshwater systems in Slovenia (Valentić et al. 2022, 2024), in shore sediments of the Zeta, Morača, and Bojana rivers in Montenegro (Bošković et al. 2023), and in cave sediments from both remote and frequently visited caves connected to the Reka/Timavo River in NE Italy (Bruschi et al. 2026). In Croatia, MP research remains heavily biased toward the Adriatic Sea, particularly beach sediments (Blašković et al. 2017, Calore and Fraticelli 2022, Gomiero et al. 2018, Maršić-Lučić et al. 2018), and to a lesser extent toward estuaries (Parać et al. 2022) or terrestrial systems in the non-karstic parts of the country (Burghardt et al. 2025, Ćaleta et al. 2025), while freshwater systems are still underrepresented.

1.4. The Krka River

The Krka River is a medium-sized karst river located in the Dinaric karst region of the Republic of Croatia, flowing into the Adriatic Sea as an estuary. The river drains predominantly carbonate terrain and has a catchment area of approximately 2,657 km². Its total length is about 73 km, of which roughly 49 km represent freshwater flow, while the estuarine section extends for an additional 23.5 km. The source of the Krka River is located at the base of the Dinara Mountain, near the Town of Knin, which had 11,633 inhabitants according to the 2021 census. From its source, the river flows through a series of karst valleys (poljes) and canyon formations before reaching the Adriatic Sea. The Krka canyon is formed within the Dinaric carbonate platform and is composed mainly of limestone and dolomite bedrock. In its freshwater course, the Krka River receives five tributaries: Krčić, Kosovčica, Orašnica, Butižnica, and Čikola (Cukrov et al. 2008, Žutinić et al. 2020).

A distinctive feature of the Krka River is the presence of seven major tufa (travertine) barriers formed by the precipitation of calcium carbonate from dissolved calcium bicarbonate under a combination of specific physicochemical conditions and biological activity. These deposits create a series of cascades and waterfalls along the river course, which alter flow velocity and direction, resulting in alternating lotic and lentic microhabitats that strongly

influence ecosystem structure and functioning. Owing to its exceptional natural value, a large part of the river basin has been protected as Krka National Park since 1985 (Lojen et al. 2004, NN 05 1985).

Despite relatively low population density in the catchment, the Krka River is exposed to anthropogenic pressures, primarily from industrial and municipal wastewater discharges located approximately 2 km upstream of the National Park boundary near the Town of Knin (Filipović Marijić et al. 2018). Industrial pollution originates from artificial basins next to a screw manufacturing and galvanizing facility operating since 1956, which has been associated with several environmental incidents and is situated approximately 3.3 km west of the Krka National Park. During periods of high water, untreated wastewater used to enter Krka's tributary, the Orašnica River, and subsequently the Krka River. Although a dam separating the basins from the river system was elevated in 2014 to reduce direct discharge, the karstic nature of the substrate allows pollutants to infiltrate groundwater and reach the Krka River through underground flow paths. Chemical analyses of wastewater from these basins revealed elevated concentrations of oils, volatile organic compounds, trace metals and metalloids, chlorides, and aromatic hydrocarbons, including toluene, ethene, benzene, and xylene (Kisić et al. 2019). In addition, untreated municipal wastewater from the Town of Knin has also been regularly discharged into the Krka River downstream of the industrial site, and previous studies have reported degraded water quality at this location, indicated by differences in pH, COD, nutrient and trace metal concentrations, as well as microbiological parameters (Cukrov et al. 2008, 2012, Filipović Marijić et al. 2018, Sertić Perić et al. 2018).

According to the Water Status Report of Surface Waters in the Republic of Croatia in 2024, the Krka River generally exhibits good chemical status and moderate ecological status/potential, primarily due to biological quality elements (Josip Juraj Strossmayer Water Institute 2025). Research conducted to date has focused mainly on the Krka National Park area and the estuary, including studies of metal concentrations in sediments (Cukrov and Barišić 2006, Cukrov et al. 2013, 2020, 2024) and water (Cukrov et al. 2008, 2012, Cindrić et al. 2015), carbohydrates (Tepić et al. 2007), and dissolved organic matter (Marcinek et al. 2020). Microplastic pollution has so far been investigated only in the lower Krka estuary, representing the first assessment of MPs in this system (Parać et al. 2022).

A limited number of studies have examined metal concentrations in the freshwater course upstream of the Krka National Park (Cukrov et al. 2008, 2012, Filipović Marijić et al. 2018,

Sertić Perić et al. 2018). These investigations reported elevated concentrations of several elements, particularly near Knin, and documented significant deterioration of physicochemical conditions downstream of industrial and municipal discharge points. Although metal concentrations in the water column are generally low, which is typical of karst rivers, pronounced increases in Fe and Mn, up to 17- and 38-fold, respectively, have been recorded relative to the river source (Filipović Marijić et al. 2018, Sertić Perić et al. 2018). Overall, existing studies indicate moderate pollution levels but consistently emphasize the need for continued monitoring and targeted research to better understand pollutant dynamics and protect this ecologically valuable yet vulnerable karst river system from point-source pollution.

2. Biological effects of pollutants on aquatic organisms

2.1. Metals

From a biological perspective, metals are commonly classified as essential or non-essential elements. Essential metals (e.g., Cu, Fe, Mo, Zn) play key physiological roles as structural or functional components of enzymes, hormones, and other metalloproteins involved in electron transport, oxygen binding, hydrolysis reactions, and redox processes. In contrast, non-essential metals (e.g., Cd, Hg, Pb) have no known biological function and are toxic even at low concentrations. Although essential metals can also exert toxic effects when present above their optimal levels, the toxicity of non-essential metals largely results from their chemical similarity to essential elements, enabling them to enter cells via the same transport pathways and interfere with the structure and function of critical biomolecules (Sharma and Agrawal 2005).

Aquatic organisms can accumulate metals through direct uptake from water via body surfaces or gills, ingestion of polluted food and sediments, or a combination of these exposure routes. In simpler aquatic organisms, uptake across the body surface is often dominant, whereas in more complex organisms, such as fish, metal uptake occurs primarily through the gills and digestive tract (Garai et al. 2021). As a result, metals can accumulate in specific tissues and organs, potentially leading to adverse biological effects.

Metal exposure can induce toxic effects at multiple levels of biological organization. At the organism level, these include morphological abnormalities, behavioral alterations, and physiological impairments such as reduced growth, fertility, and organ function. At the cellular level, metals can inhibit enzymatic activity, alter protein structure and function, disrupt mitochondrial processes and membrane integrity, and cause DNA damage. A central mechanism underlying metal toxicity is oxidative stress, characterized by excessive production of reactive oxygen species, which can damage lipids, proteins, membranes, and nucleic acids, ultimately impairing cellular energy metabolism and viability (Green and Planchart 2018, Zheng et al. 2025).

To counteract metal-induced toxicity, aquatic organisms possess homeostatic and detoxification mechanisms that regulate internal metal concentrations or facilitate their elimination. Metals may be sequestered and immobilized in inert granules, compartmentalized within lysosomes, or bound to metal-binding proteins such as metallothioneins. In parallel, antioxidant defense systems, including enzymatic antioxidants (e.g., catalase, superoxide dismutase, glutathione peroxidase, glutathione S-transferase) and low-molecular-weight antioxidants (e.g., glutathione, vitamins C and E), play a crucial role in mitigating oxidative stress. The extent of metal accumulation and toxicity is influenced by abiotic factors (e.g., temperature, pH, salinity) and biotic traits (e.g., feeding strategy, size, age, and reproductive status), as well as tissue-specific affinities that make certain organs particularly suitable as bioindicator tissues (Kraemer et al. 2006, Zheng et al. 2025).

In recent years, the emerging field of environmental metallomics (environmetallomics) has advanced the understanding of metal behavior in biological systems by integrating information on metal speciation, distribution, and molecular binding with biological effects and environmental exposure (Chen et al. 2020). This integrative approach has highlighted the importance of considering metals not only as bulk concentrations, but also in terms of their chemical form, intracellular localization, and interactions with biomolecules. Nevertheless, despite these conceptual and methodological advances, substantial gaps remain in the understanding of metal uptake pathways, intracellular transport, biotransformation, and elimination in aquatic organisms, particularly under environmentally realistic conditions and complex pollutant mixtures. Current research increasingly emphasizes the need to assess combined metal exposures, species- and tissue-specific responses, and the role of environmental factors in modulating oxidative stress and toxicity. Long-term and field-based studies are considered essential for validating laboratory findings, while the application of

antioxidant and other molecular biomarkers has been identified as a key priority for environmental monitoring and ecological risk assessment (Zheng et al. 2025, Chen et al. 2020).

In the Dinaric karst region, numerous studies have documented metal pollution in freshwater ecosystems, focusing primarily on metal concentrations in water, sediments, and selected tissues of aquatic organisms. These investigations include analyses of metals in fish tissues from Hutovo Blato (Has-Schön et al. 2008), Plitvice Lakes National Park (Vukosav et al. 2014), and the Raša River (Kljaković-Gašpić et al. 2022), aquatic macrophytes from Skadar Lake (Krivokapić 2021), and benthic invertebrates such as the mussel *Unio crassus* from the Mrežnica River (Kiralj et al. 2023). In addition to field surveys, laboratory-based studies have demonstrated cytotoxic effects of water samples from Raša coal-mine discharges on fish cell lines (Medunić et al. 2020). Collectively, these studies provide valuable evidence of metal presence and biological effects in karst freshwater systems, but they largely focus on single environmental compartments or selected tissues.

Within the Krka River system, previous investigations have demonstrated that municipal and industrial wastewater inputs near the town of Knin negatively influence fish, in which increased accumulation of metal(loid)s and altered physiological responses compared to the reference site at the river source were recorded (Dragun et al. 2018, Filipović Marijić et al. 2018, 2022, Mijošek et al. 2019, 2022). However, no studies to date have simultaneously examined metal(loid) concentrations in water, sediments, aquatic organisms (fish and intestinal parasites acanthocephalans), and fish gut content within the boundaries of the Krka National Park.

2.2. Microplastics

Biological effects of MP exposure have been more extensively investigated in marine organisms, while evidence for freshwater taxa is comparatively scarce, both in terms of the number of studies and the diversity of organisms examined. Available freshwater studies nevertheless suggest that many of the physical effects observed in marine species are also relevant in freshwater systems (Eerkes-Medrano et al. 2015).

Beyond their physical presence, MPs represent a complex chemical stressor. Plastics commonly contain additives such as flame retardants, plasticizers, and bisphenols that can be

released during environmental weathering or digestion. In freshwater environments, MPs can additionally adsorb a wide range of external pollutants, including pharmaceuticals, pesticides, fertilizers, and metals. Their high adsorption capacity is enhanced by small particle size, hydrophobicity, and high surface-area-to-volume ratios, while photo-oxidative weathering increases surface polarity and charge, facilitating metal binding. As a result, MPs can act as vectors that transport and release associated chemicals within the digestive tract of aquatic organisms, potentially increasing internal exposure to toxic substances (Naqash et al. 2020, Parker et al. 2021).

Following ingestion, MPs may exert effects at multiple levels of organization. At the organism level, MP exposure has been associated with starvation due to buildup and blockage of the gastrointestinal tract, reduced growth, impaired reproduction, behavioral abnormalities, and decreased mobility. At the tissue and cellular levels, MPs can induce tissue damage, inflammation, oxidative stress, immune suppression, endocrine disruption, neurotoxicity, and genetic damage, often accompanied by altered antioxidant status and changes in gene expression. Inhibition of acetylcholinesterase activity and increased oxidative stress have been reported in freshwater biota exposed to MPs (Bhuyan 2022, Naqash et al. 2020, Hampuwo et al. 2026).

Fish are a particular focus of freshwater MP research due to their ecological relevance and importance as a protein source for humans. The biological fate of MPs after ingestion depends on particle size, shape, and polymer type. Larger MPs are typically retained within the gastrointestinal tract, where they may cause physical damage but are expelled as pseudofeces. Smaller MPs and nanoplastics, however, can cross the intestinal barrier and translocate to internal tissues. While egestion can be relatively rapid for some species and particle types, retention times vary widely, with fibrous MPs showing higher persistence than fragments or pellets (Parker et al. 2021, Khan et al. 2025). Within fish, translocated MPs have been recovered from liver, gills, muscle and brain, suggesting some risk of MP trophic transfer (Cera et al. 2020, Parker et al. 2021). Experimental exposure studies, such as those conducted on brown trout (*Salmo trutta*), demonstrate that small MPs (1–5 μm) can translocate from the intestine to the liver and muscle, while larger particles (10 μm) remain largely confined to the gut, with some biochemical responses indicating impaired digestive and antioxidant enzyme activity (Hampuwo et al. 2026).

Despite rapid growth in MP research, major knowledge gaps remain. Most studies are laboratory-based and rely on juvenile fish, limiting ecological realism and the ability to generalize findings across life stages and sexes. There is a strong need for comparative laboratory–field studies using wild fish to assess environmentally relevant exposure scenarios, as well as for research addressing MP ingestion, accumulation, transport, and elimination dynamics. The role of MPs as vectors for metals and persistent organic pollutants, remains insufficiently resolved. Integrated approaches that combine chemical characterization with physiological, molecular, and ecological endpoints are essential to assess the long-term risks of MPs to freshwater biota (Bhuyan 2022, Naqash et al. 2020, Khan et al. 2025).

In karst freshwater systems of the Dinaric region, data on MP intake by organisms and biological effects are particularly limited. To date, MP pollution has been documented in cave and surface crustaceans from the sinking Pivka River in the Slovenian karst (Jemec Kokalj et al. 2025) and in farmed *Cyprinus carpio* from Croatia (Savoca et al. 2021). To our knowledge, no studies have investigated MP presence in wild freshwater fish from Croatian rivers. This lack of data represents a critical gap in understanding MP exposure pathways, ecological impacts, and potential risks to protected karst freshwater ecosystems and the human food web.

3. Bioindicator organisms

Measurements of pollutant concentrations in water provide information on the chemical status of an aquatic system at the time of sampling but, due to the dynamic nature of freshwater environments, such measurements are often insufficient to assess long-term exposure and biological effects. Pollutants in natural waters occur as complex mixtures whose toxicity may be modified by synergistic or antagonistic chemical interactions, and their potential to interact with aquatic organisms is strongly influenced by fluctuating physicochemical conditions and bio- or phototransformation processes. As a result, chemical monitoring alone has limited capacity to predict ecological consequences or to reflect cumulative impacts on aquatic biota (Holt and Miller 2011, Li et al. 2010).

To overcome these limitations, bioindicator organisms are widely used to assess the long-term effects of environmental pollution. Bioindicators are organisms whose presence, absence, abundance, or measurable physiological, biochemical, or behavioral responses provide information on the environmental conditions of their habitat (Holt and Miller 2011, Van der Oost et al. 2003). Unlike physical and chemical analyses, bioindicators integrate the combined effects of multiple stressors over extended periods and reflect the biologically relevant fraction of pollutants, including those that are unmeasured or present at low concentrations (Holt and Miller 2011). Bioindicator organisms are particularly valuable in freshwater ecosystems, where pollutant concentrations in water may fluctuate rapidly and where long-term exposure occurs primarily through sediments and food webs. Common bioindicators of freshwater quality include benthic invertebrates such as bivalves and crustaceans, then fish as organisms on the top of the aquatic food chain, as well as primary producers and planktonic organisms (Kumari and Paul 2020).

The effectiveness of a bioindicator organism depends on specific biological and ecological characteristics. An ideal bioindicator organism should be abundant, widely distributed, and exhibit limited mobility, ensuring site specificity, as well as moderate tolerance to environmental variability that allows sensitivity to pollution exposure without rapid population loss. Additional desirable traits include a defined ecological niche, participation in food webs, sufficient generation time to integrate exposure, and predictable responses to specific pollutants. Practical considerations such as ease of sampling, identification, handling, and cost-effectiveness are also critical for routine monitoring. In some cases, organisms that accumulate pollutants to levels exceeding those in the surrounding environment are used as sentinels, providing indirect estimates of environmental pollution through bioaccumulation (Holt and Miller 2011, Kumari and Paul 2020, Li et al. 2010).

However, biomonitoring does not replace chemical analyses but complements them, as bioindicators have certain limitations, including sensitivity to natural variability, scale-dependent responses and the risk of oversimplifying complex systems. Moreover, it may be difficult to attribute observed biological effects to specific pollutants or to extrapolate responses from individuals to population or ecosystem levels. For this reason, bioindicator-based approaches are most effective when applied alongside targeted chemical analyses (Holt and Miller 2011, Van der Oost et al. 2003).

Biomonitoring uses various methods of monitoring the state of ecosystems by determining biological changes in indicator organisms, i.e. their organs and tissues, which enables the detection of harmful effects. Changes within a biological system that indicate exposure to, or sublethal effects of, environmental pollutants are called biomarkers. They can occur at any level of biological organization, with molecular biomarkers responding first, followed by biochemical, physiological, and eventually morphological or histological changes (Hemmadi 2017). While higher-level biomarkers (e.g., reproduction, mortality, or shifts in community structure) are more ecologically relevant, lower-level biomarkers (e.g., molecular and cellular responses) are more sensitive and serve as early warning indicators of pollution (Hemmadi 2017, Okwuosa et al. 2019).

Overall, bioindicator organisms remain among the most ecologically relevant tools for assessing freshwater ecosystem status. When carefully selected and interpreted within an integrated monitoring framework, they provide robust insight into the long-term impacts of pollution, complement chemical data, and support informed environmental management and conservation strategies (Holt and Miller 2011).

3.1. Ecotoxicity tests

Ecotoxicity tests are standardized laboratory bioassays used to evaluate the effects of environmental pollutants on living organisms under controlled conditions, with the aim of assessing potential ecological risks. These tests were initially developed to support environmental regulation and therefore focused on acute exposure of experimental organisms to single substances and simple endpoints such as mortality, prioritizing simplicity, reproducibility, and cost-effectiveness (Bernhardt et al. 2017, Menghini et al. 2023).

Although classical toxicity tests are essential for understanding mechanisms of toxic action and comparing the relative toxicity of chemicals, they have limited ecological relevance when applied to natural systems. Single-species and single-compound tests therefore provide limited insight into mixture effects, species-specific sensitivity, trophic transfer, and indirect ecological consequences (Bernhardt et al. 2017).

To characterize the ecotoxicity of complex environmental mixtures, including undetected and unmeasured substances, current approaches increasingly emphasize whole effluent toxicity testing combined with multiple bioassays representing different trophic levels and biological

complexity, together with utilization of sublethal endpoints (Menghini et al. 2023, Vosylienė 2007). While whole effluent toxicity testing is applied in regulatory contexts, establishing clear links between observed toxic effects and environmental conditions remains challenging. Consequently, integrative testing strategies are increasingly recommended to improve ecological relevance and interpretability (Menghini et al. 2023, Vosylienė 2007).

Primary producers and primary consumers are central to freshwater ecotoxicity testing due to their ecological relevance and sensitivity to changes in the environment. The freshwater alga *Pseudokirchneriella subcapitata* is widely used in phytotoxicity assays because of its rapid growth and high sensitivity. Among invertebrates, the cladoceran *Daphnia magna* is one of the most commonly used species in zootoxicity testing, due to its broad distribution, short life cycle, easy maintenance and sensitivity to numerous pollutants. Both species are supported by extensive toxicity databases and standardized guidelines for regulatory use (Radix et al. 2000, Weyers et al. 2000, Moreira-Santos et al. 2004).

Despite extensive laboratory-based research, ecotoxicity data for complex environmental samples, particularly in karst freshwater systems and combining tests on algae and daphnids, remain scarce. A study on ecotoxicity of river water has been conducted in the Sava River in Croatia (Källqvist et al. 2008), but, to our knowledge, there is no study incorporating ecotoxicity testing of freshwaters in Dinaric karst. Given the strong hydrological connectivity and high variability of karst environments, there is a clear need for studies that apply standardized bioassays to wastewater and receiving surface waters under environmentally realistic conditions, using a combination of aquatic test organisms from various trophic groups and comparing their sensitivity. Such research would address a critical knowledge gap in ecologically meaningful assessments of pollutant toxicity and in linking biological responses to their chemical drivers in karst ecosystems.

3.2. Fish as bioindicator organisms

Fish are among the most widely used bioindicator organisms in freshwater ecosystems. They play a major ecological role in aquatic food webs, and the information they provide on the uptake, transfer, and biological effects of pollutants is of high ecological relevance. In most aquatic environments, fish occupy the highest or upper trophic levels, particularly omnivorous and carnivorous species, which are particularly useful for the integrated assessment of water-borne, diet-borne and sediment-deposited toxins. Furthermore, as an

important component of human nutrition, fish are relevant for evaluating potential risks to human health through bioaccumulation and biomagnification of pollutants (Okwuosa and Eyo 2019, Parente and Hauser-Davis 2013).

Besides that, fish possess several more biological and practical advantages as bioindicator organisms. They are widely distributed across aquatic habitats and their relatively large body size enables the collection of multiple tissue samples for parallel analyses. Their generally long lifespan allows the assessment of both short-term and chronic exposure to pollutants. In addition, fish integrate exposure from multiple pathways, including water and diet, and can accumulate metals and other pollutants in various organs, thereby reflecting environmental pollution over time. Extensive data are available for many species, further supporting their application in environmental monitoring (Chovanec et al. 2003, Okwuosa and Eyo 2019).

Fish are also sensitive models for research in biochemistry and comparative physiology. Because they inhabit diverse environments and are continuously exposed to fluctuating environmental conditions, they are suitable for both field and laboratory-based studies. Furthermore, fish can serve as indicators of sublethal effects, since exposure to low pollutant concentrations may induce measurable biochemical, cellular, or physiological responses long before mortality occurs (Okwuosa and Eyo 2019, Parente and Hauser-Davis 2013).

Despite these advantages, certain limitations must be considered. Fish mobility, particularly in migratory species, can complicate the identification of precise pollution sources and the duration of exposure. Therefore, careful species selection and consideration of ecological and behavioural characteristics are essential for reliable environmental assessments (Chovanec et al. 2003). Overall, fish represent integral indicators of aquatic ecosystem status, providing valuable insight into pollutant distribution, ecological effects, and potential risks to higher trophic levels, including humans.

3.2.1. Fish intestine as an indicator organ

In studies assessing pollutant exposure, accumulation, and toxicity in wild fish, the liver and gills are traditionally the most frequently analyzed tissues. The liver is highly metabolically active and represents the site of pollutant detoxification, while the gills serve as a major interface for uptake of pollutants from water. Muscle, blood, and kidney tissues are also commonly examined. In contrast, the intestine has long remained an overlooked

compartment, although its relevance as a target and indicator organ has increasingly been recognized (Chovanec et al. 2003, Hemmadi 2017, Lapointe and Couture 2009).

The gastrointestinal tract represents a critical interface between the organism and its environment. As a selectively permeable barrier, the intestinal epithelium regulates the nutrient, electrolyte and water absorption while protecting the organism from pathogens and foreign substances through immunogenic and non-immunogenic mechanisms (Marinsek et al. 2022). In recent decades, it is recognized that intestine plays an important role in pollutant uptake and detoxification, especially for metals. Increasing evidence suggests that dietary metal uptake via the intestine may exceed uptake from water through the gills and skin (Campbell et al. 2005, Lapointe and Couture 2009, Okwuosa and Eyo 2019). Consequently, the intestine is gaining prominence as a bioindicator tissue in environmental monitoring (Mijošek et al. 2021a, Marinsek et al. 2022).

Recent studies have demonstrated that exposure to environmental pollutants, including metals, MPs, pharmaceuticals, and pesticides, can induce morphological and functional alterations in fish intestine. Reported effects include reduction of the villi, disruption of the mucous layer, inflammatory responses, and fibrosis (Barišić et al., 2018, Dane and Şişman 2020, Marinsek et al. 2022). Such alterations may impair nutrient absorption, barrier integrity, and overall physiological homeostasis.

Although diet-borne metal uptake and associated toxicity have been investigated under laboratory conditions, these studies typically focus on acute exposure to one or a few metals at concentrations exceeding those found in natural environments (Creighton and Twining 2010, Ojo and Wood 2008, Omer et al. 2012). Field-based investigations conducted under environmentally realistic conditions remain limited. Metal accumulation and their biological effects in the intestines of wild freshwater fish have been reported in several systems, including Lithuanian freshwaters (Staniskiene et al. 2006), the Yangtze River (Zhang et al. 2007), Porsuk Dam Lake (Uysal 2011), the Danube River (Jarić et al. 2011), the Sava River (Filipović Marijić et al. 2012, 2014), the Ilova River (Mijošek et al. 2021a), and the North Macedonian rivers (Filipović Marijić et al. 2023). However, studies specifically addressing dietary metal uptake in wild fish from Dinaric karst systems remain scarce.

Similarly, ingestion of MPs by wild freshwater fish has been widely documented in European rivers, including the Widawa River (Kuśmierek and Popiołek 2020), the Mura River (Bogdan et al. 2022), the Kifissos River (Koutsikos et al. 2023), and the Danube River (Števove et al.

2025). Nevertheless, no published peer-reviewed studies to date have reported microplastic ingestion or associated intestinal effects in wild freshwater fish from the Dinaric karst region.

3.2.2. Brown trout (*Salmo trutta* Linnaeus, 1758)

Brown trout (*Salmo trutta*) is an autochthonous freshwater fish species in Croatia belonging to the family Salmonidae. It is indigenous to Europe, North Africa and western Asia and represents the most widespread and abundant native trout species in Europe, largely due to its strong adaptive capacity and ability to colonize diverse freshwater habitats. It is also highly valued as a food resource and a popular species in recreational fisheries (Klemetsen et al. 2003).

This rheophilic species primarily inhabits the upper and middle reaches of rivers, preferring cold, clear, fast-flowing waters with temperatures ranging from 2 to 16 °C. Anadromous forms are absent from the Mediterranean Sea. Adult individuals are opportunistic predators that feed on a wide range of organisms, including smaller fish, amphibians, mollusks, crustaceans, and aquatic insects and their larvae, placing them at high trophic levels within freshwater food webs. Depending on environmental conditions and age, brown trout can reach lengths of 15–70 cm and weights from 100 g to 6 kg. Sexual maturity is typically attained at 2–3 years of age, with spawning occurring during colder periods, usually beginning in autumn. Females construct nests (redds) in the substrate and cover the fertilized eggs with gravel and stones after spawning (Klemetsen et al. 2003, Mrakovčić et al. 2006).

According to the Red Book of Freshwater Fish of Croatia, brown trout is classified as a vulnerable species. Major threats include water pollution and hydromorphological alterations such as river damming and hydropower development, which restrict migration to upstream spawning grounds. Stocking practices may further affect the genetic integrity of native populations and complicate the taxonomic status of the species (Mrakovčić et al. 2006).

As a species present year-round in the Krka River, brown trout represents a suitable model organism for environmental monitoring and assessment of freshwater ecosystem health. Metal accumulation and toxicity in *Salmo trutta* from the Krka River have been investigated in the liver (Dragun et al. 2018) and in the intestine (Barišić et al. 2018, Mijošek et al. 2019, 2021b).

3.3. Acanthocephalans as bioindicator organisms

Acanthocephalans (phylum Syndermata), or thorny-headed worms, are a monophyletic group of obligate endoparasites that inhabit the intestinal tract of vertebrates, primarily fish. Approximately 1,300 species have been described, exhibiting considerable diversity in morphology, life cycle strategies, host specificity, habitat, and geographic distribution (Perrot-Minnot et al. 2023). Their life cycle includes arthropod intermediate hosts, and transmission occurs through trophic interactions when vertebrates ingest infected prey (Kennedy 2006).

Morphologically, acanthocephalans exhibit extreme morphological reduction and specialization for parasitism. They lack circulatory, respiratory, and digestive systems, and consequently are attached to the host intestine using a retractable proboscis with curved hooks. They absorb nutrients from the host intestinal lumen directly through their body wall (Herlyn and Taraschewski 2017, Kennedy 2006). Although infections may cause local tissue damage and immune responses in fish, they are typically not associated with severe pathology or mortality (Barišić et al. 2018, Dezfuli et al. 2008a). Beyond their biological role as parasites, acanthocephalans are ecologically significant because they can alter food web dynamics by manipulating the behavior of their intermediate hosts, thereby enhancing trophic transmission (Kennedy 2006). Importantly, they have also emerged as valuable organisms in environmental parasitology, a discipline focused on interactions between parasites, pollutants, and host health (Sures et al. 2017).

Acanthocephalans are particularly notable for their exceptional capacity to accumulate toxic trace metals. Toxic metals are absorbed through the tegument by the same pathways used for essential metals due to their chemical similarity. These parasites can accumulate metals to levels several thousand times higher than those measured in host tissues, exceeding the accumulation capacity of many conventional bioindicators (Filipović Marijić et al. 2013, 2014, Mijošek et al. 2022, Sures 2017). As a result, acanthocephalans act as biological sinks within the host intestine, reducing metal availability to host organs. In some cases, infected fish exhibit lower internal pollutant concentrations and reduced oxidative stress, suggesting a potential detoxification effect (Filipović Marijić et al. 2013, Hassanine and Al-Hasawi 2021, Mijošek et al. 2022, Sures 2017). The ratio of metal concentrations in acanthocephalans to those in host tissue is expressed as the bioconcentration factor (BCF). Because acanthocephalans have relatively short lifespans (approximately 50–140 days) compared to

their fish hosts, BCF values can reflect recent exposure to metals. Higher ratios indicate recent pollution, whereas lower ratios suggest longer-term exposure (Sures et al. 1999).

Despite their advantages, acanthocephalans also present limitations as bioindicator organisms. In case of migratory species, the mobility of their hosts can introduce spatial variability in pollutant accumulation, potentially complicating site comparisons. In addition, parasites are relatively small, may be difficult to sample, and have shorter lifespans than many free-living indicator organisms (Sures et al. 1999).

Although acanthocephalans are widely recognized as promising bioindicator organisms, research remains limited to relatively few groups worldwide (Sures et al. 2017). Most previous studies on parasite–pollutant interactions in freshwaters have focused on larval stages in intermediate crustacean hosts, whereas effects in definitive fish hosts are less thoroughly investigated. Moreover, studies on adult acanthocephalans have predominantly focused on comparing metal concentrations in parasites and other bioindicator organisms (Chunchukova et al. 2020, Chunchukova and Kuzmanova 2017, Duarte et al. 2020, Filipović Marijić et al. 2013, 2014, Mijošek et al. 2022, Nachev and Sures 2016), whereas the mechanisms underlying parasite-mediated detoxification, metal uptake and accumulation, protection against metal toxicity, and the effects of pollutants on the parasites themselves remain largely unresolved. Future research should adopt interdisciplinary and mechanistic approaches, including omics-based methods, to elucidate the physiological processes governing metal binding, detoxification, and parasite–host interactions under pollutant exposure (Perrot-Minnot et al. 2023). Strengthening this mechanistic understanding will improve the application of acanthocephalans as bioindicators, which could improve the assessment of exposure and impact of metals on freshwater organisms.

3.3.1. *Dentitruncus truttae* Šinžar, 1955

Dentitruncus truttae is an endemic freshwater acanthocephalan species restricted to limited areas of Bosnia and Herzegovina, Italy, and Croatia. It belongs to the family Leptorhynchoididae (Palaeacanthocephala) and is the only member of the genus *Dentitruncus*. Morphologically, it is characterized by 18 longitudinal rows of hooks on the proboscis, typically with 18 hooks per row. Unlike most acanthocephalans, whose hooks have smooth surfaces, scanning electron microscopy has revealed distinct surface striations on the hooks of *D. truttae* (Dezfuli et al. 2008b).

The most common definitive host is *Salmo trutta*, although the species has also been recorded in other freshwater fishes, including *Salmo obtusirostris*, *Anguilla anguilla*, *Thymallus thymallus*, and *Coregonus clupeoides*. Amphipods of the genera *Gammarus* and *Echinogammarus* serve as intermediate hosts (Moravec 2004, Vardić Smrzlić et al. 2013). This parasite is often characterized by high prevalence and, in some cases, high infection intensity, occasionally occupying a substantial portion of the intestinal lumen of the host (Barišić et al. 2018, Mijošek et al. 2022, Vardić Smrzlić et al. 2013).

Pathogenicity in definitive hosts depends on the intensity of infection and the depth of penetration of the parasite proboscis into the intestinal tissue. Unlike most acanthocephalans that only damage the mucosal layers, *D. truttae* penetrates deeply into the intestinal wall, inducing pronounced inflammatory and immune responses. Increased numbers of rodlet cells, mast cells, and fibroblasts, as well as inflammatory, necrotic, and hyperplastic alterations, have been documented in infected *S. trutta* (Dezfuli et al. 2008a, Barišić et al. 2018).

Metal accumulation in *D. truttae* has been investigated in specimens collected from *S. trutta* in the Krka River, where high total metal concentrations were reported in whole body of parasite (Mijošek et al. 2022). Furthermore, ultrastructural analyses combining transmission electron microscopy (TEM) and NanoSIMS have provided insight into element localization within different body parts of this acanthocephalan (Filipović Marijić et al. 2023a). Taken together, its high prevalence, pronounced host interactions, and confirmed ability to accumulate metals make *D. truttae* a particularly relevant model for advancing research in environmental parasitology and investigate important mechanistic aspects of efficient pollutant uptake and accumulation, as well as host–parasite interactions.

4. Assessing bioavailability and toxicity of metals

4.1. Distribution of metals among subcellular fractions

When evaluating metal toxicity in aquatic organisms, total tissue concentrations alone provide limited insight into biological risk. At the cellular level, biotic systems have evolved control mechanisms to minimize accumulation of reactive metal species and to facilitate optimal utilization of essential metals (Vijver et al. 2004). Only a fraction of the accumulated

metal participates in metabolic processes and might be potentially toxic, whereas another fraction is detoxified or sequestered through physiological regulatory mechanisms (Wallace et al. 2003). Consequently, assessment of subcellular metal distribution has emerged as a powerful approach for estimating their bioavailability in an organism and potential toxicity following bioaccumulation. A widely applied approach involves successive differential centrifugation followed by heat treatment of the cytosolic fraction. The field of metallomics was subsequently developed and defined as the comprehensive analysis of all forms of metal(loid)s in cells or tissues (Szpunar 2004, Wallace et al. 2003).

Within cells, metals are distributed among distinct compartments, such as organelles (e.g., mitochondria, microsomes and lysosomes), intracellular granules and cytosol. The biologically available fraction generally comprises metals associated with organelles and heat-denatured cytosolic proteins such as enzymes, often referred to as the metal-sensitive fraction (MSF), which represents metabolically active and potentially toxic metals. In contrast, metals bound to heat-stable cytosolic proteins such as metallothioneins or stored in metal-rich granules constitute the biologically detoxified metal fraction (BDM), reflecting sequestration processes. In addition, the trophically available metal (TAM) fraction represents the portion that may be transferred to predators. It excludes granules (Wallace et al. 2003).

The analysis of subcellular metal partitioning enables differentiation between detoxified and sensitive bioavailable metal pools and provides insight into the strategies that organisms use to cope with metal exposure (Rolland et al. 2025). When detoxification mechanisms are overwhelmed, excess metals may bind to sensitive targets such as enzymes or organelles, leading to cellular dysfunction and toxic effects (Vijver et al. 2004). Therefore, the distribution of metals among subcellular fractions is more indicative of potential toxicity than total body burden.

Short-term exposure typically induces the synthesis of metal-binding proteins such as metallothioneins, reflecting an active detoxification response. Under chronic exposure, metals are increasingly stored in inert granules, which may persist for long periods and influence accumulation and elimination patterns. Consequently, this approach identifies subcellular targets of accumulated metals and helps to understand how some organisms are more tolerant or sensitive to highly polluted environments, as well as how some elements induce greater damage than others (Rolland et al. 2025, Vijver et al. 2004).

Despite its relevance, information on subcellular metal distribution in fish remains largely limited to liver, gills, and gonads (Campbell et al. 2005, Caron et al. 2018, Desjardins et al. 2022, Giguère et al. 2006, Urien et al. 2018a), while data for the intestine are extremely scarce and restricted to a small number of elements (Oyoo-Okoth et al. 2012). Most studies report total metal concentrations in the intestine, which do not distinguish between bioavailable and detoxified forms. However, rare comparisons of total and cytosolic metal concentrations in freshwater fish intestines have confirmed that total concentrations overestimate metabolically available fractions (Filipović Marijić and Raspor 2012, Mijošek et al. 2019). In addition, fish frequently host intestinal parasites that may alter their metal regulation capacity (Oyoo-Okoth et al. 2010). Overall, data on the subcellular distribution and bioavailability of diet-borne metals in the fish intestine remain scarce, limiting accurate assessment of their toxicological significance.

4.2. Distribution of metals among cytosolic biomolecules

Tolerance to metal toxicity observed in some organisms can be linked to protective mechanisms that regulate metal uptake, subcellular distribution, and excretion, and include binding to various cellular ligands (Rainbow 2002, Rosabal 2015). Although subcellular fractionation provides valuable information on general metal partitioning into “sensitive” and “detoxified” pools, it does not identify specific metal-binding biomolecules nor clarify their structural or functional significance. A detailed understanding of metal distribution among cytosolic biomolecules is therefore essential for elucidating both detoxification processes and mechanisms of metal toxicity (Urien et al. 2018b).

Within the cytosol, metals are generally considered metabolically available and soluble. Metals associated with heat-denaturable proteins are regarded as biologically active and potentially toxic, as they may inhibit enzymatic activity, displace essential elements, or promote ROS formation. In contrast, metals bound to heat-stable proteins, particularly MTs or MT-like proteins, are interpreted as detoxified forms reflecting protective sequestration mechanisms (Urien et al. 2018b).

A commonly used methodological approach in metalloprotein research combines size-exclusion high-performance liquid chromatography (SEC-HPLC) with inductively coupled plasma mass spectrometry (ICP-MS). Size-exclusion chromatography separates cytosolic biomolecules according to molecular size, while ICP-MS enables sensitive,

element-specific detection of associated metals. Given the complexity of the cytosolic matrix, comprising proteins, peptides, and low-molecular-weight ligands, this hyphenated technique represents a powerful screening tool for assessing metal distribution among biomolecules of different sizes (Krasnići et al. 2014, Strižak et al. 2014).

The SEC-HPLC–ICP-MS approach has been widely applied in aquatic ecotoxicology. Cytosolic metal distribution has been investigated in several freshwater fish species, including liver and gills of *Squalius cephalus* (Krasnići et al. 2013, 2014), liver of *Salmo trutta* (Dragun et al. 2018), liver of *Perca flavescens* (Caron et al. 2018), liver and gonads of *Catostomus commersonii* (Urien et al. 2018b), liver and gills of *Squalius vardarensis* (Krasnići et al. 2019) and liver and gills of *Carassius gibelio* (Dragun et al. 2020). However, intestinal tissue remains largely underrepresented and has been examined only in *Salmo trutta* (Mijošek et al. 2021b).

Thus, detailed characterization of cytosolic metal distribution moves beyond total cytosolic concentration measurements and provides mechanistic insight into how organisms regulate, tolerate, or succumb to metal stress. Such an approach may be particularly valuable for elucidating metal-handling strategies in acanthocephalans, for which comparable metallomic investigations are currently lacking.

4.3. Biochemical biomarkers

Adverse effects of environmental pollutants at the population level are often difficult to detect in wild organisms, as they typically become evident only after prolonged exposure, when damage may already be irreversible. In contrast, toxic effects first occur at the cellular and molecular levels. Detecting these early responses is therefore essential for timely environmental assessment at low pollution levels (Van der Oost et al. 2003).

Biochemical biomarkers are measurable changes in cellular structures or biochemical functions that occur in response to pollutant exposure and serve as early warning indicators of anthropogenic stress. However, their responses are rarely driven solely by pollution, as they are influenced by intrinsic factors (e.g., age, sex, health, nutritional and reproductive status) and extrinsic factors (e.g., dose, exposure duration and route, environmental conditions and interactions with other chemicals). To account for this variability, a multi-biomarker approach is strongly recommended, as it enables a more reliable distinction between natural variability

and anthropogenic impact and provides a more comprehensive evaluation of biological responses to pollution (Ryan and Hightower 1996, Van der Oost et al. 2003).

A well-established biomarker of metal exposure is metallothionein (MT), a low-molecular-weight, cysteine-rich, metal-binding, inducible protein located primarily in the cytoplasm. Metallothioneins play a key role in maintaining homeostasis of essential metals such as Cu and Zn and in detoxifying toxic metals like Cd, Hg, Ag, and Pt. A well-established correlation exists between MT induction and intracellular metal concentrations, making MTs reliable indicators of fish metal exposure (Hemmadi 2017).

In addition to MTs, various inducible cytosolic proteins are rapidly synthesized in response to environmental stressors such as heat, UV radiation, metal(loid)s, organic pollutants and plastics. While non-specific, the concentration of total cytosolic proteins (TP) reflects cumulative biological impact of multiple factors and serves as a biomarker of general stress. Many of these proteins are highly conserved across taxa, making them broadly applicable in ecotoxicological studies (Sanders and Dyer 1994).

Metals and MP are known to induce oxidative stress by generating reactive oxygen species (ROS) or by disrupting antioxidant defenses, leading to cellular damage. As a result, biomarkers of oxidative stress are widely used in ecotoxicological studies to assess the impact of pollutants in aquatic organisms (Hemmadi 2017).

One of the most commonly used biomarkers of oxidative damage is malondialdehyde (MDA), a reactive byproduct of lipid peroxidation. Transition metals such as Cd, Co, Cu, Hg, Ni, Pb, Fe, Sn, and V cause the peroxidation of polyunsaturated fatty acids in cell membranes, resulting in the formation of lipid peroxy radicals and degradation products like MDA. Although not the only end-product of lipid peroxidation, nor a substance generated exclusively by it, MDA is widely accepted as a reliable indicator of oxidative stress-induced lipid damage in fish tissues (Hemmadi 2017, Rizzo 2024).

In the enzymatic antioxidant defense system, primary enzymes directly neutralize ROS, providing the first line of defense against oxidative stress. Superoxide dismutase (SOD) catalyzes the conversion of the superoxide radical into molecular oxygen and hydrogen peroxide, which is then broken down into water and oxygen by catalase (CAT). Together, the SOD–CAT system plays a central role in protecting cells from oxidative stress and these enzymes are widely used as biomarkers in ecotoxicological studies (Hemmadi 2017).

Secondary antioxidant enzymes support the primary defense system. For example, the phase II detoxification enzyme glutathione S-transferase (GST) contributes to the elimination of xenobiotics and protects cells from oxidative damage by reducing hydroperoxyl groups in oxidized membrane phospholipids (Hayes et al. 2005, Hellou et al. 2012).

Another important component of the antioxidant defense is the non-enzymatic antioxidant glutathione (GSH), a ubiquitous thiol-containing tripeptide involved in neutralizing ROS, maintaining redox balance, and stabilizing cell membranes. It also serves as a substrate for GST-mediated conjugation reactions and plays an important role in the detoxification of metals such as Cd and Cu through binding to their thiol groups. Due to its sensitivity to oxidative changes, GSH is frequently used as a biomarker of metal-induced oxidative stress in fish (Hemmadi 2017, Hayes et al. 2005).

Furthermore, the glycolytic enzyme lactate dehydrogenase (LDH) that catalyzes the reversible reduction of pyruvate to lactate is commonly used as a biomarker of tissue metabolic capacity, anaerobic metabolism and organ or tissue lesions. In fish, LDH activity has also been applied to assess the effects of chemical stress (de Almeida et al. 2019, Osman et al. 2010).

An ideal biomarker of environmental pollution should be sensitive, chemically specific, cost-effective, measurable in small amounts, available by non-invasive techniques and quantitatively related to exposure levels. Moreover, it should be more responsive than conventional endpoints such as growth, survival, or reproduction, while still maintaining ecological relevance. Although substantial progress has been made, there remains a need for early-warning signs that are both sensitive to sublethal concentrations and ecologically relevant (Hellou 2012, Ryan and Hightower 1996, Van der Oost et al. 2003).

Recent research emphasizes the importance of integrating multiple biomarkers into standardized assessment framework for a more comprehensive evaluation of metal exposure and associated cellular damage. However, further field validation across various species and ecosystems is required to establish basal concentrations of biomarkers. In particular, synergistic and antagonistic effects of pollutant mixtures on biochemical biomarkers, as well as tissue-specific response patterns beyond the liver, remain insufficiently characterized. Distinguishing pollution-induced changes from natural biomarker variability would enable more robust conclusions and facilitate comparisons among ecologically similar systems worldwide (Zeng et al. 2025).

Although several studies have investigated intestinal biomarker responses to pollutant exposure in freshwater fish under laboratory conditions (Huang et al. 2022, Sakalli et al. 2018, Teodorescu et al. 2012, Zhang et al. 2021), and some studies on wild fish have reported histopathological alterations (Barišić et al. 2018, Marinsek et al. 2018), data on biochemical biomarkers specifically measured in the intestine of wild freshwater fish remain extremely limited (Filipović Marijić et al. 2023b, Mijošek et al. 2019). Furthermore, many biomarkers commonly used to assess metal and MP exposure have not yet been systematically evaluated in the intestinal tissue of freshwater fish. To date, biochemical biomarker responses to environmental pollution have not been investigated in acanthocephalans. Considering their exceptional capacity to accumulate metals and their ecological relevance in host–parasite–pollutant interactions, this represents a significant and unexplored research area.

4.4. Gene expression profiling

In recent years, molecular approaches have increasingly been incorporated into ecotoxicological studies to gain mechanistic insight into organismal responses to environmental stressors. Among these approaches, transcriptomic analysis based on RNA sequencing (RNA-seq) has become a powerful tool for identifying genes and pathways involved in specific biological processes (Huang et al. 2016, Martin and Wang 2011).

Ribonucleic acids (RNAs) represent the transcribed output of the genome, the transcriptome, reflecting which genes are actively expressed under particular conditions. With the development of affordable next-generation sequencing technologies, high-throughput RNA-seq has become the preferred method for comprehensive transcriptome profiling. RNA-seq enables both functional annotation of genes and differential gene expression analysis, allowing the identification of molecular pathways that respond to environmental stressors (Raghavan et al. 2022).

Transcriptomic analyses can be performed either using a reference-guided or a *de novo* assembly approach. Reference-guided assembly requires an available genome sequence of the studied species or a closely related organism, to which sequencing reads are mapped. In contrast, *de novo* transcriptome assembly reconstructs transcripts directly from sequencing reads without prior genomic information. Recent technological advances have made *de novo* reconstruction reliable and efficient, which is particularly valuable for non-model organisms

lacking genomic resources, such as acanthocephalans (Huang et al. 2016, Martin and Wang 2011, Raghavan et al. 2022).

Studies investigating gene expression responses to metal exposure in fish intestine have predominantly been conducted under laboratory conditions and have focused on a limited number of candidate genes and metals (Bai et al. 2019, Hoseini et al. 2022, Kwong et al. 2011, Zhang et al. 2019). In contrast, transcriptome-wide analyses in natural populations remain scarce (Uren Webster et al. 2013). Even more limited is the application of transcriptomic approaches to parasitic helminths.

Although advances in high-throughput sequencing have substantially improved our understanding of genomic diversity, phylogeny, metabolic pathways, and host–parasite interactions in helminths (Coghlan et al. 2019, Hotez et al. 2008), genomic and transcriptomic data for Acanthocephala are still extremely limited. Compared to other helminth phyla, such as Nematoda and Platyhelminthes, this group remains understudied, likely due to its limited direct relevance to human health (Perrot-Minnot et al. 2023). Despite approximately 1,300 described acanthocephalan species, genomic and transcriptomic resources have only recently become available for a single species, *Pomphorhynchus laevis* (Mauer et al. 2020).

Importantly, the molecular mechanisms underlying the remarkable capacity of acanthocephalans to accumulate extremely high metal concentrations remain unexplored. Identifying gene sequences encoding proteins involved in metal uptake, transport, binding, and detoxification, and comparing their expression under different gradients of environmental pollution, represents a critical first step toward understanding the molecular basis of metal handling in these parasites. Such knowledge would provide novel insight into both parasite biology and host–parasite interactions in polluted freshwater ecosystems.

5. Aims, research objectives and hypotheses

The objective of this thesis is assessment of the exposure, uptake, distribution and toxic effects of pollutants (metal(loid)s and MPs) in the intestine of fish and their intestinal parasites, acanthocephalans.

Hypotheses:

1) Fish intestine has mechanisms of diet-borne pollutant regulation which can be used as early biological responses to pollutant exposure

2) Toxicity of pollutants depends on subcellular distribution and binding to specific biomolecules in fish intestine and acanthocephalans

3) The transcriptome of acanthocephalans reflects a specific lifestyle, and gene expression of acanthocephalans and fish intestines indicates environmental pollution levels

Publications

Publication No. 1: Long-term and seasonal trends of water parameters in the karst riverine catchment and general literature overview based on CiteSpace

Environmental Science and Pollution Research (2024) 31:3887–3901
https://doi.org/10.1007/s11356-023-31418-3

RESEARCH ARTICLE

Long-term and seasonal trends of water parameters in the karst riverine catchment and general literature overview based on CiteSpace

Sara Šariri[1] · Damir Valić[1] · Tomislav Kralj[1] · Želimira Cvetković[2] · Tatjana Mijošek[1] · Zuzana Redžović[1] · Ivana Karamatić[1] · Vlatka Filipović Marijić[1]

Received: 1 September 2023 / Accepted: 4 December 2023 / Published online: 14 December 2023

Abstract

Although Europe is the continent with the highest proportion of karst areas, where hydrological systems are essential but extremely sensitive, data on the ecological status of karst riverine catchments are scarce. The aim of the present study was to assess the spatial and temporal (long-term and seasonal) variability of the physico-chemical and organic water parameters in the headwaters of the Krka River and its tributaries, as representatives of a typical karst ecosystem, situated in one of the largest karst areas in Europe, Dinarides in Croatia. It is affected in its upper reaches by improperly treated wastewaters, so anthropogenic influences and ecological status were estimated with the aim to present consequences of pollution exposure and importance of strict monitoring of such sensitive karst ecosystems worldwide. Results indicated degraded water quality, poor ecological status, and disturbed seasonal fluctuations at wastewater-influenced sites, primarily due to high levels of nutrients and organic matter. However, improvement was observed downstream in the Krka National Park, confirming the self-purification as important processes in dynamic karst rivers. Natural seasonality, observed at sites without wastewater influence, was mainly driven by fluctuations in water levels and primary production during the year. Literature analysis by CiteSpace pointed to scarce data on this topic worldwide (China and the USA account for 49% of all publications) and in Europe (34%). Therefore, such study is a valuable contribution in presenting the long-term and seasonal variability of ecological water parameters and in providing a more comprehensive understanding of the health of catchment under influence of multiple stressors.

Keywords Physico-chemical parameters · Organic parameters · Wastewaters · Water quality · Krka River · Scientometric analysis · CiteSpace

Introduction

Karst areas are one of the most diverse landscapes in the world, with outstanding natural, cultural, and hydrogeological values. Highly important components of the karst areas are hydrological systems, since they are key factors in the karstification process, which act not only as a natural sink for atmospheric CO_2, but also as water resources for human consumption, aquatic ecosystems, soil formation, and agricultural irrigation (Goldscheider 2019). Their importance is also reflected in the fact that many karst terrains have been declared protected areas. In fact, 23% of all national parks in Europe are partially or mostly karstic, which corresponds to the percentage of karst in the land area of Europe (21.6%) (Chen et al. 2017; Goldscheider 2019; Goldscheider et al. 2020; Telbisz and Mari 2020).

Accordingly, many of the unique karst phenomena and surface and subsurface biodiversity depend on the good quality of karst water systems (Goldscheider 2019). The main factors affecting water quality in karst are diffuse pollution from agricultural lands and point source pollution from landfills and improperly treated wastewater. In karst

Responsible Editor: Philippe Garrigues

✉ Vlatka Filipović Marijić
vfilip@irb.hr

[1] Ruđer Bošković Institute, Bijenička Cesta 54, Zagreb, Croatia

[2] Teaching Institute for Public Health Dr. Andrija Štampar, Mirogojska Cesta 16, Zagreb, Croatia

areas, pollutants can move rapidly and unfiltered from the surface to groundwater through sinkholes and fracture networks in the bedrock (Ford and Williams 2007; Yue et al. 2019). Due to the unique hydrologic characteristics and dynamic interactions with groundwater, karst hydrologic systems can exhibit large variations in water levels and water quality parameters and therefore be particularly difficult to predict and manage. However, it is critical to study temporal trends since current changes in climate and human activities significantly affect water quality (Alamdari et al. 2022). Monitoring both long-term and seasonal trends in physico-chemical and organic parameters contributes to a better understanding of natural variability and enables a timely response to observed deviations that could be harmful to the ecosystem or local population.

Typical example of the karst river catchment, not only protected as a natural park, but also anthropogenically impacted by wastewater and agricultural runoff, is the Krka River in Dinaric karst region in Croatia. Based on the intercalibration river typology, it belongs to the IC type R-M2 Mediterranean rivers with catchment area of 100–1000 km^2, mixed geology (except non-siliceous), and high seasonality (Schöll et al. 2012). The Krka River springs at the base of Dinara Mountain near the Town of Knin (8300 inhabitants), after which it flows downstream through a series of valleys (poljes) and canyon formations until reaching the Adriatic Sea near the Town of Šibenik (42600 inhabitants). Along the course of the Krka River, there are seven prominent tufa deposits forming barrages and cascades which cause the water to change flow and velocity with alternating lotic and lentic microhabitats. Since 1985, part of the Krka River watercourse has been protected as National Park (GRC 1985). While the upper course of the Krka River is known for its exceptional beauty, species richness, and sensitivity, necessitating the monitoring and estimation of its water quality, there are only few papers that indicate the physico-chemical parameters of this region (Cukrov et al. 2008; Filipović Marijić et al. 2018; Sertić Perić et al. 2018).

General review of the literature data showed that research on water quality of European karst waters is scarce and mostly focused on groundwater and springs (Hoaghia et al. 2021; Puig et al. 2017) and lake systems (Barešić et al. 2011; Sertić Perić et al. 2011; Sironić et al. 2017; Vurnek et al. 2021), while physico-chemical and organic water parameters in surface karst rivers are less frequently studied. In order to obtain a systematic and objective overview of a research domain, scientometric analysis software CiteSpace is increasingly used (Li et al. 2022; Yang et al. 2023; Zhong et al. 2022). CiteSpace can map a set of bibliographic records as a several types of networks, such as co-cited documents, collaborating countries, or co-occurring keywords, where the nodes represent the objects of analysis (e.g., cited references, countries, keywords), and the links describe the relationship between these nodes. Citation burst of a node, i.e., a keyword, reflects an increase in its citation frequency in a short period of time related to a particular topic within a research area (Chen 2006, 2017). Although there are two studies that have used CiteSpace to analyze the current state of research on karst in general (Zhao et al. 2021) and karst groundwater pollution (Zhou et al. 2020), to our knowledge, no attempt was made to use CiteSpace to visualize the literature data related to water quality parameters and quality status of karst rivers.

Accordingly, the main aim of the present paper was to assess long-term trends of the physico-chemical (turbidity, temperature, conductivity, total dissolved solids (TDS), pH, dissolved oxygen, saturated oxygen, dissolved CO_2, chemical oxygen demand (COD), ammonium, total nitrogen, nitrate, nitrite, total phosphorus) and organic (total organic carbon (TOC), dissolved organic carbon (DOC), mineral oils, phenols) water parameters in the Krka River and get general conclusions on theirs seasonal and spatial variability in the karst ecosystem. Specifically, the impact of wastewater discharges on ecological status and seasonality in the dynamic karst area was evaluated, as well as the physico-chemical properties of the industrial and municipal wastewaters, with the aim to give insights for further monitoring and protection of this sensitive karst area. As a general overview, scientometric data of the current research situation, the main topic categories, and developing trends in this field worldwide and in Europe were presented based on CiteSpace analysis.

Materials and methods

Study area

To maintain the water quality of a river, monitoring and management at the catchment level are recommended, as tributaries can significantly influence the spatial and temporal dynamics of the river water quality (Calmuc et al. 2020). Therefore, this study included sampling sites of the whole upper catchment of the Krka River and presented for the first time its water quality since previous included only a few sampling sites in the upper reaches and omitted the influence of the tributaries (Fig. S1). A total of eight sampling sites, differing by anthropogenic influences, were investigated:

A. Sites without direct anthropogenic influence: KRS (1) — the source of the Krka River (a reference site); TKR (4) — the Krčić Stream (flows into the Krka River near its source)

B. Anthropogenically influenced sites: TKO (5) — the Kosovčica River (flows near the Knauf gypsum factory, which has caused several ecological incidents); TOR (6) — the Orašnica River (passes by the screw factory and its basins with technological wastewater); KRK-MWW (2) — Krka watercourse influenced by the municipal wastewater outlets from the Town of Knin; TBU (7) — the Butišnica River (flows through the area influenced by agricultural runoff and numerous septic tanks from the surrounding settlements near the Town of Knin, but also from Bosnia and Herzegovina); KBL-NP (3) — Brljan Lake (located in the Krka National Park, downstream from the other sites and providing insight into the ecological status of the park)
C. Wastewater sampled directly from basin: IWW (8) — industrial wastewater from the screw factory.

As seen, the main point sources of pollution in the Krka River are industrial and municipal wastewaters discharged into the river without adequate purification treatment (Filipović Marijić et al. 2018). The industrial wastewaters come from the artificial basins near the screw factory, located 3.3 km west of the Krka National Park. It has been active since 1956 and is known for numerous ecological incidents (DLS 2018; Kisić et al. 2019), especially due to the karst nature of the soil, allowing industrial wastewaters to reach the groundwater and enter the nearby Orašnica and Krka rivers through the underground fracture networks. Previous analyses of this water confirmed a high concentration of oil, volatile organic compounds, trace metals and metalloids, chlorides, and aromatic hydrocarbons such as toluene, ethene, benzene, and xylene (DLS 2018; Filipović Marijić et al. 2018; Kisić et al. 2019). However, there are no previous data for organic pollutants in the Krka River and its tributaries, so concentrations of total phenols and mineral oils were presented for the first time in this study. Municipal wastewaters from the Town of Knin are also regularly discharged into the Krka River without appropriate treatment. The municipal outlet is located downstream of the factory and about 2 km upstream from the border of the National Park. Previous studies reported poor water quality at this location, and parameters such as pH, COD, nutrient and trace metal concentrations, as well as microbiological parameters reflected the impact of sewage effluents (Filipović Marijić et al. 2018; Sertić Perić et al. 2018).

Despite the decades long influence of wastewaters in the upper reaches of the Krka River and vicinity of the Krka National Park, long-term trends in water quality parameters in this area are still unknown. As there have been some ecological incidents in this area in the past, and some industrial pollutants remain in the sediment of water bodies even after the pollution sources are no longer present, it is important to assess the long-term changes in water quality parameters (Dragun et al. 2022). Other factors such as changes in climate, surrounding land cover and land use may also affect water quality and potentially be reflected in long-term trends (Alamdari et al. 2022). Maintaining good ecological status of the water at the tufa barriers downstream is a top priority task and a long-term objective of Krka National Park, as the biotic communities at the barriers and the process of tufa deposition depend on it (Gulin et al. 2021).

Sampling procedure

Water sampling was conducted in each season of 2021: Winter (January 28), Spring (April 25–27), Summer (July 20), and Autumn (October 18–20). The only exception of this seasonal sampling dynamic was the Krčić Stream (TKR), which went dry in summer and autumn and measurement of organic parameters. After the first sample analysis in January, there was a need to monitor other organic parameters besides TOC and DOC, at anthropogenically impacted sites. Therefore, concentration of total phenols and mineral oils (total hydrocarbons) was also measured during the next three sampling campaigns at the reference (KRS) and pollution impacted sites (KRK-MWW, TOR, TBU, and IWW) in the same water samples as TOC and DOC. For the chemical laboratory analysis of physico-chemical parameters, river water samples were collected manually in polyethylene plastic bottles, while those for organic parameters were collected in glass bottles. The samples were stored in the dark at temperatures up to 8 °C until analysis. The schematic framework of the methodological procedure can be seen in Fig. S2.

Analyses of physico-chemical and organic water parameters

A total of 18 physicochemical parameters were analyzed; among them, temperature, pH, conductivity, dissolved oxygen concentration and saturation, and TDS were measured in situ at 0.1 m depth using portable field probes (Mettler Toledo, precision of ± 0.2; ± 0.01; ± 0.5%; ± 1,5%; ± 0.5%, respectively). In situ measurements were not performed only for industrial wastewater, because immersion of probes in the water of such poor quality could damage them, so only pH, conductivity, and TDS were measured subsequently in filtered samples. Concentrations of nutrients (ammonium, nitrite, nitrate, total nitrogen, and phosphorus), turbidity, COD, and dissolved CO_2 were determined in the laboratory using the respective standardized methods (Hach Lange 2013; Baird and Bridgewater 2017). The concentration of total nitrogen was determined by UV spectrophotometric method with alkaline potassium persulfate digestion. Total phosphorus was analyzed colorimetrically, by ascorbic acid method. COD was measured with potassium permanganate and sulfuric acid following standard procedure HRN

EN ISO 8467:2001. Total dissolved CO_2 was analyzed by standard titration procedure using Na_2CO_3 and phenolphthalein. Declared uncertainties of spectrophotometer used for the listed measurements (Hach Lange) are < 1% for 0.50–2.0 Abs at 546 nm. Among organic water parameters, TOC and DOC were measured according to the method HRN EN 1484:2002 (±4.40%) using TOC analyzer TOC-VCSH + ASI–V + SSM-5000A (Shimadzu), while qualitative analysis and concentration measurements of phenols and mineral oils were performed according to ASTM D 4763-06 (2020) using the Fluo-Imager MB53 (Skalar Analytical B.V.).

The overall assessment of the water quality was performed according to the Directive on water quality status of the Government of the Republic of Croatia, which defines the limit values for "very good," "good," and "below good" ecological status of the main types of water bodies present in Croatia (GRC 2019). According to ecological and physicochemical characteristics, majority of investigated Krka River watercourse fits to a national type HR-R_12: medium and large upland river, as a 73-km-long karst river flowing in the Dinaric Western Balkan ecoregion (ER5; sensu Illies 1978; GRC 2019). Industrial wastewater parameters were compared with the emission limit values defined by the Regulation on limit values for wastewater emissions (GRC 2020).

Literature collection and scientometric visualization by CiteSpace

Prior to CiteSpace analysis, literature datasets on water quality of karst rivers worldwide and on European karst rivers were collected separately. For both datasets, the Web of Science (WoS) Core Collection was used as the data collection platform. In creating both datasets, papers on marine environments were filtered out. Therefore, the topics "karst" AND "water quality" AND "river" NOT "marine" NOT "ocean" were used for global scientometric dataset, and a total of 237 publications from 1995 to 2022 were found. For the second dataset, containing research papers on karst rivers in Europe, the topics "Europe" AND "karst" AND "river" were chosen and 61 publications from 1999 to 2022 were found. For both datasets, literature data were stored as complete records and cited references.

A scientometric analysis was then performed using CiteSpace 6.1.R6 (Basic). To analyze the collaborative network and identify the most important countries in the karst river water quality research worldwide, the network was constructed by setting the node type to "country" and the node rendering mode to "tree ring history," so that each node represents a country and the concentric citation rings represent the number of citations for the country in the corresponding years. The size of the node indicates the number of papers published in that country, and the links between nodes indicate the collaboration between co-authors from different countries (Chen 2006, 2017). A cluster analysis was conducted to analyze the main themes and developing trends in the research on karst river water quality worldwide and on European karst rivers. For this purpose, the node type was set to "reference and keyword," combining document co-citation network and keyword co-occurrence network. In the co-citation network, each node represents a research paper, and the link between them represents that they were co-cited in the later literature. In the keyword co-occurrence network, each node represents a keyword, and the linked nodes co-occur in the same paper (Chen 2006, 2017). The network nodes were then clustered. For the first dataset, "title words" were chosen as the source to label clusters and for the second dataset, "keywords" were chosen.

Results and discussion

Spatial differences and long-term trends in the Krka River

Physico-chemical water parameters

At all sampling sites along the karst Krka River and its tributaries, water temperature, pH, and dissolved oxygen saturation were within the range typical for karst rivers (Table S1), while their spatial distribution followed the trends previously recorded in the Dinaric karst watercourses (Cukrov et al. 2008; Filipović Marijić et al. 2018; Sertić Perić et al. 2018; Terzić et al. 2014; Žutinić et al. 2020). Specifically, average pH increased in the downstream direction of the main Krka River flow (7.48–8.02), while dissolved CO_2 concentration showed the opposite trend, decreasing 4.9–3.3 mg L^{-1} (Table S1). Both trends could be explained by CO_2 degassing, as previously noted by Srdoč et al. (1986), Cukrov et al. (2008), Sironić et al. (2017), and Žutinić et al. (2020). The temperature increase was evident in the downstream direction of the Krka River and in the four tributaries in summer (10.5–20.4 °C), while it was mostly comparable and uniform between all sites in other seasons (Table S1). Turbidity trend pointed to low levels at the river source and in the national park as expected (0–1 FAU), with increasing levels at the tributaries (1–9 FAU), especially showing the influence of industrial discharge to clearness of water at nearby TOR. The highest turbidity value was found at KRK-MWW (4–10 FAU) and IWW (15–2355), clearly reflecting impact of municipal and industrial wastewaters, respectively (Table S1).

Anthropogenic influences were also reflected in the increase of dissolved ion content downstream, as evidenced by conductivity and TDS, which levels were much higher

at IWW than any other freshwater sampling site. If IWW is excluded, the highest TDS and conductivity values were measured in the tributaries TKO, TBU, and TOR (Table S1), probably originating from agricultural runoff at TBU and industrial wastewater at TOR. Both of these influences are present in the catchment of TKO, but, since the Kosovčica River flows through an area composed of gypsum and anhydrite rock mass, it is also enriched by sulfates from the underlying bedrock, which might explain maximum TDS values at this site (Mihaljević et al. 2011; Terzić et al. 2014). In addition, increased nitrate, total nitrogen, and total phosphorus concentrations at the IWW and KRK-MWW compared to the other sites confirmed industrial and municipal wastewaters as an important source of these nutrients (Table S1). Our results on COD, total phosphorus, total nitrogen, and nitrate concentrations were higher compared to the karst Mrežnica River, which has been historically contaminated with industrial waste (Dragun et al. 2022). However, nutrient concentrations were still lower than those in the agriculture-impacted Karašica River and the Vučica River, non-karstic Croatian rivers with the same catchment size as the Krka River, indicating the importance and positive effect of the groundwater sources and water turbulence for the water quality of the karst catchment (Amić and Tadić 2018).

Long-term trends of the physico-chemical water parameters could be evaluated for pH, temperature, conductivity, and dissolved oxygen concentration at KRS, KRK-MWW, and KBL-NP (Fig. 1), since the data for mentioned parameters were previously published for the same sampling locations along the Krka River (Cukrov et al. 2008; Filipović Marijić et al. 2018; Rovan et al. 2021; Sertić Perić et al. 2018; Terzić et al. 2014; Žutinić et al. 2020). All selected sampling campaigns were performed in autumn to omit seasonal influences and the results confirmed an increase in physico-chemical water parameters from KRS, as an unpolluted and most upstream location, downstream along the Krka River in each period, except dissolved oxygen concentrations which were mostly comparable among the sampling sites. Comparison over the years showed comparable levels of most of the parameters, with exception of few peaks downstream (mostly 2008, 2018,

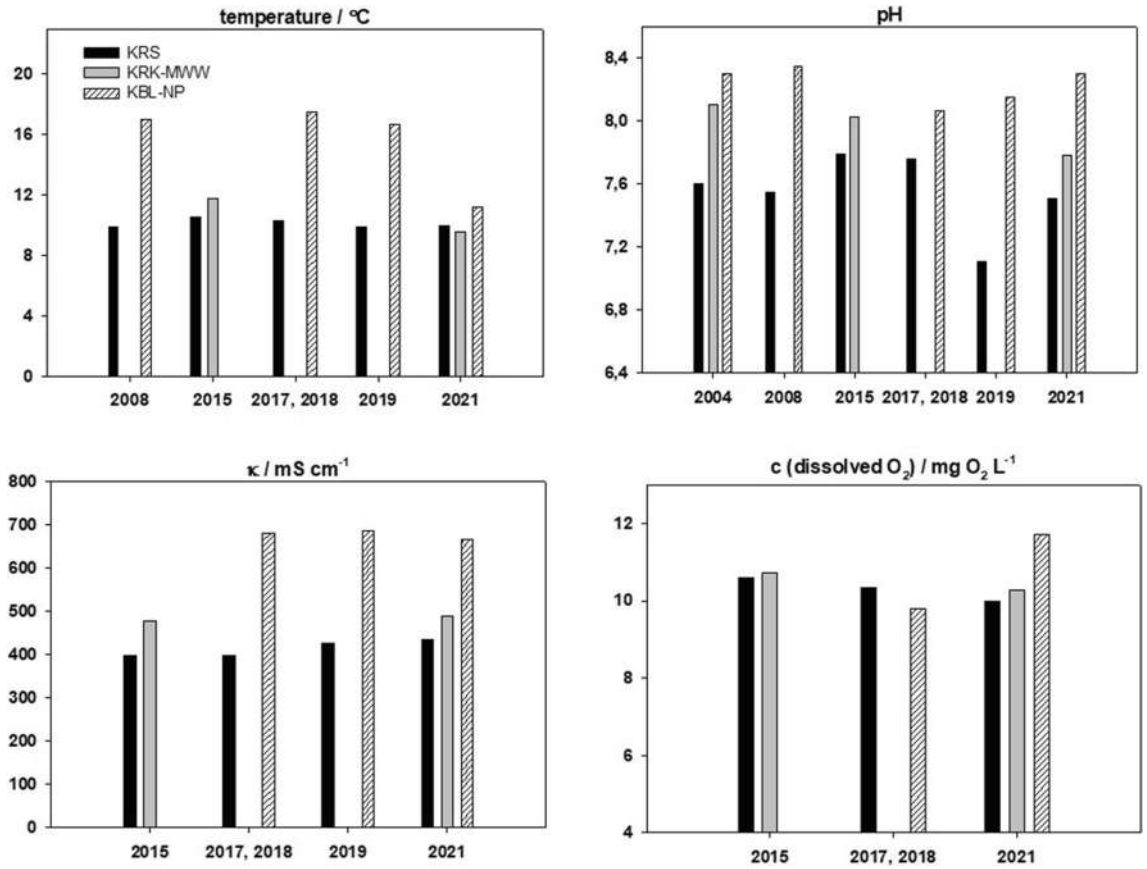

Fig. 1 Long-term trends of the average water temperature, pH value, conductivity (κ), and dissolved oxygen concentration along the sampling sites 1, 2, and 3 in the Krka River watercourse in autumn season. Data are related to the following publications: 2004 — Cukrov et al. (2008); 2008 — Terzić et al. (2014); 2015 — Filipović Marijić et al. (2018) and Sertić Perić et al. (2018); 2017 and 2018 — Žutinić et al. (2020); 2019 — Rovan et al. (2021); 2021 — from this study

2019; Fig. 1), probably reflecting influence of few ecological incidents (DLS 2018; Kisić et al. 2019).

When considering IWW and Regulation on limit values for wastewater emissions (GRC 2020), water quality of samples taken in 2021 was worse compared to samples taken in 2015 (Filipović Marijić et al. 2018) due to much higher conductivity, TDS, dissolved CO_2, ammonium and total nitrogen concentrations, and especially turbidity (55 times higher average levels) and COD (46 times higher average levels) in 2021. But for these data, possible coincidence of the moment of sampling with the wastewater discharge should be considered. On the contrary, lower values of the same parameters at nearby TOR in our study than 2018 could possibly be due to the gradual purification since 2014, when the dam between industrial wastewaters and the Orašnica River was built and mitigated the overflow of the wastewater during high water levels.

Organic water parameters

Spatial differences in TOC and DOC values in the natural karst system pointed to the lowest organic matter values at KRS and TBU (Table S2) and showed comparable values to the TOC results obtained previously in the Krka River (Žutinić et al. 2020) and other karst sources in the Dinaric mountain range (Matić et al. 2013), as well as to the DOC values reported for the Krka River (Cukrov et al. 2012; Strmečki et al. 2018; Žutinić et al. 2020). As expected, the highest TOC and DOC levels were recorded at IWW, as a site impacted by industrial effluent. Besides IWW, maximum TOC and DOC concentrations were obtained in TOR and KRK in all seasons, reflecting the impact of industrial and municipal wastewaters on these locations, respectively (Table S2). Although presented results on organic content pointed to some impact of wastewaters on the karst ecosystem, the average DOC concentrations in the Krka River were still lower than in the other European rivers such as Douro (2.4 mg L^{-1}) and Loire (3.9 mg L^{-1}) (Abril et al. 2002).

The impact of wastewaters on the river water quality was also reflected in content of mineral oils and total phenols. Mineral oil concentrations in our study area ranged from below 0.005 to 56.811 mg L^{-1} (Table S2). Values over 0.005 mg L^{-1} were found not only at TOR and IWW in all three seasons in which they were measured, but also at KRK-MWW in summer and autumn (Table S2). For total phenols, IWW was the only site where concentrations over 0.005 mg L^{-1} were observed (0.047 mg L^{-1} in summer and 0.182 mg L^{-1} in autumn) (Table S2). Such results not only suggested that the main sources of organic carbon, mineral oils, and phenols in the Krka River and its tributaries are industrial, but they also indicated the presences of municipal wastewaters discharged into the watercourse without adequate treatment (Filipović Marijić et al. 2018).

Our results represent one of the first data reported for organic water parameters in the upper reaches of the Krka River. Long-term trends could therefore not be presented, except the comparison with TOC and DOC values reported for KRS and KBL-NP by Strmečki et al. (2018) and Žutinić et al. (2020). In these studies, TOC concentration was 1.44 mg L^{-1} at KRS and 1.56 mg L^{-1} at KBL-NP, while DOC levels were mostly below 1.00 mg L^{-1}, therefore confirming comparable values with our data, except much higher levels in our study at KRK-MWW, TOR, and especially IWW, as a result of direct impact of wastewater discharges (Table S2). In addition, results for mineral oils and total phenols in the Krka River were recorded only between 1969 and 1978 (Munjko 1979), being much higher (0.7–5.4 mg L^{-1} for mineral oils and 0.0–7.0 mg L^{-1} for total phenols) compared to 2021, but here differences in analytical methodology should be considered.

Seasonal differences in the Krka River

Physico-chemical water parameters

Seasonality of specific physico-chemical water parameters in the karst catchment was estimated in the Krka River for the first time. The water level of this karst watercourse followed common trend for temperate climate zone, with the highest levels in winter and spring (219 cm in January; 117 cm in April) and decreased in summer and autumn (77 cm in July; 80 cm in October), being in accordance with the precipitation regime (Croatian Meteorological and Hydrological Service). Water temperature also followed the trend specific for temperate climate zone with the highest levels in April and July at downstream locations, while stable values were confirmed at karst river source (10–11 °C) (Table S1).

Seasonal variations of the most physico-chemical water parameters were not specific, especially at the wastewater impacted sites IWW and KRK-MWW, since temporal variations at these sites mostly depend on the moment of the wastewater discharge. Regarding other sites, variations in the dissolved nutrient and total solid levels pointed to the influence of the rainfall and water level regime. Generally, elevated nitrite concentrations were recorded during the wet season (winter and spring) at all locations except TOR in autumn, probably reflecting the impact of nearby IWW where the highest nitrite levels were recorded in autumn (Fig. 2a; Table S1). An increase in nitrite or nitrate levels during a rainy period was commonly observed in rivers and groundwater (Huebsch et al. 2014; Yue et al. 2018), especially in regions with a Mediterranean climate, characterized by large differences in precipitation between seasons, when nitrate peaks are often observed after the summer drought (Bernal et al. 2005). In our study, nitrate concentrations peaked in autumn, which coincided with the

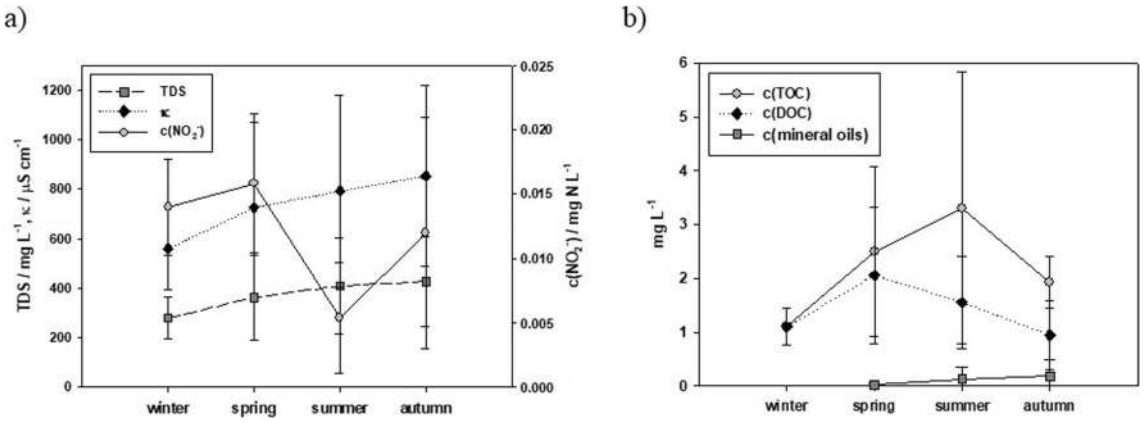

Fig. 2 Seasonal dynamics of **a** the average values of TDS, electrical conductivity (κ) and nitrites measured at six sampling sites in the Krka River catchment (locations 1, 3–7) and **b** the average TOC, DOC, and mineral oil concentrations measured at three sampling sites in the Krka River catchment (locations 1, 6, 7)

end of the summer drought and low water levels (77 cm in July) and the beginning of the rainy periods (Fig. S3) that cause surface runoff. Although point sources of pollution (such as industrial wastewaters and sewage effluents) have a big impact on nitrogen levels in aquatic environments, typically the main sources of nitrogen are the chemical fertilizers from the soil in the river catchment (Huebsch et al. 2014; Malá et al. 2022; Schliemann et al. 2021; Wang et al. 2020). During low flows in the dry summer season, nitrogen from organic matter and fertilizers cannot be transported into receiving water so they are stored in farmland or infiltrated into groundwater. Then, in the wet season, precipitation accelerates surface runoff and subsurface flow, flushing the accumulated nitrogen from soils into rivers, what can also be related to our study (Glavan and Pintar 2010; Huebsch et al. 2014; Wang et al. 2020; Xu et al. 2019).

On the other hand, average values of TDS and electrical conductivity were higher during the dry season (summer and autumn) (Fig. 2a), being in accordance with the results of Jebreen et al. (2018) and might be the result of the lower water levels and less effective purification processes in the river and its tributaries (Filipović Marijić et al. 2018). In addition, generally higher levels of COD, ammonium, and total nitrogen were recorded in April and of total phosphorus in July, but mostly due to their increased levels at TOR and TKO (Table S1). These are locations under the impact of nearby industry, TOR of screw factory and TKO gypsum facilities and probably reflect specific impact of pollution related to discharge peaks and as such, cannot be related to natural seasonality.

Organic water parameters

Measured organic water parameters had the highest values at the wastewater impacted locations, KRK-MWW and IWW, but without common seasonal trends since these values probably reflect discharge peaks. Still, the highest values of TOC and DOC at IWW were especially evident in spring (Table S2), coinciding with the higher values of physico-chemical parameters at the nearby site TOR, which may reflect the timing of wastewater discharge in this season (Table S1). If wastewater impacted sites are excluded, mineral oils showed a tendency to increase in dry periods, after agricultural activities and during low water levels in summer (77 cm) and autumn (80 cm) (Table S2; Fig. S3). Strmečki et al. (2018) reported the highest TOC values at KBL-NP in spring and explained it as the result of autochthonous phytoplankton production. The DOC concentrations measured by Marcinek et al. (2020) in the Krka River estuary (approximately 33 km downstream of the sampling sites in this study) were also higher in summer than in winter. In our study, the highest TOC and DOC concentrations in the river watercourse were recorded in spring and summer (Fig. 2b), especially at TOR as the location directly impacted by the wastewater effluents. Therefore, our results may reflect increased biomass of primary producers in the river system and increased agricultural activities in the catchment area (Cukrov et al. 2012; Stanley et al. 2012), but again were additionally influenced by wastewater discharge from the nearby screw factory and cannot only be presented as natural seasonal variations of organic matter in the river.

Ecological status of the Krka River

Physico-chemical water parameters

According to the Directive on water quality status of the Government of the Republic of Croatia (GRC 2019), the ecological status of a water body can be classified as "very good," "good," or "below good" based on the limit values

for pH, COD, and concentration of ammonium, nitrate, total nitrogen, and total phosphorus. In our study, the ecological status of water from the reference site was very good considering all parameters except ammonium concentrations in spring and autumn (0.02 mg N L^{-1}) and pH value in winter (7.29) (Fig. 3). Ecological status of water at KRS was previously classified as very good by Hrvatske vode (2016), Filipović Marijić et al. (2018), and Sertić Perić et al. (2018), including also ammonium concentrations (below 0.01 mg N L^{-1}) and pH value (7.4–8.5). As there are not some specific sources of pollution here, such data can be classified as occasional disturbances due to the complex subsurface hydrological systems in karstified regions and big catchment area of the river source (Bonacci et al. 2006; Ravbar and Kovačič 2014). Moreover, the Krčić Stream flows into the Krka River near its source so TKR might have a direct impact on KRS water quality. Most parameters at TKR were within the range for very good ecological status (Fig. 3) and values typical for karst streams, comparable to Kolda et al. (2019), who confirmed pristine oligotrophic conditions in the Krčić Stream.

However, physico-chemical parameters measured in the other downstream tributaries pointed to ecological status below good in all seasons at KRK-MWW, TOR, and TKO, mainly due to high concentrations of nutrients and COD (Fig. 3), confirming long-term influence of municipal and industrial wastewaters from the Town of Knin (8300 inhabitants), screw factory, and gypsum factory, respectively (Filipović Marijić et al. 2018; Magdaleno et al. 2001; Mihaljević et al. 2011; Sertić Perić et al. 2018). Considering the other parameters, which were not defined in the Directive (GRC 2019), the highest water turbidity, TDS, conductivity, and total nitrogen concentrations were recorded at KRK-MWW, TOR, and TKO, indicating anthropogenic degradation of water quality compared to the reference site (Table S1). Higher turbidity at KRK-MWW might be the result of microbial activity, typical for municipal wastewater outlets as already confirmed by Kapetanović et al. (2009) and Filipović Marijić et al. (2018), while extremely high turbidity at IWW is the result of high content of mineral and fuel oils in these wastewaters.

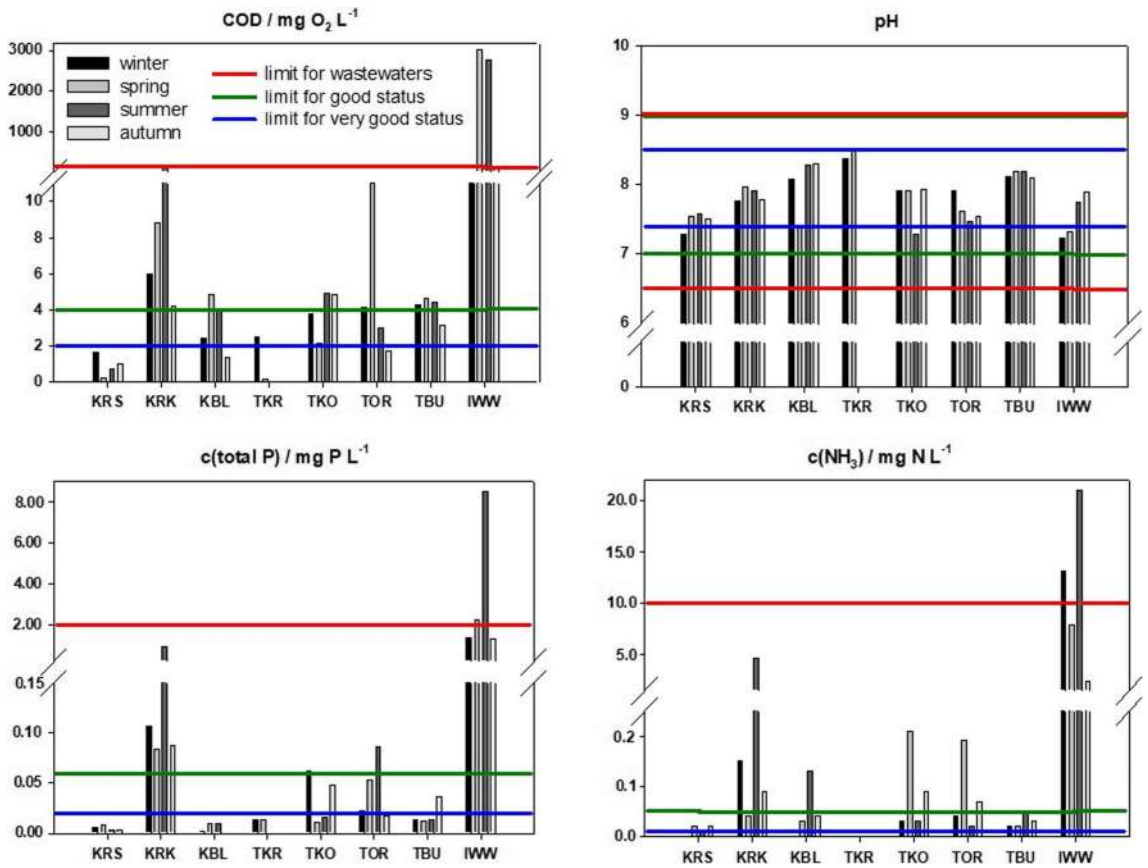

Fig. 3 Comparison of physico-chemical water parameters in the Krka River catchment with limit values for "very good" and "good" ecological status (locations 1–7) according to the Directive on water quality status (2019) and limit values for "good" quality of wastewaters (location 8) according to Regulation on limit values for wastewater emissions (2020). As defined, upper and lower limits are presented for the pH value and the upper limit for all other parameters

The water parameters at TBU were within the limits for very good or good ecological status, depending on the season, except COD, which exceeded the limit of 4 mg O_2 L^{-1} in all seasons except autumn. Higher nutrient concentrations, TDS, and conductivity than at the reference site were also observed, possibly indicating the impact of agricultural activities on the quality of the Butišnica River (Divya and Belagali 2012) (Fig. 3).

Water from KBL-NP, the only sampling site situated in the Krka National Park, had mostly very good quality compared to the other sampling sites. The only parameters that exceeded the limit values for good ecological status according to GRC (2019) were COD and ammonium concentrations in spring and summer (Fig. 3). Good water quality of the Brljan Lake may be the result of limited anthropogenic activities within the borders of the Krka National Park, sedimentation due to the lower water velocity in the lake, positive effect of aquatic macrophytes, and mixing with new freshwater originating from the Zrmanja River which enters into the Krka by underground springs (Cukrov et al. 2008; Srivastava et al. 2008). Self-purification of surface karst rivers downstream of the pollution source has also been previously reported by Cukrov et al. (2008) and Malá et al. (2022).

Compared to the other sites, much higher concentrations of ammonium, total nitrogen, nitrates, nitrites, total phosphorus, and COD were determined at KRK-MWW, indicating deteriorated water quality due to urban wastewater effluents (Filipović Marijić et al. 2018; Schliemann et al. 2021; Xu et al. 2019). However, dissolved oxygen saturation at KRK-MWW was quite high (91.6–97.9%), contrary to the most sites near the municipal wastewater outlets (Magdaleno et al. 2001; Olatunde et al. 2015). These results are in accordance with the results from 2017 (104.0%, 114.3%) and 2018 (99.8%) and might be explained by the oxygen production by submerged aquatic macrophytes, abundant at the KRK–MWW sampling site, which compensates oxygen loss due to biodegradation of organic matter (Filipović Marijić et al. 2018; Malá et al. 2022; Sertić Perić et al. 2018). Based on the results of the present study, it is important to connect the Town of Knin to a wastewater treatment plant. According to Malá et al. (2022), this is a factor that influences the quality of surface waters in karst areas more than the population size of a municipality and that could significantly reduce the concentrations of ammonium and total phosphorus.

The quality of industrial wastewater (sampling site IWW) was poor throughout the whole year, especially in summer when all parameters, except pH, exceeded the limits set by the Regulation on limit values for wastewater emissions (GRC 2020) (Fig. 3). Moreover, the highest concentrations of some nutrients were also measured in autumn, when they were about five times (total nitrogen) and even nine times (nitrites) above the emission limit values for pollutants in wastewater prior to their discharge into the surface waters.

Organic water parameters

There are not defined limits for organic water parameters (TOC, DOC, mineral oils, total phenols) in natural freshwater systems related to specific ecological status, but only for wastewater emissions (GRC 2020), and are defined as 10 mg L^{-1} mineral oils, 0.10 mg L^{-1} total phenols, and 30 mg L^{-1} TOC. In industrial wastewater near the Krka River (IWW), these regulatory limits were exceeded for mineral oil concentrations in all investigated seasons (24.902–56.811 mg L^{-1}), phenols in autumn (0.181 µg L^{-1}), and TOC in spring (100 mg L^{-1}) (Fig. 4) with around three times higher levels than the permissible limit (GRC 2020).

The Regulation does not specify a limit value for the concentration of DOC, but they were also the highest at IWW, followed by KRK-MWW, in accordance with all other organic parameters and, therefore, confirming elevated levels of organic matter at municipal and industrial wastewater impacted sites (Table S2). The lack of adequate treatment process resulting in such high hydrocarbon concentration in the wastewater discharged into the environment poses

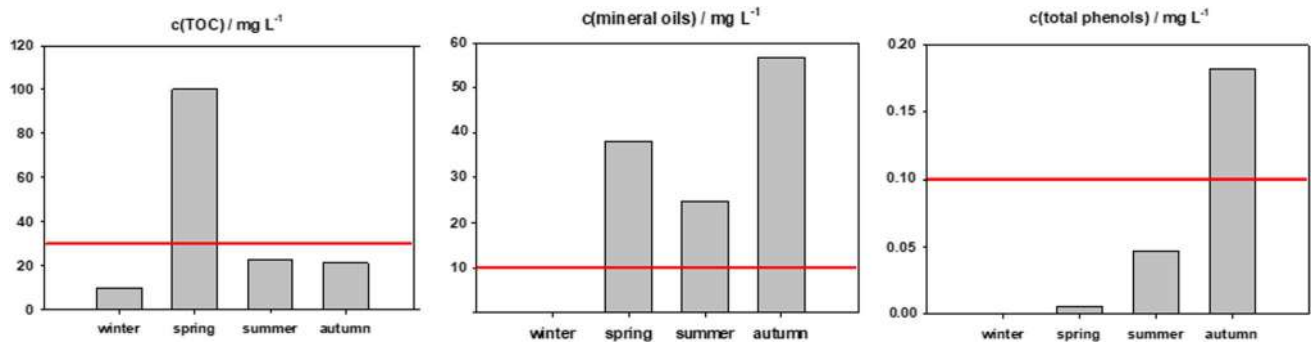

Fig. 4 Comparison of organic water parameters of industrial wastewaters (location 8) with defined emission limit values for pollutants in wastewater (red line) prior to their discharge into the surface waters, according to the Regulation on limit values for wastewater emissions (2020)

a threat to the Krka National Park (Filipović Marijić et al. 2018). Therefore, immediate remediation of the basins with industrial wastewater from the screw factory is necessary.

Our study provided the first data on organic water parameters in the upper reaches of the Krka River and confirmed the impact of wastewater discharges on the concentration of mineral oils in this ecosystem, so further assessment of organic pollutant exposure is recommended. Integrated approach of water quality assessment and maintenance of good water quality in the lower part of the Krka River is also recommendable not only for nature conservation, but also for the drinking water supply of the Town of Šibenik (Ravbar and Kovačič 2014).

Scientometric literature analysis using CiteSpace

According to the CiteSpace literature analysis, most research on these topics was conducted in Asia (38%), Europe (34%), and North America (22%). This distribution differs somewhat from the proportion of karst areas on these continents (Europe 21.8%, North America 19.6%, Asia 18.6%), likely due to factors such as the availability of research funding or the number of research institutions (Goldscheider et al. 2020). The most productive countries were China with 85 papers and the USA with 57 papers, accounting for 49% of all publications (Fig. S4). According to their betweenness centrality, China (0.56), Germany (0.42), the USA (0.17), the Czech Republic (0.15), and Switzerland (0.13) played a central role in establishing collaborations with other countries. The leading European countries by number of publications were Germany (16 papers), Croatia (15 papers), and Spain (9 papers). According to Chen et al. (2017), carbonate rocks cover 50.5% of Croatia, 29.2% of Spain, and only 21.4% of Germany.

Worldwide literature dataset

Literature set after combining the topics "karst," "water quality," and "river," and not including the "marine environment," resulted in 237 papers worldwide, suggesting that water quality parameters in karst rivers are not commonly studied overall. A total of 18 clusters were identified from the co-citation network of references and keywords and labeled using the log-likelihood ratio (LLR) algorithm (Fig. 5). Based on the input dataset, four major research areas on water quality of karst waters were identified for the period 1995–2022: First ranked was cluster #0, labeled "Southwest China" (size = 69 nodes, mean silhouette value = 0.808), and

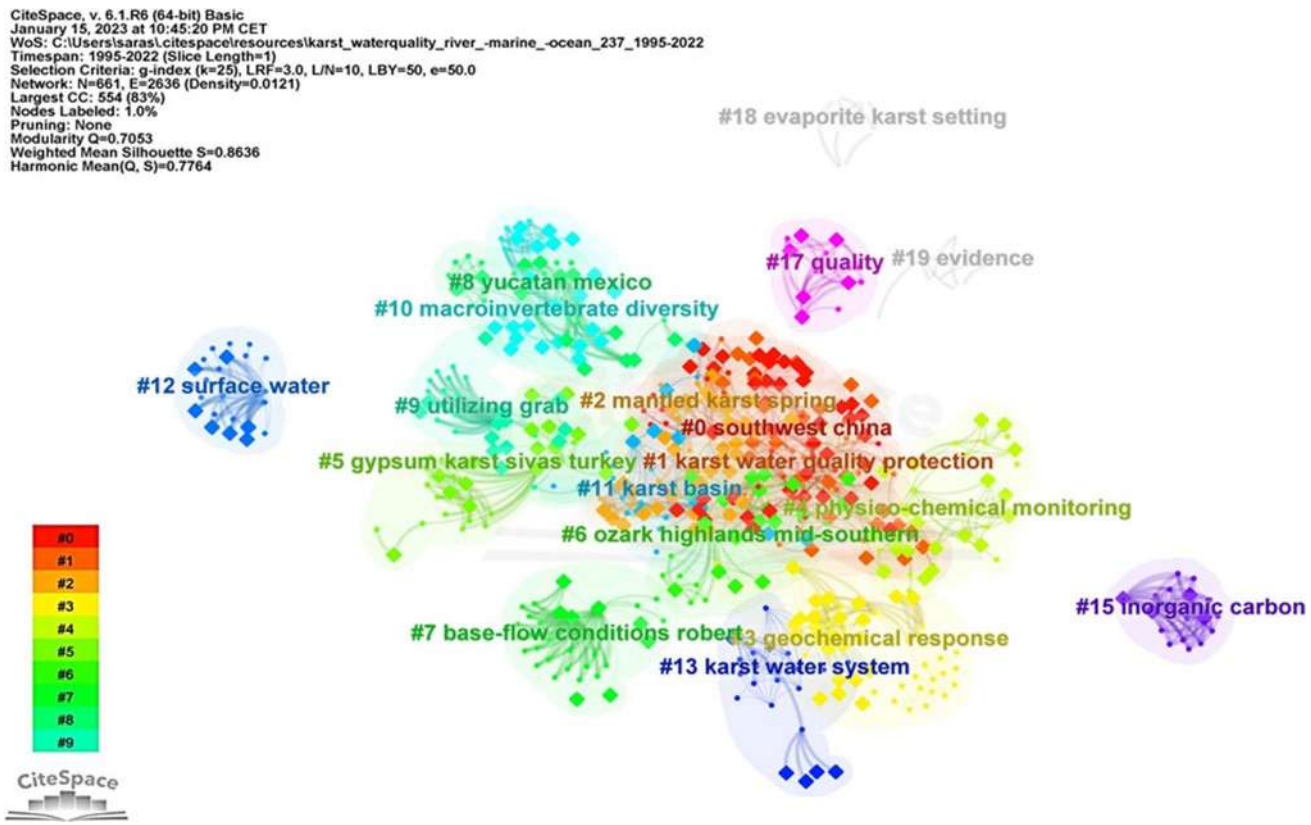

Fig. 5 Clustered network of co-cited references (dots) and co-occurring keywords (diamonds) created from literature connecting topics "karst," "water quality," and "river." Cluster labels were determined from title words using the log-likelihood algorithm

contained mainly literature on hydro(geo)chemical variations in groundwater and rivers in subtropical karst areas in southwest China characterized by monsoon climate. The second was cluster #1, labeled "karst water quality protection" (size = 54, mean silhouette value = 0.722), which focused on the pollution of karst waters by nitrates from fertilizers and the prevention of pollution from agricultural land. Third ranked was cluster #2, labeled "mantled karst spring" (size = 49, mean silhouette value = 0.770), and literature in this cluster mainly measured bacterial pathogens and heavy metals in karst waters to assess the health risk when using these waters as a drinking water source. The fourth cluster was cluster #3, labeled "geochemical response" (size = 49, mean silhouette value = 0.940), and it was focused on monitoring the hydrochemical and hydrodynamic behaviors of karst springs and rivers (Fig. 5).

Based on the mean year of publications of each cluster (Fig. 6), it can be concluded that the focus of karst water quality research has shifted from case studies of hydrologic connections and water quality in specific karst systems (1993–1999, clusters #7, 12, 17, 18, 19) to developing sampling strategies, studying the influence of land use on water quality and biota, monitoring hydrochemical and hydrodynamic changes, and using macroinvertebrate diversity as a bioindicator of karst water quality (2001–2008, clusters #0, 3, 5, 8, 9, 10, 15). The most active topics during the most recent period (2009–2014, clusters #1, 2, 4, 6, 11, 13) involved human impact on karst groundwater quality, monitoring of physico-chemical parameters, environmental isotopes, heavy metals, and bacterial pathogens at the catchment scale, as well as identifying sources of these pollutants. Therefore, the main topic of our study fits into the current framework of the global research and complement the sparse database on long-term and seasonal trends of water quality parameters in surface karst rivers. These results are relevant not only for the Dinaric karst, but also for other geologically similar karst landscapes distributed worldwide (Ford and Williams 2007; Goldscheider et al. 2020).

European literature dataset

Scientometric analyses of the 1999–2022 literature connecting the topics "Europe," "karst," and "river" identified a total of 12 clusters, labeled using the latent semantic indexing (LSI) algorithm (Fig. 7). After examining the characteristic keywords for each cluster, resulting main research areas are those focused on organisms dependent on karst waters, especially macroinvertebrates and plants: cluster #0 "dinaric karst" (aquatic beetles and

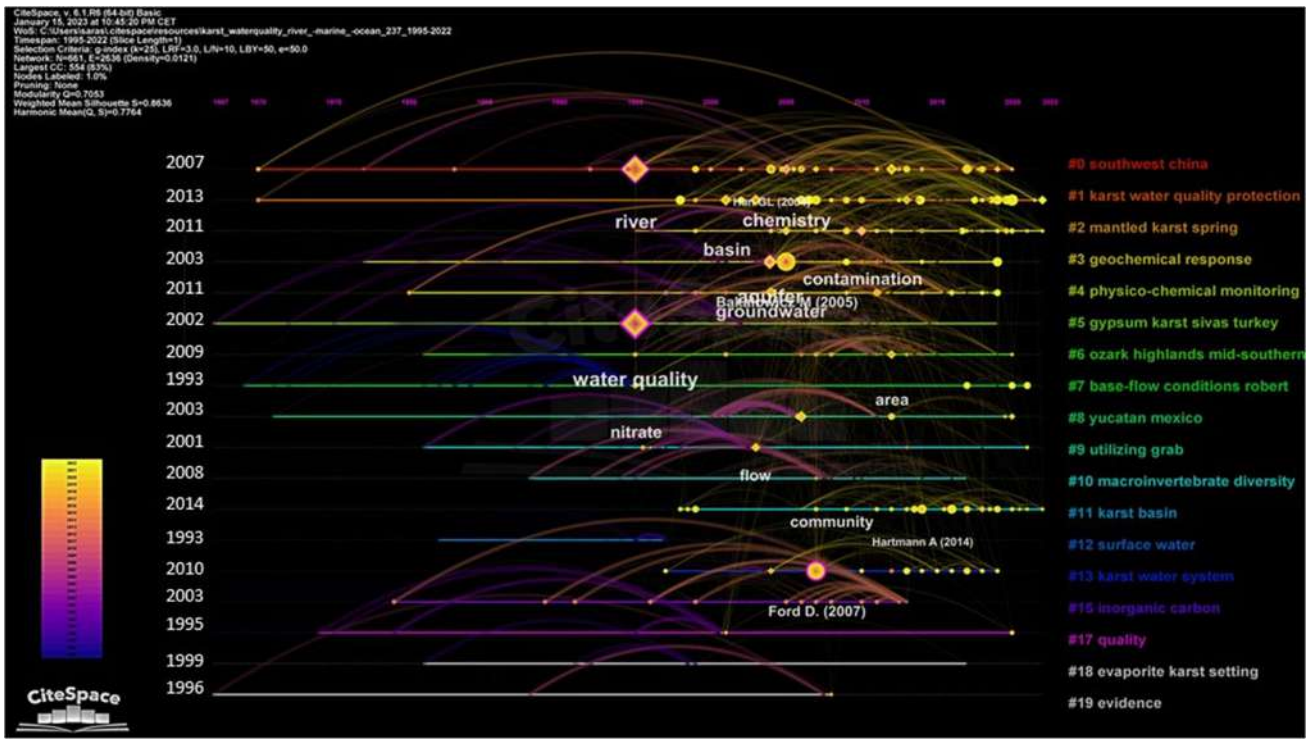

Fig. 6 Timeline view of clustered network of co-cited references (dots) and co-occurring keywords (diamonds) created from literature connecting topics "karst," "water quality," and "river." The numbers on the left are the mean years of each cluster's publications. The color of the links indicates when citations were made

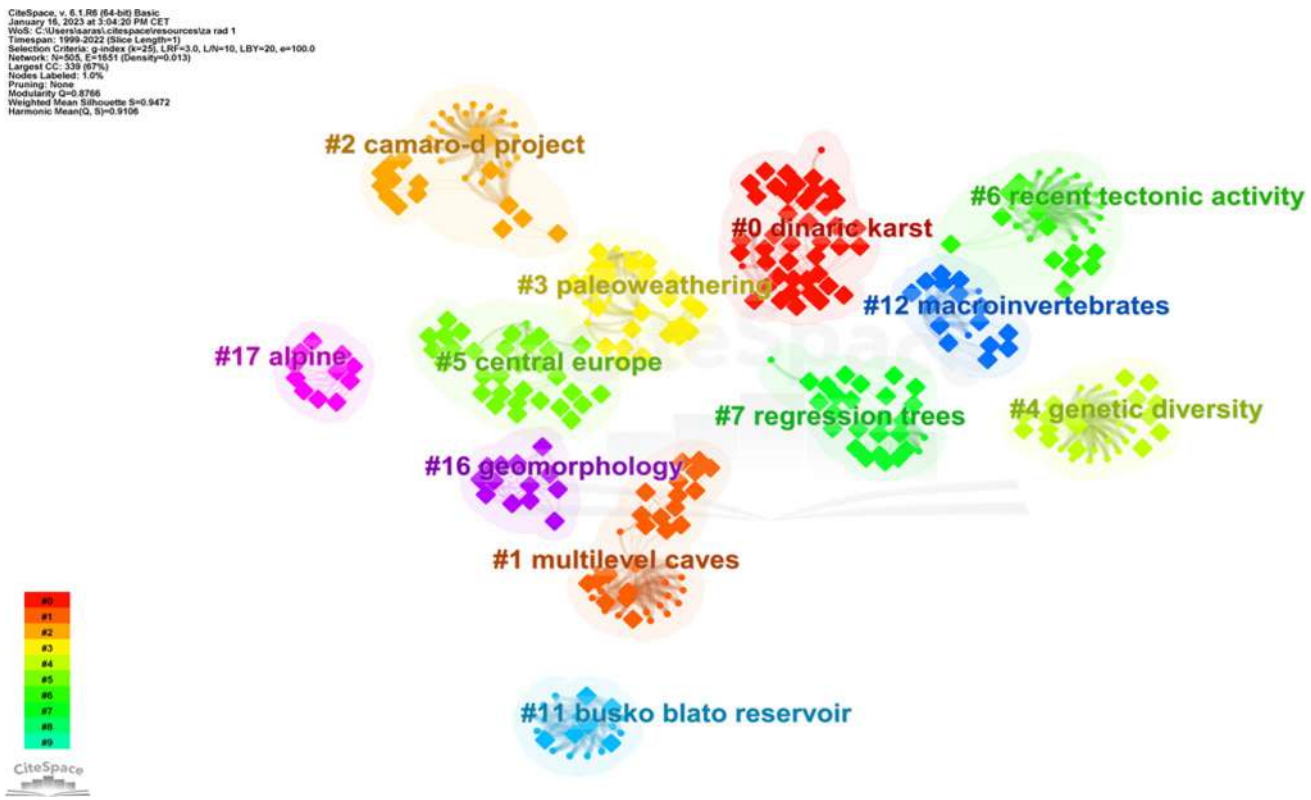

Fig. 7 Clustered network of co-cited references (dots) and co-occurring keywords (diamonds) created from literature connecting topics "Europe," "karst," and "river." Cluster labels were determined from keywords using the latent semantic indexing algorithm

macrophytes), cluster #4 "genetic diversity" (phylogeny and population dynamics), cluster #7 "regression trees" (endemic crustaceans), cluster #12 "macroinvertebrates," and cluster #17 "alpine" (changes in plant communities in Europe). The second group of research areas focused on geology and geomorphology: cluster #1 "multilevel caves" (radiocarbon dating and travertine deposits), cluster #3 "paleoweathering" (paleogeomorphology), cluster #5 "central Europe" (reconstruction of hydro-geomorphic processes), cluster #6 "recent tectonic activity" (geological mapping and modelling), and cluster #16 "geomorphology" (Holocene tufa changes in response to human impacts and climate change). The third, smallest group focused on water quality parameters: cluster #2 "camaro-d project" (hydrochemical characteristics of the karst river basin and impact of land use on water quality) and cluster #11 "busko blato reservoir" (trophic index, eutrophication, nutrients) (Fig. 7). Since CiteSpace analysis confirmed that there are only few data on physico-chemical and organic water parameters for the European karst rivers, the present field study results are important for understanding hydrological systems similar to not only the Krka River, in the Dinaric karst region in Croatia (e.g., Plitvice Lakes), but also other south-eastern European countries such as Slovenia (e.g., the Reka River), Bosnia and Herzegovina (e.g., the Pliva River), Montenegro (e.g., the Tara River), Albania (e.g., the Osum River), and Italy (e.g., the Sorgue River) (Stevanović et al. 2016; Stevanović and Milanović 2023).

Timeline report by the average year of publications in each cluster from the Fig. 7 revealed the following current research areas related to European karst rivers: (a) aquatic macroinvertebrate distribution and population history using DNA barcoding and species distribution modeling ("regression trees," 2016); (b) the reconstruction of hydro-geomorphic processes based on tree-ring data to identify hydro-meteorological triggers ("central Europe," 2016); (c) the study of Holocene tufa changes in response to human impacts and climate change ("geomorphology," 2019). The focus of this research domain on global issues such as biodiversity loss and climate change was also confirmed by citation burst analysis, which identified climate change, Europe, and diversity as keywords with the strongest citation burst (with citation burst strengths 3.01, 2.54 and 2.39 respectively). Although these issues are important, human-induced degradation of water quality is also a major environmental problem in the modern world and requires attention.

Conclusions

Presented concentrations and seasonal and long-term changes in physico-chemical and organic water parameters are among the rare data for karst rivers in Europe and the first data for the upper reaches of the Krka River in Croatia. In this study, the impact of anthropogenic activities on the sensitive karst ecosystem was also estimated, confirming that industrial and municipal wastewaters alter water quality and disturb natural seasonal variations. The impact of wastewater discharges as point sources of pollution to the river was found to be more severe than those of diffuse pollution from agricultural runoff. They were identified as the main source of nutrients and organic matter affecting the water quality and causing deteriorated ecological status of the surrounding area. Although the upper reaches of the river were affected by the wastewater discharges, our results indicated very good water quality downstream, in the national park, confirming the efficiency and importance of self-purification and underground flows in the complex hydrological karst systems. This self-regulation was also reflected in mostly stable long-term trends of water parameters along the river over the last 10–20 years. At sites with little or no wastewater influence, seasonal variations in dissolved nutrients and total solids reflected precipitation and water level regimes, while organic water parameters reflected changes in water levels, primary producer biomass, and intensity of agricultural activities in the watershed. Presented data thus contribute to the understanding of the dynamics of karst ecological indicators and the effects of wastewater pollution in complex and valuable karst river ecosystems and indicate the need of strict monitoring and protection. According to CiteSpace visualization, there are only few data on physico-chemical and organic water parameters for the karst rivers in Europe available, while keywords with the strongest citation burst are climate change (3.01), Europe (2.54), and diversity (2.39). Scientometric analysis of the global literature revealed that most research on these topics was conducted in Asia (38%), Europe (34%), and North America (22%), changing the focus from case studies of hydrologic connections and water quality to the recent studies on human impact on karst ecosystem and monitoring and identification of specific pollutants. Thus, CiteSpace analysis confirmed human-induced degradation of water quality as a major environmental problem in the modern world which requires significant attention.

Supplementary Information The online version contains supplementary material available at https://doi.org/10.1007/s11356-023-31418-3.

Author contribution The manuscript was written through contributions of all authors. Sara Šariri — investigation; resources; data curation; visualization; formal analysis; writing — original draft; writing — review and editing. Damir Valić — investigation; resources; writing — review and editing. Tomislav Kralj — investigation; resources; writing — review and editing. Želimira Cvetković — investigation; data curation; formal analysis; writing — review and editing. Tatjana Mijošek — investigation; resources; data curation; writing — review and editing. Zuzana Redžović — investigation; resources; writing — review and editing. Ivana Karamatić — investigation; resources; writing — review and editing. Vlatka Filipović Marijić — conceptualization; methodology; funding acquisition; resources; supervision; project administration; investigation; data curation; formal analysis; writing — original draft; writing — review and editing. All authors read and agreed to publish the final manuscript.

Funding This study was funded by the Croatian Science Foundation within the project no. IP-2020–02-8502 "Integrated evaluation of aquatic organism responses to metal exposure: gene expression, bioavailability, toxicity and biomarker responses" (BIOTOXMET).

Data Availability The datasets used and/or analyzed during the current study are available from the corresponding author on reasonable request.

Declarations

Ethical approval Not applicable.

Consent to participate Not applicable.

Consent for publication Not applicable.

Competing interests The authors declare no competing interests.

References

Abril G, Nogueira M, Etcheber H, Cabeçadas G, Lemaire E, Brogueira MJ (2002) Behaviour of organic carbon in nine contrasting European estuaries. Estuar Coast Shelf Sci 54:241–262

Alamdari N, Claggett P, Sample DJ, Easton ZM, Yazdi MN (2022) Evaluating the joint effects of climate and land use change on runoff and pollutant loading in a rapidly developing watershed. J Clean Prod 330:129953

Amić A, Tadić L (2018) Analysis of basic physical-chemical parameters, nutrients and heavy metals content in surface water of small catchment Area of Karašica and Vučica Rivers in Croatia. Environments 5:20

ASTM D 4763-06 (2020) Standard practice for identification of chemicals in water by fluorescence spectroscopy. STANDARD by ASTM International 12/15/2020

Baird R, Bridgewater L (2017) Standard methods for the examination of water and wastewater. 23rd edition. American Public Health Association (APHA), Washington D.C.

Barešić J, Horvatinčić N, Roller-lutz Z (2011) Spatial and seasonal variations in the stable C isotope composition of dissolved inorganic carbon and in physico-chemical water parameters in the Plitvice Lakes system. Isot Environ Health Stud 47:316–329

Bernal S, Butturini A, Sabater F (2005) Seasonal variations of dissolved nitrogen and DOC:DON ratios in an intermittent Mediterranean stream. Biogeochemistry 75:351–372

Bonacci O, Jukić D, Ljubenkov I (2006) Definition of catchment area in karst: case of the rivers Krčić and Krka, Croatia. Hydrol Sci J 51:682–699

Calmuc M, Calmuc V, Arseni M, Topa C, Timofti M, Georgescu LP, Iticescu C (2020) A comparative approach to a series of physico-chemical quality indices used in assessing water quality in the Lower Danube. Water 12(11):3239

Chen C (2006) CiteSpace II: Detecting and visualizing emerging trends and transient patterns in scientific literature. J Am Soc Inf Sci Technol 57:359–377
Chen C (2017) Science mapping: a systematic review of the literature. J Data Inf Sci 2:1–40
Chen Z, Auler AS, Bakalowicz M, Drew D, Griger F, Hartmann J, Jiang G, Moosdorf N, Richts A, Stevanović Z, Veni G, Goldscheider N (2017) The World Karst Aquifer Mapping project: concept, mapping procedure and map of Europe. Hydrogeol J 25:771–785
Cukrov N, Cmuk P, Mlakar M, Omanović D (2008) Spatial distribution of trace metals in the Krka River, Croatia: an example of the self-purification. Chemosphere 72:1559–1566
Cukrov N, Tepić N, Omanović D, Lojen S, Bura-Nakić E, Vojvodić V, Pižeta I (2012) Qualitative interpretation of physico-chemical and isotopic parameters in the Krka River (Croatia) assessed by multivariate statistical analysis. Int J Environ Anal Chem 92:1187–1199
Divya J, Belagali SL (2012) Impact of chemical fertilizers on water quality in selected agricultural areas of Mysore district, Karnataka, India. Int J Environ Sci 2:1449–1458
DLS (2018) Expert base for application for the issuance of an environmental permit: DIV d.o.o., screw factory, branch office Knin (REV1), RN/2015/0424 [In Croatian] https://knin.hr/wp-content/uploads/2018/07/1-SP_DIV_FINAL_REV1_F.pdf. Accessed 3 November 2021
Dragun Z, Stipaničev D, Fiket Ž, Lučić M, Udiković Kolić N, Puljko A, Repec S, Šoštarić Vulić Z, Ivanković D, Barac F, Kiralj Z, Kralj T, Valić D (2022) Yesterday's contamination–a problem of today? The case study of discontinued historical contamination of the Mrežnica River (Croatia). Sci Total Environ 848:157775
Filipović Marijić V, Kapetanović D, Dragun Z, Valić D, Krasnići N, Redžović Z, Grgić I, Žunić J, Kružlicová D, Nemeček P, Ivanković D, Vardić Smrzlić I, Erk M (2018) Influence of technological and municipal wastewaters on vulnerable karst riverine system, Krka River in Croatia. Environ Sci Pollut Res 25:4715–4727
Ford D, Williams PD (2007) Karst hydrogeology and geomorphology. John Wiley & Sons
Glavan M, Pintar M (2010) Impact of point and diffuse pollution sources on nitrate and ammonium ion concentrations in the karst-influenced Temenica river. Fresenius Environ Bull 19:1005–1014
Goldscheider N (2019) A holistic approach to groundwater protection and ecosystem services in karst terrains. Carbonates Evaporites 34:1241–1249
Goldscheider N, Chen Z, Auler AS, Bakalowicz M, Broda S, Drew D, Hartmann J, Jiang G, Moosdorf N, Stevanović Z, Veni G (2020) Global distribution of carbonate rocks and karst water resources. Hydrogeol J 28:1661–1677
Government of the Republic of Croatia (GRC) (1985) Act on the Proclamation of Krka National Park Official Gazette of the Republic of Croatia No. 5 [In Croatian]
Government of the Republic of Croatia (GRC) (2019) Directive on water quality status. Official Gazette of the Republic of Croatia No. 96 [In Croatian]
Government of the Republic of Croatia (GRC) (2020) Regulation on limit values for wastewater emissions. Official Gazette of the Republic of Croatia No. 26 [In Croatian]
Gulin V, Kepčija RM, Perić MS, Felja I, Fajković H, Križnjak K (2021) Environmental and periphyton response to stream revitalization–a pilot study from a tufa barrier. Ecol Indic 126:107629
Hach Lange GmbH (2013) Water analysis guide, DOC316.53.01336 1st edn. Loveland, USA
Hoaghia MA, Moldovan A, Kovacs E, Mirea IC, Kenesz M, Brad T, Cadar O, Micle V, Levei EA, Moldovan OT (2021) Water quality and hydrogeochemical characteristics of some karst water sources in Apuseni Mountains, Romania. Water 13(6):857
HRN EN 1484 (2002) Water analysis - guidelines for the determination of total organic carbon (TOC) and dissolved organic carbon (DOC)
HRN EN ISO 8467 (2001) Water quality -- determination of permanganate index (ISO 8467:1993; EN ISO 8467:1995)
Hrvatske vode (2016) Report on the state of surface waters in the Republic of Croatia in 2014 [In Croatian]
Huebsch M, Fenton O, Horan B, Hennessy D, Richards KG, Jordan P, Goldscheider N, Butscher C, Blum P (2014) Mobilisation or dilution? Nitrate response of karst springs to high rainfall events. Hydrol Earth Syst Sci 18:4423–4435
Illies J (1978) Limnofauna Europaea. A checklist of the animals inhabiting European inland waters, with accounts of their distribution and ecology (except Protozoa) [in German]. Gustav Fischer Verlag, Stuttgart, New York, Amsterdam
Jebreen H, Wohnlich S, Banning A, Wisotzky F, Niedermayr A, Ghanem M (2018) Recharge, geochemical processes and water quality in karst aquifers: Central West Bank, Palestine. Environ Earth Sci 77:1–16
Kapetanović D, Dragun Z, Valić D, Teskeredžić Z, Teskeredžić E (2009) Enumeration of heterotrophs in river water with spread plate method: comparison of yeast extract agar and R2A agar. Fresenius Environ Bull 18:1276–1280
Kisić I, Zgorelec Ž, Galić M, Delač D (2019) Analysis of mud and water in lagoons polluted by waste materials in Knin [In Croatian] https://knin.hr/wp-content/uploads/2019/07/Zavrsno-izvijesce-Analiza-mulja-DIV-ove-lagune.pdf Accessed 3 November 2021
Kolda A, Petrić I, Mucko M, Gottstein S, Žutinić P, Goreta G, Ternjej I, Rubinić J, Radišić M, Udovič MG (2019) How environment selects: resilience and survival of microbial mat community within intermittent karst spring Krčić (Croatia). Ecohydrol 12:e2063
Li M, Wang Y, Xue H, Wu L, Wang Y, Wang C, Gao X, Li Z, Zhang X, Hasan M, Alrugi M, Bokhari A, Han N (2022) Scientometric analysis and scientific trends on microplastics research. Chemosphere 304:135337
Magdaleno A, Puig A, de Cabo L, Salinas C, Arreghini S, Korol S, Bevilacqua S, López L, Moretton J (2001) Water pollution in an urban Argentine river. Bull Environ Contam Toxicol 67:0408–0415
Malá J, Hübelová D, Schrimpelová K, Kozumplíková A, Lejska S (2022) Surface watercourses as sources of karst water pollution. Int J Environ Sci Technol 19:3503–3512
Marcinek S, Santinelli C, Cindrić AM, Evangelista V, Gonnelli M, Layglon N, Mounier S, Lenoble V, Omanović D (2020) Dissolved organic matter dynamics in the pristine Krka River estuary (Croatia). Mar Chem 225:103848
Matić N, Miklavčić I, Maldini K, Tomas D, Cuculić V, Cardellini C, Frančišković-Bilinski S (2013) Geochemical and isotopic characteristics of karstic springs in coastal mountains (Southern Croatia). J Geochem Explor 132:90–110
Mihaljević Z, Ternjej I, Stanković I, Ivković M, Želježić D, Mladinić M, Kopjar N (2011) Assessment of genotoxic potency of sulfate-rich surface waters on medicinal leech and human leukocytes using different versions of the Comet assay. Ecotoxicol Environ Saf 74:1416–1426
Munjko I (1979) Determination of phenolic and extractable substances in surface waters of the Adriatic and Black Sea basins [In Croatian]. Ribar Croat J Fish 34:100–105
Olatunde OS, Olalekan FS, Beatrice OO, Bhekumusa XJ, Zacheaus OO, Kehinde AN (2015) Nutrient enrichment and hypoxia threat in urban surface water. Clean - Soil Air Water 43:205–209
Puig R, Soler A, Widory D, Mas-Pla J, Domènech C, Otero N (2017) Characterizing sources and natural attenuation of nitrate contamination in the Baix Ter aquifer system (NE Spain) using a multi-isotope approach. Sci Total Environ 580:518–532

Ravbar N, Kovačič G (2014) Vulnerability and protection aspects of some Dinaric karst aquifers: a synthesis. Environ Earth Sci 74:129–141
Rovan L, Zuliani T, Horvat B, Kanduč T, Vreča P, Jamil Q, Čermelj B, Bura-Nakić E, Cukrov N, Štrok M, Lojen S (2021) Uranium isotopes as a possible tracer of terrestrial authigenic carbonate. Sci Total Environ 797:149103
Schliemann SA, Grevstad N, Brazeau RH (2021) Water quality and spatio-temporal hot spots in an effluent-dominated urban river. Hydrol Process 35:e14001
Schöll F, Birk S, Böhmer J (2012) XGIG Large river intercalibration exercise – WFD intercalibration phase 2: milestone 6 report – BQE: Phytobenthos. Eur Comm Direct Gen JRC Joint Res Centre Inst Environ Sustain 73
Sertić Perić M, Miliša M, Matoničkin Kepčija R, Primc-Habdija B, Habdija I (2011) Seasonal and fine-scale spatial drift patterns in a tufadepositing barrage hydrosystem. Fundam Appl Limnol 178:131–145
Sertić Perić M, Matoničkin Kepčija R, Miliša M, Gottstein S, Lajtner J, Dragun Z, Filipović Marijić V, Krasnići N, Ivanković D, Erk M (2018) Benthos-drift relationships as proxies for the detection of the most suitable bioindicator taxa in flowing waters–a pilot-study within a Mediterranean karst river. Ecotoxicol Environ Saf 163:125–135
Sironić A, Barešić J, Horvatinčić N, Brozinčević A, Vurnek M, Kapelj S (2017) Changes in the geochemical parameters of karst lakes over the past three decades–The case of Plitvice Lakes, Croatia. Appl Geochem 78:12–22
Srdoč D, Krajcar-Bronić I, Horvatinčić N, Obelić B (1986) Increase of 14C activity of dissolved inorganic carbon along a river course. Radiocarbon 28:515–521
Srivastava J, Gupta A, Chandra H (2008) Managing water quality with aquatic macrophytes. Rev Environ Sci Biotechnol 7:255–266
Stanley EH, Powers SM, Lottig NR, Buffam I, Crawford JT (2012) Contemporary changes in dissolved organic carbon (DOC) in human-dominated rivers: is there a role for DOC management? Freshw Biol 57:26–42
Stevanović Z, Krešić N, Kukuric N (2016) Karst without boundaries. 23, CRC Press/Balkema, London
Stevanović Z, Milanović P (2023) South-eastern Dinaric karst: contrasts in water treasury. Environ Earth Sci 82(9):1–15
Strmečki S, Ciglenečki I, Udovič MG, Marguš M, Bura-Nakić E, Dautović J, Plavšić M (2018) Voltammetric study of organic matter components in the upper reach of the Krka River, Croatia. Croat Chem Acta 91:1–8
Telbisz T, Mari L (2020) The significance of karst areas in European national parks and geoparks. Open Geosci 12:117–132
Terzić J, Marković T, Reberski JL (2014) Hydrogeological properties of a complex Dinaric karst catchment: Miljacka Spring case study. Environ Earth Sci 72:1129–1142
Vurnek M, Brozinčević A, Matoničkin Kepčija R, Frketić T (2021) Analyses of long-term trends in water quality data of the Plitvice Lakes National Park. Fundam Appl Limnol 194:155–169
Wang F, Chen H, Lian J, Fu Z, Nie Y (2020) Seasonal recharge of spring and stream waters in a karst catchment revealed by isotopic and hydrochemical analyses. J Hydrol 591:125595
Xu J, Jin G, Tang H, Mo Y, Wang YG, Li L (2019) Response of water quality to land use and sewage outfalls in different seasons. Sci Total Environ 696:134014
Yang L, Sun Y, Zhang L (2023) Microreactor technology: identifying focus fields and emerging trends by using CiteSpace II. ChemPlusChem 88(1):e202200349
Yue FJ, Li SL, Zhong J, Liu J (2018) Evaluation of factors driving seasonal nitrate variations in surface and underground systems of a karst catchment. Vadose Zone J 17:1–10
Yue FJ, Waldron S, Li SL, Wang ZJ, Zeng J, Xu S, Zhang ZC, Oliver DM (2019) Land use interacts with changes in catchment hydrology to generate chronic nitrate pollution in karst waters and strong seasonality in excess nitrate export. Sci Total Environ 696:134062
Zhao Y, Jiang Y, Zhou Z, Yang Z (2021) Global trends in karst-related studies from 1990 to 2016: a bibliometric analysis. Alex Eng J 60:2551–2562
Zhong D, Li Y, Huang Y, Hong X, Li J, Jin R (2022) Molecular mechanisms of exercise on cancer: a bibliometrics study and visualization analysis via CiteSpace. Front Mol Biosci 8:797902
Zhou Y, Wu X, Jia C, Liu S, Gao Y (2020) Bibliometric analysis of research progress on karst groundwater pollution. IOP Conf Ser: Earth Environ Sci 568:012040
Žutinić P, Kulaš A, Levkov Z, Šušnjara M, Orlić S, Kukić S, Goreta G, Valić D, Udovič MG (2020) Ecological status assessment using periphytic diatom communites-case study Krka River. Maced J Ecol Environ 22:29–44

Publication No. 2: Spatial and temporal variability of dissolved metal(loid)s in water of the karst ecosystem: consequences of long-term exposure to wastewaters

Environmental Technology & Innovation 32 (2023) 103254

Contents lists available at ScienceDirect

Environmental Technology & Innovation

journal homepage: www.elsevier.com/locate/eti

Spatial and temporal variability of dissolved metal(loid)s in water of the karst ecosystem: consequences of long-term exposure to wastewaters

Tatjana Mijošek [a], Zorana Kljaković-Gašpić [b], Tomislav Kralj [a], Damir Valić [a], Zuzana Redžović [a], Sara Šariri [a], Ivana Karamatić [a], Vlatka Filipović Marijić [a,*]

[a] Ruđer Bošković Institute, Bijenička c. 54, 10000 Zagreb, Croatia
[b] Institute for Medical Research and Occupational Health, Ksaverska c. 2, 10000 Zagreb, Croatia

ARTICLE INFO

Article history:
Received 5 May 2023
Received in revised form 4 June 2023
Accepted 13 June 2023
Available online 19 June 2023

Keywords:
Wastewater pollution
Metal toxicity
The Krka River
Heavy metals
Anthropogenic impact
Water quality

ABSTRACT

The metal(loid) variability in the sensitive karst ecosystem was addressed as possible indicator of short- and long-term exposure to the wastewaters, recognized as the main metal contamination sources. Industrial and municipal wastewaters are released without proper purification only 2 km upstream from the Krka National Park (KNP) in Croatia. The variability of dissolved metal(loid)s was studied in four seasons and eight locations: Krka River source (reference site, KRS), municipal wastewaters from the Town of Knin (KRK), industrial wastewaters from the screw factory (IWW), Brljan Lake in the KNP (KBL), and the tributaries Krčić (TKR), Kosovčica (TKO), Orašnica (TOR) and Butišnica (TBU). Water taken directly from IWW had several times higher concentrations of all elements than other locations and indicated industrial wastewater as the primary Mn, Zn, Co, Cs, and Fe source. Tributary Orašnica, flowing by IWW, was the most affected site, although higher metal concentrations were also found at other locations compared to KRS. Overall, spatial metal contamination followed the order: TOR>KRK>TKO>TBU>KBL>KRS. Seasonality was not pronounced, although the highest levels for most metals were observed in summer, dry season when the self-purification processes are reduced. Almost all elements had low tendency to bind with particles, therefore showing high presence in dissolved fraction and confirming their bioavailability and potential toxicity. Although metal concentrations increased over time, they were still low compared to metal-contaminated rivers. However, observed metal exposure and inter-site differences present a warning and indicate the need for the targeted continuous monitoring of potential hotspots to protect this karst ecosystem.

1. Introduction

Karst aquifers are considered extremely sensitive ecosystems, susceptible to contamination due to their unique hydrological (rapid flow of contaminants through fractures), morphological (presence of numerous cavities) and geological (fractured carbonates) characteristics (Brinkmann and Parise, 2012; Campanale et al., 2022; Kovačič and Ravbar, 2003; Padilla and Vesper, 2018; Selak et al., 2022). Contaminants are easily dispersed and transported over long distances in

* Correspondence to: Laboratory for Biological Effects of Metals, Division for Marine and Environmental Research, Ruđer Bošković Institute, Bijenička c. 54, 10000 Zagreb, Croatia.
E-mail address: vfilip@irb.hr (V. Filipović Marijić).

https://doi.org/10.1016/j.eti.2023.103254

karst aquifers, whether through sinking streams, caves, sinkholes or open fractures and shafts in carbonate rocks, which are characterized by conduit porosity and highly permeable zones (Padilla and Vesper, 2018; Kalhor et al., 2019). In addition, the porosity and high sediment content of karst aquifers allow significant storage capacity for various types of contaminants, which can then be released into the water column slowly and over a long time (Padilla et al., 2011; Padilla and Vesper, 2018; Vadillo and Ojeda, 2022).

Among contaminants, metal(loid)s always pose a major threat due to their enhanced releases from natural and anthropogenic sources, persistence, toxicity and possible accumulation. As seasonal variations in precipitation regime, temperature, interflow or groundwater flow have a significant impact on river discharge and consequently on the concentration of metals in river water (Vega et al., 1998), the assessment of spatial, as well as temporal variability of metal(loid) concentrations is important for the ecological characterization of aquatic ecosystems and estimation of water quality.

Although groundwater from karst aquifers is one of the most important drinking water sources and reservoirs (Bakalowicz, 2005), not many studies have focused on the water quality assessment of the karst rivers in Europe, even worldwide, as confirmed by Šariri et al. (submitted for publication) using CiteSpace. Namely, combination of the keywords "karst", "water quality" and "river" resulted in only 237 published papers around the world, mostly in China and USA. Further, only small portion of these papers deals with water pollution and anthropogenically-induced degradation, which was indicated as major environmental problem investigated in the modern world. Since many karst terrains in the world have also been declared protected areas due to their biotic and abiotic values together with high sensitivity and vulnerability (Telbisz and Mari, 2020), special awareness and establishment of permanent monitoring and protection measures in such areas are necessary.

The Krka River is a typical karst river in the Dinaric region of Croatia, the largest part of which has been declared a national park, with the aim of protecting and preserving this region of exceptional natural value characterized by tufa-barriers, waterfalls and great plant and animal biodiversity. Although most of the Krka River watercourse is relatively sparsely populated and seemingly pristine, the upper part is exposed to anthropogenic influences including industrial and municipal wastewaters, agricultural runoff, fertilizers, tourism and gypsum factory (Cukrov et al., 2008; Filipović Marijić et al., 2018). In recent years, the limited number of studies in the upper course of the Krka River investigated the potential threat to the national park and confirmed ecological disturbances and negative impact of wastewaters by variety of physico-chemical and microbiological parameters and metal(loid) contamination at the sites downstream of the wastewater's discharges in the period 2004–2021 (Cukrov et al., 2008, 2012; Filipović Marijić et al., 2018; Sertić Perić et al., 2018; Šariri et al., submitted for publication). As for the temporal changes of metal(loid)s in water, previous studies in the upper part of the Krka River covered only some seasons in a limited spatial area (usually two characteristic locations, pristine and contaminated) or presented only few elements (Cukrov et al., 2012; Filipović Marijić et al., 2018; Sertić Perić et al., 2018), while a comprehensive study covering temporal changes in all four seasons at a number of target locations in the wider area was never conducted. Therefore, we presented for the first time long-term trends in variability of 20 metal(loid) concentrations in the karst river and estimated the use of their current and long-term levels as chemical indicators of pollution impacts.

As a continuation of the mentioned research in this important area, we aimed to conduct a comprehensive study of the metal exposure assessment of the upper part of the Krka River by: (a) characterizing for the first time seasonal dynamics of metal(loid) concentrations at locations of variable pollution impact; (b) comparing the results with previously reported data to assess long-term trends and changes in metal concentrations; (c) estimating and comparing the bioavailability of 20 elements at unpolluted and polluted sites by calculating ratios of dissolved to total metal concentrations; (d) characterizing the main pollution sources and their direct and long-term impact on the Krka River watercourse; (e) identifying the influence and consequences of long-term exposure to industrial and municipal wastewaters on this sensitive ecosystem.

2. Materials and methods

2.1. Study area

Presented research was conducted in the Dinaric karst Krka River in Dalmatian part of Croatia. Although its lower part is protected as a national park, the upper course of the river is nowadays under influence of anthropogenic activities, which mostly include technological wastewaters from the screw factory, municipal wastewaters from the Town of Knin and agricultural runoff (Filipović Marijić et al., 2018; Sertić Perić et al., 2018). Wastewater outlets represent serious threat for the living world of the Krka River, as well as for the KNP, considering that wastewater is discharged into the river without adequate treatment only about 2 km upstream of the KNP border (Fig. S1). Previous research in this area has pointed to ecological disturbances and evidently higher metal concentrations and negative impact downstream of the existing wastewater outlets (Filipović Marijić et al., 2018). Conductivity, chemical oxygen demand, levels of ammonium, total nitrogen and phosphorus, nitrates and bacteria counts were below good water quality status even near the border of the KNP (Filipović Marijić et al., 2018). Further, 2–400 times higher levels of Al, Co, Fe, Li, Mn, Ni, Sr, Ti, and Zn were previously recorded in the technological/municipal wastewaters and the locations under the anthropogenic influence downstream of the Town of Knin (Filipović Marijić et al., 2018; Sertić Perić et al., 2018) compared to the Krka River source.

Therefore, to make comprehensive spatial and temporal assessment of environmental conditions in the upper part of the Krka River, 8 locations were selected: Krka River source without known anthropogenic impact as the reference site (KRS), downstream of the municipal wastewaters of the Town of Knin (KRK), industrial wastewaters from the screw factory (IWW), Brljan Lake situated in the Krka National Park (KBL), tributary Krčić flowing near the Krka River source (TKR), tributary Kosovčica influenced by gypsum factory (TKO), tributary Orašnica which flows along IWW (TOR) and tributary Butišnica, affected by agricultural activities (TBU) (Fig. S1).

2.2. Water sampling

The river water samples for the analysis of inorganic elements, except total mercury (THg), were collected in pre-cleaned polyethylene bottles in triplicates in all four seasons during 2021. Exception was TKR, where water was not collected in summer and autumn since this tributary had dried up. In all samplings, appropriate aliquots from each bottle were transferred into pre-cleaned 20-mL polyethylene bottles for determination of total metal concentrations. Other aliquots from each bottle were filtered using a 0.45-μm pore diameter cellulose acetate filter (Sartorius, Germany) mounted on syringes for the measurements of dissolved metal(loid) concentrations. All samples were acidified with concentrated nitric acid (Rotipuran Supra 69%, Carl Roth, Germany) and stored at 4 °C before analysis in the laboratory.

Water samples for THg analysis were collected concurrently with the collection of samples for other elements according to the method described by Bravo et al. (2018). Briefly, unfiltered and filtered (0.45-μm CA filters; Sartorius, Germany) water samples for the analysis of total and dissolved THg fraction and corresponding locational blanks were collected in pre-cleaned 100-mL amber borosilicate glass bottles, acidified with hydrochloric acid (HCl, 30%, Suprapur, Merck, Darmstadt, Germany) and stored at 4 °C in plastic zip-sealed bags for further THg analyses.

2.3. Measurements of trace and macroelement concentrations in water samples

Concentrations of trace and macroelements in collected and acidified water samples were measured directly, without prior dilution using inductively coupled plasma mass spectrometry (ICP-MS) on an Agilent 7500cx instrument (Agilent Technologies, Tokyo, Japan) under working conditions presented in Table S1. Helium and hydrogen collision gases were used to remove interference and an internal standard solution containing 3 $\mu g\ L^{-1}$ Ge, Rh, Tb, Lu and Ir (SCP Science, Quebec, Canada) was used to correct for instrumental drifts and plasma fluctuations. Standard solutions used for external calibration were prepared from individual PlasmaCAL Single-Element Standard solutions (SCP Science, Quebec, Canada). The preparation and analysis of samples were carried out in a laboratory with a HVAC system (Heating, Ventilating and Air Conditioning) combined with HEPA filters. The limits of detection (LODs) of the analyzed elements ranged from 0.0005 $\mu g\ L^{-1}$ for Cs to 30 $\mu g\ L^{-1}$ for K (individual LOD values are given in Table S2). Three standard certified reference materials (NIST SRM 1643e, NIST SRM 1643f, NRCC SLRS-5) were analyzed as part of quality control. The accuracy for the analyzed elements in the referent water samples was within ±10% of the certified values, with recoveries ranging from 92% (Ni) to 109% (Ba). Detailed data on all elements in reference materials is given in Table S2.

2.4. Measurements of mercury in water samples

Concentrations of THg in filtered and un-filtered water samples were analyzed directly, using cold-vapor atomic absorption spectrometry (CV-AAS) on AMA 254 Mercury Analyzer (LECO, Korea). Briefly, an aliquot of the water sample was added to the sample boat and gradually heated to 750 °C. After thermal decomposition and catalytic removal of impurities, mercury vapors were concentrated on a gold trap. Mercury was then released from the gold trap by heating to 900 °C and measured on the detector. Standard solutions used for external calibration were prepared from standard solution of inorganic mercury (10 $mg\ L^{-1}$; Inorganic Ventures, Christiansburg, USA). The LOD of the method was 0.03 $\mu g\ L^{-1}$. Standard certified reference material NIST SRM 1641e was analyzed with each batch of samples as part of quality control, with recoveries ranging from 95% to 101% of the certified value.

2.5. Data processing and statistics

Statistical analyses and creation of images was performed in SigmaPlot 11.0 for Windows. We presented data on metal concentrations as mean ± standard deviation (S.D.). Variability of metal concentrations in water samples between the sites and seasons was tested using two-way ANOVA and Holm-Sidak test. In all cases level of significance was set at $p < 0.05$. As TKR was dried up in two seasons, it was not analyzed and presented in graphs. Statistically significant differences between sites within each season are always indicated with different numbers in the graphs: 0 Significant difference from all other locations; 1–6 Significant difference from the location indicated by a specific number as follows: 1—KRS; 2—KRK; 3—KBL; 4—TOR; 5—TBU; 6—TKO. Differences between seasons for each location are indicated by different letters or asterisk: * Significant difference between all seasons; a-d Significant difference from season indicated by a specific letter as follows: a—winter; b—spring; c—summer; d—autumn.

3. Results and discussion

3.1. Concentration ranges of dissolved metal(loid)s in IWW, point source of pollution

Data related to the inadequately purified wastewaters from the screw factory were characterized and presented separately from other riverine locations, as an artificial pool presenting point source of pollution and the most serious threat for the whole karst ecosystem of the Krka River. The concentrations of trace elements in IWW were in the following ranges, depending on the season ($\mu g\ L^{-1}$): 50-3850 (Mo<Ba<Mn≤Fe≤Sr<Zn); 0.5–10 (As<Cu<Cr<Ni≤Co); 0.001–0.5 (Tl<Cd<Cs≤Se<Sb) (Table S3). Macroelements were found in the following concentration ranges (mg L^{-1}): Ca (424–1560) > Na (102–246) ≥ K (85.7–318) > Mg (16.4–27.1). We have also measured THg in waters, but all the values, even at IWW, were close to the limit of detection (0.03 $\mu g\ L^{-1}$), indicating there was no significant pollution with total mercury in this area. Contrary to expectations, given that the values of certain physico-chemical parameters and nutrients (chemical oxygen demand (COD), ammonium, nitrites, total nitrogen, phosphorus) at this location exceeded the regulatory emission limits (Šariri et al. submitted for publication), obtained concentrations of investigated elements in IWW in all seasons were below the legally defined threshold values for wastewater emissions (GRC, 2020). This particularly applies to As, Ba, Cd, Co, Cr, Cu, Fe, Mn, Ni, Se and Zn concentrations, which were many times lower than prescribed by the regulation.

Concentrations of most elements at IWW were significantly higher compared to all riverine locations, and especially compared to the river source water (KRS) with up to 46689 times higher values for Mn, 566 for Zn, 405 for Co, 263 for Cs, 114 for Fe and 80 for Ni, depending on the season (Table S3). That could be expected considering that these are all elements often used in the industry of iron and steel alloys, as present in this area (Filipović Marijić et al., 2018; Sertić Perić et al., 2018). Besides KRS, significant differences in metal(loid) levels were also found between IWW and other locations, even TOR, as presumably the most contaminated site on the Krka River, which is directly influenced by IWW due to possible spillover of wastewaters during rains and/or floods, and karst porosity.

Comparison of our data with the previous research of these technological wastewaters in autumn 2015 (Filipović Marijić et al., 2018) indicated a significant increase in the concentrations of many elements (including As, Ba, Cr, Cu, Mo, Sr, Ca, K, Mg), but also a decrease in the concentrations of Cd, Fe, Mn, Ni, Se and Zn over time at the IWW. Since concentrations of most of the "industrial" elements (Fe, Mn, Ni, Zn) at the IWW were lower in 2021 than in 2015, this may reflect positive improvements in the treatment of the wastewater and construction of the dam between the waste basins and TOR to prevent spillover of wastewater. As a follow up to 2015 research, the study of the of organic and inorganic pollution in sludge and waters in lagoons in the immediate vicinity of the screw factory in 2019 showed extreme contamination with different types of hydrocarbons, while sludge, as the only medium in which inorganic pollutants were measured, was highly contaminated with Zn, Cr, Ni, Mn, Al, Mg, Ca and K (Kisić et al., 2019), many of which were also highly increased in this research. Therefore, enhanced metal releases are still evident and are a cause for concern due to the karst nature of the terrain, which allows industrial wastewaters to reach the groundwater and enter the Krka River through the numerous underground fracture networks.

3.2. Concentration ranges of dissolved metal(loid)s in the Krka River catchment

Generally, element concentrations in the Krka River watercourse were in the following ranges ($\mu g\ L^{-1}$): ≤ 0.5 (Tl≤Cs<Cd<Sb≤Se≤As; Fig. 1); 0.5–3.0 (Co≤Cu<Mo≤Cr; Fig. 2); 3.0–2800 (Zn≤Ba≤Ni≤Mn≤Fe≤Sr; Fig. 3). As expected, the highest metal concentrations in water were observed for macroelements (0.2–300 mg L^{-1}, K<Na≤Mg<Ca; Fig. 4). Since THg concentrations of more than 50% of samples at all locations and seasons were below the LOD of the used method and the other values were only slightly higher than the LOD, THg was not further presented and discussed.

Among investigated elements, only Cd, Hg and Ni are regulated by Croatian and European legislations (EPCEU, 2013; GRC, 2019) and Cd and Hg are additionally considered as priority hazardous substances by the Water Framework Directive (EPCEU, 2013). According to these legislations, tolerable annual average concentrations of dissolved forms ($\mu g\ L^{-1}$) are 0.15 for Cd and 4 for Ni, while maximum allowable concentrations (MAC; $\mu g\ L^{-1}$) are 0.9 for Cd, 34 for Ni, and 0.07 for THg, respectively. Even the highest concentrations of Cd measured in our study were around 7 times lower than the recommended values, while THg values, being below 0.03 $\mu g\ L^{-1}$, were also few times lower than the recommended MAC, indicating the good condition of the upper reaches of the Krka River with regard to Cd and THg concentrations. Several times lower values compared to the recommended annual average were also observed for Ni, except for the values at KRK and TOR in winter (∼29 $\mu g\ L^{-1}$ and ∼14 $\mu g\ L^{-1}$, respectively) (Fig. 3), which were close to the MAC.

Maximum concentrations of most elements were obtained at TOR and KRK, directly impacted by industrial and municipal wastewaters, respectively. As exception, Cd and Tl had the highest concentrations at the reference site KRS (Fig. 1), probably reflecting the geological background of the catchment area. This applies especially to Cd considering that Jurassic dolomites, as the main feature of the geological background of the Krka River basin, may contain naturally high Cd concentrations (Cukrov et al., 2008).

Comparison of the obtained values with already available data on metal(loid) concentrations in the Krka River in period from 2004 to 2015 (Cukrov et al., 2008, 2012; Filipović Marijić et al., 2018) revealed mostly higher values in our research, indicating an increase of concentrations of most elements over time (Table S4). That was especially evident for Cr, Cu,

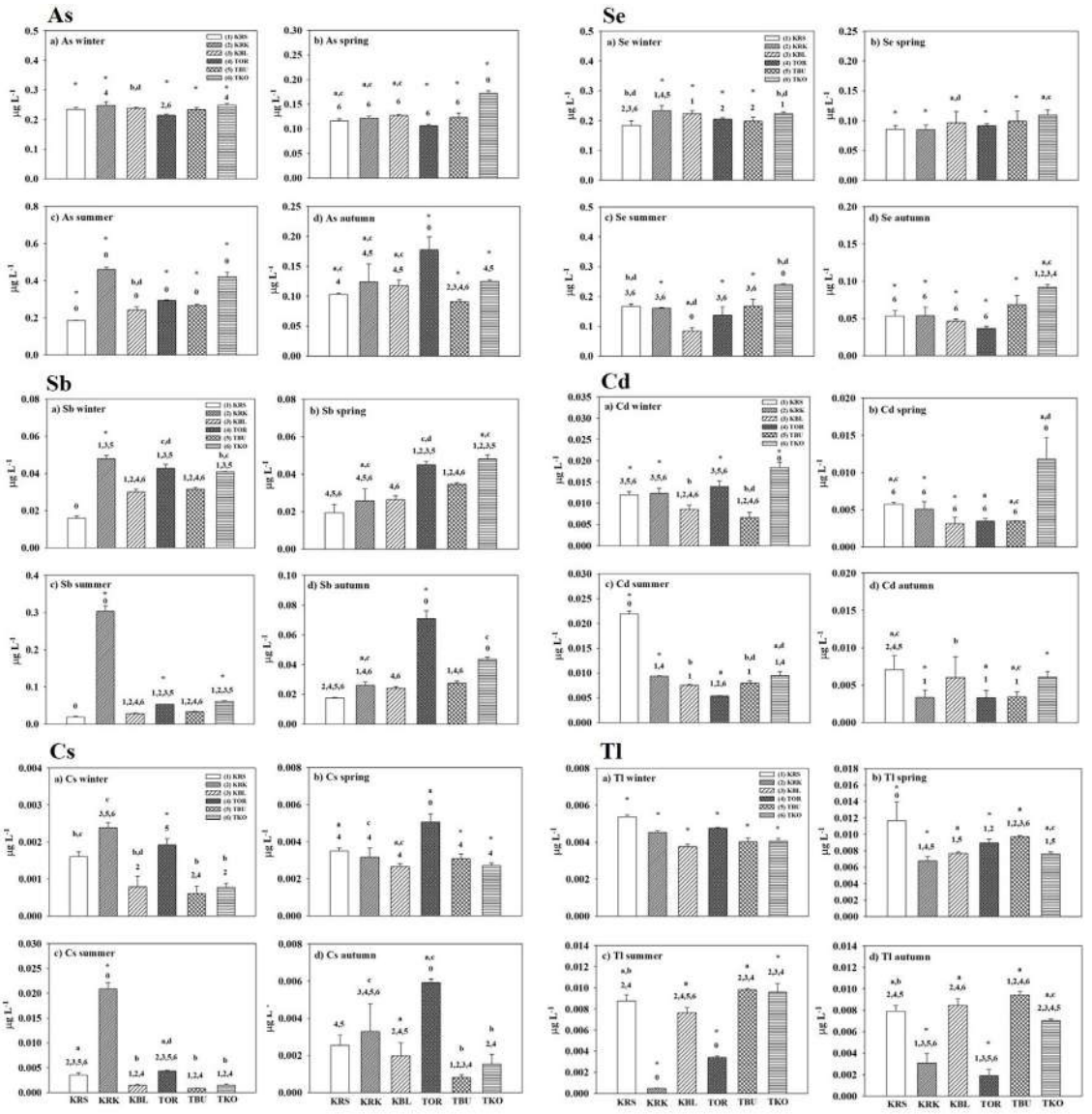

Fig. 1. Dissolved concentrations of metal(loid)s with maximum average concentrations $\leq 0.5\ \mu g\ L^{-1}$ in water from six sites of the Krka River sampled in four seasons. The description of the labels (numbers and letters) are given in Section 2.5 "Data processing and statistics".

Fe, Mn and Ni, which are all often used in industrial and agricultural activities. The only elements whose concentrations were mostly comparable in all research during the past 18 years are Mo, Sb, Se, Tl and Zn (Table S4). Comparison with another research conducted only in the Kosovčica River (TKO) in 2011 also indicated an increase in concentrations of Cd, Cr, Sr, Zn, and especially Fe and Mn during 11 years (Ternjej et al., 2014). Although "industrial" elements measured directly at IWW showed certain decrease over the years, the same trend could not be seen in the Krka River watercourse probably as a consequence of long-term contamination, whereby sediments serve as the potential sink and, in the case of resuspension, important source of metals over longer period (Filipović Marijić et al., 2018).

Comparison of our results with the data for typical Croatian karst ecosystems with low level of anthropogenic pollution, such as Plitvice Lakes and Una River, showed lower concentrations of all elements except Cd, and Mg in the Plitvice Lakes, and Ba, Ca, and Mn in the Una River (Dautović, 2006; Dautović et al., 2014). Since Ca, Cd and Mg are elements characteristic for the karst ecosystems, these differences are due to differences in natural characteristics of the areas of origin and dependence on the weathering of the dolomite carbonates (Hartmann et al., 2014). Comparison with the karst Mrežnica River showed comparable concentrations of most elements at the reference sites of both rivers. However, higher concentrations of Ba, Cr, Cu, Fe, Mn, Ni, Sr, Zn, Ca, K, and Na were observed in anthropogenically affected sites of the Krka River (Dragun et al., 2022). Although concentrations of most of the elements mentioned above, except Ba, Na and Sr, are

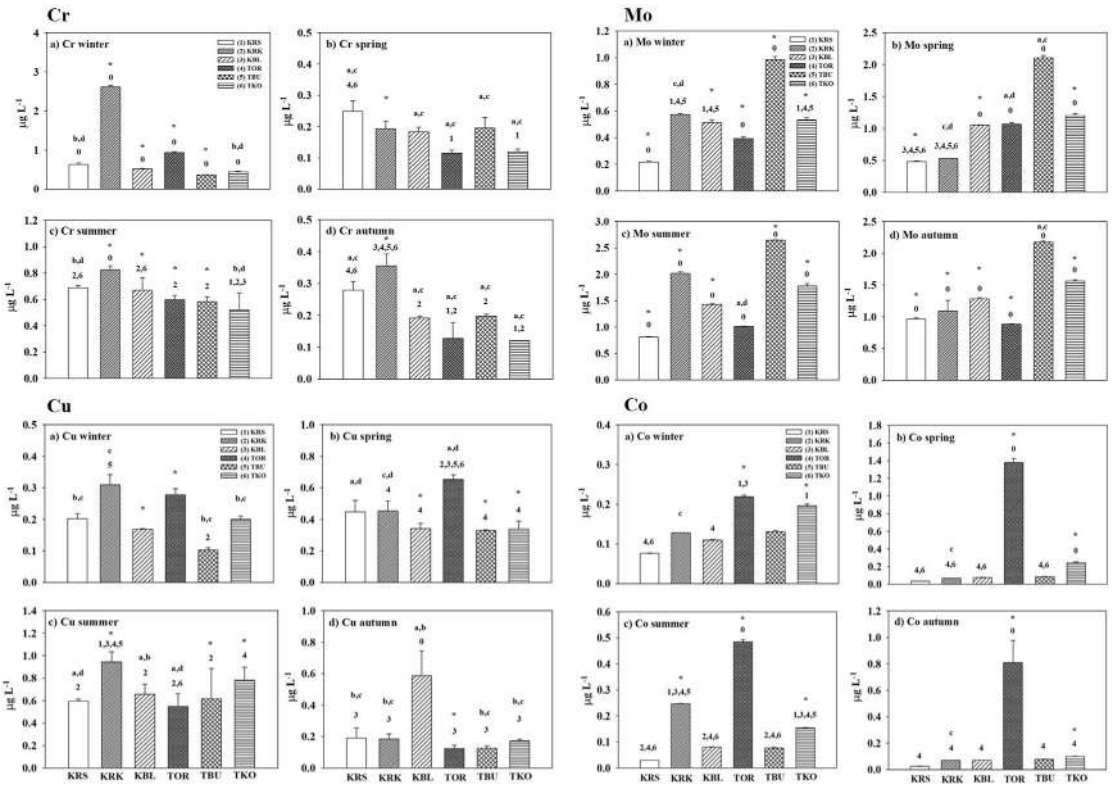

Fig. 2. Dissolved concentrations of metal(loid)s with maximum average concentrations 0.5–3 μg L^{-1} in water from six sites of the Krka River sampled in four seasons. The description of the labels (numbers and letters) are given in Section 2.5 "Data processing and statistics".

naturally higher in the soils of coastal Croatia (where Krka River is located) than in central Croatia (location of Mrežnica River) due to differences in geologic and lithogenic composition in these two regions (Halamić and Miko, 2009; Halamić et al., 2012), Krka River water samples probably also reflect a more significant impact of the active screw factory on the Krka River compared to the influence of the former textile industry (closed in 2015) which was located on the Mrežnica River.

However, although the Krka River is more contaminated than those pristine Croatian karst ecosystems mentioned above, comparison with other Croatian rivers of different degrees of contamination (Sava, Ilova and Sutla rivers) pointed to lower concentrations of most elements in the Krka River than in those moderately to heavily contaminated rivers (Table S4). The main exceptions were Co, Cr, Cu, Mn and Ni which sometimes showed even higher concentrations at some sites of the Krka River than at the polluted sites of the Sava, Sutla and Ilova rivers (Dragun et al., 2009, 2011; Filipović Marijić et al., 2016; Mijošek et al., 2020).

Based on the above, the water quality of the Krka River is still mostly good considering metal contamination and the impact of wastewaters and agriculture can be considered as moderate. Nevertheless, we were still able to recognize possible threats for the whole karst ecosystem, especially national park (Figs. 1–4).

3.3. Spatial and temporal variability of dissolved metal(loid) concentrations in the upper part of the Krka River catchment

Metal(loid) concentrations varied considerably between sites and seasons (Figs. 1–4), although elements accumulation was shown to be more site than season dependent. Therefore, temporal (4 seasons) and spatial trends (8 locations, including tributaries) of metal(loid) concentrations were presented for the first time for the upper part of the Krka River watercourse showing some specific but also long-term trends.

3.3.1. Spatial variability of dissolved metal(loid) concentrations in the upper course of the Krka River basin

Concentrations of dissolved metal(loid)s in water mostly pointed to significant element increases at anthropogenically affected sites compared to the reference location, but differences between all sites were often observed (Figs. 1–4). Concentrations of elements at TKR, sampled only in two seasons, were in similar ranges as KRS in winter and spring, so it can be considered as an additional reference site. Spatial differences were only sometimes comparable, but generally, concentrations of Co, Fe, K, Mn and Zn were the highest at TOR, of Cr and Cu at KRK, of Ca and Se at TKO, of Mg, Mo,

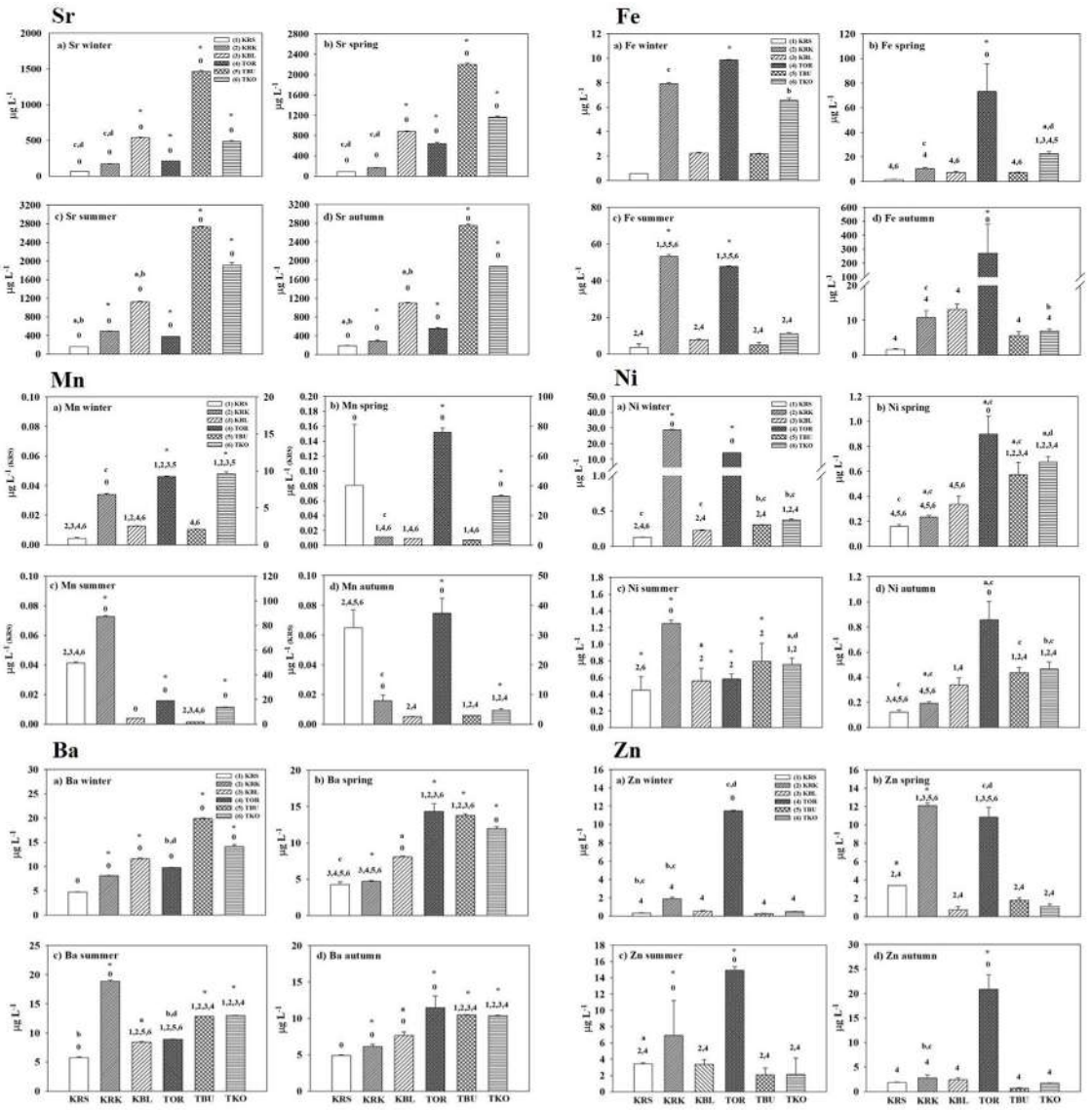

Fig. 3. Dissolved concentrations of metal(loid)s with maximum average concentrations ≥ 3 μg L^{-1} in water from six sites of the Krka River sampled in four seasons. The description of the labels (numbers and letters) are given in Section 2.5 "Data processing and statistics".

and Sr at TBU, and of Cd and Tl at KRS, while other elements showed considerable variations depending on the season (Figs. 1–4). Overall, metal contamination followed the order: TOR>KRK>TKO>TBU>KBL>KRS.

Altogether, the most pronounced spatial differences existed between KRS and the two wastewater impacted sites, TOR and KRK (Figs. 1–4). That was especially evident for Ba, Co, Fe, K, Na, Ni, Sb and Zn, as consistent with the previous research in this area (Cukrov et al., 2008; Filipović Marijić et al., 2018). Many of these elements, including Co, Fe, Ni and Zn are regularly used in different kinds of industrial activities (Wang et al., 2005; Sertić Perić et al., 2018; Gemeda et al., 2021). If KRK and TOR are compared, Mg, K, Ca, Na, Mn, Zn, Ba and Sr were mostly significantly higher at TOR, influenced by industrial wastewaters, while As, Cr, and Mo had higher concentrations at KRK, influenced by municipal wastewaters. Therefore, TOR, a potential recipient of waters from IWW, represents a direct connection and the most significant source of metal(loid)s contamination directly in the Krka River watercourse.

Nevertheless, many significant differences were also observed between other two tributaries (TBU and TKO) and KRS (Figs. 1–4). If TBU and TKO are compared, more elements had higher concentrations in TKO, except Ba, Cr, Mg, Mo, Sr, and Tl, which were higher in TBU, probably as a result of more extensive agricultural activity in this area and nearby field Kninsko polje. Tributary Kosovčica is also influenced by agriculture from the nearby Kosovo polje, but also by gypsum factory, whose wastewaters, resulting from mining activities and gypsum production, may be contaminated with variety of

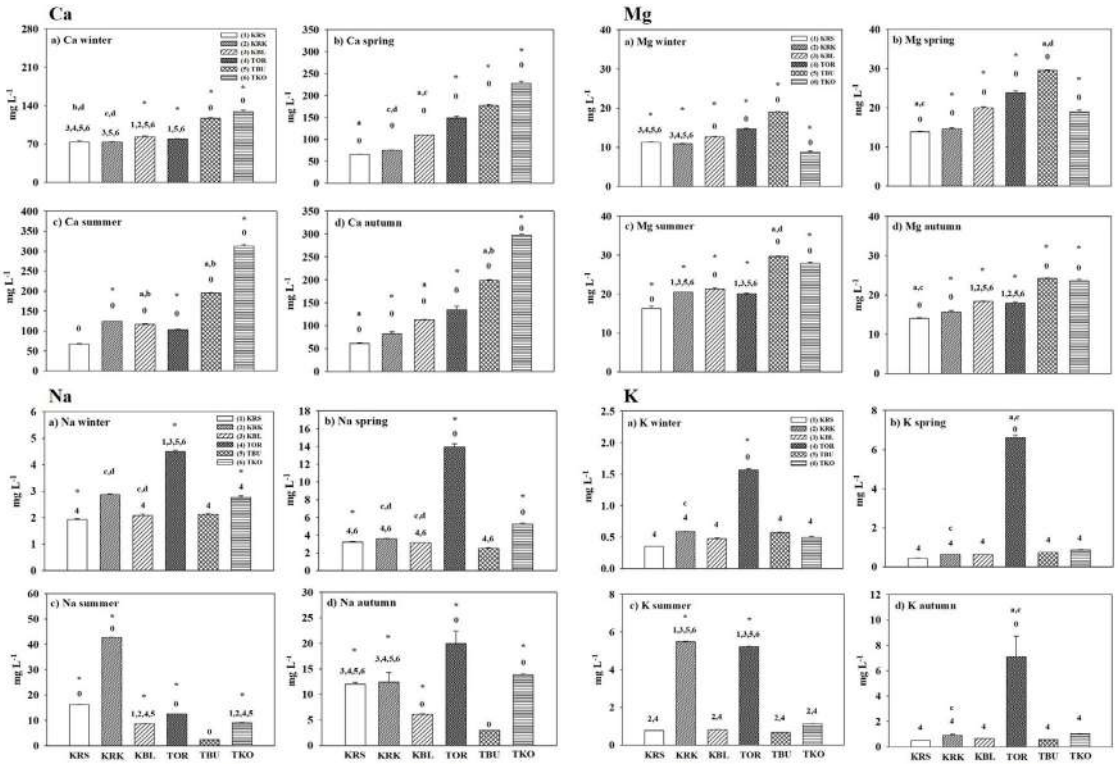

Fig. 4. Dissolved concentrations of macroelements in water from six sites of the Krka River sampled in four seasons. The description of the labels (numbers and letters) are given in Section 2.5 "Data processing and statistics".

metals (Carbonell-Barrachina et al., 2002; Mihara et al., 2008; Ternjej et al., 2014). In the previous research of Ternjej et al. (2014), investigating the impact of gypsum mine water on organisms in Kosovčica River, concentrations of most elements were mostly lower than in our research, indicating an increase of the pollution impact over time. However, concentrations at TBU and TKO are still mostly lower than at KRK and TOR, with the exceptions of Ca, Cd, Mg, Mo, Sb, Se, and Sr in some seasons (Figs. 1–4), which are elements that can often be found in fertilizers and/or phosphogypsum (Carbonell-Barrachina et al., 2002; Thomas et al., 2012; Mijošek et al., 2020). Concentrations of Cd and Tl tended to be higher in the reference site than in the downstream, anthropogenically affected sites of the Krka River. Martinez et al. (2002) assumed that elevated Cd concentrations in river sources are often associated with leaching of soil enriched with organic matter and sulphur. Another explanation is that limestones and dolomites, predominant in Dinaric area, are enriched with Cd compounds in karst areas (Cukrov et al., 2008).

Comparison of concentrations of metal(loid)s at KBL, chosen site located in the protected KNP, with river source water (KRS) showed higher concentrations of Ba, Ca, Cu, Fe, Mg, Mo, and Sr, and lower of Cd, Cs, Mn, and Na at KBL (Figs. 1–4), while concentrations of other elements were comparable. In general, metal concentrations were higher in the anthropogenically affected sites than in KBL, while the higher levels in the national park were found for Mo and Tl than in TOR, for Sr than in KRK and TOR, and for Cs than in TBU (Figs. 1–3). Such trends confirm that the impact of wastewaters is still not significant in the area of KNP. However, enhanced accumulation of some elements and higher concentrations of many elements compared to the river source, represent a possible danger to preserving this sensitive ecosystem in the future. This is still not cause for concern since numerous small cascade lakes are formed by tufa-barriers in the central course of the Krka River and they serve as traps for trace elements, resulting in self-purification of the water and prevention of downstream metal(loid)s increase (Cukrov et al., 2008). This process is enabled by the strong and intensive sedimentation, which starts in KBL, so even lower metal concentrations can probably be expected in the area of the KNP in the downstream direction (Cukrov et al., 2008). This is also supported by a comparison of physico-chemical parameters, which over the years did not show an evident increase in pollution impact in the area of KNP (Filipović Marijić et al., 2018; Šariri et al., submitted for publication).

Observed differences in metal concentrations between sites were generally supported by the spatial distribution of physico-chemical parameters (Šariri et al., submitted for publication). Namely, waters at TOR, KRK and TKO were classified as waters below good quality (GRC, 2019) in all seasons due to COD and content of nutrients, which, together with metal accumulation, confirmed long-term impact of municipal and industrial wastewaters (Mihaljević et al., 2011; Ternjej et al., 2014; Filipović Marijić et al., 2018; Sertić Perić et al., 2018; Šariri et al., submitted for publication). On the other hand, the

best ecological conditions considering physico-chemical parameters were confirmed in KRS and TKR, which were classified as waters of very good quality, while the water parameters at TBU were either within the range for very good or good ecological status (GRC, 2019), all supporting the patterns of metal accumulation in our research (Šariri et al., submitted for publication), but also previous findings of Filipović Marijić et al. (2018).

3.3.2. Temporal variability of dissolved metal(loid) concentrations in the Krka River basin

Temporal variability of metal(loid) concentrations may depend on different factors such as water level and flow, rain intensity, soil erosion, pH values, water hardness, agricultural activities or wastewater discharge. In our research, higher water levels representing wet seasons were recorded in winter and spring (219 cm in January; 117 cm in April) and lower in summer and autumn as dry seasons (77 cm in July; 80 cm in October), according to Croatian Meteorological and Hydrological Service.

Dissolved concentrations of many metal(loid)s often differed considerably between seasons in many locations (Figs. 1–4). However, the uniform seasonal variations pattern of most elements was not obvious, except for significantly higher values observed in summer at most locations, probably due to the lowest water level (77 cm), which additionally reduces the dilution effects and the self-purification ability of the Krka River. The high summer concentrations pattern was evident for Cs, Cu, Mg, Mo, Na, Sb, Sr, and mostly for As, Ba, and Ca (Figs. 1–4). On the contrary, the lowest concentrations of Ca, Co, Cs, Cu, Fe, K, Mg, Mn, Mo, Na, Sr, Tl, and Zn were observed in winter (Figs. 1–4), the season specified by the highest precipitation, when high water level and water velocity contribute to the dilution and more effective purification processes which decrease metal concentrations. However, some elements showed the opposite trend and the highest concentrations in winter were mostly observed for Cd, Cr, Ni and Se, as well as for As and Ba in some locations (Figs. 1–3), probably due to considerable rainfalls which wash down the waste and can cause soil erosion and metal desorption from sediments to the water column (Dural et al., 2007; Gunes, 2022). Some of these elements, like As, Cd, Cr, and Ni, are often found in fertilizers (Thomas et al., 2012) and additional rains or floods can contribute to the wash-up of agricultural soils to the river water (Mijošek et al., 2020).

Most elements showed differences among seasons in almost all locations, except Fe, K, Mn, Sb and Zn, which showed poor temporal changes compared to other elements (Figs. 1–4). Namely, significant differences between seasons were observed for Fe and K only at KRK and TOR, for Mn and Sb at KRK, TOR and TKO, and for Zn in KRS, KRK and TOR, showing that temporal variability of many elements at the wastewater impacted sites probably often depends on their (ir)regular wastewaters discharges.

Therefore, seasonal changes in the dissolved metal(loid)s concentrations are partially influenced by wastewaters inputs and partially by the rainfalls and water level, which were at a maximum in winter and a minimum in summer.

Previous research by Filipović Marijić et al. (2018) in this area, which covered only two seasons (spring and autumn), pointed to significantly higher levels of majority of elements in dry season. That was not the case in our study, but such inter-annual differences are normal for water samples, depending on the changes in flood season duration, rain intensity or the level of anthropogenic pressure (Guo et al., 2022). This highlights the need of long-term monitoring, to get the most reliable results and accurate estimation of water quality of the ecosystem.

3.4. Ratios of dissolved and total metal(loid) concentrations in the upper course of the Krka River

Dissolved elements are easily transported over longer distances and are much more available, and, as such, are potentially more toxic to aquatic organisms than the elements which are mostly attached to particles (Janssen et al., 2003; de Paiva Magalhães et al., 2015; Adams et al., 2020). Therefore, it is important to know the distribution of elements between dissolved and particulate phase since average ratios of dissolved and total concentrations of elements might give us basic information on the metal(loid)s behavior in the Krka River and their tendency to bind with particulate matter (Table 1). It is commonly expected that the dissolved concentrations of trace metals in waters, which are available to aquatic organisms, are lower than the total concentrations of those elements (Cleven et al., 2005).

All macroelements were almost completely ($\geq$95%) present in the dissolved fraction in all locations of the Krka River, regardless of the season (Table 1). Many trace elements (Co, Sb, Ba, Se, Sr and Mo) also showed high presence (>90%) in dissolved fraction. Average ratios of dissolved to total concentrations of Tl, Ni, As, Mn, Cr, Cd and Cu ranged between 70 and 90% pointing to their still relatively low affinity of binding to particles in this ecosystem and high bioavailability for organisms. Average ratio of Zn was 68.6%, while the only elements with average presence in dissolved form below 50% were Cs and Fe (Table 1), pointing to their predominant association with particles and/or suspended matter and consequently lower risk of manifestations of their toxicity.

Regarding the spatial distribution of the dissolved/total ratios, the presence of macroelements in dissolved form at the IWW location did not differ significantly from the locations in the Krka River watercourse. However, majority of trace elements, including Co, Ba, Se, Mo, As, Cr, Cu, Zn and Fe, showed lower ratios of dissolved to total concentrations at IWW than other locations, indicating higher portion of trace metals associated to particulate matter of the industrial source (Table 1). Smaller spatial differences were also evident between other locations in the Krka River, showing lower ratios of many elements (Se, Sb, Co, Tl, Ni, As, Mn, Cr, Cd, Cu, Fe) in some of the anthropogenically affected locations (e.g. KRK, TOR, TBU, TKO), which have more particulate and suspended matter from an anthropogenic source. This is also supported by the highest values of TDS, TOC and DOC recorded previously in IWW and anthropogenically influenced sites of the

Table 1
Average ratios of dissolved and total metal(loid) concentrations in the investigated locations of the Krka River in four seasons.

	Mg	Na	Mo	K	Sr	Se	Ca	Ba	Sb	Co	Tl	Ni	As	Mn	Cr	Cd	Cu	Zn	Cs	Fe
	%	%	%	%	%	%	%	%	%	%	%	%	%	%	%	%	%	%	%	%
IWW																				
average	100.3	102.1	90.5	98.6	96.8	85.9	99.1	87.0	84.1	74.9	75.5	79.1	60.1	89.8	14.8	91.6	32.6	58.1	96.1	4.0
SD	4.4	5.6	13.8	2.8	3.6	10.1	5.7	17.2	15.0	39.3	3.4	31.6	26.1	11.8	11.1	21.1	20.0	44.4	4.9	2.2
KRS																				
average	100.8	101.2	98.1	98.8	98.1	97.8	95.6	95.6	86.0	95.5	98.2	88.2	92.9	76.6	86.9	92.4	74.8	68.0	64.9	33.3
SD	4.5	8.1	2.8	3.8	5.0	11.4	11.3	7.7	7.4	3.7	5.2	5.8	4.8	7.4	12.4	10.7	47.9	57.5	22.3	26.5
KRK																				
average	103.1	102.1	96.8	99.8	98.7	93.8	99.8	93.8	98.1	90.3	79.5	92.0	89.9	91.9	91.3	65.8	65.8	78.4	54.6	24.1
SD	3.3	5.4	7.5	3.2	3.0	22.1	4.3	2.2	17.8	6.1	33.8	14.5	11.8	10.0	15.1	33.0	35.5	6.5	12.5	8.5
KBL																				
average	102.8	102.7	100.2	98.8	99.6	103.2	96.4	98.2	94.3	96.3	97.4	84.0	92.1	79.8	89.4	72.6	73.0	61.1	42.6	35.4
SD	4.4	4.7	3.5	4.6	2.8	6.0	6.0	2.8	3.7	6.8	14.7	12.4	5.3	14.9	6.2	6.2	17.9	13.4	27.8	36.1
TOR																				
average	101.4	102.2	100.7	98.4	98.3	98.0	97.4	95.4	95.2	88.4	76.8	82.2	74.6	89.3	57.6	37.2	72.1	62.8	50.4	25.6
SD	4.1	4.8	2.9	2.7	2.1	15.8	4.7	3.7	5.7	11.3	14.0	24.5	6.6	9.4	14.0	16.7	17.8	21.0	28.5	27.4
TBU																				
average	102.5	100.5	100.7	99.1	98.6	98.4	94.6	96.3	86.0	86.1	88.3	89.6	87.6	63.2	72.1	81.8	82.4	74.6	32.2	19.5
SD	3.9	5.8	3.9	4.2	2.3	13.3	1.4	2.3	9.5	19.1	11.8	9.9	10.9	24.0	3.3	15.6	29.2	33.1	29.2	17.1
TKO																				
average	103.6	102.4	101.7	100.3	100.3	97.0	97.9	98.0	97.7	86.0	84.2	86.8	83.3	78.0	69.8	76.8	55.4	66.7	22.9	10.8
SD	3.5	5.4	2.4	3.2	2.3	17.1	4.1	1.8	5.8	14.1	8.4	7.8	7.6	25.8	20.0	5.7	13.9	28.0	12.8	2.3
Average*	102.4	101.9	99.7	99.2	98.9	98.0	97.0	96.2	92.9	90.4	87.4	87.1	86.7	79.8	77.9	71.1	70.6	68.6	44.6	24.8
SD	1.1	0.8	1.9	0.7	0.8	3.0	1.8	1.7	5.5	4.5	9.0	3.6	6.9	10.3	13.5	18.9	9.2	6.7	15.3	9.1
RSD	1.0	0.8	1.9	0.7	0.9	3.1	1.9	1.7	5.9	5.0	10.3	4.1	7.9	12.9	17.3	26.5	13.0	9.8	34.3	36.6

*Final average value corresponds to the locations in the Krka River watercourse, without IWW which were separated as in the whole paper.

Krka River (Šariri et al., submitted for publication) which are all well known to complex trace elements (Buffle, 1988). Seasonal patterns were not always uniform and were probably caused by both natural and anthropogenic environmental conditions. Average ratios of dissolved and total metal(loid) concentrations in locations of the Krka River followed the order: Mg>Na>Mo>K>Sr>Se>Ca>Ba>Sb>Co>Tl>Ni>As>Mn>Cr>Cd>Cu>Zn>Cs>Fe (Table 1).

Altogether, high variability in average ratios of dissolved and total metal(loid) concentrations between locations, supported by higher RSD values (>15%), were confirmed only for Cr, Cd, Cs and Fe (Table 1), possibly as a consequence of irregular discharges of these elements from industry, agriculture and municipal activities. Although more particulate matter at wastewater impacted locations can bind higher amount of some metals and decrease their dissolved concentrations, generally much higher concentrations at these sites, despite binding capacity, still point to significant risk of negative effects on the Krka River and possible toxic effects for biota.

4. Conclusions

Conducted research showed spatial and temporal variations in metal(loid) concentrations in the Krka River, reflecting direct and long-term consequences of wastewater discharges and physico-chemical water properties in this sensitive karst area. The highest element concentrations were mostly observed in summer, as the dry season characterized by the lowest water level and poor purification processes in the river and its tributaries. Dissolved metal concentrations indicated clean, pristine conditions at the river source, while industrial wastewaters contained the highest concentrations of all elements, particularly Mn, Zn, Co, Cs, and Fe, than other locations. The most significant impact of IWW was observed at its closest site TOR, which turned out to be the most contaminated site in the upper reaches of the Krka River. Although IWW was found to be the most important source of many elements, municipal effluents of the Town of Knin, agricultural practice, and gypsum factory were the main route of contamination with As, Ca, Cr, Mg, Mo, and Sr, showing the highest concentrations in KRK, TBU or TKO. Brljan Lake (KBL), as the location in the KNP, had higher concentrations of Ba, Ca, Cu, Fe, Mg, Mo, and Sr than KRS. However, most of the levels were still much lower than at other anthropogenically affected locations, confirming the moderate impact of the contamination sources on the KNP and self-purification processes specific to karst flow systems.

Most elements, except for Zn, Cs and Fe, were present in dissolved fraction with >70%, showing a low tendency to bind with particulate matter and suggesting possible high risk of toxicity during time. The long-term comparisons showed increased concentrations of most elements over time in the Krka River watercourse, especially for Cr, Cu, Fe, Mn, and Ni, as elements often used in industrial activities. Altogether, the influence of industrial and municipal activities over time still seems moderate in the Krka River but observed differences and metal increases emphasize possible accumulation over time. Therefore, continuous monitoring and control of contamination sources and adequate wastewater treatment are required to protect this karst ecosystem.

Our study contributes to a better understanding of the dynamics of dissolved and total metal(loid) concentrations in sensitive karst river systems under anthropogenic impact, represented by the Krka River, a typical karst basin of the Dinaric region, which is one of the largest karst areas in Europe. In this way, both the vulnerability of the karst ecosystem in general and the potential threat to the Krka National Park were assessed.

CRediT authorship contribution statement

Tatjana Mijošek: Validation, Formal analysis, Investigation, Writing – original draft, Writing – review & editing. **Zorana Kljaković-Gašpić:** Validation, Formal analysis, Investigation, Writing – original draft, Writing – review & editing. **Tomislav Kralj:** Investigation. **Damir Valić:** Investigation. **Zuzana Redžović:** Investigation. **Sara Šariri:** Formal analysis, Investigation. **Ivana Karamatić:** Investigation. **Vlatka Filipović Marijić:** Conceptualization, Investigation, Resources, Writing – original draft, Writing – review & editing, Supervision, Project administration, Funding acquisition.

Declaration of competing interest

The authors declare that they have no known competing financial interests or personal relationships that could have appeared to influence the work reported in this paper.

Data availability

Data will be made available on request.

Acknowledgments

This work has been supported by Croatian Science Foundation under the project "Integrated evaluation of aquatic organism responses to metal exposure: gene expression, bioavailability, toxicity and biomarker responses" (BIOTOXMET; IP-2020-02-8502). Ministry of Science and Education of the Republic of Croatia is acknowledged for institutional funding of the Laboratory for Biological Effects of Metals.

Appendix A. Supplementary data

Supplementary material related to this article can be found online at https://doi.org/10.1016/j.eti.2023.103254.

References

Adams, W., Blust, R., Dwyer, R., Mount, D., Nordheim, E., Rodriguez, P.H., Spry, D., 2020. Bioavailability assessment of metals in freshwater environments: A historical review. Environ. Toxicol. Chem. 39 (1), 48–59.

Bakalowicz, M., 2005. Karst groundwater: a challenge for new resources. Hydrogeol. J. 13 (1), 148–160. http://dx.doi.org/10.1007/s10040-004-0402.

Bravo, A.G., Kothawala, D.N., Attermeyer, K., Tessier, E., Bodmer, P., Amouroux, D., 2018. Cleaning and sampling protocol for analysis of mercury and dissolved organic matter in freshwater systems. MethodsX 5, 1017–1026. http://dx.doi.org/10.1016/j.mex.2018.08.002.

Brinkmann, R., Parise, M., 2012. Karst environments: problems, management, human impacts, and sustainability. J. Caves Karst Stud. 74 (2), 135–136. http://dx.doi.org/10.4311/2011JCKS0253.

Buffle, J., 1988. Complexation reactions in aquatic systems: an analytical approach. Ellis - Horwood Ltd, Chichester, England.

Campanale, C., Losacco, D., Triozzi, M., Massarelli, C., Uricchio, V.F., 2022. An overall perspective for the study of emerging contaminants in Karst aquifers. Resources 11 (105), http://dx.doi.org/10.3390/resources11110105.

Carbonell-Barrachina, A., DeLaune, R.D., Jugsujinda, A., 2002. Phosphogypsum chemistry under highly anoxic conditions. Waste Mgmt 22, 657–665.

Cleven, R., Nur, Y., Krystek, P., van den Berg, G., 2005. Monitoring metal speciation in the rivers meuse and rhine using DGT. Water Air Soil Pollut. 165, 249–263.

Cukrov, N., Cmuk, P., Mlakar, M., Omanović, D., 2008. Spatial distribution of trace metals in the Krka River, Croatia. An example of the selfpurification. Chemosphere 72 (10), 1559–1566. http://dx.doi.org/10.1016/j.chemosphere.2008.04.038.

Cukrov, N., Tepić, N., Omanović, D., Lojen, S., Bura-Nakić, E., Vojvodić, V., Pižeta, I., 2012. Qualitative interpretation of physico-chemical and isotopic parameters in the Krka River (Croatia) assessed by multivariate statistical analysis. Int. J. Environ. An. Ch. 92 (10), 1187–1199. http://dx.doi.org/10.1080/03067319.2010.550003.

Dautović, J., 2006. Determination of Metals in Natural Waters using High Resolution Inductively Coupled Plasma Mass Spectrometry Bachelor of Science thesis. University of Zagreb (in Croatian).

Dautović, J., Fiket, Ž., Barešić, J., Ahel, M., Mikac, N., 2014. Sources, distribution and behavior of major and trace elements in a complex karst lake system. Aquat. Geochem. 20 (1), 19–38. http://dx.doi.org/10.1007/s10498-013-9204-9.

de Paiva Magalhães, D., da Costa Marques, M.R., Baptista, D.F., Buss, D.F., 2015. Metal bioavailability and toxicity in freshwaters. Environ. Chem. Lett. 13, 69–87.

Dragun, Z., Kapetanović, D., Raspor, B., Teskeredžić, E., 2011. Water quality of medium size watercourse under baseflow conditions: the case study of river Sutla in Croatia. Ambio 40 (4), 391–407. http://dx.doi.org/10.1007/s13280-010-0119-z.

Dragun, Z., Roje, V., Mikac, N., Raspor, B., 2009. Preliminary assessment of total dissolved trace metal concentrations in Sava river water. Environ. Monit. Assess. 159, 99–110.

Dragun, Z., Stipaničev, D., Fiket, Ž., Lučić, M., Udiković Kolić, N., Puljko, A., Repec, S., Šoštarić Vulić, Z., Ivanković, D., Barac, F., Kiralj, Z., Kralj, T., Valić, D., 2022. Yesterday's contamination–A problem of today? The case study of discontinued historical contamination of the Mrežnica River (Croatia). Sci. Total Environ. 848, 157775.

Dural, M., Goksu, M.Z.L., Ozak, A.A., 2007. Investigation of heavy metal levels in economically important fish species captured from the Tuzla Lagoon. Food Chem 102, 415–421. http://dx.doi.org/10.1016/j.foodchem.2006.03.001.

European Parliament and the Council of the European Union (EPCEU), 2013. Directive 2013/ 39/EU of the European parliament and of the council of 12 2013 amending directives 2000/60/EC and 2008/105/EC as regards priority substances in the field of water policy. O. J. L. 226. p. 1.

Filipović Marijić, V., Kapetanović, D., Dragun, Z., Valić, D., Krasnići, N., Redžović, Z., Grgić, I., Žunić, J., Kružlicová, D., Nemeček, P., Ivanković, D., Vardić Smrzlić, I., Erk, M., 2018. Influence of technological and municipal wastewaters on vulnerable karst riverine system, Krka River in Croatia. Environ. Sci. Pollut. Res. 25, 4715–4727. http://dx.doi.org/10.1007/s11356-017-0789-1.

Filipović Marijić, V., Sertić Perić, M., Matoničkin Kepčija, R., Dragun, Z., Kovarik, I., Gulin, V., Erk, M., 2016. Assessment of metal exposure, ecological status and required water quality monitoring strategies in small- to medium-size temperate rivers. J. Environ. Sci. Health A 51 (4), 309–317.

Gemeda, F.T., Guta, D.D., Wakjira, F.S., Gebresenbet, G., 2021. Occurrence of heavy metal in water, soil, and plants in fields irrigated with industrial wastewater in Sabata town, Ethiopia. Environ. Sci. Pollut. Res. 28, 12382–12396. http://dx.doi.org/10.1007/s11356-020-10621-6.

Government of the Republic of Croatia (GRC), 2019. Directive on water quality status. Official gazette of the republic of Croatia no. 96 (NN 96/19).

Government of the Republic of Croatia (GRC), 2020. Regulation on limit values for waste water emissions. Official gazette of the Republic of Croatia no. 26 (NN 26/20).

Gunes, G., 2022. The change of metal pollution in the water and sediment of the Bartın River in rainy and dry seasons. Environ. Eng. Res. 27, 200701.

Guo, W., Zou, J., Liu, S., Chen, X., Kong, X., Zhang, H., Xu, T., 2022. Seasonal and spatial variation in dissolved heavy metals in Liaodong Bay, China. Int. J. Environ. Res. Public Health 19 (608), http://dx.doi.org/10.3390/ijerph19010608.

Halamić, J., Miko, S. (Eds.), 2009. Geochemical Atlas of the Republic of Croatia. Croatian Geological Survey, Zagreb.

Halamić, J., Peh, Z., Miko, S., Galović, L., Šorša, A., 2012. Geochemical atlas of Croatia: Environmental implications and geodynamical thread. J. Geochem. Explor. 115, 36–46. http://dx.doi.org/10.1016/j.gexplo.2012.02.006.

Hartmann, A., Goldscheider, N., Wagener, T., Lange, J., Weiler, M., 2014. Karst water resources in a changing world: Review of hydrological modeling approaches. Rev. Geophys. 52, 218–242.

Janssen, C.R., Heijerick, D.G., De Schamphelaere, K.A.C., Allen, H.E., 2003. Environmental risk assessment of metals: tools for incorporating bioavailability. Environ. Int. 28, 793–800.

Kalhor, K., Ghasemizadeh, R., Rajić, L., Alshawabkeh, A., 2019. Assessment of groundwater quality and remediation in karst aquifers: A review. Groundw. Sustain. Dev. 8, 104–121. http://dx.doi.org/10.1016/j.gsd.2018.10.004.

Kisić, I., Zgorelec, Ž., Galić, M., Delač, D., 2019. Analysis of Mud and Water in Lagoons Polluted By Waste Materials in Knin. Zagreb, https://knin.hr/wp-content/uploads/2019/07/Zavrsno-izvijesce-Analiza-mulja-DIV-ove-lagune.pdf.

Kovačič, G., Ravbar, N., 2003. Karst aquifers vulnerability or sensitivity? Acta Carsologica 32, 307–314.

Martinez, C.E., McBride, M.B., Kandianis, M.T., Duxbury, J.M., Yoon, S., Bleam, W.F., 2002. Zinc sulfur and cadmium-sulfur association in metalliferous peats: evidence from spectroscopy, distribution coefficients, and phytoavailability. Environ. Sci. Technol. 36, 3683–3689.

Mihaljević, Z., Ternjej, I., Stanković, I., Ivković, M., Želježić, D., Mladinić, M., Kopjar, N., 2011. Assessment of genotoxic potency of sulfate-rich surface waters on medicinal leech and human leukocytes using different versions of the Comet assay. Ecotoxicol. Environ. Safety 74, 1416–1426.

Mihara, N., Soya, K., Kuchar, D., Fukuta, T., Matsuda, H., 2008. Utilization of calcium sulfide derived from waste gypsum board for metal-containing wastewater treatment. Glob. NEST J. 10, 101–107.

Mijošek, T., Filipović Marijić, V., Dragun, Z., Ivanković, D., Krasnići, N., Redžović, Z., Sertić Perić, M., Vdović, N., Bačić, N., Dautović, J., Erk, M., 2020. The assessment of metal contamination in water and sediments of the lowland Ilova river (Croatia) impacted by anthropogenic activities. Environ. Sci. Pollut. Res. 27, 25374–25389.

Padilla, I.Y., Irizarry, C., Steele, K., 2011. Historical contamination of groundwater resources in the north coast karst aquifer of Puerto Rico. Dimension 25 (3), 7–12.

Padilla, I.Y., Vesper, D.J., 2018. Fate, transport, and exposure of emerging and legacy contaminants in karst systems: State of knowledge and uncertainty. In: White, W., Herman, J., Herman, E., Rutigliano, M. (Eds.), Karst Groundwater Contamination and Public Health. In: Advances in Karst Science, Springer, Cham, http://dx.doi.org/10.1007/978-3-319-51070-5_5.

Šariri, S., Valić, D., Kralj, T., Cvetković, Ž., Mijošek, T., Redžović, Z., Karamatić, I., Filipović Marijić, V., n.d. Long-term and seasonal trends of water parameters in the karst riverine catchment and general literature overview based on CiteSpace. Appl. Water Sci. (submitted for publication).

Selak, A., Reberski, J.L., Klobučar, G., Grčić, I., 2022. Ecotoxicological aspects related to the occurrence of emerging contaminants in the Dinaric karst aquifer of Jadro and Žrnovnica springs. Sci. Total Environ. 825, 153827.

Sertić Perić, M., Matoničkin Kepčija, R., Miliša, M., Gottstein, S., Lajtner, J., Dragun, Z., Filipović Marijić, V., Krasnići, N., Ivanković, D., Erk, M., 2018. Benthos-drift relationships as proxies for the detection of the most suitable bioindicator taxa in flowing waters – a pilot-study within a Mediterranean karst river. Ecotoxicol. Environ. Safety 163, 125–135. http://dx.doi.org/10.1016/j.ecoenv.2018.07.068.

Telbisz, T., Mari, L., 2020. The significance of karst areas in European national parks and geoparks. Open Geosci. 12, 117–132.

Ternjej, I., Mihaljević, Z., Ivković, M., Previšić, A., Stanković, I., Maldini, K., Želježić, D., Kopjar, N., 2014. The impact of gypsum mine water: a case study on morphology and DNA integrity in the freshwater invertebrate, Gammarus balcanicus. Environ. Pollut. 189, 229–238. http://dx.doi.org/10.1016/j.envpol.2014.03.009.

Thomas, E.Y., Omueti, J.A.I., Ogundayomi, O., 2012. The effect of phosphate fertilizer on heavy metal in soils and *Amaranthus caudatus*. Agric. Biol. J. N. Am. 3, 145–149.

Vadillo, I., Ojeda, L., 2022. Carbonate aquifers threatened by contamination of hazardous anthropic activities: Challenges. Curr. Opin. Environ. Sci. Health 26, 100336. http://dx.doi.org/10.1016/j.coesh.2022.100336.

Vega, M., Pardo, R., Barrado, E., Deban, L., 1998. Assessment of seasonal and polluting effects on the quality of river water by exploratory data analysis. Water Res. 32 (12), 3581–3592.

Wang, X.S., Qin, Y., Sang, S.X., 2005. Accumulation and sources of heavy metals in urban topsoils: a case study from the city of Xuzhou, China. Environ. Geol 48, 101–107. http://dx.doi.org/10.1007/s00254-005-1270-x.

Publication No. 3: Association of toxic effects and the quality of surface water and wastewater: Application under environmental conditions and literature overview by CiteSpace

Journal of Contaminant Hydrology 274 (2025) 104667

Contents lists available at ScienceDirect

Journal of Contaminant Hydrology

journal homepage: www.elsevier.com/locate/jconhyd

Association of toxic effects and the quality of surface water and wastewater: Application under environmental conditions and literature overview by CiteSpace

Sara Šariri [a], Želimira Cvetković [b], Tatjana Mijošek Pavin [a], Zorana Kljaković-Gašpić [c], Damir Valić [a], Tomislav Kralj [a], Amalia Brkić [d], Zuzana Redžović [d], Vlatka Filipović Marijić [a,*]

[a] Ruđer Bošković Institute, Bijenička cesta 54, 10000 Zagreb, Croatia
[b] Teaching Institute for Public Health Dr. Andrija Štampar, Mirogojska cesta 16, Zagreb, Croatia
[c] Institute for Medical Research and Occupational Health, Ksaverska 2, 10000 Zagreb, Croatia
[d] Department of Biology, Faculty of Science, University of Zagreb, Horvatovac 102a, 10000 Zagreb, Croatia

ARTICLE INFO

Keywords:
Physical and chemical parameters
Metal(loid) exposure
Ecotoxicity
Microbiotests
Scientometric analysis

ABSTRACT

Monitoring of wastewaters is crucial for the protection of surface waters and should contain quality and toxicity analyses to ensure safety of aquatic organisms. In this study, the impacts of industrial and municipal wastewaters were assessed by examining the responses of organisms from different trophic levels, *Pseudokirchneriella subcapitata* (microalgae) and *Daphnia magna* (crustaceans), together with physical and chemical water parameters and total metal(loid) concentrations, separately in wastewater lagoons and four nearby sites in the karst Krka River in spring, summer and autumn. The sites in close proximity to the inappropriately treated wastewaters exhibited diminished ecological status, especially regarding COD, nutrients, turbidity, mineral oils, and elevated concentrations of metals (Cd, Co, Cu, Fe, Na, Ni, and Zn). Toxicity effects were confirmed for surface river water near the municipal wastewater outlet (hazard class III) and for basins with industrial wastewater (hazard class IV). Although such approach enabled determination of the toxic hazard of complex mixtures in aquatic environments, literature overview by CiteSpace showed that data in this field are limited and that European countries dominate in this area of research. In addition, multivariate statistical analysis confirmed association of water quality data and toxic effects and the importance of microbiotests in assessment of ecologically relevant risks for aquatic organisms.

1. Introduction

The karst environment is among the most fragile and vulnerable on Earth. In karst regions, water infiltrates rapidly through a highly interconnected network of conduits, caves, and sinkholes formed within soluble carbonate or evaporite bedrock (Parise et al., 2015; Ford and Williams, 2007). Even minor, diffuse inputs at the surface (such as agricultural runoff, septic effluent, or accidental spills) can quickly propagate throughout the entire system, making karst aquifers especially susceptible to contamination (White, 2002). However, many urban areas in karst regions face water quality degradation due to limited or no sewer systems and wastewater treatment plants, resulting in discharge of municipal and industrial wastewaters into karst streams without appropriate treatment (Ford and Williams, 2007; Hillebrand et al., 2012; Malá et al., 2022). Given that karst groundwater supplies up to 25 % of the world's drinking water, preserving its quality is of critical importance (Goldscheider and Drew, 2007).

The methods for assessing the quality of water systems provided in the Water Framework Directive (WFD, Commission Directive 2013/39/EU) mainly focus on single chemical analyses (Kortenkamp et al., 2019). However, this approach is often insufficient for quality control purposes, since chemical compounds occur as mixtures in the environment.

* Corresponding author at: Laboratory for Biological Effects of Metals, Division for Marine and Environmental Research, Ruđer Bošković Institute, Bijenička c. 54, 10000 Zagreb, Croatia.
E-mail addresses: ssariri@irb.hr (S. Šariri), zelimira.cvetkovic@stampar.hr (Ž. Cvetković), tmijosek@irb.hr (T. Mijošek Pavin), zorana@imi.hr (Z. Kljaković-Gašpić), dvalic@irb.hr (D. Valić), Tomislav.Kralj@irb.hr (T. Kralj), abrkic@stud.biol.pmf.hr (A. Brkić), zuzana.redzovic@biol.pmf.hr (Z. Redžović), vfilip@irb.hr (V. Filipović Marijić).

https://doi.org/10.1016/j.jconhyd.2025.104667
Received 14 February 2025; Received in revised form 9 June 2025; Accepted 30 June 2025
Available online 2 July 2025

Consequently, it is hard to predict physical, chemical and biological impact of pollutants, especially due to their antagonistic and synergistic effects in mixtures (Mendonça et al., 2013). To fully capture the integrated biological risks posed by these mixtures, there is growing recognition of the need for ecotoxicity testing in karst rivers. In the ecotoxicological testing of mixtures, the contributions and interactions of the individual mixture components are often investigated in the laboratory. However, it is strongly recommended to complement this approach with whole effluent toxicity testing, which characterizes the ecotoxicity of an entire mixture (including undetected and unmeasured substances) and provides an overall assessment of cumulative biological effects (Maloney et al., 2023; Menghini et al., 2023). Although whole effluent toxicity testing is applied in regulatory context, especially in the USA and Canada, linking toxic effects and environmental conditions is still challenging (Vosylienė, 2007). Increasingly, it is proposed to combine multiple bioassays, include organisms with different biological complexity and trophic roles, and expand the range of quantifiable endpoints (Menghini et al., 2023; Vosylienė, 2007).

Algae form the base of aquatic food webs and are widely used in phytotoxicity testing due to their sensitivity to chemical and biological changes in the environment (Burton Jr. et al., 2002). When compared to other species, algae are more sensitive to a diverse range of potential contaminants, including metals and organic pollutants, and to fluctuations in physical and chemical parameters (Tousova et al., 2018; Xin et al., 2021). Among aquatic invertebrates, daphnids are commonly used in zootoxicity assays due to their broad distribution in a wide range of habitats, sensitivity to numerous environmental contaminants, relatively small size, short life cycle and easy maintenance in the laboratory (Persoone et al., 2009). Essentially, the algae *Pseudokirchneriella subcapitata* (Korshikov) F. Hindák, 1990 (initially named *Selenastrum capricornutum* Printz, 1914 and renamed *Raphidocelis subcapitata* (Korshikov) Nygaard, 1987) and the crustacean *Daphnia magna* Straus, 1820 are among the most frequently used and recommended species for freshwater toxicity testing, supported by standardized protocols and extensive data on their responses to a range of contaminants (Radix et al., 2000; Weyers et al., 2000; Moreira-Santos et al., 2004).

Although whole effluent toxicity assessment was developed in the 1950s, research combining tests on algae and daphnids appears to have begun in the 1990s, partially due to the development of "Toxkit" microbiotests. Unlike earlier bioassays, these commercially available tests contained dormant eggs of selected invertebrate species, immobilized microalgae, or ciliate protozoans and were maintenance-free, resulting in high popularity among researchers in many countries (Persoone et al., 2003). The majority of toxicity tests involving algae and daphnids were conducted to determine the toxicity of a specific chemical substance or compound (Garric et al., 2007; Hund-Rinke et al., 2018), while fewer studies were conducted using effluents or environmental water samples (Kusui et al., 2014; Luan et al., 2020).

In order to estimate possible relation between the toxic effects of contaminants and their concentrations and sources under the real environmental conditions, our study was performed in the karst Krka River. It is an ideal environment for conducting such research due to the pristine water at the river source and the direct influence of the mixtures of contaminants from industrial and municipal wastewaters downstream. As a result, ambient river samples and wastewater outlet samples differ in their physical, chemical and organic water parameters, as well as metal(loid) concentrations (Filipović Marijić et al., 2018; Sertić Perić et al., 2018; Mijošek et al., 2023). To assess rapid and ecologically relevant evaluation of toxicity in complex environmental samples, we applied standardized microbiotests using two aquatic species from different trophic levels: the green alga *Pseudokirchneriella subcapitata* (primary producer) and the freshwater crustacean *Daphnia magna* (primary consumer). The main objective was to compare experimental and environmental data, i.e. the results of toxicity tests on two species with physical and chemical parameters and metal concentrations in surface freshwater and in wastewaters. Possible relationship between the toxic effects and the effects of pollution on the living organisms in the complex and sensitive karst ecosystem was estimated, thus providing new data expressing the causal relationship between the mixture of pollutants and the toxic effects in environmental samples. To support and contextualize our findings, we also conducted a scientometric analysis using CiteSpace software. This analysis aimed to identify global research trends, major thematic clusters, and existing knowledge gaps in the field of ecotoxicological assessments of wastewaters and surface waters, particularly with respect to studies using multiple test organisms under environmentally relevant conditions. By integrating scientometric insights with original experimental data, we provide both new ecotoxicological information for the Krka River and a broader perspective on how this research contributes to the advancement of knowledge in karst aquatic ecosystems. Finally, we assessed the potential and limitations of microbiotests for the detecting and quantifying exposure to environmental pollutants and for linking toxic effects to their chemical causes.

2. Materials and methods

2.1. Sampling procedures

Field research was conducted in the upper part of the Krka River, involving surface water at four localities along the river watercourse. Additionally, industrial wastewater from the basins of the nearby screw factory was directly sampled. Sampling was performed in spring (April 25–27), summer (July 20) and autumn (October 18–20) of 2021. Water samples and in situ measurements were taken at a depth of 0.1 m, approximately 1 m from the riverbank, involving the source of the Krka River, considered as a reference station without direct anthropogenic impact (KRS); Krka River watercourse downstream of the industrial wastewaters and along the municipal wastewater discharge of the Town of Knin (KRK); tributary Orašnica, which passes along the lagoons with industrial wastewater (TOR); tributary Butišnica, mainly influenced by agricultural runoff (TBU); lagoons with industrial wastewater from the screw factory (IWW) (Fig. S1). Air distance from KRS was 2.8 km for TOR, 2.9 km for IWW, 3.7 km for KRK and 4.1 km for TBU. Detailed data on ecological status, long term trends in physical and chemical water parameters and dissolved metal(loid) concentrations were recently described by Šariri et al. (2024) and Mijošek et al. (2023).

2.2. Analyses of the physical and chemical water parameters

The pH and total dissolved solids (TDS) were measured in situ using portable field meters (Mettler Toledo), with exception of industrial wastewater, which was filtered in the laboratory prior to the measurements of pH and TDS due to its extremely poor quality. Other physical and chemical parameters (ammonia, nitrate, total nitrogen and phosphorus, turbidity, chemical oxygen demand (COD) and dissolved CO_2), were analyzed in the laboratory using the respective standardized methods (Hach Lange GmbH, 2013; APHA, 2018) as described by Šariri et al. (2024), total organic carbon (TOC) and dissolved organic carbon (DOC) according to HRN EN 1484 (Croatian Normative Document, 2002), while phenols and mineral oils according to ASTM D 4763-6 (2020). Surface river water data were compared with the values outlined in the Directive on water quality status issued by the Government of the Republic of Croatia (Official Gazette of the Republic of Croatia NN 96/, 2019, 2019; Official Gazette of the Republic of Croatia NN 96/, 2019), which defines the limit values for the ecological status of various types of water bodies, categorizing them as "very good", "good", or "below good". The industrial wastewater data were compared with the emission limit values defined by the Regulation on limit values for wastewater emissions (Official Gazette of the Republic of Croatia NN 26/2020, 2020). The aforementioned documents convey the EU Water Framework Directive (Official Gazette of the Republic of Croatia NN 96/2019, 2019; Official Gazette of the Republic of Croatia NN 26/2020, 2020).

2.3. Measurements of total metal(loid) concentrations in water

Mijošek et al. (2023) provided a detailed description of water sampling, as well as the procedure we utilized for the analysis of the total macro and trace elements in water samples using inductively coupled plasma mass spectrometry (ICP-MS, Agilent 7500cx, Agilent Technologies, Tokyo, Japan). For the elements examined, the limits of detection (LODs) varied from 0.0005 μg L^{-1} for Cs to 30 μg L^{-1} for K. As part of quality control, three certified standard reference materials (NRCC SLRS-5, NIST SRM 1643e, and NIST SRM 1643f) were analyzed, and the recoveries ranged from 92 % (Ni) to 109 % (Cd) (Table S1).

2.4. Toxicity tests

The toxicity of the samples to aquatic organisms was tested using the Microbiotests Toxkits supplied by MicroBioTestsInc. as Algaltoxkit F™ (2004) and Daphtoxkit F™ magna (2001), which follow the standardized methods and ensure reliable and comparable results (Vosylienė, 2007). Each water sample was collected in 1 L glass bottle, and then stored at 4 °C until the start of the experiments within 48 h after the sampling. Based on estimation on water quality of the river water samples and according to the kit manufacturer instructions (ISO standard 8692, 2012; ISO standard 6341, 2012) water from KRS and TBU was not additionally diluted (used as 100 % concentration), while other water samples were diluted with standard freshwater (used as algal culturing medium and hatching medium for crustaceans and provided with necessary nutrients). They were applied in the following concentration ranges: TOR as 100 % and 50 % concentrations, KRK as 100 %, 50 % and 25 % concentrations and IWW as 100 %, 50 %, 25 %, 12.5 % and 6.25 % concentrations.

2.4.1. Algal growth inhibition test

The green microalgae were de-immobilized from alginate beads for determination of algal growth inhibition after 72 h, according to ISO standard 8692 (2012). The test vials were incubated under controlled conditions in an incubator TC 135 S (Aqualytic, Germany) at 23 ± 2 °C with continuous illumination of 10,000 lx for 24, 48 and 72 h. Optical density (OD) was measured at wavelength of 670 nm by UV–Vis spectrophotometer DR6000 (Hach, SAD), which was zero-calibrated with algal growth medium. The cell density of algal stock was adjusted to approximately $1*10^6$ cells/ml, according to OD/N regression, and initial cell density in each test vial was $1*10^4$ cells/ml. The growth and inhibition rate were calculated using the data from OD measurement for every volume of water sample and the control. Six replicates of controls (untreated) and three replicates of each test water concentration were prepared and applied, followed by triplicate measurements. Potassium dichromate ($K_2Cr_2O_7$) was used as positive control to ensure the validity of the test method. Since the industrial wastewaters were colored, a dilution series without algae was prepared for the IWW samples and used to zero-calibrate the spectrophotometer prior to the daily measurement of OD in the algae-IWW dilutions to minimize interference.

2.4.2. Daphnia immobilization test

The toxicity tests on *D. magna* were carried following ISO 6341 standard method (ISO standard 6341, 2012). *D. magna* were hatched from dormant eggs (ephippia) in three days under continuous illumination (6000 lx) at 20–22 °C. Neonates (younger than 24 h) were exposed to the undiluted and diluted samples for 24 h and 48 h at a temperature of 20 °C in darkness. Twenty neonates were used for each sample in a series of four wells; each well contained 10 mL of sample and 5 neonates. The toxicity of each sample was evaluated by the estimation of *D. magna* immobilization rates based on the number of dead or immobilized water fleas compared to the number of active organisms tested. Potassium dichromate ($K_2Cr_2O_7$) was used as positive control to ensure the validity of the test method.

2.4.3. Toxicity evaluation

Toxicity was evaluated by means of toxicity effect and the effective concentration. The toxicity effect was expressed as percentage of mortality/immobilization (*Daphnia* test) or inhibition (Algae test), depending on the effect criterion of the respective assay. The effective concentration (EC_{50}, % *v*/v), causing immobilization or inhibition in 50 % of the tested population, was calculated using nonlinear regression analysis (ISO standard 8692, 2012) and performed with software for automated data analysis of *Algaltoxkit* and *Daphtoxkit* results, provided by the kit manufacturer MicroBio Tests Inc. All results are presented as mean ± standard deviation (S.D.). The toxicity data were also classified according to the hazard classification system as shown in Table S2 (Persoone et al., 2003), by using the equation $TU = 100/EC_{50}$ to transform toxicity values (EC_{50}) into Toxic Units (TU).

2.5. Statistical and scientometric analysis

2.5.1. Statistics

Statistical analyses and calculations were done using SigmaPlot 11.0 (Systat Software, USA), and SPSS Statistics 20.0 (IBM). Total metal(loid) concentrations are presented as mean ± S.D. Variability of total metal (loid) concentrations in water samples between the sites and seasons was performed using two-way ANOVA and Holm-Sidak test. Statistically significant differences between sites in each season are marked with different numbers: 0 – significantly different site from all other sites; 1–5 - significantly different site from the sites indicated by specific number as follows: 1- KRS; 2- TOR; 3- KRK; 4- TBU; 5- IWW; differences between seasons for each location are marked with different letters or asterisk: * - significantly different season from all other seasons; a-c - significantly different season from the seasons indicated by specific letter as follows: a - spring; b - summer; c - autumn. Reduction of dimensionality of a multivariate data set was performed by the Principal Component Analysis (PCA).

2.5.2. Scientometric analysis by CiteSpace

The scientometric analysis of the literature on testing the toxicity of effluents with algae and crustaceans was performed using CiteSpace 6.1. R6 (Basic). CiteSpace is a Java application for analyzing and visualizing scientific literature developed by Dr. Chaomei Chen and is increasingly used to identify trends and provide an objective overview of a state of the art. Based on a set of publications, it can create various types of visual analysis maps in which the objects of analysis (e.g., cited references, countries, keywords, etc.) are represented as nodes of a network and linked based on the relationships between them (co-citation, collaboration, co-occurrence, etc.). The importance of each node in a network is proportional to its Betweenness Centrality (BC) value, while Citation Burst (CB), representing an increase in the citation frequency of a node (i.e., a keyword) in a short period of time, can indicate an increase in interest in a particular topic within a research area (Chen, 2006). The burst strength, calculated using Kleinberg's algorithm, quantifies the intensity of this increase, helping to identify emerging trends or influential topics in a research field (Kleinberg, 2002).

In this study, a dataset was created by searching the topics "alga" AND "daphnia" AND "effluents" AND "toxicity" in the Web of Science Core Collection (WoS), to collect scientific literature combining the whole effluent toxicity testing using both organisms. WoS was used because it proved to be the best data source for the CiteSpace analysis (Mostafaie et al., 2021). The document types and time of publications were not specified. A total of 125 publications from 1992 to 2022 were found and stored as complete records and cited references. To analyze the collaborations and identify the most important countries in this research domain, a network was created with node type = country, time slice = one year, scale factor k = 15, and node rendering mode = tree ring history. For the same dataset, keyword co-occurrence analysis, clustering, and burst detection were also used to identify the most active topics in the research domain. Accordingly, the node type was changed

to keyword, and the other parameters remained the same. After clustering the network nodes, cluster labels were determined based on the title words using the log-likelihood ratio (LLR) algorithm.

3. Results and discussion

Karst catchments are vulnerable areas due to the porous nature of karst landscapes which can lead to the pollution of surface and groundwater sources, representing a threat to drinking water supplies. For this reason, the monitoring of water's physical and chemical factors holds great importance, as they serve as reliable indicators of the overall condition. However, it is also beneficial to involve organisms, as they can predict potential threats to aquatic species (Blanck et al., 1984).

3.1. Trends of the physical and chemical water properties

Detailed characterization on physical and chemical conditions of the Krka River and adjacent industrial wastewaters were previously published by Šariri et al. (2024), so in this study we focused on varying degrees of anthropogenic influence among four sampling locations of the Krka River and assessed the conditions of industrial wastewaters (Table 1). According to limit values for surface water bodies categorized in the Directive (Official Gazette of the Republic of Croatia NN 96/2019, 2019), only water from the reference site, KRS, could be regarded as water of "very good" quality in all seasons, except ammonium concentrations, which were in "good" quality range. When compared to other locations, KRS exhibited the highest level of clarity and the lowest concentrations of TDS, ammonium, nitrogen, nitrates and phosphorus in all seasons. Most parameters at TOR and KRK frequently exceeded the limit values and did not meet the desired quality standards, especially during summer and autumn, while TBU water was of "very good" or "good" quality according to the regulations. This confirmed deteriorated environmental conditions in tributaries which are directly influenced by wastewaters (Table 1). Based on the physico-chemical characterization, the ecological water status in the upper course of the Krka River generally adhered to the following order: KRS > TBU > TOR > KRK.

Physical and chemical properties of IWW exceeded emission limit values for many parameters set up for wastewaters (Official Gazette of the Republic of Croatia NN 26/2020, 2020). Organic parameters were the highest in IWW, but their higher levels were reflected in surface waters of KRK and TOR, which are located in the vicinity of municipal and industrial wastewater discharges, respectively. Therefore, contrary to physical and chemical parameters, concentrations of mineral oils, TOC, DOC and dissolved CO_2 tended to be higher at KRK than TOR, suggesting municipal wastewaters as the primary source of organic compounds in the Krka River (Table 1).

3.2. Trends of the total metal(loid) concentrations in water

The average total concentrations of almost all elements were highest in the IWW basins and were significantly higher than at the other sites in the Krka River across all seasons (Table S3). Levels of Fe, Zn, Cs and Co were up to 1778 times, 1207 times, 450 times and 450 times higher at IWW than at TBU and KRS, respectively. Such trend is consistent with the "good" to "very good" ecological status of TBU and KRS (Table 1). Moreover, concentrations of several metal(loid)s at IWW were higher than at TOR (Cs: 91×, Zn: 65×, Cu: 63×, As: 30×), the site nearest to basins with industrial wastewater and characterized as having a "below good" ecological status in the Krka River (Table 1). Given the widespread industrial application of the aforementioned elements, particularly Fe and Cu in a screw production, it is evident that the IWW has a strong influence and presents a potential danger for aquatic organisms in the Krka River (Filipović Marijić et al., 2018; Mijošek et al., 2023).

The differences among the sampling sites in the Krka River, excluding IWW, mostly were not statistically significant and were still rather low and typical for karst ecosystems (Table S3), suggesting the efficiency of self-purification process (Filipović Marijić et al., 2018; Cukrov et al., 2008). Nevertheless, average concentrations of As, Cd, Co, Cu, Fe, Na, Ni, and Zn were clearly higher at TOR and KRK, influenced by wastewater discharges, than at KRS and TBU (Table S3).

Seasonal patterns for the majority of elements showed higher levels in summer than in other two seasons, probably as a consequence of low water levels during summer months. A similar trend was not seen in IWW, where metal(loid) concentrations (particularly As, Cu, Fe, and Ni) (Table S3) and organic matter (Table 1) peaked in spring, probably signifying the moment of wastewater discharge (Šariri et al., 2024). Similar patterns of increasing metal(loid) concentrations and higher TOC and DOC values were also noted at other locations, mostly in the

Table 1
Physical, chemical and organic parameters of surface waters of the Krka River (sampling sites 1–4) and of industrial wastewater (sampling site 5) in three sampling seasons (spring, summer and autumn) of 2021. According to the limit values for surface water bodies (sampling sites 1–4), those parameters which are categorized in the Directive (Official Gazette of the Republic of Croatia NN 96/2019, 2019) are presented as italic for "very good", underlined for „good" and bold for „bellow good" ecological status, while parameters above emission limit values set for wastewater (sampling site 5) emissions (Official Gazette of the Republic of Croatia NN 26/2020, 2020) are presented as bold/underlined.

Sampling	Spring					Summer					Autumn				
	(25.-27.4.2021)					(20.7.2021)					(18.-20.10.2021)				
Parameters	1 KRS	2 KRK	3 TOR	4 TBU	5 IWW	1 KRS	2 KRK	3 TOR	4 TBU	5 IWW	1 KRS	2 KRK	3 TOR	4 TBU	5 IWW
Turbidity / FAU	0	4	8	3	2355	0	4	3	4	35	0	5	2	1	15
Total dissolved solids (TDS) / mg L^{-1}	193.9	215	564	440	1642	226	291	320	440	2750	216	291	403	478	5290
pH	*7.54*	*7.97*	*7.61*	*8.20*	7.32	*7.58*	*7.92*	*7.48*	*8.20*	7.75	*7.51*	*7.78*	*7.54*	*8.10*	7.89
Dissolved CO_2 / mg L^{-1}	4.7	31	2.7	1.1	14.01	4	4.1	1.7	1.6	8.8	5.7	3.6	2	4.9	9.1
Chemical oxygen demand (COD) /mg O_2 L^{-1}	*0.19*	**8.83**	**11**	**4.6**	**3030**	*0.72*	**165.5**	3.02	**4.41**	**2770**	*0.98*	**4.18**	*1.74*	3.11	101.7
Ammonium / mg N L^{-1}	0.02	0.04	**0.19**	0.02	7.88	*0.01*	**4.6**	0.02	0.05	**21**	0.02	**0.09**	**0.07**	0.03	2.4
Total nitrogen / mg N L^{-1}	*0.1*	0.8	**1.9**	*0.6*	**21.2**	*0.2*	**6.5**	*0.5*	0.8	**60**	*0.3*	**3**	**1.8**	0.8	**69**
Nitrate / mg N L^{-1}	*0.08*	*0.15*	*0.22*	*0.11*	**7.09**	*0.04*	*0.41*	*0.02*	0.1	**3.07**	*0.11*	*0.21*	*0.25*	*0.03*	**3.07**
Total phosphorus / mg P L^{-1}	*0.009*	**0.084**	0.053	*0.012*	**2.21**	*0.003*	**0.89**	**0.086**	*0.014*	**8.54**	*0.004*	**0.087**	*0.017*	0.037	1.3
Mineral oils / µg L^{-1}	< 5	< 5	56.7	< 5	**38,177**	< 5	1863	380	< 5	**24,902**	< 5	1787	540	< 5	**56,811**
Phenols / µg L^{-1}	< 5	< 5	< 5	< 5	< 5	< 5	< 5	< 5	< 5	46.8	< 5	< 5	< 5	< 5	**182**
Total organic carbon (TOC) / mgL^{-1}	1.476	1.552	4.321	1.694	**100.0**	1.064	6.783	6.042	2.798	22.82	1.557	8.164	1.775	2.468	21.18
Dissolved organic carbon (DOC) / mgL^{-1}	1.381	1.496	3.519	1.272	76.36	0.876	5.483	2.517	1.272	11.97	0.268	7.794	1.535	1.021	20.36

summer (Table S3).

3.3. Toxicity evaluation

In addition to the analysis of physical, chemical and organic parameters and total metal(loid) concentrations, which provide an assessment of the present conditions and require long-term monitoring, biological analyses can give insight in potential toxicity and anthropogenic impact on the aquatic organisms within the sensitive karst ecosystem. Moreover, the inclusion of toxicity biotests has become increasingly important for potential hazards evaluation (Wolska et al., 2007).

3.3.1. Toxicity effects

The samples of surface Krka River water (sites KRK, TBU, TOR and KRK) mostly did not show toxic effect regarding *Daphnia* toxicity test (0–20 % immobilization in all sites and seasons of 2021). Slightly higher toxic effect was observed at TOR and KRK than at other sites, probably confirming impact of industrial and municipal wastewaters at these locations (Fig. 1). Inhibition of algae growth varied more among sites and seasons than immobilization of daphnids, also indicating marginal effects in undiluted water samples from TOR (26.7 % in autumn, Fig. 1c) and KRK (46.0 % in summer and 82.7 % in autumn, Fig. 1b, c). In spring, toxic effects on algae were less pronounced, but still detected at all locations (6.08–28.0 %, Fig. 1a). Contrary, the wastewater at IWW exhibited high toxicity in both tests. During the spring, the toxic effect of undiluted and 50 %-diluted IWW samples was confirmed by the 94.4 % to 98.9 % inhibition of phytoplankton growth and the 100 % immobilization of *D. magna* (Fig. 1a). Industrial wastewaters showed lower toxic effects in summer than in spring (84.6 % inhibition of algae growth; 20 % immobilization of *D. magna,* Fig. 1b), which coincides to lower levels of metal(loid)s and some physical and chemical water parameters at that location (Tables 1, S3).

Differences between seasons were more pronounced in *Daphnia* test, where the toxic effect recorded for IWW in summer was 5 times lower than in spring (Fig. 1a, b). In autumn, the inhibition of algae growth was 98.3 % and immobilization of *D. magna* 100 % (Fig. 1c), which corresponded to the maximum levels of phenols, mineral oils, total nitrogen and TDS compared to spring and summer (Table 1). Overall, impact of physical and chemical disturbances and contaminant mixtures resulted in the highest toxicity observed at IWW, but also toxic effects were recorded at locations near wastewater outlets in the Krka River (Fig. 1). Comparison of the two testing organisms, primary producer and primary consumer, indicated that algae *P. subcapitata* was more sensitive to pollution than *D. magna*, with a higher percentage of toxic effect evident in all seasons (Fig. 1). In addition, water from KRK and TOR had a discernible effect solely on algae, with the exception of spring when minor effects were observed on both algae and daphnids (Fig. 1a). These findings are consistent with previous studies, reporting that among four toxicity tests to 16 chemicals algae were more sensitive compared to bacteria, rotifers and *D. magna* (Radix et al., 2000), and that *P. subcapitata* was shown as very sensitive to herbicides and fungicides (Yeh and Chen, 2006), both of which may be present in the area of the Town of Knin due to agricultural practices. Still, the proposed limitation of algae as primary producers is their inability to predict chronic toxicity to higher organisms, necessitating the further use of invertebrates like *D. magna*.

3.3.2. Hazard toxicity classification

Based on hazard classification system (Table S2) (Persoone et al., 2003), only KRK water showed acute toxicity (TU = 2, hazard class III) for both tested species when surface river water was considered, indicating high sensitivity of the karst river water to the pressure of organic compounds. Industrial wastewater was classified as high acute toxicity (TU = 18 for daphnids and 32 for algae, hazard class IV) (Table 2). Generally, our results confirmed toxic effects of water from sites with direct influence of municipal (KRK) and industrial (IWW) wastewaters. Calculated EC_{50} (% *v*/v) for KRK river water was 50 for both testing organisms and for IWW 5.55 for *D. magna* and 3.125 for *P. subcapitata* (Table 2). In summary, the increase in toxicity of the analyzed river and wastewater samples follows the order: KRS $\leq$ TBU $<$ TOR $<$ KRK $<$ IWW.

3.4. Association of water quality and toxic effects on aquatic organisms

Our results pointed to the toxic effects recorded at site of the Krka River directly influenced by municipal wastewaters (KRK). Although situated in the vicinity and under the influence of IWW, site TOR was not classified as being acutely toxic (Table 2), indicating a higher sensitivity of the karst river water to the pressure of organic compounds, which are usually abundant in municipal wastewaters (KRK), rather than to the higher metal concentrations resulting from IWW. However, due to the complexity of the environmental conditions and physical and chemical matrix, it is extremely challenging, if not impossible, to establish a complete link with their respective degrees of toxicity. This is also in agreement with reports from similar studies on complex samples in which no clear relationship between the ecotoxicological findings and the results of the chemical analyses could be established (Persoone et al., 2003).

Accordingly, we performed Principal Component Analysis (PCA) to correlate results obtained by microbiotests (toxicity) with chemical analyses (metal(loid) levels and physical and chemical parameters), considering the sites with the highest hazard toxicity class, and one of them belonging to the Krka River watercourse (KRK) and the other to the basins with industrial wastewater (IWW). Two components, using Varimax rotation with Kaiser Normalization, were extracted explaining 66.7 % of variance at KRK and 65.7 % at IWW (Fig. 2). At both locations, association among different metal(loid)s was specific for the first component, while most of the organic parameters and data on toxic effects on algae were associated in the second component. Specifically, at KRK in the first component all metal(loid)s with COD, total N, total P and ammonium were extracted, while second component combined toxic effect on algae with TDS, turbidity, TOC, DOC and mineral oils. At IWW the first component combined metal(loid)s, dissolved CO_2, COD, TOC, DOC and nitrates, while in the second component toxic effects on algae were linked with TDS, mineral oils, phenols, but also Zn and Cs (Fig. 2). Such integrated approach confirmed municipal wastewaters as the primary source of organic compounds in the Krka River, with the highest influence on toxic impact on algae inhibition growth. Also, previous conclusion on seasonal variability of parameters at KRK showed the same patterns of toxic effects with TOC and DOC, mineral oils, nitrates, ammonium, nitrogen and TDS, but most of the metal(loid) concentrations did not show similar pattern among seasons (Tables 1, S3), what was reflected in multivariate analysis. On the other hand, the relationship between physical and chemical variations and toxic effects was probably more specific in the basins into which wastewater is directly discharged (IWW), due to the lack of natural seasonality, circulation and self-purification, as well as the specific composition (metal(loid)s used in industry) and timing of wastewater discharge (Šariri et al., 2024).

3.5. CiteSpace analysis of the literature data

A comprehensive search of the WoS database revealed that 125 publications were published worldwide between 1992 and 2022 using a combination of the terms “alga,” “daphnia”, “effluents”, and “toxicity”, presenting a relatively small number. Nevertheless, the number of publications in this research domain is increasing, with the majority of publications from our dataset published in recent years (41 % between 2016 and 2022), highlighting both the current relevance of the topic and the continued scarcity of experimental data, such as the toxicity assessment of the Krka River presented above (Fig. S2).

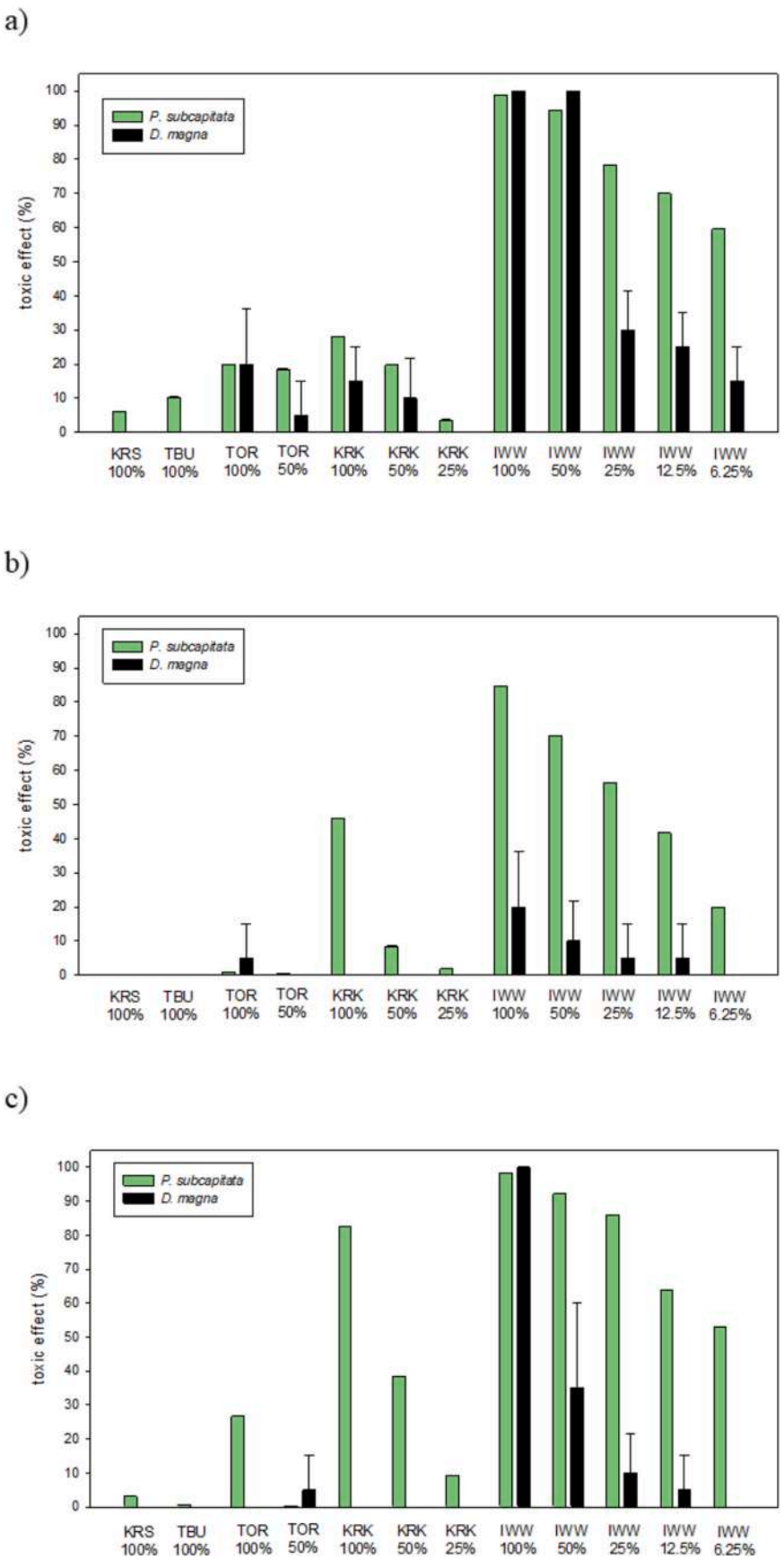

Fig. 1. Toxic effects (%) on *Pseudokirchneriella subcapitata* and *Daphnia magna* using dilution series of river water (sampling sites: KRS, TBU, TOR, KRK- 25; 50; 100 %) and wastewater (sampling site: IWW- 6.25; 12.5; 25; 50; 100 %) sampled in: a) spring; b) summer; c) autumn of 2021. The values of the standard deviations range from 0.02 % to 0.18 % for the growth inhibition of *P. subcapitata* and from 0.00 % to 25.17 % for the immobilization of *D. magna*.

Table 2
Toxicity classification for analyzed samples of the river water and wastewater from the Krka River catchment.

Sampling sites	Testing organism	EC_{50}% (vol/vol)	Toxicity unit (TU)	Hazard class	Toxicity
KRS	*D. magna*	> 100	< 0.4	I	No acute toxicity
	P. subcapitata	> 100	< 0.4	I	No acute toxicity
TBU	*D. magna*	> 100	< 0.4	I	No acute toxicity
	P. subcapitata	> 100	< 0.4	I	No acute toxicity
TOR	*D. magna*	> 100	< 0.4	I	No acute toxicity
	P. subcapitata	> 100	< 0.4	I	No acute toxicity
KRK	*D. magna*	50	2	III	Acute toxicity
	P. subcapitata	50	2	III	Acute toxicity
IWW	*D. magna*	5.55	18	IV	High acute toxicity
	P. subcapitata	3.125	32	IV	High acute toxicity

3.5.1. The country collaboration analysis

Research connecting terms "alga," "daphnia", "effluents" and "toxicity" was conducted in a total of 37 countries, with most articles published by authors from Germany (13), Italy (13), the United States (13), England (12), and Portugal (12) (Fig. S3). However, it contained only 65 links between nodes and 57 % of the included countries had a BC of 0.00, showing the significant lack of international collaborations in this research domain. Similar to the number of publications, the highest BC values were found in European countries, namely Germany (0.44), Belgium (0.27), England (0.19), Italy (0.17), and Portugal (0.13), probably due to common project funding opportunities and similar environmental standards and regulations related to biomonitoring and effluent toxicity control. Among non-European countries, the United States and Japan had the highest BC.

3.5.2. The keyword co-occurrence analysis

Apart from the basic keywords "toxicity" and "effluent", the top three keywords in terms of frequency and centrality were "*Daphnia magna*" (43 occurrences, centrality of 0.77), followed by "pharmaceutical" (15 occurrences, centrality of 0.18), and "acute toxicity" (12 occurrences, centrality of 0.19). Burst detection of keywords, as indicators of emerging trends, showed that the keywords "test" and "chemical" appeared more frequently in the papers published in the early 2000s, while more keywords started to burst since 2013 (Fig. 3). Although our dataset contained the papers published in 1992–2022 period, no significant trend keyword was observed until 2000. The keywords with the most recent bursts were "removal", "waste water", "pharmaceutical", "toxicity" and "risk assessment". Among them, "pharmaceutical", "toxicity" and "risk assessment" were used in the early 2000s but gained more attention after 2015, 2017 and 2020, respectively. On the other hand, "removal" and "waste water" appeared in publications for the first time in recent years and bursted shortly after. These are also two keywords with the highest burst strength (3.36 and 3.15). Although our experimental study does not fall under the currently prominent topic of contaminant removal, such as the elimination of pharmaceuticals from wastewater, burst detection of keywords confirmed that toxicity testing and the environmental risk assessment of wastewater remain highly relevant. A distinctive contribution of our research lies in the assessment of surface waters within a karst ecosystem and the integration of toxicity results with environmental data - both of which are relatively understudied areas not reflected among the most frequently cited keywords.

The network of keywords was divided into 12 clusters (Fig. 4). The largest cluster, resulting from this analysis, labeled as "#0 emerging contaminant" (size 46, silhouette 0.752), contained many more members than other clusters. The size of the second largest cluster, labeled as "#1 hospital wastewater" (silhouette value 0.906), was 29. Both of them contained research papers that used a battery of toxicological tests, primarily to assess the toxicity of pharmaceuticals, but also disinfectants, illicit drugs, pesticides and persistent organic pollutants from wastewater and diffuse pollutant sources. However, cluster #1 contained much older publications (mean year 2005) than cluster #0 (mean year 2013).

Based on the mean years of publications in the obtained clusters, studies have previously been focused on assessing toxicity of environmental samples (#3 combination effect (2007)) and effluents from hospitals, industries and mines (#1 hospital wastewater (2005), #10

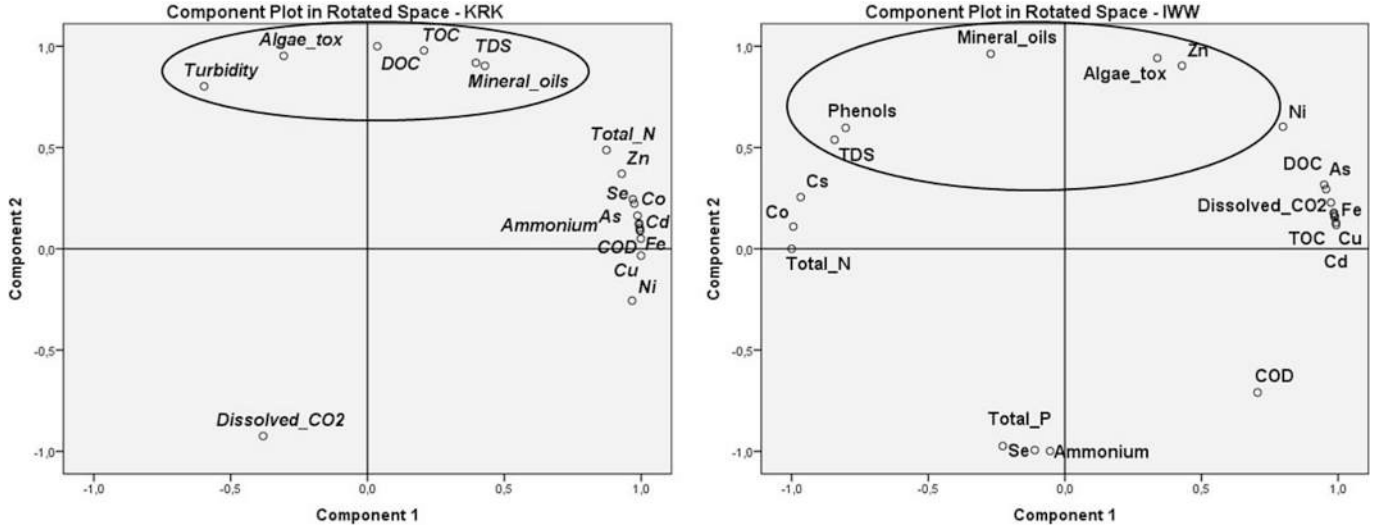

Fig. 2. Principal component plot using Varimax rotation for toxic impact observed on algae (Algae_tox) and physical and chemical parameters at site under the direct influence of municipal wastewaters (KRK) and industrial wastewater from the basins of the screw factory (IWW), showing association of parameters in two principal components (circled parameters are associated with toxic effects on algae).

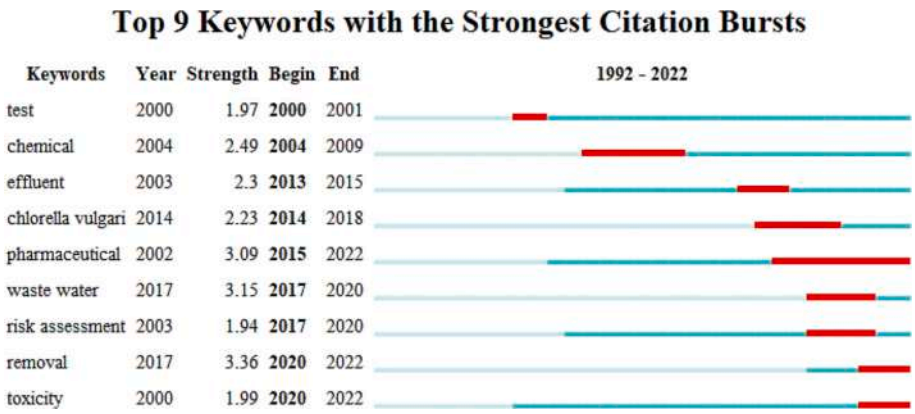

Fig. 3. Keywords indicating the major trends in research connecting topics "alga", "daphnia", "effluents" and "toxicity" from 1992 to 2022. The period in which each keyword occurs most frequently in the analyzed literature is highlighted in red. (For interpretation of the references to colour in this figure legend, the reader is referred to the web version of this article.)

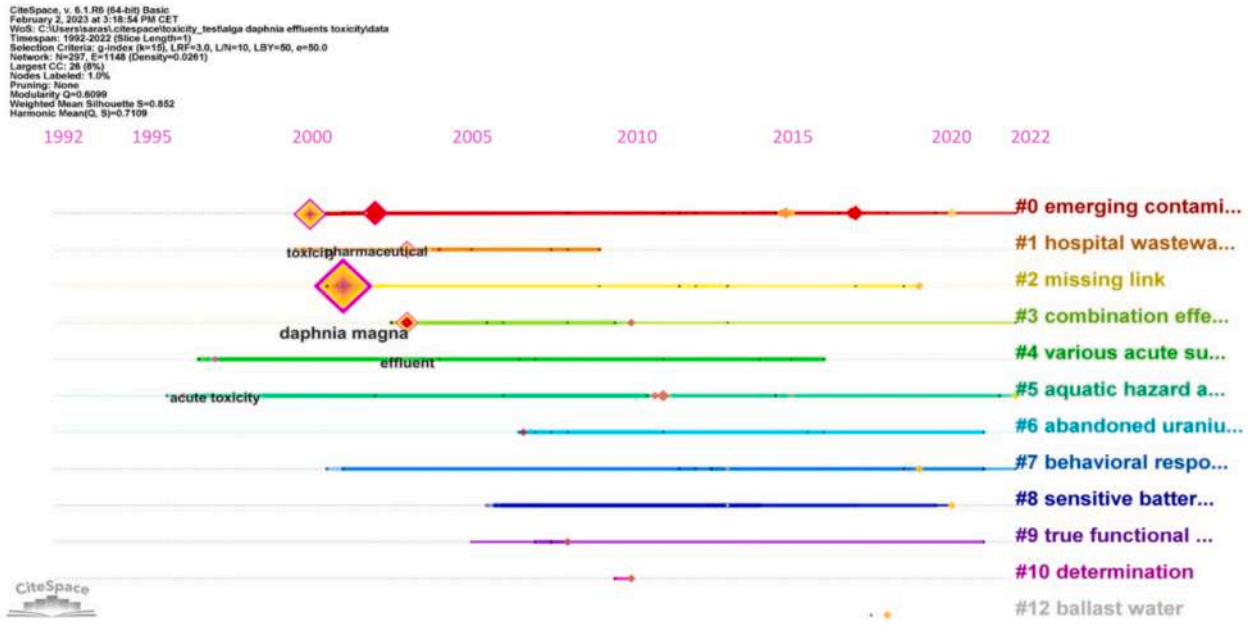

Fig. 4. Timeview of the clustered network of co-occurring keywords (diamonds) created from the literature linking the topics "alga", "daphnia", "effluents" and "toxicity".

determination (2010), #6 abandoned uranium mine (2010)), but also of specific contaminants in environmental samples (#1 hospital wastewater (2005), #5 aquatic hazard assessment (2009), #9 true functional environmental genomics (2009)), shifting from acute to sublethal toxicity indicators and linking laboratory and field effects (#4 various acute sublethal (2005), #2 missing link (2008), #9 true functional environmental genomics (2009)). Research on effluent toxicity to algae and daphnids has increased over the past decade, and recent studies have focused on assessing the effects of exposure to emerging contaminants and metals using the battery of toxicity tests (#0 emerging contaminant (2013), #8 sensitive battery (2013)), the use of sublethal endpoints in toxicity tests (#0 emerging contaminant (2013), #7 behavioral responses (2014)), and the effects of water treatment methods prior to discharge to the environment on its toxicity (#0 emerging contaminant (2013), #7 behavioral responses (2014), #12 ballast water (2018)).

Both the keyword burst detection and clustering results pointed to the same research trend over the last decade: the use of the battery of toxicity tests to evaluate the effects of mixtures of compounds present in wastewater effluents and, consequently, surface waters. This mainly included emerging contaminants, but also metals to a lesser extent. Since the results of toxicity tests of wastewaters were often highly variable due to their complex composition and different sensitivity of model organisms in bioassays, it was concluded that the use of a battery of toxicity tests with organisms of different trophic levels is a more effective approach (Liwarska-Bizukojc, 2022). In line with this current state of the art, our experimental study on the Krka River contributes novel data on a karst ecosystem by utilizing organisms from two distinct trophic levels, testing whole effluents and surface waters rather than isolated chemicals in laboratory settings, and linking observed toxic effects with metal contamination.

The clustering and burst detection results indicated that the toxicity of pharmaceuticals to aquatic ecosystems was recognized as an important research topic in early 2000s (leading to the discovery of other similarly hazardous compounds in wastewater effluents) and continues to be studied in recent years under the group term "emerging contaminants". Emerging contaminants are diverse chemical compounds (pharmaceuticals, illicit drugs, personal care products, etc.) that often

enter surface waters with wastewater, for which there are no environmental monitoring regulations, and which have recently been recognized as concerning aquatic pollutants due to their adverse effects on the endocrine system of humans and wildlife. Since only few of these compounds have been toxicologically evaluated and there are ongoing policy initiatives to standardize their research and propose regulations, it is understandable that research on effluent toxicity to algae and daphnids has prioritized "emerging contaminants" in recent years (Petrie et al., 2015). Although emerging contaminants were not included in the present toxicity study on the Krka River, we plan to address this in the future research by investigating microplastics -highly prevalent wastewater-related contaminants whose toxic effects remain largely unknown. This planned work will further enhance our understanding of pollution-related risks in karst aquatic ecosystems and contribute to more comprehensive environmental monitoring strategies.

4. Conclusions

Based on the physical and chemical thresholds set in the Croatian Regulation, poor water quality was found in the basins with wastewater from the screw factory (IWW) and downstream in the Krka River, especially at the site directly exposed to the municipal wastewater outlets (KRK). Higher concentrations of mineral oils, TOC, DOC and dissolved CO_2 at KRK indicated municipal wastewaters as the primary source of organic compounds, while concentrations of total metal(loid)s in water confirmed IWW as an important source of pollution in the Krka River, especially of metal(loid)s used in industry (Cr, Cu, Fe, or Ni).

Generally, toxic effects on *Pseudokirchneriella subcapitata* and *Daphnia magna* were consistent with the chemical data recorded in the Krka River, resulting in acute toxicity (TU = 2, hazard class III) at KRK, which is contaminated by organic compounds. Moreover, high acute toxicity was found at IWW (TU = 18 for daphnids and 32 for algae, hazard class IV), basins with industrial wastewater. Algae were shown to be more sensitive to wastewater pollution than crustaceans. Moreover, integral view on ecotoxicological effects and physical and chemical parameters based on multivariate PCA analysis confirmed stronger association of certain organic compounds with the toxic effects on algae than of metal(loid) concentrations.

CiteSpace, a scientometric analysis tool applied to global publications on effluent toxicity, has shown that research on algae and daphnids has increased over the past decade, focusing on emerging contaminants (mainly pharmaceuticals and metals) using the battery of toxicity tests. Based on the Betweenness Centrality, European countries play the key role in these scientific topics. These findings indicate that our study is among the few that presents a holistic assessment of the mixture of contaminants and their toxicity. While incorporating current recommendations and aligning with recent research trends identified through CiteSpace, our work provides a comprehensive and ecologically valuable evaluation of the effects of toxic compounds and the relationship between water quality parameters and toxicity in a complex and vulnerable karst river system, which is an ecosystem that remains underrepresented in toxicity studies.

CRediT authorship contribution statement

Sara Šariri: Investigation, Writing – review & editing, Formal analysis, Writing – original draft. **Želimira Cvetković:** Supervision, Data curation, Writing – review & editing, Investigation, Writing – original draft, Formal analysis. **Tatjana Mijošek Pavin:** Writing – review & editing, Formal analysis, Writing – original draft, Investigation. **Zorana Kljaković-Gašpić:** Writing – review & editing, Investigation, Formal analysis. **Damir Valić:** Investigation. **Tomislav Kralj:** Investigation. **Amalia Brkić:** Formal analysis, Writing – review & editing. **Zuzana Redžović:** Investigation. **Vlatka Filipović Marijić:** Writing – original draft, Project administration, Supervision, Funding acquisition, Writing – review & editing, Resources, Investigation.

Funding

This work was financially supported by The Croatian Science Foundation within the project no. IP-2020-02-8502, "Integrated evaluation of aquatic organism responses to metal exposure: gene expression, bioavailability, toxicity and biomarker responses" (BIOTOXMET).

Declaration of competing interest

The authors declare that they have no known competing financial interests or personal relationships that could have appeared to influence the work reported in this paper.

Acknowledgment

The authors would like to acknowledge colleagues whose valuable help contributed to this research, Zvjezdana Šoštar Vulić for the measurement of physical and chemical water parameters, Ivana Karamatić in performing toxicity testing and Dr. Zrinka Dragun for the measurement of total metal concentrations.

Appendix A. Supplementary data

Supplementary data to this article can be found online at https://doi.org/10.1016/j.jconhyd.2025.104667.

Data availability

The authors declare that the data supporting the findings of this study are available within the paper and its Supplementary Information files. Should any raw data files be needed in another format they are available from the corresponding author upon reasonable request.

References

Algaltoxkit FTM™, 2004. Freshwater Toxicity Test with Microalgae, Standard Operational Procedure. MicroBio Tests Inc, p. 36.
APHA (American Public Health Association), 2018. Standard Methods for the Examination of Water and Wasterwater, 23rd ed. USA.
ASTM Designation: D 4763-6, 2020. Standard Practice for Identification of Chemicals in Water by Fluorescence Spectroscopy.
Blanck, H., Wallin, G., Wängberg, S.Å., 1984. Species-dependent variation in algal sensitivity to chemical compounds. Ecotoxicol. Environ. Saf. 8 (4), 339–351.
Burton Jr., G.A., Denton, D.L., Ho, K., Ireland, D.S., 2002. Sediment toxicity testing: issues and methods. In: Handbook of Ecotoxicology, 2nd ed. CRC Press, pp. 111–150.
Chen, C., 2006. CiteSpace II: detecting and visualizing emerging trends and transient patterns in scientific literature. J. Am. Soc. Inf. Sci. Technol. 57 (3), 359–377.
Croatian Normative Document HRN EN 1484, 2002. Water Analysis - Guidelines for the Determination of Total Organic Carbon (TOC) and Dissolved Organic Carbon (DOC), [Ispitivanje vode - Smjernice za određivanje ukupnoga organskog ugljika (UOU) i otopljenoga organskog ugljika (OOU)]. Croatian Standards Institute.
Cukrov, N., Cmuk, P., Mlakar, M., Omanović, D., 2008. Spatial distribution of trace metals in the Krka River, Croatia: an example of the self-purification. Chemosphere 72 (10), 1559–1566.
Daphtoxkit FTM™ magna, 2001. Crustacean Toxicity Test for Freshwater, Standard Operational Procedure. MicroBio Tests Inc, p. 27.
Filipović Marijić, V., Kapetanović, D., Dragun, Z., Valić, D., Krasnići, N., Redžović, Z., Grgić, I., Žunić, J., Kružlicová, D., Nemeček, P., Ivanković, D., Vardić, Smrzlić I., Erk, M., 2018. Influence of technological and municipal wastewaters on vulnerable karst riverine system, Krka River in Croatia. Environ. Sci. Pollut. Res. 25, 4715–4727.
Ford, D., Williams, P., 2007. Karst Hydrogeology and Geomorphology. John Wiley & Sons.
Garric, J., Vollat, B., Duis, K., Péry, A., Junker, T., Ramil, M., Fink, G., Ternes, T.A., 2007. Effects of the parasiticide ivermectin on the cladoceran *Daphnia magna* and the green alga *Pseudokirchneriella subcapitata*. Chemosphere 69 (6), 903–910.
Goldscheider, N., Drew, D., 2007. Methods in Karst Hydrogeology: IAH: International Contributions to Hydrogeology, 26, 1st ed. CRC Press. https://doi.org/10.1201/9781482266023.
Hach Lange GmbH, 2013. Water Analysis Guide, Loveland, USA, 1st ed. DOC316.53.01336.
Hillebrand, O., Nödler, K., Licha, T., Sauter, M., Geyer, T., 2012. Caffeine as an indicator for the quantification of untreated wastewater in karst systems. Water Res. 46 (2), 395–402.

Hund-Rinke, K., Schlich, K., Kühnel, D., Hellack, B., Kaminski, H., Nickel, C., 2018. Grouping concept for metal and metal oxide nanomaterials with regard to their ecotoxicological effects on algae, daphnids and fish embryos. NanoImpact 9, 52–60.
ISO standard 6341, 2012. Water Quality. Determination of the Inhibition of the Mobility of *Daphnia magna* Straus (Cladocera, Crustacea) — Acute Toxicity Test. ISO, Geneva.
ISO standard 8692, 2012. Water Quality - Fresh Water Algal Growth Inhibition Test with Unicellular Green Algae. ISO, Geneva.
Kleinberg, J., 2002. Bursty and hierarchical structure in streams. In: Proceedings of the Eighth ACM SIGKDD International Conference on Knowledge Discovery and Data Mining, pp. 91–101.
Kortenkamp, A., Faust, M., Backhaus, T., Altenburger, R., Scholze, M., Müller, C., Ermler, S., Posthuma, L., Brack, W., 2019. Mixture risks threaten water quality: the European collaborative project SOLUTIONS recommends changes to the WFD and better coordination across all pieces of European chemicals legislation to improve protection from exposure of the aquatic environment to multiple pollutants. Environ. Sci. Eur. 31 (1), 1–4.
Kusui, T., Takata, Y., Itatsu, Y., Zha, J., 2014. Whole effluent toxicity assessment of industrial effluents in Toyama, Japan with a battery of short-term chronic bioassays. J. Water Environ. Technol. 12 (1), 55–63.
Liwarska-Bizukojc, E., 2022. Evaluation of ecotoxicity of wastewater from the full-scale treatment plants. Water 14 (20), 3345.
Luan, X., Liu, X., Fang, C., Chu, W., Xu, Z., 2020. Ecotoxicological effects of disinfected wastewater effluents: a short review of in vivo toxicity bioassays on aquatic organisms. Environ. Sci.: Water Res. Technol. 6 (9), 2275–2286.
Malá, J., Hübelová, D., Schrimpelová, K., Kozumplíková, A., Lejska, S., 2022. Surface watercourses as sources of karst water pollution. Int. J. Environ. Sci. Technol. 19 (5), 3503–3512.
Maloney, E.M., Villeneuve, D.L., Jensen, K.M., Blackwell, B.R., Kahl, M.D., Poole, S.T., Vitense, K., Feifarek, D.J., Patlewicz, G., Dean, K., Tilton, C., Randolph, E.C., Cavallin, J.E., LaLone, C.A., Blatz, D., Schaupp, C.M., Ankley, G.T., 2023. Evaluation of complex mixture toxicity in the Milwaukee estuary (WI, USA) using whole-mixture and component-based evaluation methods. Environ. Toxicol. Chem. 42 (6), 1229–1256.
Mendonça, E., Picado, A., Paixão, S.M., Silva, L., Barbosa, M., Cunha, M.A., 2013. Ecotoxicological evaluation of wastewater in a municipal WWTP in Lisbon area (Portugal). Desalin. Water Treat. 51 (19–21), 4162–4170. https://doi.org/10.1080/19443994.2013.768021.
Menghini, M., Pedrazzani, R., Feretti, D., Mazzoleni, G., Steimberg, N., Urani, C., Zerbini, I., Bertanza, G., 2023. Beyond the black box of life cycle assessment in wastewater treatment plants: which help from bioassays? Water 15 (5), 960.
Mijošek, T., Kljaković-Gašpić, Z., Kralj, T., Valić, D., Redžović, Z., Šariri, S., Karamatić, I., Filipović Marijić, V., 2023. Spatial and temporal variability of dissolved metal (loid) s in water of the karst ecosystem: consequences of long-term exposure to wastewaters. Environ. Technol. Innov. 32, 103254.
Moreira-Santos, M., Soares, A.M., Ribeiro, R., 2004. An *in situ* bioassay for freshwater environments with the microalga *Pseudokirchneriella subcapitata*. Ecotoxicol. Environ. Saf. 59 (2), 164–173.
Mostafaie, A., Cardoso, D.N., Kamali, M., Loureiro, S., 2021. A scientometric study on industrial effluent and sludge toxicity. Toxics 9 (8), 176.
Official Gazette of the Republic of Croatia NN 26/2020, 2020. Rulebook on Wastewater Emission Limit Values [Pravilnik o graničnim vrijednostima emisija otpadnih voda, on Croatian]. Available online: https://narodne-novine.nn.hr/clanci/sluzbeni/2020_03_26_622.html (assessed August 2022).
Official Gazette of the Republic of Croatia NN 96/2019, 2019. Regulation on Water Quality Standards [Uredba o standardu kakvoće voda, on Croatian]. Available online: https://narodne-novine.nn.hr/clanci/sluzbeni/2019_10_96_1879.html (assessed August 2022).
Parise, M., Ravbar, N., Živanović, V., Mikszewski, A., Kresic, N., Mádl-Szőnyi, J., Kukurić, N., 2015. Hazards in karst and managing water resources quality. In: Karst Aquifers—Characterization and Engineering. Springer International Publishing, Cham, pp. 601–687.
Persoone, G., Marsalek, B., Blinova, I., Törökne, A., Zarina, D., Manusadzianas, L., Nalecz-Jawecki, G., Tofan, L., Kolar, B., 2003. A practical and user-friendly toxicity classification system with microbiotests for natural waters and wastewaters. Environ. Toxicol. Int. J. 18 (6), 395–402.
Persoone, G., Baudo, R., Cotman, M., Blaise, C., Thompson, K.C., Moreira-Santos, M., Vollat, B., Törökne, A., Han, T., 2009. Review on the acute *Daphnia magna* toxicity test–evaluation of the sensitivity and the precision of assays performed with organisms from laboratory cultures or hatched from dormant eggs. Knowl. Manag. Aquat. Ecosyst. 393, 01.
Petrie, B., Barden, R., Kasprzyk-Hordern, B., 2015. A review on emerging contaminants in wastewaters and the environment: current knowledge, understudied areas and recommendations for future monitoring. Water Res. 72, 3–27.
Radix, P., Léonard, M., Papantoniou, C., Roman, G., Saouter, E., Gallotti-Schmitt, S., Thiébaud, H., Vasseur, P., 2000. Comparison of four chronic toxicity tests using algae, bacteria, and invertebrates assessed with sixteen chemicals. Ecotoxicol. Environ. Saf. 47 (2), 186–194. https://doi.org/10.1006/eesa.2000.1966.
Šariri, S., Valić, D., Kralj, T., Cvetković, Ž., Mijošek, T., Redžović, Z., Karamatić, I., Filipović Marijić, V., 2024. Long-term and seasonal trends of water parameters in the karst riverine catchment and general literature overview based on CiteSpace. Environ. Sci. Pollut. Res. 31 (3), 3887–3901. https://doi.org/10.1007/s11356-023-31418-3.
Sertić Perić, M., Matoničkin Kepčija, R., Miliša, M., Gottstein, S., Lajtner, J., Dragun, Z., Filipović Marijić, V., Krasnići, N., Ivanković, D., Erk, M., 2018. Benthos-drift relationships as proxies for the detection of the most suitable bioindicator taxa in flowing waters–a pilot-study within a Mediterranean karst river. Ecotoxicol. Environ. Saf. 163, 125–135.
Tousova, Z., Froment, J., Oswald, P., Slobodník, J., Hilscherova, K., Thomas, K.V., Tollefsen, K.E., Reid, M., Langford, M.K., Blaha, L., 2018. Identification of algal growth inhibitors in treated waste water using effect-directed analysis based on non-target screening techniques. J. Hazard. Mater. 358, 494–502.
Vosylienė, M.Z., 2007. Review of the methods for acute and chronic toxicity assessment of single substances, effluents and industrial waters. Acta Zool. Litu. 17 (1), 3–15.
Water Framework Directive (WFD, Commission Directive 2013/39/ EU).
Weyers, A., Sokull-Klüttgen, B., Baraibar-Fentanes, J., Vollmer, G., 2000. Acute toxicity data: a comprehensive comparison of results of fish, Daphnia, and algae tests with new substances notified in the European Union. Environ. Toxicol. Chem. Int. J. 19 (7), 1931–1933.
White, W.B., 2002. Karst hydrology: recent developments and open questions. Eng. Geol. 65 (2–3), 85–105.
Wolska, L., Sagajdakow, A., Kuczyńska, A., Namieśnik, J., 2007. Application of ecotoxicological studies in integrated environmental monitoring: possibilities and problems. TrAC Trends Anal. Chem. 26 (4), 332–344.
Xin, X., Huang, G., Zhang, B., 2021. Review of aquatic toxicity of pharmaceuticals and personal care products to algae. J. Hazard. Mater. 410, 124619.
Yeh, H.J., Chen, C.Y., 2006. Toxicity assessment of pesticides to *Pseudokirchneriella subcapitata* under air-tight test environment. J. Hazard. Mater. 131 (1–3), 6–12.

Publication No. 4: Interrelation between environmental conditions, acanthocephalan infection and metal(loid) accumulation in fish intestine: an in-depth study

Environmental Pollution 356 (2024) 124358

Contents lists available at ScienceDirect

Environmental Pollution

journal homepage: www.elsevier.com/locate/envpol

Interrelation between environmental conditions, acanthocephalan infection and metal(loid) accumulation in fish intestine: an in-depth study☆

Tatjana Mijošek [a], Sara Šariri [a], Zorana Kljaković-Gašpić [b], Željka Fiket [a], Vlatka Filipović Marijić [a,*]

[a] Ruđer Bošković Institute, Bijenička cesta 54, Zagreb, Croatia
[b] Institute for Medical Research and Occupational Health, Ksaverska 2, 10000 Zagreb, Croatia

ARTICLE INFO

Keywords:
Bioaccumulation
Biodilution
Brown trout
Acanthocephalans
Trace elements
Bioconcentration factors

ABSTRACT

Metal(loid) bioaccumulation in acanthocephalans (*Dentitruncus truttae*) and intestines of fish (*Salmo trutta*) from the Krka River, influenced by industrial and municipal wastewaters, was investigated in relation to exposure to metal(loid)s from fish gut content (GC), water, and sediment to estimate potentially available metal (loid)s responsible for toxic effects and cellular disturbances in biota. Sampling was performed in two seasons (spring and autumn) at the reference site (river source, KRS), downstream of the wastewater outlets (Town of Knin, KRK), and in the national park (KNP). Metal(loid) concentrations were measured by ICP-MS. The highest accumulation of As, Ba, Ca, Cu, Fe, Pb, Se and Zn was observed mainly in organisms from KRK, of Cd, Cs, Rb and Tl at KRS, and of Hg, Mn, Mo, Sr and V at KNP. Acanthocephalans showed significantly higher bioaccumulation than fish intestine, especially of toxic metals (Pb, Cd and Tl). Metal(loid) bioaccumulation in organisms partially coincided to exposure from water, sediments and food, while in GC almost all elements were elevated at KNP, reflecting the metal(loid) exposure from sediments. Seasonal differences in organisms and GC indicated higher metal (loid) accumulation in spring, which follows enhanced fish feeding rates. Higher number of acanthocephalans in the intestine influenced biodilution process and lower concentrations of metal(loid)s in fish, indicating positive effects of parasites to their host, as supported by high values of bioconcentration factors. Fish intestine and acanthocephalan *D. truttae* were confirmed as sensitive indicators of available metal fraction in conditions of generally low environmental exposure in karst ecosystem. Since metal(loid) accumulation depended on ecological, chemical and biological conditions, but also on the dietary habits, physiology of organisms and parasite infection, continuous monitoring is recommended to distinguish between the effects of these factors and environmental exposure when assessing dietary associated metal(loid) exposure in aquatic organisms.

1. Introduction

Metal(loid)s occur naturally in the environment, but their presence has rapidly increased as a result of anthropogenic activities such as mining, traffic, smelting, agriculture, and the release of industrial or municipal waste. This is of particular concern in freshwater karst ecosystems, characterized by numerous caves, sinkholes, and open fractures in carbonate rocks that, because of high porosity and permeability, allow rapid flow but also significant storage of contaminants, including metal(loid)s, which can be released into the water column over time (Padilla and Vesper, 2018).

The most commonly used bioindicator organisms in freshwater ecosystems are bivalves, crustaceans and fish. In recent decades, parasites have also been recognized as potential bioindicators of water quality, leading to the establishment of the field of Environmental Parasitology (Sures et al., 2017). Among them, acanthocephalans have been proposed as promising bioindicators of metal exposure (Filipović Marijić et al., 2013; Nachev and Sures, 2016; Mehana et al., 2020). Further, accumulated metals in acanthocephalans represent a biologically available fraction, since contaminants have to cross the tegument

☆ This paper has been recommended for acceptance by Wen Chen.

* Corresponding author. Laboratory for Biological Effects of Metals Division for Marine and Environmental Research Ruđer Bošković Institute Bijenička c. 54, 10000 Zagreb, Croatia.
E-mail address: vfilip@irb.hr (V. Filipović Marijić).

https://doi.org/10.1016/j.envpol.2024.124358
Received 3 April 2024; Received in revised form 22 May 2024; Accepted 9 June 2024
Available online 11 June 2024

and membranes and might positively or negatively affect their hosts (Sures et al., 2017; Molbert et al., 2020). Given their widespread distribution and high prevalence, parasites should not be neglected in environmental research as being a crucial link for the correct interpretation of field studies.

Due to the complexity of dietary metal(loid) uptake, correlation to food sources depends on metal(loid) bioavailability in the ingested food and selectivity in metal(loid) accumulation to intestinal tissue in order to maintain homeostasis. Consequently, the uptake and potential toxicity of dietary metal(loid)s have been studied predominantly under controlled laboratory conditions (Ojo and Wood, 2007; Creighton and Twining, 2010). A drawback of these studies is that they mostly employ higher concentrations of metals and shorter exposure times than in natural conditions (Giguère et al., 2004). There have been limited studies on the metal levels in the intestine of indigenous freshwater fish (Dallinger and Kautzky, 1985; Sures et al., 1999; Giguère et al., 2004; Filipović Marijić and Raspor, 2010, 2012; Mijošek et al., 2019, 2022), leaving much of the research on metal uptake from diet under field conditions largely unexplored.

Previous studies involving biota from the Krka River have already confirmed negative impact of urban and industrial wastewaters at the KRK site near the Town of Knin in terms of increased accumulation of metal(loid)s and disruption of biomarker responses in organisms compared to the reference site represented by the Krka River source, which is not under known anthropogenic impact and, according to previous studies, not characterized by stress responses (Dragun et al., 2018; Filipović Marijić et al., 2018; Mijošek et al., 2019, 2022). However, there have been no investigations that concurrently examined the concentrations of metal(loid)s in sediments, organisms, and the intestinal contents of fish within the boundaries of the national park.

As a continuation of the research in this important area, we measured total concentrations of 22 metal(loid)s in the intestine and gut content (GC) of brown trout *Salmo trutta* and in acanthocephalan *Dentitruncus truttae* from three locations with varying levels of contamination (reference site – river source upstream of the wastewater discharge; pollution impacted site near the Town of Knin – downstream of the wastewater discharge; and the most downstream location directly in the Krka National Park). Additionally, due to significance of dietborne metal uptake, metal(loid)s were measured in fish gut contents (GC) to investigate possible bioavailability and metal(loid) transfer from food to fish. Metal(loid) concentrations were also measured in water and sediment samples, and the relation of environmental conditions with accumulation in organisms was evaluated. This comprehensive investigation was conducted with the following objectives: 1) comparison of bioaccumulated metal(loid) concentrations between fish intestine and acanthocephalans; 2) determination of spatial and seasonal variability of metal(loid) concentrations in fish, acanthocephalans and gut content and their connection to environmental metal(loid) exposure (water and sediment); 3) analysis of possible association of bioaccumulated metal (loid) concentrations with the fish size, sex, condition, feeding habits and acanthocephalan infection rate; 4) evaluation of the intestine and acanthocephalans as bioindicators of metal(loid) exposure and their bioavailable levels and 5) assessment of the overall impact of industrial and municipal wastewaters on the Krka National Park.

2. Materials and methods

2.1. Research area

Significant part of the Krka River watercourse is protected as the Krka National Park, which is in last decades influenced by extensive tourism, industrial and municipal wastewaters, agriculture and fertilizers, especially in the upper river basin only 2 km upstream of the border of the Krka National Park (Cukrov et al., 2008; Filipović Marijić et al., 2018; Sertić Perić et al., 2018). Based on the results on water quality from previous studies (Filipović Marijić et al., 2018) and current sampling campaigns (Mijošek et al., 2023; Šariri et al., 2024, Table S1), three sites were selected for organisms and sediment sampling – Krka River source (KRS) as the reference site, location downstream of the wastewater outlets and Town of Knin (KRK) as the presumed contaminated site, and the third site in the area of the national park near the Brljan Lake (KNP) (Fig. 1). Detailed description, as well as results on the water analyses were given by Mijošek et al. (2023) and Šariri et al. (2024).

2.2. Sampling procedures

2.2.1. Organisms

Samplings were conducted in April and October 2021 at the three above described sites. Electrofishing, carried out according to Croatian standard HRN EN 14011 (2005), was chosen for fish sampling. Fish were kept aerated in the plastic tanks filled with water.

2.2.2. Water

At each location, river water samples were collected in precleaned polyethylene bottles in triplicates. Appropriate aliquots from each bottle were then filtered into pre-cleaned polyethylene bottles using a cellulose acetate filter with a pore diameter of 0.45 μm (Sartorius, Germany) to measure dissolved metal(loid)s, acidified with concentrated HNO_3 (Rotipuran Supra 69%, Carl Roth, Germany) and stored at 4 °C before further analysis.

2.2.3. Sediments

Surface sediments (upper 10 cm) were sampled only once in 2021 from the same sites as fish. We collected approximately 0.5 kg of surface and near surface sediment at each site using plastic spatulas and bags for the storage. Samples were transported to the laboratory at 4 °C and then stored at − 20 °C.

2.3. Procedure of biometric analysis, tissue dissection and storage

Fish were anesthetized immediately after the sampling using tricaine methane sulphonate (MS 222, Sigma Aldrich) according to the Ordinance on the protection of animals used for scientific purposes (NN 55, 2013). Firstly, basic biometric data (total length and body weight) were taken for each fish. Further, organ (liver, gonads, viscera) dissection was performed on ice to collect the data for calculation of biometric indices. Gonads also served for the sex determination. The posterior part of the intestine was isolated, cleaned from the exterior fat and gut content, and examined for the presence of acanthocephalans. The gut content of each fish was separated and stored. After isolating and quantifying acanthocephalans from the intestines of each fish, the prevalence and intensity of infection were calculated. All samples were subsequently stored in liquid nitrogen until transportation to the laboratory, where they were kept at −80 °C until analyses.

2.4. Acid digestion of biological samples and sediments

2.4.1. Biological samples

Prior to acid digestion, acanthocephalans from the same fish were pooled together to enable reliable measurements (3–24 individuals). Fish intestine and acanthocephalans were digested with HNO_3 (Rotipuran® Supra 69%, Carl Roth, Germany) and 30% H_2O_2 (Suprapur, Merck, Germany) at 85 °C for 3.5 h, as described by Mijošek et al. (2022). Gut contents of fish were digested under the same conditions using the mixture of HNO_3 (Rotipuran® Supra 69%, Carl Roth, Germany) and HF (Suprapur, Merck, Germany).

2.4.2. Sediments

Sediment samples were air-dried, homogenized in agate mill and sediment subsamples were digested in a two-step digestion procedure performed using microwawe oven (Multiwave ECO, Anton Paar,

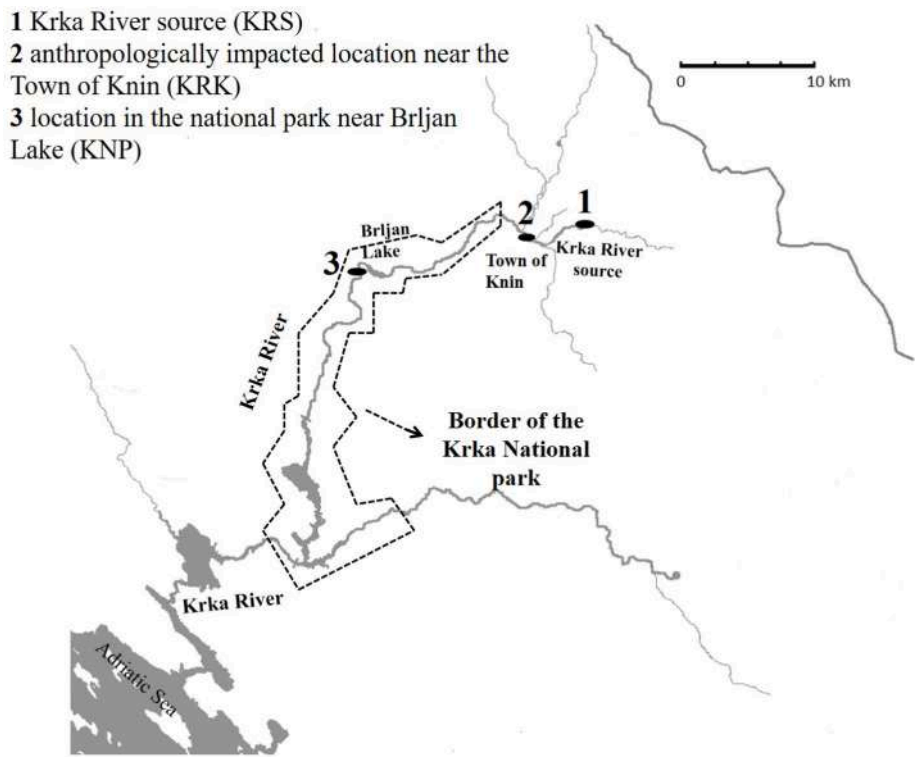

Fig. 1. Study area with marked sampling sites on the Krka River (1 – Krka River source; 2 – Krka River near the Town of Knin; 3 – location in the national park near the Brljan Lake).

Austria). Mixture of 4 mL HNO_3 (65%, p.a., Kemika, Croatia), 1 mL HCl (TraceSELECT, Fluka, Germany), and 1 mL HF (TraceSELECT, Fluka, Germany) is used in the first step, followed by the addition of 6 mL H_3BO_3 (Fluka, Switzerland), as described by Fiket et al. (2017).

2.5. ICP-MS measurements

Concentrations of trace and macroelements in water, organisms and GC were measured using an Agilent 8800 instrument (Agilent Technologies, USA) as presented in Table S2. To reduce interference, cell (helium and hydrogen) and reaction (oxygen) gases were used. Ultrapure Mili-Q water (Barnstead Smart2Pure Water Purification System, Thermo Scientific, Langenselbold, Germany) was used for preparation of standards and samples, and washing the dishes and disposable plastics. Acidified water samples underwent analysis without dilution, whereas the biological samples were diluted 10–13 times with a solution containing 1% (v/v) of purified nitric acid [HNO_3, 65%, p.a., Merck; purified by quartz sub-boiling distillation using the Milestone SubPUR system (Milestone S.r.l., Sorisole, Italy)] and hydrochloric acid (HCl, 30%, Suprapur®, for trace analysis, Supelco®). An internal standard solution containing 3 μg L^{-1} of internal standards (Ge, Rh, Tb, Lu, and Ir) (SCP Science, Canada) was used to correct instrumental drifts and plasma fluctuations. Standard solutions used for external calibration were prepared from individual PlasmaCAL Single-Element Standard solutions which were obtained from SCP Science, Quebec, Canada. Four standard certified reference materials [IAEA-407 (fish tissue), ERM-BB422 (fish muscle), ERM-CE278 (mussel tissue), NIST SRM 1577a (bovine liver)] were analyzed with the samples as part of quality control. The accuracy of the method for the elements in the referent biological samples mostly fell within a range of ±10%, with the recoveries varying from 90.4% for rubidium (Rb) to 110% for cadmium (Cd). Detailed information on the limits of detection (LODs) and the recoveries for each element and certified reference material in water and biological samples are presented in Tables S3 and S4.

Total element concentrations in sediments were measured using triple quadrupole inductively coupled plasma mass spectrometer (ICP-QQQ, Agilent 8900, USA). Analytical quality control was performed by simultaneous analysis of procedural blanks and certified reference materials of stream sediment NCS DC 73309 (GBW 07311) (China National Analysis Center for Iron and Steel, China). Recoveries in the referent sample were in range 91–104%, depending on the element.

2.6. Data processing and statistical methods

2.6.1. Biological and chemical data

Prevalence (number of infected fish) and mean intensity of infections (number of parasites per fish individuals) were calculated to describe acanthocephalan epidemiology. Bioconcentration factors (BCFs) were calculated as ratios between the element concentrations in acanthocephalans and fish intestine. Ratios between metal(loid) concentrations in fish intestine and gut contents, as well as in acanthocephalans and gut contents, were calculated as percentages and considered as the indication of possible metal(loid) bioavailability from the dietborne uptake.

Metal(loid) concentrations are presented as average values ± standard deviation and expressed in μg L^{-1} for water, μg kg^{-1} or mg kg^{-1} of wet weight (w.w.) for organisms and GC, and mg kg^{-1} or g kg^{-1} d.w. for sediments.

2.6.2. Statistical methods

Statistical analyses were done in SigmaPlot 11.0 (Systat Software, USA) and Microsoft Office Excel 2007. Metal(loid) concentrations in fish, acanthocephalans, GC, and water were compared between three sample locations using Kruskal-Wallis one-way analysis of variance on ranks, followed by Dunn's or Tukey's tests. Mann-Whitney *U* test was applied to test the data variability between the two seasons. Due to normal distribution of data on sediment samples, spatial differences were tested using one-way ANOVA using Holm-Sidak method. Differences were considered significant when $p < 0.05$. Correlations between parameters were calculated using Spearman correlation analysis and correlation coefficients and levels of significance were indicated in the

text and all are reported in tables in supplementary material.

3. Results and discussion

3.1. Main biometric characteristics of fish and acanthocephalans

No significant spatial differences were observed in total length (TL), total body mass (TM), and biometric indices of fish. Nevertheless, there were notable seasonal differences in TL and TM, with higher values observed in autumn, as the spawning period of this species, than in spring at all locations (Table 1). GSI values were also higher in autumn at all locations. However, these seasonal differences were not statistically significant at KNP, likely as a consequence of sporadic sampling of a few small, reproductively immature individuals and generally lower number of fish captured at this site in the spring. There were no significant differences depending on the fish sex.

All fish were infected with acanthocephalan *D. truttae* and there were no significant spatial differences in mean intensity of parasites in any season. The mean intensities and number of parasites were higher in autumn than in spring at all locations (Table 1). Comparable epidemiological characteristics have already been reported for the period 2005–2016 (Vardić Smrzlić et al., 2013; Filipović Marijić et al., 2022; Mijošek et al., 2022), probably all related to the life-cycle of gammarids, intermediate hosts of acanthocephalans. Gammarids reproduce mainly in late summer and autumn, leading to a higher abundance of acanthocephalans due to higher presence of gammarids in fish food.

To describe the relationship of this host-parasite system, we examined the correlations of parasite abundance and fish size and condition (FCI). Given the strong correlation between TL and TW ($r = 0.887–1.000$, $p < 0.001$, depending on the site and season), we opted to utilize TM as the variable to describe fish size in order to prevent issues with multicollinearity. For this purpose, all data were tested together. A significant positive correlation ($r = 0.478$, $p < 0.001$) was established between the abundance of parasites and fish TM, while no correlation was observed between abundance and FCI, confirming that acanthocephalans do not have negative effect on the fish fitness. Similar to findings of Vardić Smrzlić et al. (2013) an d Mijošek et al. (2022) for *D. truttae*, we observed higher prevalence of infection in male than in female fish, but not statistically significant.

3.2. Main environmental conditions

3.2.1. Concentrations of dissolved metal(loid)s in water

The recent comprehensive study on the dissolved metal(loid)s in water samples from eight locations along the upper stretch of the Krka River (Mijošek et al., 2023) revealed that industrial wastewaters from the screw factory (IWW) represent the most significant source of metal (loid)s in the Krka River primarily through the Orašnica River, a tributary that is directly influenced by the wastewaters due to potential spillover during heavy rains. Metal(loid) concentrations were also increased near the municipal outlet of the Town of Knin (KRK) in comparison to the river source (KRS) and location in national park (KNP).

At the three locations where fish were sampled, a few distinct patterns of metal(loid)s in the dissolved fraction were observed: As, Fe, Mg, Mn, Na, and Rb were predominantly the highest at KRK, while Ba, Ca, Mo, Sr, and V were the highest at KNP, and Tl was the highest at KRS. (Table S1). Seasonal differences between spring and autumn were not clearly distinguishable between the three sites, which is in line with results of our comprehensive data covering metal(loid) concentrations across eight locations, with no significant differences observed between spring and autumn (Table S1, Mijošek et al., 2023). Furthermore, spatial distribution of metal(loid)s coincided with water physico-chemical parameters, which were below good at KRK due to high concentrations of nutrients and COD in both seasons. Regarding Krka River source (KRS) and location in the national park (KNP), mostly very good ecological status was indicated (Mijošek et al., 2023; Šariri et al., 2024). The same pattern was observed for metal(loid) concentrations, wherein the lowest concentrations were found at KRS, followed by the highest concentrations of many elements at KRK and a subsequent gradual decrease at KNP, with the exception of Ba, Ca, Mo, Sr and V, which increased to their maximum concentrations at KNP (Table S1). Cukrov et al. (2008) verified the existence of a self-purification mechanism in the Krka River, starting in the Brljan Lake and progressing through subsequent tufa barriers, resulting in decreased metal(loid) concentrations in water downstream of the pollution sources. Moreover, groundwater input of clean water from the Zrmanja River also contributes to the decrease in water trace metal concentrations in a downstream way of contamination in the Krka River (Cukrov et al., 2008). Hence, elevated concentrations of many elements at KNP in comparison to KRS suggested potential future threats to this protected area, especially since measuring contaminants solely in water is inconclusive due to water discharge fluctuations and short resident times, making it a less reliable method of assessment (Salati and Moore, 2010; Algül and Beyhan, 2020).

3.2.2. Metal(loid) concentrations in sediments

Concentrations of majority of elements in sediment samples showed significant site-specific differences (Table S5). Potassium, Na and all

Table 1
Biometric characteristics (mean ± S.D.) of *S. trutta* caught in the Krka River at the reference (Krka River source, KRS), contaminated site (near Town of Knin, KRK) and location in the national park near Brljan Lake (KNP) in two sampling campaigns and basic epidemiological characteristics of acanthocephalans hosted in the brown trout. Statistically significant differences between two seasons at each sampling site are marked with asterisk (*) and between sampling sites within the same season are assigned with different superscript letters.

	Krka River source (KRS)		Town of Knin (KRK)		Krka National Park (KNP)	
	Spring 2021 n = 10	Autumn 2021 n = 10	Spring 2021 n = 6	Autumn 2021 n = 11	Spring 2021 n = 5	Autumn 2021 n = 7
Total length (cm)	22.66 ± 4.57*	28.81 ± 3.88*	22.10 ± 6.07*	29.28 ± 3.09*	19.08 ± 4.64*	27.56 ± 4.45*
Body mass (g)	120.09 ± 59.44*	237.46 ± 90.05*	132.03 ± 119.81*	248.15 ± 85.06*	86.94 ± 85.06*	224.93 ± 109.99*
FCI (g cm^{-3}*100)	0.92 ± 0.10	0.95 ± 0.08	0.97 ± 0.10	0.95 ± 0.07	1.01 ± 0.13	0.99 ± 0.12
HSI (%)	1.10 ± 0.23	1.42 ± 0.53	1.34 ± 0.53	1.37 ± 0.47	1.34 ± 0.34	1.23 ± 0.31
GSI (%)	0.50 ± 0.43*	4.56 ± 4.18*	0.24 ± 0.06 *	4.33 ± 4.67*	0.32 ± 0.16	2.55 ± 2.56
VSI (%)	9.55 ± 1.46	12.54 ± 5.27	8.59 ± 1.99	11.77 ± 4.61	9.82 ± 1.52	10.27 ± 2.33
Sex (F/M/ND)	4/6/0	5/4/1	4/2/0	6/5/0	4/1/0	3/4/0
Epidemiological characteristics of acanthocephalans						
Prevalence (number and % of infected trouts)	10, 100%	10, 100%	6, 100%	11, 100%	5, 100%	7, 100%
Mean intensity of infection (mean ± S.D.)	40.2 ± 27.9	60.8 ± 32.1	17.3 ± 15.2*	67.0 ± 30.7*	16.0 ± 16.6*	82.6 ± 52.2*
Total number of parasites	402	608	104	737	80	578

FCI – Fulton condition index; HSI –hepatosomatic index; GSI –gonadosomatic index; VSI – viscerosomatic index; ND – not determined.

trace elements in sediments exhibited the highest concentrations at the location in close proximity to Brljan Lake in KNP (Table S5). The sole deviations from this pattern were noted for Mg and Ca, with the highest average concentrations at KRS and KRK, respectively. River source is a reference site without the known pollution sources, characterized by the strong flow and low sedimentation rate, which explains the lowest concentrations of most elements at this site, both in sediments and water. However, only few kilometers downstream from the KRS, municipal wastewaters of the Town of Knin cause the increase in metal (loid) concentrations, which is the highest in downstream lake systems which serve as sink for metals due to intensive sedimentation and low flow (Chon et al., 2012). The water flow rate decreases in a downstream direction and lowers the transmission strength and carries smaller sediments particles which sink and deposit over longer time, and during such extensive sedimentation metal(loid)s bind to these particles and precipitate in sediments, consequently reducing metal(loid) concentrations in water in the process of self-purification (Cukrov et al., 2008).

It is obvious that negative influence of anthropogenic activities is observed in the area of the national park according to the sediment analyses (Table S5), which act as a sink, but also the source of many contaminants, including metal(loid)s (Chon et al., 2012). Metal(loid)s are not permanently bound to sediments and can be released into the water at any time depending on pH, temperature or flow which affect metal balance and remobilization between the sediments and water and consequently, cause possible toxic effects in biota. Therefore, both water and sediments, in addition to food can serve as sources of metal (loid)s for organisms, which will be discussed further.

3.3. Metal(loid) concentrations in biota

3.3.1. Metal(loid) accumulation in fish intestine

Metal(loid) accumulation in fish intestine followed the order K > Na > Mg ≥ Ca for macroelements and Zn > Fe > Rb > Cu ≥ Se > Mn > Sr > Cd ≥ Co ≥ As > Mo > Tl > Ba ≥ Cr > V ≥ Hg > Pb ≥ Cs for trace elements (Figs. 2–5), similar to the brown trout sampled in 2015/2016 (Mijošek et al., 2022). Our findings are consistent with prior research that reported the highest levels of essential elements as Zn, Fe, and Cu in the intestines of various fish species, including perch (Sures, 2002), European chub (Filipović Marijić and Raspor, 2010), or barbel (Nachev and Sures, 2016). When comparing the current state of accumulation of elements in brown trout intestines with that of previous research that focused on two locations in Krka River (KRS and KRK), it is evident that Ca, Cs, K, Mg, Na, Rb and Tl remained relatively constant, whereas bioaccumulation of Cd, Co, Cu, Fe, Mn, Se, Sr and Zn increased with time (Figs. 2–5, Mijošek et al., 2022). Only Pb concentrations were found to be around 3–5 times lower in the present research compared to previous study, owing to possibly lower concentrations of this element in sediment or gut content samples which are related to uptake sources and were not analyzed in the previous study. Given the widespread utilization of Cu, Fe, Mn, and Zn in the industrial, municipal, and agricultural processes, our findings suggest the intensifying impact of wastewaters on biota. This is particularly worrisome in unexplored region of the national park, where fish frequently exhibited maximum concentrations of certain elements compared to locations upstream. These patterns are consistent with the analysis of metal(loid)s in water samples, which confirmed that the majority of values in 2021, particularly for Cr, Cu, Fe, and Mn, were higher than those recorded between 2004 and 2015, probably all as a consequence of industrial and agricultural activities in the region (Mijošek et al., 2023).

We further investigated the potential influence of size (represented by TM) and sex on metal(loid) accumulation in the intestine. The influence of FCI was not considered since the differences in FCI between sites and seasons were negligible and not significant (Table 1). Spearman's correlation coefficients for the associations between TM and metal(loid) concentrations in fish intestine are presented in Table S6. Only a few notable correlations were observed between the concentrations of elements in the intestine and TM. A statistically significant ($p < 0.05$ in all cases) decrease with increasing TM was found for V ($r = -0.886$) at KRK in spring, Cd ($r = -0.767$) and Cs ($r = -0.833$) at KRS in spring, and Cs ($r = -0.786$) at KNP in autumn. Conversely, significant increase was detected for Mg ($r = 0.667$) at KRS in spring and As ($r = 0.609$) at KRK in autumn. Fish often show variations in metal-size associations, usually as a result of differences in their metabolic rates, detoxification systems or feeding habits (Nikolić et al., 2021). The influence of fish sex on bioaccumulation of metal(loid)s in fish intestine was evaluated using pooled data for each sex. Statistical analysis showed there were no significant differences, although average values of majority of elements were slightly higher in females, possibly due to factors such as food preferences or specificities of the reproductive cycle (Rajkowska and Protasowicki, 2013). Overall, the impact of fish biometric parameters on metal(loid)s accumulation in the intestine of brown trout was mainly negligible.

3.3.2. Metal(loid) accumulation in acanthocephalans

Macroelements followed the order K > Na ≥ Ca > Mg, and trace elements: Zn > Fe > Cu > Mn > Sr ≥ Rb > Cd ≥ Tl ≥ Se > Pb > Ba > As > Co ≥ Hg ≥ Cr ≥ Mo ≥ V > Cs (Figs. 2–5), as in previous research from 2015/2016 (Mijošek et al., 2022). Unlike in fish, concentrations of the majority of elements did not vary between the studies, indicating the absence of temporal trends, with the exception of Cd, Cu, Mn, and Zn, which were mostly higher in the current research, implying continuous contamination impact of the screw factory. Our two studies present the only data on metal(loid) accumulation in this endemic acanthocephalan species and both indicated the certain level of environmental deterioration over time. Additionally, concentrations of As, Ba, Cr, Hg, Mo and V in *D. truttae* were now measured for the first time.

Contrary to positive association between parasite abundance and fish size, we observed a negative correlation between metal(loid)s accumulation in acanthocephalans and fish TM for many metal(loid)s, especially in autumn (Table S6). Hence, significant negative correlations were observed for Mn at KRS ($r = -0.800$; $p < 0.01$) in the spring, as well as for Tl at KNP ($r = -0.750$; $p < 0.05$), Cd ($r = -0.700$; $p < 0.05$), Pb ($r = -0.624$; $p < 0.05$), Rb ($r = -0.886$; $p < 0.05$) and Tl ($r = -0.627$; $p < 0.05$) at KRK, and Ba ($r = -0.661$; $p < 0.05$), Co ($r = -0.745$; $p < 0.05$), Fe ($r = -0.709$; $p < 0.05$), Pb ($r = -0.767$; $p < 0.05$), Cd ($r = -0.758$; $p < 0.01$), Tl ($r = -0.806$; $p < 0.01$), Cu ($r = -0.830$; $p < 0.001$) and Se ($r = -0.879$; $p < 0.001$) at KRS in the autumn. Higher concentrations of metal(loid)s in acanthocephalans from smaller fish may be associated with higher metabolic and feeding rates in smaller specimens, both of which decline with fish aging (Farkas et al., 2003).

Analyses of associations between metal(loid)s accumulation in the intestines of brown trout and in acanthocephalans failed to uncover many consistent correlations when data were stratified by season and location. However, upon analyzing the pooled data, many positive correlations were identified [$p < 0.05$ for As ($r = 0.369$), and Se ($r = 0.360$), $p < 0.01$ for Cd ($r = 0.441$), Hg ($r = 0.400$), Mn ($r = 0.468$), Mo ($r = 0.372$), Pb ($r = 0.331$) and Zn ($r = 0.409$), $p < 0.001$ for Ba ($r = 0.615$), Ca ($r = 0.600$), Cs ($r = 0.794$), Cu ($r = 0.478$), Rb ($r = 0.660$), Sr ($r = 0.819$; p), Tl ($r = 0.511$), and V ($r = 0.519$)], suggesting that fish and parasites exhibit similar biological responses. All results on this association are presented in Table S7.

Although various studies (Sures, 2002; Filipović Marijić et al., 2013; Brázová et al., 2015) demonstrated that acanthocephalan-infected fish have lower metal concentrations than the uninfected ones, the 100% prevalence of acanthocephalans in our research prevented us from testing this hypothesis (Table 1). However, we observed notable differences in the accumulation of metal(loid)s in the intestine based on the number of acanthocephalans in fish. In particular, statistically significant inverse relationships between the abundance of acanthocephalans in fish and the concentrations of As ($r = -0.545$; $p < 0.001$), Cr ($r = -0.571$; $p < 0.001$), Mn ($r = -0.446$; $p < 0.001$), Se ($r = -0.523$; $p < 0.001$), V ($r = -0.507$; $p < 0.001$), Mo ($r = -0.392$; $p < 0.01$), Ba ($r =$

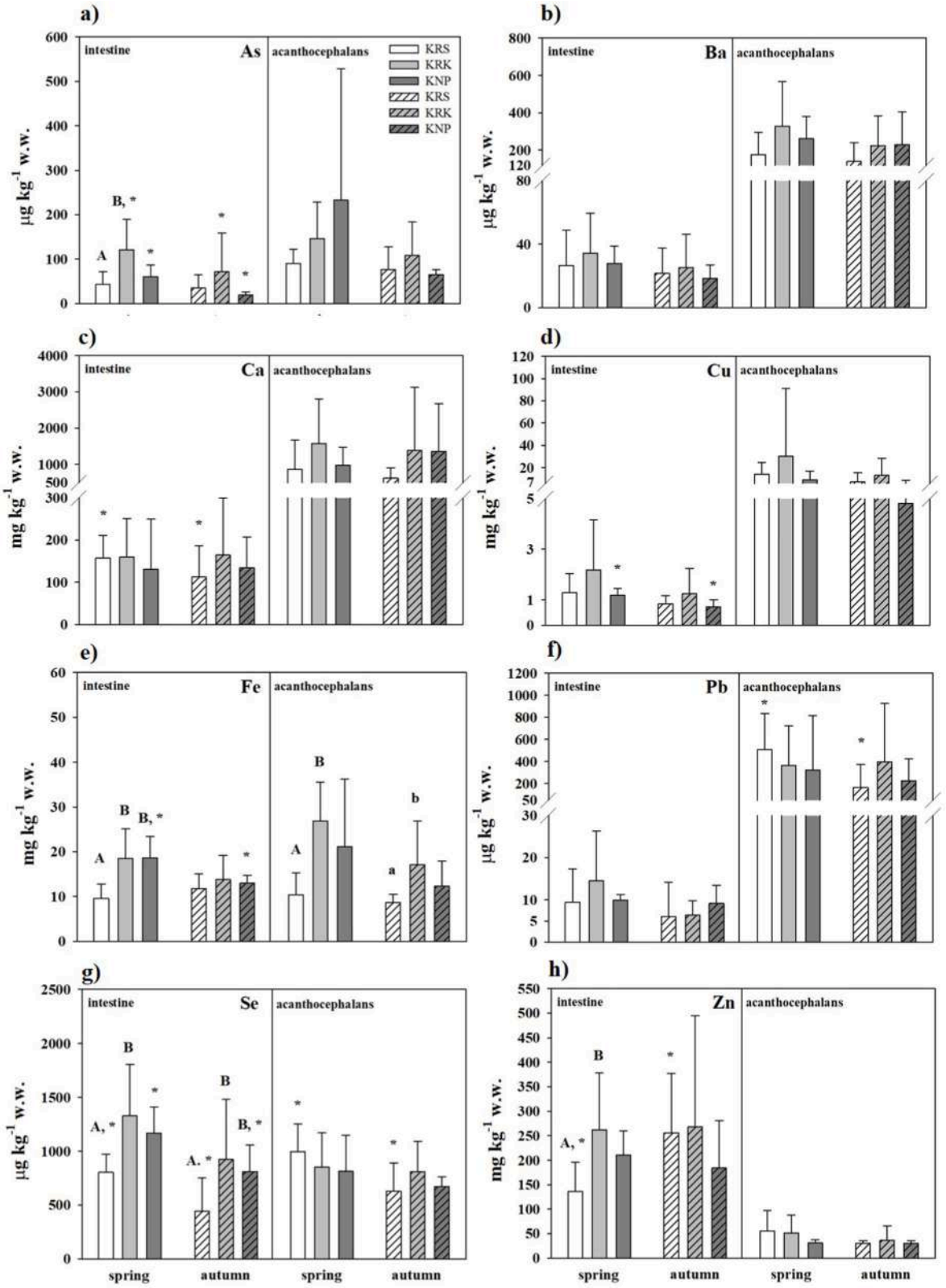

Fig. 2. Concentrations (mg kg^{-1} or µg kg^{-1} on wet mass basis) of six elements in the intestine of brown trout *S. trutta* and acanthocephalans *D. truttae* from three sites of the Krka River in two sampling campaigns (spring and autumn) that showed enhanced accumulation at the contaminated site, KRK. Different letters refer to significant differences of metal(loid) concentrations among three locations in spring (capital letters) and autumn (small letters), while statistically significant differences between two seasons at each sampling site are marked with asterisk (*).

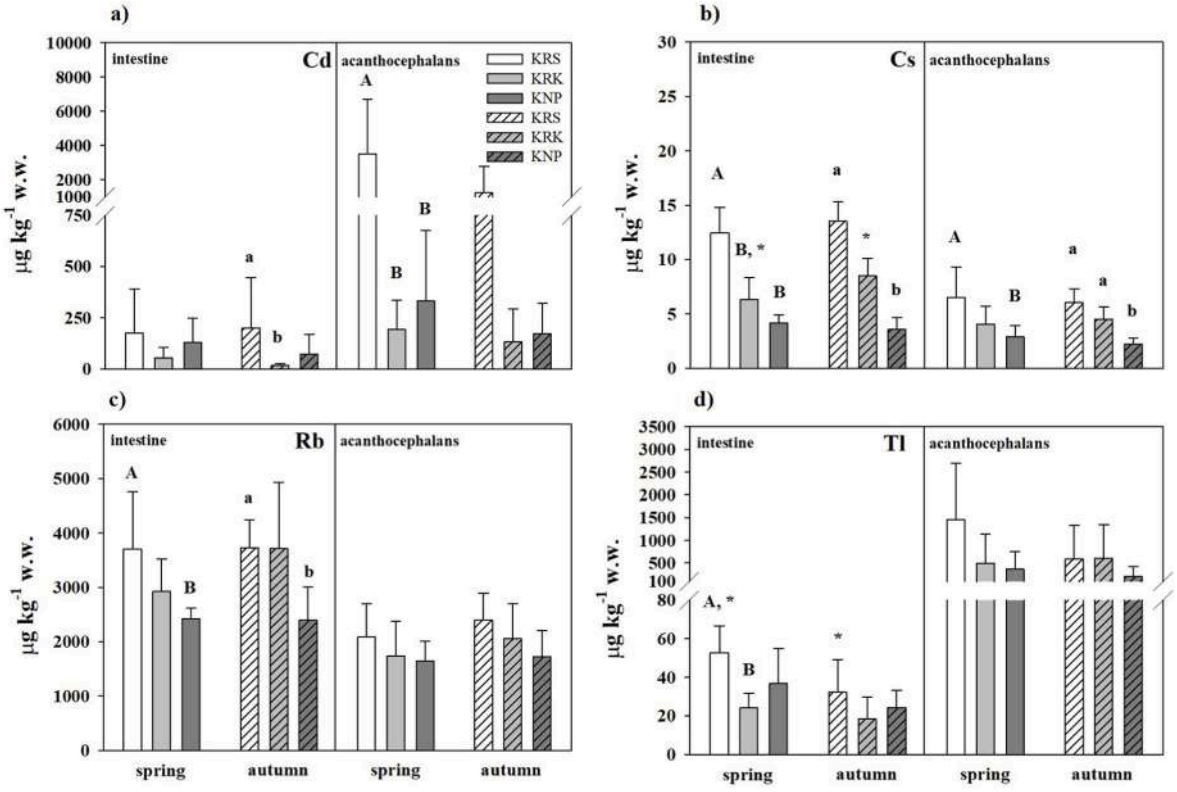

Fig. 3. Concentrations (µg kg^{-1} on wet mass basis) of four elements in the intestine of brown trout *S. trutta* and acanthocephalans *D. truttae* from three sites of the Krka River in two sampling campaigns (spring and autumn) that showed enhanced accumulation at the reference site, KRS. Different letters refer to significant differences of metal(loid) concentrations among three locations in spring (capital letters) and autumn (small letters), while statistically significant differences between two seasons at each sampling site are marked with asterisk (*).

−0.326, $p < 0.05$), Cu ($r = -0.351$, $p < 0.05$), and Fe ($r = -0.339$, $p < 0.05$) in the intestine of fish was established. Correlation analysis is presented in Table S8. This suggests that fish with greater infection levels absorbed lower concentrations of these elements via the intestinal wall, as consistent with the possible protective and beneficial role for their fish hosts (Sures, 2002; Nachev and Sures, 2016; Mehana et al., 2020).

Continuing to analyze the potential impact of acanthocephalan infrapopulation sizes on metal(loid) accumulation mechanisms within parasites (Table S8), we observed that larger infrapopulations had lower concentrations of Co ($r = -0.545$; $p < 0.001$), Cr ($r = -0.500$; $p < 0.001$), V ($r = -0.646$; $p < 0.001$), Zn ($r = -0.475$; $p < 0.001$), As ($r = -0.414$; $p < 0.01$), Fe ($r = -0.453$; $p < 0.01$), Mg ($r = -0.406$; $p < 0.01$), Mo ($r = -0.466$, $p < 0.01$), Ba ($r = -0.333$, $p < 0.05$) and Se ($r = -0.361$, $p < 0.05$) compared to smaller infrapopulations. Sures et al. (1999) previously reported that concentrations of several elements within the parasite *Acanthocephalus lucii* decreased as the infrapopulation of *A. lucii* in fish increased. Similar findings were reported by Brázová et al. (2015), who recorded that a high intensity of infection was associated with lower heavy metal concentration in *A. lucii* and *Proteocephalus percae*, and by Hassanine et al. (2018) regarding the inverse relationship between metal concentrations in the acanthocephalan *Sclerocollum saudii* and the size of its infrapopulation in fish *Siganus rivulatus*. It is still unclear whether our findings support the traditionally accepted concept of intraspecific competition among acanthocephalans for the absorption of metals from fish intestine (Sures, 2002; Hassanine and Al-Hasawi, 2021) or the more recent hypothesis of biodilution of elements in the fish host proposed by Duarte et al. (2020). The latter concept proposes that in larger parasite populations, elements may be dispersed among all parasite individuals, leading to reduced metal(loid) concentrations in both parasites and fish. In the investigation of the accumulation of 12 trace metals in the muscle, intestine, and liver of the white mullet and its intestinal parasites, Leite et al. (2023) also noted that the size of the parasite infrapopulation had an effect on the concentrations of trace metals in the parasites, with smaller infrapopulations accumulating a greater quantity of metals. Regarding the host, fish with a more severe parasitic infection had reduced concentrations of Cd exclusively in the muscle tissue, while no significant differences were detected with regard to other tissues or metals. They also explained this phenomenon by biodilution, resulting from the increased biomass of the host-parasite system and the fact that after metal is excreted in the intestine, reabsorption by fish does not occur because metal is captured by the parasite at the infection site.

Therefore, as parasites can be found in every free-living organism in all ecosystems there is a need of investigating their impact on environmental health and biological responses of organisms (Timi and Poulin, 2020). Our results confirmed that accumulation in acanthocephalans may have implications for accumulation levels in fish, that they have high accumulation potential and response fast, as well as possible negative and positive effects on intermediate and final hosts (Sures, 2002; Sures et al., 2017). However, it is challenging and almost impossible to distinguish in field conditions acanthocephalan from environmental impact because parameters as season, abundance of intermediate hosts, sex of the hosts, as well as their biometric characteristics may sometimes impact epidemiological characteristics of acanthocephalans and cannot always be excluded. That highlights the complexity of the host-parasite relationship, as well as of the assessment of contamination exposure. Still, good freshwater ecosystem management plans and monitoring programs should always contain physico-chemical factors, water and sediment analyses, fish, but also parasites to interpret the data and results from the field studies as accurate as possible.

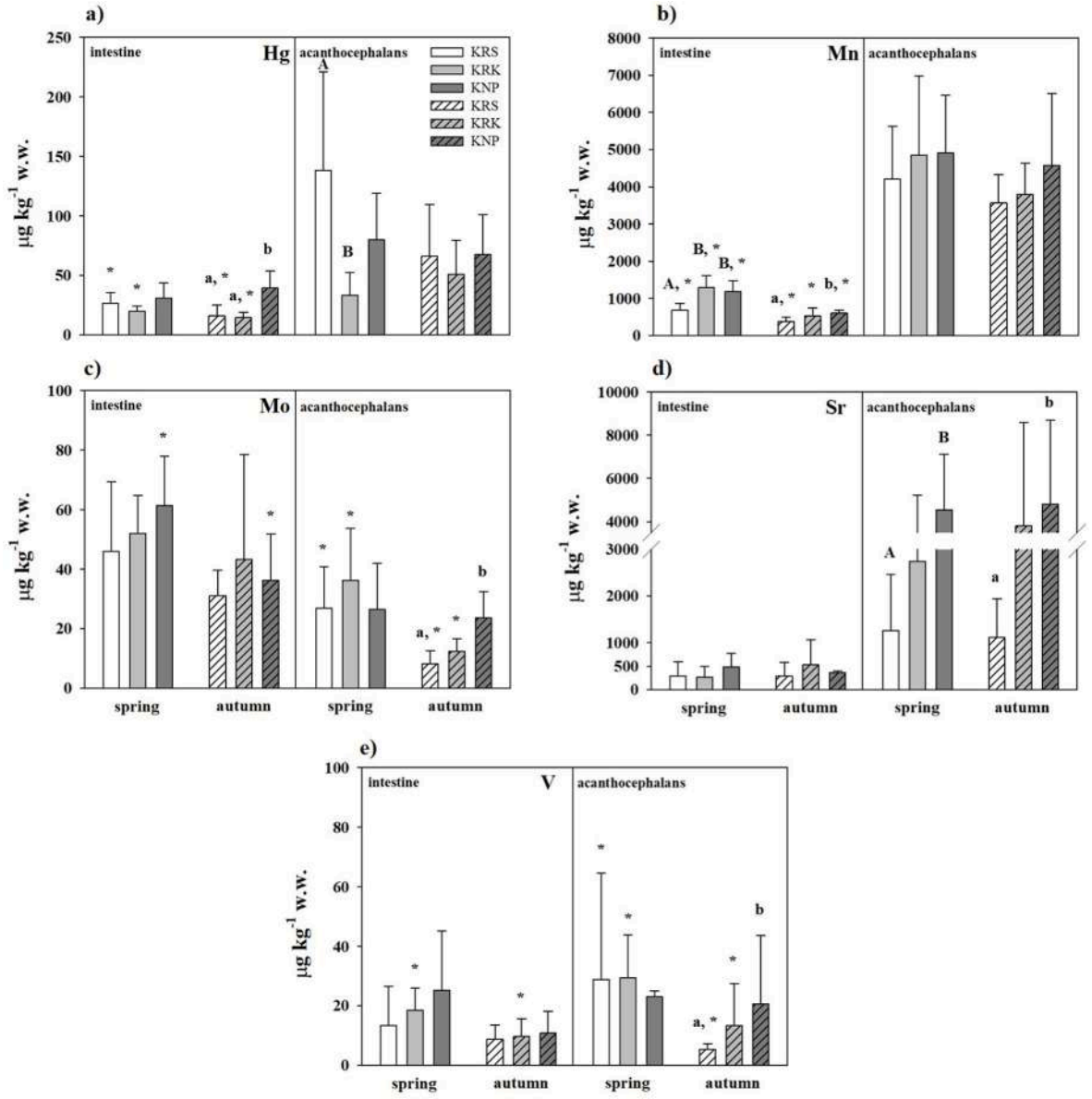

Fig. 4. Concentrations (µg kg^{-1} on wet mass basis) of five elements in the intestine of brown trout *S. trutta* and acanthocephalans *D. truttae* from three sites of the Krka River in two sampling campaigns (spring and autumn) that showed enhanced accumulation at the site in the national park, KNP. Different letters refer to significant differences of metal(loid) concentrations among three locations in spring (capital letters) and autumn (small letters), while statistically significant differences between two seasons at each sampling site are marked with asterisk (*).

3.3.3. Spatial differences in metal(loid) accumulation

Fish intestine and acanthocephalans showed variable spatial differences which were not always statistically significant but could be mostly grouped in four patterns: 1) elements with higher concentrations at the contaminated site, KRK; 2) elements with higher concentrations at the reference site, KRS; 3) elements with higher concentrations at the site in national park, KNP; 4) elements with unclear trends (Figs. 2–5).

Statistically significant differences in metal(loid) accumulation between sites in the fish were observed for Cs, Mn, Rb and Se during both seasons. For As, Co, Fe, Tl, and Zn, these differences were evident only in spring, whereas for Cd and Hg only in autumn (Figs. 2–5). The highest levels of certain elements were recorded at different locations: 1) As, Mn, Se, Zn at KRK; 2) Cd, Cs, Rb, Tl at KRS; and 3) Co, Hg, Mn at KNP. Similar patterns were previously documented for brown trouts from KRS and KRK collected in 2015/2016, with no sampling conducted at KNP during that period (Mijošek et al., 2022). These patterns could not be fully explained by uptake from water or sediments alone, suggesting the importance of long-term dietborne metal(loid) uptake and feeding preferences. Namely, As, Se and Zn were found in higher concentrations in fish from KRK (Fig. 2), but not in the water or sediment samples from that site (Tables S1 and S5). Similarly, Cs and Rb concentrations in fish (Fig. 3b and c) did not correspond to their levels in water or sediments; in water, the levels were either similar across sites or the highest at KRK (Table S1) whereas for sediments, they were highest at KNP (Table S5). Bioaccumulation of Co, Fe, Hg and Mn in fish could mostly be explained by their uptake and remobilization from sediments, while concentrations of Tl and Cd in fish from the reference site seemed to be more closely related to their concentrations in water than sediment samples (Tables S1 and S5). Concentrations of Cd and Tl tended to be higher in fish from the KRS (Fig. 3), possibly due the prevalence of Cd-enriched limestones and dolomites in Dinaric karst (Cukrov et al., 2008). In addition to natural and anthropogenic causes, food preferences can significantly affect metal accumulation in the intestine, since dietborne metal uptake may be of equal or greater importance than waterborne

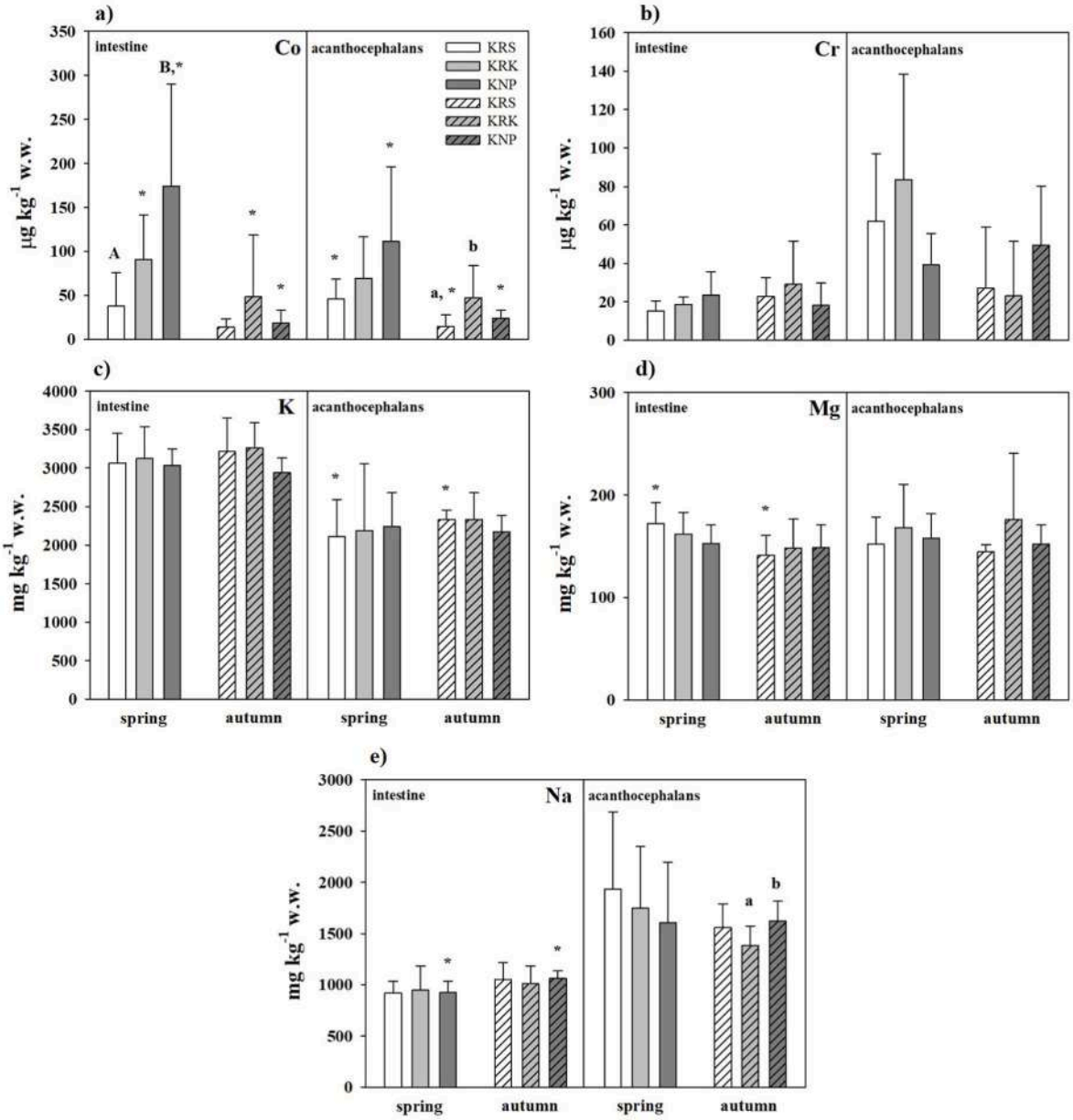

Fig. 5. Concentrations (mg kg^{-1} or µg kg^{-1} on wet mass basis) of five elements in the intestine of brown trout *S. trutta* and acanthocephalans *D. truttae* from three sites of the Krka River in two sampling campaigns (spring and autumn) that showed unclear trends of accumulation. Different letters refer to significant differences of metal(loid) concentrations among three locations in spring (capital letters) and autumn (small letters), while statistically significant differences between two seasons at each sampling site are marked with asterisk (*).

uptake for some elements, including Tl (Lapointe and Couture, 2009).

Acanthocephalans showed significant spatial differences for Cs, Fe, and Sr in both seasons, while variations for Cd, Co, Hg, Mo, Na, and V were apparent during only one season (Figs. 2–5), which partially corresponded to patterns in the intestines. Similar to previous research of Mijošek et al. (2022), the highest levels of certain metals in fish parasites were found at the following locations: 1) Co and Fe at KRK; 2) Cd and Cs at KRS; and 3) Mo, Na, Sr, and V at KNP. In contrast to the accumulation of Cd, Co, Cs, and Hg in parasites, which, similar to the intestinal accumulation, was largely unrelated to exposure from water and sediments, the highest accumulation of Mo, Sr, and V at KNP was concurrent with their highest levels in water, sediment and GC samples from that site (Tables S1, S5 and S9). Patterns of other elements might be associated with long-term feeding preferences of their fish hosts or natural geological background. Although there were notable differences in the average values of other elements in acanthocephalans across different sites, these variations were not statistically significant due to the high variability and high standard deviations in metal(loid) concentrations among individual acanthocephalans, as already stated for different acanthocephalan species (Filipović Marijić et al., 2013; Nachev and Sures, 2016; Mijošek et al., 2022).

3.3.4. *Temporal differences in metal(loid) accumulation*

Seasonal variations of metal(loid) concentrations in the intestine of brown trout were mostly not uniform and could not be extrapolated to all locations (Figs. 2–5). Nevertheless, more elements showed higher levels in spring compared to autumn, with significant differences observed for Ca, Hg, Mg, Mn, Se, and Tl at KRS, As, Co, Hg, Mn, and V at KRK, and As, Co, Cu, Fe, Mn, Mo, and Se in KNP. Conversely, greater accumulation of Cs at KRK, Na at KNP, and Zn at KRS was observed during the autumn (Figs. 2–5). Various biotic and abiotic factors, in addition to exposure conditions, can influence seasonal variability in

Table 2
Bioconcentration factors ($c_{[parasite]}/c_{[host\ intestine]}$) for *D. truttae* calculated with respect to intestinal tissue of *S. trutta*. Bioconcentration factors over 1 are marked in bold, indicating higher accumulation in acanthocephalans than fish.

	Krka River source (KRS)		Town of Knin (KRK)		Krka National Park (KNP)	
	Spring 2021	**Autumn 2021**	**Spring 2021**	**Autumn 2021**	**Spring 2021**	**Autumn 2021**
As	**3.5 ± 3.2**	**6.0 ± 6.8**	**1.3 ± 1.0**	**3.1 ± 2.5**	**2.1 ± 1.5**	**3.6 ± 1.1**
Ba	**9.2 ± 6.9**	**9.7 ± 9.2**	**15.0 ± 20.6**	**11.9 ± 12.5**	**10.9 ± 5.7**	**9.4 ± 2.6**
Cd	**86.0 ± 192.2**	**8.5 ± 10.1**	**4.9 ± 4.6**	**16.5 ± 28.6**	**9.4 ± 16.2**	**15.0 ± 21.2**
Co	**2.0 ± 1.5**	**1.5 ± 1.3**	0.8 ± 0.4	**3.0 ± 4.5**	1.0 ± 0.7	**2.1 ± 1.4**
Cr	**4.0 ± 1.4**	**1.6 ± 2.3**	**4.8 ± 4.8**	**1.2 ± 1.5**	**2.2 ± 1.6**	**4.0 ± 2.9**
Cs	0.5 ± 0.2	0.5 ± 0.1	0.7 ± 0.2	0.5 ± 0.1	0.7 ± 0.3	0.6 ± 0.2
Cu	**14.6 ± 12.8**	**7.7 ± 7.4**	**7.3 ± 8.9**	**10.1 ± 11.8**	**9.2 ± 9.4**	**7.7 ± 7.9**
Fe	**1.1 ± 0.5**	0.8 ± 0.3	**1.5 ± 0.4**	**1.4 ± 0.9**	**1.1 ± 0.6**	1.0 ± 0.5
Hg	**5.5 ± 3.0**	**3.7 ± 1.8**	**1.3 ± 1.1**	**3.6 ± 2.1**	**2.9 ± 1.8**	**1.8 ± 0.8**
Mn	**6.3 ± 1.8**	**9.8 ± 2.9**	**3.7 ± 1.0**	**8.1 ± 2.8**	**4.6 ± 2.3**	**7.5 ± 3.8**
Mo	0.6 ± 0.1	0.3 ± 0.2	0.7 ± 0.4	0.3 ± 0.1	0.5 ± 0.3	0.8 ± 0.5
Pb	**74.1 ± 68.6**	**20.0 ± 30.6**	**31.4 ± 27.8**	**46.4 ± 53.0**	**28.1 ± 42.8**	**34.4 ± 46.7**
Rb	0.6 ± 0.2	0.7 ± 0.2	0.6 ± 0.2	0.6 ± 0.1	0.7 ± 0.1	0.7 ± 0.1
Se	**1.3 ± 0.4**	**1.8 ± 0.9**	0.7 ± 0.3	**1.1 ± 0.6**	0.7 ± 0.3	0.9 ± 0.3
Sr	**5.8 ± 6.3**	**5.5 ± 2.3**	**9.7 ± 4.0**	**6.3 ± 3.9**	**9.7 ± 3.0**	**8.3 ± 4.6**
Tl	**29.3 ± 27.2**	**16.0 ± 18.0**	**22.2 ± 34.4**	**30.9 ± 35.4**	**13.7 ± 18.6**	**9.0 ± 8.9**
V	**2.0 ± 1.5**	0.6 ± 0.2	**1.7 ± 0.6**	**1.2 ± 0.6**	**1.4 ± 1.1**	**2.1 ± 1.3**
Zn	0.4 ± 0.3	0.1 ± 0.1	0.2 ± 0.1	0.2 ± 0.2	0.2 ± 0.0	0.2 ± 0.1
Ca	**4.3 ± 3.0**	**6.0 ± 1.8**	**9.3 ± 4.8**	**9.1 ± 9.5**	**5.9 ± 2.1**	**6.5 ± 4.0**
K	0.7 ± 0.2	0.7 ± 0.1	0.7 ± 0.3	0.7 ± 0.1	0.7 ± 0.2	0.7 ± 0.1
Mg	0.9 ± 0.2	0.9 ± 0.4	1.0 ± 0.2	**1.1 ± 0.4**	**1.1 ± 0.3**	**1.1 ± 0.3**
Na	**2.1 ± 0.9**	**1.5 ± 0.2**	**1.9 ± 0.6**	**1.4 ± 0.3**	**1.8 ± 0.7**	**1.5 ± 0.2**

metal accumulation. For example, differences in growth, metabolism rate or water parameters like temperature, pH, or water hardness may influence bioaccumulation in organisms. Further, food type or feeding rates can also significantly affect bioaccumulation (Farkas et al., 2003) and these differences were clearly observed during fish dissection. Specifically, we observed high gut fullness index in nearly all fish during spring. The feeding intensity was lower in autumn with the higher proportion of half-empty to empty stomachs. Greater diversity of the gut contents was also observed in spring, which contributed to the higher metal (loid) concentrations in fish GC in that season as will be further discussed. This observation is in accordance with research reporting maximum feeding rates of trouts in spring (Debeljak, 1986; Kara and Alp, 2005). Fullness indices of the brown trouts were also already found to be the lowest in autumn, increasing from winter to summer (Kara and Alp, 2005).

Higher accumulation in spring than autumn was also observed in acanthocephalans, although less pronounced, and engaged different elements than in fish intestines. Namely, concentrations of Co, Mo, Pb, and V at KRS, Mo and V at KRK, and Co at KNP were significantly higher in spring than in autumn (Figs. 2, 4 and 5). Potassium was significantly higher in autumn compared to spring in acanthocephalans from KRS, while other elements did not display significant seasonal variations (Figs. 2–5). According to Nachev and Sures (2016), seasonality in metal accumulation in parasites can be explained by acanthocephalan transmission, maturation in the intestine of the hosts, or by physiological or behavioral changes of their final hosts, such as mobility or alterations in food preferences.

3.3.5. *Bioconcentration factors (BCFs)*

To define the relation of metal(loid) concentrations in acanthocephalans and fish intestine, we calculated BCFs (Table 2). Due to the different life spans of acanthocephalans and fish, high BCFs indicate recent metal exposures, while lower ratios represent continuous, longer exposure (Sures et al., 1999).

Our research supported findings of superior efficiency of metal(loid) accumulation in acanthocephalans compared to fish (Filpović Marijić et al., 2013; Nachev and Sures, 2016; Sures et al., 2017; Mijošek et al., 2022). Acanthocephalans showed higher accumulation of As, Ba, Cd, Cr, Cu, Hg, Mn, Pb, Sr, Tl, Ca, and Na in all sites and seasons, and of Co, Fe, and V in majority of cases (Table 2). The only elements with lower accumulation in acanthocephalans than in fish intestine (BCF<1) were Cs, Mo, Rb, Zn and K, with the occasional inclusion of Co, Se, V and Mg in a few instances (Table 2). This is in accordance with a recent research conducted on the Krka River, which found that the same few elements accumulated more in fish intestines than in acanthocephalans (Mijošek et al., 2022). Both investigations confirmed remarkably efficient accumulation of potentially highly toxic elements (Pb, Cd and Tl), which goes in favor of possible protection of the infected fish (Sures, 2002; Filipović Marijić et al., 2013; Mehana et al., 2020; Molbert et al., 2020). Moreover, high BCF values observed for Pb, Cd, Tl, Cu, Ba, Mn, Sr, Ca, and Hg (Table 2) suggest the likelihood of recent high exposure to these elements in the Krka River.

Although we expected to observe some significant spatial or temporal trends regarding BCF values, the number of distinctive patterns was limited (Table 2). Still, the maximum BCFs in both seasons for As, Hg, Mn, and Se were observed at KRS, for Ba and Ca at KRK, and for Sr at KNP, showing that used acanthocephalan species provides a valuable biological response even at the site of the minimal metal(loid) exposure, KRS. Regarding seasonal changes, only the BCFs for Fe, Na, and Sr were higher in spring compared to autumn at all sites, whereas the opposite trend was seen for As, Mn and Pb (Table 2). These trends could not be associated with the metal(loid) exposure from water or sediments, but rather to factors such as age, physiology, reproductive stage or size of the acanthocephalans or fish host (Filipović Marijić et al., 2013; Sures et al., 2017).

The BCF ranges for most elements in the current research were comparable to the 2015/2016 study on the same host-parasite system (Table 2, Mijošek et al., 2022). However, the BCF values for Pb were 2–8 times greater in the current study, which can be attributed to the aforementioned decrease in Pb concentrations in fish intestines nowadays. In summary, while there is a lack of additional research pertaining to this particular ecosystem and species, our data suggests that *D. truttae* is a promising indicator, even in ecosystems characterized by low to moderate metal (loid) exposure, such as the karst Krka River.

3.4. *Metal(loid) accumulation in gut contents (GC)*

Dietborne metal(loid) uptake was considered through measuring metal(loid) concentrations in GC of fish. The sequences of macroelements (Ca > Na > K > Mg) and trace elements (Fe > Zn > Sr ≥ Mn > Cu

> Ba ≥ V ≥ Cr ≥ Co ≥ Rb ≥ Pb ≥ Cd ≥ As > Se ≥ Mo > Cs > Tl > Hg) (Table S9) were notably different in comparison to fish intestine (Figs. 2–5), indicating that metal(loid) accumulation depends on the bioavailability of metal(loid)s in fish diet. Further, fish have the ability to regulate metal uptake from food into the tissue depending on the specific requirements of organisms (Clearwater et al., 2000), which is reflected in different efficiency of metal absorption. Similar patterns and differences in metal accumulation (Cd, Cu, Fe, Mn, and Zn) between fish intestine and GC have been reported for the European chub from the Sava River (Filipović Marijić and Raspor, 2012,2013). As brown trout is an omnivorous species, the gut contents included a variety of species like insect larvae, detritus, plants, gammarids, and small mollusks. This led to high variations in metal(loid) concentrations among individual fish (Table S9). For example, the higher average contents of Ca and Sr in GC compared to fish intestine is associated to the prevalence of gammarids as a favored food source for many fish, and crustacean exoskeletons are particularly rich in Ca and Sr (Greenaway, 1985), but only a small portion of these elements is bioavailable to organisms. To our knowledge, this is the first report on metal(loid)s in GC of brown trouts, so comparison with previous data was not possible.

Spearman correlation analyses revealed sporadic associations between concentrations of metal(loid)s in GC and fish intestine or acanthocephalans. More frequently, we observed negative correlation between metal(loid)s in GC and fish size (TM), which corresponds to higher metabolic needs and feeding rates during the development in early stages (Farkas et al., 2003).

3.4.1. Spatial differences

Statistically significant spatial differences were observed for most elements, except Ba, Ca, Mg, Na, Se, Sr and Tl (Table S9). The levels of most of the remaining elements were highest in GC of fish from KNP, similar to spatial distribution observed in sediment samples (Tables S5 and S9). During dissection, particles of sediments could be observed in GC of many fish, suggesting that sediments play a significant role in the absorption of metals through the diet and may pose a threat to organisms in the area of the national park and sensitive lake systems in case of the prolonged exposure. Exceptionally, Cd concentrations in GC were highest at KRS, while Cu concentrations in GC were highest at KRK, which aligns with the spatial distribution of Cu in fish intestine and acanthocephalans (Fig. 2d and 3a). Overall, metal(loid) concentrations in GC of fish were typically the lowest at KRS, demonstrating the lowest metal(loid) exposure at this location, which corresponded to water and sediment samples.

3.4.2. Temporal differences

The majority of elements in GC had higher concentrations in spring than autumn, with the highest number of statistically significant differences at KRS (Table S9). As already mentioned, higher gut fullness indices were found in spring, a season characterized by maximum feeding rates for this species, as well as greater variability of the prey, which led to the increased metal(loid) accumulation in spring. A similar pattern was also observed in parasites and intestine, which further suggests that the uptake of metal(loid)s through the diet influences the responses of organisms, prompting us to investigate their relationships further.

3.4.3. Relationships between metal(loid) concentrations in fish intestine and acanthocephalans to gut contents

To compare levels of metal(loid)s in biological samples to those found in GC, as an important uptake route, we calculated average ratios between the concentrations of metal(loid)s in the intestine of fish and GC (INT/GC), as well as in acanthocephalans and GC (AC/GC) (Table S10). With this approach, we were able to evaluate and estimate the potential bioavailability of metal(loid)s from food to organisms. However, it is important to keep in mind that this is only an estimate since the metal(loid)s found in the GC reflect the source of metal(loid)s in the food at the time of sampling, whereas organisms accumulate metal(loid)s over a longer period of time and exhibit a more chronical response.

Nevertheless, it can be presumed that the bioavailability of As, Ba, Ca, Cr, Cu, Fe, Mn, Pb, Sr, and V from food to the fish intestine may be minimal, since the majority of the INT/GC ratios for these elements were <15%, suggesting that their absorption is physiologically regulated and not dependent on their quantity in the food source. Although concentrations of these elements in GC were predominantly highest at KNP, the calculated ratios were either similar across all locations or the lowest at KNP (Table S10). With the exception of Cd and Pb, the lowest values of the AC/GC ratios were found once more for As, Ba, Ca, Cr, Fe, Mn, Sr, and V, confirming low bioavailability of these elements from food. Low values mostly up to 50% were also observed for Co, Cs, and Mo for both fish intestine (INT/GC) and acanthocephalans (AC/GC) (Table S10), suggesting that although concentrations of these elements in the GC are elevated (Table S9), their burden is significantly lower in fish intestine and parasites. This indicates that a large portion of these elements is excreted via the faeces (Dallinger and Kautzky, 1985).

Thallium, Se, Hg, Rb, K and Zn exhibited remarkable luminal absorption efficiency, as evidenced by their substantially higher concentrations in the intestine and acanthocephalans compared to GC (Table S10). In addition, Cd, Cu, and Pb were also accumulated more efficiently in acanthocephalans than GC and fish intestine showing that they may selectively accumulate certain elements over others, potentially influencing the overall element distribution within the fish host and providing a protective role for the fish host when exposed to potentially toxic elements (Sures, 2002). Understanding these differences in element accumulation is important since it can provide valuable insights into the dynamics of host-parasite interactions and their impact on element cycling in aquatic ecosystems. To our knowledge, there is no available research that compares metal(loid) accumulation in acanthocephalans and fish gut content. However, Dallinger and Kautzky (1985) published data on Cd, Cr, Cu, Mn, Pb and Zn concentrations in the intestine and GC of species *Salmo gairdneri* from Augraben River and Leiferer Graben River in Italy. The obtained ratios of Cd, Cu, Mn and Zn were similar to those in our research, whereas Cr and Pb appeared to be less bioavailable in our study. Further, Filipović Marijić and Raspor (2012) reported comparable ratios to those found in the present research for European chub (Zn > Cd ≥ Cu > Fe ≥ Mn). Prior studies have consistently shown that fish intestines contain very high levels of Zn, serving as an important storage location for Zn in many fish species (Dallinger and Kautzky, 1985; Rajkowska and Protasowicki, 2013). In addition, it is also important to consider the potential influence of thiol-containing proteins, which can be found in even higher quantities in fish intestines compared to liver and gills, as indicated in previous studies on various fish species (Roesijadi et al., 2009; Filipović Marijić and Raspor, 2010), including brown trout from the Krka River (Mijošek et al., 2019). Given the high affinities of Zn and Hg for thiol-containing proteins like metallothioneins (MTs) (Roesijadi et al., 2009), it is possible that MTs may serve as potential binders of Zn and Hg, leading to their substantially higher intestinal concentrations compared to GC. Further, Hg, but also Rb and Se, are among rare elements for which biomagnification in food webs is suggested (Campbell et al., 2005; Córdoba-Tovar et al., 2022). High accumulation and absorption of K in the intestine in comparison with other macrolements has also been previously described by Bucking and Wood (2006). Also, accumulation of K, Se, and Zn over time is probably related to their important biological roles (e.g. as a part of different enzymes, metallothioneins, or K^+ channels).

However, it is consistently challenging to make a clear distinction between the uptake through the alimentary tract (dietborne uptake) and absorption through the gills (waterborne uptake) in the field studies. Moreover, the composition and metal(loid) content of fish diet are extremely heterogenous, making it impossible to establish a direct link between a specific food source and the fish.

4. Conclusions

This study provided information on total concentrations of 22 metal (loid)s in the intestine of brown trout *S. trutta*, fish gut content, and acanthocephalan species *D. truttae*. Concentrations of As, Ba, Cr, Hg, Mo, and V in parasites provide the first-ever information on this endemic acanthocephalan species, as well as metal(loid)s in GC of brown trouts, serving as an indication of metal intake through food sources. Although often neglected in fish ecology and ecotoxicology, parasites were integrated in the study to achieve more complete understanding of fish biology and to realize influence of parasitic infections on fish responses. Acanthocephalans and GC were also applied to assess possible bioavailability of metal(loid)s to fish intestinal tissue and intestinal parasites.

Great efficiency of metal(loid) accumulation in acanthocephalans was confirmed for many elements, especially potentially toxic ones such as Pb, Cd, and Tl. With few exceptions, concentrations of various elements were found to be the highest at different sites: As, Ba, Ca, Cu, Fe, Pb, Se, and Zn at KRK; Cd, Cs, Rb, and Tl at KRS; and Hg, Mn, Mo, Sr, and V at KNP. These patterns corresponded only partially to metal(loid) exposure through water and/or sediments, and indicated that differences in metal (loid) bioaccumulation were strongly related to the biology and ecology of host and parasite species, dietary habits, and the presence of acanthocephalans in the fish intestine. Metal(loid) concentrations in GC were generally the highest at KNP, reflecting the spatial distribution of metal(loid)s in river surface sediment. Ratios between metal accumulation in the intestine and GC, and acanthocephalans and GC, indicate potential low bioavailability of As, Ba, Ca, Cr, Cu, Fe, Mn, Pb, Sr, and V from the dietary sources, while high absorption of Tl, Se, Hg, Rb, K and Zn is suggested. However, that should be interpreted with caution since concentrations in GC represent the metal(loid) burden in the moment of sampling, while concentrations in organisms reflect chronic exposure, which might give different response.

We observed a biodilution effect associated with increased acanthocephalan mean intensity. This requires further investigations of other species exposed to different levels to evaluate the potential benefits to hosts and parasites. Comparison with previous research in this area revealed an increase of Cd, Cu, Mn, and Zn concentrations, pointing to the still negative influence of the industrial and municipal wastewater outlets on the Krka National Park.

According to collected data, wastewater discharges near the border of Krka National Park currently have a moderate impact. However, concerning tendencies of frequently highest metal(loid) concentrations in sediments, GC and occasionally even in organisms from the KNP indicate the need for more thorough and frequent monitoring of this area. Besides water and sediment as potential environmental sources of metal(loid)s, future monitoring programs should always consider the dietary effects of metal(loid) exposure and the presence of acanthocephalan parasites as possible important contribution factors to metal (loid) input, which would enable more reliable interpretations of results in all ecosystems. Based on given data, we recommend for future studies to inspect fish for the presence of other parasites like trematodes as well, while for the analysis of dietary habits, it would be relevant to classify the gut content in herbal and animal material to identify the most common groups of insects and gammarids to possibly evaluate the contribution of each group to metal(loid) uptake in fish. Further, estimation of bioavailable, and thus possibly toxic metal(loid)s, whose binding to sensitive biomolecules may actually change their molecular function, structure and/or dynamics in the cell, is a next crucial step in metal(loid) risk assessment.

CRediT authorship contribution statement

Tatjana Mijošek: Writing – review & editing, Writing – original draft, Investigation, Formal analysis. **Sara Šariri:** Writing – review & editing, Investigation, Formal analysis. **Zorana Kljaković-Gašpić:** Writing – review & editing, Writing – original draft, Investigation. **Željka Fiket:** Writing – review & editing, Investigation. **Vlatka Filipović Marijić:** Writing – review & editing, Writing – original draft, Supervision, Resources, Project administration, Investigation, Funding acquisition.

Declaration of competing interest

The authors declare that they have no known competing financial interests or personal relationships that could have appeared to influence the work reported in this paper.

Data availability

Data will be made available on request.

Acknowledgements

This research has been supported by the Croatian Science Foundation under the project "Integrated evaluation of aquatic organism responses to metal exposure: gene expression, bioavailability, toxicity and biomarker responses" (BIOTOXMET; IP-2020-02-8502). The authors would like to acknowledge Dr. Zuzana Redžović, Dr. Damir Valić and Dr. Tomislav Kralj for their valuable help in the field work and Dr. Tatjana Ocrt and Dr. Ankica Sekovanić for their valuable help in the ICP-MS measurements.

Appendix A. Supplementary data

Supplementary data to this article can be found online at https://doi.org/10.1016/j.envpol.2024.124358.

References

Algül, F., Beyhan, M., 2020. Concentrations and sources of heavy metals in shallow sediments in Lake Bafa, Turkey. Sci. Rep. 10, 11782.
Brázová, T., Hanzelová, V., Miklisová, D., Šalamún, P., Vidal-Martínez, V.M., 2015. Host-parasite relationships as determinants of heavy metal concentrations in perch (*Perca fluviatilis*) and its intestinal parasite infection. Ecotoxicol. Environ. Saf. 122, 551–556.
Bucking, C., Wood, C.M., 2006. Gastrointestinal processing of Na^+, Cl^-, and K^+ during digestion: implications for homeostatic balance in freshwater rainbow trout. Am. J. Physiol. Regul. Integr. Comp. Physiol. 291 (6), 1764–1772.
Campbell, L.M., Fisk, A.T., Wang, X., Köck, G., Muir, D.C.G., 2005. Evidence for biomagnification of rubidium in freshwater and marine food webs. Can. J. Fish. Aquat. Sci. 62 (5), 1161–1167.
Chon, H.-S., Ohandja, D.-G., Voulvoulis, N., 2012. The role of sediments as a source of metals in river catchments. Chemosphere 88, 1250–1256.
Clearwater, S.J., Baskin, S.J., Wood, C.M., McDonald, D.G., 2000. Gastrointestinal uptake and distribution of copper in rainbow trout. J. Exp. Biol. 203, 2455–2466.
Córdoba-Tovar, L., Marrugo-Negrete, J., Barón, P.R., Díez, S., 2022. Drivers of biomagnification of Hg, as and Se in aquatic food webs: a review. Environ. Res. 204, 112226.
Creighton, N., Twining, J., 2010. Bioaccumulation from food and water of cadmium, selenium and zinc in an estuarine fish, *Ambassis jacksoniensis*. Mar. Pollut. Bull. 60, 1815–1821.
Cukrov, N., Cmuk, P., Mlakar, M., Omanović, D., 2008. Spatial distribution of trace metals in the Krka River, Croatia. An example of the self-purification. Chemosphere 72 (10), 1559–1566.
Dallinger, R., Kautzky, H., 1985. The importance of contaminated food for the uptake of heavy metals by rainbow trout (*Salmo gairdneri*): a field study. Oecologia 67, 82–89.
Debeljak, L., 1986. The nutrition of brown trout (*Salmo fario*) in Bager reservoir and Lepenica Stream. J. Ichthos. 3, 1–7.
Dragun, Z., Filipović Marijić, V., Krasnići, N., Ivanković, D., Valić, D., Žunić, J., Kapetanović, D., Vardić Smrzlić, I., Redžović, Z., Grgić, I., Erk, M., 2018. Total and cytosolic concentrations of twenty metals/metalloids in the liver of brown trout *Salmo trutta* (Linnaeus, 1758) from the karstic Croatian river Krka. Ecotoxicol. Environ. Saf. 147, 537–549.
Duarte, G.S.C., Lehun, A.L., Leite, L.A.R., Consolin-Filho, N., Bellay, S., Takemoto, R.M., 2020. Acanthocephalans parasites of two Characiformes fishes as bioindicators of cadmium contamination in two neotropical rivers in Brazil. Sci. Total Environ. 738, 140339.
Farkas, A., Salánki, J., Specziár, A., 2003. Age- and size-specific patterns of heavy metals in the organs of freshwater fish *Abramis brama* L. populating a low-contaminated site. Water Res. 37, 959–964.

Filipović Marijić, V., Raspor, B., 2010. The impact of the fish spawning on metal and protein levels in gastrointestinal cytosol of indigenous European chub. Comp. Biochem. Physiol., C 708, 133–138.
Filipović Marijić, V., Raspor, B., 2012. Site-specific gastrointestinal metal variability in relation to the gut content and fish age of indigenous European chub from the Sava River. Water Air Soil Pollut. 223, 4769–4783.
Filipović Marijić, V., Vardić Smrzlić, I., Raspor, B., 2013. Effect of acanthocephalan infection on metal, total protein and metallothionein concentrations in European chub from a Sava River section with low metal contamination. Sci. Total Environ. 463–464, 772–780.
Filipović Marijić, V., Kapetanović, D., Dragun, Z., Valić, D., Krasnići, N., Redžović, Z., Grgić, I., Žunić, J., Kružlicová, D., Nemeček, P., Ivanković, D., Vardić Smrzlić, I., Erk, M., 2018. Influence of technological and municipal wastewaters on vulnerable karst riverine system, Krka River in Croatia. Environ. Sci. Pollut. Res. 25, 4715–4727.
Filipović Marijić, V., Mijošek, T., Dragun, Z., Retzmann, A., Zitek, A., Prohaska, T., Bačić, N., Redžović, Z., Grgić, I., Krasnići, N., Valić, D., Kapetanović, D., Žunić, J., Ivanković, D., Vardić Smrzlić, I., Erk, M., 2022. Application of fish calcified structures as indicators of metal exposure in the freshwater ecosystem. Environments 9, 14.
Fiket, Ž., Mikac, N., Kniewald, G., 2017. Mass fractions of forty-six major and trace elements, including rare earth elements, in sediment and soil reference materials used in environmental studies. Geostand. Geoanal. Res. 41, 123–135.
Giguère, A., Campbell, P.G.C., Hare, L., McDonald, D.G., Rasmussen, J.B., 2004. Influence of lake chemistry and fish age on cadmium, copper, and zinc concentrations in various organs of indigenous yellow perch (*Perca flavescens*). Can. J. Fish. Aquat. Sci. 61 (9), 1702–1716.
Greenaway, P., 1985. Calcium balance and moulting in the Crustacea. Biol. Rev. Cambridge Philos. Soc 60, 425–454.
Hassanine, R., Al -Hasawi, Z., Hariri, M., Touliabah, H., 2018. *Sclerocollum saudii* (acanthocephala: cavisomidae) as a sentinel for heavy-metal pollution in the red Sea. J. Helminthol. 93, 177–186.
Hassanine, R., Al-Hasawi, Z., 2021. Acanthocephalan Worms mitigate the harmful impacts of heavy metal pollution on their fish hosts. Fishes 6, 49.
HRN EN 14011, 2005. Fish Sampling by Electric Power. Croatian Standard Institute, Zagreb (In Croatian).
Kara, C., Alp, A., 2005. Feeding habits and diet composition of brown trout (*Salmo trutta*) in the upper streams of river Ceyhan and river Euphrates in Turkey. Turk. J. Vet. Anim. Sci. 29, 417–428.
Lapointe, D., Couture, P., 2009. Influence of the route of exposure on the accumulation and subcellular distribution of nickel and thallium in juvenile fathead minnows (*Pimephales promelas*). Arch. Environ. Contam. Toxicol. 57, 571–580.
Leite, L.A.R., Agostinho, B.N., Oliveira, S.L.P., Pedreira Filho, W.D.R., de Azevedo, R.K., Abdallah, V.D., 2023. Trace metal accumulation is infrapopulation-dependent in acanthocephalans parasites of the white mullet (*Mugil curema*) from an estuarine environment of southeastern Brazil coast. Mar. Pollut. Bull. 194 (Pt. B), 115374.
Mehana, E.E., Khafaga, A.F., Elblehi, S.S., Abd El-Hack, M.E., Naiel, M.A.E., Bin-Jumah, M., Othman, S.I., Allam, A.A., 2020. Biomonitoring of heavy metal pollution using acanthocephalans parasite in ecosystem: an updated overview. Animals (Basel) 10, 811.
Mijošek, T., Filipović Marijić, V., Dragun, Z., Ivanković, D., Krasnići, N., Erk, M., Gottstein, S., Lajtner, J., Sertić Perić, M., Matoničkin Kepčija, R., 2019. Comparison of electrochemically determined metallothionein concentrations in wild freshwater salmon fish and gammarids and their relation to total and cytosolic metal levels. Ecol. Indicat. 105, 188–198.
Mijošek, T., Filipović Marijić, V., Dragun, Z., Ivanković, D., Krasnići, N., Erk, M., 2022. Efficiency of metal bioaccumulation in acanthocephalans, gammarids and fish in relation to metal exposure conditions in a karst freshwater ecosystem. J. Trace. Elem. Med. Biol. 73, 127037.
Mijošek, T., Kljaković-Gašpić, Z., Kralj, T., Valić, D., Redžović, Z., Šariri, S., Karamatić, I., Filipović Marijić, V., 2023. Spatial and temporal variability of dissolved metal(loid)s in water of the karst ecosystem: consequences of long-term exposure to wastewaters. Environ. Technol. Innov. 32, 103254.
Molbert, N., Alliot, F., Leroux-Coyau, M., Mèdoc, V., Biard, C., Meylan, C.S., Jacquin, L., Santos, R., Goutte, A., 2020. Potential benefits of acanthocephalan parasites for chub hosts in polluted environments. Environ. Sci. Technol. 54, 5540–5549.
Nachev, M., Sures, B., 2016. Seasonal profile of metal accumulation in the acanthocephalan *Pomphorhynchus laevis*: a valuable tool to study infection dynamics and implications for metal monitoring. Parasit. Vectors 9, 300–308.
Nikolić, D., Skorić, S., Janković, S., Hegediš, A., Djikanović, V., 2021. Age-specific accumulation of toxic metal(loid)s in northern pike (*Esox lucius*) juveniles. Environ. Monit. Assess. 193, 229.
NN 55, 2013. Ordinance on the Protection of Animals Used for the Scientific Purposes [Pravilnik o zaštiti životinja koje se koriste u znanstvene svrhe].
Ojo, A.A., Wood, C.M., 2007. In vitro analysis of the bioavailability of six metals via the gastro-intestinal tract of the rainbow trout (*Oncorhynchus mykiss*). Aquat. Toxicol. 83, 10–23.
Padilla, I.Y., Vesper, D.J., 2018. Fate, transport, and exposure of emerging and legacy contaminants in karst systems: state of knowledge and uncertainty. In: White, W., Herman, J., Herman, E., Rutigliano, M. (Eds.), Advances in Karst Science. Springer, Cham. Karst Groundwater Contamination and Public Health.
Rajkowska, M., Protasowicki, M., 2013. Distribution of metals (Fe, Mn, Zn, Cu) in fish tissues in two lakes of different trophy in Northwestern Poland. Environ. Monit. Assess. 185, 3493–3502.
Roesijadi, G., Rezvankhah, S., Perez-Matus, A., Mitelberg, A., Torruellas, K., Van Veld, P. A., 2009. Dietary cadmium and benzo(a)pyrene increased intestinal metallothionein expression in the fish *Fundulus heteroclitus*. Mar. Environ. Res. 67 (1), 25–30.
Salati, S., Moore, F., 2010. Assessment of heavy metal concentration in the Khoshk River water and sediment, Shiraz, Southwest Iran. Environ. Monit. Assess. 164, 677–689.
Sertić Perić, M., Matoničkin Kepčija, R., Miliša, M., Gottstein, S., Lajtner, J., Dragun, Z., Filipović Marijić, V., Krasnići, N., Ivanković, D., Erk, M., 2018. Benthos-drift relationships as proxies for the detection of the most suitable bioindicator taxa in flowing waters – a pilot-study within a Mediterranean karst river. Ecotoxicol. Environ. Saf. 163, 125–135.
Sures, B., Steiner, W., Rydlo, M., Taraschewski, H., 1999. Concentrations of 17 elements in the Zebra Mussel (*Dreissena polymorpha*), in different tissues of perch (*Perca fluviatilis*), and in perch intestinal parasites (*Acanthocephalus lucii*) from the subalpine lake Mondsee, Austria. Environ. Toxicol. Chem. 18, 2574–2579.
Sures, B., 2002. Competition for minerals between *Acanthocephalus lucii* and its definitive host perch (*Perca fluviatilis*). Int. J. Parasitol. 32, 1117–1122.
Sures, B., Nachev, M., Selbach, C., Marcogliese, D.J., 2017. Parasite responses to pollution: what we know and where we go in 'Environmental Parasitology'. Parasit. Vectors 10, 65–83.
Šariri, S., Valić, D., Kralj, T., Cvetković, Ž., Mijošek, T., Redžović, Z., Karamatić, I., Filipović Marijić, V., 2024. Long-term and seasonal trends of water parameters in the karst riverine catchment and general literature overview based on CiteSpace. Environ. Sci. Pollut. Res. 31, 3887–3901.
Timi, J.T., Poulin, R., 2020. Why ignoring parasites in fish ecology is a mistake. Int. J. Parasitol. 50, 755–761.
Vardić Smrzlić, I., Valić, D., Kapetanović, D., Dragun, Z., Gjurčević, E., Ćetković, H., Teskeredžić, E., 2013. Molecular characterisation and infection dynamics of *Dentitruncus truttae* from trout (*Salmo trutta* and *Oncorhynchus mykiss*) in Krka River, Croatia. Vet. Parasitol. 197, 604–613.

Publication No. 5: Biomarker-based assessment of sublethal metal exposure in brown trout and parasites acanthocephalans from a protected karst river

Environmental Toxicology and Pharmacology 119 (2025) 104823

Contents lists available at ScienceDirect

Environmental Toxicology and Pharmacology

journal homepage: www.elsevier.com/locate/etap

Biomarker-based assessment of sublethal metal exposure in brown trout and parasites acanthocephalans from a protected karst river

Sara Šariri [a], Tatjana Mijošek Pavin [a], Zuzana Redžović [b], Zoran Kiralj [a], Dušica Ivanković [a], Vlatka Filipović Marijić [a,*]

[a] Ruđer Bošković Institute, Bijenička cesta 54, Zagreb 10000, Croatia
[b] Faculty of Science, Division of Zoology, Horvatovac 102a, Zagreb 10000, Croatia

ARTICLE INFO

Keywords:
Cytosolic proteins
Dentitruncus truttae
Environmental parasitology
Fish intestine
Karst ecosystems
Biomarkers

ABSTRACT

Karst freshwater ecosystems are especially susceptible to metal pollution, even in protected areas. Present study assessed biomarker responses in intestine of *Salmo trutta* and their intestinal parasites acanthocephalans at three sites along the karst Krka River: river source, a wastewater-impacted site, and a site within the Krka National Park. Biomarkers of metal exposure, general stress, lipid peroxidation, antioxidant defense, and tissue metabolic activity were analyzed in relation to season, fish biometry, cytosolic metal(loid) concentrations, and parasite burden. Fish from both the wastewater-impacted site (KRK) and the national park site (KNP) showed moderate stress and significantly elevated lipid peroxidation compared to the river source. Correlation analysis revealed stronger biomarker–metal associations in spring, and higher stress in smaller fish with lower parasite burdens. This study provides rare data on biomarker responses in fish intestine and the first data on metallothionein and cytosolic protein levels in acanthocephalans, which exhibited higher biomarker values than host tissue. These results support biomarker use for early detection of sublethal contamination.

1. Introduction

Protected areas are essential for nature conservation, but in aquatic systems, boundaries of the reserve rarely encompass the entire watershed, allowing pollution to affect even strictly protected areas such as national parks (Fernández-Trujillo et al., 2021). Among pollutants, trace metals are particularly concerning due to their persistence, accumulation in sediments and biota, and potential to induce oxidative stress and other toxic effects in aquatic organisms (Hemmadi, 2017; Rizzo, 2024). This issue is critical in karst environments, where porous carbonate bedrock offers little natural filtration, allowing pollutants to travel long distances with minimal attenuation (Schiperski et al., 2016).

When assessing the ecological status of aquatic ecosystems, certain organisms can serve as bioindicators, providing insight into the conditions of their habitat (Colin et al., 2016). Fish, especially higher trophic-level species, are key bioindicators of metal pollution in aquatic environments (Okwuosa et al., 2019). While most studies focus on muscle, blood, liver, kidney, or gill tissues (Hemmadi, 2017), the intestine is increasingly recognized for its role in metal uptake and detoxification and is gaining importance as a bioindicator tissue (Mijošek et al., 2021). In fact, some research suggests that dietary metal uptake through the intestine may surpass uptake from water via the gills and skin (Okwuosa et al., 2019). Intestinal parasites acanthocephalans (Acanthocephala) can also serve as effective bioindicators, often accumulating metals at higher levels than host tissues, surrounding water, or other organisms (Nachev and Sures, 2016; Sures, 2001). They may even function as metal sinks, potentially reducing host metal burdens (Sures, 2001; Filipović Marijić et al., 2014).

Changes within a biological system that indicate exposure to, or sublethal effects of, environmental contaminants such as metals are called biomarkers. They can occur at any level of biological organization, with molecular responses appearing first, followed by biochemical, physiological, and eventually morphological or histological changes (Hemmadi, 2017). While higher-level biomarkers are more ecologically relevant, lower-level biomarkers are more sensitive and serve as early warning indicators of contamination (Hemmadi, 2017; Sures, 2001). However, data on biomarker responses in the intestinal tissue of wild fish from karst ecosystems remain extremely limited (Mijošek et al.,

* Correspondence to: Laboratory for Biological Effects of Metals, Division for Marine and Environmental Research, Ruđer Bošković Institute, Bijenička c. 54, Zagreb 10000, Croatia.
E-mail address: vfilip@irb.hr (V. Filipović Marijić).

https://doi.org/10.1016/j.etap.2025.104823
Received 23 July 2025; Received in revised form 19 September 2025; Accepted 22 September 2025
Available online 25 September 2025

2019a), and no study has yet examined biochemical biomarkers in acanthocephalans.

This study addresses these gaps by assessing biomarker responses in the intestine of brown trout (*Salmo trutta* Linnaeus, 1758) from the karst Krka River in Croatia, a system known for tufa deposition and diverse habitats supporting endemic, rare, and threatened species (Bonacci et al., 2017). The lower course of the river was proclaimed a national park, but upstream section is impacted by inadequately purified industrial and municipal wastewaters. Compared to pristine conditions at the river source, chemical status of river at the site near the wastewater discharges is degraded (Mijošek et al., 2023; Šariri et al., 2024). Further downstream, within the Krka National Park, overall water quality improves, but metal concentrations remain elevated in fish intestinal tissue, acanthocephalans, and especially in fish gut contents and river sediments (Mijošek et al., 2023; Šariri et al., 2024; Mijošek et al., 2024). While previous studies have reported the effects of wastewater on trout populations directly exposed to these discharges (Mijošek et al., 2019a), the condition of fish within the downstream protected area, where metal accumulation has been detected, remains unknown.

Therefore, the aim of the present study was to assess the impact of contaminants, primarily metals, using a multi-biomarker approach in the intestinal tissue of *S. trutta* and their intestinal parasites acanthocephalans (*Dentitruncus truttae* Sinzar, 1955), in both a wastewater-affected section of the river and downstream within the Krka National Park. Set of applied biomarkers involved metallothioneins (MTs) as specific indicators of metal exposure and total cytosolic proteins (TP) as indicators of general stress (Hemmadi, 2017; Sanders and Dyer, 1994). Malondialdehyde (MDA) served as a marker of oxidative damage through lipid peroxidation (Hemmadi, 2017; Rizzo, 2024). Antioxidant defenses were assessed through the primary enzymes superoxide dismutase (SOD) and catalase (CAT), the secondary enzyme glutathione S-transferase (GST), and the non-enzymatic tripeptide glutathione (GSH) (Hemmadi, 2017; Hayes et al., 2005). Lactate dehydrogenase (LDH) was measured as an indicator of metabolic capacity and anaerobic activity of the tissue (Osman et al., 2010).

2. Materials and methods

2.1. Study area and fish sampling

This study was conducted in the upper reaches of the karst Krka River during spring (April) and autumn (October) of 2021. Brown trout (*Salmo trutta* Linnaeus, 1758) were sampled at three locations along the river: the source (KRS), representing an unpolluted reference site; KRK, located near municipal wastewater discharges from the town of Knin and downstream of a tributary influenced by industrial effluents; and KNP, a site downstream of a tufa lake within the Krka National Park (Fig. S1). Water quality has previously been assessed through physicochemical and organic parameter analysis, metal concentration measurements, and ecotoxicological testing on water fleas and microalgae (Mijošek et al., 2023; Šariri et al., 2024, 2025a). Moreover, metal concentrations have been measured in river sediment, fish intestinal tissue, gut content, and acanthocephalans (Mijošek et al., 2024).

Fish were collected by electrofishing in accordance with the Croatian standard HRN EN 14011 (HRN EN 14011, 2005) approved by Croatian Ministry of Agriculture, with 24 specimens sampled at KRS and 26 at each of the KRK and KNP sites. Immediately after capture, fish were transferred alive to a field laboratory in oxygen-aerated tanks containing river water from the respective sites. Prior to dissection, fish were euthanized using tricaine methanesulfonate (MS-222) (Sigma-Aldrich, USA) following the dosage described by Topić Popović et al. (2012), in compliance with the Croatian Ordinance on the Protection of Animals Used for Scientific Purposes (NN 55, 2013). Fish sacrifice and tissue dissection was performed in the laboratory authorized for fish sacrifice and work with fish body, organs and tissues by the Ministry of Agriculture, Veterinary and Food Safety Department (License number: HR-POK-025).

For each individual, total length, body mass, liver mass, and gonad mass were recorded, and additionally Fulton's condition index (FCI) (Ricker, 1975), hepatosomatic index (HSI) (Heidinger and Crawford, 1977), and gonadosomatic index (GSI) were calculated (Wootton, 1990). The intestine was isolated on ice, cleared of external fat, and carefully opened with a longitudinal incision along the intestinal wall. After removal of gut content, intestinal parasites acanthocephalans were counted, removed with tweezers, and frozen in cryotubes in liquid nitrogen. Intestinal tissue was weighed and also stored in liquid nitrogen. All samples were kept at −80 °C until further analysis.

2.2. Preparation of intestinal tissue and acanthocephalans for biomarker analyses

Prior to the biomarker analyzes, portions of the posterior intestine were excised, weighed, and homogenized on ice using a combination of an Ultra-Turrax T25 homogenizer (IKA, Germany) and a Potter-Elvehjem homogenizer (Glas-Col, USA). The homogenizers were thoroughly rinsed between each specimen. All procedures were conducted on ice or in pre-cooled centrifuges to preserve sample integrity. All aliquots for each analysis were taken in duplicate and stored at −80 °C until further use.

For the analysis of MT, TP, MDA, CAT, GST, LDH and cytosolic metal concentrations, tissue was homogenized in five volumes of ice-cold buffer containing 100 mM Tris-HCl/base (pH 8.1), 1 mM dithiothreitol (DTT) (Sigma-Aldrich, USA), 0.5 mM phenylmethylsulfonyl fluoride (PMSF) (Sigma-Aldrich, USA), and 0.006 mM leupeptin (Sigma-Aldrich, USA), following established protocols (Mijošek et al., 2019a; Marijić and Raspor, 2010). The homogenates were centrifuged in an Avanti J-E centrifuge (Beckman Coulter, USA) under different conditions, to separate different cellular fractions, depending on the biomarker: at 3000 × g for 10 min at 4 °C for MDA analysis; at 10,000 × g for 30 min at 4 °C for CAT, GST and LDH activity and total protein concentration; at 50,000 × g for 2 h at 4 °C resulting cytosolic fraction was used for MT, TP, and metal concentration analyses. Detailed description of the cytosolic fraction digestion procedure and the determination of macro and trace elements by ICP-MS is provided in Supplementary File S2.2, while the corresponding results on cytosolic element concentrations in fish are presented in Table S1.

For GSH analysis, samples were homogenized in five volumes of ice-cold 5 % sulfosalicylic acid (SSA) (Kemika, Croatia), followed by centrifugation at 11,000 × g for 10 min at 4 °C. Cytosolic SOD activity was determined using the Superoxide Dismutase Assay Kit, Item No. 706002 (Cayman Chemical, USA). According to the manufacturer's protocol, tissue was first homogenized in five volumes of cold 20 mM HEPES buffer (pH 7.2) containing 1 mM EGTA, 210 mM mannitol, and 70 mM sucrose per gram of tissue, and then centrifuged at 10,000 × g for 15 min at 4 °C. The resulting supernatant was used for both SOD activity and protein measurement.

Acanthocephalan samples were processed similarly to fish intestinal tissue. After weighing, multiple specimens from the same fish (mean ± SD: 4 ± 1) were pooled to obtain sufficient mass for biomarker analysis. Whole organisms were homogenized in 15 volumes of ice-cold buffer containing 100 mM Tris-HCl/base (pH 8.1 at 4 °C), 1 mM DTT, 0.5 mM PMSF, and 0.006 mM leupeptin using a Potter-Elvehjem homogenizer. The homogenates were centrifuged at 50,000 × g for 2 h at 4 °C (Avanti J-E centrifuge with adapters for 1.5 mL tubes), and the resulting supernatants (cytosolic fractions) were collected in duplicate and stored at −80 °C until further analysis. Due to the limited cytosolic volume, it was not possible to measure the full set of biomarkers and metal concentrations as in fish tissues. Given the parasites' known efficiency in metal accumulation, MT and TP levels were prioritized.

2.3. Biomarker analyses

Because *Dentitruncus truttae* specimens are small and yield limited sample volumes, MT concentrations were measured by differential pulse voltammetry—a highly sensitive electrochemical method requiring minimal volume of sample (Adam et al., 2008). For consistency, fish MT levels were measured using the same technique. All other biomarkers were determined spectrophotometrically with an Infinite® 200 PRO microplate reader (Tecan, Switzerland).

2.3.1. MT analysis

Cytosolic samples from fish and acanthocephalans were heat-treated at 85 °C for 10 min prior to MT analysis to denature high molecular weight proteins and isolate the thermostable protein fraction containing MT. After centrifugation at 10,000 × g for 15 min at 4 °C using a Biofuge Fresco centrifuge (Heraeus, Germany), the denatured proteins were pelleted and discarded, and the MT-rich supernatant was used for MT analysis by differential pulse voltammetry. The modified Brdička procedure (Raspor et al., 2001) was applied using a 797 VA Computrace voltammetric measuring stand (Metrohm, Switzerland) with a three-electrode system. The supporting electrolyte consisted of a 1:1 mixture of 2 M NH_4Cl/NH_4OH and 1.2×10^{-3} M $Co(NH_3)_6Cl_3$ (pH = 9.5). The applied measurement parameters were set according to Mijošek et al. (2018). Final MT concentrations were calculated from the calibration curve using a commercially available rabbit liver MT-2 standard (Enzo Life Sciences, USA) and expressed as milligrams of MT per gram of tissue wet weight (mg g^{-1} w.w.).

2.3.2. TP analysis

Total protein concentrations in cytosolic samples from fish and acanthocephalans were determined in triplicates using the method of Lowry et al. (1951) and the absorbance was measured at 750 nm. A standard curve (0–2 mg mL^{-1}) was prepared using bovine serum albumin (BSA) (Serva, Germany), and results were expressed as milligrams of TP per gram of tissue wet weight (mg g^{-1} w.w.).

2.3.3. MDA analysis

MDA concentration was determined spectrophotometrically using a method adapted from Botsoglou et al. (1994) and Ringwood et al.(2003), which is based on the reaction of MDA with 2-thiobarbituric acid (TBA). Absorbance was measured at 535 nm. 1,1,3,3-Tetramethoxypropane (TEP) (Aldrich, USA), dissolved in 1 N HCl, was used to prepare the MDA standard curve (0–50 μmol L^{-1}) in 100 mM Tris-HCl/Base buffer and final MDA concentrations were expressed as nanomoles per gram of tissue wet weight (nmol g^{-1} w.w.).

2.3.4. SOD analysis

Cytosolic SOD activity was measured in duplicates using the Cayman's Superoxide Dismutase Assay Kit (Cayman Chemical, USA), which is based on the generation of superoxide radicals through the reaction of hypoxanthine with xanthine oxidase. In the absence of SOD, these radicals react with a tetrazolium salt to produce a formazan dye, the absorbance of which was measured at 460 nm over a 3-minute period. One unit of SOD was defined as the amount of enzyme required to achieve 50 % dismutation of the superoxide radical, expressed as the change in absorbance per minute at 25 °C and pH 8.0. The assay detects Cu/Zn-SOD, Mn-SOD, and Fe-SOD. A standard curve was prepared using bovine erythrocyte Cu/Zn-SOD provided in the kit, and SOD activity was calculated following the manufacturer's protocol.

The results were normalized to protein content in the corresponding cytosolic fraction. Protein concentrations were determined by the Bradford method (Bradford, 1976) and absorbance was measured at 595 nm to avoid potential interference from the homogenization buffer (HEPES) with the Lowry method (Lowry et al., 1951). Protein concentrations were calculated using a BSA (Serva, Germany) standard curve ranging from 0.0625 to 0.5 mg mL^{-1} . Final SOD activity was expressed as units per milligram of cytosolic protein (U mg^{-1} prot.).

2.3.5. CAT analysis

CAT activity was determined in triplicates according to the method described by Claiborne (Claiborne, 1985) and modified for microplate assays by Li and Schellhorn (Li and Schellhorn, 2007). Samples were mixed with 15.8 mM hydrogen peroxide (H_2O_2, Suprapur®, Merck, Germany) and the decomposition of H_2O_2 was monitored by measuring absorbance at 240 nm every 10 s for a total of nine intervals at 25 °C. One unit of CAT activity was defined as the amount of enzyme that degrades 1 μmol of H_2O_2 per minute (μM min^{-1}). Activity was calculated as units per milliliter (U mL^{-1}) using a molar extinction coefficient of 43.6 M^{-1} cm^{-1} (Aebi, 1984), and normalized to protein content measured according to Lowry et al. (1951) to final unit per milligram of protein (U mg^{-1} prot.).

2.3.6. GSH analysis

Total GSH concentrations were determined spectrophotometrically using the DTNB–glutathione reductase recycling assay, based on the method by Tietze (1969) and adapted for microplate from Rahman et al. (2006). The assay relies on the reduction of 5,5′-dithio-bis(2-nitrobenzoic acid) (DTNB) by GSH to form the yellow-colored 5-thio-2-nitrobenzoic acid (TNB), which absorbs at 412 nm. The absorbance was recorded every 60 s for six intervals at 30 °C. GSH (Sigma-Aldrich, USA) standards (3.125–25 nM mL^{-1}) were prepared in 0.5 % sulfosalicylic acid (SSA) and a calibration curve was used to calculate the GSH levels. 1 % SSA was used as a blank. Final results were expressed as nanomoles of GSH per gram of tissue wet weight (nmol g^{-1} w.w.).

2.3.7. GST analysis

GST activity was measured in triplicate according to the method of Habig et al. (1974), modified and adapted for use in microplates by Kiralj et al. (2025). The assay is based on the GST-catalyzed conjugation of reduced GSH with 1-chloro-2,4-dinitrobenzene (CDNB), forming a product with maximum absorbance at 340 nm, which was recorded every 15 s for 3 min (13 intervals total) at 28 °C. One unit of GST activity was defined as the amount of enzyme that catalyzes the formation of 1 μmol of the CDNB–GSH conjugate per minute (μM min^{-1}). Activity was calculated using a molar extinction coefficient of 9.6 mM^{-1} cm^{-1} and expressed as units per milligram of protein (U mg^{-1} prot.), based on the protein concentrations previously determined in the post-mitochondrial fraction according to Lowry et al. (1951).

2.3.8. LDH analysis

LDH activity was measured according to the method of Bergmeyer et al. (1965), which is based on the enzymatic oxidation of D-lactate in the presence of NAD^+, resulting in the formation of pyruvate and NADH. Absorbance at 340 nm was measured every 20 s for three minutes at 25 °C. Enzyme activity was calculated using the molar extinction coefficient of NADH (6.22 mM^{-1} cm^{-1}) and expressed as micromoles of NADH oxidized per minute per milligram of protein (U mg^{-1} prot.).

2.4. Statistical analysis

Statistical analyses and data visualization were performed using SigmaPlot 11.0 (Systat Software, USA) and RStudio (R version 4.4.3, R Core Team). Data are presented as mean ± standard deviation (SD), and statistical significance was accepted at $p < 0.05$. Due to occasional violations of normality and homogeneity of variance, seasonal differences in biomarker responses were assessed using the non-parametric Mann–Whitney *U* test, while differences between sampling sites were tested using the Kruskal–Wallis one-way analysis of variance. Correlations among biomarkers and other parameters were evaluated using Spearman's rank correlation coefficient. Graphs were generated in R using the packages *ggplot2*, *patchwork*, *openxlsx*, *corrplot*, and *RColorBrewer*.

3. Results

3.1. Biometric and epidemiological characterization of fish used in the study

A total of 76 fish were analyzed in this study, including 29 males (38 %), 46 females (61 %), and one juvenile. The sex ratio was the same in both seasons. Since none of the measured biomarkers differed significantly between males and females, all individuals were analyzed together. Biometric parameters of fish were statistically significant for the average body mass and total length, which were higher in autumn at all sites. FCI and HSI were higher in spring than in autumn, with FCI significantly higher at KRK and HSI at KNP (Table 1). GSI was higher in autumn, showing significant differences at KRS and KRK. Spatial difference showed that fish from KNP had lower body mass and length compared to other locations, statistically significant only when compared with fish from KRS in spring (Table 1).

Intestinal parasites acanthocephalans were present in nearly all brown trout specimens analyzed in this study (prevalence 92–100 % across seasons and sampling sites, Table 1). Only one acanthocephalan species, *Dentitruncus truttae*, was identified. Although infection intensity varied considerably among individual fish, it was generally higher in autumn than in spring at all sites, with a statistically significant increase at KRK, where the mean number of parasites per fish in autumn was 5.6 times greater than in spring.

3.2. Biomarker of metal exposure (MT) in fish and acanthocephalans

MT concentrations were consistently higher in acanthocephalans than in fish intestine across all sites and seasons (Fig. 1). The average levels in fish intestine ranged 0.675(±0.146)–1.883(±0.807) mg g^{-1} w.w. and in *D. truttae* 1.56(±0.27)–2.53(±0.86) mg g^{-1} w.w. (Fig. 1).

Seasonal variation showed for both fish intestinal tissue and parasites higher levels in spring, being significant in fish from KRK and KNP and in acanthocephalans from KRS (Fig. 1). Spatial differences were significant in autumn, with higher MT levels in fish intestine at KRS than at KRK, whereas no significant differences were observed in spring, despite a tendency for higher concentrations at downstream sites (Fig. 1). Spearman correlation across the full dataset showed no significant relationship between MT levels in fish intestine and in acanthocephalans from the same hosts, indicating distinct biological responses and patterns of MT induction. Acanthocephalans also showed partially opposite spatial trends compared with intestinal tissue, although these differences were not significant.

3.3. Biomarker of general stress (TP) in fish and acanthocephalans

TP levels were consistently higher in acanthocephalans than in fish intestine across all sites and seasons, with differences exceeding those observed for MT (Fig. 1). Average TP concentrations ranged 48.2(±9.0)-67.0(±12.6) mg g^{-1} w.w. in fish intestine and 80.3(±37.2)-132.7 (±49.2) mg g^{-1} w.w. in *D. truttae* (Fig. 2). Similar to the seasonal pattern of MT, TP concentrations in both fish and acanthocephalans were higher in spring than in autumn (Fig. 2). Spatial patterns differed between hosts and parasites, with no statistically significant site-specific differences. Individual variability of MT and TP levels was much higher in acanthocephalans than in fish intestine, especially in spring.

3.4. Biomarkers of oxidative stress in fish

3.4.1. Biomarker of lipid peroxidation (MDA)

Average MDA concentrations ranged 106(±21)-161(±38) nmol g^{-1} w.w., depending on the site and season. They indicated generally higher oxidative stress-induced lipid peroxidation in spring than in autumn, significantly at KRK (Fig. 3). Spatially, MDA levels were highest in fish from KNP and lowest in those from KRS (Fig. 3). In spring, they were significantly higher at KRK and KNP compared to KRS, while in autumn at KNP compared to the other sites.

3.4.2. Biomarkers of antioxidant defense (SOD, CAT, GSH, GST)

In the fish intestine, antioxidant defense biomarkers showed site- and season-dependent patterns. SOD activity (2.51(±1.27)–3.74(±1.56) U mg^{-1} prot.) and CAT activity (13.82(±3.78)–21.70(±5.78) U mg^{-1} prot.) tended to be higher in spring and at downstream sites, particularly KNP, but without significant differences (Fig. 4a,b). GSH concentrations (1100(±181)–1542(±336) nmol g^{-1} w.w.) followed the same seasonal trend and were significantly elevated in spring at KRK and KNP, with downstream sites showing generally higher values than the reference site, but spatial differences were not statistically significant (Fig. 4c). In contrast, GST activity (0.039(±0.009)–0.075(±0.026) U mg^{-1} prot.) was consistently higher in autumn, with significant differences at KRS and showed a decreasing trend downstream, particularly pronounced in autumn when activity at KRS was significantly higher than at KNP (Fig. 4d).

3.5. Biomarker of tissue metabolic activity (LDH) in fish

LDH activity in *S. trutta* intestine ranged 0.169(±0.032)–0.220 (±0.030) U mg^{-1} prot. (Fig. 5), representing the first available data for this species. Activity was generally higher in autumn than in spring, with significant differences at KRS and KRK. Spatially, LDH tended to slightly decrease downstream (from KRS to KNP), showing seasonal and spatial

Table 1
Biometric characteristics (mean ± SD) of *Salmo trutta* from the Krka River source (KRS), contaminated site near the Town of Knin (KRK), and location in the national park (KNP) across two sampling campaigns, including basic epidemiological data on acanthocephalan infection. Statistically significant seasonal differences at each site are marked with asterisk ($p < 0.05$, Mann-Whitney U-test). Differences between sites within the same season are indicated by different superscript letters ($p < 0.05$, Kruskal Wallis test with Dunn's test for all-pairwise comparisons).

	Krka River source (KRS)		Town of Knin (KRK)		Krka National Park (KNP)	
	spring 2021	autumn 2021	spring 2021	autumn 2021	spring 2021	autumn 2021
	n = 12	n = 12	n = 13	n = 13	n = 13	n = 13
total length (cm)	22.9 ± 4.7*^{C}	28.2 ± 4.0*	20.2 ± 4.6*	34.3 ± 17.5*	17.5 ± 3.3*^{A}	26.2 ± 6.2*
body mass (g)	124.6 ± 63.6*^{C}	224.6 ± 90.3*	97.6 ± 85.8*	257.1 ± 80.7*	63.4 ± 55.0*^{A}	195.7 ± 125.7*
FCI (g cm^{-3} × 100)	0.94 ± 0.09	0.95 ± 0.07	1.00 ± 0.08*	0.88 ± 0.26*	1.02 ± 0.10	0.94 ± 0.11
HSI (%)	1.08 ± 0.21 ^{C}	1.49 ± 0.64	1.37 ± 0.42	1.71 ± 0.74 ^{C}	1.45 ± 0.38*^{A}	1.04 ± 0.38*^{B}
GSI (%)	0.53 ± 0.38*^{B}	4.78 ± 3.89*	0.23 ± 0.10*^{A}	5.60 ± 4.91*	0.31 ± 0.15	2.77 ± 3.53
sex (number of F/M/n.d.)	6/6/0	7/4/1	7/6/0	8/5/0	10/3/0	8/5/0
parasite infection prevalence (number and % of infected fish)	11, 92 %	12, 100 %	12, 92 %	13, 100 %	12, 92 %	12, 92 %
parasite infection intensity (number of parasites per fish)	38 ± 27^{B}	55 ± 32	11 ± 12*^{A}	62 ± 30*	13 ± 12	51 ± 52
total number of parasites	461	662	149	811	174	664

FCI – Fulton's condition index, HSI –hepatosomatic index, GSI –gonadosomatic index, n.d. – not determined

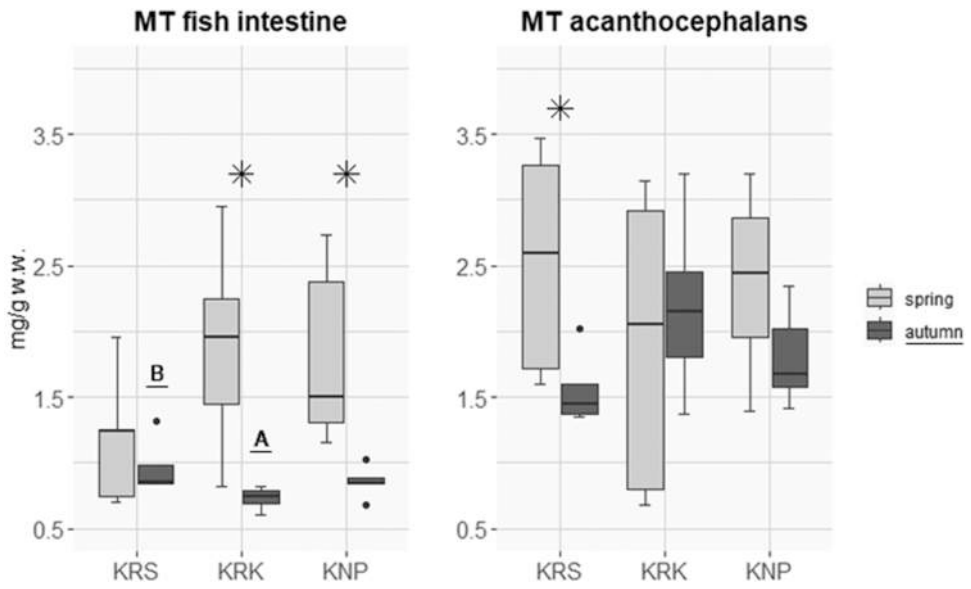

Fig. 1. Electrochemically determined metallothionein concentrations (MT) in the intestinal tissue of *Salmo trutta* and in their intestinal parasites (*Dentitruncus truttae*, Acanthocephala) from three sites along the Krka River - Krka River source (KRS), Krka near the Town of Knin (KRK) and Krka National Park (KNP). Data are presented as the median (line in the box), 25th and 75th percentiles (boundaries of the box), nonoutlier minimum and maximum (whiskers below and above the box) and outliers. Statistically significant differences among different locations within the same season are indicated in different letters ($p < 0.05$, Kruskal Wallis test with Dunn's test for all-pairwise comparisons) and between two seasons at the same location with an asterisk ($p < 0.05$, Mann-Whitney U-test).

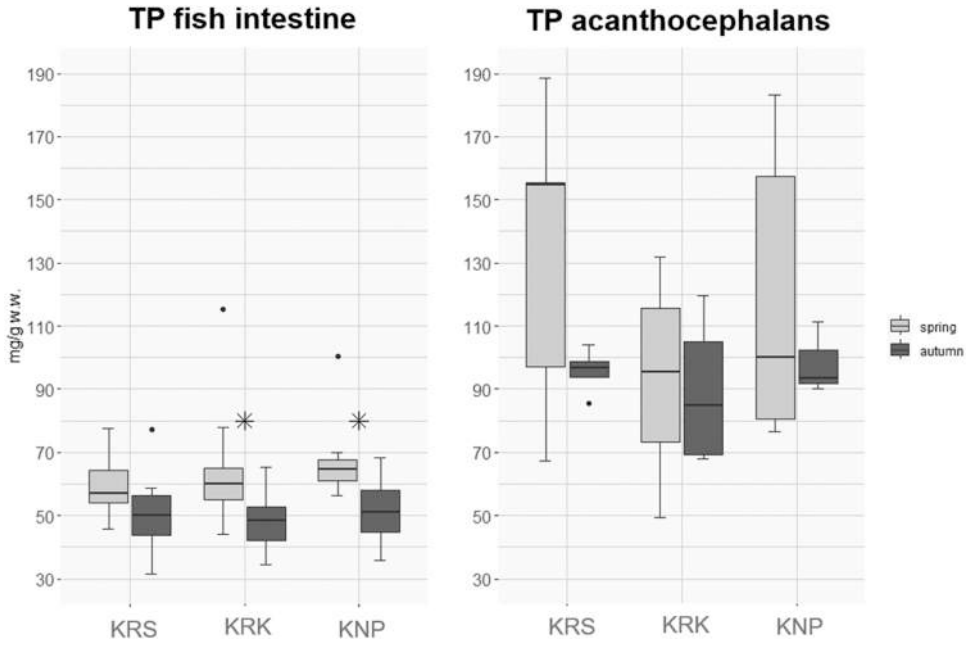

Fig. 2. Concentrations of total cytosolic proteins (TP) in the intestinal tissue of *Salmo trutta* and in their intestinal parasites (*Dentitruncus truttae*, Acanthocephala) from three sites along the Krka River- Krka River source (KRS), the Town of Knin (KRK) and Krka National Park (KNP). Data are presented as the median (line in the box), 25th and 75th percentiles (boundaries of the box), nonoutlier minimum and maximum (whiskers below and above the box) and outliers. Statistically significant differences between two seasons at the same location are indicated with an asterisk ($p < 0.05$, Mann-Whitney U-test).

patterns similar to GST but opposite to other biomarkers (Fig. 5).

3.6. Correlation of fish biomarker responses with cytosolic metal(loid) levels and biometric and epidemiological parameters

Most biomarkers showed significantly ($p < 0.05$) positive correlations with a greater number of cytosolic metals in spring compared to autumn (Fig. 6a). In spring, TP, MDA, and SOD were associated with multiple metals (Co, Cu, Fe, Mn, Mo, Ni, Se) while in autumn, significant correlations were scarce and limited mainly to Cd, Cu and Zn. GSH was positively correlated with Fe and Zn in spring and with As in autumn. Overall, Co, Cu, Mo, Fe, Mn, and Ni were the metals most consistently linked to biomarker responses.

As fish mass was highly correlated with length ($r = 0.987$ in spring and 0.978 in autumn, $p < 0.05$), only mass was selected as a biometric characteristic for testing relations with biomarker responses. Most biomarkers were significantly ($p < 0.05$) negatively correlated with fish body mass and acanthocephalan infection intensity, indicating higher

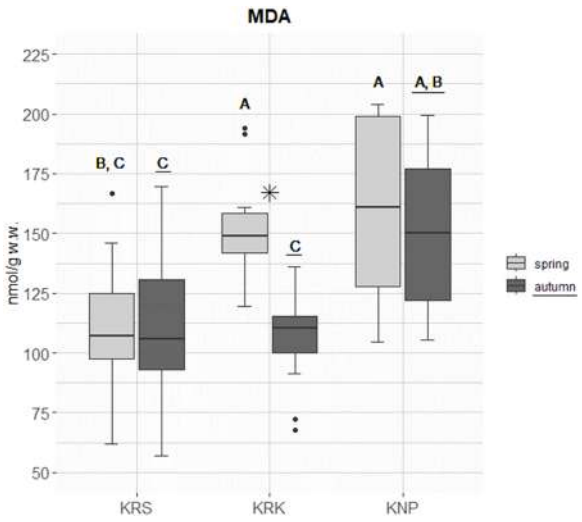

Fig. 3. Concentrations of malondialdehyde (MDA) in the intestinal tissue of *Salmo trutta* from three sites along the Krka River - Krka River source (KRS), the Town of Knin (KRK) and Krka National Park (KNP). Data are presented as the median (line in the box), 25th and 75th percentiles (boundaries of the box), nonoutlier minimum and maximum (whiskers below and above the box) and outliers. Statistically significant differences among different locations within the same season are indicated in different letters ($p < 0.05$, Kruskal Wallis test with Dunn's test for all-pairwise comparisons) and between two seasons at the same location with an asterisk ($p < 0.05$, Mann-Whitney U-test).

general and oxidative stress in smaller fish and in those with lower parasite burdens (Fig. 6b). In spring, TP, MDA, CAT and GSH were all inversely related to both fish body mass ($r = -0.450$ for TP, -0.606 for MDA, -0.595 for CAT, -0.664 for GSH) and acanthocephalan infection intensity ($r = -0.419$ for TP, -0.638 for MDA, -0.636 for CAT, and -0.581 for GSH). In autumn, SOD activity was negatively correlated with FCI ($r = -0.512$) and parasite infection intensity ($r = -0.458$). In contrast, LDH activity correlated significantly positive with fish body mass ($r = 0.483$) and parasite infection intensity ($r = 0.411$) and negatively with HSI ($r = -0.389$) (Fig. 6b).

4. Discussion

4.1. Biometric and epidemiological characterization of fish used in the study

Average body mass and total length of fish from all sampling sites were significantly higher in autumn than in spring. Such pattern agrees with our previous observations in the Krka River (Mijošek et al., 2019a), coincides with the brown trout spawning period and reflects the presence of more mature individuals (Smialek et al., 2021). Lower FCI and HSI in autumn, together with higher GSI, likely resulted from energy reallocation from somatic growth to gonad development during the pre-spawning and spawning periods, leading to reduced body condition and increased gonad mass (Flores et al., 2019; Kara and Alp, 2005). At KNP, where fish were generally smaller and possibly younger, elevated GSI in autumn was less pronounced, suggesting incomplete sexual maturity.

Infection with *D. truttae* was highly prevalent, consistent with previous reports from the Krka River (Mijošek et al., 2024; Vardić Smrzlić et al., 2013; Mijošek et al., 2022). Higher infection intensity in autumn reflected the reproductive cycle of the parasite's intermediate hosts, gammarids, which are more abundant during this season (Kennedy, 1985). Overall, biometric parameters of fish and acanthocephalan infection were mostly influenced by fish physiology and parasite life cycle, respectively, without direct connection to the contaminant exposure.

4.2. Biomarker of metal exposure (MT) in fish and acanthocephalans

Intestinal MT concentrations were comparable with the previously reported average levels of 0.85–1.5 mg g^{-1} w.w. in the intestines of brown trout from the Krka River (2015/2016) (Mijošek et al., 2019b). Comparison with other freshwater fish from Croatian lowland rivers, such as Prussian carp (*Carassius gibelio*) and the European chub (*Squalius cephalus*), which exhibited higher average intestinal MT levels (2.5–3 mg g^{-1} w.w.) (Mijošek et al., 2021; Marijić and Raspor, 2010), indicated species-specific variability and possible differences in metal exposure and conditions in karst and lowland rivers.

While metallothioneins and metallothionein-like proteins have previously been identified in the transcriptome of *D. truttae*, their concentrations have not yet been quantified or compared with the host tissues (Šariri et al., 2025b). Consistently higher MT levels in acanthocephalans than in fish intestine may reflect previously observed higher accumulation of Cd, Cu and Pb in parasites (bioconcentration factors 4.9–86) (Mijošek et al., 2024), as these metals are among the strongest MT inducers (Viarengo et al., 1999). Other elements also accumulated to a greater extent in acanthocephalans (Mijošek et al., 2024), which may have further contributed to the MT induction.

To our knowledge, MT levels in acanthocephalans have so far only been reported by Petrlova et al (Petrlova et al., 2007). for *Acanthocephalus lucii* and *Acanthocephalus anguillae,* where very low concentrations were detected, but using a different electrochemical technique. The higher concentrations observed in our study likely reflect methodological and possible species-specific differences.

Previous results on metal levels in this study area showed that their seasonal differences in water were not significant (Mijošek et al., 2023), while higher metal accumulation in fish intestinal tissue and parasites was observed in spring (Mijošek et al., 2024), as also confirmed by our data on cytosolic metal levels (Table S1). Such patterns contributed to higher MT levels in spring, especially at KNP, where increased intestinal MTs were also consistent with higher metal levels in gut content and sediments. Our results suggest that diet may also represent an important source of metal accumulation in the intestinal tissue and parasites (Mijošek et al., 2024), and indicated the importance of applying intestine as a bioindicator tissue. Elevated MTs in spring likely reflect increased feeding, metabolic activity, and dietary metal uptake (Mijošek et al., 2024; Marijić and Raspor, 2010).

In autumn, significantly elevated MT levels in the intestine of fish from KRS were associated with higher Cd accumulation, an important MT inducer (Wang et al., 2014), consistently reported in previous studies on brown trout from the Krka River (Mijošek et al., 2019a, 2019b), as well as in current data (Mijošek et al., 2024). By contrast, Cu and Zn were more elevated in fish from KRK and KNP, particularly in spring (Table S1) (Mijošek et al., 2024), suggesting that multiple metals contributed to MT synthesis. Therefore, MT concentrations did not follow a uniform spatial or temporal pattern, making it difficult to establish a clear relationship with any single element. Such variability reflects the combined effects of exposure, water chemistry, season, age, sex, reproduction, and feeding status, which all should be considered for the proper data interpretation (Marijić and Raspor, 2010).

Future research should address the potential effects of acanthocephalan prevalence and infection intensity on MT levels in both parasites and hosts, to better define variations in MT levels and their dependence on different abiotic and biotic parameters. To our knowledge, this relation has not yet been investigated.

4.3. Biomarker of general stress (TP) in fish and acanthocephalans

TP concentrations in fish were comparable to those reported for brown trout from the Krka River in 2015/2016 (Mijošek et al., 2019a) and slightly lower than values reported for *S. cephalus* from the Sava River (Marijić and Raspor, 2010). Data on TP in helminths and invertebrates are limited, and to our knowledge, no values have been

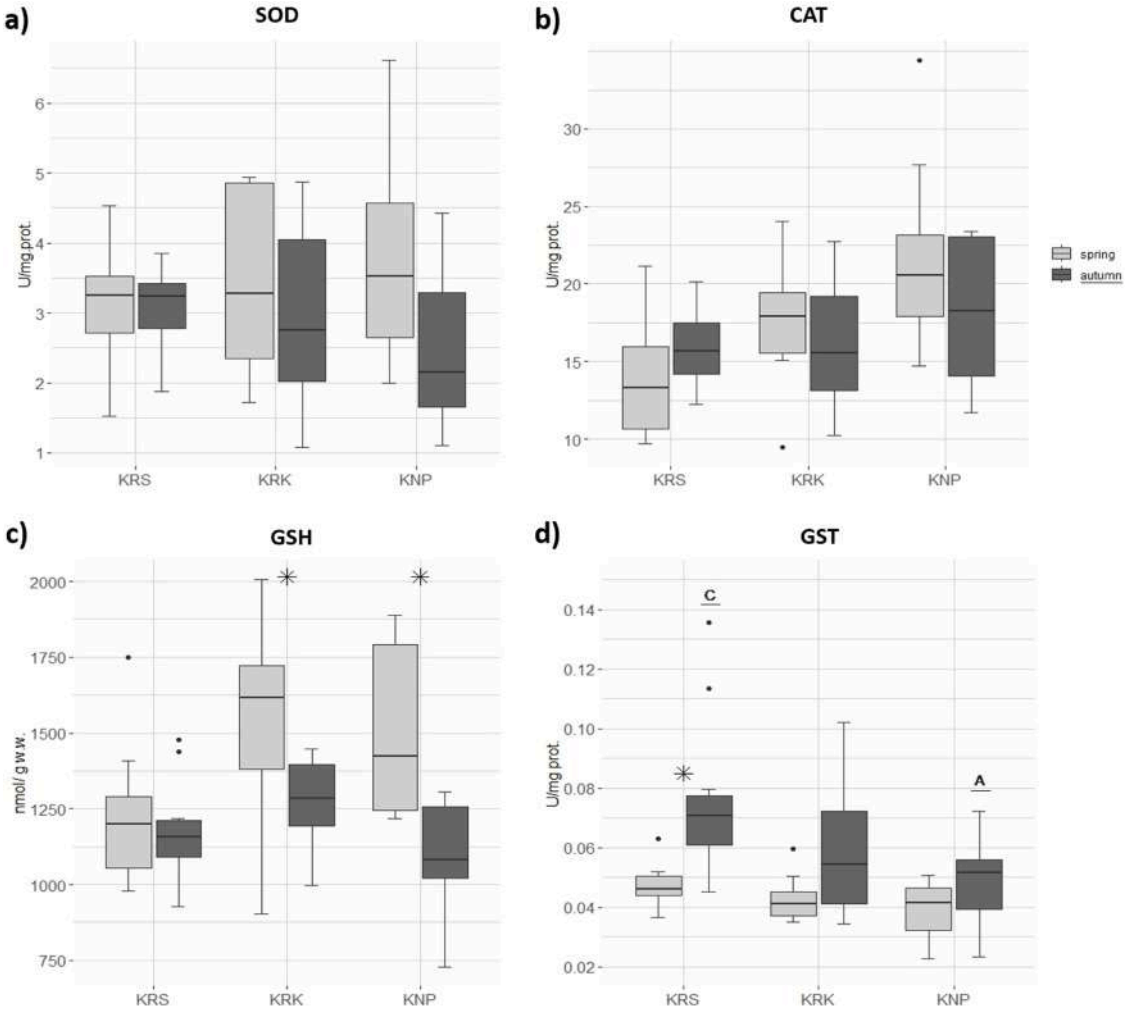

Fig. 4. Activity of enzymes a) superoxide dismutase (SOD), b) catalase (CAT), d) glutathion-S-transferase (GST) and c) concentration of glutathione (GSH) in the intestinal tissue of *Salmo trutta* from three sites along the Krka River - Krka River source (KRS), the Town of Knin (KRK) and Krka National Park (KNP). Data are presented as the median (line in the box), 25th and 75th percentiles (boundaries of the box), nonoutlier minimum and maximum (whiskers below and above the box) and outliers. Statistically significant differences among different locations within the same season are indicated in different letters ($p < 0.05$, Kruskal Wallis test with Dunn's test for all-pairwise comparisons) and between two seasons at the same location with an asterisk ($p < 0.05$, Mann-Whitney U-test).

reported for any Acanthocephala species to date. TP concentrations in *D. truttae* exceeded those reported for marine and freshwater mussels (*Mytilus edulis*, *Unio crassus*) and amphipods (*Gammarus duebeni*), indicating a potential taxon-specific pattern (Kiralj et al., 2025; Lysenko et al., 2014).

Higher TP levels in spring corresponded with increased fish activity and metabolic demands (Kara and Alp, 2005), as well as elevated intestinal metal and MT levels observed in our study (Table S1) (Mijošek et al., 2024). These seasonal differences were reflected in increased cytosolic protein synthesis in both fish and acanthocephalans. Additionally, the higher individual variability of MT and TP in acanthocephalans compared to fish intestine was also observed for metal levels, further supporting the link between stress biomarkers and metal exposure (Mijošek et al., 2024).

4.4. Biomarkers of oxidative stress in fish

4.4.1. Biomarker of lipid peroxidation (MDA)

Average MDA concentrations in the present study were similar to previously measured metal concentrations in trout intestine, which ranged 147(±37)–166(±41) nmol g^{-1} w.w. in 2015/2016 (Mijošek et al., 2019a). However, these values are considerably higher than, for example, those reported for the liver and kidney of cultivated rainbow trout (*Oncorhynchus mykiss*) (Elia et al., 2018), liver and muscle of cultivated brown trout (*S. trutta*) (Mila-Kierzenkowska et al., 2005) and intestine of wild Vardar chub (*Squalius vardarensis*) (Dragun et al., 2017), wild *C. gibelio* (Mijošek et al., 2021) and coral trout (*Plectropomus leopardus*), used as a control in an experiment (Lin et al., 2023).

Spatial differences indicated an elevation of oxidative stress in a downstream direction, especially at KNP. Metals are one of the main causes of oxidative stress in fish (Birnie-Gauvin et al., 2017), and the highest metal(loid) concentrations in sediment and fish gut content from this site compared to other locations were consistent with MDA increase. A similar spatial pattern was observed for cytosolic levels of Ba, Mn, Mo, Ni in both seasons, Co and V in spring, and Pb in autumn (Table S1). However, other known oxidative stress-inducing metal(loid)s, As, Cu, Fe, Pb, and Se, were most elevated in the intestinal tissue of fish from KRK, while Cd was highest in those from KRS (Mijošek et al., 2024). Previously measured metal(loid) concentrations in fish intestine were generally higher in spring, with the highest levels of Hg, Mn, Mo and V recorded at KNP (Mijošek et al., 2024). These findings confirm that, although elevated lipid peroxidation at KNP is consistent with the highest metal(loid) levels in sediment and gut content of fish from this site, it cannot be attributed to metal(loid) exposure alone, but rather reflects a complex interaction of various contaminants.

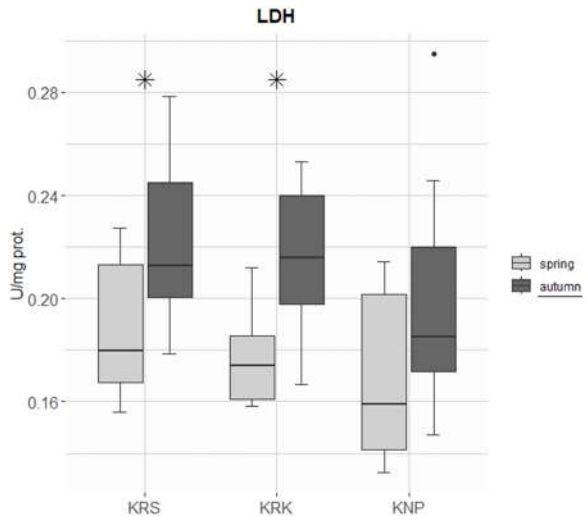

Fig. 5. Activity of lactate dehydrogenase (LDH) in the intestinal tissue of *Salmo trutta* from three sites along the Krka River - Krka River source (KRS), the Town of Knin (KRK) and Krka National Park (KNP). Data are presented as the median (line in the box), 25th and 75th percentiles (boundaries of the box), nonoutlier minimum and maximum (whiskers below and above the box) and outliers. Statistically significant differences between two seasons at the same location are indicated with an asterisk ($p < 0.05$, Mann-Whitney U-test).

4.4.2. Biomarkers of antioxidant defense (SOD, CAT, GSH, GST)

SOD activity was measured for the first time in the intestinal tissue of brown trout (*S. trutta*). Average values were generally lower than in the intestine of other freshwater species used as control groups in experimental studies (Lin et al., 2023; Jiang et al., 2016; Xie et al., 2019; Wang et al., 2022), but comparable to wild African bonytongue (*Heterotis niloticus*) (Akinsanya et al., 2020), and lower than SOD activities in blood serum, liver, or muscle of freshwater fishes (Mila-Kierzenkowska et al., 2005; Kovacik et al., 2019; Li et al., 2022; Radovanović et al., 2010).

CAT activities (13.82–21.70 U mg^{-1} prot.) were similar to those previously measured in the intestine of brown trout from the Krka River (Mijošek et al., 2019a) and higher than values reported for intestine (Jiang et al., 2016; Xie et al., 2019; Wang et al., 2022), blood serum (Kovacik et al., 2019), or muscle (Radovanović et al., 2010) of other freshwater species. However, they were lower than activities reported for the intestine of *P. leopardus* (Lin et al., 2023) and liver of *Barbus barbus* (Radovanović et al., 2010).

GSH concentrations were consistent with those found in *S. trutta* from the Krka River and *C. gibelio* from the Ilova River (Mijošek et al., 2021, 2019a). They were also comparable to levels in muscle, liver, and kidney of cultivated *O. mykiss* (Elia et al., 2018; Eyckmans et al., 2011), but lower than concentrations reported for the intestine of cultivated *Ctenopharyngodon idella* (Jiang et al., 2016) and the liver of wild gudgeon (*Gobio gobio*) and roach (*Rutilus arcasii*) from the Bernesga River (Almar et al., 1998).

GST activity, also reported here for the first time in trout intestine, was lower than values measured in the intestine of cultivated *C. idella* (Jiang et al., 2016) and liver of several freshwater fish species (Almar et al., 1998; Abdallah et al., 2024; Frank et al., 2011), but comparable to the activities in the liver of wild chub (*Leuciscus cephalus*) (Frank et al., 2011) and gills of wild *Astyanax altiparanae* (Vieira et al., 2017).

Overall, antioxidant defense biomarker responses in the intestinal tissue revealed higher oxidative stress downstream (KRK and KNP) than at the river source (KRS), particularly in spring, consistent with higher MDA, greater metal accumulation in the river sediment and fish gut content, and slightly worse physico-chemical river conditions (Šariri et al., 2024; Mijošek et al., 2024; Kara and Alp, 2005). Among antioxidants, GSH and CAT showed the most pronounced elevation in fish experiencing oxidative damage. However, these primary defense mechanisms were clearly insufficient to fully prevent lipid peroxidation and formation of MDA.

Unlike other biomarkers, GST activity showed opposite seasonal and spatial trends, being higher in autumn and decreasing downstream. This may indicate enzyme suppression or a dominant reliance on other antioxidant pathways in response to metal exposure, which was higher in spring and at KRK and KNP. However, antioxidant levels can be influenced by numerous non-contaminant factors, including food availability, reproductive status, growth rate, and seasonal metabolic fluctuations (Pavlović et al., 2010). In fish, lower metabolic rates are generally associated with reduced antioxidant defense, but individual enzymes may respond differently depending on the physiological context (Pavlović et al., 2010).

Finally, the divergent patterns of GSH and GST can be partly explained by their multifunctional roles. Beyond oxidative defense, GSH contributes to metal chelation, nutrient metabolism, immune regulation, and redox signaling, whereas GST participates in xenobiotic detoxification and transport of hormones and metabolites (Hayes et al., 2005; Pompella et al., 2003). The observed increase in GSH alongside reduced GST activity during spring may therefore reflect a combined effect of elevated nutrient intake, metal exposure, and seasonal metabolic shifts.

4.5. Biomarker of tissue metabolic activity (LDH) in fish

LDH activity in *S. trutta* intestine was generally lower than the values reported for liver, gill, brain, gonad, and muscle tissues of wild Mozambique tilapia (*Oreochromis mossambicus*) from the Bhima River (Kumar et al., 2017), in the liver and muscles of African catfish (*Clarias gariepinus*) from the Nile River (Osman et al., 2010), and in the gills of Atlantic salmon (*Salmo salar*) used as controls in experiments (Gagnon and Holdway, 1999).

Spatial and temporal trends of LDH activity contrasted with many literature reports where elevated LDH activity is commonly associated with pollution exposure and oxidative stress (Osman et al., 2010; Kumar et al., 2017). Notably, LDH activity in the intestine of *Carassius auratus gibelio* increased at moderate Cu^{2+} exposure (100 μg L^{-1}) but decreased at higher concentrations (250 μg L^{-1}), suggesting LDH suppression under more severe metal stress (Teodorescu et al., 2012).

However, in this study, pollution in the Krka River was likely not severe enough to suppress LDH activity at downstream sites in spring. Therefore, the elevated autumn levels were more likely linked with moderate fasting, typical for trouts during their spawning period (Kara and Alp, 2005). Increased LDH activity in response to short-term fasting, supporting gluconeogenesis, has been reported in the liver of *O. mykiss* (Fernández-Muela et al., 2023) and *Labeo rohita* (Yengkokpam et al., 2013). To our knowledge, the relationship between feeding rate and LDH activity in fish intestinal tissue has not yet been investigated.

4.6. Correlation of fish biomarker responses with cytosolic metal(loid) levels and biometric and epidemiological parameters

Biomarker responses (TP, MDA, SOD, CAT, GSH) showed more positive correlations with cytosolic metal levels in fish intestine in spring, reflecting seasonally higher tissue accumulation (Mijošek et al., 2024). Cobalt, Cu, Mo, Fe, Mn and Ni were most frequently associated with biomarker responses. Based on our previous analyses of river water, the main source of these elements in the Krka River catchment seem to be industrial and/or municipal wastewater, with an exception of Mo, which mainly originates from agricultural runoff and septic tanks (Mijošek et al., 2023). In river sediments and gut content isolated from fish intestine, these metals showed the increasing trend from the river source to the sites downstream of wastewater outlets (Mijošek et al., 2024). All these elements have previously been linked to the oxidative stress (Briffa et al., 2020), but biomarker responses in the present study

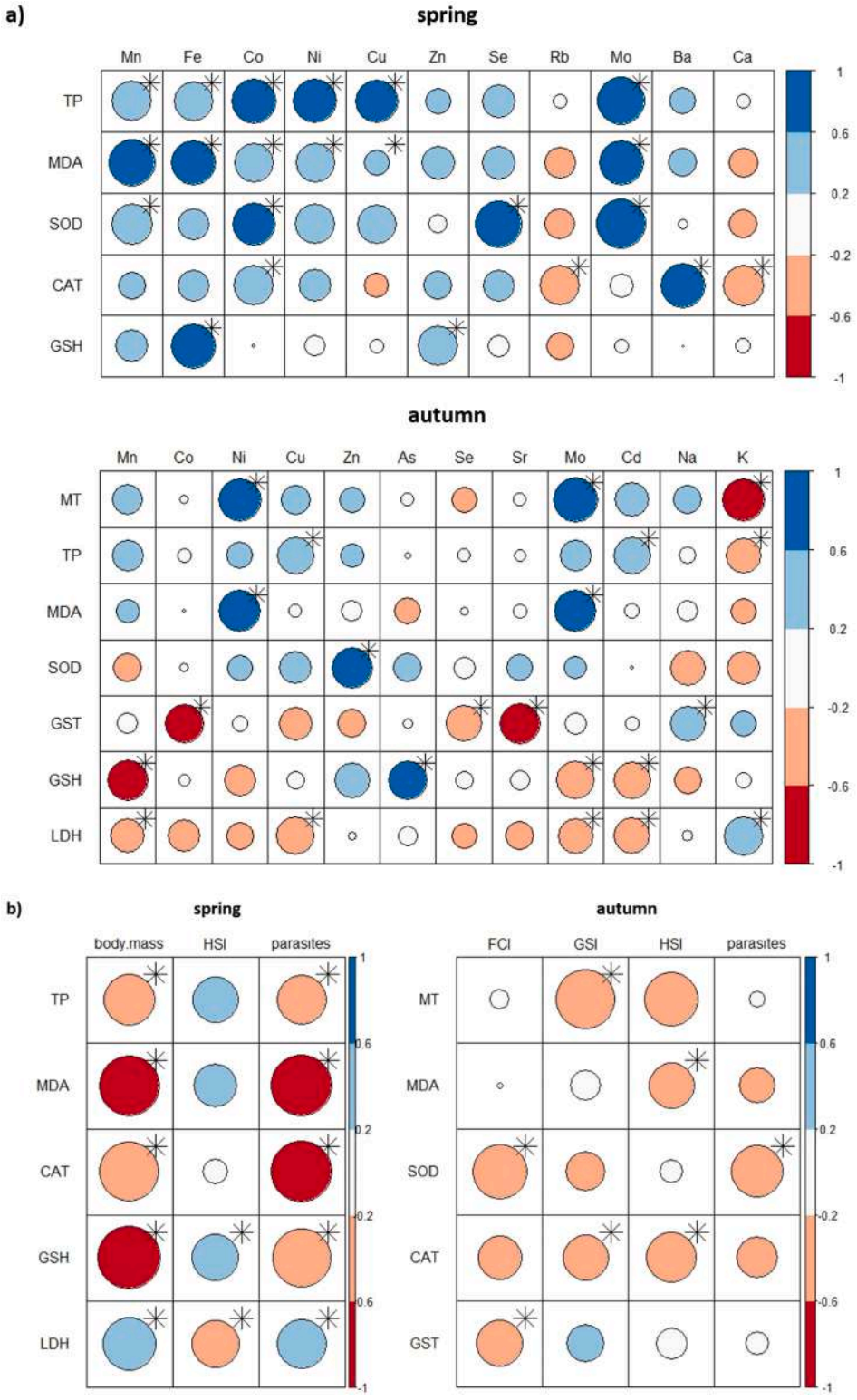

Fig. 6. Spearman correlation matrix between intestinal biomarkers and a) concentrations of cytosolic intestinal metal(loid)s, b) biometric and epidemiological parameters of *S. trutta* from the Krka River. Circle area is proportional to the absolute value of the correlation coefficient and an asterisk denotes significance ($p < 0.05$). FCI – Fulton's condition index, GSI – gonadosomatic index, HIS – hepatosomatic index, parasites – number of acanthocephalans per fish.

could not be explained entirely by metal exposure.

Negative correlations of TP, MDA, CAT and GSH with fish body mass pointed to higher general and oxidative stress in smaller fish, likely due to the higher metabolic activity and greater sensitivity in younger fish to metal load (Mijošek et al., 2024). In contrast, LDH activity was positively correlated with fish mass. The observed pattern of higher LDH activity in larger fish with more parasites, lower energy reserves, and lower metal accumulation, confirmed that fasting, rather than metal exposure, had a greater influence on this biomarker.

Parasite-related effects were also evident in the present study. Negative correlations of TP, MDA, CAT, GSH, LDH and SOD with intensity of parasite infection indicated reduced stress in heavily infected

fish. The TP correlation aligns with findings by Hassanine and Al-Hasawi (2021), who reported that acanthocephalan infection reduced elevated liver enzyme levels in fish. Fish infected with more acanthocephalans also exhibited lower oxidative damage in spring, consistent with findings in *S. cephalus* from the Marne River, where infected individuals showed reduced oxidative damage compared to uninfected ones, regardless of their pollutant load (Molbert et al., 2020). In *H. niloticus*, significantly lower intestinal SOD and MDA levels were observed in acanthocephalan-infected individuals (Bamidele et al., 2022), and similar reductions in hepatic GST and SOD activity were reported in fish infected with intestinal nematodes (Hursky and Pietrock, 2015). Such trends once more suggest possible protective role of acanthocephalans (Filipović Marijić et al., 2014; Mijošek et al., 2024), not only in regard to metal accumulation, but also biomarker responses. The strongest effect of infection intensity was observed for MDA and CAT levels, where higher parasite loads corresponded to lower lipid peroxidation and consequently reduced need for antioxidant defense. Contrary to findings by Frank et al (Frank et al., 2011)., no evidence was found in this study for decreased GST activity associated with intestinal parasite infection.

Altogether, seasonal and spatial patterns, metal correlations, and host-parasite effects highlight the complexity of biomarker responses in wild fish. Elevated oxidative stress and antioxidant activity downstream reflected higher contaminant exposure, especially of metals, but parasite infection was shown to modulate these responses and, in some cases, appeared protective. These findings emphasize the intestine and acanthocephalans as sensitive indicators of metal exposure in the Krka River and underline the need to integrate multiple biomarkers with ecological and physiological factors when assessing fish health in natural ecosystem.

5. Conclusions

Presented study assessed biomarker responses in the intestine of *Salmo trutta* from three sites along the karst Krka River, providing one of the first comprehensive multi-biomarker datasets on fish intestine and the first reporting of SOD, GST, and LDH activities in the intestine of brown trouts. Biomarker responses varied more with season than location, with spring marked by greater metal exposure, general stress, oxidative damage, and antioxidant defense.

Fish from sites downstream of wastewater discharges exhibited moderate, but significant oxidative stress responses compared to fish from the pristine river source, consistent with elevated metal concentrations in fish gut contents and sediments. Biomarker responses were assessed for the first time in fish from the Krka National Park, where the effects of wastewater contamination were not reflected in water quality or differences in fish biometric parameters. Therefore, detection at the biochemical level underscores the value of biochemical biomarkers and intestinal tissue as early indicators of sublethal pollution effects.

This study also provides one of the first data on MT and TP responses in fish intestinal parasites acanthocephalans and first ever for the species *D. truttae*. Biomarker levels were consistently higher in parasites than in host tissue, confirming their potential as complementary bioindicators, though further studies are needed to clarify their responses and host–parasite interactions.

Overall, this study demonstrates that even in seemingly well-preserved environments such as Krka National Park, sublethal contamination can be traced at the biochemical level. The combined use of multiple host and parasite biomarkers provides an early-warning tool for detecting hidden physiological stress in freshwater organisms and strengthens the basis for including intestinal tissue and parasites in ecotoxicological studies.

CRediT authorship contribution statement

Zoran Kiralj: Supervision, Investigation. **Zuzana Redžović:** Writing – review & editing, Methodology, Investigation. **Vlatka Filipović Marijić:** Writing – review & editing, Validation, Supervision, Resources, Project administration, Funding acquisition, Conceptualization. **Dušica Ivanković:** Writing – review & editing, Supervision, Methodology. **Tatjana Mijošek Pavin:** Writing – review & editing, Validation, Supervision, Investigation, Formal analysis. **Sara Šariri:** Writing – original draft, Visualization, Investigation, Formal analysis.

Funding

This study was funded by the Croatian Science Foundation within project no. IP-2020-02-8502 "Integrated evaluation of aquatic organism responses to metal exposure: gene expression, bioavailability, toxicity and biomarker responses" (BIOTOXMET).

Declaration of Competing Interest

The authors declare that they have no known competing financial interests or personal relationships that could have appeared to influence the work reported in this paper

Acknowledgements

The authors would like to acknowledge Ivana Karamatić and Yasir Al-Marsoomi for their assistance with laboratory analyses, and Damir Valić, Ivana Karamatić, and Tomislav Kralj for their support during fieldwork.

Appendix A. Supporting information

Supplementary data associated with this article can be found in the online version at doi:10.1016/j.etap.2025.104823.

Data availability

Data will be made available on request.

References

Abdallah, S.M., Muhammed, R.E., Mohamed, R.E., El Daous, H., Saleh, D.M., Ghorab, M. A., Chen, S., El-Sayyad, G.S., 2024. Assessment of biochemical biomarkers and environmental stress indicators in some freshwater fish. Environ. Geochem. Health 46 (11), 464. https://doi.org/10.1007/s10653-024-02226-6.

Adam, V., Baloun, J., Fabrik, I., Trnkova, L., Kizek, R., 2008. An electrochemical detection of metallothioneins at the zeptomole level in nanolitre volumes. Sensors 8 (4), 2293–2305. https://doi.org/10.3390/s8042293.

Aebi, H., 1984. Catalase in vitro. In: in: Methods in enzymology, 105. Academic press, pp. 121–126. https://doi.org/10.1016/S0076-6879(84)05016-3.

Akinsanya, B., Ayanda, I.O., Fadipe, A.O., Onwuka, B., Saliu, J.K., 2020. Heavy metals, parasitologic and oxidative stress biomarker investigations in *heterotis niloticus* from lekki lagoon, lagos, Nigeria. Toxicol. Rep. 7, 1075–1082. https://doi.org/10.1016/j.toxrep.2020.08.010.

Almar, M., Otero, L., Santos, C., Gallego, J.G., 1998. Liver glutathione content and glutathione-dependent enzymes of two species of freshwater fish as bioindicators of chemical pollution. J. Environ. Sci. Health B. 33 (6), 769–783. https://doi.org/10.1080/03601239809373177.

Bamidele, A., Omoregie, I.P., Esen, U., Saliu, J.K., 2022. Biosequestration potentials of *tenuisentis niloticus* (Meyer, 1932) (Acanthocephala: Tenuisentidae) on organochlorine pesticide burden in *heterotis niloticus* (Cuvier, 1829) (Actinopterygii: Arapaimidae) from lekki lagoon, lagos, Nigeria. Environ. Chall. 6, 100414. https://doi.org/10.1016/j.envc.2021.100414.

Bergmeyer, H.U., Bernt, E., Hess, B., 1965. Lactic dehydrogenase. In: Bergmeyer, H.U. (Ed.), Methods of Enzymatic Analysis. Academic Press, p. 231. https://doi.org/10.1016/B978-0-12-395630-9.50134-1.

Birnie-Gauvin, K., Costantini, D., Cooke, S.J., Willmore, W.G., 2017. A comparative and evolutionary approach to oxidative stress in fish: a review. Fish Fish 18 (5), 928–942. https://doi.org/10.1111/faf.12215.

Bonacci, O., Andrić, I., Roje-Bonacci, T., 2017. Hydrological analysis of skradinski buk tufa waterfall (Krka River, Dinaric karst, Croatia). Environ. Earth Sci. 76 (19), 669. https://doi.org/10.1007/s12665-017-7023-9.

Botsoglou, N.A., Fletouris, D.J., Papageorgiou, G.E., Vassilopoulos, V.N., Mantis, A.J., Trakatellis, A.G., 1994. A rapid, sensitive, and specific thiobarbituric acid method for measuring lipid peroxidation in animal tissues, food, and feedstuff samples. J. Agric. Food Chem. 42, 1931–1937. https://doi.org/10.1021/jf00045a019.

Bradford, M.M., 1976. A rapid and sensitive method for the quantitation of microgram quantities of protein utilizing the principle of protein-dye binding. Anal. Biochem 72 (1-2), 248–254. https://doi.org/10.1016/0003-2697(76)90527-3.

Briffa, J., Sinagra, E., Blundell, R., 2020. Heavy metal pollution in the environment and their toxicological effects on humans. Heliyon 6 (9), e04691. https://doi.org/10.1016/j.heliyon.2020.e04691.

Claiborne, A., 1985. Catalase activity. In: Greenwald, R.A. (Ed.), CRC Handbook of Methods for Oxygen Radical Research. CRC Press, Boca Raton FL, pp. 283–284. https://doi.org/10.1201/9781351072922.

Colin, N., Porte, C., Fernandes, D., Barata, C., Padrós, F., Carrassón, M., Monroy, M., Cano-Rocabayera, O., de Sostoa, A., Piña, B., Maceda-Veiga, A., 2016. Ecological relevance of biomarkers in monitoring studies of macro-invertebrates and fish in Mediterranean rivers. Sci. Total Environ. 540, 307–323. https://doi.org/10.1016/j.scitotenv.2015.06.099.

Dragun, Z., Filipović Marijić, V., Krasnići, N., Ramani, S., Valić, D., Rebok, K., Kostov, V., Jordanova, M., Erk, M., 2017. Malondialdehyde concentrations in the intestine and gills of vardar chub (*squalius vardarensis* Karaman) as indicator of lipid peroxidation. Environ. Sci. Pollut. Res 24, 16917–16926. https://doi.org/10.1016/j.ecoenv.2016.03.006.

Elia, A.C., Capucchio, M.T., Caldaroni, B., Magara, G., Dörr, A.J.M., Biasato, I., Biasibetti, E., Righetti, M., Pastorino, P., Prearo, M., Gai, F., Schiavone, A., Gasco, L., 2018. Influence of *hermetia illucens* meal dietary inclusion on the histological traits, gut mucin composition and the oxidative stress biomarkers in rainbow trout (*oncorhynchus mykiss*). Aquaculture 496, 50–57. https://doi.org/10.1016/j.aquaculture.2018.07.009.

Eyckmans, M., Celis, N., Horemans, N., Blust, R., De Boeck, G., 2011. Exposure to waterborne copper reveals differences in oxidative stress response in three freshwater fish species. Aquat. Toxicol. 103 (1-2), 112–120. https://doi.org/10.1016/j.aquatox.2011.02.010.

Fernández-Muela, M., Bermejo-Poza, R., Cabezas, A., Pérez, C., González de Chavarri, E., Díaz, M.T., Torrent, F., Villarroel, M., De la Fuente, J., 2023. Effects of fasting on intermediary metabolism enzymes in the liver and muscle of rainbow trout. Fishes 8 (1), 53. https://doi.org/10.3390/fishes8010053.

Fernández-Trujillo, S., López-Perea, J.J., Jiménez-Moreno, M., Martín-Doimeadios, R.C. R., Mateo, R., 2021. Metals and metalloids in freshwater fish from the floodplain of tablas de daimiel national park, Spain. Ecotoxicol. Environ. Saf. 208, 111602. https://doi.org/10.1016/j.ecoenv.2020.111602.

Filipović Marijić, V., Vardić Smrzlić, I., Raspor, B., 2014. Does fish reproduction and metabolic activity influence metal levels in fish intestinal parasites, acanthocephalans, during fish spawning and post-spawning period? Chemosphere 112, 449–455. https://doi.org/10.1016/j.chemosphere.2014.04.086.

Flores, A., Wiff, R., Ganias, K., Marshall, C.T., 2019. Accuracy of gonadosomatic index in maturity classification and estimation of maturity ogive. Fish. Res. 210, 50–62. https://doi.org/10.1016/j.fishres.2018.10.009.

Frank, S.N., Faust, S., Kalbe, M., Trubiroha, A., Kloas, W., Sures, B., 2011. Fish hepatic glutathione-S-transferase activity is affected by the cestode parasites *schistocephalus solidus* and *ligula intestinalis*: evidence from field and laboratory studies. Parasitology 138 (7), 939–944. https://doi.org/10.1017/S003118201100045X.

Gagnon, M.M., Holdway, D.A., 1999. Metabolic enzyme activities in fish gills as biomarkers of exposure to petroleum hydrocarbons. Ecotoxicol. Environ. Saf. 44 (1), 92–99. https://doi.org/10.1006/eesa.1999.1804.

Habig, W.H., Pabst, M.J., Jakoby, W.B., 1974. Glutathione S-transferase. J. Biol. Chem. 25, 7130–7139. https://doi.org/10.1016/s0021-9258(19)42083-8.

Hassanine, R., Al-Hasawi, Z., 2021. Acanthocephalan worms mitigate the harmful impacts of heavy metal pollution on their fish hosts. Fishes 6 (4), 49. https://doi.org/10.3390/fishes6040049.

Hayes, J.D., Flanagan, J.U., Jowsey, I.R., 2005. Glutathione transferases. Annu. Rev. Pharmacol. Toxicol. 45 (1), 51–88. https://doi.org/10.1146/annurev.pharmtox.45.120403.095857.

Heidinger, R.C., Crawford, S.D., 1977. Effect of temperature and feeding rate on the liversomatic index of largemouth bass, *micropterus salmoides*. J. Fish. Res. Board Can. 34, 633–638. https://doi.org/10.1139/f77-099.

Hemmadi, V., 2017. A critical review on integrating multiple fish biomarkers as indicator of heavy metals contamination in aquatic ecosystem. Int. J. Bioassays 6 (9), 5494–5506. https://doi.org/10.21746/ijbio.2017.9.5.

HRN EN 14011, 2005. Fish sampling by electric power. Croatian Standard Institute, Zagreb (in Croatian).

Hursky, O., Pietrock, M., 2015. Intestinal nematodes affect selenium bioaccumulation, oxidative stress biomarkers, and health parameters in juvenile rainbow trout (*oncorhynchus mykiss*). Environ. Sci. Technol. 49 (4), 2469–2476. https://doi.org/10.1021/es5048792.

Jiang, J., Wu, X.Y., Zhou, X.Q., Feng, L., Liu, Y., Jiang, W.D., Wu, P., Zhao, Y., 2016. Glutamate ameliorates copper-induced oxidative injury by regulating antioxidant defences in fish intestine. Br. J. Nutr. 116 (1), 70–79. https://doi.org/10.1017/S0007114516001732.

Kara, C., Alp, A., 2005. Feeding habits and diet composition of brown trout (*salmo trutta*) in the upper streams of river ceyhan and river Euphrates in Turkey. Turk. J. Vet. Anim. Sci. 29 (2), 417–428.

Kennedy, C.R., 1985. Regulation and dynamics of acanthocephalan populations. In: Crompton, D.W.T., Nickol, B.B. (Eds.), Biology of the Acanthocephala. Cambridge University Press, pp. 385–416.

Kiralj, Z., Dragun, Z., Lajtner, J., Trgovčić, K., Mijošek Pavin, T., Bušić, B., Ivanković, D., 2025. Changes in subcellular responses in the digestive gland of the freshwater mussel *unio crassus* from historically contaminated environment. Fishes 10 (7), 317. https://doi.org/10.3390/fishes10070317.

Kovacik, A., Tvrda, E., Miskeje, M., Arvay, J., Tomka, M., Zbynovska, K., Andreji, J., Hleba, L., Kovacikova, E., Fik, M., Cupka, P., Nahacky, J., Massanyi, P., 2019. Trace metals in the freshwater fish *cyprinus carpio*: effect to serum biochemistry and oxidative status markers. Biol. Trace Elem. Res. 188, 494–507. https://doi.org/10.1007/s12011-018-1415-x.

Kumar, N., Krishnani, K.K., Meena, K.K., Gupta, S.K., Singh, N.P., 2017. Oxidative and cellular metabolic stress of *oreochromis mossambicus* as biomarkers indicators of trace element contaminants. Chemosphere 171, 265–274. https://doi.org/10.1016/j.chemosphere.2016.12.066.

Li, X., Naseem, S., Hussain, R., Ghaffar, A., Li, K., Khan, A., 2022. Evaluation of DNA damage, biomarkers of oxidative stress, and status of antioxidant enzymes in freshwater fish (*labeo rohita*) exposed to pyriproxyfen. Oxid. Med. Cell. Longev. 2022 (1), 5859266. https://doi.org/10.1155/2022/5859266.

Li, Y., Schellhorn, H.E., 2007. Rapid kinetic microassay for catalase activity. J. Biomol. Tech. 18 (4), 185.

Lin, Z., Pan, L., Xie, R., Li, L., Wen, J., Zhou, X., Dong, X., Xie, S., Tan, B., Liu, H., 2023. Effects of dietary artemisinin on growth performance, digestive enzyme activity, intestinal microbiota, antioxidant capacity and immune biomarkers of coral trout (*plectropomus leopardus*). Aquac. Rep. 29, 101525. https://doi.org/10.1016/j.aqrep.2023.101525.

Lowry, O.H., Rosebrough, N.J., Farr, A.L., Randall, R.J., 1951. Protein measurement with the folin phenol reagent. J. Biol. Chem. 193, 265–275. https://doi.org/10.1016/S0021-9258(19)52451-6.

Lysenko, L., Kantserova, N., Käiväräinen, E., Krupnova, M., Shklyarevich, G., Nemova, N., 2014. Biochemical markers of pollutant responses in macrozoobenthos from the White sea: intracellular proteolysis. Mar. Environ. Res. 96, 38–44.

Marijić, V.Filipović., Raspor, B., 2010. The impact of fish spawning on metal and protein levels in gastrointestinal cytosol of indigenous european chub. Comp. Biochem. Physiol. C. Toxicol. Pharm. 152 (2), 133–138. https://doi.org/10.1016/j.cbpc.2010.03.010.

Mijošek, T., Erk, M., Filipović Marijić, V., Krasnići, N., Dragun, Z., Ivanković, D., 2018. Electrochemical determination of metallothioneins by the modified Brdička procedure as an analytical tool in biomonitoring studies. Croat. Chem. Acta 91 (4), 475–480. https://doi.org/10.5562/cca3444.

Mijošek, T., Filipović Marijić, V., Dragun, Z., Krasnići, N., Ivanković, D., Erk, M., 2019a. Evaluation of multi-biomarker response in fish intestine as an initial indication of anthropogenic impact in the aquatic karst environment. Sci. Total Environ. 660, 1079–1090. https://doi.org/10.1016/j.scitotenv.2019.01.045.

Mijošek, T., Filipović Marijić, V., Dragun, Z., Ivanković, D., Krasnići, N., Erk, M., Gottstein, S., Lajtner, J., Sertić Perić, M., Matoničkin Kepčija, R., 2019b. Comparison of electrochemically determined metallothionein concentrations in wild freshwater salmon fish and gammarids and their relation to total and cytosolic metal levels. Ecol. Indic. 105, 188–198. https://doi.org/10.1016/j.ecolind.2019.05.069.

Mijošek, T., Filipović Marijić, V., Dragun, Z., Krasnići, N., Ivanković, D., Redžović, Z., Erk, M., 2021. First insight in trace element distribution in the intestinal cytosol of two freshwater fish species challenged with moderate environmental contamination. Sci. Total Environ. 798, 149274. https://doi.org/10.1016/j.scitotenv.2021.149274.

Mijošek, T., Filipović Marijić, V., Dragun, Z., Ivanković, D., Krasnići, N., Erk, M., 2022. Efficiency of metal bioaccumulation in acanthocephalans, gammarids and fish in relation to metal exposure conditions in a karst freshwater ecosystem. J. Trace Elem. Med. Biol. 73, 127037. https://doi.org/10.1016/j.jtemb.2022.127037.

Mijošek, T., Kljaković-Gašpić, Z., Kralj, T., Valić, D., Redžović, Z., Šariri, S., Karamatić, I., Filipović Marijić, V., 2023. Spatial and temporal variability of dissolved metal(loid) s in water of the karst ecosystem: consequences of long-term exposure to wastewaters. Environ. Technol. Innov. 32, 103254. https://doi.org/10.1016/j.eti.2023.103254.

Mijošek, T., Šariri, S., Kljaković-Gašpić, Z., Fiket, Ž., Filipović Marijić, V., 2024. Interrelation between environmental conditions, acanthocephalan infection and metal (loid) accumulation in fish intestine: an in-depth study. Environ. Pollut. 356, 124358. https://doi.org/10.1016/j.envpol.2024.124358.

Mila-Kierzenkowska, C., Woźniak, A., Woźniak, B., Drewa, G., Chęsy, B., Drewa, T., Krzyyska-Malinowska, E., Cerafícki, R., 2005. Activity of superoxide dismutase (SOD) and concentration of thiobarbituric acid reactive substances (TBARS) in liver and muscles of some fish. Acta Biol. Hung. 56 (3-4), 399–401. https://doi.org/10.1556/abiol.56.2005.3-4.21.

Molbert, N., Alliot, F., Leroux-Coyau, M., Médoc, V., Biard, C., Meylan, S., Jacquin, L., Santos, R., Goutte, A., 2020. Potential benefits of acanthocephalan parasites for chub hosts in polluted environments. Environ. Sci. Technol. 54 (9), 5540–5549. https://doi.org/10.1021/acs.est.0c00177.

Nachev, M., Sures, B., 2016. Environmental parasitology: parasites as accumulation bioindicators in the marine environment. J. Sea Res. 113, 45–50. https://doi.org/10.1016/j.seares.2015.06.005.

NN 55, Ordinance on the Protection of Animals Used for Scientific Purposes [Pravilnik o zaštiti životinja koje se koriste u znanstvene svrhe], 2013.

Okwuosa, O.B., Eyo, J.E., Omovwohwovie, E.E., 2019. Role of fish as bioindicators: a review. Iconic Res. Eng. J. 2 (11), 1456–8880. ⟨https://www.researchgate.net/publication/357255031⟩.

Osman, A.G., Abd-El–Baset, M., AbuelFadl, K.Y., GadEl-Rab, A.G., 2010. Enzymatic and histopathologic biomarkers as indicators of aquatic pollution in fishes. Nat. Sci. 2 (11), 1302–1311. ⟨https://www.researchgate.net/publication/259667787⟩.

Pavlović, S.Z., Mitić, S.S.Borković., Radovanović, T.B., Perendija, B.R., Despotović, S.G., Gavrić, J.P., Saičić, Z.S., 2010. Seasonal variations of the activity of antioxidant defense enzymes in the red mullet (*mullus barbatus* l.) from the adriatic sea. Mar. Drugs 8 (3), 413–428. https://doi.org/10.3390/md8030413.

Petrlova, J., Krizkova, S., Zitka, O., Hubalek, J., Prusa, R., Adam, V., Wang, J., Beklova, M., Sures, B., Kizek, R., 2007. Utilizing a chronopotentiometric sensor technique for metallothionein determination in fish tissues and their host parasites.

Sens. Actuators B Chem. 127 (1), 112–119. https://doi.org/10.1016/j.snb.2007.07.025.
Pompella, A., Visvikis, A., Paolicchi, A., Tata, V.De, Casini, A.F., 2003. The changing faces of glutathione, a cellular protagonist. Biochem. Pharm. 66 (8), 1499–1503. https://doi.org/10.1016/S0006-2952(03)00504-5.
Radovanović, T.B., Borković-Mitić, S.S., Perendija, B.R., Despotović, S.G., Pavlović, S.Z., Cakić, P.D., 2010. Z.S. Saičlć, Superoxide dismutase and catalase activities in the liver and muscle of barbel (Barbus barbus) and its intestinal parasite (*pomphoryinchus laevis*) from the Danube river, Serbia. Arch. Biol. Sci. 62 (1), 97–105. https://doi.org/10.2298/ABS1001097R.
Rahman, I., Kode, A., Biswas, S.K., 2006. Assay for quantitative determination of glutathione and glutathione disulfide levels using enzymatic recycling method. Nat. Protoc. 1, 3159–3165. https://doi.org/10.1038/nprot.2006.378.
Raspor, B., Paić, M., Erk, M., 2001. Analysis of metallothioneins by the modified Brdička procedure. Talanta 55, 109–115. https://doi.org/10.1016/S0039-9140(01)00399-X.
Ricker, W.E., 1975. Computation and interpretation of biological statistics of fish populations. B. Fish. Res. Board Can. 191, 1–382.
Ringwood, A.H., Hoguet, J., Keppler, C.J., Gielazyn, M.L., Ward, B.P., Rourk, A.R., 2003. Cellular biomarkers (lysosomal destabilization, glutathione & lipid peroxidation) in three common estuarine species: a methods handbook. Mar. Resour. Res. Inst. South Carol. Dep. Nat. Resour. 1–45.
Rizzo, M., 2024. Measurement of malondialdehyde as a biomarker of lipid oxidation in fish. Am. J. Anal. Chem. 15 (9), 303–332.
Sanders, B.M., Dyer, S.D., 1994. Cellular stress response. Environ. Toxicol. Chem. 13 (8), 1209–1210. https://doi.org/10.1002/etc.5620130801.
Šariri, S., Cvetković, Ž., Mijošek Pavin, T., Kljaković-Gašpić, Z., Valić, D., Kralj, T., Brkić, A., Redžović, Z., Filipović Marijić, V., 2025a. Association of toxic effects and the quality of surface water and wastewater: application under environmental conditions and literature overview by CiteSpace. J. Contam. Hydrol. 274, 104667. https://doi.org/10.1016/j.jconhyd.2025.104667.
Šariri, S., Valić, D., Kralj, T., Cvetković, Ž., Mijošek, T., Redžović, Z., Karamatić, I., Marijić, V.Filipović., 2024. Long-term and seasonal trends of water parameters in the karst riverine catchment and general literature overview based on CiteSpace. Environ. Sci. Pollut. Res. 31 (3), 3887–3901. https://doi.org/10.1007/s11356-023-31418-3.
Šariri, S., Vardić Smrzlić, I., Mijošek Pavin, T., Filipović Marijić, V., 2025b. First insight into metal binding proteins from the de novo transcriptome of acanthocephalan parasite *dentitruncus truttae*. Sci. Rep. 15 (1), 26152.
Schiperski, F., Zirlewagen, J., Scheytt, T., 2016. Transport and attenuation of particles of different density and surface charge: a karst aquifer field study. Environ. Sci. Technol. 50 (15), 8028–8035. https://doi.org/10.1021/acs.est.6b00335.
Smialek, N., Pander, J., Geist, J., 2021. Environmental threats and conservation implications for atlantic salmon and brown trout during their critical freshwater phases of spawning, egg development and juvenile emergence. Fish. Manag. Ecol. 28 (5), 437–467. https://doi.org/10.1111/fme.12507.
Sures, B., 2001. The use of fish parasites as bioindicators of heavy metals in aquatic ecosystems: a review. Aquat. Ecol. 35, 245–255. https://doi.org/10.1023/A:1011422310314.
Teodorescu, D., Munteanu, M.C., Staicu, A.C., Dinischiotu, A.N.C.A., 2012. Changes in lactate dehydrogenase activity in *carassius auratus gibelio* (L. Pysces) kidney, gills and intestine induced by acute exposure to copper. Rom. Biotechnol. Lett. 17 (6), 7873–7880.
Tietze, F., 1969. Enzymic method for quantitative determination of nanogram amounts of total and oxidized glutathione: applications to mammalian blood and other tissues. Anal. Biochem 27, 502–522. https://doi.org/10.1016/0003-2697(69)90064-5.
Topić Popović, N., Strunjak-Perović, I., Čož-Rakovac, R., Barišić, J., Jadan, M., Peršin Beraković, A., Sauerborn Klobučar, R., 2012. Tricaine methane-sulfonate (MS-222) application in fish anaesthesia. J. Appl. Ichthyol. 28 (4), 553–564. https://doi.org/10.1111/j.1439-0426.2012.01950.x.
Vardić Smrzlić, I., Valić, D., Kapetanović, D., Dragun, Z., Gjurčević, E., Ćetković, H., Teskeredžić, E., 2013. Molecular characterisation and infection dynamics of *dentitruncus truttae* from trout (*salmo trutta* and *oncorhynchus mykiss*) in krka river, Croatia. Vet. Parasitol. 197 (3/4), 604–613. https://doi.org/10.1016/j.vetpar.2013.07.014.
Viarengo, A., Burlando, B., Dondero, F., Marro, A., 1999. R. Fabbri, metallothionein as a tool in biomonitoring programmes. Biomarkers 4 (6), 455–466. https://doi.org/10.1080/135475099230615.
Vieira, C.E.D., Costa, P.G., Cabrera, L.C., Primel, E.G., Fillmann, G., Bianchini, A., dos Reis Martinez, C.B., 2017. A comparative approach using biomarkers in feral and caged neotropical fish: implications for biomonitoring freshwater ecosystems in agricultural areas. Sci. Total Environ. 586, 598–609. https://doi.org/10.1016/j.scitotenv.2017.02.026.
Wang, W.C., Mao, H., Ma, D.D., Yang, W.X., 2014. Characteristics, functions, and applications of metallothionein in aquatic vertebrates. Front. Mar. Sci. 1, 34. https://doi.org/10.3389/fmars.2014.00034.
Wang, C., Yuan, Z., Li, J., Liu, Y., Li, R., Li, S., 2022. Acute effects of antimony exposure on adult zebrafish (*danio rerio*): from an oxidative stress and intestinal microbiota perspective. Fish. Shellfish Immunol. 123, 1–9. https://doi.org/10.1016/j.fsi.2022.02.050.
R.J. Wootton, Ecology of teleost fishes, Chapman and Hall, Fish and Fisheries Series 777 1. London, New York, 1990.
Xie, D., Li, Y., Liu, Z., Chen, Q., 2019. Inhibitory effect of cadmium exposure on digestive activity, antioxidant capacity and immune defense in the intestine of yellow catfish (*pelteobagrus fulvidraco*). Comp. Biochem. Physiol. C. Toxicol. Pharm. 222, 65–73. https://doi.org/10.1016/j.cbpc.2019.04.012.
Yengkokpam, S., Debnath, D., Pal, A.K., Sahu, N.P., Jain, K.K., Norouzitallab, P., Baruah, K., 2013. Short-term periodic feed deprivation in *labeo rohita* fingerlings: effect on the activities of digestive, metabolic and anti-oxidative enzymes. Aquaculture 412, 186–192. https://doi.org/10.1016/j.aquaculture.2013.07.025.

Publication No. 6: First insight into metal binding proteins from the de novo transcriptome of acanthocephalan parasite *Dentitruncus truttae*

scientific reports

Check for updates

OPEN

First insight into metal binding proteins from the *de novo* transcriptome of acanthocephalan parasite *Dentitruncus truttae*

Sara Šariri, Irena Vardić Smrzlić✉, Tatjana Mijošek Pavin & Vlatka Filipović Marijić✉

Acanthocephala are parasites increasingly used as bioindicators of environmental quality due to their ability to effectively accumulate metals. However, the mechanisms of metal homeostasis in them remain unclear as there has been only one genomic study on Acanthocephala species (*Pomphorhynchus laevis*). In the present study, the transcriptome of the freshwater acanthocephalan *Dentitruncus truttae* was assembled *de novo* and analyzed for orthologs and metal-binding proteins (MBPs), which were compared between two acanthocephalans and taxa related to them phylogenetically or by lifestyle. MBPs were characterized using the PFAM database and the MeBiPred software. Orthology analysis revealed that 75% of orthogroups were species-specific, with *D. truttae* sharing most orthologues (21% of non-species-specific) with *P. laevis*. The proteome of *D. truttae* consisted of 14.5% MBPs, predominantly zinc-binding proteins such as zinc finger proteins. Phylogenetic analysis of metalloproteases (zinc-binding), iron-sulphur protein group (iron-binding) and nickel-binding ureases/hydrogenases showed that the analyzed sequences are fairly conserved across all taxonomic groups, with a particularly high conservation in Acanthocephala and Rotifera. Protein sequences that could not be described using the PFAM database were grouped into three clusters characterized by a high preference for binding zinc and copper. This study provides the first transcriptomic insights into *D. truttae* and its MBPs, contributing to future research of the molecular mechanisms underlying metal accumulation in acanthocephalans. These findings may highlight their potential as bioindicators, reveal mechanisms of tolerance to toxic metals, and improve our understanding of their ecological adaptations and roles in aquatic ecosystems.

Keywords RNA sequencing, *de novo* transcriptome, Fish parasite, MeBiPred, Metal-binding proteins

Acanthocephala, also known as thorny-headed worms, are a monophyletic group of obligate endoparasites found worldwide in arthropods and vertebrates, primarily fishes. They are recognized as model species for various research areas including host–parasite interactions, evolution of parasitic life cycles, environmental parasitology, taxonomy, phylogeography and behavioral ecology[1]. *Dentitruncus truttae* Šinžar, 1955, an acanthocephalan freshwater species, is found in restricted areas of Bosnia and Herzegovina, Italy, and Croatia. It belongs to the family Leptorhynchoididae Witenberg, 1932 (Palaeacanthocephala) and is the only member of the genus *Dentitruncus*. This species is characterized by 18 longitudinal rows of hooks on its proboscis, with 18 hooks per row (occasionally 19–20). High infestation intensity of *D. truttae* has been reported in its native habitat, the Krka river in Croatia[2–4].

The definitive host of *D. truttae* is primarily the brown trout (*Salmo trutta* Linnaeus, 1758), while intermediate hosts include crustaceans from the genera *Gammarus* and *Echinogammarus*[2,5]. *D. truttae*, like other acanthocephalans, effectively accumulates metals, especially toxic metals, making it a bioindicator of anthropogenic metal pollution in aquatic environments[4,6,7]. In addition, infection with these parasites has been associated with reduced accumulation of toxic metals in the fish host[6,7]. Thus, *D. truttae* is significant not only as a pathogen of salmonid fish commonly consumed by humans, but also as an evolutionarily intriguing species of acanthocephalan, and as a potential bioindicator of metal pollution in freshwater ecosystems.

Transcriptome analysis enables genome-wide identification of novel genes and protein families, including metal-binding proteins (MBPs)[8–16], which are essential for understanding metal homeostasis in Acanthocephala.

Ruđer Bošković Institute, Bijenička cesta 54, Zagreb 10000, Croatia. ✉email: Irena.Vardic.Smrzlic@irb.hr; vfilip@irb.hr

Acanthocephalans, lacking a digestive system, absorb nutrients and accumulate metals, especially toxic ones[4,7,17–20], likely due to competition for essential elements and enhanced uptake via bile salts, which form bioavailable metal complexes[17,21–24]. Reliant on host-derived steroids and fatty acids, they efficiently absorb bile salts, inadvertently taking up toxic metals[6,25,26]. Mechanisms of metal homeostasis remain unclear, with molecular data available only for a single acanthocephalan species, *Pomphorhynchus laevis*.

The identification of MBPs typically involves annotating assembled transcripts using databases such as PFAM, Swiss-Prot and NR (Non-Redundant) which combine sequence alignment, domain identification and functional annotations[27]. Predictive tools like MeBiPred, which assess metal-binding potential based on sequence information of proteins that interact with ubiquitous metal ligands such as zinc (Zn), copper (Cu), cobalt (Co) and others essential for life yet toxic in excess[28–31]. The identified MBPs could then be compared in different but evolutionarily related taxa, which would provide valuable insights into their functions, evolutionary conservation and adaptations.

This study aimed to assemble and analyze the *de novo* transcriptome of *D. truttae* with a focus on identifying orthologous genes and characterizing MBPs in detail. By generating the first publicly available transcriptome for the family Leptorhynchoididae Witenberg, 1932, this research provides a foundation for addressing questions related to the phylogeny, taxonomy, diversity and evolution of Acanthocephala. Additionally, the ecological roles of MBPs in metal accumulation and host–parasite interactions are explored, offering insights into the broader significance of *D. truttae* as both a bioindicator and a model species.

Results

De Novo assembly of the *D. truttae* transcriptome

A total of 102.66 Gb of clean reads (98.51% of raw reads) were generated from the eight samples of *D. truttae* (Table S1), with an average of 42.7 million clean reads and 34.2 million total mapped reads. The Trinity assembler generated 129,887 transcripts with an average length of 915 bp and an N50 of 1193 bp and a total of 61,570 unigenes with an average length of 817 bp and an N50 of 1027 bp. The total length of the transcriptome was 118,871,775 bp when considering the transcripts, whereas it was 50,302,772 bp when accounting for the unigenes. Most transcripts and unigenes were 300 bp to 500 bp in length (38.6% of transcripts and 47.1% of unigenes), and 8.9% of transcripts and 7.0% of unigenes were larger than 2,000 bp (Fig. S1). The longest sequence was 15,212 bp, and the shortest sequence was 301 bp for both the transcript and unigene databases. BUSCO assessment of the completeness of the *D. truttae* transcriptome assemblies revealed a high quality of the assembled transcripts (Fig. S2). The percentage of fragmented reads was low (3% for Trinity.fasta and 4.8% for unigene.fasta sequences), while the percentage of missing reads was higher (25.2% for Trinity.fasta and 26.8% for unigene.fasta sequences) (Fig. S2).

Functional annotation

The statistics of the genes successfully annotated by each database can be found in Table 1, which shows that 40.6% of the unigenes were annotated in at least one database.

After GO analysis, a total of 18,017 unigenes were assigned to the three main GO categories: 50.4% to biological processes (BP), with 25 subcategories; 24.8% to cellular component (CC), with five subcategories; and 24.8% to molecular function (MF), with 12 subcategories (Fig. 1). The highest number of unigenes in BP was associated with cellular processes (27.9%), metabolic processes (22.0%) and biological regulation (10.4%). Further analysis of the biological processes at GO levels 3 and 4 showed that most of the genes were associated with metabolism and its regulation, organization and biogenesis of cellular components, biosynthesis, and regulation of response to stimuli, localization and transport. In the CC category, unigenes were abundant as cellular anatomical entities (46.3%), intracellular entities (28.3%) and protein-containing complexes (19.6%). Most of these genes were associated with organelles and membranes. Most of the unigenes in the MF category were associated with binding (46.3%), catalytic activity (31.5%) and transporter activity (7.2%) and were linked to the binding of nucleic acids, nucleoside phosphates, ions and signaling receptors, as well as to the activity of transferases, peptidases, hydrolases, and transmembrane transporters.

	Number of unigenes	Percentage (%)
Total Unigenes	61,570	100.00
Annotated in at least one database	25,002	40.60
Annotated in PFAM (Protein family)	18,022	29.27
Annotated in GO	18,017	29.26
Annotated in NR	14,662	23.81
Annotated in SwissProt	8976	14.57
Annotated in KO (KEGG orthology)	7616	12.36
Annotated in KOG	6729	10.92
Annotated in NT (NCBI nucleotide sequences)	2806	4.55
Annotated in all databases	996	1.61

Table 1. Proportion of genes successfully annotated in the *D. truttae de novo* transcriptome across different databases with percentages calculated relative to the total unigene count.

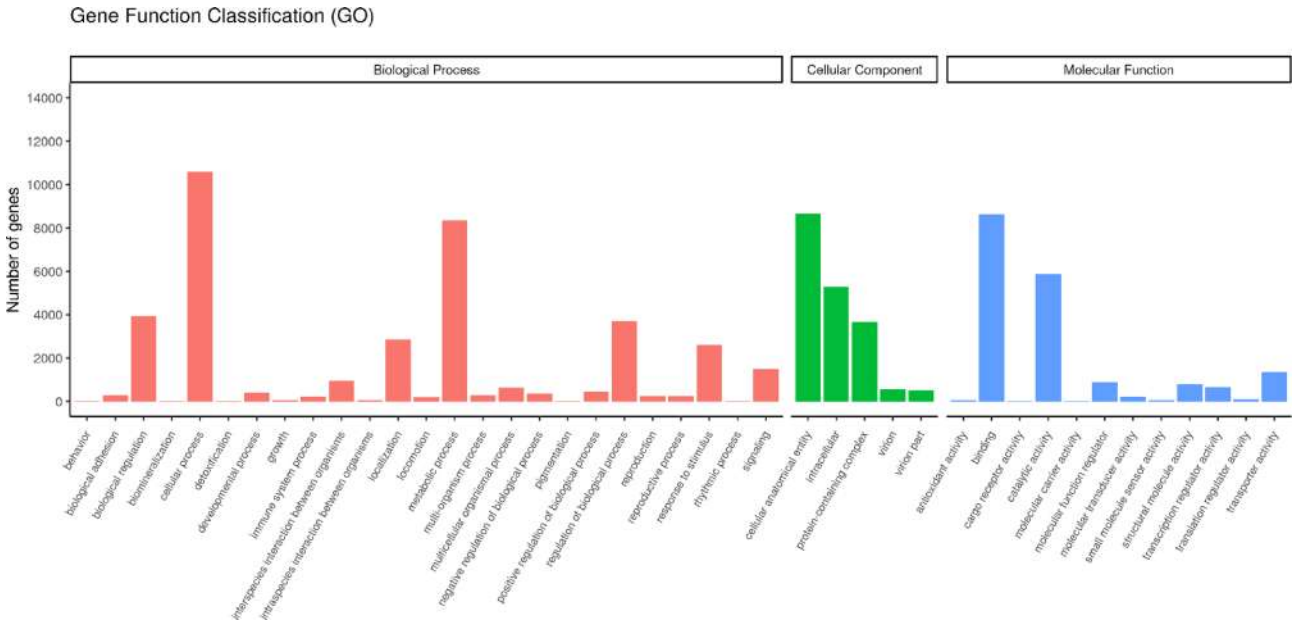

Fig. 1. Classification of *D. truttae* unigenes annotated in the Gene Ontology (GO) database into three functional GO categories: biological process (BP), cellular component (CC) and molecular function (MF).

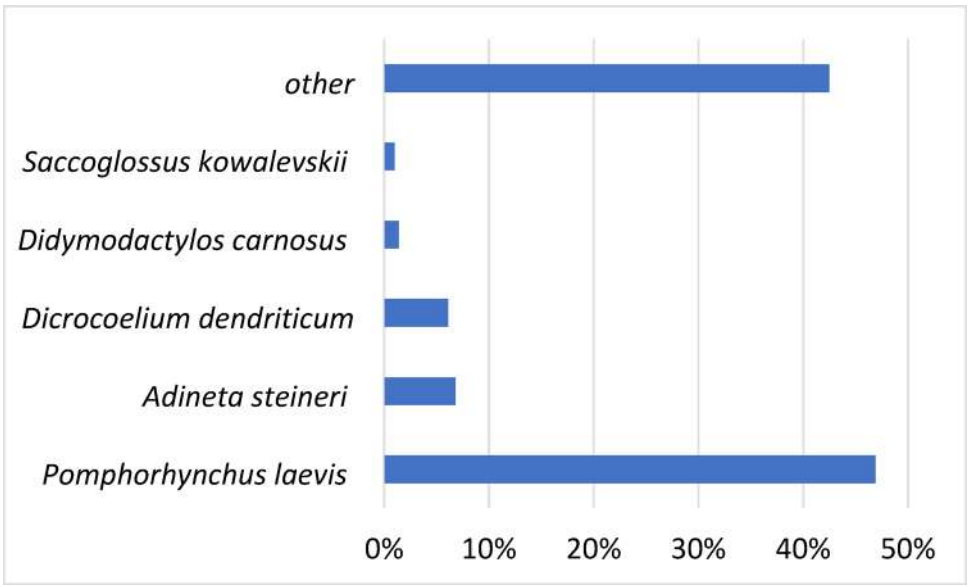

Fig. 2. Species distribution of *D. truttae* unigenes annotated in the NR database (NCBI non-redundant protein sequences). This graph shows the percentage of unigenes that match sequences from different species showing the top five most represented species.

A total of 14,662 unigenes were annotated by matching them to the NR database and used to further determine the GO terms and KEGG pathways. According to the species distribution of the sequences annotated in the NR database, 46.9% of the matched unigenes showed similarities with sequences of *Pomphorhynchus laevis* (Acantocephala), followed by *Dicrocoelium dendriticum* (Platyhelminthes, Trematoda) (6.1%), *Didymodactylos carnosus* (Rotifera) (1.4%), *Adineta steineri* (Rotifera) (6.8%), *Saccoglossus kowalevskii* (Hemichordata) (1.0%), *Rotaria magnacalcarata* (Rotifera) (1.0%), and others (42.5%) (Fig. 2).

Only a small proportion of unigenes matched sequences from the fish host *Salmo trutta* (0.91%), with an additional 0.91% matched sequences from *Salmo salar* and 0.53% from *Oncorhynchus mykiss*. This suggests that contamination with DNA from parasite hosts was not significant.

According to the KOG function classification, 6,729 of 14,662 unigenes (45.9%) were annotated and classified into 25 functional categories based on their predicted functions. Among them, the largest group was

"General function prediction only" (11.2% genes), followed by "Signal transduction mechanisms" (11.1%), "Posttranslational modification, protein turnover, chaperones" (10.4%), "Translation, ribosomal structure and biogenesis" (8.5%) and "Transcription" (6.8%) (Fig. S3). The least represented categories were "extracellular structures" (0.4%) and "cell motility" (0.2%).

A total of 7,616 out of 14,662 unigenes (51.9%) were assigned to 303 KEGG pathways belonging to seven KO pathway level 1 categories (markers B, C, E, G, M, N, and O in Fig. 3). Most genes (58.2%) belonged to "BRITE Hierarchies" (B), while only 1.2% belonged to "Not Included in Pathway or BRITE" (N) (Fig. S4).

Most of the unigenes in the largest subcategory of the "BRITE Hierarchies", "Genetic information processing", were included in the pathways "Membrane trafficking" (15.9%), "Chromosome and associated proteins" (11.9%), "Messenger RNA biogenesis" (8.0%) and "Spliceosome" (7.9%) (Fig. S5). The pathways that contained the largest number of unigenes in the category "Signaling and Cellular Processes" were "Exosome" (31.3%) and "Cytoskeleton proteins" (17.2%), while those in the "Metabolism" category were "Peptidases and inhibitors" (26.3%), "Protein phosphatases and associated proteins" (25.1%) and "Protein kinases" (25.0%). Within "Genetic Information Processing" category the subcategory "Translation" contained the most unigenes associated with the KEGG pathways "Ribosome" (39.4%), "Ribosome biogenesis in eukaryotes" (21.0%) and "mRNA surveillance pathway" (17.2%).

Identification of orthologous sequences

OrthoFinder has been used to identify orthogroups, i.e. groups of genes that share a common ancestor and provide important insights into gene function, evolutionary history and species adaptations among *D. truttae*, *Pomphorhynchus laevis* (Acanthocephala), *Adineta steineri*, *Rotaria socialis*, *Brachionus calyciflorus* (Rotifera), *Ancylostoma ceylanicum*, *Trichinella nativa* (Nematoda), *Dicrocoelium dendriticum* (Platyhelminthes, Trematoda) and *Saccoglossus kowalevskii* (Hemichordata). The analysis assigned 169,531 genes from these nine species (66.1% of the total) to 49,452 orthogroups. Half of the assigned genes were present in orthogroups with four or more genes (G50 = 4) and were contained in the largest 12,529 orthogroups (G50 = 12,529), emphasizing the comprehensive nature of the orthogroup assignments and their evolutionary significance.

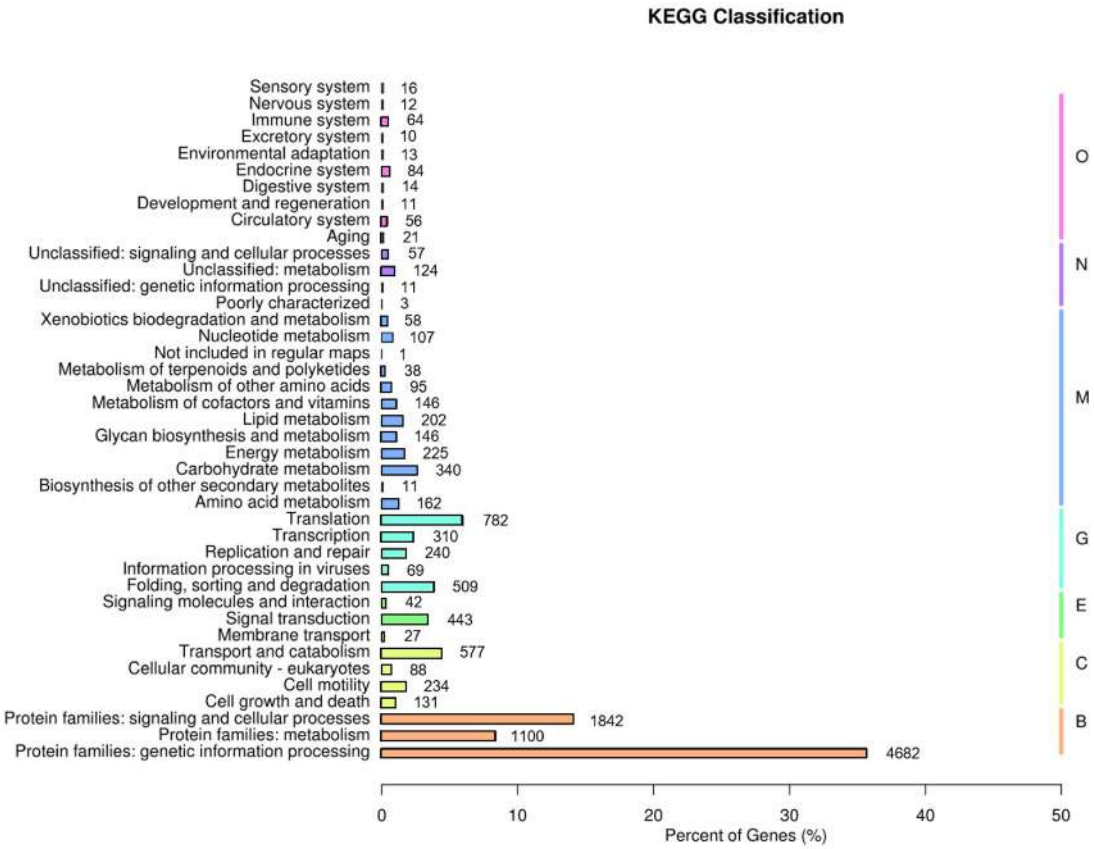

Fig. 3. Functional classification of annotated genes based on the KEGG database[68–70]. KEGG functional categories are grouped into two major classifications: KEGG Pathways, which include categories such as Metabolism (M), Genetic Information Processing (G), Environmental Information Processing (E), Cellular Processes (C), Organismal Systems (O), and Not Included in Pathway or BRITE (N), and BRITE Hierarchy, which includes higher-level functional groupings such as "Protein families: metabolism", "Protein families: genetic information processing" and "Protein families: signaling and cellular processes" (represented by code B).

	Acanthocephala		Rotifera			Nematoda		Platyhelminthes	Hemichordata
	D. truttae	*P.* laevis	*A. steineri*	*R.* socialis	*B. calyciflorus*	*A. ceylanicum*	*T. nativa*	*D. dendriticum*	*S. kowalevskii*
Number of genes	**13,457**	13,055	50,525	33,717	24,404	65,583	16,586	16,907	22,132
Number of genes in orthogroups	**10,345**	6423	42,052	20,137	10,413	53,574	10,603	9055	6929
Number of unassigned genes	**3112**	6632	8473	13,580	13,991	12,009	5983	7852	15,203
% of genes in orthogroups	**76.9**	49.2	83.2	59.7	42.7	81.7	63.9	53.6	31.3
% of unassigned genes	**23.1**	50.8	16.8	40.3	57.3	18.3	36.1	46.4	68.7
Number of orthogroups containing species*	**3512**	1875	17,845	13,944	3812	13,538	3088	2610	2456
% of orthogroups containing species	**7.1**	3.8	36.1	28.2	7.7	27.4	6.2	5.3	5.0
Number of species-specific orthogroups	**3432**	1737	5734	1828	3224	13,438	2938	2550	2209
Number of genes in species-specific orthogroups	**10,144**	6214	17,858	5274	9623	53,337	10,324	8960	6565
% of genes in species-specific orthogroups	**75.4**	47.6	35.3	15.6	39.4	81.3	62.2	53.0	29.7

Table 2. Species-specific statistics of orthofinder orthogroup analysis among coding sequences of *D. trutta* and eight phylogenetically or lifestyle-related species with reference genomes available in the NCBI database: *Pomphorhynchus laevis*, *Adineta steineri*, *Rotaria socialis*, *Brachionus calyciflorus*, *Ancylostoma ceylanicum*, *Trichinella nativa*, *Dicrocoelium dendriticum* and *Saccoglossus kowalevskii*. *Number of orthogroups containing species – total number of orthogroups in which the species listed at the top of the column is present.

	Acanthocephala		Rotifera			Nematoda		Hemichordata	Platyhelminthes
	D. truttae	*P.* laevis	*A. steineri*	*R.* socialis	*B. calyciflorus*	*A. ceylanicum*	*T. nativa*	*S. kowalevskii*	*D. dendriticum*
D. truttae		**31**	**24**	**24**	**13**	**22**	**15**	**11**	**9**
P. laevis			78	82	55	8	14	30	10
A. steineri				12,768	490	38	76	157	27
R. socialis					488	37	79	152	27
B. calyciflorus						19	59	94	14
A. ceylanicum							22	26	14
T. nativa								29	12
S. kowalevskii									20
D. dendriticum									

Table 3. Number of shared orthogroups among the acanthocephalans *Dentitruncus truttae* and *Pomphorhynchus laevis* and other species related by phylogeny or lifestyle.

While over 80% of genes in *A. steineri* (83.2%), and *A. ceylanicum* (81.7%) were assigned to orthogroups, more than half of the genes in *P. laevis* (50.8%), *B. calyciflorus* (57.3%), and *S. kowalevskii* (68.7%) remained unassigned (Table 2, Fig. S6), highlighting differences in gene assignment rates and the varying degrees of genomic characterization among species.

Only two orthogroups contained genes from all nine species, and neither of these was a single-copy orthogroup. The majority of orthogroups were species-specific, with 37,090 orthogroups (75.0%) containing 128,299 genes (50.0% of the total). The number of species-specific genes ranged from 5,274 (15.6%) in *R. socialis* to 53,337 (81.3%) in *A. ceylanicum* (Table 2, Fig. S6), illustrating the considerable variability in gene distribution and species-specific evolution across the dataset.

The highest number of shared orthogroups was observed among the rotifer species and between them and *S. kowalevskii* (Hemichordata) (Table 3). Notably, 10,144 (75.4%) *D. truttae* genes were found in species-specific orthogroups, with only 1.5% shared across different species. The species sharing the highest proportion of orthogroups with *D. truttae* were *P. laevis* (20.8% of shared orthogroups), *A. steineri* (16.1%), *R. socialis* (16.1%) and *A. ceylanicum* (14.8%) (Fig. S7), highlighting patterns of gene conservation and divergence across species.

The shared orthogroups provide valuable insights into evolutionary relationships and functional similarities, helping to distinguish conserved genes that are shared across species from species-specific genes that reveal evolutionary pressures and functional innovations. For instance, the extensive sharing of orthogroups among rotifers and *S. kowalevskii* suggests conserved functional roles and evolutionary constraints linked to their shared aquatic habitats and developmental biology. Among the species analyzed, *A. steineri* and *R. socialis* shared the highest number of orthogroups (12,768), reflecting their close phylogenetic relationship within Bdelloidea rotifers and high genomic similarity. Conversely, the lower level of shared orthogroups between *P. laevis* and *D. truttae*, despite their phylogenetic proximity as parasitic organisms, suggests divergent evolutionary pressures potentially related to host specialization and life cycle adaptations.

Interestingly, *P. laevis* shared more orthogroups with rotifers than with *D. truttae*, which contrasts with expected phylogenetic relationships and ecological similarities. This pattern indicates that evolutionary convergence in certain genes related to environmental adaptation may have occurred between *P. laevis* and the

rotifers. Furthermore, the identification of 12 *P. laevis* genes with multiple orthologs in *D. truttae* implies post-speciation gene duplication events, contributing to potential functional diversification.

Orthogroup analysis thus highlights not only evolutionary ancestry but also gene family expansions, contractions, and functional adaptations specific to ecological niches, demonstrating its importance for comparative genomics by helping researchers understand how gene duplication, loss, and retention shape genomes over time. The distribution of orthogroups across species emphasizes both conserved genetic pathways and species-specific innovations that reflect adaptive strategies within their respective clades.

Metal-binding proteins

After the entire proteome of *D. truttae* (13,457 protein sequences) was submitted to the MeBiPred server for prediction of metal-binding properties, 1,944 protein sequences (14.5%) were characterized as metal-binding (Supplementary File 2, Supplementary File 2a), with a remarkable distribution across different metal ions. Zinc-binding proteins were the most abundant (53.8%, 1,052 proteins), followed by iron- (13.6%, 266 proteins) and nickel-binding proteins (11.4%, 233 proteins) (Fig. 4). A relatively low number of copper- (5.0%, 98 proteins) and cobalt-binding proteins (2.5%, 49 proteins) were predicted, while manganese-binding proteins bind to 8.0% (157 proteins) of MBPs in *D. truttae* (Fig. 4). Proteomic analysis of *P. laevis* (GCA_012934845.2) showed a similar metal-binding pattern, with 15.5% (2,029 protein sequences) of the proteome exhibiting metal-binding properties (Supplementary File 2, Fig. 4 Supplementary File 2b). Zinc-binding proteins were also the most abundant MBPs (47.2%, 958 proteins), followed by iron- (15.6%, 317 proteins) and nickel- (11.4%, 231 proteins) binding proteins, with a similar low prediction of manganese- (9.7%, 196 proteins), copper- (4.4%, 90 proteins) and cobalt- (2.9%, 58 proteins) ion-binding proteins. However, 796 of the total MBPs in *D. truttae* were predicted to bind two or more ions, compared to 832 in *P. laevis* (Supplementary File 2).

Of the 1,944 protein sequences predicted as MBPs by the MeBiPred software, 1,383 were described by the PFAM database (e-value threshold is 0.01) as having specific protein domains. Of these, 265 were associated with binding of zinc ions (Supplementary File 3), 23 with nickel ions (Supplementary File 4), 22 with copper ions (Supplementary File 5), 11 with iron ions (Supplementary File 6) and no protein sequence was associated with a specific domain for cobalt binding. When we analyzed the zinc-binding proteins in *D. truttae*, the majority (246 protein sequences) was classified as zinc finger proteins and 13 as metalloproteases (Supplementary File 3, Fig. 5). Zinc fingers, a common motif, are particularly involved in gene regulation, which may explain their prevalence among the proteins in these organisms. However, as metalloproteases are a more homogeneous protein group, we further analyzed 13 protein sequences from *D. truttae* for their similarity and agreement with the NCBI GenBank data (Fig. 5). These proteins could support nutrient acquisition and stress resistance by breaking down host or environmental proteins, managing oxidative stress, and adapting to metal-rich environments, potentially enhancing parasite survival. The phylogenetic tree showed a division of the sequences into five not clearly delimited clusters consisting of matrixin, reprolysin and some proteins with functions unknown by PFAM (Supplementary File 3, Fig. 5). The heatmap results showed that the metalloproteases of Acanthocephala (mainly matrixins and reprolysins) are highly conserved with *P. laevis* (Fig. 5). In cases where the NCBI database did

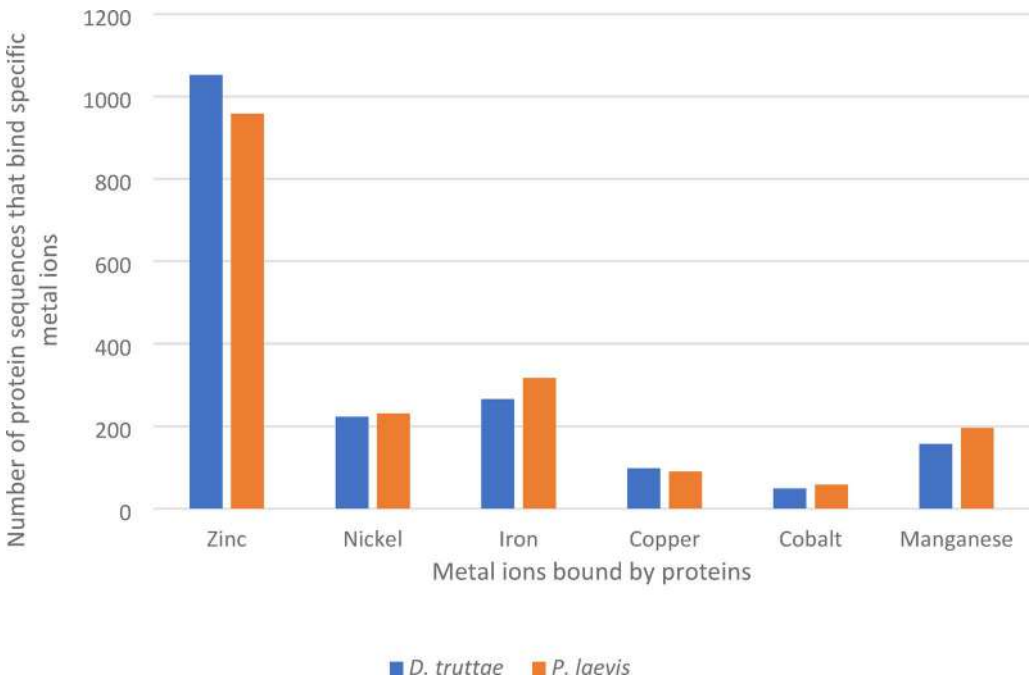

Fig. 4. Comparison of the number of metal-binding proteins that bind different metal ions (zinc, nickel, iron, copper, cobalt, manganese) in two Acanthocephala species, *D. truttae* and *P. laevis*, according to the MeBiPred analysis.

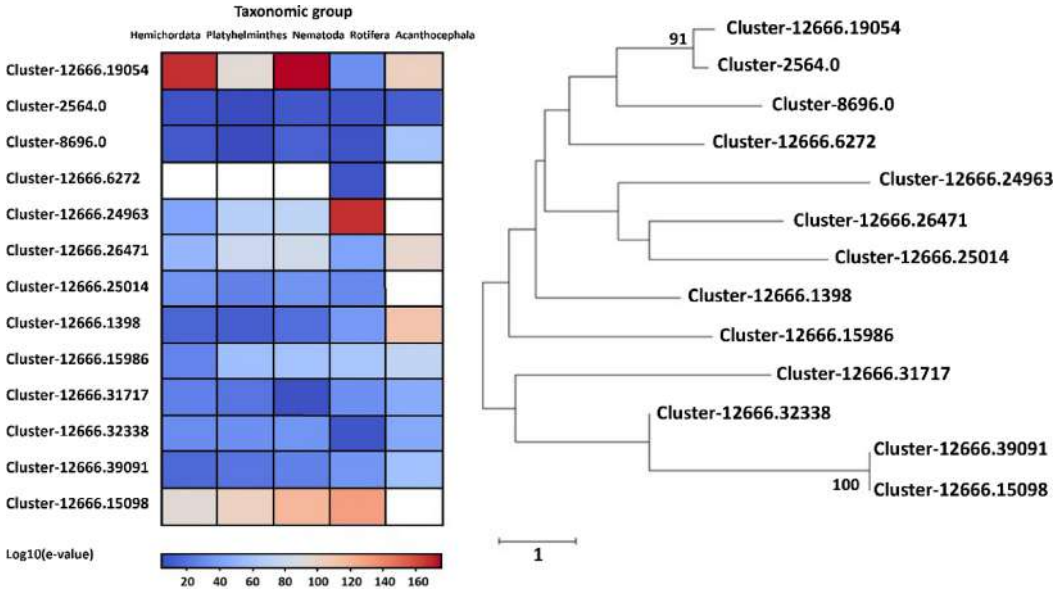

Fig. 5. Phylogenetic analysis of *D. truttae* zinc metalloproteases using 1000 replicates and Whelan Goldman + Freq Model. Only bootstrap values ≥ 70% are shown. The tree is drawn to scale, with branch lengths representing the number of substitutions per site, as indicated by the scale bar. The heatmap represents log10-transformed e-values from alignments against sequences from Acanthocephala, Rotifera, Nematoda, Platyhelminthes, and Hemichordata, with red indicating significant alignments and blank boxes representing no similar sequences.

not contain data for *P. laevis* homologues, the metalloprotease sequences of *D. truttae* showed more similarities with evolutionarily close Rotifera and parasitic Nematoda. Only one sequence (Cluster-12666.19054) was an exception, showing the highest degree of similarity to Nematoda and Hemichordata. These proteins may play a crucial role in nutrient acquisition and stress resistance by degrading host tissue and remodeling of extracellular matrix components.

Nineteen sequences have been described that bind iron, eight of which have been identified as the iron-sulfur group (Supplementary File 6, Fig. 6). These iron-sulfur binding and zinc-finger proteins may contribute to parasitic adaptation by facilitating survival in metal-rich host environments, possibly through improved redox homeostasis and protection against oxidative stress. When we analyzed these sequences in a phylogenetic tree, two main clusters emerged (Fig. 6). One cluster consisted of two proteins with predicted NADH-ubiquinone oxidoreductase-G iron-sulfur binding region (Cluster-12666.43560 and Cluster-12666.33394) and one zinc-finger (Cluster-12666.179). Only one sequence (Cluster-12666.33394) showed a higher degree of similarity to other Acanthocephala species (P.laevis) and Rotifera, shown in red squares in the heatmap. Other cluster contained more variable sequences, two of which (Cluster-12666.14469 and Cluster-12666.28221) showed the highest similarity to P.laevis and Rotifera.

When we analyzed the nickel-binding proteins in *D. truttae*, 23 were PFAM described as nickel ureases/hydrogenases (Supplementary File 4). The phylogenetic tree, which consisted of similar protein sequences from invertebrates, showed three major clusters that are not clearly variable in the PFAM definition (Fig. 7). The heatmap showed the highest degree of similarity with other Acanthocephala (*P. laevis*) and Rotifera, and one sequence (Cluster-12666.195031) had no similar homologues other than the taxonomic group Hemichordata, with a high degree of similarity (Fig. 7). These nickel-binding proteins likely support parasite adaptation by contributing to nitrogen metabolism and mitigating the toxic effects of metal accumulation by enhancing survival in metal-rich host environments through processes such as urease-driven ammonia detoxification and redox balance maintenance.

Of the 19 sequences identified as potential invertebrate metallothioneins by HMMER using the PFAM database, five were characterized as MBPs by MeBiPred (Supplementary File 7). Of these five proteins, one was identified by the NR database as most similar to *Pomphorhynchus laevis* (Acanthocephala), two had identical amino acid sequences and were most similar to *Trichinella patagoniensis* (Nematoda), one was most similar to *Branchiostoma belcheri* (Cephalochordata) and one sequence showed no significant similarity in blasting to a sequence in the NCBI database.

Interestingly, the protein sequence that was most similar to *T. patagoniensis* (55.6%) also had the highest similarity to plant metallothioneins (87.7% and 86.1% for *Carpus fangiana* and *Corylus avellane*, respectively). No other organisms, except plants and *T. patagoniensis*, showed such a high degree of similarity. Metallothioneins are known for their chelating properties for metal ions, which could help parasites such as *P. laevis* and *T. patagoniensis* to cope with metal toxicity while contributing to redox regulation and resistance to oxidative stress during parasitism.

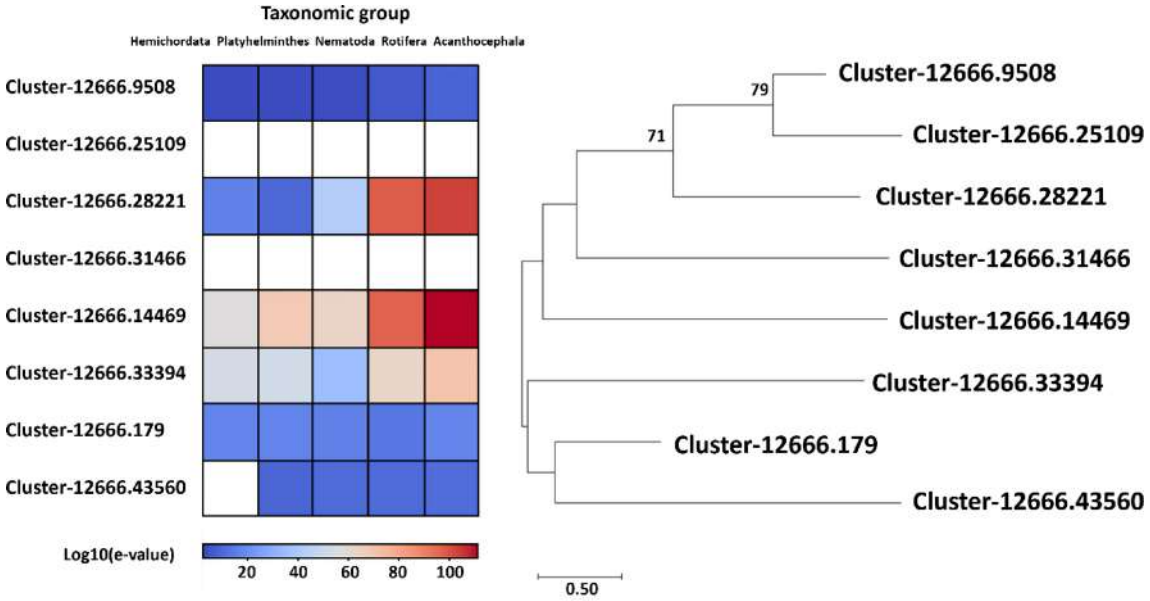

Fig. 6. Phylogenetic analysis of *D. truttae* iron-sulfur proteins using 1000 replicates and Whelan Goldman + Freq Model. Only bootstrap values ≥ 70% are shown. The tree is drawn to scale, with branch lengths representing the number of substitutions per site, as indicated by the scale bar. The heatmap represents log10-transformed e-values from alignments against sequences from Acanthocephala, Rotifera, Nematoda, Platyhelminthes, and Hemichordata, with red indicating significant alignments and blank boxes representing no similar sequences.

To further explore evolutionary relationships, we constructed a phylogenetic tree and heatmap for the remaining two metallothionein sequences. The results confirmed their highest similarity with sequences from the closely related acanthocephalan *P. laevis* and various species of Rotifera (Fig. 8). These observations support the hypothesis that metallothioneins are critical for survival in dynamic, metal-rich environments and contribute to the evolutionary success of parasitic species inhabiting a range of ecological niches.

To group the remaining 561 protein sequences for which we could not find characteristic metal-binding domains in the PFAM database, we categorized them according to the predictions of the MeBiPred software for specific metal binding (Fig. 9). The hierarchical cluster map visualized patterns in their metal binding preferences, based on which these 561 proteins were divided into three main clusters, the largest of which is subdivided into two subclusters (Fig. 9, Supplementary File 8). These two subclusters (protein 1 and 2 in Fig. 9) showed similar binding preferences, characterized by higher binding of Zn, Ni, Co and Cu ions, while lower binding preferences were observed for Mn and Mg ions. The members of the second cluster were characterized by the highest preference for the binding of Ca and the lowest for the binding of Mn. The third cluster consisted of proteins with a high preference for binding Cu and a low preference for binding Fe and Mg ions (Fig. 9). It is evident that all clusters had an almost equal preference for binding Zn ions, while Mg, Fe and Mn were bound with the lowest preference.

To refine our analysis of metal-binding proteins (MBPs), we focused on protein groups with specific metal-binding domains using HMMER (HMMER package, Seed Alignment, e-value threshold of $1e^{-5}$). The analysis revealed that most MBPs in *D. truttae* belonged to the PFAM family "ABC transporter", with seven sequences, followed by "solute carrier family 39 member 10", "Ctr copper transporter family", "Metallothionein", and "ABC transporter transmembrane region" (two sequences each) and "Cation efflux family", "Inositol polyphosphate kinase", and "Glutathione S-transferase, N-terminal domain" (one sequence each).

Comparative analysis with organisms from Rotifera, Nematoda, Trematoda and Hemichordata revealed the greatest similarities between the acanthocephalans *D. truttae* and *P. laevis*, and between members of Nematoda (*Trichinella nativa* and *Trichinella patogoniensis*) and Trematoda (*Dicrocoelium dendriticum*). Members of the phylum Rotifera had a significantly higher number of genes (Table 2) and consequently a higher number of proteins belonging to the analyzed PFAM groups containing metal-binding domains (Table 4, Supplementary File 9). The PFAM group "ABC transporter" consistently contained the highest number of proteins. However, only a small proportion (11.0-24.0%) were predicted as MBPs by the MeBiPred software (Table 4, Supplementary File 9).

Interestingly, *D. truttae* possessed two MBPs from the "Ctr copper transporter family", a feature it shared with *Brachionus plicatilis* and *Saccoglossus kowalevskii*, whereas organisms with larger genomes generally possessed only one or no protein from this family (Table 4). Remarkably, *D. truttae* also contained an MBP from the "metallothionein" family, which was absent in the other organisms analyzed (Supplementary File 9).

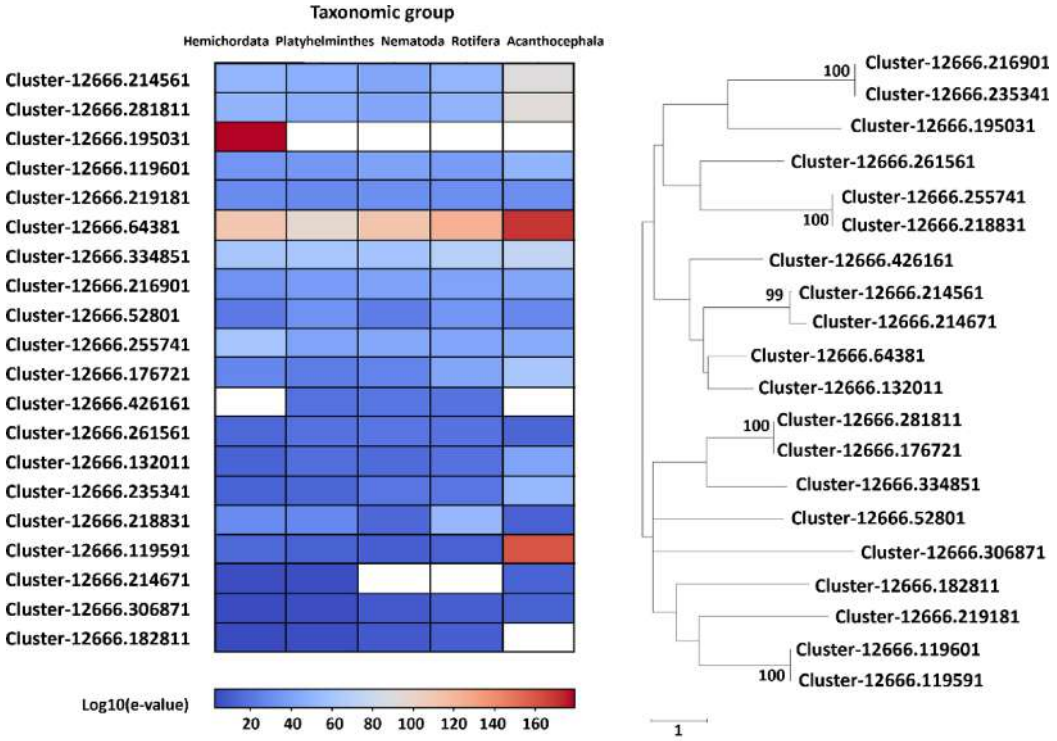

Fig. 7. Phylogenetic analysis of *D. truttae* nickel urease/hydrogenase proteins using 1000 replicates and Whelan Goldman + Freq Model. Only bootstrap values ≥ 70% are shown. The tree is drawn to scale, with branch lengths representing the number of substitutions per site, as indicated by the scale bar. The heatmap represents log10-transformed e-values from alignments against sequences from Acanthocephala, Rotifera, Nematoda, Platyhelminthes, and Hemichordata, with red indicating significant alignments and blank boxes representing no similar sequences.

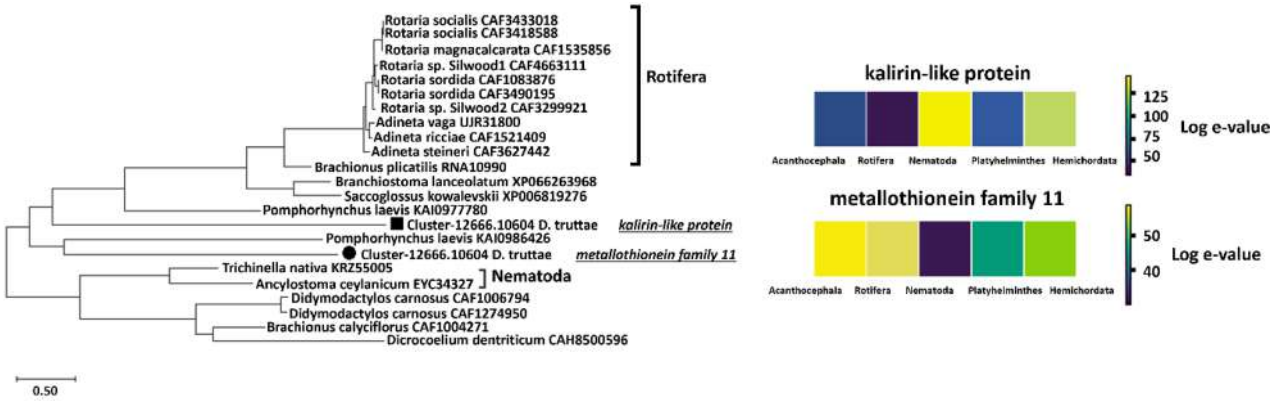

Fig. 8. Phylogenetic analysis of two *D. truttae* metallothioneins using 1000 replicates and JTT matrix-based Model. The threshold for displaying bootstrap support values was 70%. The tree is drawn to scale, with branch lengths representing the number of substitutions per site, as indicated by the scale bar. The black circle and square in the tree indicate two *D. truttae* metallothionein protein sequences which were identified as kalirin-like protein and a member of metallothionein family 11. The heatmap represents log10-transformed e-values from alignments against sequences from Acanthocephala, Rotifera, Nematoda, Platyhelminthes, and Hemichordata, with purple indicating significant alignments and yellow boxes representing less matching sequences.

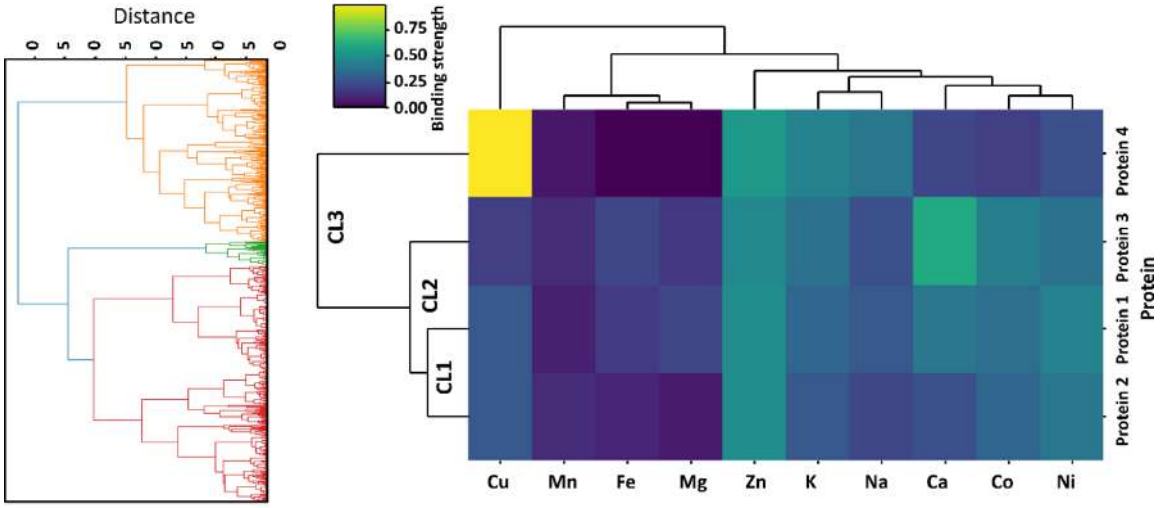

Fig. 9. Hierarchical clustering heatmap of *D. truttae* metal-binding proteins lacking PFAM annotation, grouped into three clusters (CL1, CL2, and CL3) based on predicted metal-binding affinities. Binding strength values are color-coded, ranging from low (dark purple) to high (yellow), as indicated by the scale. The dendrograms represent hierarchical relationships among both proteins (right) and metal ions (top), based on binding preferences for Cu, Mn, Fe, Mg, Zn, K, Na, Ca, Co, and Ni (Supplementary File 8).

In the "Cation efflux family", *P. laevis* contained proteins that were characterized as metal tolerance proteins in the Swiss-Prot database but were classified as non-metal-binding proteins by MeBiPred (clusters 12666.22969, 12666.23553, 12666.31057 and 12666.31058). In addition, no MBPs from *D. truttae* were identified within the family "Heavy-metal-associated domain", a result consistent with most of the parasitic organisms analyzed (Table 4).

One MBP belonging to the family "ABC transporter transmembrane region" (ATP-binding cassette) was identified in *D. truttae* and showed high sequence similarity to the hypothetical protein GJ496_010402 from *P. laevis*. However, this protein was predicted by MeBiPred to be non-metal-binding (Table 4, Supplementary File 2).

Discussion

As the entire transcriptome has only been published for a single species from the order Acanthocephala, the transcriptome sequence of *D. truttae* represents a valuable resource to advance research and improve our understanding of this group of parasites. We have particularly emphasized their physiologically fascinating and ecologically important ability to accumulate high concentrations of metals, the molecular mechanism of which is not yet understood. The *D. truttae* transcriptome, based on unigenes, spans 50.3 million bp, which exceeds the lengths reported for the transcriptomes of the acanthocephalan (*P. laevis*, 33.8 million bp) and two rotifers (*Brachionus manjavacas*, 40.1 million bp; and *Rotaria magnacalcarata*, 40.0 million bp) - based on filtered contigs[32]. Differences in the length distribution of transcripts and unigenes are to be expected due to the limitations of sequencing technology and biological variability[33]. The low percentage of fragmented reads in our assembly indicates that reconstruction successfully captured most of the expected single-copy orthologs. However, the relatively high percentage of missing reads may reflect transcript variability or species-specific factors in this *de novo* transcriptome analysis.

As expected, a higher proportion of *D. truttae* unigenes (40.6%) were annotated in at least one database compared to 30% of *P. laevis* transcripts matched with counterparts in a custom database[32]. This difference likely reflects the inclusion of *P. laevis* and other closely related species in the NCBI database following the earlier studies. However, only 14.6% of our transcriptome data matched the SwissProt database, while 29.3% matched entries in the PFAM or GO databases. This is due to the fact that PFAM and GO provide more comprehensive and domain-based annotations covering a broad range of proteins and functions, whereas SwissProt provides highly curated annotations that focus on a narrower set of well-characterized proteins and may exclude novel or less-characterized proteins in *D. truttae*.

The results of the GO annotation of *D. truttae* unigenes were consistent with those of the GO analysis of the *P. leavis* transcriptome[32]. Our findings support those of Mauer et al. (2020) who reported that a significant proportion of the acanthocephalan transcriptome is dedicated to metabolism - an adaptation likely linked to their parasitic lifestyle and reliance on nutrient uptake via their body surface (e.g. GO term “binding”)[32]. While the distribution of biological process (BP) subcategories were similar in *D. truttae* and *P. laevis*, the molecular function (MF) categories related to binding, catalytic activity and transporter activity were more abundant in *D. truttae*. These proportions were comparable to those observed in the rotifer *Brachionus koreanus*[32,34], indicating possible shared physiological traits related to environmental adaptation.

PFAM groups		Acanthocephala		Rotifera				Nematoda			Platyhelminthes	Hemichordata
		Dentitruncus truttae	*Pomphorhynchus laevis*	*Adineta steineri*	*Rotaria socialis*	*Brachionus calyciflorus*	*Brachionus plicatilis*	*Ancylostoma ceylanicum*	*Trichinella nativa*	*Trichinella patagoniensis*	*Dicrocoelium dendriticum*	*Saccoglossus kowalevskii*
Name	PFAM no.	Number of metal-binding proteins within PFAM group/number of PFAM group members										
ABC transporter	PF00005	**7/46**	3/36	72/299	21/179	17/113	11/93	30/238	11/46	8/58	8/51	13/118
Cation efflux family	PF01545	**1/13**	0/7	11/48	0/32	1/15	1/15	12/23	1/12	0/7	2/6	2/10
ZIP Zinc transporter	PF02535	**2/12**	2/15	6/32	4/26	0/15	1/17	10/52	10/19	7/15	1/12	1/21
Ctr Copper transporter family	PF04145	**2/3**	0/1	0/12	0/8	1/5	2/5	0/15	0/1	0/1	0/2	2/7
P5-type ATPase cation transporter	PF12409	**0/1**	0	0/1	0/1	0/5	0/2	0/6	0/1	0/3	1/1	0/2
Ferritin-like domain	PF00210	**0/13**	1/3	0/5	0/7	0/15	0/11	0/3	0/1	0/1	0/3	0/4
Metallothionein	PF01439	**1/1**	0	0	0	0	0	0	0	0/1	0	0
Copper permeases	PF00403	**0/2**	0/1	0/6	1/7	0/3	0/2	5/8	0/3	0/6	0/4	1/7
Sco1 chaperons	PF03770	**1/4**	0/4	0/8	1/5	0/2	0/2	1/8	1/3	3/6	2/6	0/4
ATP-binding cassette	PF00664	**2/17**	0/9	49/153	2/55	2/41	3/35	6/116	1/10	1/20	0/18	3/53
Glutathione S-transferase	PF02798	**0/16**	0/17	2/83	3/33	1/27	0/27	0/35	2/6	3	2/22	8/54

Table 4. Number of MBPs confirmed by the MeBiPred in selected metal-binding PFAM groups in Acanthocephala and related species.

The species distribution of the sequences annotated in the NR database was consistent with expectations, given the scarcity of genomic and transcriptomic data available for acanthocephalans. As anticipated, the highest sequence similarity was with *P. laevis*, the only acanthocephalan species for which both genome and transcriptome data are available[32]. Mauer et al. (2020) also identified similarities between sequences from Acanthocephala, Rotifera (especially Bdelloidea), and Platyhelminthes[32]. The resemblance to bdelloid rotifers likely reflects the phylogenetic relatedness of these taxa, while the similarity to trematodes may be due to shared adaptations to a parasitic lifestyle.

Given the parasitic nature of *D. truttae*, there was a high probability of contamination of the studied parasite with the host fish tissue. However, the low percentage of matched sequences confirmed that this contamination was negligible. Similarly, Mauer et al. (2020) reported that only 4% of the contigs of *P. laevis* matched sequences in the genome and transcriptome database of its fish host (*Cyprinus carpio* Linnaeus, 1758), confirming that host contamination was insignificant[32]. The results of the KOG classification of *D. truttae* unigenes were comparable to those of the nematode *Angiostrongylus cantonensis* and the cestode *Taenia pisiformis*[35,36]. Although "general function prediction only" was not the largest cluster in these two organisms, this is not surprising in *D. truttae* due to the limited amount of genomic and transcriptomic data available for acanthocephalans. The occurrence of KEGG Orthology terms in the analysis of *D. truttae* was similar to that of *Trichinella pseudospiralis* and *T. spiralis*, especially in the KEGG BRITE categories[37]. This suggests a comparable metabolic profile, reflecting the evolutionary and functional parallels between these parasitic species.

The high percentage (> 20%) of genes that could not be assigned to an orthogroup in the OrthoFinder analysis could be due to incorrectly assembled or annotated genes or poor species sampling[38,39]. However, this result is not unexpected, as we are working with a non-model organism whose genome has not yet been sequenced. As Acanthocephala is a large taxonomic group for which only a single genome has been published[32], we considered that Acanthocephala species are phylogenetically distant from other well-studied taxa[40], limiting the ability to refine species selection due to the scarcity of available comparative genomic data. Given that we used NCBI reference genome data for all species except *D. truttae*, we did not interpret unassigned genes as assembly errors, but instead chose to report the full set of results. The high number of potentially species-specific genes and the low number of single-copy orthogroups are consistent with the diversity and phylogenetic distance of the species included in the analysis[38,39]. However, the percentage of species-specific genes is notably higher than the values commonly reported in the literature[41,42]. For comparison, an analysis of the transcriptomes of larvae of the parasitic nematode *Anisakis pegreffii* revealed that 58.1% of all unigenes obtained by *de novo* assembly were novel and that only 41.9% corresponding to previously known genes. This finding supports the hypothesis that the high specificity may reflect the lack of comprehensive comparative transcriptomic data rather than methodological issues[43].

The percentage of metal-binding proteins in a proteome can vary depending on the organism and the specific environment. However, it is generally estimated that 20–30% of all proteins in a typical proteome are metal-binding, with the majority of binding the essential metals, such as Ca^{2+} and Mg^{2+}. Using MeBiPred software, our analysis predicted 14.5% of proteins binding the corresponding ions (Fe, Ca, Na, K, Mg, Mn, Cu, K, Co, and Ni), similar to another Acanthocephala *P. laevis* (15.5%). This percentage is slightly lower than that of the reference proteome of the alga *Micromonas pusilla* (19.4%), which was analyzed using the same method[30]. This lower number could be a consequence of the two-tiered approach of the software, since some proteins classified as members of the families that bind metals according to the Swissprot or PFAM databases were characterized by MeBiPred as non-metal-binding.

The predominance of zinc-binding proteins, which account for 53.8% of MBPs in *D. truttae* and 47.2% in *P. laevis*, emphasizes the essential role of zinc in various biological processes. Zinc is crucial for DNA replication, repair, transcription and protein synthesis and thus essential for cellular functions. Zinc fingers, a common motif, are particularly involved in gene regulation, which may explain its prevalence among the proteins in these organisms. The dominance of zinc finger proteins in *D. truttae* (246 sequences) is consistent with observations in other invertebrates and eukaryotic organisms such as *Caenorhabditis elegans* (Nematoda)[44] and *Drosophila melanogaster* (Arthropoda)[45], in which zinc fingers also represent a large proportion of the proteome, reflecting their essential role in regulating gene expression during development, differentiation, and stress response. Zinc finger motifs, abundant in these proteomes, may reflect the evolutionary pressure to maintain robust transcriptional control mechanisms in dynamic host environments.

Phylogenetic analysis of metalloproteases, another group of zinc-binding protein in *D. truttae*, shows that the sequences for reprolysin and matrixin do not form distinct clusters but are dispersed across different clusters. Very strong evolutionary conservation or functional similarity between the metalloproteases of *D. truttae* and *P. laevis* was expected, since they both belong to Acanthocephala. Rotifera, Nematoda and Hemichordata showed a slightly lower level of conservation, while Platyhelminthes showed a moderate range of low e-values in BLAST alignments, suggesting a somewhat reduced degree of conservation. Metalloproteases in Acanthocephala are predicted to degrade extracellular matrix (ECM) components, facilitating the tissue invasion, immune evasion, and nutrient acquisition. These processes are similarly observed in nematodes and parasitic platyhelminths, suggesting convergent evolution driven by parasitic lifestyles. However, the differences in sequence conservation among taxonomic groups (e.g., lower conservation in platyhelminths) may point to unique evolutionary adaptations in acanthocephalans[46,47]. The analyzes of MBPs defined by PFAM as iron-binding in *D. truttae* were focused on the iron-sulfur group. Iron-sulfur proteins are involved in electron transfer and enzyme catalysis. They are ubiquitous and are found in all domains of life. In Acanthocephala they may play a role in the metabolic processes and energy production. As parasites, Acanthocephala can be confronted with fluctuating and rather low oxygen levels in their host's intestine, which requires a flexible metabolic adaptation. Their adaptations include: (1) a relatively low metabolic demand, so that diffusion is sufficient for gas exchange, and (2) the ability for anaerobic metabolism, which is useful in the low-oxygen environment of their hosts' gut[48]. Acanthocephala

may have adapted mitochondrial function through iron-sulfur proteins in complex I and complex II to flexibly switch between aerobic and anaerobic metabolic pathways. Acanthocephala also possesses machinery for the assembly of iron-sulfur clusters, as we found some of its components in the proteome of *D. truttae*, based on the definition of PFAM domains (frataxin or frataxin-like and ferredoxin or ferredoxin-like proteins). Due to the low e-values obtained from the BLAST alignments, the degree of concordance between the sequences of *D. truttae* and *P. laevis* was, as expected, the highest. Nematoda, Platyhelminthes, and Hemichordata also show very low e-values in most cases, suggesting conserved sequences, though with some slight variations. A few outliers with higher e-values (e.g. 0.001 for Nematoda, 0.028 for Platyhelminthes) may suggest some divergence and possible adaptations of acanthocephalan proteins compared to these taxonomic groups. Nickel-binding proteins, although less abundant, play a key role in the activity of certain enzymes such as urease and hydrogenases, which are involved in nitrogen metabolism and energy production[49]. The presence of nickel-binding proteins suggests that *D. truttae* requires nickel for certain metabolic functions, particularly those related to environmental adaptability. The analyzed sequences are highly conserved, particularly in Acanthocephala and Rotifera. The variations in e-values across taxonomic groups (e.g. in Nematoda) may suggest that these sequences have diverged functionally or evolutionarily from the Acanthocephalan sequences.

561 protein sequences that had no characteristic metal-binding domains based on the PFAM database, were grouped using MeBiPred software to predict their metal-binding preferences. This approach enabled categorization of proteins based on their predicted ability to bind specific metal ions. The hierarchical cluster map was used to visualize the patterns in metal-binding preferences, resulting in the identification of three main clusters (Fig. 9, Supplementary File 8). An important observation across all clusters is the almost equal preference for Zn ions. This likely reflects the importance of Zn as a ubiquitous metal cofactor involved in a variety of biological functions, such as enzyme catalysis, structural stabilization, and regulation of protein-DNA interactions[50]. Overall, the proteins in all clusters show a lower preference for binding Mg, Fe and Mn. This suggests that the remaining proteins are not as strongly involved in functions where these metals play critical roles, or that they are specialized in functions involving other transition metals, particularly Zn, Ni, Co, and Cu. The Zn and Cu binding preferences indicate functions in metalloenzymes, redox biology, or metal ion transport, while the Ca preference indicates calcium-dependent signalling or structural functions[16]. Proteins with low Fe binding preference may not be involved in iron-sulfur cluster formation or electron transport, but their high affinity for other metals suggests alternative biological pathways. These findings highlight the critical role of zinc-binding proteins in parasite survival, supporting enzyme catalysis, structural stabilization, and immune evasion. The low preference for iron-binding proteins suggests an adaptation to avoid host-imposed iron limitations, favouring zinc, copper, and nickel-dependent pathways instead. This may enhance parasite resilience against host defences and oxidative stress. Additionally, calcium-binding proteins indicate roles in signalling and motility, aiding host invasion. Environmentally, parasites may influence zinc and copper cycling in ecosystems, while their reduced reliance on iron and magnesium suggests minimal contribution to traditional iron-sulfur and electron transport processes. Overall, these adaptations reflect a strategic shift in metal utilization, impacting both host-parasite interactions and environmental metal cycling.

We have decided to narrow our analyses strictly to the several specific PFAM protein groups known to be involved in metal binding. The group with the largest number of proteins was PF00005, which includes ABC transporters. This was expected, as this group contains a large family of proteins responsible for the translocation of a variety of compounds across biological membranes. The finding that only 11.0–24.0% of the ABC transporters are predicted by MeBiPred to be metal-binding proteins suggests that although the "ABC transporter" family contains proteins that can transport metal ions, this is not the main function of most of them. *D. truttae* had an MBP from a member of the "metallothionein" family PF01439, which appears to be closest to the Class II metallothioneins, under PFAM number PF00131. The metallothionein-like protein type 2 (MT-2) is expressed in a wide range of organisms from different kingdoms, including animals, plants, fungi and even some bacteria. Various invertebrates, including mollusks and arthropods, express MT-2, which helps detoxify heavy metals accumulated from their environment[51,52]. Although proteins in the family "Heavy-metal-associated domain" are found in both microorganisms and mammals and transport heavy metals, they do not appear to play a role in Acanthocephala, as we did not find MBPs in *D. truttae* or *P. laevis*. Two members of the "ATP-binding cassette" protein group had metal-binding properties, and only one of them had the highest percentage of sequence similarity with the similar protein sequence of *P. laevis*, which in contrast was characterized as non-metal-binding. Whether this difference is a consequence of the two-tiered method used by the MeBiPred software to identify metal binding, or because the sequences were too different, remains to be clarified in future studies. Data availability is a major limitation in this study due to the lack of reference genomes and general molecular data on Acanthocephala in databases. In contrast to model organisms with extensive reference genomes and databases, there are no previously published genomic resources for *D. truttae*, making comparative analyses challenging. A limiting factor in our research on MBPs could also be the limited capacity of protein databases and software. The MeBiPred software has been trained and optimised based on well-characterised model organisms[28]. Its performance may decrease when applied to non-model organisms with unique or poorly studied molecular features. In addition, the PFAM database is more comprehensive for well-studied model organisms. For organisms that are not model organisms, such as Acanthocephala, the database may lack annotations for certain proteins or domains that are unique to these species. The PFAM approach is based on sequence homology and Hidden Markov Models (HMMs), which can miss highly divergent sequences or novel protein domains that are not captured by existing HMM profiles. The focus of the study on samples of *D. truttae* from the Krka River limits its scope, as genetic divergence between the Croatian population and the populations in Bosnia[53] and Italy may exist, leading to a lack of generalisability to the entire range of the species. Regarding sample composition, while pooling helped minimize individual variability, it may have masked variations in MBP expression between individual parasites.

Future research on MBPs could explore comparative transcriptomics to reveal metal-binding gene expression, qRT-PCR and functional assays to validate MBP activities, and environmental sampling with lab exposure to study metal concentration effects. Single-cell proteomics may also uncover cell-specific MBP expression and low-abundance proteins.

Conclusions

In this study, we present the first draft of the entire transcriptome, which is representative of adults of both sexes of the freshwater acanthocephalan *Dentitruncus truttae*. This is the first publicly available transcriptome of the family Leptorhynchoididae and serves as a valuable addition to the field of environmental parasitology The dataset, which yielded an average of 12.8 Gb of clean reads, was analyzed alongside the transcriptome and genome data of *Pomphorhynchus laevis*—the only acanthocephalan sequenced to date - and revealed a 47% sequence similarity highlighting conserved genomic regions within acanthocephalans. Orthology assessments across species of Rotifera, Nematoda, Platyhelminthes and Hemichordata emphasise the evolutionary proximity of *D. truttae* to *P. laevis*, followed by Rotifera and Nematoda. The comprehensive annotation of the transcriptome of *D. truttae* using seven databases reveals a strong enrichment of genes related to metabolic processes — a likely adaptation to its parasitic lifestyle characterised by nutrient uptake via the body surface. The transcriptome of *D. truttae* provides valuable insights into its role in environmental surveillance and host-parasite coevolution, particularly in salmonids. Due to the increasingly recognized importance of the ability of acanthocephalans to effectively accumulate toxic metals and influence the metal exposure of their hosts, this study also focused on metal-binding proteins (MBPs).

The analysis revealed numerous MBPs, particularly zinc-binding proteins, as well as others that interact with nickel, iron and copper. These proteins, which are associated with stress responses, detoxification and metal transport, can serve as biomarkers for metal exposure and bioaccumulation. By identifying genes that are upregulated in response to metal accumulation, diagnostic tests, such as qPCR panels, can track environmental contamination based on changes in *D. truttae* gene expression. As a freshwater species that bioaccumulates metals, *D. truttae* provides species-specific molecular indicators of ecosystem health, while comparative studies can reveal conserved metal-binding pathways for universal biomarkers in all aquatic systems. The transcriptome also sheds light on molecular mechanisms of metal tolerance, contributing to conservation and bioremediation strategies, such as recombinant protein production for metal sequestration or engineering bioindicator organisms. Insights into host-parasite interactions reveal genes related to immune modulation, nutrient uptake, and defense evasion, indicating that *D. truttae* thrives in metal-rich environments by imposing selective pressure on its host's detoxification and immune responses. This could lead to a co-evolutionary "arms race" in which the genomes of host and parasite adapt to environmental stressors such as metal pollution. Genetic models built from transcriptomic data can simulate coevolutionary processes and predict how host-parasite dynamics evolve under environmental pressure. This research explains phenomena such as parasite resistance, host tolerance, and the evolutionary effects of metal stress on immune gene selection and deepens our understanding of the ecological and evolutionary consequences in aquatic ecosystems.

Overall, the transcriptomes of acanthocephalans seem to be streamlined and specialized for their parasitic lifestyle. They focus on genes necessary for survival and reproduction in their hosts, in contrast to free-living organisms, which have more complex and diverse transcriptomes, reflecting their adaptability to different environmental conditions and ecological niches. The results presented provide a valuable basis for further investigations of metal homeostasis in these parasites and for solving many questions about the phylogeny, taxonomy, diversity and evolution of Acanthocephala.

Materials and methods

Sampling

The adult parasites used for analysis in this study were collected from the intestines of brown trout caught in the Krka River in Croatia. The Krka River is a typical karst river that flows through the Dinaric ecoregion of the Western Balkans and discharges into the Adriatic Sea. Sampling was conducted in April 2021 at two sites in the upper reaches of the river: (1) the river source (KRS), known for its high water quality, and (2) approximately four kilometers downstream (KRK), near the Town of Knin (population: 8,300), which is impacted by industrial (screw factory) and municipal wastewater discharges (Fig. S8). Previous studies have indicated differences in metal accumulation and stress responses between fish from these two sites[54,55].

Fish were collected by electrofishing in accordance with the Croatian standard protocol HRN EN 14,011 (2005)[56]. The fish were anesthetized and sacrificed using unbuffered tricaine methane sulfonate (MS 222, Sigma Aldrich) following the Ordinance on the protection of animals used for scientific purposes[57] at a concentration of 50 mg/L, as recommended by Topić Popović et al. (2016) and Xu et al. (2008)[58,59]. To minimize individual variability, six acanthocephalan specimens were isolated from the intestine of each fish, rinsed in phosphate-buffered saline (pH 7.4), pooled, placed in cryotubes and frozen in liquid nitrogen. Upon return to the laboratory, these pooled samples were stored at -80 °C until further analysis. Each pooled sample was visually inspected to confirm the presence of both male and female individuals, ensuring balanced representation to avoid potential bias from sex differences during transcriptomic analysis and to maximize transcript coverage[32].

Total RNA extraction and RNA sample quality control

Workflow for the RNA-Seq analysis and Identification of MBPs in *D. truttae* is summarized in Fig. S9. Total RNA was extracted from the pooled samples (each containing six parasite specimens) using a Direct-zol™ RNA Miniprep Kit (Zymo Research) according to the manufacturer's instructions. Prior to RNA isolation, the samples were homogenized using an Ultra Turrax T8 homogenizer (Ika Werke). RNA quantification was initially

performed spectrophotometrically (BioSpec-nano, Shimadzu), and degradation or possible contamination was assessed by 1% agarose gel electrophoresis. After confirming their appropriate concentration and quality, samples were sent to Novogene (UK) Company Limited (https://www.novogene.com/us-en/) for commercial cDNA library preparation and RNA sequencing. Only high-quality total RNA (RIN > 7.5, without impurities) was used for further cDNA library construction and sequencing: five from the river source and three from the downstream anthropogenically impacted site.

Library construction and sequencing

Libraries were prepared using the Illumina TruSeq RNA-Seq protocol, and sequencing was performed on an Illumina HiSeq 2500 platform, generating 150 bp paired-end reads with the TruSeq PE Cluster Kit v3 (Illumina). The raw data were stored in FASTQ format and quality of each RNA-Seq library was reviewed with FastQC software[60]. All the samples had a Q30 Phred score > 90% and a Q20 Phred score > 96% (Table S1). The raw reads were deposited in the Sequence Read Archive (SRA) database (NCBI accession number: PRJNA1123588). Clean reads were obtained by removing adapters, poly-N sequences, and reads containing more than 50% low-quality bases (Qphred ≤ 5) using the FASTQ Toolkit (v2.2.5 within BaseSpace).

Transcriptome assembly and annotation

Trinity was used for *de novo* transcriptome assembly due to its effectiveness in reconstructing full-length transcripts and isoforms from RNA-seq data in the absence of a reference genome[61]. The assembly was performed using default parameters optimized for transcriptome data. Detailed information about the workflow is available at https://github.com/trinityrnaseq/trinityrnaseq. CORSET was used to reduce redundancies in the Trinity assembly by clustering transcripts based on shared mapping events and expression patterns, producing a non-redundant set of representative sequences[62]. Further details about the workflow are available at https://github.com/Oshlack/Corset/wiki. The completeness of the transcriptome assembly (Trinity.fasta, unigene.fasta, and cluster.fasta) was assessed using Benchmarking Universal Single-Copy Orthologs (BUSCO) software[63] by searching each assembly for the presence of eukaryotic "core" genes, using the Metazoa database as the reference (database: metazoa_odb10).

To ensure reliable gene annotation and comprehensive coverage, from basic sequence alignment to advanced functional and pathway analysis, and a thorough understanding of gene function, a multi-database approach was used, comprising seven annotation databases, each with specific software and stringent parameters. These databases included the NT database (NCBI BLAST; threshold: $1e^{-5}$); NR, SwissProt, and KOG databases (DIAMOND; threshold: $1e^{-5}$)[64]; PFAM (HMMER; threshold: 0.01)[65]; GO (Blast2GO and Novogene scripts; threshold: $1e^{-6}$)[66,67]; and KEGG database (KAAS; threshold: $1e^{-5}$)[68–70].

The use of 0.01 as a threshold for the e-value in the PFAM database was a reasonable compromise and balance between sensitivity and specificity[71,72] to capture a broader range of potential matches[73].

Identification of orthologous sequences

Orthologous were identified using OrthoFinder (v2.5.5)[39] by comparing the predicted coding sequences (CDS) of *D. truttae* with the genomic coding sequences of eight species available in the NCBI database: *Pomphorhynchus laevis* (GCA_012934845.2), *Adineta steineri* (GCA_905250115.1), *Rotaria socialis* (GCA_905331475.1), *Brachionus calyciflorus* (GCA_002922825.1), *Ancylostoma ceylanicum* (GCA_000688135.1), *Trichinella nativa* (GCA_001447565.2), *Dicrocoelium dendriticum* (GCA_944474145.2) and *Saccoglossus kowalevskii* (GCF_000003605.2). BLAST all-v-all sequence similarity searches were conducted using DIAMOND[64]. Orthologous genes were defined as pairs of genes descended from a single gene in the last common ancestor of two species, while orthogroups represented sets of genes descended from a single ancestral gene shared across multiple species[39].

Metal-binding protein identification

The investigation of metal-binding proteins (MBPs) in Acanthocephala species, such as *Dentitruncus truttae*, is essential for understanding the mechanisms underlying the bioaccumulation of metals in these parasites and their broader ecological roles. MBPs contribute to critical parasitic adaptation processes, including the degradation of host proteins and tissues (zinc-binding metalloproteases), respiration and energy production (iron-sulfur proteins), metabolic flexibility in nutrient-limited environments (nickel-binding ureases and hydrogenases), and protection against metal-induced oxidative stress (metallothioneins). These proteins also hold significant promise as biomarkers for environmental metal dynamics, offering insights into both host-parasite interactions and the impacts of metal contamination in aquatic ecosystems[16].

To systematically study MBPs in *D. truttae*, several key bioinformatics and analytical steps were implemented. Firstly, the transcriptome of *D. truttae* was translated into amino acid sequences by extracting coding regions (CDS) from the assembled unigene sequences using the standard codon Table (5' to 3' orientation). The translated sequences were subjected to BLAST (Basic Local Alignment Search Tool) searches against the NR (Non-Redundant Protein) and Swissprot databases. The NR database was utilized for comprehensive sequence coverage, maximizing the likelihood of detecting homologous proteins across a broad range of species. The SwissProt database, known for its manually curated, high-quality annotations, was used to ensure accurate and reliable functional predictions, reducing the risk of erroneous annotations.

For unigenes that did not produce significant matches in the BLAST analysis, TransDecoder (v3.0.1) was employed to predict coding regions and determine the directionality of the sequences. This step was critical for refining annotations and identifying potentially novel coding sequences that might represent species-specific or less characterized MBPs. Once coding regions were confirmed, *Me*Bi*Pred*, a machine learning-based software specifically designed for predicting metal-binding proteins from sequence-derived features, was used to identify

MBPs in *D. truttae*[28]. This tool follows a two-tiered approach, as described in Dedman et al. (2024), allowing for a robust and precise prediction of MBPs[30].

The predicted MBPs were classified into homogeneous groups based on their binding specificity for zinc (zinc-binding metalloproteases), iron (iron-sulfur proteins), nickel (nickel-binding ureases and hydrogenases) and metallothioneins (Supplementary File 3, 4, 6 and 7).

The MBPs identified in *D. truttae* were compared to related proteins in *Pomphorhynchus laevis* using data from GenBank (NCBI accession GCA_012934845.2) to investigate potential evolutionary and functional differences between the two species. The protein sequences were aligned using MUSCLE 3.8.31 to ensure accurate sequence homology assessments. Phylogenetic analysis was performed using MEGA X with the Maximum Likelihood method and the Whelan Goldman + Freq model, generating phylogenetic trees to visualize evolutionary relationships.

To further assess sequence similarity and potential homologues, BLASTp searches were conducted against annotated proteins from taxonomic groups including Acanthocephala (taxid:10232), Rotifera (taxid:10190), Nematoda (taxid:6231), Platyhelminthes (taxid:6157) and Hemichordata (taxid:10219). This taxonomic range was chosen to detect homologous MBPs across closely and distantly related taxa, providing insights into the conservation and divergence of metal-binding functionalities.

The resulting e-values from BLASTp alignments were transformed with the negative logarithm (base 10) to enhance the visualization of sequence similarity. Heatmaps were generated using Python's Seaborn library (the heatmap() function)[74] to illustrate these patterns across multiple taxa, facilitating the identification of potential homologues and highlighting shared or unique MBPs. The heatmaps enabled the detection of conserved MBPs that may play universal roles in parasitic adaptation and revealed proteins with species-specific functions potentially linked to the environmental conditions faced by *D. truttae*. The next step was the functional characterisation of MBPs by identifying specific protein families with conserved domains associated with MBPs. For this purpose, we used the PFAM database due to its comprehensive coverage, robust statistical models (Hidden Markov Models, HMMs) and high-quality curated entries[75]. Protein sequences were scanned for conserved domains using PFAM seed alignments and the corresponding profile HMMs for different MBP families from the PFAM database. Key MBP families involved in metal homeostasis, transport and detoxification were selected to cover a range of biological functions important for parasite adaptation to metal-rich environments and included domains under the PFAM numbers: PF00005 and PF00664 (ABC transporters), PF01545 (cation efflux family), PF02535 (ZIP-zinc transporter), PF04145 (Ctr-copper transporter), PF00131 and PF07846 (metallothioneins), PF02798 (glutathione S-transferase), PF03770 (sco1 chaperones), PF12409 (P-type ATPase cation transporter), PF00210 (ferritin-like domains) and PF00403 (copper permeases). We used a strict e-value < $1e^{-5}$, which minimises the number of false-positive hits and ensures that only domain hits with high confidence associated with metal-binding functions are selected.

Data availability

Data is provided within the manuscript or supplementary information files. RNA sequencing data from the present study have been submitted to the NCBI Sequence Read Archive under accession number PRJNA1123588 and are available from June 1, 2025, at https://www.ncbi.nlm.nih.gov/sra/PRJNA1123588. Previously published datasets used in this study are available at NCBI: for *Pomphorhynchus laevis* at https://www.ncbi.nlm.nih.gov/datasets/genome/GCA_012934845.2/, for *Adineta steineri* at https://www.ncbi.nlm.nih.gov/datasets/genome/GCA_905250115.1/, for *Rotaria socialis* at https://www.ncbi.nlm.nih.gov/datasets/genome/GCA_905331475.1/, for *Brachionus calyciflorus* at https://www.ncbi.nlm.nih.gov/datasets/genome/GCA_002922825.1/, for *Brachionus plicatilis* at https://www.ncbi.nlm.nih.gov/datasets/genome/GCA_003710015.1/, for *Ancylostoma ceylanicum* at https://www.ncbi.nlm.nih.gov/datasets/genome/GCA_000688135.1/, for *Trichinella nativa* at https://www.ncbi.nlm.nih.gov/datasets/genome/GCA_001447565.2/, for *Trichinella patagoniensis* at https://trace.ncbi.nlm.nih.gov/Traces? run=SRR1971737, for *Dicrocoelium dendriticum* at https://www.ncbi.nlm.nih.gov/datasets/genome/GCA_944474145.2/, and for *Saccoglossus kowalevskii* at https://www.ncbi.nlm.nih.gov/datasets/genome/GCF_000003605.2/.

Received: 8 October 2024; Accepted: 11 July 2025
Published online: 18 July 2025

References

1. Perrot-Minnot, M. J. et al. Hooking the scientific community on thorny-headed worms: interesting and exciting facts, knowledge gaps and perspectives for research directions on Acanthocephala. *Parasite* **30**, 23 (2023).
2. Vardić Smrzlić, I. et al. Molecular characterisation and infection dynamics of *Dentitruncus truttae* from trout (*Salmo trutta* and *Oncorhynchus mykiss*) in Krka river, Croatia. *Vet. Parasitol.* **197**, 604–613 (2013).
3. Barišić, J. et al. Evaluation of architectural and histopathological biomarkers in the intestine of brown trout (*Salmo trutta* linnaeus, 1758) challenged with environmental pollution. *Sci. Total Environ.* **642**, 656–664 (2018).
4. Mijošek, T. et al. Efficiency of metal bioaccumulation in acanthocephalans, Gammarids and fish in relation to metal exposure conditions in a karst freshwater ecosystem. *J. Trace Elem. Med. Bio.* **73**, 127037. https://doi.org/10.1016/j.jtemb.2022.127037 (2022).
5. Moravec, F. Metazoan Parasites of Salmonid Fishes of Europe. Academia, Prague, ISBN 80-200-1189–7, 510 pp (2004).
6. Sures, B. Accumulation of heavy metals by intestinal helminths in fish: an overview and perspective. *Parasitology* **126**, 7, S53–S60 (2003).
7. Filipović Marijić, V., Vardić Smrzlić, I. & Raspor, B. Effect of acanthocephalan infection on metal, total protein and Metallothionein concentrations in European Chub from a Sava river section with low metal contamination. *Sci. Total Environ.* **463**, 772–780 (2013).
8. Prajapati, M. R., Singh, J., Kumar, P. & Dixit, R. De Novo transcriptome analysis and identification of defensive genes in Garlic (*Allium sativum* L.) using high-throughput sequencing. *J. Genet. Eng. Biotechnol.* **21** (1), 56. https://doi.org/10.1186/s43141-023-00499-5 (2023).

9. Yepiskoposyan, H. et al. Transcriptome response to heavy metal stress in Drosophila reveals a new zinc transporter that confers resistance to zinc. *Nucleic Acids Res.* **34** (17), 4866–4877. https://doi.org/10.1093/nar/gkl606 (2006).
10. Chandrangsu, P., Rensing, C. & Helmann, J. Metal homeostasis and resistance in bacteria. *Nat. Rev. Microbiol.* **15**, 338–350. https://doi.org/10.1038/nrmicro.2017.15 (2017).
11. Pang, C. N. et al. Transcriptome and network analyses in *Saccharomyces cerevisiae* reveal that amphotericin B and lactoferrin synergy disrupt metal homeostasis and stress response. *Sci. Rep.* **7** (1), 40232. https://doi.org/10.1038/srep40232 (2017).
12. Zhang, X. et al. High-throughput identification of heavy metal binding proteins from the Byssus of Chinese green mussel (*Perna viridis*) by combination of transcriptome and proteome sequencing. *PLoS One*. **14** (5), e0216605. https://doi.org/10.1371/journal.pone.0216605 (2019).
13. Suo, N. et al. Transcriptome analysis reveals molecular underpinnings of common carp (*Cyprinus carpio*) under hypoxia stress. *Front. Genet.* **13**, 907944. https://doi.org/10.3389/fgene.2022.907944 (2022).
14. Xu, R. et al. Transcriptome-Wide analysis revealed the influential role of PbrMTP (Metal tolerance Protein) in the growth and fruit development of Chinese white Pear. *J. Plant. Growth Regul.* **1–15** https://doi.org/10.1007/s00344-023-11107-8 (2023).
15. Raza, A. et al. Transcriptomics, proteomics, and metabolomics interventions prompt crop improvement against metal(loid) toxicity. *Plant. Cell. Rep.* **43** (3), 80. https://doi.org/10.1007/s00299-024-03153-7 (2024).
16. Permyakov, E. A. & Metal *Binding Proteins Encyclopedia* **1**(1), 261–292 ; https://doi.org/10.3390/encyclopedia1010024 (2021).
17. Sures, B. & Reimann, N. Analysis of trace metals in the Antarctic host-parasite system *Notothenia coriiceps* and *Aspersentis megarhynchus* (Acanthocephala) caught at King George island, South Shetland Islands. *Polar Biol.* **26**, 680–686. https://doi.org/10.1007/s00300-003-0538-4 (2003).
18. Thielen, F., Zimmermann, S., Baska, F., Taraschewski, H. & Sures, B. The intestinal parasite *Pomphorhynchus laevis* (Acanthocephala) from Barbel as a bioindicator for metal pollution in the Danube river near budapest, Hungary. *Environ. Pollut.* **129** (3), 421–429. https://doi.org/10.1016/j.envpol.2003 (2004).
19. Filipović Marijić, V., Vardić Smrzlić, I. & Raspor, B. Does fish reproduction and metabolic activity influence metal levels in fish intestinal parasites, acanthocephalans, during fish spawning and post-spawning period? *Chemosphere* **112**, 449–455. https://doi.org/10.1016/j.chemosphere.2014.04.086 (2014).
20. Sures, B., Nachev, M., Pahl, M., Grabner, D. & Selbach, C. Parasites as drivers of key processes in aquatic ecosystems: facts and future directions. *Exp. Parasitol.* **180**, 141–147. https://doi.org/10.1016/j.exppara.2017.03.011 (2017).
21. Oyoo-Okoth, E. et al. Parasites modify sub-cellular partitioning of metals in the gut of fish. *Aquat. Toxicol.* **106–107**, 76–84. https://doi.org/10.1016/j.aquatox.2011.10.014 (2012).
22. Sures, B. Competition for minerals between *Acanthocephalus lucii* and its definitive host perch (*Perca fluviatilis*). *Int. J. Parasitol.* **32** (9), 1117–1122. https://doi.org/10.1016/s0020-7519(02)00083-8 (2002).
23. Hassanine, R. M. E., Al-Hasawi, Z. M., Hariri, M. S. & Touliabah, H. E. *Sclerocollum saudii Al-Jahdali*, 2010 (Acanthocephala: Cavisomidae) as a Sentinel for heavy-metal pollution in the red sea. *J. Helminthol.* **93** (2), 177–186. https://doi.org/10.1017/S0022149X18000044 (2019).
24. Leite, R. L. A., Filho, D. R. P., de Azevedo, W. & Abdallah, V. D. R.H Patterns of distribution and accumulation of trace metals in *Hysterothylacium* sp. (Nematoda), *Phyllodistomum* sp. (Digenea) and in its fish host *Hoplias malabaricus*, from two neotropical rivers in southeastern Brazil. *Environ Pollut* 277, 116052; (2021). https://doi.org/10.1016/j.envpol.2020.116052
25. Sures, B. & Siddall, R. Pomphorhynchus laevis: the intestinal acanthocephalan as a lead sink for its fish host, Chub (Leuciscus cephalus). *Exp. Parasitol.* **93** (2), 66–72. https://doi.org/10.1006/expr.1999.4437 (1999).
26. Zimmermann, S. et al. Biological availability of traffic-related platinum-group elements (palladium, platinum, and rhodium) and other metals to the zebra mussel (Dreissena polymorpha) in water containing road dust. 21(12):2713-8. *Environ Toxicol Chem.* (2002).
27. Raghavan, V., Kraft, L., Mesny, F. & Rigerte, L. A simple guide to de Novo transcriptome assembly and annotation. *Brief. Bioinform.* **23** (2), 1–30. https://doi.org/10.1093/bib/bbab563 (2022).
28. Aptekmann, A. A. et al. A powerful tool to discover metal binding proteins. *Nucleic Acid Res.* **38** (14), 3532–3540. https://doi.org/10.1093/bioinformatics/btac358 (2021).
29. Dixit, H., Kulharia, M. & Verma, S. K. Metal-binding proteins and proteases in RNA viruses: unravelling functional diversity and expanding therapeutic horizons. *J. Virol.* **97** (12), e01399–e01323. https://doi.org/10.1128/jvi.01399-23 (2023).
30. Dedman, C. J., Fournier, M. & Rickaby, R. E. Alterations in metalloprotein abundance under ocean warming in the marine green Alga *Micromonas pusilla* using the Mebipred predictive tool. *Algal Res.* **78**, 103412. https://doi.org/10.1016/j.algal.2024.103412 (2024).
31. Dixit, H., Upadhyay, V., Kulharia, M. & Verma, S. K. The study of metalloproteome of DNA viruses: identification, functional annotation, and diversity analysis of viral Metal-Binding proteins. *J. Proteome Res.* **23** (9), 4014–4026. https://doi.org/10.1021/acs.jproteome.4c00358 (2024).
32. Mauer, K. et al. The genome, transcriptome, and proteome of the fish parasite *Pomphorhynchus laevis* (Acanthocephala). *PloS One*. **15** (6), e0232973. https://doi.org/10.1371/journal.pone.0232973 (2020).
33. Moreton, J., Izquierdo, A. & Emes, R. D. Assembly, assessment, and availability of de Novo generated eukaryotic transcriptomes. *Front. Genet.* **6**, 361. https://doi.org/10.3389/fgene.2015.00361 (2016).
34. Lee, B. Y. et al. Whole transcriptome analysis of the monogonont rotifer *Brachionus Koreanus* provides molecular resources for developing biomarkers of carbohydrate metabolism. *Comp. Biochem. Phys. D.* **14**, 33–41 (2015).
35. Chen, L. et al. Comparative transcriptomes analysis of *Taenia pisiformis* at different development stages. *BioRxiv Preprint At.* https://doi.org/10.1101/490276 (2018).
36. Yue, G. et al. Transcriptome profiling of male adult *Angiostrongylus cantonensis*. *Iran. J. Parasitol.* **18** (3), 382–389 (2023).
37. Korhonen, P. K. et al. Enhanced genomic and transcriptomic resources for *Trichinella pseudospiralis* and *T. spiralis* to underpin the discovery of molecular differences between stages and species. *Int. J. Mol. Sci.* **25** (13), 7366. https://doi.org/10.3390/ijms25137366 (2024).
38. Emms, D. M. & Kelly, S. OrthoFinder: solving fundamental biases in whole genome comparisons dramatically improves orthogroup inference accuracy. *Genome Biol.* **16**, 1–14 (2015).
39. Emms, D. M. & Kelly, S. OrthoFinder: phylogenetic orthology inference for comparative genomics. *Genome Biol.* **20**, 1–14 (2019).
40. Dunn, C. W., Giribet, G., Edgecombe, G. D. & Hejnol, A. Animal phylogeny and its evolutionary implications. *Annu. Rev. Ecol. Evol. S.* **45**, 371–395. https://doi.org/10.1146/annurev-ecolsys-120213-091627 (2014).
41. Lizano, A. M., Smolina, I., Choquet, M., Kopp, M. & Hoarau, G. Insights into the species evolution of Calanus copepods in the Northern seas revealed by de Novo transcriptome sequencing. *Ecolog Evol.* **12** (2), e8606 (2022).
42. Metivier, J. C. & Chain, F. J. Diversity in expression biases of Lineage-Specific genes during development and anhydrobiosis among tardigrade species. *Evol. Bioinform.* **18**, 1–10. https://doi.org/10.1177/11769343221140277 (2022).
43. Nam, U. H., Kim, J. O. & Kim, J. H. De Novo transcriptome sequencing and analysis of (Nematoda: Anisakidae) third-stage and fourth stage larvae. *J. Nematol.* **52** (1), 1–16 (2020).
44. Earley, B. J., Mendoza, A. D., Tan, C. H. & Kornfeld, K. Zinc homeostasis and signaling in the roundworm *C. elegans*. *Biochim. Biophys. Acta Mol. Cell. Res.* **1868** (1), 118882. https://doi.org/10.1016/j.bbamcr.2020.118882 (2021).
45. Missirlis, F. Regulation and biological function of metal ions in Drosophila. *Curr. Opin. Insect Sci.* **47**, 18–24. https://doi.org/10.1016/j.cois.2021.02.002 (2021).

46. Bruschi, F. et al. Matrix metalloproteinase (MMP)-2 and MMP-9 as inflammation markers of *Trichinella spiralis* and *Trichinella pseudospiralis* infections in mice. *Parasite Immunol.* **36** (10), 540–549. https://doi.org/10.1111/pim.12138 (2014).
47. Hambrook, J. R., Kaboré, A. L., Pila, E. A. & Hanington, P. C. A metalloprotease produced by larval *Schistosoma mansoni* facilitates infection establishment and maintenance in the snail host by interfering with immune cell function. *PLoS Pathog.* **14** (10), e1007393. https://doi.org/10.1371/journal.ppat.1007393 (2018).
48. Near, T. J. Acanthocephalan phylogeny and the evolution of parasitism. *Integr. Comp. Biol.* **42** (3), 668–677. https://doi.org/10.1093/icb/42.3.668 (2002).
49. Tsang, K. L. & Wong, K. B. Moving nickel along the hydrogenase-urease maturation pathway. *Metallomics* **14** (5), mfac003. https://doi.org/10.1093/mtomcs/mfac003 (2022).
50. Kambe, T., Tsuji, T., Hashimoto, A. & Itsumura, N. The physiological, biochemical, and molecular roles of zinc transporters in zinc homeostasis and metabolism. *Physiol. Rev.* **95** (3), 749–784 (2015).
51. Amiard, J. C., Amiard-Triquet, C., Barka, S., Pellerin, J. & Rainbow, P. S. Metallothioneins in aquatic invertebrates: their role in metal detoxification and their use as biomarkers. *Aquat. Toxicol.* **76** (2), 160–202. https://doi.org/10.1016/j.aquatox.2005.08.015 (2006).
52. Parameswari, E., Ilakiya, T., Davamani, V., Kalaiselvi, P. & Sebastian, S. P. Metallothioneins: Diverse Protein Family to Bind Metallic Ions. *IntechOpen*. (2021). Available at https://doi.org/10.5772/intechopen.97658
53. Vardić Smrzlić, I., Čolić, B., Kapetanović, Šariri, S. & Mijošek, T. Filipović marijić, V. Phylogeny and genetic variability of rotifer's closest relatives acanthocephala: an example from Croatia. *Hydrobiologia* **851**, 2845–2860. https://doi.org/10.1007/s10750-023-05372-7 (2024).
54. Mijošek, T. et al. Evaluation of multibiomarker response in fish intestine as an initial indication of anthropogenic impact in the aquatic karst environment. *Sci. Total Environ.* **660**, 1079–1090 (2019).
55. Mijošek, T. et al. Spatial and Temporal variability of dissolved metal(loid)s in water of the karst ecosystem: consequences of long-term exposure to wastewaters. *Environ. Technol. Inno*. **32**, 103254. https://doi.org/10.1016/j.eti.2023.103254 (2023).
56. HRN EN 14011 Fish Sampling by Electric Power. Croatian Standard Institute, Zagreb. (in Croatian) (2005).
57. Official, G. no. 55. Ordinance on the Protection of Animals Used for Scientific Purposes. (2013). Available at https://narodne-novine.nn.hr/clanci/sluzbeni/2013_05_55_1129.html. (in Croatian).
58. Topić Popović, N. et al. Native Prussian carp (*Carassius gibelio*) health status, biochemical and histological responses to treated wastewaters. *Environ. Pollut*. **218**, 689–701 (2016).
59. Xu, D. H., Shoemaker, C. A. & Klesius, P. H. Effect of Tricaine methanesulfonate on survival and reproduction of the fish ectoparasite *Ichthyophthirius multifiliis*. *Parasitol. Res.* **103**, 979–982 (2008).
60. Cock, P. J., Fields, C. J., Goto, N., Heuer, M. L. & Rice, P. M. The Sanger FASTQ file format for sequences with quality scores, and the solexa/illumina FASTQ variants. *Nucleic Acids Res.* **38** (6), 1767–1771. https://doi.org/10.1093/nar/gkp1137 (2010).
61. Grabherr, M. G. et al. Full-length transcriptome assembly from RNA-Seq data without a reference genome. *Nat. Biotechnol.* **29** (7), 644–652. https://doi.org/10.1038/nbt.1883 (2011).
62. Davidson, N. M. & Oshlack, A. Corset: enabling differential gene expression analysis for *de Novo* assembled transcriptomes. *Genome Biol.* **15** (7), 1–14. https://doi.org/10.1186/s13059-014-0410-6 (2014).
63. Simão, F. A., Waterhouse, R. M., Ioannidis, P. & Kriventseva, E. V. & Zdobnov EM. BUSCO: assessing genome assembly and annotation completeness with single-copy orthologs. *Bioinformatics* **31**(19), 3210–3212 ; https://doi.org/10.1093/bioinformatics/btv351
64. Buchfink, B., Xie, C. & Huson, D. H. Fast and sensitive protein alignment using DIAMOND. *Nat. Methods*. **12** (1), 59–60. https://doi.org/10.1038/nmeth.3176 (2015).
65. Finn, R. D. et al. The PFAM protein families database: towards a more sustainable future. *Nucleic Acids Res.* **44**, 279–285 (2016).
66. Götz, S. et al. High-throughput functional annotation and data mining with the Blast2GO suite. *Nucleic Acids Res.* **36** (10), 3420–3435. https://doi.org/10.1093/nar/gkn176 (2008).
67. Young, M. D., Wakefield, M. J., Smyth, G. K. & Oshlack, A. Gene ontology analysis for RNA-seq: accounting for selection bias. *Genome Biol.* **11**, 1–12. https://doi.org/10.1186/gb-2010-11-2-r14 (2010).
68. Kanehisa, M., Furumichi, M., Sato, Y., Matsuura, Y. & Ishiguro-Watanabe, M. KEGG: biological systems database as a model of the real world. *Nucleic Acids Res. 53 (D1)*, D672–D677 (2025). [pubmed] [doi].
69. Kanehisa, M. Toward Understanding the origin and evolution of cellular organisms. *Protein Sci.* **28**, 1947–1951 (2019). [pubmed] [doi].
70. Kanehisa, M. & Goto, S. KEGG: Kyoto encyclopedia of genes and genomes. *Nucleic Acids Res.* **28**, 27–30 (2000). [pubmed] [doi].
71. Sheng, M. et al. Co-expression network database for de Novo transcriptome assembly of *Paeonia lactiflora*.Pall. *Front. Genet.* **11**, 570138. https://doi.org/10.3389/fgene.2020.570138 (2020).
72. Yang, M., Derbyshire, M. K., Yamashita, R. A. & Marchler-Bauer, A. NCBI's conserved domain database and tools for protein domain analysis. Current Protocols in Bioinformatics, 69, e90; (2020). https://doi.org/10.1002/cpbi.90 (2020).
73. Kress, A., Poch, O., Lecompte, O. & Thompson, J. D. Real or fake? Measuring the impact of protein annotation errors on estimates of domain gain and loss events. *Front. Bioinform.* **3**, 1178926. https://doi.org/10.3389/fbinf.2023.1178926 (2023).
74. Waskom, M. L. Seaborn: statistical data visualization. *J. Open. Source Softw.* **6** (60), 3021 (2021).
75. Eddy, S. R. Accelerated profile HMM searches. *PLoS Comput. Biol.* **7** (10). https://doi.org/10.1371/journal.pcbi.1002195 (2011). e1002195.

Acknowledgements

The authors would like to acknowledge dr. Zuzana Redžović, dr. Damir Valić, dr. Tomislav Kralj, Ivana Karamatić and Camille Boucaud for their valuable help in the field work and isolation of acanthocephalans from the gut of brown trouts.

Author contributions

SŠ checked the RNA concentration and quality, performed the data analyses, prepared the graphical material, wrote the first draft, and reviewed and edited the manuscript. IVS extracted the RNA from the samples, checked the RNA concentration and quality, arranged and organized the sample shipment and bioinformatic analyses with Novogene, performed the data analyses, prepared the graphical material, wrote the first draft, and reviewed and edited the manuscript. TMP isolated the parasites from the fish intestine and prepared them for RNA extraction and reviewed the manuscript. VFM isolated the parasites from the fish intestine, prepared them for RNA extraction, designed the study, secured funding, managed project administration and coordination, and reviewed and edited the manuscript. All the authors have read and approved the final manuscript.

Funding

This study was funded by the Croatian Science Foundation within project no. IP-2020-02-8502 "Integrated eval-

uation of aquatic organism responses to metal exposure: gene expression, bioavailability, toxicity and biomarker responses" (BIOTOXMET).

Declarations

Competing interests
The authors declare no competing interests.

Additional information
Supplementary Information The online version contains supplementary material available at https://doi.org/10.1038/s41598-025-11623-5.

Correspondence and requests for materials should be addressed to I.V.S. or V.F.M.

General discussion

1. Environmental exposure conditions in the Krka River

Assessment of biological responses to pollution requires understanding the environmental conditions to which organisms were exposed. To characterize pollutant pressure within the Krka River system, physicochemical and organic parameters, metal(loid) concentrations, MP occurrence, and ecotoxicological responses were evaluated across seasons and along a spatial gradient encompassing the river source (KRS), wastewater-affected sites downstream of municipal (KRK) and industrial discharges (IWW), major tributaries (TKR, TKO, TOR, and TBU), and a downstream location within Krka National Park (KNP) (Publication No. 1).

The obtained results revealed a clear anthropogenic pressure gradient in the upper reaches of the river. Pristine conditions were recorded at KRS, characterized by low nutrient and metal concentrations and preserved seasonal variability typical of karst freshwater systems. As exception, Cd and Tl had the highest concentrations at KRS, probably reflecting the geological background of the catchment area. Jurassic dolomites, as the main feature of the geological background of the Krka River basin, may contain naturally high Cd concentrations. In contrast, locations influenced by municipal and industrial wastewaters exhibited deteriorated water quality and disrupted natural seasonal dynamics, primarily due to high levels of nutrients, metals and organic matter (Filipović Marijić et al. 2018, Publication No. 1, Publication No. 2).

Municipal wastewaters from the Town of Knin represented the dominant source of nutrients and organic matter in the Krka River. Their influence was reflected in increased turbidity, chemical oxygen demand, nutrients, TOC, DOC, mineral oils, and elevated concentrations of many dissolved metal(loid)s at KRK. Industrial wastewaters (IWW) constituted the main source of metal pollution, particularly Mn, Zn, Co, Cs, Fe, Cr, Cu, and Ni, with the strongest impact detected in the adjacent Orašnica tributary (TOR), identified as the most metal polluted location in the study area. In addition, the Kosovčica tributary contributed to dissolved ion load in the Krka River, as indicated by elevated conductivity and TDS concentration at TKO (Publication No. 1, Publication No. 2).

Despite anthropogenic inputs upstream, water quality improved downstream at KNP. Lower pollutant levels and partial restoration of natural seasonal dynamics confirmed the efficiency

and importance of self-purification and underground flows in the complex hydrological karst systems (Cukrov et al. 2008, Publication No. 1, Publication No. 2). However, nearly all metals in sediments exhibited the highest concentrations at KNP, indicating continued downstream transport and accumulation of pollutants (Publication No. 4). This pattern reflects hydrological characteristics of the Krka River, where decreasing flow velocity and increased sedimentation in downstream lake systems promote the deposition of fine particles to which metal(loid)s from upstream wastewaters can bind. As a result, sediments act as important long-term sinks for pollutants, contributing to the reduction of dissolved metal concentrations in the water column through natural self-purification processes. Nevertheless, metal(loid)s are not permanently immobilized in sediments and may be remobilized under changing environmental conditions such as variations in pH, temperature, or hydrological regime. Consequently, sediments may also represent potential secondary sources of pollution and contribute to ongoing exposure of aquatic organisms in the Krka River ecosystem, particularly through trophic transfer (Publication No. 4).

Spatial patterns indicated that organisms inhabiting the study area experienced combined exposure to variant pollutants, with metal(loid)s coinciding with water physico-chemical parameters and overall combined pollution pressure decreasing in the following order: KRK > TOR > TKO > TBU > KNP > KRS (Publication No. 1, Publication No. 2). At the three locations where fish were sampled, a few distinct patterns of metal(loid)s in the dissolved water fraction were observed: As, Fe, Mg, Mn, Na, and Rb were predominantly the highest at KRK, while Ba, Ca, Mo, Sr, and V were the highest at KNP, and Cd and Tl was the highest at KRS. Despite moderate absolute metal concentrations compared with heavily polluted river systems, their predominance in the dissolved fraction (>70%) indicated high environmental mobility and potential for biological uptake, as dissolved elements are more readily transported and generally more bioavailable and toxic to aquatic organisms than particle-bound forms (Publication No. 2). In contrast, Cs and Fe occurred predominantly in particulate form (<50% dissolved), suggesting reduced possibility of direct biological uptake.

Seasonal differences were less pronounced, although elevated metal levels during summer low-flow conditions suggested increased exposure risk during periods of reduced dilution and self-purification capacity (Publication No. 2). Generally higher metal(loid) concentrations in the Krka River were detected during the present study compared to the earlier studies conducted between 2004 and 2015, particularly for Cr, Cu, Fe, Mn and Ni, suggesting a

gradual increase of these elements over time likely related to ongoing industrial and agricultural activities (Publication No. 2).

Microplastics were detected for the first time in the upper Krka River, including polystyrene and polyamide particles in the industrial wastewater, introducing an additional stressor potentially interacting with metal toxicity (Appendix A). Although metals showed limited association with particulate matter (except in the industrial wastewaters, where higher portion of trace metals was associated to particulate matter), combined exposure to dissolved pollutants and MPs may contribute to complex biological effects requiring further investigation.

Ecotoxicological assays using *Pseudokirchneriella subcapitata* and *Daphnia magna* supported chemical observations, revealing acute toxicity at KRK (hazard class III) and high acute toxicity in IWW (hazard class IV), with algae showing greater sensitivity than crustaceans (Publication No. 3). These findings confirm that pollutants present in the river were biologically active and capable of inducing toxic effects at lower trophic levels, supporting environmentally relevant exposure conditions for higher trophic aquatic organisms inhabiting the study area.

Taken together, the investigated system represents a heterogeneous exposure environment in which aquatic organisms were subjected to spatially variable but chronic mixtures of dissolved metals, organic compounds, and MPs. Although the Krka River in its upper course is more polluted than pristine karst ecosystems such as Plitvice Lakes and Una River, metal concentrations remain generally lower than in several moderately to heavily polluted Croatian rivers such as the Sava, Ilova and Sutla. Nevertheless, localized upstream point sources created conditions of elevated exposure to biologically available and potentially toxic pollutants, particularly for elements such as Co, Cr, Cu, Mn and Ni, which occasionally reached comparable or higher levels than those reported from more polluted systems. Thus, despite the overall moderate pollution status, the presence of biologically available pollutants and confirmed biological toxicity indicates environmentally relevant exposure conditions for aquatic organisms. This environmental framework forms the basis for interpreting pollutant uptake, accumulation, and biological responses observed in fish intestine and their acanthocephalan parasites.

2. Biological responses in *Salmo trutta*

2.1. Pollutant uptake in the digestive system of *Salmo trutta*

To investigate pollutant accumulation and toxicity in the fish intestine, *Salmo trutta* Linnaeus, 1758, a representative fish species of the Krka River ecosystem, was sampled at KRS, KRK, and KNP. All examined individuals were infected with intestinal parasites acanthocephalans, species *Dentitruncus truttae* Šinžar, 1955 (Publication No. 4). Although the presence of intestinal parasites in fish represents a natural component of the Krka River ecosystem, it may influence the accumulation and biological effects of environmental pollutants.

Metal(loid) concentrations in the intestine of *S. trutta* likely reflected both environmental exposure and dietary uptake pathways. Metal(loid) accumulation followed the order K > Na > Mg ≥ Ca for macroelements and Zn > Fe > Rb > Cu ≥ Se > Mn > Sr > Cd ≥ Co ≥ As > Mo > Tl > Ba ≥ Cr > V ≥ Hg > Pb ≥ Cs for trace elements (Publication No. 4). Fish intestines often contain very high concentrations of Zn, serving as an important storage site for this element in many fish species. When comparing the current accumulation of elements in intestines of *S. trutta* with that of previous research in 2015/2016 conducted at KRS and KRK, levels of Cd, Co, Cu, Fe, Mn, Se, Sr and Zn concentrations were higher (Mijošek et al. 2022). Spatial differences in intestinal metal(loid) concentrations partly corresponded with environmental pollution patterns observed in water and sediments (Publication No. 4).

Elevated levels of As, Mn, Se, and Zn were detected in fish from KRK, consistent with increased pollutant input from municipal wastewater. In contrast, higher Cd, Cs, Rb and Tl concentrations observed in fish from KRS were probably associated with their natural occurrence in the Dinaric karst geology and their presence in dissolved form in river water. However, the spatial distribution of several elements could not be fully explained by water or sediment concentrations alone, highlighting the importance of diet-borne metal uptake (Publication No. 4).

In addition, a significant inverse relationship between the abundance of acanthocephalans and intestinal concentrations of several elements (As, Cr, Mn, Se, V, Mo, Ba, Cu, and Fe) was observed, suggesting that higher parasite burdens may reduce metal accumulation in fish tissues, possibly through metal uptake and sequestration by parasites (Filipović Marijić et al. 2004, Publication No. 4).

Analysis of gut content (GC) further supported the importance of dietary exposure. Metal(loid) composition in GC differed markedly from that in intestinal tissue, indicating selective absorption and physiological regulation of metal uptake from food. In general, metal concentrations in GC were lowest in fish from KRS and highest in fish from KNP, corresponding to elevated metal levels in surface sediments. Sediment particles were frequently observed in gut contents, suggesting that ingestion of sediment-associated material contributes to dietary exposure. Seasonal differences also supported the role of trophic uptake, as most elements showed higher concentrations in intestinal tissue and GC during spring, when feeding intensity and prey diversity were greatest (Publication No. 4).

Nevertheless, ratios between metal concentrations in the intestine and GC indicated potentially low bioavailability of As, Ba, Ca, Cr, Cu, Fe, Mn, Pb, Sr, and V from dietary sources, whereas Tl, Se, Hg, Rb, K, and Zn exhibited relatively efficient intestinal absorption, possibly due to binding to thiol-containing proteins. Overall, these results indicate that metal accumulation in the fish intestine reflects a combination of environmental exposure, dietary intake, parasite-mediated metal sequestration, and physiological regulation of metal uptake (Publication No. 4).

Synthetic polymers were also detected in gut contents (Appendix A). The dominant types were polyamide, ethylene-vinyl acetate, and styrene-ethylene-butylene, while ethylene-acrylic acid and polyethylene occurred in smaller amounts. Their presence indicates exposure of fish to riverine microplastics, potentially related to nearby roads and municipal wastewater discharge. Polyamide was the only polymer detected both in water and fish gut contents, whereas the remaining polymers were compartment-specific, suggesting multiple diffuse sources. However, these preliminary findings do not allow clear identification of emission sources or direct links between fish diet and detected MPs. Considering that sediments represent major sinks for MPs, future studies should include sediment analyses to better constrain their distribution and trophic transfer within the ecosystem (Appendix A).

2.2. Biological responses in intestine of *Salmo trutta* on molecular level

Transcriptomic comparison of intestinal tissue of *Salmo trutta* between KRK and KRS revealed substantial molecular differences, with 14,280 differentially expressed genes (DEGs), most of which were upregulated in fish from KRK (Appendix D). Functional enrichment analyses indicated that these genes were mainly associated with increased cellular activity, including biological processes such as ribosome biogenesis, protein catabolic

processes, nucleobase-containing small molecule metabolism, and chromatin organization. Enrichment of cellular components - ribosomes, organelles, mitochondria, and chromosomes; together with molecular functions related to RNA binding, isomerase, hydrolase, GTPase, and structural molecule activity, further suggested elevated transcriptional, translational, and metabolic activity in intestinal tissue of fish from KRK. Increased energetic and biosynthetic demands could be associated with coping with chronic environmental stress (Mitra et al. 2020, Oleksiak 2008).

KEGG pathway enrichment analysis supported this interpretation. Upregulated pathways were primarily related to proteostasis, energy metabolism, and innate immune responses, including proteasome, phagosome, and thermogenesis pathways (Appendix D). These processes are commonly involved in cellular stress responses and defense mechanisms, indicating increased metabolic demands and activation of protective mechanisms in intestinal tissue of fish from KRK (Mitra et al. 2020). In contrast, several pathways associated with digestion and metabolism were downregulated in fish from KRK, including bile and pancreatic secretion, retinol metabolism, steroid hormone biosynthesis, cholesterol metabolism, and metabolism of xenobiotics by cytochrome P450 (Appendix D). This pattern suggests reduced intestinal capacity for detoxification, lipid and vitamin metabolism, and digestive processes in fish from KRK.

Taken together, the observed transcriptomic patterns suggest a shift in intestinal physiological priorities in fish from KRK, characterized by enhanced cellular activity, immune defense, energy demand, and protein turnover, accompanied by reduced digestive, detoxification, and lipid metabolic functions. These responses align with the observed higher metal(loid) concentrations in intestinal tissue and gut content at KRK, indicating continuous exposure of the intestine to environmental pollutants through both waterborne and dietborne pathways. Activation of stress- and immune-related pathways, together with increased protein turnover, may therefore represent early molecular adjustments of intestinal tissue to heterogeneous exposure conditions, preceding more pronounced physiological or pathological alterations.

However, these responses likely reflect the combined influence of environmental pollution and other site-specific ecological factors, such as differences in diet composition. While Acanthocephala were observed in intestinal samples from both sites, we found no evidence to suggest that their presence contributed to the observed transcriptomic differences. Overall,

these findings highlight intestinal tissue as a key interface where environmental exposure may trigger early molecular responses to complex pollutant mixtures in riverine ecosystems.

2.3. Biological responses in intestine of *Salmo trutta* on cellular level

To gain insight into the bioavailability and potential toxicity of accumulated elements in the intestine of *Salmo trutta*, their distribution among subcellular fractions was investigated (Appendix B). Fractions obtained by differential centrifugation were grouped into metal-sensitive fractions (MSF), comprising organelles and heat-denatured cytosolic proteins (HDP), and biologically detoxified metal pools (BDM), consisting of metals bound to heat-stable cytosolic proteins (HSP) and those stored in metal-rich granules. This separation provides an indication of whether metals in intestinal tissue remain metabolically active or are sequestered in detoxified cellular compartments under increased accumulation.

To evaluate cellular responses to metal accumulation, several biochemical biomarkers were measured in major intracellular compartments (Publication No. 5). These included metallothionein (MT) as a biomarker of metal exposure, total cytosolic proteins (TP) as a general stress indicator, malondialdehyde (MDA) as a marker of lipid peroxidation, antioxidant defense biomarkers (GSH and the enzymes SOD, CAT, and GST), and lactate dehydrogenase (LDH) as an indicator of tissue metabolic activity. Metal concentrations were additionally determined in the cytosolic fraction to assess the proportion of metals associated with soluble intracellular components. Together, these approaches provide complementary information on both the intracellular fate of metals and the physiological responses of intestinal tissue.

Cytosolic metal concentrations were comparable with previous observations for *S. trutta* from the Krka River and followed similar spatial and temporal patterns as total intestinal concentrations (Publication No. 4, Publication No. 5). The results of subcellular metal distribution analysis showed that essential elements Cu, Fe, Se, and Zn were predominantly associated with MSF, reflecting their physiological roles in metabolically active cellular compartments (Appendix B). In contrast, non-essential elements Sr, As, and Tl, were largely partitioned into BDM pools, indicating sequestration within detoxified compartments. The only exception was Mn, an essential element showing pronounced association with

detoxification fractions, which may reflect tissue-specific regulation or interactions with other essential metals (Appendix B).

Element-specific patterns further illustrated the diversity of intracellular metal handling. Zinc and Fe increasingly accumulated in metal-rich granules with rising exposure, whereas Cu and Se were mainly associated with HSP, suggesting regulation through thiol-rich metal-binding molecules such as metallothioneins (Appendix B). Manganese and Sr were also redistributed away from MSF fractions along the bioaccumulation gradient, indicating efficient cellular regulation. Arsenic and Tl were primarily associated with HSP, although a slight increase of Tl in the sensitive HDP fraction may indicate early cellular disturbance. Overall, these patterns suggest that intestinal cells possess effective mechanisms to regulate intracellular metal availability through sequestration processes that limit interactions with sensitive cellular structures (Appendix B).

Biochemical biomarker responses were broadly consistent with this pattern of regulated but ongoing exposure (Publication No. 5). Fish from sites downstream of wastewater inputs showed moderate but significant oxidative stress compared with the river source, reflected by elevated lipid peroxidation and increased activity of several antioxidant defenses. These responses coincided with higher metal concentrations in sediments, gut contents, and intestinal tissue at downstream sites, suggesting that continuous pollutant exposure probably contributes to increased oxidative pressure in intestinal cells. Elevated GSH and CAT activities in fish experiencing higher oxidative damage further indicated activation of primary antioxidant defenses. However, these mechanisms were not sufficient to fully prevent lipid peroxidation, suggesting that detoxification capacity was partly challenged under environmental exposure conditions, consistent with results of gene expression analysis. Although oxidative stress at the downstream site KNP coincided with the highest metal levels in sediments and gut contents, these responses cannot be exclusively attributed to metal toxicity, as they likely integrate the cumulative effects of multiple factors (Publication No. 5).

Seasonal differences between spring and autumn provided additional context for these patterns. Spring was characterized by higher metal accumulation in intestinal tissue and cytosol, accompanied by stronger biomarker responses and more correlations between biomarkers and cytosolic metal concentrations (Publication No. 5). Because seasonal differences in metal concentrations in river water were minimal, this pattern likely reflects increased feeding activity and dietary metal uptake during spring period of higher metabolic

demand. Consistently, MT concentrations were also elevated in spring, supporting the role of cytosolic metal-binding proteins in regulating accumulated metals. Nevertheless, MT levels did not follow a uniform spatial pattern, indicating that their induction is influenced by multiple metals as well as physiological factors such as feeding activity and metabolic state (Publication No. 5).

Several metals, particularly Co, Cu, Mo, Fe, Mn, and Ni, showed the strongest associations with biomarker responses (Publication No. 5). Combined with subcellular partitioning patterns, these observations suggest that Cu was mainly regulated through binding to HSP fractions, likely involving metallothionein or glutathione complexes. In contrast, Fe and Mn appeared to be efficiently detoxified in granules, which may limit their direct contribution to oxidative stress responses (Appendix B).

Biomarker responses were also influenced by ecological and physiological factors. Smaller fish exhibited higher general stress, oxidative damage and antioxidant activity, consistent with their higher metabolic rates and potentially greater sensitivity to pollutants (Publication No. 5). Parasite infection further modified these responses. Fish harboring higher numbers of acanthocephalans showed reduced general stress, oxidative damage, antioxidant activity and tissue metabolic activity. This pattern aligns with previous findings indicating that acanthocephalans can reduce the pollutant burden of host tissues. Parasite infection may therefore partly mitigate oxidative stress by influencing metal bioavailability within the host (Publication No. 5).

Taken together, these results indicate that intestinal tissue of *S. trutta* functions as a dynamic interface where environmental exposure, dietary uptake, and host-parasite interactions collectively shape cellular responses to pollutant mixtures. Subcellular metal partitioning demonstrates that intestinal cells can effectively regulate intracellular metal availability through sequestration in detoxified compartments. Nevertheless, the moderate oxidative stress responses observed downstream of wastewater inputs suggest that these mechanisms cannot fully prevent cellular stress under chronic environmental exposure (Appendix B, Publication No. 5).

These biochemical responses are consistent with transcriptomic patterns observed in intestinal tissue, which likely reflected an energetic trade-off under chronic environmental stress, where cellular resources are increasingly allocated to maintenance and defense processes rather than routine physiological activities (Appendix D). Biomarker responses also

revealed stress effects in fish from the Krka National Park, where pollution was not evident from water quality data alone (Publication No. 5). This finding highlights the value of biochemical biomarkers in intestinal tissue as sensitive indicators of sublethal environmental stress. Altogether, the integration of transcriptomic patterns, metal subcellular distribution, and biomarker responses demonstrates that intestinal tissue represents a sensitive early-warning bioindicator of the biological consequences of complex pollutant exposure in freshwater ecosystems.

2.4. Biological responses in intestine of *Salmo trutta* on organismal level

To evaluate whether the observed molecular and cellular responses translate to effects at the level of the whole organism, fish total length (TL), total body mass (TM), Fulton's condition index (FCI), hepatosomatic index (HSI), and gonadosomatic index (GSI) were compared between sampling sites and seasons.

Similarly to biochemical biomarkers, seasonal effects were more pronounced than spatial ones. No significant differences were observed in TL, TM, or biometric indices of *S. trutta* among the studied locations, except for slightly smaller individuals recorded at KNP in spring. No significant differences were detected between sexes (Publication No. 4, Publication No. 5).

Clear seasonal differences were observed, with significantly higher TL and TM in autumn than in spring at all sampling sites (Publication No. 4, Publication No. 5). This pattern coincides with the spawning period of *S. trutta* and reflects the presence of more mature individuals during autumn sampling, consistent with previous observations in the Krka River and the reproductive cycle of the species (Mijošek et al. 2019, Publication No. 4, Publication No. 5). Lower FCI and HSI in autumn, together with higher GSI values, likely reflect the seasonal redistribution of energy reserves from somatic growth to gonad development during the pre-spawning and spawning periods, leading to reduced body condition and increased gonad mass. At the KNP site, where fish were generally smaller and likely younger, seasonal differences in GSI were less pronounced, suggesting incomplete sexual maturity (Publication No. 4, Publication No. 5). Overall, biometric parameters of fish appeared to be primarily influenced by natural physiological processes rather than pollutant exposure. In contrast,

intestinal tissue showed clear seasonal and spatial patterns at lower levels of biological organization.

Altogether, the results indicate that pollutant exposure in the Krka River induces measurable biological responses in intestinal tissue of *S. trutta* at molecular and cellular levels, but these disturbances do not scale up to detectable effects at the level of the whole organism. Instead, these responses likely represent early adaptive adjustments and serve as early-warning indicators of environmental stress before impacts become evident at higher levels of biological organization.

3. Biological responses in *Dentitruncus truttae*

Intestinal parasites acanthocephalans were present in nearly all *Salmo trutta* specimens examined in this study, with prevalence ranging from 92 to 100 % across sampling sites and seasons (Publication No. 4, Publication No. 5). Only one species, *Dentitruncus truttae*, was identified. These epidemiological characteristics were comparable with previous reports from the Krka River system (Vardić Smrzlić et al. 2013, Filipović Marijić et al. 2022, Mijošek et al. 2022). Infection intensity showed no clear spatial differences but was consistently higher in autumn than in spring (Publication No. 4, Publication No. 5). This seasonal pattern most likely reflects the life cycle of the parasite's intermediate hosts, amphipods of the genus *Gammarus*. Gammarids reproduce predominantly during late summer and autumn, resulting in greater availability of infected intermediate hosts and consequently higher transmission of *D. truttae* to fish during this season (Kennedy 2006).

Parasite abundance was positively related to fish body mass, indicating that larger individuals accumulate more parasites, while no relationship was observed with FCI (Publication No. 4). This suggests that infection with *D. truttae* does not substantially impair host condition. Overall, the epidemiological patterns observed in this study appear to be primarily driven by host feeding and parasite life cycle dynamics, rather than by pollutant exposure.

3.1. Metal accumulation and bioconcentration in *Dentitruncus truttae*

The acanthocephalans exhibited high accumulation capacity for a wide range of elements (Publication No. 4). Element concentrations followed patterns similar to those reported in

previous study, with macroelements occurring in the order K > Na ≥ Ca > Mg and trace elements following the order Zn > Fe > Cu > Mn > Sr ≥ Rb > Cd ≥ Tl ≥ Se > Pb > Ba > As > Co ≥ Hg ≥ Cr ≥ Mo ≥ V > Cs. Although concentrations of most metals in both fish intestine and acanthocephalans were comparable to those measured in 2015/2016, higher levels of Cd, Cu, Mn and Zn were observed in the present study in both organisms, while increases in Co, Fe, Se and Sr were detected only in fish intestine (Mijošek et al. 2022, Publication No. 4). Because fish integrate environmental exposure over longer periods due to their longer life span, they represent more reliable indicators of long-term pollution trends than parasites.

Spatial patterns of metal accumulation in parasites differed from those observed in fish intestine. The highest concentrations of Co and Fe in *D. truttae* were recorded at KRK, whereas Mo, Na, Sr and V peaked at KNP. Only Cd and Cs showed similar spatial maxima in both parasites and fish intestine, with the highest levels at KRS (Publication No. 4). This pattern likely reflects higher exposure from natural sources (Mijošek et al. 2022). Seasonal variation was also detected, with generally higher metal concentrations in spring than in autumn, although this trend was less pronounced than in fish intestine. This pattern likely reflects seasonal differences in host feeding activity and dietary metal exposure, which were also indicated by higher metal concentrations in GC and intestinal tissue during spring (Publication No. 4).

Parasite metal loads were negatively correlated with fish body mass for several elements, particularly in autumn, indicating that parasites from smaller fish accumulated higher metal concentrations (Publication No. 4). This pattern may reflect higher metabolic and feeding rates in smaller hosts, resulting in greater exposure of parasites to metals present in the intestinal lumen.

When data from all seasons and locations were pooled, numerous positive correlations were observed between metal concentrations in fish intestine and parasites, suggesting that both respond to similar environmental exposure conditions (Publication No. 4). At the same time, metal concentrations in individual parasites decreased with increasing infrapopulation size. This pattern may reflect either intraspecific competition for metal uptake among acanthocephalans within the same host or a biodilution effect, whereby elements are distributed among a larger number of parasites, resulting in lower metal(loid) concentrations in individual parasites and potentially also in the fish host (Publication No. 4).

Bioconcentration factors calculated between parasites and fish intestine further confirmed the remarkable accumulation efficiency of *D. truttae* (Publication No. 4). For most elements, particularly potentially toxic metals such as Cd, Hg, Pb and Tl, concentrations were substantially higher in parasites than in host intestinal tissue. Elevated accumulation was also observed for As, Ba, Cr, Cu, Mn, Sr, Ca and Na, indicating recent exposure of the host–parasite system to these elements. In contrast, Cs, Mo, Rb, Zn and K accumulated less in parasites than in fish intestine, which may reflect longer-term host exposure or element-specific differences in uptake and regulation (Mijošek et al. 2022, Publication No. 4).

Comparison of element concentrations between GC and *D. truttae* provided additional insight into metal bioavailability within the fish intestinal environment. Both parasites and fish intestinal tissue showed low transfer from GC for As, Ba, Ca, Cr, Fe, Mn, Sr and V, indicating limited bioavailability and likely partial elimination via feces (Publication No. 4). In contrast, Tl, Se, Hg, Rb, K and Zn showed high transfer efficiency from GC to both biological tissues. Notably, Cd, Cu and Pb were accumulated efficiently from GC by parasites but not by fish intestinal tissue (Publication No. 4). Combined with the significant inverse relationship between acanthocephalan abundance and Cu concentration in fish intestine discussed above, these patterns suggest that acanthocephalans may selectively concentrate certain metals present in the intestinal lumen, potentially influencing metal distribution between parasites and host tissues.

Taken together, the results confirm that *D. truttae* functions as an efficient biological accumulator of metals within the host intestine. By concentrating potentially toxic elements such as Cd, Pb and Tl to levels substantially higher than those found in host tissue, acanthocephalans may influence the internal distribution of metals within infected fish and potentially reduce host exposure to certain pollutants. The mechanisms underlying this remarkable accumulation capacity remain unclear but probably involve specialized metal-binding molecules and intracellular regulatory pathways within parasite tissues, which are examined in the following sections.

3.2. Biological responses in *Dentitruncus truttae* on molecular level

To better understand the mechanisms underlying the remarkable metal accumulation capacity of acanthocephalans, the transcriptome of *D. truttae* was assembled *de novo* and analyzed with particular emphasis on proteins involved in metal binding, transport and detoxification (Publication No. 6). Because genomic resources for Acanthocephala are extremely limited and the entire transcriptome has previously been published only for a single species, *Pomphorhynchus laevis*, (family Pomphorhynchidae), the transcriptome of *D. truttae* represents an important molecular resource. It also provides a valuable framework for functional interpretation of metal-related processes in this parasite group, as the first transcriptome from Leptorhynchoididae family.

Comparative analysis revealed approximately 47% sequence similarity with *P. laevis*, highlighting conserved genomic regions within acanthocephalans (Publication No. 6). Functional annotation of the *D. truttae* transcriptome showed strong enrichment of genes associated with metabolic processes and binding functions, likely reflecting adaptation to a parasitic lifestyle characterized by nutrient uptake through the body surface. Similar patterns reported for *P. laevis* suggest that acanthocephalan transcriptomes are streamlined and specialized for survival and reproduction in host intestine, rather than for ecological versatility typical of free-living organisms (Publication No. 6).

Within this framework, particular attention was directed toward metal-binding proteins (MBPs), which may contribute to the exceptional ability of acanthocephalans to accumulate and tolerate high concentrations of metals. Approximately 14–15% of predicted proteins in *D. truttae* were identified as MBPs, a proportion similar to that reported for *P. laevis*. However, this estimate may be influenced by the lack of molecular data available for acanthocephalans (Publication No. 6).

Among these proteins, Zn-binding proteins were by far the most abundant (54% of all predicted MBPs), followed by Fe- and Ni-binding proteins. The dominance of zinc-binding motifs, particularly zinc-finger proteins, reflects their central role in gene regulation, cellular stability and stress responses. A smaller group of Zn-binding proteins identified in the transcriptome included metalloproteases such as reprolysins and matrixins, enzymes involved in host–parasite interactions that facilitate nutrient acquisition and enhance parasite stress tolerance (Publication No. 6).

Proteins associated with Fe–S clusters were also abundant (14% of all predicted MBPs) and likely contribute to electron transfer and energy metabolism. In acanthocephalans, such proteins may support metabolic flexibility under the fluctuating and low-oxygen conditions characteristic of the host intestinal environment, enabling shifts between aerobic and anaerobic metabolic pathways. In addition, Ni-binding proteins were detected (11% of MBPs), many associated with enzymes such as ureases or hydrogenases, suggesting roles in nitrogen metabolism, energy production, redox balance and environmental adaptation within the host intestine (Publication No. 6).

Analysis of conserved protein domains associated with metal homeostasis further revealed that most detected proteins belonged to the ABC transporter family. However, only a small proportion of these transporters were predicted to bind metals, indicating that metal transport is not their primary function. In contrast, a metallothionein-like protein which appears to be closest to the Class II metallothioneins (MT-2) was identified in *D. truttae*. The metallothionein-like proteins type 2 are expressed in a wide range of organisms to bind and detoxify heavy metals, providing a plausible molecular mechanism contributing to the high metal accumulation observed in acanthocephalans (Publication No. 6).

Interestingly, a substantial fraction of predicted MBPs (29%) lacked known PFAM metal-binding domains but still showed a high predicted preference for binding Zn and low preference for binding Mg, Fe, and Mn. These proteins may represent poorly characterized or potentially acanthocephalan-specific metal-binding systems, suggesting that additional mechanisms of metal regulation remain to be discovered in this parasite group (Publication No. 6).

Overall, the transcriptomic data indicate that *D. truttae* possesses a diverse set of proteins capable of binding, transporting and regulating metals. The predominance of Zn-dependent proteins, together with the presence of MT-like proteins and metal-associated enzymes, suggests that *D. truttae* relies on specialized molecular mechanisms for metal detoxification rather than ABC transporters. These findings provide the first molecular insight into MBPs in *D. truttae* and offer a mechanistic framework for interpreting the exceptionally high metal concentrations observed in acanthocephalans relative to their hosts (Publication No. 6).

Differences in gene expression were analyzed between *D. truttae* isolated from fish sampled at KRS and KRK (Appendix D). Overall, transcriptional differences were moderate and did not indicate a dominant or highly specialized biological response. Differential gene

expression analysis identified 594 DEGs, of which 58% were upregulated at KRK compared to KRS, yet GO enrichment did not reveal any significantly overrepresented biological processes (BP), cellular components (CC), or molecular functions (MF) (Appendix D).

In contrast, KEGG pathway analysis indicated regulation of pathways primarily associated with cellular stress responses and energy metabolism (Appendix D). Parasites from KRK showed increased activity of pathways related to glycolysis/gluconeogenesis and several stress-associated signaling processes, suggesting metabolic adjustments that may support survival under environmentally challenging conditions. Activation of calcium- and lipid-mediated signaling pathways, together with shifts in tryptophan metabolism, indicates enhanced regulation of cellular defense mechanisms. At the same time, pathways linked to proteostasis, oxidative phosphorylation and mitochondrial function were relatively downregulated, which may reflect altered energy metabolism and increased oxidative stress in parasites from KRK. These patterns are broadly consistent with the environmental context of the KRK site, where somewhat higher metal(loid) concentrations were observed accumulated in acanthocephalans, fish intestinal tissue and gut content, indicating continuous exposure of parasites to environmental pollutants (Appendix D, Publication No. 4).

Expression patterns were validated by qPCR, for which three candidate reference genes were tested. EIF showed the highest expression stability and was used for relative quantification. To our knowledge, this study provides the first validated set of reference genes for *D. truttae*, offering a useful resource for future transcriptomic and ecotoxicological studies (Appendix D).

Together, the presence of diverse metal-binding proteins and the relatively moderate transcriptional response suggest that *D. truttae* is intrinsically well adapted to metal-rich intestinal environments, enabling efficient accumulation and tolerance of metals.

3.3. Biological responses in *Dentitruncus truttae* on cellular level

To our knowledge, this study provides the first data on metal(loid) concentrations in the cytosolic fraction of acanthocephalans, representing the biologically available metal pool within parasite cells. Cytosolic concentrations in *D. truttae* followed the order Zn ≥ Fe > Mn > Cu > Se > Cd > As > Tl, with Zn markedly exceeding all other elements (Appendix C). A similar pattern was observed in whole-body concentrations (Publication No. 4), highlighting

the central physiological role of Zn in parasite metabolism. Comparison with the intestinal cytosol of the host revealed different accumulation patterns, as Cu, Mn and Cd levels were higher in parasites, whereas Zn, Fe, Se, As and Tl were lower (Mijošek et al. 2019, Publication No. 5). Notably, these trends differ from whole-tissue comparisons, where Fe, As, Tl, Cu and Cd accumulated to higher total levels in *D. truttae* than in the host intestine, potentially suggesting selective intracellular distribution and regulated metal handling in the parasite (Publication No. 4).

The present study also provides one of the first insights into stress biomarkers in acanthocephalans and the first data for *D. truttae* (Publication No. 5). MT concentrations were consistently higher in parasites than in host intestinal tissue, likely reflecting the higher levels of accumulated MT-inducing metals such as Cd, Cu and Pb in acanthocephalans (Publication No. 4). These findings complement the transcriptomic detection of metallothionein-like proteins in *D. truttae*, providing physiological evidence for their role in metal binding and detoxification (Publication No. 6). TP concentrations were also higher in parasites than in host tissue, exceeding values reported for several aquatic invertebrates and suggesting a potentially taxon-specific pattern (Publication No. 5).

Spatial patterns of both MT and TP differed between hosts and parasites, with no statistically significant site-specific differences (Publication No. 5). In contrast, seasonal patterns were evident, with both biomarkers showing higher levels in spring, consistent with increased metal accumulation during this period. These trends correspond with elevated metabolic activity of the host and higher intestinal metal concentrations, as well as MT and TP levels observed in fish (Publication No. 4, Publication No. 5). No significant correlation was found between biomarker levels in fish intestine and in acanthocephalans from the same hosts, indicating that parasite biomarker responses are largely independent of those in host tissues. Notably, individual variability of MT and TP levels was higher in parasites than in fish intestine, a pattern also observed for metal concentrations, further supporting the link between metal exposure and biomarker responses in acanthocephalans (Publication No. 4, Publication No. 5).

To further understand how accumulated metals are handled at subcellular level in acanthocephalans, distribution of selected elements among cytosolic biomolecules of different molecular sizes in *D. truttae* was investigated using size-exclusion chromatography (SEC) coupled with inductively coupled plasma mass spectrometry (ICP-MS). Obtained

profiles represent an initial step toward characterizing and identifying specific metal-binding biomolecules in acanthocephalans, which are currently completely unknown. They revealed general patterns of intracellular metal handling and complemented the transcriptomic evidence for diverse MBPs (Appendix C).

Copper was distributed across all molecular-mass fractions, indicating association with a wide range of cytosolic biomolecules (Appendix C). The dominant peak occurred in the medium-molecular-mass (MMM) range rather than in the low-molecular-mass (LMM) fraction typically associated with metallothioneins (MTs) in fish, suggesting that Cu homeostasis in *D. truttae* relies on diverse metalloproteins and enzymes. Only in the sample with the highest cytosolic Cu levels did the high-molecular-mass (HMM) and very-low-molecular-mass (VLMM) peaks become more pronounced, indicating simultaneous induction of both high- and low-molecular-mass Cu-binding biomolecules. Sequence-based predictions identified several MT isoforms in *D. truttae*, including forms with unexpectedly high molecular masses (up to 255 kDa) that would likely elute in the MMM or HMM regions rather than in the VLMM fraction typical for vertebrate MTs (Publication No. 6). Together with different patterns of MT induction and the lack of correlation between MT levels in fish intestine and their acanthocephalan parasites, these results suggest species-specific patterns of MT induction and indicate that Cu regulation in *D. truttae* involves a broader range of MBPs than typically observed in vertebrate hosts (Appendix C, Publication No. 5).

Zinc, dominant cytosolic metal in *D. truttae*, exhibited the broadest distribution among all analyzed elements, with multiple peaks across the entire molecular-mass range, reflecting its role as an essential structural and catalytic cofactor in numerous proteins and consistent with the dominance of Zn-binding proteins identified in the transcriptome (Appendix C, Publication No. 6). With increasing Zn accumulation, all peaks increased proportionally, while the relative contribution of the MT-associated fraction remained stable, indicating that Zn was primarily bound to functional proteins rather than to newly synthesized MTs (Appendix C). In contrast, Cd showed a more restricted distribution, with a dominant peak in the VLMM fraction corresponding to MT-like proteins, indicating detoxification through binding to thiol-rich cytosolic molecules. Increasing Cd accumulation was accompanied by enhanced LMM and VLMM peaks and the appearance of an additional HMM fraction at the highest concentrations, suggesting progressive recruitment of multiple Cd-binding biomolecules (Appendix C).

Iron and Mn showed similar elution profiles, dominated by peaks in the MMM fraction with several additional peaks at higher and lower molecular masses (Appendix C). Such distributions are typical for essential metals involved in numerous enzymatic and metabolic processes. The presence of multiple peaks likely reflects binding to a range of proteins associated with energy metabolism, redox regulation and electron transfer, consistent with the Fe–S cluster proteins identified in the parasite transcriptome. Increasing concentrations of these metals generally led to a rise in MMM and VLMM peaks (Appendix C).

Selenium and As were primarily associated with VLMM fractions, with secondary peaks in the HMM range, indicating dominant binding to small cytosolic biomolecules (Appendix C). For Se, this pattern may reflect the presence of low-molecular-mass selenocompounds involved in redox regulation and selenium metabolism. Arsenic, in contrast, is a non-essential toxic metalloid and its predominance in the same fraction probably reflects nonspecific binding to thiol-containing molecules. These results suggest distinct biochemical roles despite similar chromatographic profiles. Binding of As to HMM biomolecules was unexpected and should be studied further (Appendix C).

Thallium exhibited a unique profile, eluting exclusively within a single HMM peak (Appendix C). This pattern suggests its association with a limited group of cytosolic proteins rather than with the low-molecular-mass detoxification ligands typically observed in fish. Given that Tl has no known biological function, yet showed high absorption from the GC in both acanthocephalans and fish intestine, such binding likely reflects nonspecific interactions with large proteins rather than an active detoxification mechanism (Appendix C).

Taken together, the SEC-ICP-MS profiles indicate that metals in *D. truttae* are distributed among a diverse set of cytosolic biomolecules. Essential elements such as Cu, Zn, Fe and Mn were associated with a wide range of functional proteins, whereas non-essential metals such as As and Tl were predominantly eluted within a single peak. These findings complement the transcriptomic evidence for numerous MBPs and metallothionein-like sequences in *D. truttae*, suggesting that acanthocephalans rely on a complex network of cytosolic metal-binding biomolecules that likely contributes to their remarkable metal accumulation capacity.

4. Hypothesis evaluation

1) Fish intestine has mechanisms of diet-borne pollutant regulation which can be used as early biological responses to pollutant exposure

Our results support this hypothesis. The intestine of *Salmo trutta* proved to be a sensitive and reliable bioindicator organ, reflecting environmental exposure through metal accumulation, microplastic ingestion, and measurable molecular and biochemical responses. Differences in metal transfer from the gut content to intestinal tissue indicated selective absorption and physiological regulation of uptake, while seasonal increases in intestinal metal levels highlighted the influence of feeding activity. Observed patterns of accumulation and biomarker responses corresponded to spatial differences in environmental pollution, confirming the relevance of diet-borne exposure pathways for environmental assessment.

2) Toxicity of pollutants depends on subcellular distribution and binding to specific biomolecules in fish intestine and acanthocephalans

This hypothesis is supported. The results demonstrated that total metal concentrations alone do not adequately reflect their potential toxicity. Subcellular metal distribution analysis in fish intestine showed that essential metals were primarily associated with metabolically active fractions but were redistributed away from them under elevated exposure, whereas non-essential and potentially toxic elements were largely sequestered in detoxified compartments. In addition, cytosolic metal profiles in acanthocephalan revealed that essential metals were distributed among a diverse set of biomolecules, while non-essential and toxic elements predominantly eluted within a single peak. Together, these findings confirm that pollutant toxicity is closely linked to bioavailability, subcellular distribution, and binding to specific biomolecules.

3) The transcriptome of acanthocephalans reflects a specific lifestyle, while gene expression in acanthocephalans and fish intestines indicates environmental pollution levels

Our results support this hypothesis. The transcriptome of *Dentitruncus truttae* reflected overall specialized and streamlined organization typical of parasitic organisms, but revealed a set of genes associated with metal binding proteins, potentially supporting its high metal

accumulation capacity. Gene expression patterns in both acanthocephalans and fish intestine varied in response to environmental pollution gradients, indicating that transcriptomic responses can reflect pollutant exposure. In fish intestinal tissue, these changes were more pronounced.

Conclusion

This thesis provides an integrated assessment of environmental pollution and biological responses in the karst Krka River ecosystem, influenced by industrial and municipal wastewaters. It links environmental exposure to the accumulation and toxicity of pollutants across multiple levels of biological organization in the intestine of brown trout (*Salmo trutta*) and their intestinal parasites, acanthocephalans (*Dentitruncus truttae*).

Environmental assessment revealed a clear spatial gradient of anthropogenic pressure in the upper Krka River. Municipal and industrial wastewater were important local sources of nutrients, organic matter, and metal(loid)s, while hydrological processes characteristic of karst systems contributed to downstream recovery of water quality within Krka National Park. However, the accumulation of metals in downstream sediments indicated that pollutants are redistributed within the ecosystem rather than eliminated, creating long-term environmental reservoirs of pollutants. The presence of microplastics and confirmed ecotoxicological effects in bioassays further demonstrated that aquatic organisms in upper course of the Krka River are continuously exposed to biologically available pollutant mixtures, despite the overall moderate pollution status of the ecosystem. Compared to investigations conducted in 2015/2016, concentrations of Cu and Mn increased in river water, fish intestine, and acanthocephalans, Cd and Zn increased in the intestine and acanthocephalans and Fe increased in water and fish intestine. Overall, the generally higher metal(loid) concentrations in the Krka River, along with their increased biological accumulation, may indicate intensified pollution pressure within the river catchment.

The intestine of *S. trutta* was confirmed as reliable bioindicator organ, mediating pollutant uptake and early biological responses. This study provides the first data on microplastic ingestion in native freshwater fish in Croatia and on metal accumulation in the intestine of fish sampled within Krka National Park. Metal accumulation patterns reflected a combination

of environmental exposure, dietary intake, parasite-mediated metal sequestration and physiological regulation of metal absorption. Transcriptomic analyses revealed pronounced changes in gene expression in fish from wastewater-influenced sites, including increased cellular activity, activation of stress and immune pathways, and reduced expression of genes involved in digestion and detoxification. These molecular responses were supported by biochemical biomarkers, which indicated moderate oxidative stress downstream of wastewater discharges. In addition, the study presents the first data on subcellular metal distribution in fish intestinal tissue, demonstrating that intestinal cells can effectively regulate intracellular metal availability through sequestration in detoxified compartments. Despite measurable molecular and cellular disturbances, pollutant exposure did not translate into detectable effects at the organismal level, such as fish growth or biometric indices. These findings highlight the ability of fish to compensate for moderate environmental stress and underscore the value of molecular and biochemical biomarkers as sensitive early-warning indicators capable of detecting sublethal stress effects.

The parasite *D. truttae* demonstrated exceptional metal accumulation, often exceeding concentrations in host tissues, confirming its role as both an efficient accumulator and a sensitive bioindicator of environmental pollution. The negative relationship between parasite abundance and certain metal concentrations in fish intestine further indicated that parasites influence pollutant dynamics within the host. This study presents the first draft of the entire transcriptome of *D. truttae*, representing the first publicly available transcriptome of the family Leptorhynchoididae and only the second for the entire group Acanthocephala. Transcriptomic and biochemical analyses provided initial insights into the molecular mechanisms underlying capacity for metal accumulation. The *de novo* assembled transcriptome revealed a diverse set of metal-binding proteins, including metallothionein-like proteins and numerous Zn-dependent proteins, indicating specialized mechanisms for metal binding, transport, and detoxification. Furthermore, this study reports one of the first measurements of biochemical biomarkers, metallothioneins and total cytosolic proteins, in acanthocephalans. These biomarkers consistently exhibited higher levels than in fish intestine and responded to seasonal changes in metal exposure, while appearing independent of host responses. Metal distribution among different size categories of cytosolic biomolecules in *D. truttae* was analysed for the first time, showing a complex association with cytosolic biomolecules and suggesting regulated intracellular handling rather than passive accumulation. These findings indicate that acanthocephalans are well adapted to metal-rich

intestinal environments and possess molecular mechanisms enabling efficient metal uptake and tolerance.

Overall, this study provides a comprehensive and integrative assessment of metal(loid) and microplastic contamination in a karst freshwater ecosystem, generating findings of both local and broader scientific relevance. It also delivered the first dataset on the presence of microplastics in Croatian karst rivers and their ingestion by wild freshwater fish.

A key contribution of this work is the demonstration of the fish intestine as a sensitive and informative bioindicator organ for assessing pollutant exposure and effects. The study also provides rare data on biochemical biomarkers and subcellular metal distribution in the intestine of wild freshwater fish, improving the distinction between bioavailable and detoxified metal fractions and enabling a more accurate interpretation of toxicological significance of their accumulation in tissue.

The application of standardized bioassays to wastewater and receiving surface waters under environmentally realistic conditions, using multiple aquatic organisms from different trophic groups, strengthens the ecological relevance of toxicity assessment and supports a clearer linkage between chemical exposure and biological response.

Moreover, this study presents one of the rare investigations of adult freshwater acanthocephalans as bioindicator organisms, advancing the understanding of host–parasite–pollutant interactions and contributing to the growing field of environmental parasitology. It provides the first mechanistic insights into metal handling in these parasites. The identification of gene sequences encoding metal-binding proteins, together with their expression patterns along an environmental pollution gradient, represents a critical first step towards understanding the molecular basis of their exceptional metal accumulation capacity. The characterization of biochemical biomarker responses in acanthocephalans further establishes a foundation for future research on pollutant effects in parasite systems.

Overall, the findings demonstrate the potential of both fish intestine and acanthocephalans in environmental assessments. By integrating environmental measurements with host and parasite responses across multiple levels of biological organization, this study provides a comprehensive perspective on the effects of pollutant mixtures in karst freshwater ecosystems. Such an approach enhances the accuracy of exposure and risk assessment and supports the development of more ecologically meaningful monitoring strategies. In addition,

the first transcriptomic data for *D. truttae* constitute a valuable contribution to globally relevant databases.

References

Amoatey, P., & Baawain, M. S. (2019). Effects of pollution on freshwater aquatic organisms. *Water Environment Research*, *91*(10), 1272-1287.

Bai, Z., Ren, T., Han, Y., Rahman, M. M., Hu, Y., Li, Z., & Jiang, Z. (2019). Influences of dietary selenomethionine exposure on tissue accumulation, blood biochemical profiles, gene expression and intestinal microbiota of *Carassius auratus*. *Comparative Biochemistry and Physiology Part C: Toxicology & Pharmacology*, *218*, 21-29.

Bailly-Comte, V., Jourde, H., Roesch, A., Pistre, S., & Batiot-Guilhe, C. (2008). Time series analyses for Karst/River interactions assessment: Case of the Coulazou river (southern France). *Journal of hydrology*, *349*(1-2), 98-114.

Bala, K., Nogueira, R., Darbha, G. K., & Weichgrebe, D. (Eds.). (2025). *Occurrence, Detection, and Fate of Microplastics in Freshwater Ecosystems*. Springer Nature.

Balestra, V., Vigna, B., De Costanzo, S., & Bellopede, R. (2023). Preliminary investigations of microplastic pollution in karst systems, from surface watercourses to cave waters. *Journal of Contaminant Hydrology*, 252, 104117.

Barišić, J., Marijić, V. F., Mijošek, T., Čož-Rakovac, R., Dragun, Z., Krasnići, N., ... & Erk, M. (2018). Evaluation of architectural and histopathological biomarkers in the intestine of brown trout (*Salmo trutta* Linnaeus, 1758) challenged with environmental pollution. *Science of the total environment*, *642*, 656-664.

Bernhardt, E. S., Rosi, E. J., & Gessner, M. O. (2017). Synthetic chemicals as agents of global change. *Frontiers in Ecology and the Environment*, *15*(2), 84-90.

Bhardwaj, L. K., Rath, P., Yadav, P., & Gupta, U. (2024). Microplastic contamination, an emerging threat to the freshwater environment: a systematic review. *Environmental Systems Research*, *13*(1), 8.

Bhuyan, M. S. (2022). Effects of microplastics on fish and in human health. *Frontiers in Environmental Science*, *10*, 827289.

Blašković, A., Fastelli, P., Čižmek, H., Guerranti, C., & Renzi, M. (2017). Plastic litter in sediments from the Croatian marine protected area of the natural park of Telaščica bay (Adriatic Sea). *Marine pollution bulletin*, *114*(1), 583-586.

Blettler, M. C., Abrial, E., Khan, F. R., Sivri, N., & Espinola, L. A. (2018). Freshwater plastic pollution: Recognizing research biases and identifying knowledge gaps. *Water research*, *143*, 416-424.

Boev, I., Sijakova-Ivanova, T., & Lepitkova, S. (2025). Arsenic, heavy metals and rare earth elements in travertine limestone quarry in the Mariovo area, North Macedonia. *Geologica Macedonica*, 39(1).

Bogdan, D., Kolerič, T., Meznarič, M., Kozjek, M., & Viršek, M. K. (2022). Microlitter measurement in fish Rutilus rutilus from the Slovenian part of the Mura river basin. *Acta Biologica Slovenica*, *65*(1), 80-92.

Bonacci, O., Željković, I., & Galić, A. (2013). Karst rivers' particularity: an example from Dinaric karst (Croatia/Bosnia and Herzegovina). *Environmental earth sciences*, *70*(2), 963-974.

Bondu, R., Casiot, C., Pistre, S., & Batiot-Guilhe, C. (2023). Impact of past mining activities on water quality in a karst area in the Cévennes region, Southern France. *Science of the Total Environment*, *873*, 162274.

Bošković, N., Jaćimović, Ž., & Bajt, O. (2023). Microplastic pollution in rivers of the Adriatic Sea basin in Montenegro: Impact on pollution of the Montenegrin coastline. *Science of the Total Environment*, 905, 167206.

Brázová, T., Hanzelová, V., Miklisová, D., Šalamún, P., & Vidal-Martínez, V. M. (2015). Host-parasite relationships as determinants of heavy metal concentrations in perch (*Perca fluviatilis*) and its intestinal parasite infection. *Ecotoxicology and Environmental Safety*, *122*, 551-556.

Bruschi, R., Piccardo, M., Bentivoglio, T., Anselmi, S., Cabanel, P., Bevilacqua, S., ... & Renzi, M. (2026). Microplastics in Pristine Caves of the Classic Karst (NE Italy): A First Assessment of Contamination Levels. *Microplastics*, *5*(1), 24.

Burghardt, T. E., Babić, D., Kučina, I., & Babić, D. (2025). Erosion of road markings in Croatia and estimate of contribution to microplastic pollution. *Transportation research procedia*, *83*, 561-568.

Calore, D., & Fraticelli, N. (2022). State of the art offshore in situ monitoring of microplastic. *Microplastics*, 1(4), 640-650.

Campanale, C., Losacco, D., Triozzi, M., Massarelli, C., & Uricchio, V. F. (2022). An overall perspective for the study of emerging contaminants in karst aquifers. *Resources*, 11(11), 105.

Campbell, P. G., Giguère, A., Bonneris, E., & Hare, L. (2005). Cadmium-handling strategies in two chronically exposed indigenous freshwater organisms—the yellow perch (*Perca flavescens*) and the floater mollusc (*Pyganodon grandis*). *Aquatic Toxicology*, *72*(1-2), 83-97.

Cardon, P. Y., Caron, A., Rosabal, M., Fortin, C., & Amyot, M. (2018). Enzymatic validation of species‐specific protocols for metal subcellular fractionation in freshwater animals. *Limnology and Oceanography: Methods*, *16*(9), 537-555.

Caron, A., Rosabal, M., Drevet, O., Couture, P., & Campbell, P. G. (2018). Binding of trace elements (Ag, Cd, Co, Cu, Ni, and Tl) to cytosolic biomolecules in livers of juvenile yellow perch (*Perca flavescens*) collected from lakes representing metal contamination gradients. *Environmental Toxicology and Chemistry*, *37*(2), 576-586.

Cera, A., Cesarini, G., & Scalici, M. (2020). Microplastics in freshwater: what is the news from the world?. *Diversity*, *12*(7), 276.

Chen, B., Hu, L., He, B., Luan, T., & Jiang, G. (2020). Environmetallomics: Systematically investigating metals in environmentally relevant media. *Trends in Analytical Chemistry*, *126*, 115875.

Chovanec, A., Hofer, R., & Schiemer, F. (2003). Fish as bioindicators. In *Trace metals and other contaminants in the environment* (Vol. 6, pp. 639-676). Elsevier.

Chunchukova, M., Kirin, D., & Kuzmanova, D. (2020). Arsenic content in the parasite-host systems: *Pomphorhynchus laevis-Abramis brama* and *Acanthocephalus lucii-Abramis brama*. *Scientific Papers. Series D. Animal Science*, *63*(2).

Chunchukova, M., & Kuzmanova, D. (2017). Arsenic content in parasite-host system: *Alburnus alburnus-Pomphorhynchus laevis* and the impact of the acanthocephalan on his host. *Agricultural Sciences/Agrarni Nauki*, *9*(22).

Cindrić, A. M., Garnier, C., Oursel, B., Pižeta, I., & Omanović, D. (2015). Evidencing the natural and anthropogenic processes controlling trace metals dynamic in a highly stratified estuary: The Krka River estuary (Adriatic, Croatia). *Marine pollution bulletin*, *94*(1-2), 199-216.

Creighton, N., & Twining, J. (2010). Bioaccumulation from food and water of cadmium, selenium and zinc in an estuarine fish, *Ambassis jacksoniensis*. *Marine Pollution Bulletin*, 60(10), 1815-1821.

Cukrov N, Barišić D (2006) Spatial Distribution of 40K and 232Th in Recent Sediments of the Krka River Estuary. *Croatica Chemica Acta* 79: 115-118.

Cukrov, N., Cmuk, P., Mlakar, M., & Omanović, D. (2008). Spatial distribution of trace metals in the Krka River, Croatia: an example of the self-purification. *Chemosphere*, *72*(10), 1559-1566.

Cukrov, N., Cuculić, V., Barišić, D., Lojen, S., Mikelić, I. L., Oreščanin, V., ... & Mlakar, M. (2013). Elemental and isotopic records in recent fluvio-lacustrine sediments in karstic river Krka, Croatia. *Journal of geochemical exploration*, 134, 51-60.

Cukrov, N., Cukrov, N., & Omanović, D. (2024). Early Diagenetic Processes in the Sediments of the Krka River Estuary. *Journal of marine science and engineering*, *12*(3), 466.

Cukrov, N., Doumandji, N., Garnier, C., Tucaković, I., Dang, D. H., Omanović, D., & Cukrov, N. (2020). Anthropogenic mercury contamination in sediments of Krka River estuary (Croatia). *Environmental science and pollution research*, *27*(7), 7628-7638.

Cukrov, N., Tepić, N., Omanović, D., Lojen, S., Bura-Nakić, E., Vojvodić, V., & Pižeta, I. (2012). Qualitative interpretation of physico-chemical and isotopic parameters in the Krka River (Croatia) assessed by multivariate statistical analysis. *International journal of environmental analytical chemistry*, *92*(10), 1187-1199.

Coghlan, A., Tyagi, R., Cotton, J. A., Holroyd, N., Rosa, B. A., Tsai, I. J., ... & Blaxter, M. L. (2019). Comparative genomics of the major parasitic worms. *Nature Genetics*, *51*, 163-174.

Commission Regulation (EU) 2023/2055 of 25 September 2023 amending Annex XVII to Regulation (EC) No 1907/2006 of the European Parliament and of the Council concerning the Registration, Evaluation, Authorisation and Restriction of Chemicals (REACH) as

regards synthetic polymer microparticles (Text with EEA relevance) URL: https://eur-lex.europa.eu/eli/reg/2023/2055/oj

Ćaleta, B., Hackenberger Kutuzović, B., Jug, D., Jug, I., & Hackenberger Kutuzović, D. (2025). Impact of Different Soil Tillage Practices on Microplastic Particle Abundance and Distribution. *Soil systems*, *9*(2), 63.

Dane, H., & Şişman, T. (2020). A morpho-histopathological study in the digestive tract of three fish species influenced with heavy metal pollution. *Chemosphere*, 242, 125212.

de Almeida, M. E., Batista, M. T. O., Vani, G. S., de Oliveira, M. F., Rodrigues, E., & Suda, C. N. K. (2019). Isozymes of malate-and lactate dehydrogenase of *Astyanax bimaculatus* as biomarkers of environmental impact. *Ambiente e Agua-An Interdisciplinary Journal of Applied Science*, *14*(7), 1-11.

de Araújo, G. A., Ramos, M. C. S., Carvalho, G. L. D., Camilo-Cotrim, C. F., do Amaral, R. B., Castro, Í. B., ... & Damacena-Silva, L. (2025). Microplastic contamination in wild freshwater fish: global trends, challenges and perspectives. *Environmental Pollution*, 126406.

Desjardins, K., Khadra, M., Caron, A., Ponton, D. E., Rosabal, M., & Amyot, M. (2022). Significance of chemical affinity on metal subcellular distribution in yellow perch (*Perca flavescens*) livers from Lake Saint-Pierre (QUEBEC, Canada). *Environmental Pollution*, *312*, 120077.

Dezfuli, B. S., Giovinazzo, G., Lui, A., & Giari, L. (2008a). Inflammatory response to *Dentitruncus truttae* (Acanthocephala) in the intestine of brown trout. *Fish & Shellfish Immunology*, *24*(6), 726-733.

Dezfuli, B. S., Lui, A., Giari, L., Boldrini, P., & Giovinazzo, G. (2008b). Ultrastructural study on the body surface of the acanthocephalan parasite *Dentitruncus truttae* in brown trout. *Microscopy Research and Technique*, *71*(3), 230-235.

Directive 2008/105/EC of the European Parliament and of the Council of 16 December 2008 on environmental quality standards in the field of water policy, amending and subsequently repealing Council Directives 82/176/EEC, 83/513/EEC, 84/156/EEC, 84/491/EEC, 86/280/EEC and amending Directive 2000/60/EC of the European Parliament and of the Council. URL: https://eur-lex.europa.eu/legal-content/EN/TXT/?uri=celex:32008L0105

Dragun, Z., Filipović Marijić, V., Krasnići, N., Ivanković, D., Valić, D., Žunić, J., ... & Erk, M. (2018). Total and cytosolic concentrations of twenty metals/metalloids in the liver of brown trout *Salmo trutta* (Linnaeus, 1758) from the karstic Croatian river Krka. *Ecotoxicology and environmental safety*, *147*, 537-549.

Dragun, Z., Krasnići, N., Ivanković, D., Marijić, V. F., Mijošek, T., Redžović, Z., & Erk, M. (2020). Comparison of intracellular trace element distributions in the liver and gills of the invasive freshwater fish species, Prussian carp (*Carassius gibelio* Bloch, 1782). *Science of the total environment*, *730*, 138923.

Dragun, Z., Krasnići, N., Kolar, N., Marijić, V. F., Ivanković, D., & Erk, M. (2018). Cytosolic distributions of highly toxic metals Cd and Tl and several essential elements in the liver of brown trout (*Salmo trutta* L.) analyzed by size exclusion chromatography and inductively coupled plasma mass spectrometry. *Chemosphere*, *207*, 162-173.

Duarte, G. S. C., Lehun, A. L., Leite, L. A. R., Consolin-Filho, N., Bellay, S., & Takemoto, R. M. (2020). Acanthocephalans parasites of two Characiformes fishes as bioindicators of cadmium contamination in two neotropical rivers in Brazil. *Science of the Total Environment*, *738*, 140339.

Eerkes-Medrano, D., Thompson, R. C., & Aldridge, D. C. (2015). Microplastics in freshwater systems: a review of the emerging threats, identification of knowledge gaps and prioritisation of research needs. *Water research*, *75*, 63-82.

Eftimi, R. (2020). Karst and karst water recourses of Albania and their management. *Carbonates and evaporites*, *35*(3), 1-14.

Eris, E., & Wittenberg, H. (2015). Estimation of baseflow and water transfer in karst catchments in Mediterranean Turkey by nonlinear recession analysis. *Journal of Hydrology*, *530*, 500-507.

Fernández-Ortega, J., Ulloa-Cedamanos, F., Barberá, J. A., Batiot-Guilhe, C., Jourde, H., & Andreo, B. (2024). A common framework for the development of spring water contamination early warning system in western Mediterranean karst areas: Spanish and French sites. *Science of the Total Environment,* 956, 177294.

Filipović Marijić, V., Kapetanović, D., Dragun, Z., Valić, D., Krasnići, N., Redžović, Z., ... & Erk, M. (2018). Influence of technological and municipal wastewaters on vulnerable karst

riverine system, Krka River in Croatia. *Environmental science and pollution research*, *25*(5), 4715-4727.

Filipović Marijić, V., Krasnići, N., Valić, D., Kapetanović, D., Vardić Smrzlić, I., Jordanova, M., ... & Dragun, Z. (2023b). Pollution impact on metal and biomarker responses in intestinal cytosol of freshwater fish. *Environmental science and pollution research*, *30*(23), 63510-63521.

Filipović Marijić, V., Mijošek, T., Dragun, Z., Retzmann, A., Zitek, A., Prohaska, T., ... & Erk, M. (2022). Application of calcified structures in fish as indicators of metal exposure in freshwater ecosystems. *Environments*, *9*(2), 14.

Filipović Marijić, V., & Raspor, B. (2012). Site-specific gastrointestinal metal variability in relation to the gut content and fish age of indigenous European chub from the Sava River. *Water, Air, & Soil Pollution*, *223*(8), 4769-4783.

Filipović Marijić, V., & Raspor, B. (2004). Relationship of metallothionein and metal levels with biometric parameters in different tissues of *Mullus sp*. from the Eastern Adriatic Sea. *Environmental Science Solutions: A Pan-European Perspective,* SETAC Europe, 96-96.

Filipović Marijić, V., Subirana, M. A., Schaumlöffel, D., Barišić, J., Gontier, E., Krasnići, N., ... & Erk, M. (2023a). First insight in element localisation in different body parts of the acanthocephalan *Dentitruncus truttae* using TEM and NanoSIMS. *Science of the total environment*, *887*, 164010.

Filipović Marijić, V., Vardić Smrzlić, I., & Raspor, B. (2013). Effect of acanthocephalan infection on metal, total protein and metallothionein concentrations in European chub from a Sava River section with low metal contamination. *Science of the Total Environment*, *463*, 772-780.

Filipović Marijić, V., Vardić Smrzlić, I., & Raspor, B. (2014). Does fish reproduction and metabolic activity influence metal levels in fish intestinal parasites, acanthocephalans, during fish spawning and post-spawning period?. *Chemosphere*, *112*, 449-455.

Ford, D., & Williams, P. D. (2007). *Karst hydrogeology and geomorphology*. John Wiley & Sons.

Gaillardet, J., Viers, J., & Dupré, B. (2013). Trace elements in river waters. In Treatise on geochemistry: second edition (pp. 195-235).

Galib, S. M., Mohsin, A. B. M., Parvez, M. T., Lucas, M. C., Chaki, N., Arnob, S. S., ... & Islam, M. N. (2018). Municipal wastewater can result in a dramatic decline in freshwater fishes: a lesson from a developing country. *Knowledge & Management of Aquatic Ecosystems*, (419), 37.

Gao, S., Orlowski, N., Bopf, F. K., & Breuer, L. (2024). A review on microplastics in major European rivers. *Wiley Interdisciplinary Reviews: Water*, 11(3), e1713.

Garai, P., Banerjee, P., Mondal, P., & Saha, N. C. (2021). Effect of heavy metals on fishes: Toxicity and bioaccumulation. *Journal of Clinical Toxicology*, 18(001).

Giguère, A., Campbell, P. G., Hare, L., & Couture, P. (2006). Sub-cellular partitioning of cadmium, copper, nickel and zinc in indigenous yellow perch (*Perca flavescens*) sampled along a polymetallic gradient. *Aquatic Toxicology*, *77*(2), 178-189.

Goldscheider, N., Chen, Z., Auler, A. S., Bakalowicz, M., Broda, S., Drew, D., ... & Veni, G. (2020). Global distribution of carbonate rocks and karst water resources. *Hydrogeology Journal*, *28*(5), 1661-1677.

Goldscheider, N. (2019). A holistic approach to groundwater protection and ecosystem services in karst terrains. *Carbonates and Evaporites*, *34*(4), 1241-1249.

Gomiero, A., Strafella, P., & Fabi, G. (2018). From macroplastic to microplastic litter: occurrence, composition, source identification and interaction with aquatic organisms. Experiences from the Adriatic Sea. In *Plastics in the Environment*. IntechOpen.

Green, A. J., & Planchart, A. (2018). The neurological toxicity of heavy metals: A fish perspective. *Comparative Biochemistry and Physiology Part C: Toxicology & Pharmacology*, *208*, 12-19.

Hampuwo, B., Duenser, A., Lahnsteiner, E., Friedrich, T., & Lahnsteiner, F. (2026). Size-Dependent Tissue Translocation and Physiological Responses to Dietary Polystyrene Microplastics in Salmo trutta. *Animals: an Open Access Journal from MDPI*, *16*(2), 285.

Hartmann, A., Barberá, J. A., & Andreo, B. (2017). On the value of water quality data and informative flow states in karst modelling. *Hydrology and Earth System Sciences*, *21*(12), 5971-5985.

Hassanine, R., & Al-Hasawi, Z. (2021). Acanthocephalan worms mitigate the harmful impacts of heavy metal pollution on their fish hosts. *Fishes*, *6*(4), 49.

Has-Schön, E., Bogut, I., Rajković, V., Bogut, S., Čačić, M., & Horvatić, J. (2008). Heavy metal distribution in tissues of six fish species included in human diet, inhabiting freshwaters of the Nature Park "Hutovo Blato" (Bosnia and Herzegovina). *Archives of environmental contamination and toxicology*, 54(1), 75-83.

Hayes, J. D., Flanagan, J. U., & Jowsey, I. R. (2005). Glutathione transferases. *Annual Review of Pharmacology and Toxicology*, *45*(1), 51-88.

Hellou, J., Ross, N. W., & Moon, T. W. (2012). Glutathione, glutathione S-transferase, and glutathione conjugates, complementary markers of oxidative stress in aquatic biota. *Environmental Science and Pollution Research*, *19*, 2007-2023.

Hemmadi, V. (2017). A critical review on integrating multiple fish biomarkers as indicator of heavy metals contamination in aquatic ecosystem. *International Journal of Bioassays*, *6*(9), 5494-5506.

Herlyn, H., & Taraschewski, H. (2017). Evolutionary anatomy of the muscular apparatus involved in the anchoring of Acanthocephala to the intestinal wall of their vertebrate hosts. *Parasitology research*, 116, 1207-1225.

Hillebrand, O., Nödler, K., Licha, T., Sauter, M., & Geyer, T. (2012). Caffeine as an indicator for the quantification of untreated wastewater in karst systems. *Water research*, *46*(2), 395-402.

Hoaghia, M. A., Moldovan, A., Kovacs, E., Mirea, I. C., Kenesz, M., Brad, T., ... & Moldovan, O. T. (2021). Water Quality and Hydrogeochemical Characteristics of Some Karst Water Sources in Apuseni Mountains, Romania. *Water*, *13*(6), 857.

Holt, E. A. & Miller, S. W. (2011) Bioindicators: Using Organisms to Measure Environmental Impacts. *Nature Education Knowledge* 2(2):8

Hoseini, S. M., Sinha, R., Fazel, A., Khosraviani, K., Hosseinpour Delavar, F., Arghideh, M., ... & Van Doan, H. (2022). Histopathological damage and stress‐and immune‐related genes' expression in the intestine of common carp, *Cyprinus carpio* exposed to copper and polyvinyl chloride microparticle. *Journal of Experimental Zoology Part A: Ecological and Integrative Physiology*, *337*(2), 181-190.

Hotez, P. J., Brindley, P. J., Bethony, J. M., King, C. H., Pearce, E. J., & Jacobson, J. (2008). Helminth infections: the great neglected tropical diseases. *The Journal of clinical investigation*, *118*(4), 1311-1321.

Huang, X., Chen, X. G., & Armbruster, P. A. (2016). Comparative performance of transcriptome assembly methods for non-model organisms. *BMC genomics*, *17*, 1-14.

Huang, J. N., Zhang, Y., Xu, L., He, K. X., Wen, B., Yang, P. W., ... & Chen, Z. Z. (2022). Microplastics: A tissue-specific threat to microbial community and biomarkers of discus fish (*Symphysodon aequifasciatus*). *Journal of Hazardous Materials*, *424*, 127751.

Infante, H. G., Van Campenhout, K., Blust, R., & Adams, F. C. (2002). Inductively coupled plasma time-of-flight mass spectrometry coupled to high-performance liquid chromatography for multi-elemental speciation analysis of metalloproteins in carp cytosols. *Journal of Analytical Atomic Spectrometry*, *17*(2), 79-87.

Jan, I., Ahmad, T., Wani, M. S., Dar, S. A., Wani, N. A., Malik, N. A., & Tantary, Y. R. (2022). Threats and consequences of untreated wastewater on freshwater environments. In *Microbial consortium and biotransformation for pollution decontamination* (pp. 1-26). Elsevier.

Jarić, I., Višnjić-Jeftić, Ž., Cvijanović, G., Gačić, Z., Jovanović, L., Skorić, S., & Lenhardt, M. (2011). Determination of differential heavy metal and trace element accumulation in liver, gills, intestine and muscle of sterlet (*Acipenser ruthenus*) from the Danube River in Serbia by ICP-OES. *Microchemical journal*, 98(1), 77-81.

Jemec Kokalj, A., Fišer, C., Laforsch, C., & Löder, M. G. (2025). Above and in the underground: Linking microplastic patterns in cave and surface crustaceans along a karst river stretch. *Environmental Pollution*, 126939.

Josip Juraj Strossmayer Water Institute (2025) Report on the state of surface waters in the Republic of Croatia in 2024, Class: 325-08/25-06/3 Reg. No.: 122-05/1-25-2 [in Croatian]. Zagreb, Croatia.

Kapelj, S., Loborec, J., Fiket, Ž., & Zavrtnik, S. (2025). The comparison of dissolved ionic forms of some metals (Fe, Cu, Cd, Pb, Zn) mobility in relation with intrinsic groundwater vulnerability in the industrial waste landfills, Croatia. *Environmental earth sciences*, 84(3), 94.

Källqvist, T., Milačič, R., Smital, T., Thomas, K. V., Vranes, S., & Tollefsen, K. E. (2008). Chronic toxicity of the Sava River (SE Europe) sediments and river water to the algae *Pseudokirchneriella subcapitata*. *Water research*, *42*(8-9), 2146-2156.

Kennedy, C. R. (2006). *Ecology of the Acanthocephala*. Cambridge University Press.

Khan, F. R., Clark, N., & Xu, E. G. (2025). Micro (nano) plastics in the fish gastrointestinal tract: A mini review and relevance to One Health perspective. *Current Opinion in Environmental Science & Health*, *46*, 100645.

Kiralj, Z., Dragun, Z., Lajtner, J., Trgovčić, K., Valić, D., & Ivanković, D. (2023). Accumulation of metal (loid) s in the digestive gland of the mussel *Unio crassus* Philipsson, 1788: A reliable detection of historical freshwater contamination. *Environmental pollution*, *334*, 122164.

Kisić, I., Zgorelec, Ž., Galić, M., & Delač, D. (2019). Analysis of mud and water in lagoons polluted by waste materials (Technical report commissioned by the Town of Knin) [in Croatian]. University of Zagreb, Faculty of Agriculture; Hidro.Lab. d.o.o., https://knin.hr/wp-content/uploads/2019/07/Knin-izvijesce-19-6-2019-KRAJ.pdf

Klemetsen, A., Amundsen, P. A., Dempson, J. B., Jonsson, B., Jonsson, N., O'connell, M. F., & Mortensen, E. (2003). Atlantic salmon *Salmo salar* L., brown trout *Salmo trutta* L. and Arctic charr *Salvelinus alpinus* (L.): a review of aspects of their life histories. *Ecology of freshwater fish*, *12*(1), 1-59.

Kljaković-Gašpić, Z., Sekovanić, A., Orct, T., Šebešćen, D., Klasiček, E., & Zanella, D. (2022). Potentially toxic elements in water, sediments and fish from the Karstic river (Raša River, Croatia) located in the former coal-mining area. *Toxics*, *11*(1), 42.

Koutsikos, N., Koi, A. M., Zeri, C., Tsangaris, C., Dimitriou, E., & Kalantzi, O. I. (2023). Exploring microplastic pollution in a Mediterranean river: The role of introduced species as bioindicators. *Heliyon*, *9*(4).

Kraemer, L. D., Campbell, P. G., & Hare, L. (2006). Seasonal variations in hepatic Cd and Cu concentrations and in the sub-cellular distribution of these metals in juvenile yellow perch (*Perca flavescens*). *Environmental Pollution*, *142*(2), 313-325.

Krasnići, N., Dragun, Z., Erk, M., & Raspor, B. (2014). Distribution of Co, Cu, Fe, Mn, Se, Zn, and Cd among cytosolic proteins of different molecular masses in gills of European chub (*Squalius cephalus* L.). *Environmental science and pollution research*, *21*(23), 13512-13521.

Krasnići, N., Dragun, Z., Erk, M., & Raspor, B. (2013). Distribution of selected essential (Co, Cu, Fe, Mn, Mo, Se, and Zn) and nonessential (Cd, Pb) trace elements among protein fractions from hepatic cytosol of European chub (*Squalius cephalus* L.). *Environmental science and pollution research*, *20*(4), 2340-2351.

Krasnići, N., Dragun, Z., Kazazić, S., Muharemović, H., Erk, M., Jordanova, M., ... & Kostov, V. (2019). Characterization and identification of selected metal-binding biomolecules from hepatic and gill cytosols of Vardar chub (*Squalius vardarensis* Karaman, 1928) using various techniques of liquid chromatography and mass spectrometry. *Metallomics*, *11*(6), 1060-1078.

Krivokapić, M. (2021). Study on the evaluation of (heavy) metals in water and sediment of Skadar Lake (Montenegro), with BCF assessment and translocation ability (TA) by *Trapa natans* and a review of SDGs. *Water*, *13*(6), 876.

Kumari, D., & Paul, D. K. (2020). Assessing the role of bioindicators in freshwater ecosystem. *Journal of Interdisciplinary Cycle Research*, *12*(9), 17.

Kuśmierek, N., & Popiołek, M. (2020). Microplastics in freshwater fish from Central European lowland river (Widawa R., SW Poland). *Environmental Science and Pollution Research*, *27*(10), 11438-11442.

Kwong, R. W., Andrés, J. A., & Niyogi, S. (2011). Effects of dietary cadmium exposure on tissue-specific cadmium accumulation, iron status and expression of iron-handling and stress-inducible genes in rainbow trout: influence of elevated dietary iron. *Aquatic toxicology*, *102*(1-2), 1-9.

Lapointe, D., & Couture, P. (2009). Influence of the route of exposure on the accumulation and subcellular distribution of nickel and thallium in juvenile fathead minnows (*Pimephales promelas*). *Archives of environmental contamination and toxicology*, *57*(3), 571-580.

Li, L., Zheng, B., & Liu, L. (2010). Biomonitoring and bioindicators used for river ecosystems: definitions, approaches and trends. *Procedia environmental sciences*, *2*, 1510-1524.

Lojen, S., Dolenec, T., Vokal, B., Cukrov, N., Mihelčić, G., & Papesch, W. (2004). C and O stable isotope variability in recent freshwater carbonates (River Krka, Croatia). *Sedimentology*, *51*(2), 361-375.

Malá, J., Hübelová, D., Schrimpelová, K., Kozumplíková, A., & Lejska, S. (2022). Surface watercourses as sources of karst water pollution. *International Journal of Environmental Science and Technology*, *19*(5), 3503-3512.

Maldini, K., Cukrov, N., Pikelj, K., Matić, N., & Mlakar, M. (2023). Geochemistry of Metals and Organic Matter in Water and Sediments of the Karst River Cetina, Croatia. *Water*, *15*(7), 1429.

Marcinek, S., Santinelli, C., Cindrić, A. M., Evangelista, V., Gonnelli, M., Layglon, N., Mounier, S., Lenoble, V., Omanović, D. (2020) Dissolved organic matter dynamics in the pristine Krka River estuary (Croatia). *Marine Chemistry* 225: 103848.

Marinsek, G. P., Choueri, P. K. G., Choueri, R. B., de Souza Abessa, D. M., Gonçalves, A. R. N., Bortolotto, L. B., & de Britto Mari, R. (2022). Integrated analysis of fish intestine biomarkers: Complementary tools for pollution assessment. *Marine Pollution Bulletin*, *178*, 113590.

Marinsek, G. P., de Souza Abessa, D. M., Gusso-Choueri, P. K., Choueri, R. B., Gonçalves, A. R. N., Barroso, B. V. D. A., ... & de Britto Mari, R. (2018). Enteric nervous system analyses: new biomarkers for environmental quality assessment. *Marine Pollution Bulletin*, *137*, 711-722.

Maršić-Lučić, J., Lušić, J., Tutman, P., Varezić, D. B., Šiljić, J., & Pribudić, J. (2018). Levels of trace metals on microplastic particles in beach sediments of the island of Vis, Adriatic Sea, Croatia. *Marine pollution bulletin*, 137, 231-236.

Martin, J. A., & Wang, Z. (2011). Next-generation transcriptome assembly. *Nature Reviews Genetics*, *12*(10), 671-682.

Matić, N., Maldini, K., Cuculić, V., & Frančišković-Bilinski, S. (2012). Investigations of karstic springs of the Biokovo Mt from the Dinaric karst of Croatia. *Geochemistry*, *72*(2), 179-190.

Matić, N., Maldini, K., Tomas, D., Ćuk, R., Milović, S., Miklavčić, I., & Širac, S. (2016). Geochemical characteristics of the Gacka River karstic springs (Dinaric karst, Croatia) with macroinvertebrate assemblages overview. *Environmental earth sciences*, 75(19), 1308.

Mauer, K., Hellmann, S. L., Groth, M., Fröbius, A. C., Zischler, H., Hankeln, T., & Herlyn, H. (2020). The genome, transcriptome, and proteome of the fish parasite *Pomphorhynchus laevis* (Acanthocephala). *PloS One*, *15*(6), e0232973.

Medunić, G., Bucković, D., Crnić, A. P., Bituh, T., Srček, V. G., Radošević, K., ... & Zgorelec, Z. (2020). Sulfur, metal (loid) s, radioactivity, and cytotoxicity in abandoned karstic Raša coal-mine discharges (the north Adriatic Sea). *Rudarsko-geološko-naftni zbornik*, *35*(3).

Menghini, M., Pedrazzani, R., Feretti, D., Mazzoleni, G., Steimberg, N., Urani, C., ... & Bertanza, G. (2023). Beyond the black box of life cycle assessment in wastewater treatment plants: which help from bioassays?. *Water*, *15*(5), 960.

Mijošek, T., Filipović Marijić, V., Dragun, Z., Ivanković, D., Krasnići, N., & Erk, M. (2022). Efficiency of metal bioaccumulation in acanthocephalans, gammarids and fish in relation to metal exposure conditions in a karst freshwater ecosystem. *Journal of trace elements in medicine and biology*, 73, 127037.

Mijošek, T., Filipović Marijić, V., Dragun, Z., Ivanković, D., Krasnići, N., Redžović, Z., & Erk, M. (2021a). Intestine of invasive fish Prussian carp as a target organ in metal exposure assessment of the wastewater impacted freshwater ecosystem. *Ecological indicators*, *122*, 107247.

Mijošek, T., Filipović Marijić, V., Dragun, Z., Krasnići, N., Ivanković, D., & Erk, M. (2019). Evaluation of multi-biomarker response in fish intestine as an initial indication of anthropogenic impact in the aquatic karst environment. *Science of the total environment*, 660, 1079-1090.

Mijošek, T., Filipović Marijić, V., Dragun, Z., Krasnići, N., Ivanković, D., Redžović, Z., & Erk, M. (2021b). First insight in trace element distribution in the intestinal cytosol of two freshwater fish species challenged with moderate environmental contamination. *Science of the total environment*, *798*, 149274.

Mikac, I., Fiket, Ž., Terzić, S., Barešić, J., Mikac, N., & Ahel, M. (2011). Chemical indicators of anthropogenic impacts in sediments of the pristine karst lakes. *Chemosphere*, 84(8), 1140-1149.

Miko, S., Durn, G., Adamcová, R., Čović, M., Dubikova, M., Skalský, R., ... & Ottner, F. (2003). Heavy metal distribution in karst soils from Croatia and Slovakia. *Environmental Geology*, 45(2), 262-272.

Mitra, T., Mahanty, A., Ganguly, S., & Mohanty, B. P. (2020). Transcriptomic responses to pollution in natural riverine environment in *Rita rita*. *Environmental Research*, *186*, 109508.

Moravec, F. (2004). Metazoan parasites of salmonid fishes of Europe. Academia.

Moreira-Santos, M., Soares, A. M., & Ribeiro, R. (2004). An in situ bioassay for freshwater environments with the microalga *Pseudokirchneriella subcapitata*. *Ecotoxicology and Environmental Safety*, *59*(2), 164-173.

Nachev, M., & Sures, B. (2016). Seasonal profile of metal accumulation in the acanthocephalan Pomphorhynchus laevis: a valuable tool to study infection dynamics and implications for metal monitoring. *Parasites & Vectors*, *9*(1), 300.

Naqash, N., Prakash, S., Kapoor, D., & Singh, R. (2020). Interaction of freshwater microplastics with biota and heavy metals: a review. *Environmental Chemistry Letters*, *18*(6), 1813-1824.

NN 05 (1985). Act on the Proclamation of the National Park "Krka". Official Gazette of the Republic of Croatia No. 5 [in Croatian].

Ojo, A. A., & Wood, C. M. (2008). In vitro characterization of cadmium and zinc uptake via the gastro-intestinal tract of the rainbow trout (*Oncorhynchus mykiss*): interactive effects and the influence of calcium. *Aquatic Toxicology*, *89*(1), 55-64.

Okwuosa, O. B., & Eyo, J. (2019). Role of fish as bioindicators: A Review. *IRE Journals*.

Oleksiak, M. F. (2008). Changes in gene expression due to chronic exposure to environmental pollutants. *Aquatic Toxicology*, *90*(3), 161-171.

Omer, S. A., Elobeid, M. A., Fouad, D., Daghestani, M. H., Al-Olayan, E. M., Elamin, M. H., ... & El-Mahassna, A. (2012). Cadmium bioaccumulation and toxicity in tilapia fish (*Oreochromis niloticus*). *Journal of animal and veterinary advances*, 11(10), 1601-1606.

Oppeltová, P., Vlček, V., Geršl, M., Chaloupský, P., Ulrich, O., Sedláček, J., ... & Šimečková, J. (2024). Occurrence and path pollution of emerging organic contaminants in mineral water of Hranice hypogenic Karst. *Frontiers in Environmental Science*, *12*, 1339818.

Osman, A. G., Abd-El–Baset, M., AbuelFadl, K. Y., & GadEl-Rab, A. G. (2010). Enzymatic and histopathologic biomarkers as indicators of aquatic pollution in fishes. *Natural Science*, 2(11), 1302-1311.

Oyoo-Okoth, E., Admiraal, W., Osano, O., Kraak, M. H., Gichuki, J., & Ogwai, C. (2012). Parasites modify sub-cellular partitioning of metals in the gut of fish. *Aquatic toxicology*, *106*, 76-84.

Palcsu, L., Gessert, A., Túri, M., Kovács, A., Futó, I., Orsovszki, J., ... & Koltai, G. (2021). Long-term time series of environmental tracers reveal recharge and discharge conditions in shallow karst aquifers in Hungary and Slovakia. *Journal of Hydrology: Regional Studies*, 36, 100858.

Parać, M., Cuculić, V., Cukrov, N., Geček, S., Lovrić, M., & Cukrov, N. (2022). Microplastic distribution through the salinity gradient in a stratified estuary. *Water*, *14*(20), 3255.

Parente, T., & Hauser-Davis, R. A. (2013). The use of fish biomarkers in the evaluation of water pollution. *Pollution and fish health in tropical ecosystems*, 164-81.

Parker, B., Andreou, D., Green, I. D., & Britton, J. R. (2021). Microplastics in freshwater fishes: Occurrence, impacts and future perspectives. *Fish and Fisheries*, *22*(3), 467-488.

Perrot-Minnot, M. J., Cozzarolo, C. S., Amin, O., Barčák, D., Bauer, A., Marijić, V. F., ... & Sures, B. (2023). Hooking the scientific community on thorny-headed worms: interesting and exciting facts, knowledge gaps and perspectives for research directions on Acanthocephala. *Parasite*, *30*, 23.

Radix, P., Léonard, M., Papantoniou, C., Roman, G., Saouter, E., Gallotti-Schmitt, S., ... & Vasseur, P. (2000). Comparison of four chronic toxicity tests using algae, bacteria, and invertebrates assessed with sixteen chemicals. *Ecotoxicology and Environmental Safety*, *47*(2), 186-194.

Raghavan, V., Kraft, L., Mesny, F., & Rigerte, L. (2022). A simple guide to de novo transcriptome assembly and annotation. *Briefings in bioinformatics*, *23*(2), bbab563

Rainbow, P. S. (2002). Trace metal concentrations in aquatic invertebrates: why and so what?. *Environmental pollution*, *120*(3), 497-507.

Reberski, J. L., Selak, A., Lapworth, D. J., Maurice, L. D., Terzić, J., Civil, W., & Stroj, A. (2023). Emerging organic contaminants in springs of the highly karstified Dinaric region. *Journal of hydrology*, 621, 129583.

Rizzo, M. (2024). Measurement of malondialdehyde as a biomarker of lipid oxidation in fish. *American Journal of Analytical Chemistry*, *15*(9), 303-332.

Rolland, A., Palmer, M., Chételat, J., Amyot, M., & Rosabal, M. (2025). Subcellular Partitioning of Trace Elements Is Related to Metal Ecotoxicological Classes in Livers of Fish (*Esox lucius; Coregonus clupeaformis*) from the Yellowknife Area (Northwest Territories, Canada). *Toxics*, *13*(5), 410.

Rosabal, M., Pierron, F., Couture, P., Baudrimont, M., Hare, L., & Campbell, P. G. (2015). Subcellular partitioning of non-essential trace metals (Ag, As, Cd, Ni, Pb, and Tl) in livers of American (*Anguilla rostrata*) and European (*Anguilla anguilla*) yellow eels. *Aquatic Toxicology*, *160*, 128-141.

Ryan, J. A., & Hightower, L. E. (1996). Stress proteins as molecular biomarkers for environmental toxicology. *Stress-inducible cellular responses*, 411-424.

Sanders, B. M., & Dyer, S. D. (1994). Cellular stress response. *Environmental Toxicology and Chemistry: An International Journal*, *13*(8), 1209-1210.

Sakalli, S., Giang, P. T., Burkina, V., Zamaratskaia, G., Rasmussen, M. K., Bakal, T., ... & Zlabek, V. (2018). The effects of sewage treatment plant effluents on hepatic and intestinal biomarkers in common carp (*Cyprinus carpio*). *Science of the Total Environment*, *635*, 1160-1169.

Savoca, S., Matanović, K., D'Angelo, G., Vetri, V., Anselmo, S., Bottari, T., ... & Gjurčević, E. (2021). Ingestion of plastic and non-plastic microfibers by farmed gilthead sea bream (*Sparus aurata*) and common carp (*Cyprinus carpio*) at different life stages. *Science of the total environment*, *782*, 146851.

Selak, A., Reberski, J. L., Boljat, I., & Terzić, J. (2024). Characterizing occurrence of emerging organic contaminants in Dinaric karst catchment of Jadro and Žrnovnica springs, Croatia. *Emerging contaminants*, *10*(3), 100327.

Sertić Perić, M., Miliša, M., Matoničkin Kepčija, R., Primc-Habdija, B., & Habdija, I. (2011). Seasonal and fine-scale spatial drift patterns in a tufadepositing barrage hydrosystem. *Fundamental and applied limnology*, 131-145.

Sharma, R. K., & Agrawal, M. (2005). Biological effects of heavy metals: an overview. *Journal of environmental Biology*, 26(2), 301-313.

Sironić, A., Barešić, J., Horvatinčić, N., Brozinčević, A., Vurnek, M., & Kapelj, S. (2017). Changes in the geochemical parameters of karst lakes over the past three decades–The case of Plitvice Lakes, Croatia. *Applied geochemistry*, *78*, 12-22.

Staniskiene, B., Matusevicius, P., Budreckiene, R., & Skibniewska, K. A. (2006). Distribution of heavy metals in tissues of freshwater fish in Lithuania. *Polish Journal of Environmental Studies*, *15*(4).

Strižak, Ž., Ivanković, D., Pröfrock, D., Helmholz, H., Cindrić, A. M., Erk, M., & Prange, A. (2014). Characterization of the cytosolic distribution of priority pollutant metals and metalloids in the digestive gland cytosol of marine mussels: seasonal and spatial variability. *Science of the total environment*, *470*, 159-170.

Sures, B., Nachev, M., Selbach, C., & Marcogliese, D. J. (2017). Parasite responses to pollution: what we know and where we go in 'Environmental Parasitology'. *Parasites & vectors*, *10*(1), 65.

Sures, B., Siddall, R., & Taraschewski, H. (1999). Parasites as accumulation indicators of heavy metal pollution. *Parasitology Today*, *15*(1), 16-21.

Szpunar, J. (2004). Metallomics: a new frontier in analytical chemistry. *Analytical and Bioanalytical Chemistry*, *378*(1), 54-56.

Ševove, B., Príkazská, M., Sabová, A. A., & Kováč, V. (2025). Comparison of microplastic intake in two fish species from different functional feeding groups in Europe's second-largest river. *Chemosphere*, *391*, 144721.

Tepić, N., Olujić, G., & Ahel, M. (2007). Distribution of carbohydrates in the karstic estuary of the Krka River. In Le 38e Congres de la CIESM (pp. 9-13).

Teodorescu, D., Munteanu, M. C., Staicu, A. C., & Dinischiotu, A. N. C. A. (2012). Changes in lactate dehydrogenase activity in *Carassius auratus gibelio* (L. Pysces) kidney, gills and

intestine induced by acute exposure to copper. *Romanian Biotechnological Letters*, *17*(6), 7873-7880.

Uren Webster, T. M., Bury, N., van Aerle, R., & Santos, E. M. (2013). Global transcriptome profiling reveals molecular mechanisms of metal tolerance in a chronically exposed wild population of brown trout. *Environmental science & technology*, *47*(15), 8869-8877.

Urien, N., Cooper, S., Caron, A., Sonnenberg, H., Rozon-Ramilo, L., Campbell, P. G., & Couture, P. (2018a). Subcellular partitioning of metals and metalloids (As, Cd, Cu, Se and Zn) in liver and gonads of wild white suckers (*Catostomus commersonii*) collected downstream from a mining operation. *Aquatic toxicology*, *202*, 105-116.

Urien, N., Jacob, S., Couture, P., & Campbell, P. G. (2018b). Cytosolic distribution of metals (Cd, Cu) and metalloids (As, Se) in livers and gonads of field-collected fish exposed to an environmental contamination gradient: an SEC-ICP-MS analysis. *Environments*, *5*(9), 102.

Uysal, K. (2011). Heavy metal in edible portions (muscle and skin) and other organs (gill, liver and intestine) of selected freshwater fish species. *International Journal of Food Properties*, *14*(2), 280-286.

Valentić, L., Kozel, P., & Pipan, T. (2022). Microplastic pollution in vulnerable karst environments: case study from the Slovenian classical karst region. *Acta Carsologica*, *51*(1), 79-92.

Valentić, L., Pipan, T., & Ravbar, N. (2024). Does Microplastic Pollution in the Epikarst Environment Coincide with Rainfall Flushes and Copepod Population Dynamics?. *Sustainability*, *16*(22), 10123.

Van der Oost, R., Beyer, J., & Vermeulen, N. P. (2003). Fish bioaccumulation and biomarkers in environmental risk assessment: a review. *Environmental toxicology and pharmacology*, *13*(2), 57-149.

Vardić Smrzlić, I., Valić, D., Kapetanović, D., Dragun, Z., Gjurčević, E., Ćetković, H., & Teskeredžić, E. (2013). Molecular characterisation and infection dynamics of *Dentitruncus truttae* from trout (*Salmo trutta* and *Oncorhynchus mykiss*) in Krka River, Croatia. *Veterinary Parasitology*, *197*(3-4), 604-613.

Vesper, D. J., Loop, C. M., & White, W. B. (2001). Contaminant transport in karst aquifers. *Theoretical and Applied Karstology*, *13*(14), 101-111.

Vijver, M. G., Van Gestel, C. A., Lanno, R. P., Van Straalen, N. M., & Peijnenburg, W. J. (2004). Internal metal sequestration and its ecotoxicological relevance: a review. *Environmental science & technology*, *38*(18), 4705-4712.

Vosylienė, M. Z. (2007). Review of the methods for acute and chronic toxicity assessment of single substances, effluents and industrial waters. *Acta Zoologica Lituanica*, *17*(1), 3-15.

Vukosav, P., Mlakar, M., Cukrov, N., Kwokal, Ž., Pižeta, I., Pavlus, N., ... & Omanović, D. (2014). Heavy metal contents in water, sediment and fish in a karst aquatic ecosystem of the Plitvice Lakes National Park (Croatia). *Environmental science and pollution research*, *21*(5), 3826-3839.

Vurnek, M., Brozinčević, A., Matoničkin Kepčija, R., & Frketić, T. (2021). Analyses of long-term trends in water quality data of the Plitvice Lakes National Park. *Fundamental and Applied Limnology*, 155-169.

Wallace, W. G., Lee, B. G., & Luoma, S. N. (2003). Subcellular compartmentalization of Cd and Zn in two bivalves. I. Significance of metal-sensitive fractions (MSF) and biologically detoxified metal (BDM). *Marine Ecology Progress Series*, *249*, 183-197.

Weyers, A., Sokull‐Klüttgen, B., Baraibar‐Fentanes, J., & Vollmer, G. (2000). Acute toxicity data: a comprehensive comparison of results of fish, Daphnia, and algae tests with new substances notified in the European Union. *Environmental toxicology and chemistry*, *19*(7), 1931-1933.

Yao, L., Hui, L., Yang, Z., Chen, X., & Xiao, A. (2020). Freshwater microplastics pollution: detecting and visualizing emerging trends based on Citespace II. *Chemosphere*, *245*, 125627.

Yuan, J., Li, Q., & Zhao, Y. (2022). The research trend on arsenic pollution in freshwater: a bibliometric review. *Environmental Monitoring and Assessment*, *194*(9), 602.

Yue, F. J., Waldron, S., Li, S. L., Wang, Z. J., Zeng, J., Xu, S., ... & Oliver, D. M. (2019). Land use interacts with changes in catchment hydrology to generate chronic nitrate pollution in karst waters and strong seasonality in excess nitrate export. *Science of the Total Environment*, 696, 134062.

Zait, R., Sluser, B., Fighir, D., Plavan, O., & Teodosiu, C. (2022). Priority pollutants monitoring and water quality assessment in the Siret River Basin, Romania. *Water*, 14(1), 129.

Zeng, Y., Song, Z., Song, G., Li, S., Sun, H., Zhang, C., & Li, G. (2025). Oxidative stress and antioxidant biomarker responses in fish exposed to heavy metals: a review. *Environmental Monitoring and Assessment*, *197*(8), 892.

Zhang, Q. L., Dong, Z. X., Luo, Z. W., Zhang, M., Deng, X. Y., Guo, J., ... & Lin, L. B. (2019). The impact of mercury on the genome-wide transcription profile of zebrafish intestine. *Journal of Hazardous Materials*, *389*, 121842-121842.

Zhang, Z., He, L., Li, J., & Wu, Z. B. (2007). Analysis of heavy metals of muscle and intestine tissue in fish-in Banan section of Chongqing from three gorges reservoir, China. *Polish journal of environmental studies*, *16*(6), 949.

Zhang, J., Meng, H., Kong, X., Cheng, X., Ma, T., He, H., ... & Zhang, L. (2021). Combined effects of polyethylene and organic contaminant on zebrafish (*Danio rerio*): Accumulation of 9-Nitroanthracene, biomarkers and intestinal microbiota. *Environmental Pollution*, *277*, 116767.

Žutinić, P., Kulaš, A., Levkov, Z., Šušnjara, M., Orlić, S., Kukić, S., ... & Udovič, M. G. (2020). Ecological status assessment using periphytic diatom communites-case study Krka River. *Macedonian journal of ecology and environment*, 22(1), 29-44.

Appendices

APPENDIX A: Presence of microplastics in the Krka River

1. Materials and methods

The presence of microplastics (MP) in the Krka River system was investigated in river water, industrial wastewater and fish gut content, as an initial step toward understanding MP distribution within the system and their uptake by organisms. Preliminary results were obtained from the analysis of water samples collected at the following sites: the source of the Krka River (KRS), the Orašnica River (TOR), the Krka watercourse influenced by municipal wastewater outlets from the Town of Knin (KRK), industrial wastewater from the screw factory (IWW), and the Butišnica River (TBU), as well as from gut content of *Salmo trutta* sampled at KRK. Sampling sites were described in detail in Šariri et al. (2024), and fish sampling procedures and isolation of acanthocephalans *Dentitruncus truttae* in Šariri et al. (2025).

Representative samples of river water were collected in glass bottles and stored at 4 °C. In the laboratory, each fraction was vacuum-filtered through 45 µm nitrocellulose filters (Merck Millipore, Germany), which were visually inspected for MP presence using a stereomicroscope (PLTL 2400D) equipped with a camera (Olympus SZX10, Japan) at 40× magnification.

A separate industrial wastewater sample (2 L), expected to contain the highest abundance of MP particles, was used for polymer identification by FT-IR microscopy (FT-IR-ATR 8400S, Shimadzu, Japan). This sample was filtered through gold-coated polyester membrane filters (PETG; pore size 5.0 µm; 25 mm diameter; 100/0 nm Au coating) and analyzed by FT-IR microscopy in reflection mode.

Approximately 0.2 g of fish gut content, was subjected to acid digestion using an HNO_3:HF mixture (24:1) at 85 °C for 3.5 h in a total volume of approximately 3 mL. Digestion was performed for gut content. The digested samples were subsequently filtered through gold-coated polyester filters (i3 TrackPor P; pore size 0.8 µm; 47 mm diameter; PET substrate; 100/0 nm Au coating). Filters were examined under a stereomicroscope, followed by polymer identification using FT-IR microscopy in reflection mode. Based on visual

inspection, particles were categorized by shape as filaments, fragments, foams, spheres, or films, according to Yu et al. (2023).

Infrared spectra obtained by FT-IR microscopy were compared with reference spectra from ten Shimadzu spectral libraries, including ATR-Polymer2, UV-Damaged Plastics, Thermal-Damaged Plastics, A_FoodAdditives2, ATR-Inorganic2, ATR-Organic2, T_FoodAdditives2, T-Inorganic2, T-Organic2, and T-Polymer2. A similarity score was calculated for each spectrum and is reported accordingly. Spectral matches with similarity scores >80% were classified as high confidence identifications, while scores between 70% and 80% were classified as medium confidence.

To minimize contamination, samples were covered whenever possible during field collection, transport, and laboratory analysis. All analytical procedures were conducted under laminar flow cabinets. Cotton laboratory coats were worn, and only clean glass laboratory equipment was used throughout the analysis.

2. Results and discussion

2.1. Visual inspection

Particles were visually observed in all water and biological samples, with filaments representing the predominant shape. Blue particles were most frequently detected, though black, yellow, pink, transparent, white, green, and red particles were also observed. Representative examples of particles identified under a stereomicroscope in water samples and fish gut contents are shown in Figures 1 and 2, respectively. This distribution of particle colors and shapes is consistent with previous studies reporting microplastics in European freshwater environments, where filaments typically dominate, followed by fragments (Matjašič et al. 2023, Prata et al. 2021, Scherer et al. 2020). Similar patterns have been reported in the gut contents of freshwater fish (Collard et al. 2018, Garcés-Ordóñez et al. 2020, Horton et al. 2018, Patidar et al. 2024).

Microplastic (MP) fragments and filaments are generally generated through fragmentation, abrasion, and weathering of larger plastic items (Mani et al. 2015). Synthetic filaments, often originating from textile washing, (polyester, acrylic, and polyamide (PA)), are abundant in municipal and industrial wastewater and may reach concentrations exceeding 100 filaments per liter of effluent (Browne 2015). Consequently, synthetic textiles from clothing, shopping

bags, and packaging materials are likely sources of the filaments observed in this study (Gao et al., 2024).

However, visual identification and classification of suspected MPs are inherently subjective and depend on the observer's experience and the magnification of the microscope used. This approach may underestimate smaller or transparent particles and may result in the misclassification of natural organic compounds as MPs (Prata et al. 2019, Shruti et al. 2022). Therefore, chemical characterization of visually identified particles was conducted using FT-IR microscopy to confirm polymer composition.

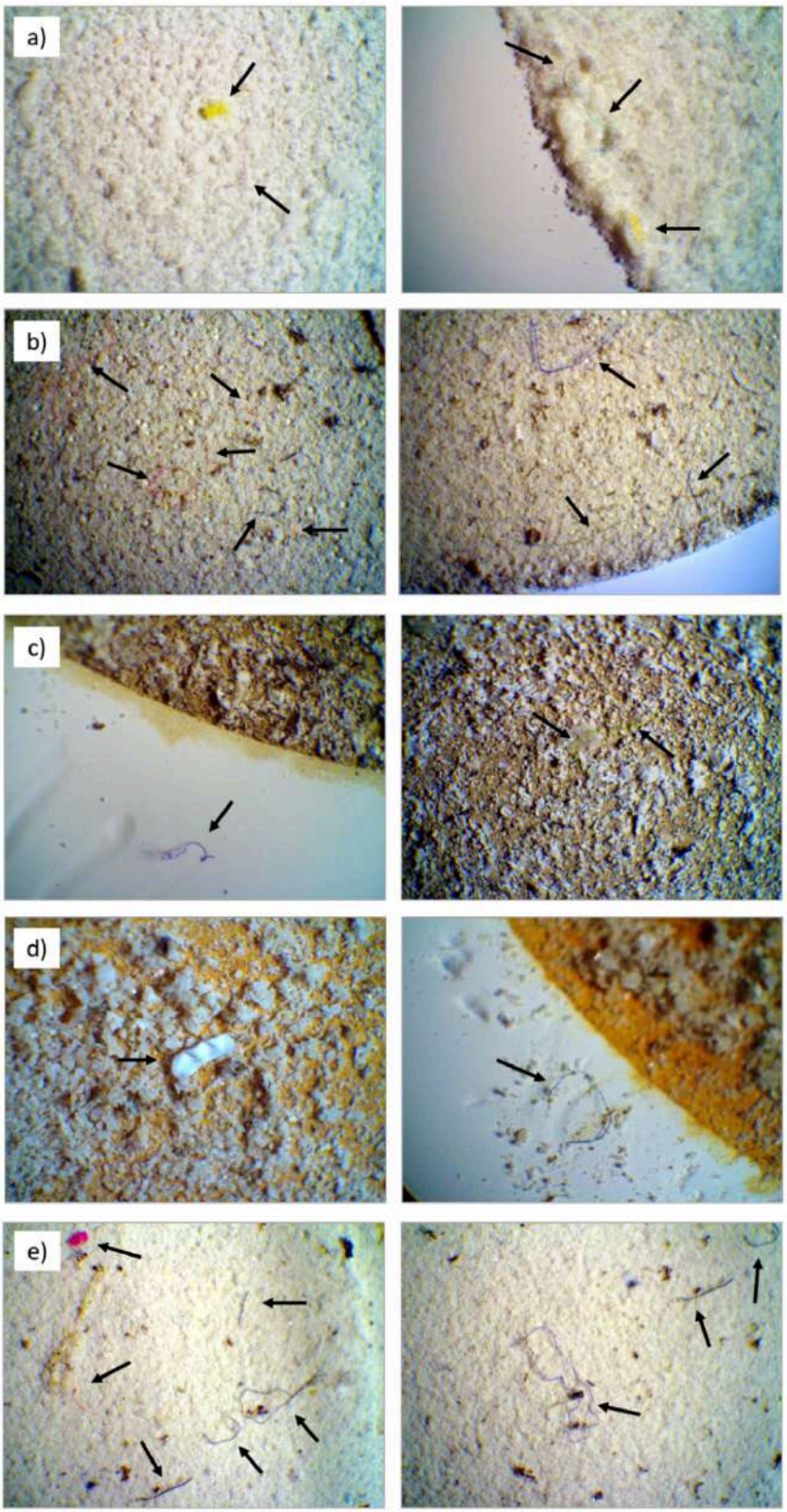

Figure 1. Particles filtered from water samples collected at the Krka River. Samples were obtained from sites a) KRS, b) TOR, c) KRK, d) IWW, and e) TBU, and examined under a stereomicroscope. Black arrows indicate particles identified as potential microplastics.

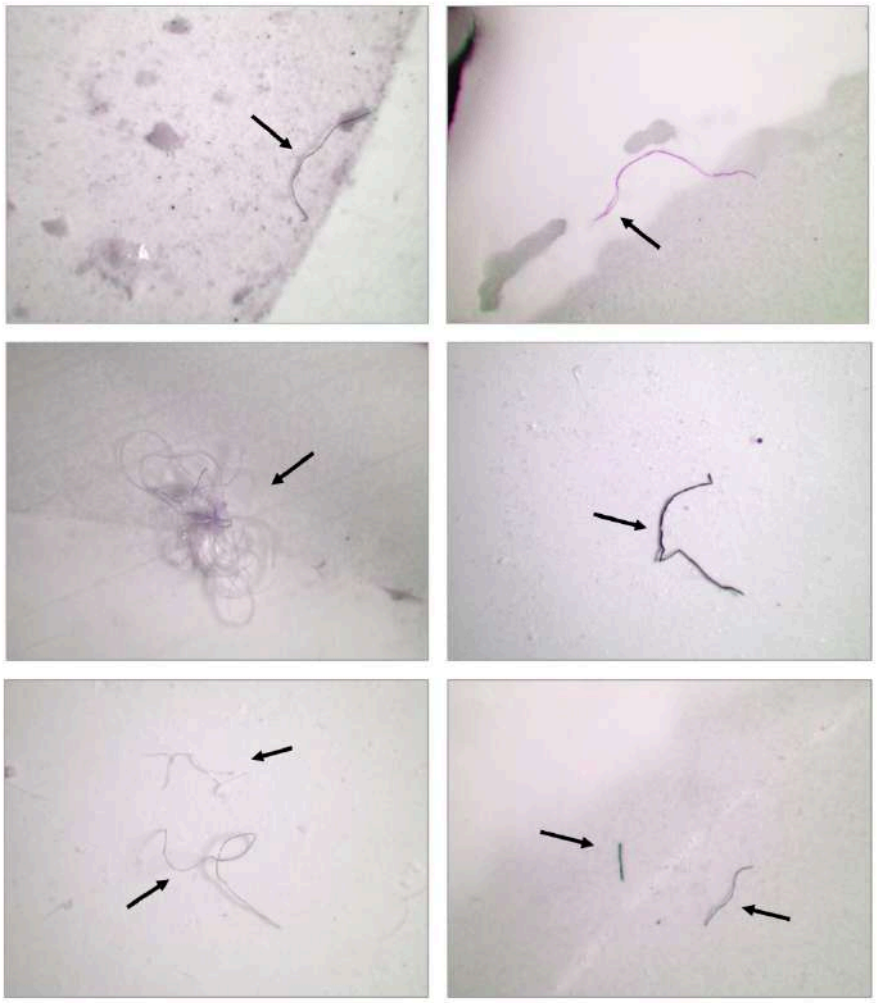

Figure 2. Particles filtered from acid digested gut content of *Salmo trutta*. Samples were collected from the Krka River near municipal outlet of the Town of Knin and examined under a stereomicroscope. Black arrows indicate particles identified as potential microplastics.

2.2. Polymer characterization

2.2.1. Industrial wastewater

FT-IR microscopy confirmed the presence of MP in industrial wastewater, specifically identifying polystyrene (PS) and thermally damaged PA (nylon) among the analyzed particles (Fig. 3). While polystyrene spherules are commonly associated with industrial sources (Mani et al. 2015), the PS particles detected in the present study are most likely secondary microplastics, originating from the fragmentation of larger plastic items. Following polymer

identification, the majority of visually classified filaments were determined to be of natural origin, predominantly cellulose. This discrepancy between visual classification and chemical composition is well documented and reflects a common limitation of stereomicroscopic identification, particularly for fibrous particles (Prata et al. 2021).

The observed polymer composition and particle morphology aligne with previous studies of industrial wastewater, where filaments tipically predominate, followed by fragments and films, and PA, cellulose acetate, and PS were reported as the dominant polymers (Haque et al. 2022).

In freshwater environments, polyethylene (PE), polypropylene (PP), and polystyrene (PS) are most frequently reported as the predominant polymers, likely reflecting their extensive production, widespread use, and relatively low densities (Cera et al. 2020, Gao et al. 2024, Mani et al. 2015, Scherer et al. 2020). Polymer density dictates vertical distribution within the water column; low-density polymers exhibit higher buoyancy and mobility, while denser particles are more prone to sedimentationgenerally exhibit higher buoyancy, facilitating their transport within the water column, whereas denser particles are comparatively less mobile and more prone to sedimentation (Gao et al. 2024). Polyethylene (PE) is extensively used in packaging materials for food and pharmaceutical products, as well as in agricultural films, while polypropylene (PP) is widely applied in single-use items such as disposable containers, cutlery, and packaging, and is also common in textiles and medical products. Polystyrene (PS), in both its rigid and foam forms, is extensively used in consumer products, household items, as well as in protective packaging, insulation, and molded industrial components (Dybka-Stępień et al. 2021, Kowalczyk et al. 2025). Collectively, these three polymer types accounted for more than 56% of the annual plastic demand in the European Union in 2019, highlighting their relevance as major environmental pollutants (Gao et al. 2024). Polyamide (PA), commonly known as nylon, is extensively used in clothing and industrial textiles, as well as in packaging materials and high-performance engineering thermoplastic for machine components, gears, and structural parts due to its strength and abrasion resistance (Kohutiar et al. 2025).

The absence of PE and PP in industrial wastewater samples likely reflects the specific industrial profile of the screw factory, which does not focus on plastic manufacturing or processing. The detection of PA and PS in industrial wastewater near the screw

manufacturing facility aligns with their common uses in industrial and manufacturing contexts.

Table 1. Particle characteristics and polymer types identified by FT-IR microscopy in industrial wastewater sampled near the Krka River.

particle type	polymer	polymer origin	polymer library name	library	score	confidence
filament	cellulose	natural	T_Microcrystalline Cellulose_101-4	T_FoodAdditives2	79.8%	moderate
fragment	polystyrene	synthetic	Polystyrene(PS)	T-Polymer2	82.8%	high
film	polyamide	synthetic	PA6-6(04)_350-2h, Nylon 6-6, 350 degrees Celsius 2hours heated	Thermal-Damaged Plastics	74.8%	moderate

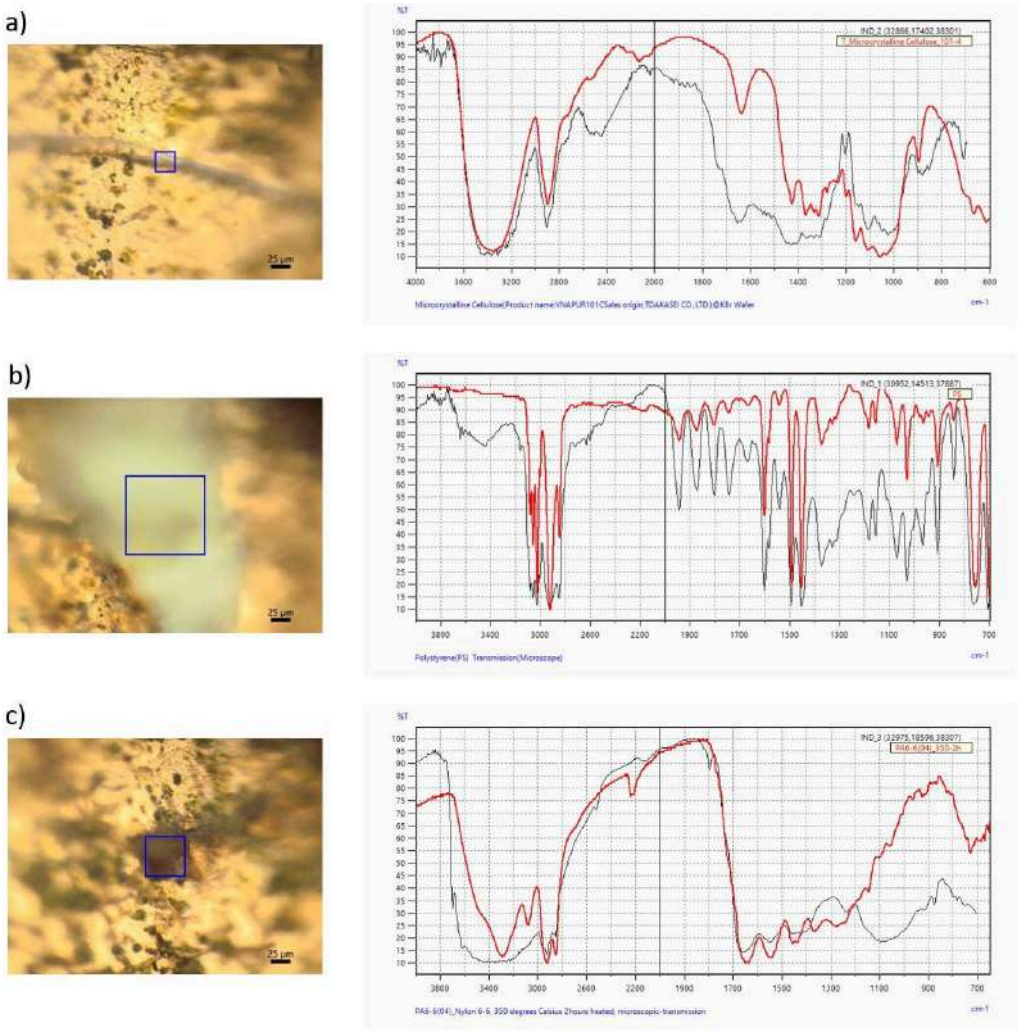

Figure 3. Representative particles isolated from industrial wastewater near the Krka River. Particles were identified by FT-IR microscopy as a) cellulose, b) polystyrene, and c) polyamide. For each particle, the IR microscope image is shown on the right, and the corresponding FT-IR spectrum of the sample (black line) overlaid with the reference library spectrum (red line) is shown on the left.

2.2.2. Fish gut content

FT-IR analysis of fish gut content revealed that most filaments were natural fibers, predominantly cellulose and cotton (Fig. 4). Given that trout feed primarily on small fish and invertebrates (Mrakovčić et al. 2006), these filaments are most likely the result of contamination, similar to what was observed in intestinal tissue. Comparable findings have been reported in other studies. In *Squalius cephalus*, 74% of analyzed particles were composed of natural organic polymers such as cellulose or could not be identified (Collard et

al. 2018), and in *Oreochromis niloticus*, 53% of particles corresponded to cellophane or cellulose (Garcia et al. 2021).

Synthetic polymers were also detected in the gut content. The dominant types were PA, EVA, and styrene-ethylene-butylene, while ethylene-acrylic acid (EAA) and PE were present in smaller amounts. Comparisons with other studies on fish gut content indicate similar patterns. In wild *Squalius cephalus*, PET, PP, polyacrylonitrile (PAN), and polyethylene-vinyl acetate (PEVA) were identified (Collard et al. 2018), and in *Rutilus rutilus*, PE, PP, and PET were most abundant (Horton et al. 2018). In various fish species from the Ebro River, FT-IR analysis revealed predominantly cellulose filaments (64%), followed by polyester, PE, PET, and PP. Other polymers, including PA, polyisoprene (PI), PS, methacrylates, and silicones, were also detected using complementary methods, with PE being the most frequently found and at the highest concentrations (Garcia-Torné et al., 2022).

The detection of styrene-ethylene-butylene may reflect the presence of styrene-butadiene rubber, a major contributor to microplastic pollution from tire abrasion in terrestrial environments. These particles can enter rivers through surface runoff and atmospheric deposition (Gao et al. 2024). Due to the shared styrene component, the FT-IR spectra of these polymers may partially overlap, particularly in weathered environmental samples, which could reduce the confidence of identification. Overall, the presence of synthetic polymers in gut content indicates exposure of fish to riverine microplastics, likely influenced by by the proximity to road networks and municipal wastewater discharge.

Table 3. Particle characteristics and polymer types identified by FT-IR microscopy in gut content of *Salmo trutta* from the Krka River

particle type	polymer	polymer origin	polymer library name	library	score	confidence
filament	cellulose	natural	T_Microcrystalline Cellulose_102-4	T_FoodAdditives2	72.5%	moderate
filament	cellulose	natural	T_Microcrystalline Cellulose_102-4	T_FoodAdditives2	83.0%	high
filament	cellulose	natural	T_Microcrystalline Cellulose_101-4	T_FoodAdditives2	83.5%	high

filament	cellulose	natural	T_Microcrystalline Cellulose_101-4	T_FoodAdditives2	86.9%	high
filament	cellulose	natural	T_Microfibrillated Cellulose_200L-4	T_FoodAdditives2	83.2%	high
filament	cotton	natural	Cotton	T-Polymer2	72.0%	moderate
fragment	polyamide	synthetic	T_Polyamide_Resin	T-Polymer2	81.2%	high
fragment	polyamide	synthetic	T_Polyamide_Resin	T-Polymer2	78.4%	moderate
fragment	polyamide	synthetic	T_Polyamide_Resin	T-Polymer2	79.0%	moderate
foam	styrene-ethylene-butylene	synthetic	Styrene-Ethylene-Butylene	T-Polymer2	77.3%	moderate
foam	styrene-ethylene-butylene	synthetic	Styrene-Ethylene-Butylene	T-Polymer3	76.5%	moderate
fragment	ethylene acrylic acid	synthetic	Ethylene Acrylic Acid(EAA)	T-Polymer2	75.9%	moderate
film	polyethylene	synthetic	Polyethylene (PE)	ATR-Polymer2	77.2%	moderate
fragment	ethylene-vinyl acetate	synthetic	Ethylene/Vinyl Acetate(EVA) Copolymer(Vinyl Acetate content 18%)	ATR-Polymer2	78.7%	moderate
fragment	ethylene-vinyl acetate	synthetic	Ethylene/Vinyl Acetate(EVA) Copolymer(Vinyl Acetate content 14%)	ATR-Polymer2	79.9%	moderate
fragment	ethylene-vinyl acetate	synthetic	EVA_20h, Ethylene Vinyl Acetate, UV Irradiation Time:20 Hours	UV-Damaged Plastics	83.0%	high

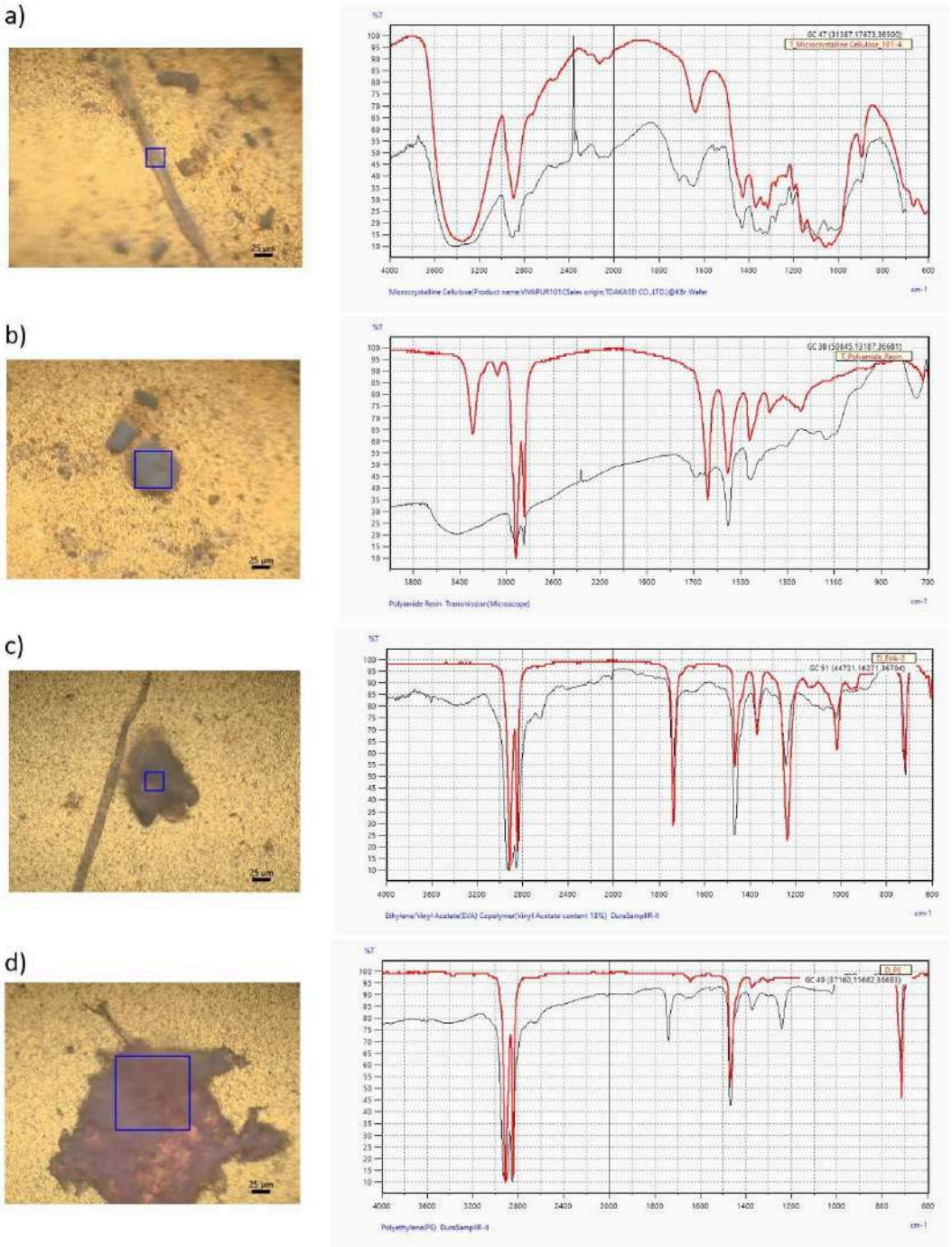

Figure 4. Representative particles isolated from gut content of *Salmo trutta* from the Krka River. Particles were identified by FT-IR microscopy as a) cellulose, b) polyamide, c) ethylene-vinyl acetate and d) polyethylene. For each particle, the IR microscope image is shown on the right, and the corresponding FT-IR spectrum of the sample (black line) overlaid with the reference library spectrum (red line) is shown on the left.

3. Conclusions

This study provides preliminary evidence of MP presence in the Krka River ecosystem, specifically in river water and the gut content of *S. trutta*. Microplastics were detected across all investigated environmental and biological compartments, confirming their widespread occurrence. Polyamide was the only polymer consistently detected both in water and fish gut content. Other polymers were compartment-specific, reflecting the diversity of MP types and suggesting multiple, diffuse sources rather than a single dominant input.

The study area is influenced by urban activities in the Town of Knin, including municipal wastewater discharge of the Town of Knin and industrial effluents from a screw factory, resulting in numerous potential MP sources. Consequently, these preliminary findings do not allow for the identification of specific emission sources or clear links between fish diet and MPs in fish gut content. Given that sediments serve as major sinks for MPs, future investigations should include sediment analysis to better constrain MP distribution and trophic interactions within the ecosystem.

The interpretation of MP occurrence in environmental and biological samples remains challenging due to methodological limitations. The lack of standardized protocols for sampling, size classification, and analytical procedures makes it difficult to distinguish true environmental pollution from artifacts introduced during sample processing (Gao et al. 2024). Despite strict laboratory precautions, background contamination, particularly from airborne cellulose fibers, was detected, consistent with previous reports (Slootmaekers et al. 2019). The extended duration of FT-IR microscopy (approximately 4-6 hours per sample), during which samples could not be covered, further increased exposure to airborne contaminants, underscoring the importance of incorporating both negative (procedural blanks) and positive controls to better assess background contamination and particle loss during sample preparation (Gao et al. 2024).

In summary, these findings highlight the need for methodologically robust, large-scale studies to quantify MP loads and identify key sinks within the Krka River system. Such efforts are essential for improving our understanding of MP dynamics and potential ecological risks in vulnerable karst freshwater ecosystems.

4. Literature

Browne, M. A. (2015). Sources and pathways of microplastics to habitats. *Marine anthropogenic litter*, 229-244.

Cera, A., Cesarini, G., & Scalici, M. (2020). Microplastics in freshwater: what is the news from the world?. *Diversity*, *12*(7), 276.

Collard, F., Gasperi, J., Gilbert, B., Eppe, G., Azimi, S., Rocher, V., & Tassin, B. (2018). Anthropogenic particles in the stomach contents and liver of the freshwater fish *Squalius cephalus*. *Science of the total environment*, *643*, 1257-1264.

Dybka-Stępień, K., Antolak, H., Kmiotek, M., Piechota, D., & Koziróg, A. (2021). Disposable food packaging and serving materials—Trends and biodegradability. *Polymers*, 13(20), 3606.

Gao, S., Orlowski, N., Bopf, F. K., & Breuer, L. (2024). A review on microplastics in major European rivers. *Wiley Interdisciplinary Reviews: Water*, *11*(3), e1713.

Garcés-Ordóñez, O., Mejía-Esquivia, K. A., Sierra-Labastidas, T., Patiño, A., Blandón, L. M., & Díaz, L. F. E. (2020). Prevalence of microplastic contamination in the digestive tract of fishes from mangrove ecosystem in Cispata, Colombian Caribbean. *Marine pollution bulletin*, *154*, 111085.

Garcia, A. G., Suárez, D. C., Li, J., & Rotchell, J. M. (2021). A comparison of microplastic contamination in freshwater fish from natural and farmed sources. *Environmental Science and Pollution Research*, 28(12), 14488-14497.

Garcia-Torné, M., Abad, E., Almeida, D., Llorca, M., & Farré, M. (2022). Assessment of micro-and nanoplastic composition (polymers and additives) in the gastrointestinal tracts of ebro river fishes. *Molecules*, *28*(1), 239.

Haque, M. M., Nupur, F. Y., Parvin, F., & Tareq, S. M. (2022). Occurrence and characteristics of microplastic in different types of industrial wastewater and sludge: A potential threat of emerging pollutants to the freshwater of Bangladesh. *Journal of Hazardous Materials Advances*, *8*, 100166.

Horton, A. A., Jürgens, M. D., Lahive, E., van Bodegom, P. M., & Vijver, M. G. (2018). The influence of exposure and physiology on microplastic ingestion by the freshwater fish *Rutilus rutilus* (roach) in the River Thames, UK. *Environmental Pollution*, *236*, 188-194.

Kohutiar, M., Kakošová, L., Krbata, M., Janík, R., Fekiač, J. J., Breznická, A., ... & Timárová, Ľ. (2025). Comprehensive review: technological approaches, properties, and applications of pure and reinforced polyamide 6 (PA6) and polyamide 12 (PA12) composite materials. *Polymers*, *17*(4), 442.

Kowalczyk, P., Kadac-Czapska, K., & Grembecka, M. (2025). Polyethylene Packaging as a Source of Microplastics: Current Knowledge and Future Directions on Food Contamination. *Foods*, *14*(14), 2408.

Mani, T., Hauk, A., Walter, U., & Burkhardt-Holm, P. (2015). Microplastics profile along the Rhine River. *Scientific reports*, *5*(1), 17988.

Matjašič, T., Mori, N., Hostnik, I., Bajt, O., & Viršek, M. K. (2023). Microplastic pollution in small rivers along rural–urban gradients: Variations across catchments and between water column and sediments. *Science of the total environment*, *858*, 160043

Mrakovčić, M., Brigić, A., Buj, I., Ćaleta, M., Mustafić, P., Zanella, D. (2006) Crvena knjiga slatkovodnih riba Hrvatske. Ministarstvo kulture, Državni zavod za zaštitu prirode, Republika Hrvatska

Patidar, K., Alluhayb, A. H., Younis, A. M., Dumka, U. C., & Ambade, B. (2024). Investigation of microplastic contamination in the gastrointestinal tract of fish: A comparative study of various freshwater species. *Physics and Chemistry of the Earth, Parts A/B/C*, *136*, 103760.

Prata, J. C., Da Costa, J. P., Duarte, A. C., & Rocha-Santos, T. (2019). Methods for sampling and detection of microplastics in water and sediment: A critical review. *Trends in Analytical Chemistry*, 110, 150-159.

Prata, J. C., Godoy, V., da Costa, J. P., Calero, M., Martín-Lara, M. A., Duarte, A. C., & Rocha-Santos, T. (2021). Microplastics and fibers from three areas under different anthropogenic pressures in Douro river. *Science of the Total Environment*, *776*, 145999

Scherer, C., Weber, A., Stock, F., Vurusic, S., Egerci, H., Kochleus, C., ... & Reifferscheid, G. (2020). Comparative assessment of microplastics in water and sediment of a large European river. *Science of the Total Environment*, *738*, 139866.

Shruti, V. C., Pérez-Guevara, F., Roy, P. D., & Kutralam-Muniasamy, G. (2022). Analyzing microplastics with Nile Red: Emerging trends, challenges, and prospects. *Journal of hazardous materials*, 423, 127171.

Slootmaekers, B., Carteny, C. C., Belpaire, C., Saverwyns, S., Fremout, W., Blust, R., & Bervoets, L. (2019). Microplastic contamination in gudgeons (*Gobio gobio*) from Flemish rivers (Belgium). *Environmental Pollution*, *244*, 675-684.

Šariri, S., Valić, D., Kralj, T., Cvetković, Ž., Mijošek, T., Redžović, Z., ... & Marijić, V. F. (2024). Long-term and seasonal trends of water parameters in the karst riverine catchment and general literature overview based on CiteSpace. *Environmental science and pollution research*, *31*(3), 3887-3901.

Šariri, S., Vardić Smrzlić, I., Mijošek Pavin, T., & Filipović Marijić, V. (2025). First insight into metal binding proteins from the de novo transcriptome of acanthocephalan parasite *Dentitruncus truttae*. *Scientific reports*, 15(1), 26152.

Yu, J. T., Diamond, M. L., & Helm, P. A. (2023). A fit‐for‐purpose categorization scheme for microplastic morphologies. *Integrated Environmental Assessment and Management*, 19(2), 422-435.

APPENDIX B: Distribution of metals among subcellular fractions of the fish intestine

1. Materials and methods

1.1. Fish sampling and sample preparation

Fish were collected from the upper part of the Krka River at three sites differing in metal pollution: near the river source, downstream of the industrial and municipal discharges near the town of Knin, and within the Krka National Park. The sampling area, site characteristics, and collection procedures have been described in detail by Šariri et al. (2025), while metal accumulation in the fish intestine and their intestinal parasites was reported by Mijošek et al. (2024).

Four specimens were selected for the analyses at each site. To examine whether and how subcellular metal partitioning changes with increasing total intestinal metal concentrations, fish from all three sites were analyzed together in order to have a broader gradient of total metal burdens.

The posterior intestine was dissected on ice, cleared of external fat, and carefully opened by a longitudinal incision along the intestinal wall. After removing the gut content and intestinal parasites, the intestinal tissue was weighed and immediately frozen in liquid nitrogen, and subsequently all samples were stored at −80 °C until further analysis.

1.2. Subcellular partitioning procedure

Intestinal tissue from each individual was homogenized in triplicate (approximately 0.2 g per replicate) in a homogenization buffer containing 25 mM Tris-HCl/base, 0.5 mM phenylmethylsulfonyl fluoride (PMSF) (Sigma-Aldrich, USA), and 0.006 mM leupeptin (Sigma-Aldrich, USA) at pH 7.4 (on ice), using a tissue-to-buffer ratio of 1:10 (g:mL). Homogenization was performed using a combination of an Ultra-Turrax T25 homogenizer (IKA, Germany) and a Potter–Elvehjem glass homogenizer (Glas-Col, USA). Both instruments were thoroughly rinsed between specimens to prevent cross-contamination.

Subcellular fractions were separated by differential centrifugation. Method was adapted from protocols previously described for fish liver by Giguere et al. (2006), Campbell et al. (2008), Kamunde and MacPhail (2011), Rosabal et al. (2015), Urien et al. (2018) and Khadra et al. (2019), and for fish intestine by Oyoo-Okoth et al. (2012).

Homogenates were first centrifuged at 1 500 × g for 15 min at 4 °C to obtain pellet P1 and supernatant S1. Fraction P1 was resuspended in 500 µL of Tris buffer and temporarily stored at −80 °C, while S1 was further centrifuged at 25 000 × g for 30 min at 4 °C, yielding pellet P2 (mitochondria) and supernatant S2. Further ultracentrifugation of S2 at 100 000 × g for 1 h at 4 °C resulted in separation of pellet P3 (microsomes/lysosomes) and supernatant S3 (cytosol).

The cytosolic fraction S3 was heat-treated to separate heat-denaturable proteins (HDP), such as cytosolic enzymes, from heat-stable proteins (HSP), such as metallothioneins and similar peptides. This was achieved by heating at 85 °C for 10 min, cooling on ice for 30 min, and

centrifuging at 50 000 × g for 20 min at 4 °C, after which HDP pelleted (P4) and HSP remained in the supernatant (S4).

Pellets P1 from the initial centrifugation were thawed, heated at 100 °C for 2 min, mixed with 500 µL 1 M NaOH, incubated at 65 °C for 60 min, and centrifuged at 10 000 × g for 10 min at 20 °C to obtain pellet P5, containing the NaOH-resistant granules, and supernatant S5, representing the cellular debris/nuclei fraction (including cell nuclei, cell membranes, intact cells, and connective tissue).

Ultracentrifugation (100 000 × g) was performed using a Sorvall WX+ Ultracentrifuge (Thermo Scientific), while all other centrifugation steps were carried out with an Avanti J-E centrifuge (Beckman Coulter, USA). All procedures were conducted on ice or in pre-cooled centrifuges to maintain sample integrity.

Based on their toxicological relevance, mitochondria, microsomes/lysosomes, and HDP are commonly considered the metal-sensitive fractions (MSF), whereas metals bound to HSP and granules represent biologically detoxified metals (BDM) (Wallace et al. 2003). The cellular debris/nuclei fraction is ambiguous, as it is unclear to what extent metals in this fraction are associated with nuclei (metal-sensitive) or with cellular debris (not considered metal-sensitive). Consequently, this fraction is typically excluded from MSF/BDM classification, although that can lead to neglect the metals bound to cell nuclei, which can be biologically relevant (Rosabal et al. 2015). It is common to use this fraction as a control for homogenization efficiency, since a low and consistent metal proportion across individuals indicates effective homogenization (Desjardins et al. 2022, Rosabal et al. 2015, Urien et al. 2018).

1.3. Subcellular Sample digestion and metal analysis

Each of the six subcellular fractions was treated with concentrated nitric acid (HNO_3) (Rotipuran® Supra 69%, Carl Roth, Germany) and left to pre-digest overnight (0.5 mL for pellets and 1 mL for supernatants). Samples were then digested in a dry oven at 85 °C for 3.5 h. Prior to analysis, digests were diluted with Milli-Q water (1:10) to achieve a final acid concentration below 10%. To ensure analytical accuracy and precision, blanks and certified reference material were processed in parallel with the samples. Pure HNO_3 served as a blank

for pellets, whereas a 1:1 mixture of HNO_3 and homogenization buffer was used for supernatants.

Elemental concentrations were determined using inductively coupled plasma mass spectrometry (ICP–MS) (Agilent 7900, Agilent Technologies, USA) equipped with an autosampler. A multi-element internal standard solution containing 50 µg L^{-1} each of Sc, Ge, Y, In, and Tb in 5% HNO_3 (CPA Chem, Bulgaria) was used to correct for instrumental drift and matrix effects. Calibration standards were prepared from certified multi-element stock solutions (CPA Chem, Bulgaria).

Recovery rates (mean ± SD, n = 6) from the ICP Water Quality Standard 5 (CPA Chem, Bulgaria) were as follows: As (104.6 ± 4.9%), Cu (95.5 ± 3.6%), Fe (99.2 ± 5.5%), Mn (101.8 ± 4.4%), Se (101.9 ± 7.1%), Sr (107.2 ± 11.8%), Tl (109.8 ± 13.7%), and Zn (104.4 ± 6.5%). The certified reference material ERM®-BB422 (fish muscle, the Institute for Reference Materials and Measurements of the European Commision's Joint Research Centre) was digested and analyzed alongside the samples. Mean recoveries (± SD, n = 2) were within certified ranges: As (114 ± 4%), Cd (103 ± 2%), Cu (98 ± 15%), Fe (97 ± 26%), Mn (107 ± 22%), Se (139 ± 10%), and Zn (90 ± 5%). Limits of detection (LOD), defined as three standard deviations of 15 blank measurements, were (ng g^{-1}): for pellets As 0.064, Cu 1.842, Fe 10.230, Mn 0.680, Se 0.015, Tl 0.015, Zn 10.878, and for supernatants As 0.049, Cu 3.132, Fe 31.855, Mn 3.908, Se 0.586, Tl 0.011, Zn 105.077. Metal concentrations in all subcellular fractions were expressed as the total metal burden (µg or ng, depending on the element) per gram of intestinal tissue wet weight (w.w.) used for subcellular fractionation.

1.4. Calculations and statistical analysis

The relative contribution of each subcellular fraction was calculated as the percentage of the metal burden in that fraction relative to the sum of metal burden across all fractions. This value was determined for each sample, and mean values were used to construct pie charts showing the average distribution of metals among subcellular fractions in the intestine.

The total concentration of each element in the intestinal tissue was calculated as the sum of concentrations measured in all six fractions. When concentrations in a fraction were below the limit of detection (LOD), half of the LOD value was used (Antweiler 2015).

All numerical results are presented as means ± standard deviations (SD). Statistical analyses and graphical visualizations were performed using SigmaPlot 11.0 (Systat Software, USA),

with a significance threshold of $\alpha = 0.05$. Differences in total intestinal metal concentrations between sexes were tested using the Mann–Whitney rank-sum test, and relationships with fish length were examined using Pearson's product–moment correlation.

Relationships between total intestinal metal concentrations and either (i) metal concentrations or (ii) relative contributions (%) in each subcellular fraction were first explored using bivariate scatterplots and Spearman correlation tests. When bivariate plots suggested potential linear relationships and assumptions of normality (Shapiro–Wilk test) and homoscedasticity were met, linear regression analyses were conducted. Proportional data were arcsine square-root transformed prior to statistical testing to meet the assumptions of linear regression. However, figures and regression lines are presented on the original percentage scale for clarity. In cases where a single data point showed strong leverage on the regression, it was excluded and the model was re-run. Points excluded from regression models were identified in the figures.

We acknowledge that subcellular metal distribution may vary between tissues, but, to our knowledge, no studies have investigated this in fish intestine to date. Existing research has focused primarily on the liver, and to a lesser extent on gonads, gills, and whole bodies (Barst et al. 2016, Eyckmans et al. 2012, Goto and Wallace 2010, Khadra et al. 2019, Lapointe and Couture 2009, Rolland et al. 2025, Urien et al. 2018). As the subcellular distribution of elements may depend on their total concentrations (Desjardins et al. 2022, Rosabal et al. 2015, Urien et al. 2018), we aimed to contextualize our findings by considering total metal concentration differences across tissues. Such differences were expected due to species-specific traits, environmental conditions, and physiological characteristics of each tissue. To enable comparison with published data, often reported in different units and standardized to tissue dry weight, we converted values to wet weight equivalents. Based on the literature, average moisture content across fish tissues was estimated at 70% (Khoddami et al. 2012, Bechtel and Oliveira 2006, Elliott 1976, Payuta and Flerova 2019, Reda and Ayu 2016, González-Félix et al. 2017). Conversions were performed using the formula: ng/g WW = nmol/g DW × molar mass (g/mol) × 0.30**.**

2. Results and discussion

2.1. Total metal(loid) concentrations

The mean (± SD) total intestinal metal(loid) concentrations across all analyzed fish specimens are shown in Table 1. The ratio of maximum to minimum concentrations decreased in the order: Sr > As > Se > Zn > Cu > Mn, Tl > Fe. Due to the strong positive correlation between fish length and body mass ($r = 0.968$, $p < 10^{-6}$), only length was used to assess the relationship between total intestinal metal(loid) concentrations and fish size. Significantly positive correlations were found for Cu ($r = 0.688$, $p < 0.05$) and As ($r = 0.778$, $p < 0.01$), and a significant negative correlation for Tl ($r = -0.618$, $p < 0.05$) and fish length. Since no significant differences in fish length and metal(loid) concentrations were observed between sexes, data from males (n = 4) and females (n = 8) were pooled for analysis.

Table 1. Summary statistics for fish length, mass, and total metal(loid) concentrations in intestinal tissue of *Salmo trutta* from the Krka River

	length (cm)	mass (g)	Zn (µg g^{-1})	Fe (µg g^{-1})	Cu (µg g^{-1})	Se (ng g^{-1})	Mn (ng g^{-1})	Sr (ng g^{-1})	As (ng g^{-1})	Tl (ng g^{-1})
mean ± SD	27.1 ± 3.8	209 ± 100	213 ± 127	9.8 ± 1.9	0.77 ± 0.40	971 ± 589	414 ± 219	334 ± 373	63.0 ± 41.2	21.7 ± 10.0
range	22–35	103–431	77–517	6.8–12.5	0.38–1.93	228–2215	245–1021	77–1174	14.4–165.0	10.7–41.6
max/min	2	4	7	2	5	10	4	15	11	4

Total intestinal metal(loid) concentrations in selected fish individuals were consistent with previous measurements in *Salmo trutta* from the same 2021 sampling campaign (Mijošek et al. 2024). As expected, the highest levels were recorded for the essential elements Zn, Fe, and Cu, due to their key physiological functions (Brucka-Jastrzêbska et al. 2009). The Zn > Fe > Cu pattern has also been reported in intestinal tissue of *S. trutta* (Mijošek et al. 2024), prussian carp (*Carassius gibelio*) (Mijošek et al. 2021), and European chub (*Squalius cephalus*) (Filipović Marijić and Raspor 2012). Total Zn and Cu levels were comparable to those found in intestine of *S. trutta* from the unpolluted Fowey River, UK (Paris et al. 2025).

In contrast, intestinal metal levels in *S. trutta* from the Çatak River, Turkey (Cilingir Yeltekin & Saglamer 2019) and Ermolinus Stream, Sardinia (Alberto et al. 2021), differed notably, most likely due to natural lithological and geochemical variation. While Fe, Cu, Mn, and As were lower in the Krka River specimens, Zn concentrations were higher. This was expected given the generally low geogenic metal burden of the Dinaric karst, compared to elevated background levels in volcanic and hydrothermally active regions of Turkey and Italy (Erenturk et al. 2014, Naitza et al. 2024). Overall, no abnormal or excessive bioaccumulation was observed, supporting the representativeness of these results for wild *S. trutta* from relatively unpolluted karst rivers, with Zn as the only potential exception.

2.2. Metal subcellular partitioning

To capture complementary aspects of subcellular partitioning, we plotted both absolute concentrations and relative contributions of metals in each fraction against the total intestinal metal concentrations. Concentration-based plots describe how much metal each fraction accumulates with increasing exposure, whereas percentage-based plots reveal shifts in the relative importance of fractions in handling the total metal burden along the bioaccumulation gradient.

The relative contribution from the debris/nuclei fraction to the total metal burden can be used as an indication of the efficacy of the homogenization procedure. In the present study, the contribution from the debris/nuclei fraction was reasonably low for most metals (≤ 30% for Fe, Mn, Sr, As and Tl) according to Rosabal et al. (2015) (Fig. 1).

To provide insights into the subcellular partitioning of metal(liod)s, their relative contributions and concentrations were compared among the subcellular fractions (e.g., mitochondria, granules) and between both toxicological compartments (MSF and BDM). Since we did not include the cellular debris/nuclei fraction in niether MSF nor BDM, as explained in section 1.2., the total sum of metal contributions of both compartments was not necessarily up to 100%. Only when the relative contribution of the debris/nuclei fraction varied along the metal bioaccumulation gradient, it was included in the analysis (Rosabal et al. 2015).

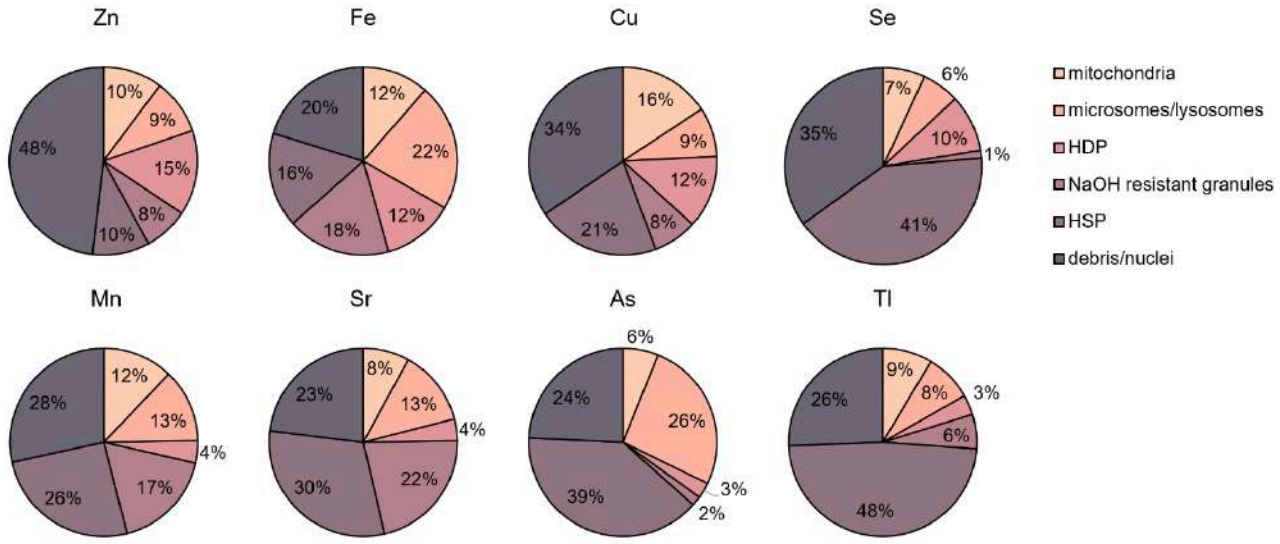

Figure 1. Average relative contributions of each subcellular fraction to the total intestinal concentration of selected metal(loid)s in *Salmo trutta* from the Krka River (n = 12).

2.2.1. Essential metals

Zinc

Total intestinal Zn levels in our study were high compared to other studies on Zn subcellular distribution in fish. They were approximately 6 times higher than in liver and up to 22 times higher than in male gonads of white sucker (*Catostomus commersonii*) from the unpolluted lake in Saskatchewan, Canada (Urien et al. 2018). They also exceeded levels reported in the liver of yellow perch (*Perca flavescens*) (Giguère et al. 2006) and were about 4 times higher than whole-body concentrations in mummichogs (*Fundulus heteroclitus*) from metal-polluted salt marshes (Goto and Wallace 2010). This difference might be tissue-specific and likely reflects the intestine's key role in Zn uptake and regulation (Ma and Wang 2024), as Cilingir Yeltekin and Saglamer (2019) reported the highest Zn accumulation in intestinal tissue among eight organs in *S. trutta macrostigma* and *Oncorhynchus mykiss*. In fact, intestine of *Rastrineobola argentea* from unpolluted sites at the Lake Victoria contained around 3 times higher Zn concentrations than those measured in the present study (Oyoo-Okoth et al. 2012). Elevated Zn may reflect dietary intake or other unmeasured factors such as infection by intestinal parasites. Fish in this study were infected with acanthocephalans (8-160 parasites per fish) and Oyoo-Okoth et al. (2012) reported that *Rastrineobola argentea* parasitized by a

cestode exhibited significantly higher intestinal Zn concentrations and significantly lower Cu concentrations compared to non-parasitized individuals.

Zinc concentrations in our study were primarily associated with the metal-sensitive (MSF) compartment (Fig. 1). In contrast to other elements, a large proportion of Zn was detected in the cell debris and nuclei fraction (on average 48%), followed by HDP (15%), while the remaining fractions contributed more or less equally to the total Zn burden. Because Zn can be associated with nuclei rather than cellular debris (e.g. zinc-finger proteins are important for gene regulation and therefore abundant in the nucleus) and because the relative contribution of the debris/nuclei fraction varied along the Zn bioaccumulation gradient, this fraction was included in the analysis for Zn (Kamaliyan and Clarke 2024, Rosabal et al. 2015).

Zn levels in all subcellular fractions were significantly positive associated with total intestinal Zn concentrations (Spearman $\rho = 0.650–0.923$, $p < 0.02$), confirmed by linear regression analyses ($p < 0.02$). Specifically, the relative importance of these increases followed the order: debris/nuclei (slope = 0.253, $R^2 = 0.684$, $n = 11$) > granules (slope = 0.154, $R^2 = 0.780$) > HDP (0.143, 0.740) > HSP (0.119, 0.828) > microsomes/lysosomes (0.101, 0.920) > mitochondria (0.0909, 0.710) (Fig. 2). However, the assumption of constant variance was not met for granules ($p = 0.007$), and this result should therefore be interpreted with caution. Although debris/nuclei exhibited the steepest slope, microsomes/lysosomes showed the strongest overall association with total Zn (highest R^2).

The relative contribution of Zn in the debris/nuclei fraction decreased with increasing intestinal Zn concentrations (slope = –0.000831, $R^2 = 0.515$, p = 0.013, $n = 11$), whereas the contribution of granules increased (slope = 0.000781, $R^2 = 0.436$, p = 0.027, $n = 11$) (Fig. 2) and no consistent changes were observed in the relative contributions of the remaining fractions.

Our results on the distribution of Zn among subcellular fractions in brown trout intestine reflect its essential role in numerous metabolic and immune processes, and gene regulation, particularly as a cofactor for many enzymes and as a key constituent of zinc-finger proteins (Mason and Jenkins 1995). Binding of Zn to metabolically active fractions (MSF) therefore does not necessarily indicate toxicity, and in fish chronically exposed to variable environmental Zn, its homeostasis is generally well regulated (Giguère et al. 2006). Given the fish intestine's central role in Zn uptake and regulation, and its typically higher total Zn levels

compared to other tissues, some differences compared with previous studies on other tissues and species were expected.

The most prominent finding of the present study was the predominance of Zn in the debris/nuclei fraction, a pattern rarely reported in fish but observed in some invertebrates, such as mussels (Sánchez-Marín et al. 2023). This fraction was also responsive to changes in total intestinal Zn, with absolute concentrations increasing but relative contributions decreasing as Zn levels rose. This divergence suggests that other fractions, particularly granules, expanded more rapidly, consistent with saturation of nuclear binding sites and the induction of detoxification or storage pools under elevated Zn exposure. A similar pattern has been reported in the liver of white sucker (*Catostomus commersonii*), where debris/nuclei concentrations increased while their proportional contribution declined with rising hepatic Zn (Urien et al. 2018). The same positive relationship of Zn concentrations in nuclei fraction and total Zn in fish intestine has also been confirmed by Oyoo-Okoth et al. (2012).

In contrast, earlier studies typically identified cytosolic fractions as the major sites of Zn storage and regulation. In the liver of yellow perch (*Perca flavescens*), for example, about half of the Zn burden was cytosolic, with HDP dominating but its relative contribution decreasing as Zn increased, while HSP showed the opposite trend (Giguère et al. 2006). Likewise, in *C. commersonii*, HDP contained the largest share of Zn in liver and ovaries, whereas testes, which contained much lower Zn levels, showed greater accumulation in mitochondria/lysosomes/microsomes fraction (Urien et al. 2018). Similarly, Oyoo-Okoth et al. (2012) reported highest intestinal Zn accumulation in cytosolic fractions, but parasitized fish accumulated significantly greater Zn levels in nuclei, mitochondria, lysosomes, and microsomes, suggesting enhanced uptake in MSF compared to non-parasitized fish. As all fish in the present study were infected with acanthocephalans, parasitism may have influenced the observed subcellular Zn distribution. Nevertheless, positive relationships of Zn in HDP and HSP with total intestinal Zn were consistent in both studies.

Substantial contribution of the HDP fraction to Zn storage in the present study was expected since many of the enzymes in this fraction, such as Cu–Zn superoxide dismutase, are metalloenzymes that use Zn as a cofactor (Kamunde and MacPhail 2011, Mason and Jenkins 1995). The relatively small share of Zn in the HSP fraction (on average 10%) probably reflects dynamic displacement by Cu, consistent with the higher binding affinity of metallothioneins for Cu than Zn (Hamilton and Mehrle 1986). Tissue-specific differences

may also contribute, according to the results in Vardar chub (*Squalius vardarensis*) that liver metallothionein isoforms bound Zn, whereas those in gills did not (Krasnići et al. 2019). Moreover, Oyoo-Okoth et al. (2012) noticed that, in the cytosolic fraction of *R. argentea* intestine, most Zn partitioned in the HSP fraction in non-parasitized individuals and in the HDP fraction in parasitized individuals. The concentrations of Zn in nuclei and organelles (mitochondria, lysosomes and microsomes) of *R. argentea* intestine were positively correlated with total intestinal Zn in both parasitized and non-parasitized *R. argentea*, but the slope was much lower in non-parasitized individuals (Oyoo-Okoth et al. 2012). The slopes in this study were even lower then in non-parasitized *R. argentea* which may reflect weaker influence of acanthocephalans to intracellular Zn distribution or weaker effect in lower concentration range.

Granules, considered of minor importance for Zn regulation in fish by some authors (Giguère et al. 2006, Kamunde and MacPhail 2011), emerged as responsive in *S. trutta* intestine, with their contribution increasing along the Zn gradient. This suggests a potential role in sequestering excess Zn. Similarly, Goto and Wallace (2010) have also reported responsiveness of granules to metal exposure in the field in mummichogs (*Fundulus heteroclitus*), although in that species Zn storage was dominated by granules (35–43%) and cytosolic fractions contributed relatively little, in contrast to our observations. These differences may be tissue-specific (intestine vs. whole body).

Copper

Average intestinal Cu levels were low compared to other Cu subcellular distribution studies. They were approximately 10 times lower than in intestinal tissue of *R. argentea* (Oyoo-Okoth et al. 2012) and liver tissue of *P. flavescens* (Desjardins et al. 2022, Giguère et al. 2006, Kraemer et al. 2006) and *C. commersonii* (Urien et al. 2018) from unpolluted sites. Compared to *C. commersonii* gonads, Cu was about 2 times lower than in females and similar to levels in males (Urien et al. 2018). It was also around 4 times lower than in whole-body *F. heteroclitus* (Goto and Wallace 2010), roughly around 3 times lower than in gills of *O. mykiss* and *Cyprinus carpio*, and around 4 times lower than in gills of gibel carp (*Carassius auratus gibelio*) (Eyckmans et al. 2012).

The majority (71%) of Cu was associated with the MSF compartment (Fig. 1). Within the MSF, debris/nuclei fraction contained the largest proportion of Cu (34%), followed by

mitochondria (16%), while a notable share (21%) was also measured in the HSP fraction, which belongs to BDM. The debris/nuclei fraction was included in this analysis of Cu because its relative contribution changed along the Cu bioaccumulation gradient, as recomanded by Rosabal et al. (2015).

Significant correlations with total intestinal Cu were observed for all fractions except HDP (Spearman $\rho = 0.608–0.853$, $p < 0.03$). Linear regression confirmed significantly positive relationships ($p < 0.02$) across all fractions, with slopes ranking as follows: HSP (0.205, $R^2 = 0.779$, $n = 11$) > HDP (0.189, $R^2 = 0.782$) > mitochondria (0.160, $R^2 = 0.865$) > debris/nuclei (0.121, $R^2 = 0.781$, $n = 11$) > microsomes/lysosomes (0.115, $R^2 = 0.909$) > granules (0.0829, $R^2 = 0.485$). While HSP and HDP exhibited the steepest slopes, indicating stronger proportional increases, microsomes/lysosomes ($R^2 = 0.909$) and mitochondria ($R^2 = 0.865$) showed the most consistent association with total Cu. Finally, the relative contribution of Cu in the debris/nuclei fraction decreased with increasing intestinal Cu concentrations (slope = –0.127, $R^2 = 0.453$, $p = 0.017$), whereas the contribution of HSP increased significantly (slope = 0.0634, $R^2 = 0.364$, $p = 0.038$) (Fig. 3).

Similar to Zn, the predominant association of Cu with the debris/nuclei fraction in the intestine of *S. trutta* was consistent with findings in mussles (Sánchez-Marín et al. 2023), but contrasted with most previous reports in fish. In studies on fish liver, Cu has typically been partitioned primarily to the HSP fraction, with additional contributions from organelles (Desjardins et al. 2022, Eyckmans et al. 2012, Giguère et al. 2006**,** Urien et al. 2018). In gonads of white suckers (*C. commersonii*), it was mostly associated with the HSP fraction in females and mitochondria/lysosomes/microsomes fraction in males, which contained lower Cu concentrations (Urien et al. 2018). In gills of three freshwater fish, Cu was mainly distributed among organelles, HSP, and HDP, although the dominant fraction varied between species (Eyckmans et al. 2012). However, dominant Cu accumulation in metal-sensitive nuclei and organelle fractions compared to cytosol (HDP and HSP) has also been recorded in previous study on fish intestine, suggesting a tissue-specific pattern (Oyoo-Okoth et al. 2012). Moreover, concentration of Cu in the cystolic fraction was particularly low in the parasitized fish due to competition for Cu between parasites and fish (Oyoo-Okoth et al. 2012).

Therefore, HSP fraction, which contains metallothioneins, may not be as central for Cu homeostasis as generally considered and other fractions may also play an important role. The

HDP fraction contains denatured enzymes and non-enzymatic proteins such as albumin and haemoglobin (Giguère et al. 2006). Elevated Cu in this fraction may indicate binding to metal-sensitive sites, potentially impairing enzyme function. Cu in the microsomes/lysosomes fraction may reflect either toxicity (microsomes) or storage/excretion (lysosomes) (Klaverkamp et al. 1991). However, as Cu is an essential element, its presence in metabolically active fractions does not necessarily indicate toxicity, particularly at the relatively low intestinal Cu concentrations observed in *S. trutta*. It is also a part of complex IV of the electron transport chain of the internal mitochondrial membrane of fish (Couture and Rajotte 2003).

Our results on positive relationship of Cu concentration in each fraction with total intestinal Cu were similar to trends previously observed in intestine of non-parasitized fish, while in parasitized fish Cu concentrations in the nuclei and organelles were negatively correlated with the total intestinal Cu concentration (Oyoo-Okoth et al. 2012). This suggests that Cu sequestration by acanthocephalans was not as strong as by cestodes or that this relationship was not visible at low Cu concentrations in *S. trutta* compared to *R. argentea*. However, results of this study were mostly similar to previous studies in fish liver, in which generally the strongest Cu increase with rising Cu burden was observed in the HSP fraction, but significant accumulation also occurred in mitochondria, microsomes/lysosomes, granules, and HDP (Desjardins et al. 2022, Giguère et al. 2006, Kamunde and MacPhail 2011, Urien et al. 2018). However, tissue-specific responses were evident: in rainbow trout, Cu increases were detected in debris/nuclei and HDP in gill tissue, while in liver, increases were found in debris/nuclei, granules, and HSP but not in organelles or HDP (Eyckmans et al. 2012). Low responsiveness of the granule fraction in the present study was contrary not only to findings on liver of rainbow trout (*Oncorhynchus mykiss*) by Eyckmans et al. (2012), but also by Kamunde and MacPhail (2011) and on whole body of mummichogs (*Fundulus heteroclitus*) by Goto and Wallace (2010). Since total Cu concentrations in these studies were higher than in *S. trutta* intestine, sequestration to the granule fraction may represent a secondary Cu-handling strategy, activated only at higher exposure levels. The increase of the relative contribution of Cu in the HSP fraction along the bioaccumulation gradient, accompanied by a decrease in the debris/nuclei fraction, suggests that excess Cu is transferred from metal-sensitive compartments to the HSP fraction for metallothioneins sequestration or GSH binding. Such redistribution is consistent with observations from fish liver and gonads, where the HSP fraction increased in relative importance with rising hepatic Cu, while contributions

other metal-sensitive fractions such as mitochondria, HDP and debris/nuclei declined (Desjardins et al. 2022, Giguère et al. 2006, Urien et al. 2018). In contrast, rainbow trout gills, and to a lesser degree those of common carp, appeared to accumulate additional Cu primarily in MSF compartment rather than in HSP (Eyckmans et al. 2012), highlighting tissue- and species-specific differences in Cu handling.

These patterns suggest that although metallothionein induction and Cu sequestration in HSP are central detoxification pathways, redistribution of Cu among other subcellular fractions can occur depending on tissue function and exposure history and is consistent with conclusions of Goto and Wallace (2010) that metals are generally equally partitioned as MSF and BDM compartments at low exposure levels. Metal–metal interactions are complex and may depend on the animal species, the metals involved and their relative concentrations as well as the exposure duration (Kamunde and MacPhail 2011). Moreover, Urien et al. (2018) suggested that in the absence of Cu or Zn overloads, these metals were mainly accumulated in organelles for metabolic purposes. Since intestine of S. *trutta* contained high Zn and low Cu concentrations compared to literature data, our results maybe confirmed this trend.

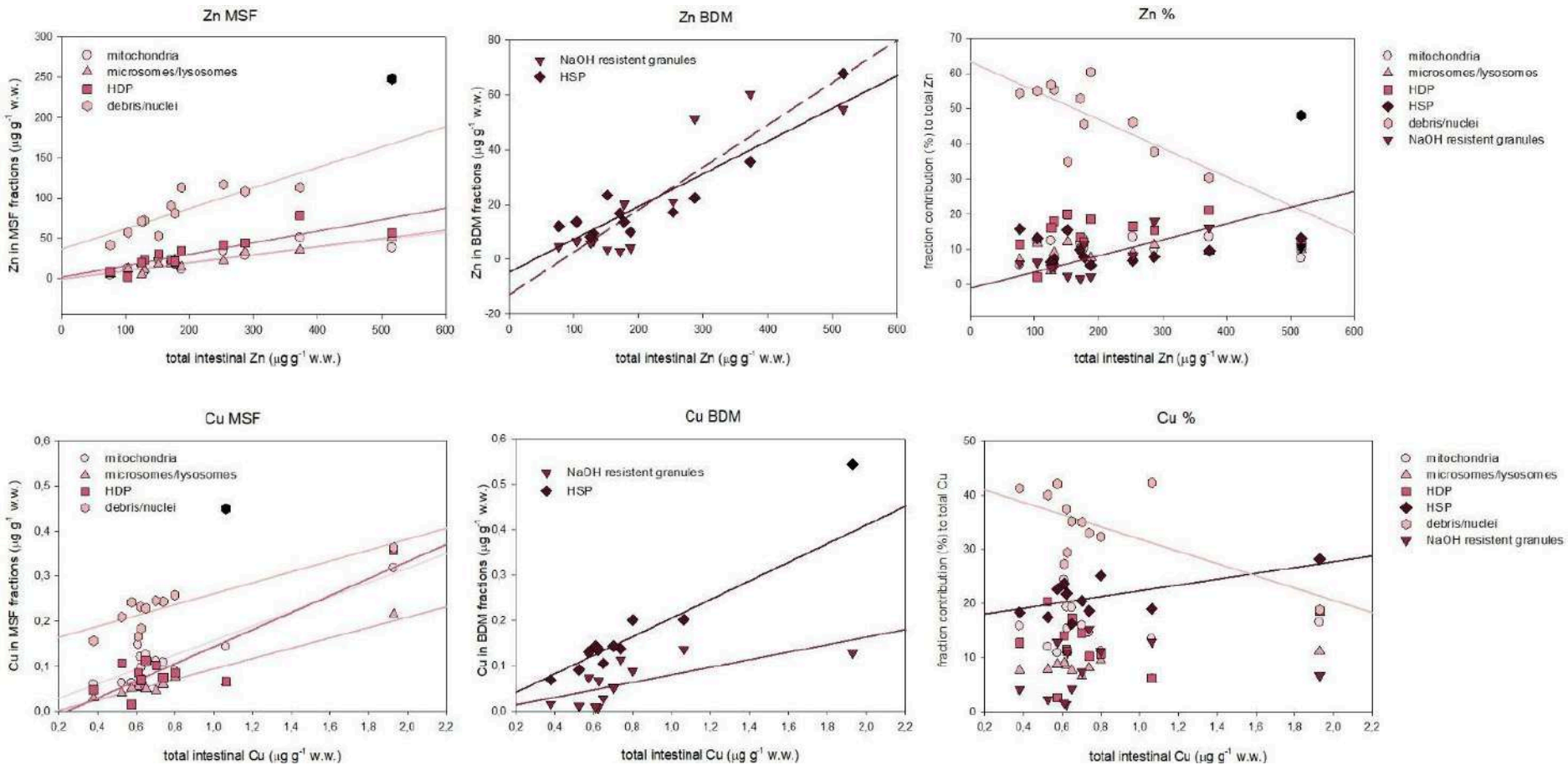

Figure 2. Relationships between total intestinal Zn and Cu concentrations and subcellular partitioning in *Salmo trutta* from the Krka River. Metal in potentially metal-sensitive fractions (MSF) is shown on the left and in biologically detoxified fractions (BDM) on the middle panel, while the right panel shows the relative contribution of each fraction to the total metal burden. Each point represents one fish (n = 12). Regression lines are shown where relationships were significant ($p < 0.05$) and dashed lines indicate that the assumption of constant variance

was not met. Black points are outliers excluded from regressions. Fraction abbreviations: HSP - heat-stable proteins, HDP- heat-denatured proteins

Iron

Iron concentrations in *S. trutta* intestine were also relatively low: about 5 times lower than in the liver of *P. flavescens* from moderately impacted lake (Desjardins et al. 2022) and up to 124 times lower than in the liver of Arctic char (*Salvelinus alpinus*) from unpolluted Arctic lakes (Barst et al. 2016).

Iron was the most evenly distributed element across subcellular fractions, consistent with its essential role in respiration and redox processes (Kurz et al. 2011). Nevertheless, it was predominantly associated with the MSF compartment (46%), particularly with the microsomes/lysosomes fraction (22%) (Fig. 1). Among fractions, only granules showed a significant positive correlation with total intestinal Fe (Spearman $\rho = 0.671$, $p = 0.0154$), which was supported by linear regression analysis (slope = 0.361, $R^2 = 0.798$, $p < 0.001$, $n = 11$) (Fig. 2). Microsomes/lysosomes also exhibited a weaker but significant increase in Fe concentrations with total Fe (slope = 0.229, $R^2 = 0.350$, $p = 0.043$). The relative contribution of granules to total Fe increased with accumulation (slope = 0.0303, $R^2 = 0.613$, $p = 0.004$, $n = 11$), highlighting them as the main responsive fraction, whereas other compartments showed no consistent trends.

The subcellular distribution of Fe in the intestine observed in this study broadly resembled patterns reported for fish liver, where Fe also accumulates predominantly in the MSF compartment (63–73%), especially in the microsomes/lysosomes and mitochondria fractions (Barst et al. 2016, Desjardins et al. 2022). Lysosomes, in particular, are recognized as important sites of Fe metabolism and storage and they usually contain relatively large amounts of redox-active Fe (Kurz et al. 2011).

However, the proportion of Fe associated with mitochondria and cytoplasm was lower in our samples than previously reported for fish liver (Barst et al. 2016, Desjardins et al. 2022). Due to the central role of Fe in cytosolic redox enzymes and in mitochondrial function, where it is incorporated into cytochromes and other respiratory chain enzymes as well as ferrochelatase, higher levels could be expected in these fractions (Kurz et al. 2011). The lower contribution observed here may therefore reflect tissue-specific physiology of the intestine, which prioritizes controlled uptake and transfer of dietary Fe, and possibly methodological constraints of subcellular fractionation.

Unlike Desjardins et al. (2022), who reported strong associations between Fe concentrations in mitochondrial and HSP fractions and the Fe bioaccumulation gradient, we found no such

responsiveness in these compartments. Instead, the most dynamic response was observed in granules, which increased in both concentration and relative contribution with rising intestinal Fe, suggesting that this fraction may play a previously underappreciated role in intestinal Fe storage or detoxification.

Considering the relatively low total Fe concentrations in the intestine of *S. trutta* compared to liver values reported in previous studies (Barst et al. 2016, Desjardins et al. 2022), and the distinct physiological roles of intestine (dietary absorption) and liver (storage and detoxification), these differences in subcellular Fe distribution are consistent with tight regulation of intestinal Fe and limited accumulation relative to hepatic tissues.

Selenium

Average intestinal Se concentration was twice as low as in liver of *S. alpinus* (Barst et al. 2016), and similar to levels in the liver, but notably higher than in gonads of *C. commersonii* — approximately 121 and 193 times higher than in female and male gonads, respectively (Urien et al. 2018).

Selenium in the intestine was partitioned more in MSF (58%) than in BDM compartment (42%). Within these, the HSP fraction dominated (41%), followed by debris/nuclei (35%), whereas the remaining fractions contributed only marginally. This pattern was also reflected across the accumulation gradient of total intestinal Se. The debris/nuclei fraction was included in Se analysis because its relative contribution changed along the Se bioaccumulation gradient (Rosabal et al. 2015). Positive correlations with total Se were observed for debris/nuclei, mitochondria, and microsomes/lysosomes (Spearman ρ = 0.809–0.858, $p < 0.0001$), although assumptions of constant variance were not met in linear regression for these fractions. By contrast, the HSP fraction showed the strongest and most consistent response. Based on regression slopes and coefficients of determination, the ranking of significant ($p < 0.02$) relationships was: HSP (slope = 0.629, $R^2 = 0.949$) > debris/nuclei (0.253, $R^2 = 0.699$) > mitochondria (0.0443, $R^2 = 0.572$) > HDP (0.0410, $R^2 = 0.581$) > microsomes/lysosomes (0.0353, $R^2 = 0.546$) > granules (0.00984, $R^2 = 0.462$). Furthermore, with increasing total intestinal Se concentration, the relative contribution of the HSP fraction increased (slope = 0.000166, $R^2 = 0.616$, $p = 0.003$), while that of debris/nuclei decreased (slope = –0.0000896, $R^2 = 0.436$, $p = 0.027$, $n = 11$).

Our findings on intestinal Se distribution in *S. trutta* were broadly consistent with patterns reported for other fish tissues. In the liver of *S. alpinus*, Se was similarly partitioned between metal-sensitive and detoxified compartments, with the latter dominated by the HSP fraction (Barst et al. 2016). In contrast, in intestine of *S. trutta* the mitochondria and HDP fractions accounted for a smaller proportion of Se, whereas the HSP and debris/nuclei fractions contributed more than reported for liver in *S. alpinus* or *C. commersonii* (Barst et al. 2016, Urien et al. 2018). Although Se in the HSP fraction may be incorporated as seleno-cysteine in thermostable metal-binding proteins such as metallothioneins, this remains speculative rather than confirmed (Barst et al. 2016, Urien et al. 2018). The relatively high proportion of Se in the debris/nuclei fraction may reflect its incorporation into nuclear selenoproteins involved in antioxidant defense and genome maintenance (Zhang et al. 2016).

The increase of Se concentrations in all subcellular fractions with rising total intestinal Se is consistent with observations in the liver of white suckers (*C. commersonii*), where the strongest increases occurred in the HDP fraction, followed by debris/nuclei, HSP, and mitochondria (Urien et al. 2018). In the gonads of *C. commersonii*, Se concentrations in all fractions also rose with increasing Se, with the greatest increases in the HDP and debris/nuclei fractions of females and in the debris/nuclei of males (Urien et al. 2018).

Changes in the relative contribution of fractions in our study also paralleled those reported for *C. commersonii* liver, where increasing allocation to the HSP fraction was accompanied by decreasing contributions from debris/nuclei and HDP (Urien et al. 2018). In *C. commersonii* gonads, however, responses diverged, with females showing a stronger contribution of HDP and males of debris/nuclei with increasing total hepatic Se (Urien et al. 2018). The association of Se with putatively metal-sensitive fractions such as HDP and nuclei in gonads was interpreted as evidence of limited detoxification capacity and possible stress (Urien et al. 2018). By contrast, in our study, despite higher total intestinal Se concentrations compared to *C. commersonii* gonads, redistribution toward the HSP fraction indicates efficient handling and detoxification in *S. trutta* intestine. Given that dietary intake is the primary route of Se exposure in fish (Hamilton 2004), these results support the presence of active, regulated mechanisms for Se uptake and detoxification in the intestine.

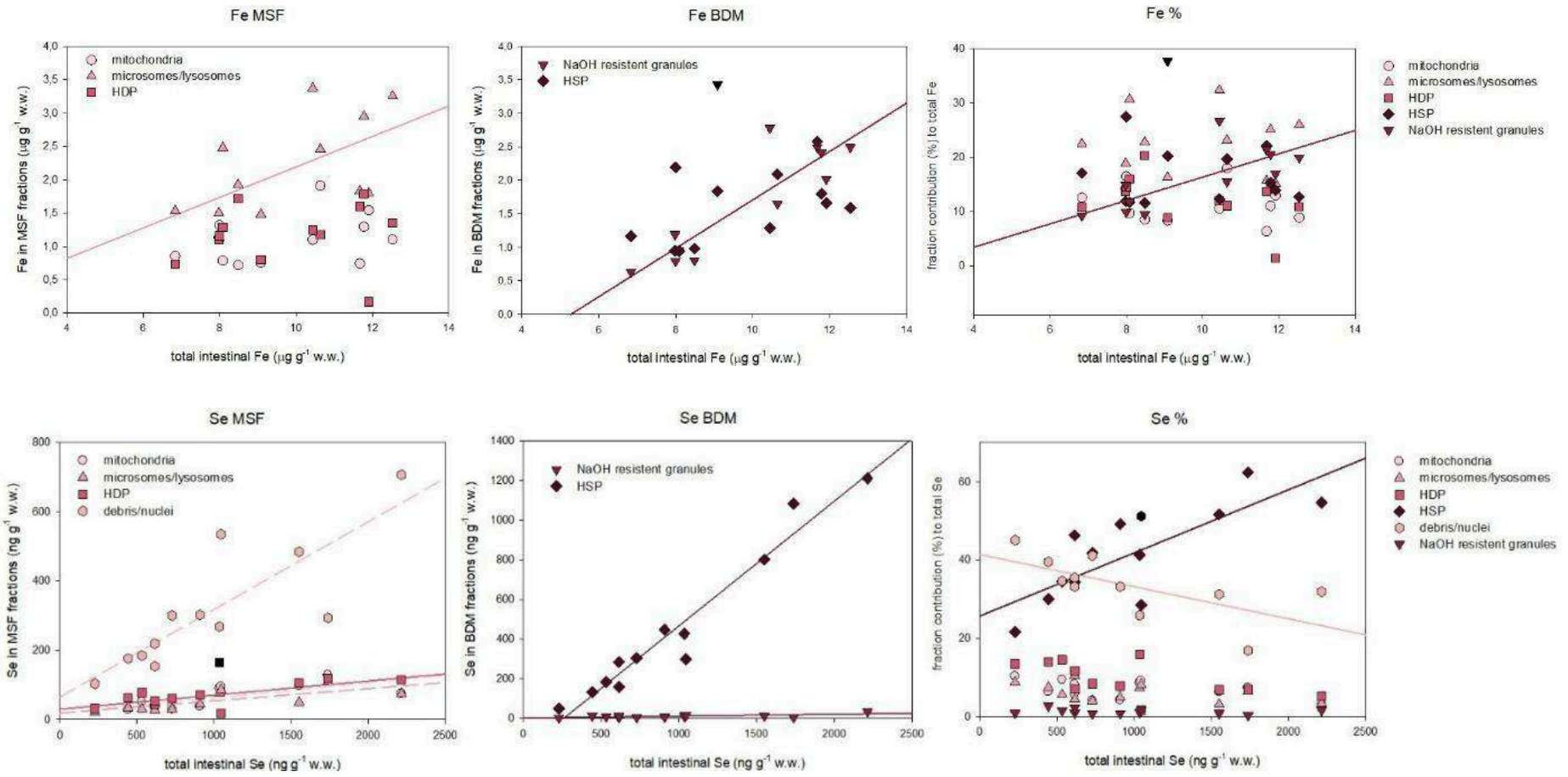

Figure 3. Relationships between total intestinal Fe and Se concentrations and subcellular partitioning in *Salmo trutta* from the Krka River. Metal in potentially metal-sensitive fractions (MSF) is shown on the left and in biologically detoxified fractions (BDM) on the middle panel, while the right panel shows the relative contribution of each fraction to the total metal burden. Each point represents one fish (n = 12). Regression lines are

shown where relationships were significant ($p < 0.05$) and dashed lines indicate that the assumption of constant variance was not met. Black points are outliers excluded from regressions. Fraction abbreviations: HSP - heat-stable proteins, HDP- heat-denatured proteins

Manganese

There is a lack of data on the subcellular distribution of Mn in fish. To our knowledge, it has only been studied in the liver of *P. flavescens* from lakes with moderate anthropogenic impact (Desjardins et al. 2022) and was sporadically mentioned in paper on Cd toxicity in liver of marine fish species *Dicentrarchus labrax* and *Solea senegalensis* (Le Croizier et al. 2019). In our study, total intestinal Mn concentration was about five times lower than the values reported in *P. flavescens*, while total concentrations for marine fish were not reported. In intestine of *S. trutta*, Mn was partitioned primarily into the BDM compartment (43%), dominated by the HSP (26%) and granules (17%). Within the MSF, microsomes/lysosomes (13%) and mitochondria (12%) contributed similarly. Significant positive correlations with total intestinal Mn were observed for HSP, granules, and mitochondria (Spearman ρ = 0.685–0.937, $p < 0.02$). Linear regression analysis identified the strongest associations with granules (slope = 0.324, R^2 = 0.809), followed by HSP (slope = 0.249, R^2 = 0.687), mitochondria (slope = 0.125, R^2 = 0.881), and HDP (slope = 0.033, R^2 = 0.740). However, the constant variance assumption was not met for HSP ($p = 0.045$), warranting caution in interpretation. Notably, microsomes/lysosomes were the only fraction whose relative contribution decreased along the Mn bioaccumulation gradient (slope = –0.000262, R^2 = 0.674, $p = 0.001$), while contributions from other fractions remained stable.

This subcellular distribution was somewhat unexpected given the essential role of Mn in organisms (Xu et al. 2023) and is in contrast with previous findings in the liver of *P. flavescens*, *D. labrax*, and *S. senegalensis*, where Mn accumulated predominantly in the MSF compartment (37–62%) (Desjardins et al. 2022, Le Croizier et al. 2019). In those studies, mitochondria and microsomes/lysosomes were the most important subcellular pools for Mn (37–50%), although HSP also accounted for a substantial proportion (23–29%) of the total Mn burden. Because Mn concentrations in our study were lower than literature values for liver, the predominance of detoxification fractions in Mn handling may reflect tissue-specific regulation or interactions with other essential metals (Fe, Zn) rather than Mn overload (Thomson et al. 1971). As feed is the dominant route for Mn acquisition in fish, the intestine plays a key role in regulating Mn absorption and excretion (Xu et al. 2023). Mn in HSP fracion might be associated to enzymes such as arginase (Wang et al. 2013) transferrin or albumin, which is involved in Mn transport from the intestine to the liver (Krasnići et al. 2013).

Differences between our results and those reported for *P. flavescens* liver were also evident in the relationships between subcellular Mn fractions and total Mn. While HSP and mitochondria were identified as responsive fractions in both liver and intestine, liver analyses showed the strongest association with microsomes/lysosomes and no significant correlation with granules (Desjardins et al. 2022). In contrast, in the intestine, granules emerged as the most responsive fraction.

Overall, the prominent role of detoxification compartments, together with the decreasing relative contribution of organelles along the Mn bioaccumulation gradient, suggests regulated sequestration rather than overt Mn toxicity in *S. trutta* intestine. Given the limited studies on Mn subcellular distribution in fish, further research is needed.

2.2.2. Non-essential metals

Strontium

Average intestinal Sr in *S. trutta* from the Krka River was about 5 times higher than levels in the liver of *P. flavescens* (Desjardins et al. 2022). To our knowledge, there are no other literature data on Sr subcellular distribution.

Strontium was almost equally partitioned between the MSF (48%) and BDM (52%) compartments. The HSP fraction was dominant (30%), followed by debris/nuclei (23%) and granules (22%). Since the relative contribution of the debris/nuclei fraction changed along the Sr bioaccumulation gradient, it was included in the analysis (Rosabal et al. 2015). All subcellular fractions were positively associated with total intestinal Sr concentrations. Significant correlations (Spearman $\rho = 0.699–0.979$, $p < 0.02$) and linear regression analyses confirmed strong positive relationships for all fractions ($p < 0.001$) as follows: HSP (slope = 0.368, $R^2 = 0.945$) > granules (0.308, 0.920) > mitochondria (0.103, 0.943, n = 11) > debris/nuclei (0.0982, 0.778, n = 11) > microsomes/lysosomes (0.0604, 0.814) > HDP (0.0336, 0.873) (Fig. 3). However, constant variance assumptions were not met for HSP ($p < 0.001$) and granules ($p = 0.008$), so these results should be interpreted with caution. In addition, the relative contributions of microsomes/lysosomes (slope = -0.000122, $R^2 = 0.639$, $p = 0.002$) and debris/nuclei (slope = -0.000149, $R^2 = 0.367$, $p = 0.037$) decreased with increasing total intestinal Sr concentrations.

The overall equal partitioning of Sr between MSF and BDM in *S. trutta* intestine was consistent with findings in *P. flavescens* liver (Desjardins et al. 2022). However, the dominant fractions differed: in *S. trutta* intestine, HSP, debris/nuclei, and granules prevailed, whereas in *P. flavescens* liver mitochondria (30%) were most important, followed by HSP (25%). The greater allocation to BDM fractions in our study may reflect higher total Sr concentrations compared to liver.

Although Sr is a non-essential element without specific transporters or binding proteins, its chemical similarity to Ca allows it to interact with Ca-binding sites, which are abundant in mitochondria and endoplasmic reticulum. Consequently, Sr is typically expected to associate with membranes or insoluble material (Cowan 2014). The notable presence of Sr in HSP and granules may reflect early sequestration or detoxification processes prior to toxicity. Once absorbed, Sr is strongly retained in calcified tissues such as bone and otoliths, while soft tissue accumulation is usually limited (Chowdhury and Blust 2011). This helps explain why Sr was detected across all subcellular fractions but was particularly concentrated in detoxification pools (HSP, granules), which can sequester excess cations and reduce their potential reactivity.

Unlike in *P. flavescens* liver, where no significant relationships were found between total Sr and concentrations in any subcellular fractions (Desjardins et al. 2022), our data revealed strong positive associations in all fractions. Desjardins et al. (2022) attributed the absence of such relationships in liver to low absorption efficiency, rapid elimination from hepatocytes, or redistribution to bone. Moreover, in liver, relative contributions of fractions remained stable across the Sr gradient, whereas in our study, contributions of microsomes/lysosomes and debris/nuclei decreased with increasing intestinal Sr. This probably suggests stronger subcellular responses at higher Sr concentrations in intestine than in liver.

Given that Sr uptake occurs primarily through the gills and dietary absorption plays a secondary role, the intestine is unlikely to be a major site of Sr regulation (Chowdhury and Blust 2011). Nevertheless, our results indicate a redistribution of Sr away from organelles and nuclei into detoxification pools, suggesting effective regulation in *S. trutta* intestine.Together, these results indicate that Sr, although non-essential, is effectively managed in intestinal tissue through detoxification fractions, while the intestine itself likely serves as a transient site of regulation before Sr is directed toward skeletal deposition.

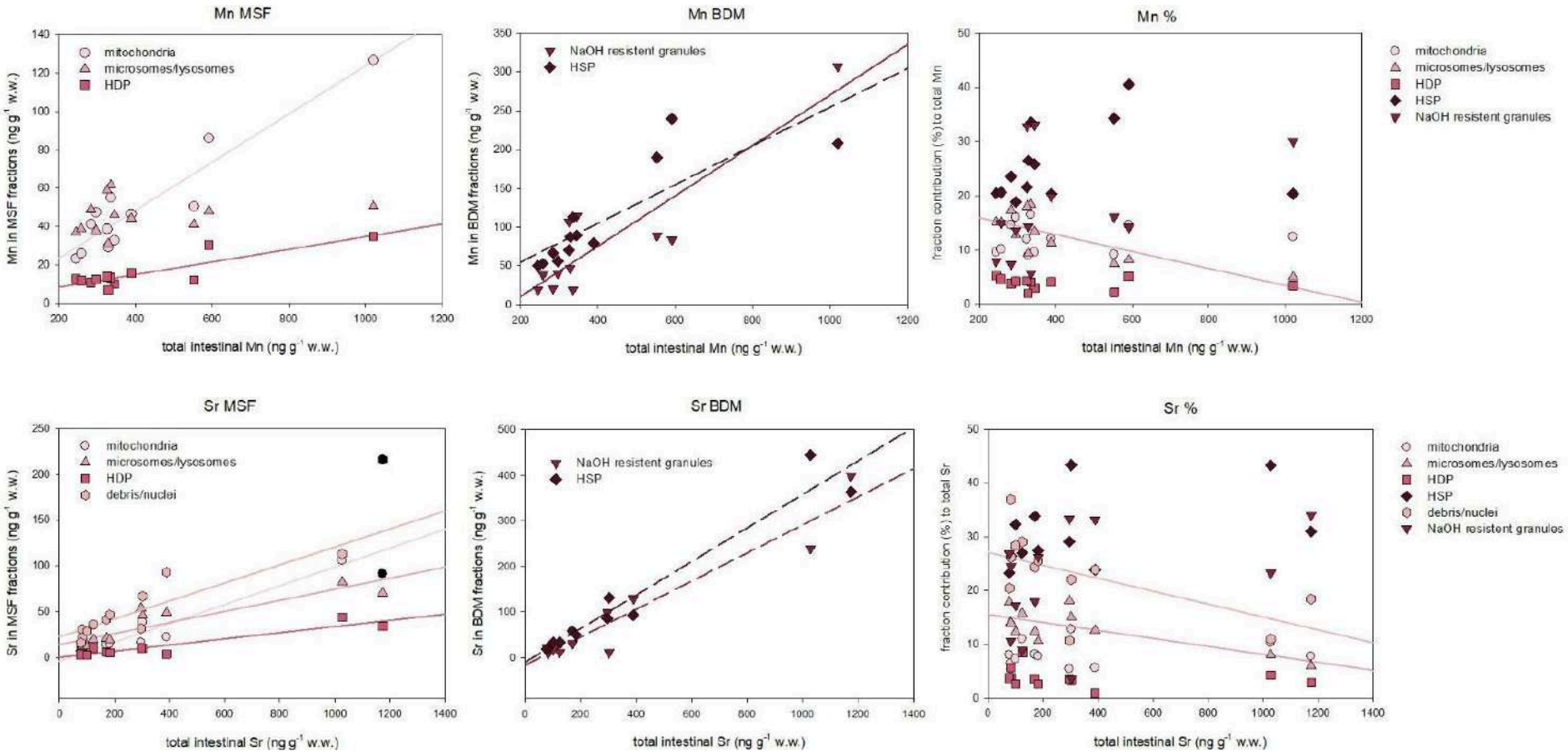

Figure 4. Relationships between total intestinal Mn and Sr concentrations and subcellular partitioning in *Salmo trutta* from the Krka River. Metal in potentially metal-sensitive fractions (MSF) is shown on the left and in biologically detoxified fractions (BDM) on the middle panel, while the right panel shows the relative contribution of each fraction to the total metal burden. Each point represents one fish (n = 12). Regression lines are shown where relationships were significant ($p < 0.05$) and dashed lines indicate that the assumption of constant variance

was not met. Black points are outliers excluded from regressions. Fraction abbreviations: HSP - heat-stable proteins, HDP- heat-denatured proteins

Arsenic

Average intestinal As concentrations in *S. trutta* were comparable to levels reported in the liver of northern pike (*Esox lucius*) and lake whitefish (*Coregonus clupeaformis*) from unpolluted sites in northern Canada (Rolland et al. 2025). They were 2 times higher than in liver and male gonads and 3 times higher than in female gonads of white suckers (*Catostomus commersonii*) from an unpolluted lake in Saskatchewan (Urien et al. 2018), but substantially lower than in the livers of American (*Anguilla rostrata*) and European eels (*A. anguilla*) from the Saint Lawrence River system and Gironde Estuary (Rosabal et al. 2015).

Consistent with expectations for non-essential elements, As was more strongly associated with the BDM compartment (41%) than the MSF (35%). The HSP fraction dominated (39%), followed by microsomes/lysosomes (26%), while other fractions contributed only marginaly to the total As burden. HSP was also the most responsive to increasing intestinal As, with mitochondria and HDP playing secondary roles. Significant positive correlations were observed between total As and concentrations in HSP, mitochondria, and HDP (Spearman ρ = 0.580–0.832, $p < 0.05$). Linear regression confirmed significant increases ($p < 0.03$), with relative importance as follows: HSP (slope = 0.411, $R^2 = 0.504$) > mitochondria (0.0559, 0.442) > HDP (0.0396, 0.407). The normality assumption was not met for HDP (Shapiro–Wilk $p = 0.001$). The relative contributions of all fractions remained stable with increasing total As.

To our knowledge, this is the first study of As subcellular distribution in fish intestine. Predominant allocation to the BDM compartment, particularly HSP, is consistent with findings in liver of *C. clupeaformis* and *E. lucius* (Rolland et al. 2025), *A. rostrata*, *A. anguilla* (Rosabal et al. 2015), liver and gonads of *C. commersonii* (Urien et al. 2018), and various tissues of *N. brasiliensis* (Hauser-Davis et al. 2022). In contrast, microsomes/lysosomes represented the second most important fraction in *S. trutta* intestine, whereas in studies on fish liver it that was mitochondria (Rolland et al. 2025, Rosabal et al. 2015). HDP and granules accounted for only a minor proportion of total As in both *S. trutta* intestine and liver studies, suggesting that these fractions play a limited role in As regulation in fish.

The predominance of HSP implies interactions with thiol-containing cytosolic ligands, such as metallothioneins and glutathione, which can immobilize and neutralize As. This is consistent with reports that organic As species (e.g. dimethylarsinous acid), which bind to

metallothioneins, are the main As forms in fish liver (Rolland et al. 2025). Furthermore, sequestration of As via induction of metallothioneins and binding to them has been reported in several fish species (He et al. 2010, Zhang et al. 2012).

The strongest responses to increasing As were in intestine of *S. trutta* observed for As concentration in HSP, followed by mitochondria and HDP, which is consistent with results from livers of *C. commersonii* (Urien et al. 2018), *A. rostrata* and *A. anguilla* (Rosabal et al. 2015). However, unlike liver, no significant associations were detected for As concentrations in microsomes/lysosomes or granules.

The relative contribution of each fraction to the total As burden did not vary significantly with increasing As concentrations in our samples, nor in the liver and gonads of *C. commersonii* (Urien et al. 2018), suggesting that no consistent defense mechanisms were activated. By contrast, in *A. rostrata* the relative contribution of the HSP fraction decreased along the As bioaccumulation gradient, while that of the metal-sensitive compartment increased, likely reflecting the higher total As concentrations in this species (Rosabal et al. 2015).

Average intestinal As concentrations in *S. trutta* were higher than in tissues of *C. commersonii* (Urien et al. 2018) but lower than in livers of *A. rostrata* and *A. anguilla* (Rosabal et al. 2015), yet the overall subcellular distribution was comparable across species. The intestine, confirmed as a main site of As uptake (Zhang et al. 2022), showed balanced partitioning between MSF and BDM, suggesting efficient sequestration. However, proportions of the As associated with MSF in *S. trutta* were non-negligible (35% vs. 20% in *C. commersonii* liver) which could potentially lead to toxicity since As has no known essential role in fish and can distupt cell functions (Hauser-Davis et al. 2022, Urien et al. 2018).

Thallium

Average Tl concentrations were similar to those measured in the liver of Arctic char (*Salvelinus alpinus*) from pristine Canadian artic lakes (Barst et al. 2026) and in American and European eels (Rosabal et al. 2015), but higher than values reported for the whole body of cultivated juvenile fathead minnows (*Pimephales promelas*) (Lapointe and Couture 2009).

Like As, and consistent with the tendency of many non-essential metals to be sequestered in detoxified pools, Tl in *S. trutta* intestine was more strongly associated with the BDM compartment (54%) than with MSF (20%). The HSP fraction accounted for the largest share of Tl (48%), while mitochondria (9%) and microsomes/lysosomes (8%) made minor contributions within MSF. Concentrations of Tl in nearly all fractions were positively correlated with total intestinal Tl (Spearman $\rho = 0.776–0.986$, $p < 0.002$). Linear regression identified HSP as the most responsive pool (slope = 0.516, $R^2 = 0.966$, $p < 0.001$), followed by microsomes/lysosomes (slope = 0.0572, $R^2 = 0.675$, $p = 0.001$), HDP (slope = 0.0481, $R^2 = 0.914$, $p < 0.001$) and mitochondria (slope = 0.0459, $R^2 = 0.596$, $p = 0.005$). The ranking of responsiveness was consistent between correlation and regression analyses. Along the Tl bioaccumulation gradient, the relative contribution of the HDP fraction increased slightly, while contributions of other fractions remained stable. The granule fraction showed a decreasing trend, although this was not statistically significant ($p = 0.052$).

Predominant Tl accumulation in the HSP fraction of the BDM in the intestine of *S. trutta* is consistant with observations in the liver of *Salvelinus alpinus* (Barst et al. 2016), *A. anguilla* and *A. rostrata* (Rosabal et al. 2015). The proportion of Tl in the cytosolic fraction (HSP + HDP, 51%) was comparable to values previously reported for *S. trutta* from the Krka River (45–70%) (Mijošek et al. 2019). Compared with *S. alpinus* liver, where 42–53% of Tl was associated with the MSF compartment (Barst et al. 2016), the intestinal distribution in *S. trutta* was more strongly biased toward BDM. Within MSF, mitochondria represented the main sink, consistent with findings in *S. alpinus* and eels (Barst et al. 2016, Rosabal et al. 2015). Granules contributed little to Tl handling in *S. trutta* (6%), whereas *P. promelas* sequestered much more Tl in this fraction (29–32%) (Lapointe and Couture 2009).

In our study, Tl concentrations in all fractions, except granules, were positively related to total intestinal Tl, a pattern identical to that reported in livers of *A. anguilla* and *A. rostrata* (Rosabal et al. 2015). Similar trends were observed in *S. alpinus* liver (Barst et al. 2016) and in whole-body *P. promelas* (Lapointe and Couture 2009), where both sensitive and detoxification compartments increased with rising exposure. In *P. promelas*, Tl exposure also enhanced the proportion bound to the HSP fraction (Lapointe and Couture 2009). The strongest responsiveness of HSP to Tl accumulation observed in our study was also consistent with results from the livers of *A. anguilla* and *A. rostrata* (Rosabal et al. 2015) and suggests that Tl interacts with metallothioneins and similar proteins. Tl(I) readily forms

stable complexes with reduced sulfur ligands (Mulkey and Oehme 1993), making binding to cysteine residues in these proteins plausible.

Although total Tl concentrations in *S. trutta* intestine were similar to those in eel livers, the sigmoidal response of Tl in granules along the bioaccumulation gradient reported in eels was absent (Rosabal et al. 2015). Instead, *S. trutta* showed a slight increase in HDP and a decline in granules with rising Tl, consistent with Rosabal et al. (2015). This may indicate limited sequestration capacity in granules at higher Tl levels, forcing greater allocation to sensitive fractions. The relatively higher proportion of Tl in granules of *P. promelas* thus may reflect lower total Tl burden in them compared to *S. trutta* and other species examined.

Our results demonstrate that Tl handling in *S. trutta* intestine is dominated by the HSP fraction, highlighting cytosolic sequestration as the primary detoxification pathway at the site of entry. Mitochondria, while contributing less overall, consistently represented the major MSF sink and may therefore be a critical target of Tl toxicity due to its ability to interfere with K^+-dependent mitochondrial processes. Compared with liver, where Tl distribution is more evenly split between BDM and MSF, the intestine showed a stronger bias toward detoxified fractions, reflecting a protective strategy to neutralize dietborne Tl before it reaches sensitive organelles. Given that diet represents the main Tl uptake pathway in *S. trutta* (Mijošek et al. 2019) and is less effectively regulated than aqueous Tl (Lapointe and Couture 2009), these findings emphasize the dual role of the intestine in both uptake or elimination of Tl.

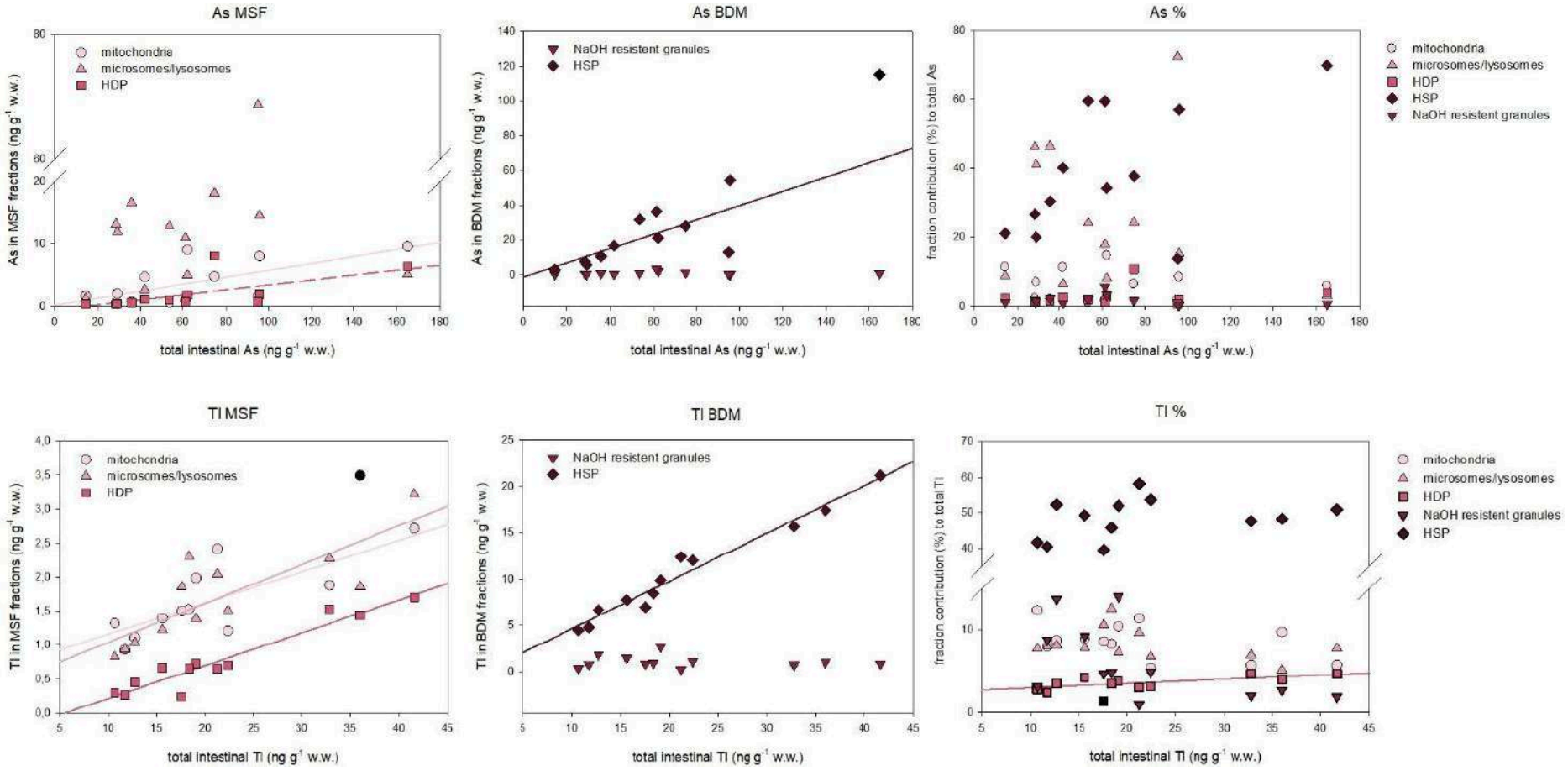

Figure 5. Relationships between total intestinal Mn and Sr concentrations and subcellular partitioning in *Salmo trutta* from the Krka River. Metal in potentially metal-sensitive fractions (MSF) is shown on the left and in biologically detoxified fractions (BDM) on the middle panel, while the right panel shows the relative contribution of each fraction to the total metal burden. Each point represents one fish (n = 12). Regression lines are shown where relationships were significant ($p < 0.05$) and dashed lines indicate that the assumption of constant variance

was not met. Black points are outliers excluded from regressions. Fraction abbreviations: HSP - heat-stable proteins, HDP- heat-denatured protein

3. Conclusions

This study provides the first characterization of subcellular distribution of essential and non-essential elements in the intestine of *Salmo trutta*, and the first report of Fe, Se, Mn, Sr, As, and Tl partitioning in any fish intestinal tissue. Essential elements were primarily associated with metal-sensitive fractions (MSF), while non-essential elements were bound mainly to biologically detoxified metal (BDM) compartments, consistent with their physiological roles. The only exception was Mn, an essential metal showing a pronounced association with detoxification fractions, suggesting tissue-specific regulation or competitive interactions with other essential metals.

Zinc and Fe increasingly accumulated in granules with rising exposure, whereas Cu and Se responses were dominated by the HSP fraction, reflecting regulation through thiol-rich proteins such as metallothioneins. Manganese and Sr were also concentrated in HSP and granules and redistributed away from MSF fractions along the bioaccumulation gradient, indicating efficient detoxification. The HSP fraction likewise played a key role in As and Tl handling, though the slight increase of Tl in the sensitive HDP fraction may signal early subcellular stress.

Overall, these results demonstrate that metal partitioning is both tissue- and species-specific, dependent on element properties and metabolic functions. The intestine of *S. trutta* exhibits effective regulation through HSP- and granule-mediated sequestration, yet element-specific patterns highlight the importance of tissue context in metal toxicokinetics. Further research is needed to elucidate the mechanisms governing subcellular allocation and their implications for metal regulation and toxicity in aquatic organisms.

4. Literature

Antweiler, R. C. (2015). Evaluation of statistical treatments of left-censored environmental data using coincident uncensored data sets. II. Group comparisons. *Environmental Science & Technology*, 49(22), 13439-13446.

Alberto, A., Francesco, C., Atzei, A., Andrea, S., Francesco, P., Carla, L., & Mariateresa, R. (2021). Heavy metal and metalloid accumulation in wild brown trout (*Salmo trutta* L., 1758 complex, Osteichthyes: Salmonidae) from a mountain stream in Sardinia by ICP-OES. *Environmental monitoring and assessment*, 193(7), 448.

Mijošek, T., Marijić, V. F., Dragun, Z., Ivanković, D., Krasnići, N., Redžović, Z., ... & Erk, M. (2019). Thallium accumulation in different organisms from karst and lowland rivers of Croatia under wastewater impact. *Environmental chemistry*, 17(2), 201-212.

Brucka-Jastrzêbska, E., Kawczuga, D., Rajkowska, M., & Protasowicki, M. (2009). Levels of microelements [Cu, Zn, Fe] and macroelements [Mg, Ca] in freshwater fish. *Journal of Elementology*, *14*(3), 437-447.

Cilingir Yeltekin, A., & Saglamer, E. (2019). Toxic and trace element levels in *Salmo trutta* macrostigma and *Oncorhynchus mykiss* trout raised in different environments. *Polish Journal of Environmental Studies*, 28(3).

Erenturk, S., Yusan, S., Turkozu, D. A., Camtakan, Z., Olgen, M. K., Aslani, M. A., ... & Isik, M. A. (2014). Spatial distribution and risk assessment of radioactivity and heavy metal levels of sediment, surface water and fish samples from Lake Van, Turkey. *Journal of Radioanalytical and Nuclear Chemistry*, *300*(3), 919-931.

Filipović Marijić, V., & Raspor, B. (2012). Site-specific gastrointestinal metal variability in relation to the gut content and fish age of indigenous European chub from the Sava River. *Water, Air, & Soil Pollution*, *223*(8), 4769-4783.

Mijošek, T., Šariri, S., Kljaković-Gašpić, Z., Fiket, Ž., & Marijić, V. F. (2024). Interrelation between environmental conditions, acanthocephalan infection and metal (loid) accumulation in fish intestine: An in-depth study. *Environmental pollution*, 356, 124358.

Mijošek, T., Marijić, V. F., Dragun, Z., Ivanković, D., Krasnići, N., Redžović, Z., & Erk, M. (2021). Intestine of invasive fish Prussian carp as a target organ in metal exposure assessment of the wastewater impacted freshwater ecosystem. *Ecological indicators*, *122*, 107247.

Naitza, S., Casini, L., Cocco, F., Deidda, M. L., Funedda, A., Loi, A., ... & Secchi, F. (2024). Post-Collisional Tectonomagmatic Evolution, Crustal Reworking and Ore Genesis along a Section of the Southern Variscan Belt: The Variscan Mineral System of Sardinia (Italy). *Minerals*, *14*(1), 65.

Paris, J. R., King, R. A., Ferrer Obiol, J., Shaw, S., Lange, A., Bourret, V., ... & Stevens, J. R. (2025). The Genomic Signature and Transcriptional Response of Metal Tolerance in Brown Trout Inhabiting Metal‐Polluted Rivers. *Molecular ecology*, *34*(1), e17591.

Eyckmans, M., Blust, R., & De Boeck, G. (2012). Subcellular differences in handling Cu excess in three freshwater fish species contributes greatly to their differences in sensitivity to Cu. *Aquatic Toxicology*, 118, 97-107.

Giguère, A., Campbell, P. G., Hare, L., & Couture, P. (2006). Sub-cellular partitioning of cadmium, copper, nickel and zinc in indigenous yellow perch (*Perca flavescens*) sampled along a polymetallic gradient. *Aquatic Toxicology*, 77(2), 178-189.

Goto, D., & Wallace, W. G. (2010). Metal intracellular partitioning as a detoxification mechanism for mummichogs (*Fundulus heteroclitus*) living in metal-polluted salt marshes. *Marine environmental research*, 69(3), 163-171.

Ma, S., & Wang, W. X. (2024). Significance of zinc re-absorption in Zn dynamic regulation in marine fish revealed by pharmacokinetic model. *Environmental Pollution*, *363*, 125106.

Khadra, M., Caron, A., Planas, D., Ponton, D. E., Rosabal, M., & Amyot, M. (2019). The fish or the egg: Maternal transfer and subcellular partitioning of mercury and selenium in Yellow Perch (*Perca flavescens*). *Science of the total environment*, *675*, 604-614.

Kraemer, L. D., Campbell, P. G., & Hare, L. (2006). Seasonal variations in hepatic Cd and Cu concentrations and in the sub-cellular distribution of these metals in juvenile yellow perch (*Perca flavescens*). *Environmental Pollution*, *142*(2), 313-325.

Barst, B. D., Rosabal, M., Campbell, P. G., Muir, D. G., Wang, X., Köck, G., & Drevnick, P. E. (2016). Subcellular distribution of trace elements and liver histology of landlocked Arctic char (*Salvelinus alpinus*) sampled along a mercury contamination gradient. *Environmental Pollution*, *212*, 574-583.

Lapointe, D., & Couture, P. (2009). Influence of the route of exposure on the accumulation and subcellular distribution of nickel and thallium in juvenile fathead minnows (*Pimephales promelas*). *Archives of environmental contamination and toxicology*, *57*(3), 571-580.

Rolland, A., Palmer, M., Chételat, J., Amyot, M., & Rosabal, M. (2025). Subcellular Partitioning of Trace Elements Is Related to Metal Ecotoxicological Classes in Livers of Fish (*Esox lucius*; *Coregonus clupeaformis*) from the Yellowknife Area (Northwest Territories, Canada). *Toxics*, *13*(5), 410.

Rosabal, M., Pierron, F., Couture, P., Baudrimont, M., Hare, L., & Campbell, P. G. (2015). Subcellular partitioning of non-essential trace metals (Ag, As, Cd, Ni, Pb, and Tl) in livers of

American (*Anguilla rostrata*) and European (*Anguilla anguilla*) yellow eels. *Aquatic Toxicology*, *160*, 128-141.

Urien, N., Cooper, S., Caron, A., Sonnenberg, H., Rozon-Ramilo, L., Campbell, P. G., & Couture, P. (2018). Subcellular partitioning of metals and metalloids (As, Cd, Cu, Se and Zn) in liver and gonads of wild white suckers (*Catostomus commersonii*) collected downstream from a mining operation. *Aquatic toxicology*, *202*, 105-116.

Kamaliyan, Z., & Clarke, T. L. (2024). Zinc finger proteins: Guardians of genome stability. *Frontiers in Cell and Developmental Biology*, *12*, 1448789.

Mason, A.Z., Jenkins, K.D. (1995). Metal detoxification in aquatic organisms. In: Tessier, A., Turner, D. (Eds.), *Metal Speciation and Bioavailability in Aquatic Systems*. John Wiley & Sons, Chichester, UK, pp. 479–608

Hamilton, S. J., & Mehrle, P. M. (1986). Metallothionein in fish: review of its importance in assessing stress from metal contaminants. *Transactions of the American Fisheries Society*, *115*(4), 596-609.

Klaverkamp, J.F., Dutton, M.D., Majewski, H.S., Hunt, R.V., Wesson, L.J. (1991). Evaluating the effectiveness of metal pollution controls in a smelter by using metallothionein and other biochemical responses in fish. In: Newman, M.C., McIntosh, A.W. (Eds.), *Metal Ecotoxicology—Concepts and Applications*. Lewis Publishers Ltd., Chelsea, MI, USA, pp. 33–64.

Couture, P., & Rajotte, J. W. (2003). Morphometric and metabolic indicators of metal stress in wild yellow perch (*Perca flavescens*) from Sudbury, Ontario: a review. *Journal of Environmental Monitoring*, *5*(2), 216-221.

Lemly, A. D. (1993). Guidelines for evaluating selenium data from aquatic monitoring and assessment studies. *Environmental monitoring and assessment*, *28*(1), 83-100.

Hamilton, S. J. (2004). Review of selenium toxicity in the aquatic food chain. *Science of the total environment*, *326*(1-3), 1-31.

Zhang, X., Zhang, L., Zhu, J. H., & Cheng, W. H. (2016). Nuclear selenoproteins and genome maintenance. *IUBMB life*, *68*(1), 5-12.

Le Croizier, G., Lacroix, C., Artigaud, S., Le Floch, S., Munaron, J. M., Raffray, J., ... & De Morais, L. T. (2019). Metal subcellular partitioning determines excretion pathways and sensitivity to cadmium toxicity in two marine fish species. *Chemosphere*, *217*, 754-762.

Thomson, A. B. R., Olatunbosun, D., & Valberg, L. S. (1971). Interrelation of intestinal transport system for manganese and iron. *The Journal of Laboratory and Clinical Medicine*, *78*(4), 642-655.

Xu, J. J., Jia, B. Y., Zhao, T., Tan, X. Y., Zhang, D. G., Song, C. C., ... & Luo, Z. (2023). Influences of five dietary manganese sources on growth, feed utilization, lipid metabolism, antioxidant capacity, inflammatory response and endoplasmic reticulum stress in yellow catfish intestine. *Aquaculture*, *566*, 739190.

Chowdhury, M. J., & Blust, R. (2011). Strontium. In: Chris M. Wood, Anthony P. Farrell, Colin J. Brauner (Eds.), *Fish Physiology*. Academic Press, Volume 31, Part B, 2011, pp. 351-390,

Cowan, J.A. (2014). Calcium. In: Maret, W., Wedd, A.G. (Eds.), *Binding, Transport and Storage of Metal Ions in Biological Cell*s. Royal Society of Chemistry, pp. 123–152.

Zhang, W., Huang, L., & Wang, W. X. (2012). Biotransformation and detoxification of inorganic arsenic in a marine juvenile fish Terapon jarbua after waterborne and dietborne exposure. *Journal of Hazardous Materials*, *221*, 162-169.

He, M., Ke, C. H., & Wang, W. X. (2010). Effects of cooking and subcellular distribution on the bioaccessibility of trace elements in two marine fish species. *Journal of Agricultural and Food Chemistry*, *58*(6), 3517-3523.

Zhang, J., Tan, Q. G., Huang, L., Ye, Z., Wang, X., Xiao, T., ... & Yan, B. (2022). Intestinal uptake and low transformation increase the bioaccumulation of inorganic arsenic in freshwater zebrafish. *Journal of Hazardous Materials*, 434, 128904.

Mulkey, J. P., & Oehme, F. W. (1993). A review of thallium toxicity. *Veterinary and human toxicology*, 35(5), 445-453.

Wang, J., Zhang, J., Li, X., Xu, H. Y., Yang, Y., Zhang, J., ... & Han, T. (2025). Metabolism of arginine in juvenile largemouth bass (*Micropterus salmoides*) after oral or intraperitoneal administration of arginine or its substrates. *Amino Acids*, *57*(1), 14.

Krasnići, N., Dragun, Z., Erk, M., & Raspor, B. (2013). Distribution of selected essential (Co, Cu, Fe, Mn, Mo, Se, and Zn) and nonessential (Cd, Pb) trace elements among protein fractions from hepatic cytosol of European chub (*Squalius cephalus* L.). *Environmental science and pollution research*, *20*(4), 2340-2351.

Krasnići, N., Dragun, Z., Kazazić, S., Muharemović, H., Erk, M., Jordanova, M., ... & Kostov, V. (2019). Characterization and identification of selected metal-binding biomolecules from hepatic and gill cytosols of Vardar chub (*Squalius vardarensis* Karaman, 1928) using various techniques of liquid chromatography and mass spectrometry. *Metallomics*, *11*(6), 1060-1078.

APPENDIX C: Distribution of metals among cytosolic proteins of acanthocephalan *Dentitruncus truttae*

1. Materials and methods

Acanthocephalans (*D. truttae*) were isolated from the intestine of *S. trutta* collected at three sites in the upper Krka River, as described in detail in Šariri et al. (2024). Several specimens from the same host fish were pooled to obtain approximately 0.09 g of tissue, which was homogenized on ice in 10 volumes of Tris-HCl homogenization buffer (1:10 w/v), following the protocol described in Šariri et al. (2025a). The cytosolic fraction was obtained by centrifugation at 50,000 × g for 120 min at 4 °C (Avanti J-E, Beckman Coulter, USA) and stored at −80 °C until analysis, according to established methods (Dragun et al. 2020, 2024). Three pooled samples per site were analyzed (n = 9).

Prior to chromatographic separation of biomolecules by molecular mass, cytosols were thawed and centrifuged at 11,000 × g for 10 min at 4 °C. Cytosolic metal-binding biomolecules were separated, and bound metals detected, using a hyphenated SEC–HPLC–ICP-MS system (HPLC: Agilent 1260 Infinity II Bio-Inert LC with a diode array detector; ICP-MS: Agilent 7900; Agilent Technologies, USA). Separation was performed on a Superdex™ 200 Increase 10/300 GL column (Cytiva) with an optimal fractionation range of 10–600 kDa. The mobile phase was 20 mM Tris-HCl buffer (Sigma

Aldrich, USA) (pH 8.1, 22 °C) at a flow rate of 0.5 mL min^{-1}. The injection volume was 100 µL, and each run lasted 60 min.

The column void volume was determined using 1 mg mL^{-1} blue dextran (2000 kDa), which eluted at 16.26 min. Column calibration was performed using six protein standards (thyroglobulin, apoferritin, β-amylase, alcohol dehydrogenase, transferrin, and superoxide dismutase) dissolved in the same 20 mM Tris buffer and run under identical conditions as the samples. Calibration details are presented in Table 1. Additionally, rabbit liver metallothionein standards (MT-1 and MT-2; Enzo Life Sciences, USA) were analyzed, as MTs are important for metal homeostasis and detoxification.

For online quantification of Cu, Zn, Cd, Fe, Mn, Se, As, and Tl, the column effluent was directly introduced into the ICP-MS nebulizer via 0.25 mm tubing, and He was used as a collision gas to minimize polyatomic interferences.

All calculations were performed in Microsoft Excel, and graphs were created in SigmaPlot 11.0 for Windows. Elution times and bioaccumulation responses were determined based on the chromatograms from all nine pooled samples, but for clarity only four representative samples are shown in figures.

Table 1. Molecular masses (MM), concentrations, and elution times (t_e) of blue dextran, the metallothionein standard, and six proteins used for calibration of the Superdex™ 200 10/300 GL size-exclusion column. The calibration line equation was: $K_{av} = -0.226 \times \log(MM) + 1.317$

protein standard	source	t_e / min	MM / kDa	concentration / mg mL^{-1}
thyroglobulin	bovine thyroid	16.79	669	5.0
apoferritin	equine spleen	17.84	443	3.0
β-amylase	sweet potato	19.49	200	4.0
alcohol dehydrogenase	*Saccharomyces cerevisiae*	20.65	150	5.0
transferrin	human	22.57	80	1.0
superoxide dismutase	bovine erythrocytes	26.38	32	5.0
MT1	rabbit liver	30.32	6.145	0.5
MT2	rabbit liver	29.47	6.145	0.5

2. Results and discussion

2.1. Cytosolic metal(loid) levels and biomolecular distribution

Among the studied elements, cytosolic concentrations in *Dentitruncus truttae* followed the order Zn > Fe > Mn > Cu > Se > Cd > As > Tl, with Zn markedly exceeding all others (Table 2). Metal concentrations measured in the whole-body samples from the same campaign showed a similar pattern: Zn > Fe > Cu > Mn > Se > Cd ≥ Tl > As (Mijošek et al. 2024). The dominance of Zn in both cytosolic and whole-body fractions indicates strong physiological regulation and its key metabolic role in *D. truttae* and follows commonly observed high Zn concentrations in fish host intestine, to which this parasite is attached during infection (Cilingir Yeltekin and Saglamer 2019, Šariri et al. 2025b2025b).

Although concentrations of these metals have been reported previously in few species of acanthocephalans, those data refer only to whole-organism levels (Mijošek et al. 2022, 2024, Nachev et al. 2013, Nachev and Sures 2016) and to our knowledge, this is the first study reporting metal(loid) concentrations specifically in the cytosolic, biologically available fraction of acanthocephalans.

Compared with the intestinal cytosol of its final host *Salmo trutta* from the Krka River, Zn, Fe, Se, As, and Tl concentrations were lower in *D. truttae*, while Cu, Mn, and Cd were higher (Mijošek et al. 2019, Šariri et al. 2025b). Relative to intermediate host *Gammarus balcanicus*, Zn, Mn, and Se were higher, Cu and As lower, and Cu, Cd, and Tl comparable, whereas compared with *Echinogammarus acarinatus*, Zn, Fe, and Mn were higher, and Cu, Cd, As, and Tl lower (Mijošek et al. 2019).

Regarding the cytosolic metal levels, in our research the following order was found in *S. trutta*: Zn > Fe > Cu > Se > Mn > Cd > As > Tl (Šariri et al. 2025b), while in the previous campaign during 2015/2016 it was Zn > Fe > Se > Cu ≥ Mn > Cd > As > Tl in *S. trutta* and Zn > Cu > Fe > Mn > Se > As ≥ Cd > Tl in gammarid species (Mijošek et al. 2019).

Table 2. Mean concentrations (± SD) of elements in the cytosolic fraction of the acanthocephalan *Dentitruncus truttae* (n = 9) isolated from the intestine of *Salmo trutta* from the Krka River

	Mn ($\mu g\ g^{-1}$)	Fe ($\mu g\ g^{-1}$)	Cu ($\mu g\ g^{-1}$)	Zn ($\mu g\ g^{-1}$)	Se ($\mu g\ g^{-1}$)	As ($ng\ g^{-1}$)	Cd ($ng\ g^{-1}$)	Tl ($ng\ g^{-1}$)
mean ± SD	1.73 ± 0.26	2.69 ± 0.67	1.09 ± 0.45	14.5 ± 1.7	0.530 ± 0.123	24.7 ± 16.3	82.6 ± 56.2	11.8 ± 10.2

Size-exclusion chromatography (SEC) coupled with inductively coupled plasma mass spectrometry (ICP-MS) was further used to determine the distribution of selected elements among cytosolic biomolecules separated according to their molecular size (Table 3). In the SEC-ICP-MS analysis of metal-binding profiles, biomolecular pools were, according to Krasnići et al. (2013), operationally defined as follows: high molecular mass (HMM; >100 kDa; elution time < 22.2 min), medium molecular mass (MMM; 30–100 kDa; 22.2–26.1 min), low molecular mass (LMM; 10–30 kDa; 26.1–29.4 min), and very low molecular mass (VLMM; <10 kDa; > 29.4 min).

Metal-binding proteins in *D. truttae* have so far been explored only through the analysis of a *de novo* assembled transcriptome (Šariri et al. 2025b). The predicted proteome was analyzed using MeBiPred software to assess potential affinities of proteins for Ca, Co, Cu, Fe, K, Mg, Mn, Na, Ni, and Zn. However, the characterization of metal-binding proteins in acanthocephalans remains challenging due to the scarcity of biochemical data for this group. Further research is therefore needed to elucidate the specific mechanisms of metal handling in these parasites.

The presented SEC-ICP-MS analysis provides a first insight into the distribution of metals among cytosolic protein fractions of *D. truttae*, representing an initial step toward identifying specific metal-binding biomolecules in the organisms characterised by effective metal accummulation, much higher than in other aquatic organisms (Mijošek et al. 2022, Sures et al. 2001). Protein separation of higher resolution could not be achieved at this stage due to the limitations of the Superdex™ 200 10/300 GL column, as evident from the chromatogram shown in Fig. 1. Following separation, UV detection at 280 nm and 254 nm showed that it was possible to detect 16 pools of biomolecules, which eluted over the entire molecular mass

range of the column, with the most prominent peaks in the VLMM range (< 1.5 kDa) at both wavelengths, indicating the predominance of small UV-reactive molecules or peptide-metal complexes within the cytosolic fraction. Biomolecule profiles were similar at both wavelenghts.

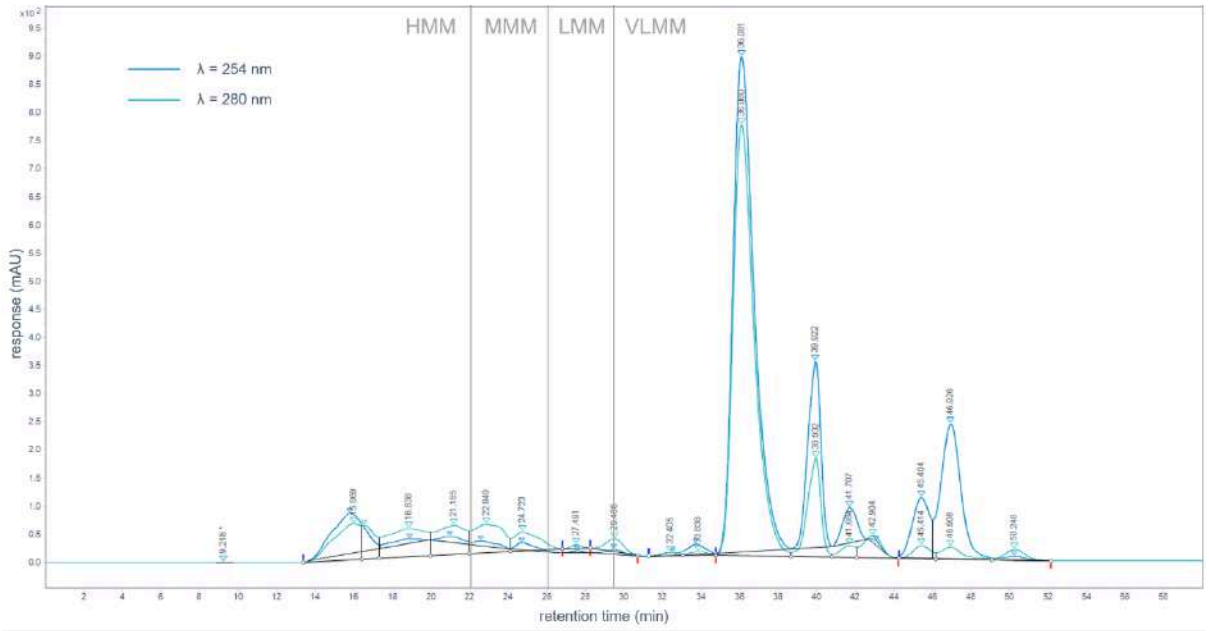

Figure 1. An example of SEC-HPLC chromatogram profile of *Dentitruncus truttae* cytosol (pooled sample of specimens isolated from one fish) after separation on Superdex™200 10/300 GL column, with UV detection at wavelengths of 280 nm and 254 nm

Table 3. Elution times (t_e) and molecular masses (MM) of cytosolic proteins from the acanthocephalan *Dentitruncus truttae*, isolated from the intestine of *Salmo trutta* from the Krka River, corresponding to the SEC-HPLC fractions (Superdex™ 200 Increase 10/300 GL column) in which each element was detected. The t_e and MM values of the most prominent peak for each element are shown in bold.

element		Cu	Zn	Fe	Se	Mn	As	Tl	Cd
[a]HMM peak 1	t_e / min	15.6 (13.5 – 16.2)	17.0 (15.5 – 17.5)	16.8 (15.0 – 17.7)	21.4 (19.2 – 23.9)	16.9 (15.5 – 17.5)	16.4 (14.7 – 17.6)	**17.0 (13.5 – 21.9)**	16.9 (16.0 – 18.0)
	MM / kDa	848 (699 - 1665)	540 (460 - 875)	576 (431 - 1028)	131 (59 - 266)	558 (460 - 875)	655 (445 - 1132)	**540 (112 - 1665)**	558 (392 - 745)
[a]HMM peak 2	t_e / min	17.0 (16.4 – 17.9)	18.9 (18.0 – 19.4)	18.6 (17.9 – 19.8)		18.6 (17.7 – 20.2)	19.2 (18.2 – 20.1)		20.5 (19.5 – 23.9)
	MM / kDa	540 (404 - 655)	293 (250 - 392)	323 (220 - 404)		323 (193 - 431)	266 (199 - 367)		175 (115 - 242)
[a]HMM peak 3	t_e / min	21.6 (21.1 – 22.9)	20.5 (19.7 – 21.0)	21.0 (20.4 – 21.4)		21.5 (19.2 – 23.9)			
	MM / kDa	123 (81 - 145)	175 (149 - 227)	149 (131 - 181)		127 (59 - 266)			
[b]MMM peak 1	t_e / min	**24.9 (24.0 – 26.5)**	22.8 (21.9 – 23.8)	22.6 (21.5 – 23.8)		**24.6 (23.8 – 26.5)**			
	MM / kDa	**42.6 (25.5 - 56.9)**	83.7 (60.7 - 111.7)	89.2 (60.7 - 127.1)		**46.9 (25.5 - 60.7)**			
[b]MMM peak 2	t_e / min		24.7 (24.3 – 25.2)	**24.7 (24.0 – 26.7)**					
	MM / kDa		45.4 (38.7 - 51.6)	**45.4 (23.9 - 56.9)**					
[c]LMM peak 1	t_e / min	27.7 (27.0 – 28.4)	26.0 (25.4 – 26.5)						26.5 (25.4 – 27.6)

	MM / kDa	17.3 (13.8 - 21.7)	29.9 (25.5 - 36.3)					25.5 (17.9 - 36.3)
[c]LMM peak 2	**t_e / min**		**27.9 (26.7 – 28.9)**					
	MM / kDa		**16.2 (11.8 - 23.9)**					
[d]VLMM peak 1	**t_e / min**	30.2 (28.9 – 32.6)	29.6 (29.0 – 31.1)	30.1 (29.0 – 31.2)	36.0 (32.9 – 38.0)	33.8 (32.7 – 34.9)	34.7 (33.6 – 37.7)	**29.5 (28.2 – 31.9)**
	MM / kDa	7.74 (3.58 - 11.76)	9.39 (5.80 - 11.39)	8.00 (5.61 - 11.39)	1.2 (0.63 - 3.25)	2.43 (1.71 - 3.47)	1.82 (0.69 - 2.59)	**9.7 (4.5 - 14.7)**
[d]VLMM peak 2	**t_e / min**	37.2 (35.6 – 37.9)	32.6 (31.6 – 33.6)	33.0 (31.8 – 34.5)	**40.4 (38.2 – 42.8)**	39.9 (38.8 – 40.9)	**39.8 (38.1 – 42.5)**	39.4 (38.5 – 40.2)
	MM / kDa	0.82 (0.65 - 1.36)	3.58 (2.59 - 4.94)	3.15 (1.94 - 4.63)	**0.29 (0.13 - 0.59)**	0.34 (0.25 - 0.49)	**0.35 (0.15 - 0.61**)	0.40 (0.31 - 0.54)
[d]VLMM peak 3	**t_e / min**	39.4 (38.3 – 41.2)	35.8 (35.0 – 37.7)		45.0 (43.0 – 47.2)		45.8 (45.0 – 47.7)	
	MM / kDa	0.4 (0.23 - 0.57)	1.28 (0.69 - 1.65)		0.07 (0.03 - 0.13)		0.05 (0.03 - 0.07)	
[d]VLMM peak 4	**t_e / min**		39.5 (38.4 – 40.3)					
	MM / kDa		0.39 (0.30 - 0.55)					

[d]VLMM peak 5	t_e / min	45.6 (44.8 – 46.7)
	MM / kDa	0.05 (0.04 - 0.07)

[a]HMM peak – a peak of trace element concentration in the cytosolic fractions with a maximum in high molecular mass protein region (>100 kDa)

[b]MMM peak – a peak of trace element concentration in the cytosolic fractions with a maximum in medium molecular mass protein region (30-100 kDa)

[c]LMM peak – a peak of trace element concentration in the cytosolic fractions with a maximum in low molecular mass protein region (10-30 kDa)

[d]VLMM peak – a peak of trace element concentration in the cytosolic fractions with a maximum in very low molecular mass protein region (<10 kDa)

2.2. Copper

Copper (Cu) showed elution peaks across all cytosolic biomolecule size categories (Fig. 2), with a greater number of distinct peaks than reported in most previous studies on cytoplasmic Cu in fish and mussels (Krasnići et al. 2019, Mijošek et al. 2021, Stržak et al. 2014). Although a dominant Cu peak could be identified, it was less pronounced compared to those of other elements, indicating Cu association with a wide variety of biomolecules and its essential biological role as signaling molecule and cofactor in numerous enzymes (Tsang et al. 2021).

In the HMM range (>100 kDa), Cu eluted in three peaks (81–145, 404–655, and 699–1665 kDa). These likely correspond to metalloproteins involved in essential physiological processes, as reported in other organisms (Dragun et al. 2018, Krasnići et al. 2014, Rosabal et al. 2016). The predicted *D. truttae* proteome includes a multicopper oxidase (Šariri et al. 2025b), and homologous enzymes in insects (Diptera) commonly exceed 100 kDa (UniProt: A0A182K9B4, A0AAG5D0M0, A0A182VTH9), matching the HMM region. 2025bPresence in this region can also include other proteins that, in other animals, were identified as β-amylase (200 kDa), transcuprein (270 kDa), hemocyanin (950 kDa in the crab *Metacarcinus magister*), cytochrome oxidase (200–1000 kDa in bovine heart), urate oxidase (120 kDa in mammalian liver), and ceruloplasmin (125 kDa in bovine and 130 kDa in human plasma) (Boivin et al. 2001, Coleman 1974, Liu et al. 2007). However, as metalloproteins in acanthocephalans have not yet been characterized, it is not possible to state with certainty which exact proteins these peaks correspond to.

The dominant Cu peak in *D. truttae* cytosol was detected in the MMM region (25.5 - 56.9 kDa), rather than in the LMM region typically associated with metallothioneins (MTs) in fish (van Campenhout et al. 2008, Krasnići et al. 2013, 2014, 2018, Caron et al. 2018, Urien et al. 2018). MTs are a family of low molecular mass, cysteine-rich proteins, which are involved in homeostasis of essential metals, like Cu and Zn, and detoxification of nonessential metals, like Ag and Cd (Viarengo and Nott 1993). Given the known affinity of Cu for MTs, dominance of Cu peak in MMM region was unexpected. A similar elution pattern has, however, been reported in nematode *Caenorhabditis elegans* and, at elevated Cu levels, in the digestive gland of the mussel *Mytilus galloprovincialis* (Hare et al. 2016, Stržak et al. 2014). An MMM Cu peak, involving proteins as albumin (66 kDa), superoxide dismutase (32 kDa) and carbonic anhydrase (29 kDa), was also previously observed in the intestine of *Salmo trutta* and in the gills of *Carassius gibelio*, but, contrary to our results, it was less pronounced

than the Cu–MT peak in VLMM (Dragun et al. 2020, Mijošek et al. 2021). Two predicted *D. truttae* Cu/Zn-SOD proteins were estimated using ProtParam at ~12 and ~43 kDa (Gasteiger et al. 2005, Šariri et al. 2025b). Ctr-family Cu transporters (20–35 kDa) were also identified, with a predicted molecular mass of 29 kDa (Šariri et al. 2025b).

In acanthocephalans, Cu may follow distinct biochemical pathways compared to fish. The dominance of MMM-bound Cu could relate to higher overall Cu accumulation in acanthocephalans or to the analysis of whole-body cytosol rather than specific tissues as usually performed in fish. An additional explanation may be the presence of MT isoforms with higher molecular masses than the MT standard used for calibration. Supporting this, one predicted *D. truttae* protein classified as Metallothionein family 11 was, based on sequence information, estimated by ProtParam tool in Expasy Server at ~44 kDa, matching the main MMM peak observed in our study (Gasteiger et al. 2005, Šariri et al. 2025b). This MT showed the greatest similarity to a protein from *Pomphorhynchus laevis*, suggesting an acanthocephalan-specific isoform. Other predicted MTs in *D. truttae*, classified as Metallothionein family 5 and most similar to *Trichinella patagoniensis*, were predicted at ~80 kDa, which is encompassed in the peak 81-145 kDa (Šariri et al. 2025b, Table 3).

One smaller Cu peak (13.8–21.7 kDa) was detected in the LMM region. This fraction may correspond to two predicted *D. truttae* galactose-1-phosphate uridyl transferase like proteins, estimated at 13 and 17 kDa, although homologs in other taxa typically exhibit masses of 43–44 kDa (UniProt: A0A6P8HBC6, A0A8C1GVF7, A0A182XFA1, A0A9J7NDS1). Comparable Cu-binding peaks have been reported in *S. trutta* liver (7–24 kDa) and in *Chaoborus* larvae, where 99% of Cu was associated with cytosolic proteins of 1.3–40 kDa (Dragun et al. 2018, Rosabal et al. 2016). Although MTs are often detected in this molecular mass range in fish (Krasnići et al. 2013, 2018, 2019, Dragun et al. 2018), in our study the VLMM peak aligned more closely with MT standards, while the MMM fraction better corresponded with predicted *D. truttae* MT isoforms.

In the VLMM range, Cu eluted as a distinct peak (3.58–11.8 kDa), coinciding with MT standards and indicative of MT-like proteins, along with two smaller peaks (0.23–0.57 and 0.65–1.36 kDa) representing very small Cu-binding molecules. A predicted *D. truttae* protein belonging to Metallothionein family 11 was estimated by ProtParam at ~44 kDa, suggesting atypical structural features or multimeric forms (Šariri et al. 2025b). A cytochrome c oxidase copper chaperone (7–9 kDa in insects) was also predicted in the *D. truttae* proteome with a

mass of ~10 kDa, consistent with this region (Šariri et al. 2025b, UniProt entries A0A9R1SUI3, A0A6P4HNK1, Q9VXY5). Additional binding to metallochaperones or other small proteins involved in intracellular Cu transport is also plausible (Loutet et al. 2015).

With increasing cytosolic Cu concentrations, all peaks increased proportionally, but the relative importance of the Cu–MT peak did not rise to the extent typically observed in fish (Mijošek et al. 2021, Urien et al. 2018, Van Campenhout et al. 2008). Only in sample with the highest Cu levels did the HMM and VLMM peaks become more pronounced, suggesting simultaneous induction of high- and low-molecular-mass Cu-binding biomolecules. Similar responses have been reported in fish, where additional HMM and LMM peaks appear at elevated cytosolic Cu concentrations (Dragun et al. 2018, Krasnići et al. 2014, 2018, Mijošek et al. 2021, Van Campenhout et al. 2010). Since the average cytosolic Cu concentration in *D. truttae* was about twice that in fish, the observed SEC-ICP-MS profiles may reflect a comparable response to higher Cu exposure, although with distinct regulation dynamics. These differences may arise from variations in exposure conditions, metabolism, or metallothionein isoform composition between parasites and their fish hosts. Sequence-based predictions revealed multiple MT isoforms in *D. truttae*, including forms with unexpectedly high molecular masses (up to 255 kDa) that would elute in MMM/HMM regions rather than in the VLMM range typically associated with MTs in vertebrates (Šariri et al. 2025b). This interpretation is supported by the different patterns of MT induction and lack of a significant relationship between MT levels in fish intestine and in their acanthocephalan parasites, indicating species-specific patterns of MT induction (Šariri et al. 2025b). Overall, the results point to a complex Cu-binding profile dominated by the MMM fraction, suggesting that Cu homeostasis in *D. truttae* relies on a broader range of metalloproteins than typically observed in their vertebrate hosts.

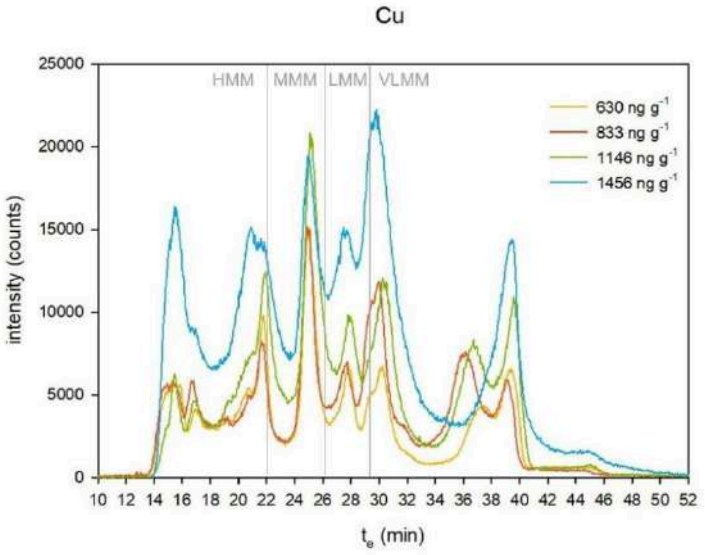

Figure 2. Representative Cu SEC-ICP-MS elution profiles showing the distribution of copper among cytosolic biomolecules of different molecular masses in the acanthocephalan *Dentitruncus truttae* collected from four individual fish

2.3. Zinc and cadmium

Zinc and Cd showed partly similar cytosolic binding patterns in *Dentitruncus truttae*, although the differences in their biological roles were still reflected in their SEC profiles. Zinc, an essential element, was associated with a wide range of cytosolic biomolecules, showing numerous poorly resolved peaks across the entire molecular mass range, while Cd, a non-essential and toxic metal, was eluted predominantly in one distinct peak wile other peaks were relatively low (Fig. 3). Among all analyzed elements, Zn showed the widest distribution with the highest number of peaks (12 in total). This is consistent with results on fish (Krasnići et al. 2013, 2014, Van Campenhout 2008) and its involvement in numerous structural and catalytic proteins (Maret and Li 2009). Cadmium association with fewer proteins reflects its lack of physiological function and preferential binding to detoxifying ligands such as MTs (Genchi et al. 2020). However, a total of five Cd peaks were recorded, contrasting observations in fish where Cd tipically eluted only within a single sharp peak associated to MTs, and no additional Cd-protein associations were observed (Caron et al. 2018, Dragun et al. 2020, Krasnići et al. 2018, 2019, Mijošek et al. 2021, Urien et al. 2018).

In the HMM region, Zn eluted in three peaks (149–227, 250–392, and 460–875 kDa), while Cd appeared in two peaks (115–242 and 392–745 kDa), with the latter detected only at high

cytosolic Cd concentrations. Zinc binding to HMM cytosolic proteins has been observed in literature and often dominates Zn elution profiles in digestive gland of mussels and gill and intestinal tissue of fish (Dragun et al. 2018, 2020, Krasnići et al. 2013, 2014, 2018, Mijošek et al. 2021, Stržak et al. 2014). This HMM range in fish has been linked to Zn association with alcohol dehydrogenase (~150 kDa), a well-known Zn-containing enzyme (Szpunar and Lobinski 1999). Considering acanthocephalans, in the predicted proteome of *D. truttae*, Zn-binding proteins were the most abundant among metal-binding proteins, including more than 240 identified zinc finger (ZNF) proteins (Šariri et al. 2025). As ZNFs are a large and diverse family with variable domain structures, they cannot be assigned to a specific MM range. Additionally, seven proteins were characterized as reprolysin (M12B) family zinc metalloproteases, enzymes involved in tissue remodeling and host–parasite interactions. They are present across animal taxa with molecular masses spanning broad ranges depending on structural complexity (Ali et al. 2014, Williams 2015). Some may correspond to the observed HMM peaks, as one was predicted in ProtParam at 226 kDa and reprolysins in insects have been reported at 160 kDa (Diptera) and 314 kDa (Coleoptera) (UniProt entries: T1PBH2, A0A1I8NDG0, A0AAW1KR02).

Binding of Cd to HMM cytosolic proteins can be considered atypical but has been observed in the digestive gland of *M. galloprovincialis*, liver of *Salmo trutta*, gills of *Squalius cephalus*, and, under high Cd exposure, the intestine of *Carassius gibelio* (Dragun et al. 2018, Krasnići et al. 2019, Mijošek et al. 2021, Stržak et al. 2014). In fish blood plasma, Cd association with HMM proteins has been linked to transferrin (~80 kDa) (Krasnići et al. 2013). Since Cd detoxification in most organisms is primarily mediated by GSH and MTs, the minor Cd peaks in the HMM range in *D. truttae* may reflect incomplete detoxification or binding to acanthocephalan-specific proteins. Our transcriptomic evidence points to the presence of unusually high-mass MT isoforms in *D. truttae*, which could possibly bind Cd and contribute to these peaks, but this should be confirmed in future studies.

Two Zn peaks were recorded (38.7–51.6 and 60.7–111.7 kDa) in the MMM region. Theymay include several Zn-binding enzymes identified in the predicted proteome of *D. truttae*. The peak corresponding to predicted *D. truttae* MT ~44 kDa was less prominent than for Cu, indicating metal-specific binding. Multiple reprolysin (M12B) metalloproteases predicted at 49, 66, 69, and 91 kDa fall within this range, as well as homologous proteins in nematodes (UniProt: A0A0D6MA85, A0AAD4N991, A0AAD4NAK5) and ticks (38–62 kDa; Ali et al. 2014). Another Zn-binding protein group that can belong to MMM in *D. truttae* (predicted 79

kDa) and nematodes (UniProt: Q21432, P98060, Q20176, P55113, Q93243) are astacins. Astacins are a family of zinc metalloproteases belonging to the peptidase family M12, which are among the most abundantly secreted proteins in helminths, facilitating infection and host establishment through tissue migration and immune evasion (Martín-Galiano and Sotillo 2022). Matrix metalloproteinases (MMPs or matrixins), another large family of metalloproteases present in the *D. truttae* proteome, may also contribute to MMM peaks. Homologous proteins with molecular masses in this range have been reported in nematodes (UniProt: A0A0B1T8S1, A0AAF5PQG4), insects (A0AAW1MER4), and echinoderms (P91953). These Zn-containing endopeptidases degrade components of the extracellular matrix and participate in numerous physiological and pathological processes, including immune responses and helminth infections. In parasitic infections of the central nervous system, MMP activity facilitates inflammatory cell and parasite migration and disrupts blood–brain barrier integrity (Bruschi and Pinto 2013). In fish, this MM range is typically associated with Zn binding to transport proteins such as albumin (66 kDa) and transferrin (~80 kDa), as well as cytosolic enzymes carbonic anhydrase (30 kDa), SOD (32 kDa), and alcohol dehydrogenase (80 kDa) (Dragun et al. 2020, Krasnići et al. 2014, 2018, 2019, Mijošek et al. 2021), reflecting the essential structural and catalytic roles of Zn in a wide range of proteins and enzymes.

Cadmium was not detected in the MMM fraction, consistent with previous studies in *Chaoborus* larvae and most fish species (Krasnići et al. 2019, Mijošek et al. 2021, Rosabal et al. 2016, Urien et al. 2018). Cadmium elution in this range has only been reported in the digestive gland of *M. galloprovincialis*, where it was linked to metallothioneins (Strižak et al. 2014). The absence of Cd in the MMM fraction in *D. truttae* therefore supports its preference for thiol-rich cytosolic ligands such as GSH and MTs rather than other cytosolic proteins.

In the LMM region, Zn eluted in two peaks (11.8–23.9 and 25.5–36.3 kDa) and Cd only in one (17.9–36.3 kDa). In several studies, peaks in this molecular mass range (10–30 kDa) have frequently been interpreted as metallothioneins (MTs), due to their correspondence with elution time of MT standards (Dragun et al. 2018, 2020, Krasnići et al. 2013, 2014, 2018, Mijošek et al. 2021, Urien et al. 2018). In the present study, the MT standard eluted at ~30 min (6 kDa), corresponding more closely to the VLMM peaks, buth higher MM of 11-18 kDa are often attributed to MT dimers and different isoforms. Further, MT and MT-like proteins have not yet been characterized in acanthocephalans, and MT isoforms in invertebrates are known to differ widely in molecular mass, ranging from 10 to 20 kDa (Strižak et al. 2014), so

LMM peaks may include MT isoforms not matching the calibration standards. The most prominent Zn peak in *D. truttae* cytosol was observed in LMM region, with a maximum at 16.2 kDa. Similarly, in *Chaoborus* larvae, approximately 80% of cytosolic Zn was bound to biomolecules of 3.1–40 kDa (Rosabal et al. 2016). Several homologs of matrix metalloproteinases (matrixins) in nematodes fall within this mass range (UniProt: A0A368FVY2, A0A1Y3E6J2, A0A0D6LR63, A0A0B1T0S8, A0A368GUR9), aligning with a predicted *D. truttae* matrixin/reprolysin (M12B) zinc metalloprotease estimated at 16 kDa (Šariri et al. 2025b). In fish hepatic cytosol, Zn in LMM region primarily associates with MTs, and enzymes like SOD isoforms (31, 15.5 or 7.75 kDa) orhemoglobin subunits (~15 kDa) (Dragun et al. 2018, Krasnići et al. 2018, 2019).

In the intestine of *S. trutta*, most Cd eluted in a peak corresponding to biomolecules of 11–18 kDa, interpreted as MT dimers, while considering that SEC–HPLC can also overestimate the molecular masses of small proteins (Krasnići et al. 2019, Mijošek et al. 2021). In *S. trutta* liver, Cd similarly eluted in the LMM region, corresponding to biomolecules of 7–24 kDa (maximum around 15 kDa), and was likewise attributed to MTs (Dragun et al. 2018).

Both Zn and Cd exhibited peaks in the VLMM region, most likely corresponding to MT-like proteins. Based on MT standards used in this study and the reported molecular masses of MTs in various invertebrates (UniProt: P17511, Q8I9B4, P80246, P33187, P55951), the Zn peak with a maximum at 9.4 kDa and the Cd peak at 9.7 kDa correspond well with MT elution. Zn showed several additional peaks within this range (0.04–11.39 kDa), consistent with strong Zn association with low-mass ligands in mussels (Ferrarello et al. 2002, Strižak et al. 2014) and fish (Dragun et al. 2018, 2020, Krasnići et al. 2013, 2018, Mijošek et al. 2021). Binding to molecules from 5.8-11.39 kDa could represent binding to MTs, but it is known that they occur in many isoforms, and their induction can be isoform- and metal-specific (Strižak et al. 2014). This phenomenon of differential metal-binding by specific MT isoforms, observed in diverse taxa, may reflect the distinct physiological roles of each isoform in metal detoxification and regulation (Krasnići et al. 2019). Zn association with molecules <5 kDa, as seen in fish gills (Dragun et al. 2020; Krasnići et al. 2014), may represent binding to metallochaperones or glutathione (GSH).

The most prominent Cd peak was recorded in the VLMM range (4.5–14.7 kDa), corresponding to the elution of MT standards, with additional minor peak occuring at 0.31–0.54 kDa. Cd binding to MTs was expected and is consistent with findings in insects

(Rosabal et al. 2016), mussels (Ferrarello et al. 2002, Strižak et al. 2014), and fish (Dragun et al. 2020, Krasnići et al. 2019, Mijošek et al. 2021, Van Campenhout et al. 2010). Strong Cd–MT binding confirm the well-known high affinity of Cd for MTs and is considered a key mechanism of protection against its toxicity (Viarengo and Nott 1993).

With increasing Zn accumulation, all Zn peaks rose proportionally. The relative contribution of the classic MT fraction did not increase, indicating that Zn was mainly bound to functional proteins rather than to newly synthesized MTs. This contrasts with most fish studies, where MT pools induction becomes more prominent at elevated Zn exposure (Dragun et al. 2020, Van Campenhout et al. 2010). Still, an exception was observed in the liver of *S. trutta*, in which increased Zn bioaccumulation resulted with higher association within the HMM region (Dragun et al. 2018). Binding to MT isoforms of higher molecular mass predicted in *D. truttae* also cannot be excluded. In contrast, higher Cd accumulation caused an increase in both LMM and VLMM peaks, along with the appearance of an additional HMM peak at the highest Cd concentration (Fig. 3). Progressive Cd binding to the MT fraction is typical and has been widely documented (Caron et al. 2018, Dragun et al. 2018, Krasnići et al. 2013, 2018, Mijošek et al. 2021, Strižak et al. 2014). The emergence of additional Cd peaks is less common but has been observed in the intestine of *Carassius gibelio* (Mijošek et al. 2021).

Overall, the Zn and Cd profiles in *D. truttae* suggest overlapping but distinct binding patterns, reflecting the contrasting physiological roles of Zn as essential metal integrated into cellular functions and Cd as non-essential metal requiring detoxification. Compared to vertebrate hosts, D. truttae appears to rely on a broader and more diverse network of metal-binding proteins, potentially including various MT isoforms, multiple metalloproteases, and Zn-dependent enzymes, highlighting a unique metallome organization in these specific group of parasites. Due to their well known role of effective accumulation of non-essential elements like Cd (Filipović Marijić et al. 2014, Mijošek et al. 2022), it is expected that they have additional defense mechanisms and detoxifying molecules.

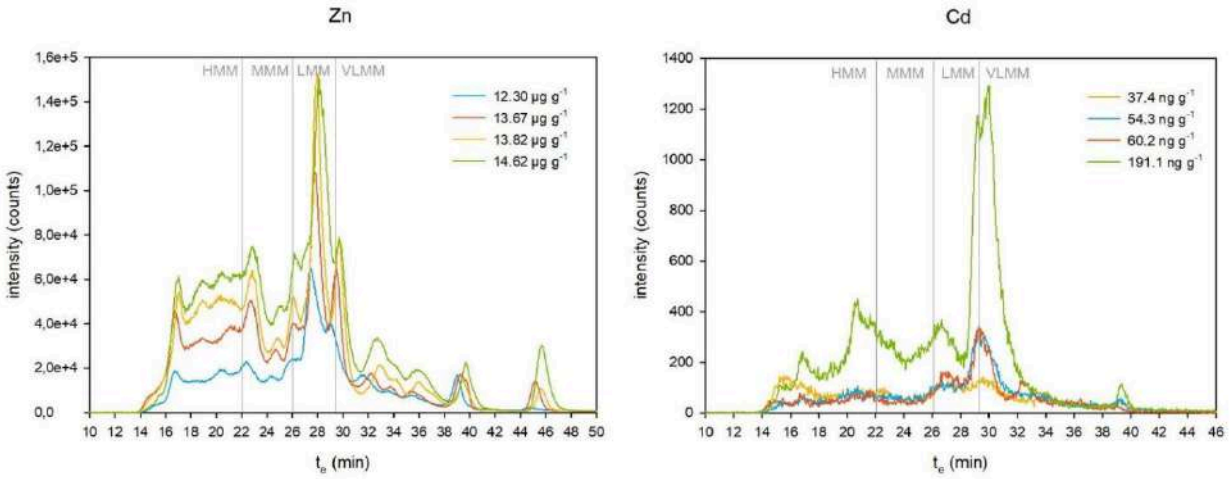

Figure 3. Representative Zn and Cd SEC-ICP-MS elution profiles showing the distribution of copper among cytosolic biomolecules of different molecular masses in the acanthocephalan *Dentitruncus truttae* collected from four individual fish

2.4. Iron and manganese

Iron and Mn exhibited broadly similar SEC–ICP–MS elution patterns, characterized by a dominant MMM peak and several minor peaks in the HMM and VLMM regions (Fig. 4). Such distribution across a wide molecular-mass range is typical for essential trace elements and agrees with previous observations in fish tissues (Krasnići et al. 2014, Mijošek et al. 2021). However, while Fe and Mn in fish organs usually elute in two, and only occasionally three to four peaks, the *D. truttae* cytosol displayed six to seven distinct peaks for both metals. A similarly complex Fe distribution was reported in the nematode *C. elegans*, where four to five peaks were detected (Hare et al. 2016), suggesting a more heterogeneous metal-binding pattern in invertebrates. This broader distribution corresponds to the diverse biochemical roles of Fe and Mn. Fe is involved in redox reactions and mitochondrial respiration, DNA synthesis and neurotransmitter production, while Mn acts as a cofactor in enzymes linked to growth, reproduction, carbohydrate and lipid metabolism, and immune function (Dragun et al. 2018, Hirst 2013, Kuhn et al. 2016, Mogobe et al. 2015). Excessive levels of either metal can be toxic and may also alter cytosolic binding patterns (Dragun et al. 2024, Kalisińska and Budis 2019).

Three HMM peaks were observed for both metals. Fe peaks were detected at 131–181 kDa, 220–404 kDa and 431–1028 kDa, while Mn peaks eluted at 59–266 kDa, 193–431 kDa and 460–875 kDa. In the predicted proteome of *D. truttae*, a putative Fe-binding protein annotated

as eukaryotic translation initiation factor 4E binding protein (EIF4EBP)/Ankyrin repeats was predicted by ProtParam at ~131 kDa, although EIF4EBP proteins are typically much smaller (around 13 kDa in some insects, UniProt entries: A0A023F7X9, T1P958, A0AAW1JKL5). This is probably a larger multidomain ankyrin-repeat protein that contains a small conserved motif similar to EIF4EBP, resulting in a false positive annotation. Similarly, a predicted 50S ribosome-binding GTPase (~105 kDa by ProtParam and similar in nematodes under UniProt entries A0A2A6BWF9 and A0A2A6BW85) is not typically Fe-binding, suggesting complicated annotation interpretation. Fe binding to HMM biomolecules is widely reported in aquatic species and is most commonly attributed to ferritin (~450 kDa), the primary Fe-storage protein (Dragun et al. 2020, 2022, Krasnići et al. 2014, 2018, 2019, Mijošek et al. 2021). A ferritin-like domain was identified in predicted protein of *D. truttae* (Šariri et al. 2025b). Although apoferritin run through the same SEC column eluted at ~443 kDa, MM of this protein estimated at only 23 kDa by ProtParam. Predominant Fe elution in the HMM region has been documented in nematode *C. elegans*, bivalves, and fish liver and intestine (Dragun et al. 2022, Ferrarello et al. 2002, Hare et al. 2016, Krasnići et al. 2019). Another Fe-binding protein refered to in the literature is transferrin, the main protein responsible for Fe transport to target organs (Ferrarello et al. 2002). It has been demonstrated that Fe profile is tissue-specific and reflects the specific function of each organ. Generally, HMM peaks in fish are far more pronounced in liver than in gills and intestine, due to the liver's dominant role in Fe storage (Dragun et al. 2020, Krasnići et al. 2018, Mijošek et al. 2021). Since *D. truttae* lacks digestive and circulatory systems, and the whole body was used in this study, some differences in SEC profiles are expected and should be interpreted cautiously. Mn was also recorded in HMM fractions in liver of several fish species, typically within 80–400 kDa, occasionally extending to ~1000 kDa (Dragun et al. 2018, 2022, Krasnići et al. 2013, 2018, 2019). Predominant binding of Mn to HMM biomolecules was reported in the liver of *S. vardarensis* and *S. cephalus* and can be explained by the essential function of these metals in the activities of numerous enzymes (Krasnići et al. 2013, 2019). Mn-binding HMM proteins reported in fish include Mn-SOD, arginase (~100 kDa both), transferrin (~80 kDa) and albumin (~66 kDa) (Krasnići et al. 2013, 2014).

Both metals showed dominant MMM peaks (Fe around 23.9–56.9 kDa, Mn around 25.5–60.7 kDa), with Fe displaying one additional peak at 60.7–127.1 kDa. Several *D. truttae* predicted proteins fall within these ranges. A putative Fe-binding protein annotated as Oxoglutarate and iron-dependent oxygenase degradation C-term was predicted by ProtParam at 57 kDa,

comparable to data on insects (UniProt entries: A0AAW1HUR6, A0ABN7AVD0). This domain belongs to the large superfamily of Fe(II)/2-oxoglutarate (2OG)-dependent oxygenases, which play important roles in a variety of catalytic reactions and are involved in fundamental biological processes (Herr and Hausinger 2018). Fe/Mn-SOD was also identified in *D. truttae* and predicted at MMs of 13 and 26 kDa, while in protists and algae they tend to be slightly bigger, in LMM and MMM ranges (UniProt A0A7G2CIC7, A0A1G4IIN1, A0A509GHP8, A0A4Y1PAR8). Several 2Fe–2S iron–sulfur cluster proteins were predicted at 11, 46, 79 and 297 kDa, consistent with known LMM–MMM ranges in invertebrates ((Uniprot A0A0B1SN13, A0A1I7VDY1, A0AAW1KJ97). Predicted catalases ranged from 10–62 kDa, with the 62 kDa protein matching catalase subunits from invertebrates (UniProt entries P17336, Q27487, P90682) and fish (Martin-Antonio et al. 2009).

The MMM region has frequently been associated with Fe- and Mn-binding biomolecules in liver, intestine and gills of fish (Dragun et al. 2020, 2022, Krasnići et al. 2013, 2018, 2019, Mijošek et al. 2021). In gill tissue, and intestine of *S. trutta*, Fe MMM peak was the dominant one (Dragun et al. 2020, Krasnići et al. 2013, 2019, Mijošek et al. 2021). Fe peaks between ~30–80 kDa have been attributed to hemoglobin (64 kDa), monomers (15 kDa), dimers (~30-31.5 kDa) and trimers (~45-47 kDa) of its subunits, transferrin (~80 kDa), ferroportin (~63 kDa), catalase subunits (~60 kDa), and myoglobin (~17 kDa) (Asmamaw 2016, Dragun et al. 2020, 2022, Krasnići et al. 2019, Mijošek et al. 2021, Wolf et al. 2007). Similarly, Mn peaks in the MMM region (typically ~35–90 kDa) have been linked to albumin (66 kDa) and transferrin (80 kDa), key Mn transport proteins (Dragun et al. 2018, 2022, Krasnići et al. 2019). Thus, the MMM Fe and Mn peaks in *D. truttae* might reflect a mixture of transport, enzymatic, and heme-associated proteins, although further biochemical validation is needed.

Peaks in LMM area were not detected for either Fe or Mn. This is consistent with most studies on mussels and fish livers and gills, where LMM peaks are typically absent (Ferrarello et al. 2002, Dragun et al. 2020, 2022, 2024, Krasnići et al. 2018, 2019). Occasional Mn LMM peaks have been reported in some fish species (Dragun et al. 2018, Krasnići et al. 2013).

Two minor VLMM peaks were recorded for Fe (1.94–4.63 and 5.61–11.39 kDa) and Mn (0.25–0.49 and 1.71–3.47 kDa). Such peaks were not reported in most studies on mussel or fish liver and gills (Dragun et al. 2018, 2024, Ferrarello et al. 2002, Krasnići et al. 2013, 2014, 2018, 2019), indicating potentially different low-molecular-mass metal ligands in *D. truttae.* Among predicted Fe-binding proteins of *D. truttae*, one sequence annotated as dynein light

chain type 1 and has a theoretical MM of 17 kDa, which corresponds to values within LMM range reported for cestodes (UniProt: A0A183TJA2, A0A183SQW8, A0A068Y4V9). Dynein is a large multisubunit complex that carries out a wide variety of tasks in the cytoplasm of most eukaryotic cells. In animal cells, it is responsible for microtubule movements and transporting various cargoes, such as vesicles, mRNA particles, and organelles (Trokter et al. 2012). However, VLMM Fe peaks are more plausibly attributed to small Fe species or low-molecular-mass ligands (such as citrate and ATP), as previously reported in *C. elegans* larvae (Hare et al. 2016) and in fish liver and intestine, where Fe and Mn were occasionally detected in VLMM fractions associated with nucleotides, citrates, pyrophosphates, amino acids, and other small complexes (Beard et al. 1996, Dragun et al. 2018, 2022, Mijošek et al. 2021).

Increasing Fe concentration was accompanied by a rise in MMM peaks and in the last VLMM peak (maxima ~3.15, 45.4 and 89.2 kDa), with the largest change in the second MMM peak (45.4 kDa). The specimen with the lowest Fe concentration lacked the first MMM peak and all VLMM peaks. This contrasts with fish liver, where Fe accumulation mainly enhances the HMM peak due to ferritin induction (Dragun et al. 2020, 2022, Krasnići et al. 2013, 2018). In fish intestine, increases may occur in either MMM or HMM fractions (Mijošek et al. 2021), whereas in *D. truttae* the response is clearly MMM-dominated. In fish gills, only slight increases in MMM peaks occur with rising Fe concentrations (Krasnići et al. 2014, 2018).

For Mn, increasing concentrations generally led to higher MMM and VLMM peaks (maxima ~0.34 and 46.9 kDa), while no clear changes occurred in other peaks. The specimen with the lowest Mn concentration lacked the third HMM peak and the final VLMM peak. Because Mn is tightly regulated within a narrow physiological range, shifts in peak profiles are typically weak or inconsistent in fish cytosols (Krasnići et al. 2013, 2018, Dragun et al. 2018, 2022). Previous studies similarly reported minimal or specimen-specific changes, with many profiles remaining nearly identical (Krasnići et al. 2018).

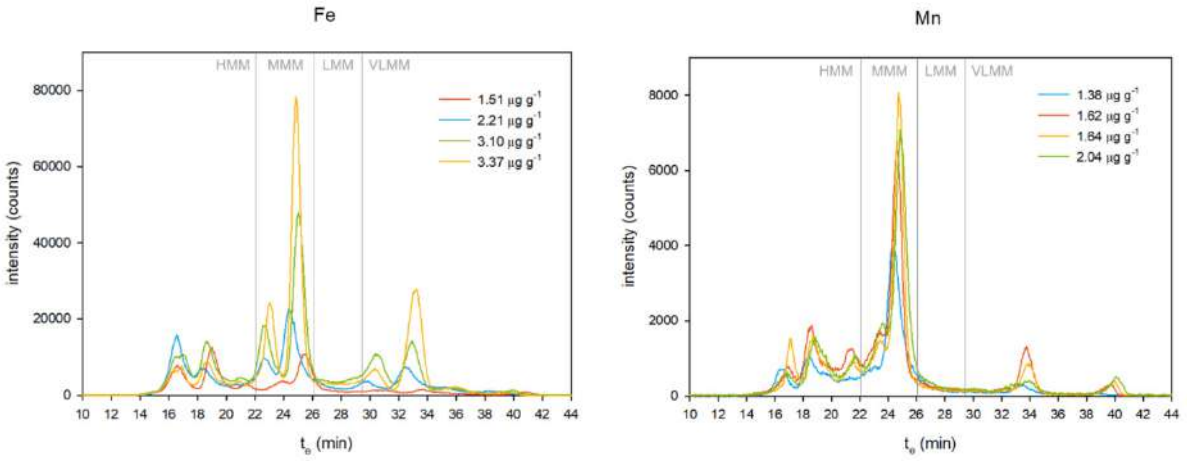

Figure 4. Representative Fe and Mn SEC-ICP-MS elution profiles showing the distribution of copper among cytosolic biomolecules of different molecular masses in the acanthocephalan *Dentitruncus truttae* collected from four individual fish

2.5. Selenium and arsenic

Selenium and As showed comparable elution patterns in *D. truttae*, with the most prominent peaks in the VLMM range and secondary peaks in the HMM range (Fig. 5). HMM peaks were relatively more important in case of Se than As. Despite similar VLMM peaks (co-elution) observed for both metalloids, previous study on fish and their distinct biochemical properties suggest that different biomolecules are involved in their intracellular handling (Urien et al. 2018). Selenium is an essential trace element incorporated mainly as selenocysteine into selenoproteins such as glutathione peroxidase and thioredoxin reductase, or nonspecifically as selenomethionine within proteins. Although it is required for cellular redox regulation, it has a narrow range between essential and threshold toxic levels (Wrobel et al. 2016, Lopez Heras et al. 2011). Selenomethionine is often the dominant Se form in aquatic organisms and plays a major role in dietary uptake and bioaccumulation (Bakke et al. 2010). In contrast, As is a non-essential toxic metalloid that binds nonspecifically to reduced thiols, including cysteine residues, zinc-finger motifs, RING-finger domains, and glutathione, often disrupting protein function and triggering cellular responses (Shen et al. 2013, Vergara-Gerónimo et al. 2021). While Se distribution in fish cytosol has been relatively well characterized, revealing species-specific patterns among leuciscid, cyprinid, and salmonid fish, corresponding data for As are largely lacking (Dragun et al. 2022, Mijošek et al. 2021). Environmental factors influence As speciation and further modulate its association with

biomolecules (Strižak et al. 2014). In *D. truttae*, four Se peaks were observed, consistent with most studies on fish (Dragun et al. 2018, 2020, 2022, Krasnići et al. 2014, 2018, Urien et al. 2018), whereas the five As peaks exceeded the number reported for fish and mussels, which is usually three or four (Strižak et al. 2014, Urien et al. 2018).

In the HMM range, one Se peak (59–266 kDa) and two As peaks (199–367 and 445–1132 kDa) were recorded in *D. truttae* cytosol. The presence of Se in HMM fractions is consistent with findings in fish organs, where Se frequently associates with higher-mass biomolecules (Dragun et al. 2018, 2020, Krasnići et al. 2014, 2018). In the liver of *S. trutta*, Se peaks in HMM biomolecule region were barely visible, while in liver of *C. gibelio*, most Se eluted in the HMM region (Dragun et al. 2018, 2020). Similar HMM maxima were reported for the liver of *S. vardarensis* (Krasnići et al. 2018). The prominence of hepatic HMM peaks in fish is attributed to the liver's central role in selenoprotein synthesis and Se catabolism (Dragun et al. 2020). Se elution in the HMM range has also been recorded in the gills of *S. cephalus* and *C. gibelio* (Krasnići et al. 2014). In the intestine of *S. trutta*, peaks in HMM region were barely visible only in some specimens, while in intestine of *C. gibelio*, a significant part of Se was eluted in HMM peaks (Mijošek et al. 2021). Since the Se HMM peak was in most fish studies wide and extended into the MMM range, it corresponded to molecular masses of several well-known selenoproteins, such as glutathione peroxidase (85 kDa, homotetramer ~96 kDa) and thioredoxin reductase (64-66 kDa) which participate in the defense against oxidative stress, and iodothyronine deiodinase (65 kDa) involved in thyroid hormone metabolism (Dragun et al. 2020, 2022, Mijošek et al. 2021, Krasnići et al. 2013).

Binding of As to HMM biomolecules was unexpected, as it does not have specific high-mass transport proteins (Shen et al. 2013). This strategy might be specific for Acanthocephala, as in previous studies on mussels and fish As elution in the HMM region was negligible (Strižak et al. 2014, Urien et al. 2018). Two HMM peaks observed in *D. truttae* probably show As binding to high-mass thiol-rich proteins or oligomeric cytosolic complexes with high cysteine content, but they need further characterization. In humans, it has been confirmed that As binds to glucocorticoid receptor, which belongs to HMM range (Bamberger et al. 1996, Spuches and Wilcox 2008). In its unliganded state, it is retained in the cytosol as part of a large heteromeric chaperone complex containing Hsp90, Hsp70, p23, and immunophilins which also have high MMs (Stancato et al. 1996).

In *D. truttae*, no peaks were detected in the MMM range for either Se or As, consistent with the literature data on mussles and various tissues from several fish species in which Se and As elution in the MMM region was negligible (Krasnići et al. 2013, 2018, Dragun et al. 2018, 2020, Strižak et al. 2014, Urien et al. 2018). However, Se association with heat-sensitive MMM proteins has been reported in hepatic and gill cytosol of *S. vardarensis* (10–140 kDa) and in hepatic cytosol of *E. lucius* the main portion of Se being eluted in this MM range (35–60 kDa) (Dragun et al. 2022, Krasnići et al. 2019). Although As binding to hemoglobin (64 kDa) and, to a lesser extent, transferrin (~80 kDa) has been demonstrated in mammalian blood (Shen et al. 2013), no corresponding peaks were observed in *D. truttae*.

No Se peaks were detected in the LMM biomolecule range in *D. truttae*. In fish such as *S. cephalus*, *S. vardarensis* and *Catostomus commersonii*, Se elution in the LMM region has been reported and attributed to selenoproteins involved in redox regulation, particularly glutathione peroxidase, whose subunits elute at approximately 23 kDa (Krasnići et al. 2013, 2014, 2018, Urien et al. 2018). Possible Se association to MTs was suggested in *S. cephalus*, although no corresponding peaks were observed in *D. truttae* (Krasnići et al. 2013). In line with previous findings from mussels and fish, As binding to LMM biomolecules was not detected (Strižak et al. 2014, Urien et al. 2018).

Three peaks were detected in the VLMM range for both Se (0.03–0.13, 0.13–0.59 and 0.63–3.25 kDa) and As (0.03–0.07, 0.15–0.61 and 0.69–2.59 kDa), with the middle peak being the most prominent. Se association with VLMM biomolecules is well documented in fish. Se elution in VLMM region was predominant in in liver of *S. trutta*, *S. vardarensis* and *C. commersonii,* gills of *C. gibelio, S. cephalus and S. vardarensis* as well as in intestine of *S. trutta*, whereas in liver of *S. cephalus, C. gibelio* and *E. lucius* it was only minor (Dragun et al. 2018, 2020, 2022, Krasnići et al. 2013, 2014, 2019, Mijošek et al. 2021). Association to VLMM compounds in fish could refer to small selenocompounds involved in antioxidant defense or Se metabolism, such as free selenocysteine (~0.2 kDa), or antioxidative compounds selenomethionine (~0.2 kDa), selenoneine (~0.5 kDa) and selenoprotein W (SelW) (~10 kDa) (Dragun et al. 2018, 2020, 2022, Krasnići et al. 2018, Mijošek et al. 2021). VLMM compounds often act as intermediates in selenoprotein biosynthesis and may be especially abundant at tissues involved in water and dietary uptake, like gills and intestine (Dragun et al. 2020). Consistent with previous studies on fish tissues, the VLMM region likely represents heat-stable selenocompounds rather than metallothionein-bound Se (Urien et al. 2018).

Predominant As elusion within the VLMM range has previously also been observed in the liver, ovaries and testes of *C. commersonii* and in the digestive gland of *M. galloprovincialis* (Strižak et al. 2014, Urien et al. 2018). Although As has strong affinity for thiol-rich molecules and can bind to low-mass stress proteins such as MT (6–7 kDa) and ubiquitin (7–8 kDa) in some taxa, literature data for fish indicate that As does not associate with MT (Shen et al. 2013, Strižak et al. 2014, Urien et al. 2018), which is consistent with the patterns observed in *D. truttae*.

In *D. truttae*, Se did not exhibit a clear pattern of peak intensification with increasing cytosolic concentrations, a trend also reported for the liver of *E. lucius* (Dragun et al. 2022). Previous studies in fish have shown that Se bioaccumulation can lead to increased peak heights in different molecular-mass fractions, but these responses are highly species- and tissue-specific. For example, in the liver, Se accumulation resulted in increased VLMM peaks in *S. trutta* and *C. commersonii*, increases in both LMM and VLMM peaks in *S. cephalus* and *S. vardarensis*, and a pronounced increase in HMM peaks in *C. gibelio* (Dragun et al. 2018, 2020, Krasnići et al. 2013, 2018, Urien et al. 2018). Responses in gill tissue were more consistent across species, with Se-responsive biomolecules occurring exclusively in the VLMM region in *C. gibelio*, *S. vardarensis* and *S. cephalus* (Dragun et al. 2020, Krasnići et al. 2014, 2018). In intestinal tissue, Se responded within both the HMM and VLMM ranges in *C. gibelio*, whereas only VLMM-associated biomolecules were observed in *S. trutta* (Mijošek et al. 2021).

In *D. truttae*, increasing As concentrations were associated with increased hight of the second VLMM peak (0.15–0.61 kDa), consistent with findings in the liver and testes of *C. commersonii* (Urien et al. 2018). However, previous studies suggest that As exposure does not necessarily induce specific As-binding biomolecules, but rather that As likely binds to cytosolic compounds that are constitutively present or induced by other environmental stressors, including co-occurring trace elements. This interpretation is supported by observations in mussels, where LMM peak area was negatively correlated with cytosolic As levels, indicating a limited role in As detoxification (Strižak et al. 2014).

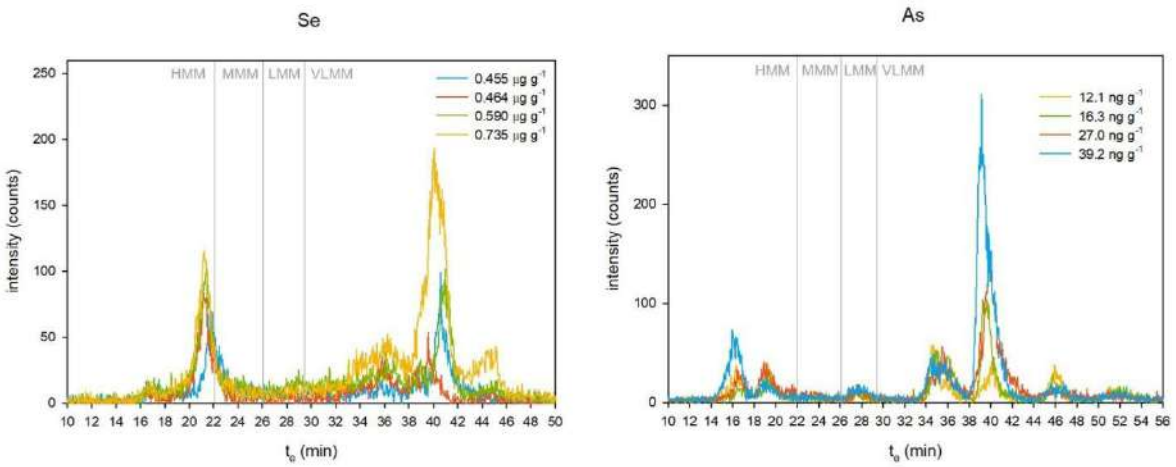

Figure 5. Representative Se and As SEC-ICP-MS elution profiles showing the distribution of copper among cytosolic biomolecules of different molecular masses in the acanthocephalan *Dentitruncus truttae* collected from four individual fish

2.6. Thallium

Thallium was the only metal in *D. truttae* that eluted entirely within a single peak in the HMM region (112–1665 kDa) (Fig. 6). Such a distribution pattern is characteristic of non-essential and highly toxic metals that associate with a limited set of cytosolic biomolecules, and it aligns with reports of Tl eluting in one or two peaks in fish and Chaoborus larvae (Caron et al. 2018, Dragun et al. 2018, Rosabal et al. 2016). Tl has no known biological function and is extremely toxic even at low concentrations due to its interference with potassium-dependent processes (Avendaño-Briseño et al. 2025). In the liver of *S. trutta*, the primary Tl peak was also detected in the HMM range and was linked to enzymes aldehyde dehydrogenase (187 kDa) and (Na^+/K^+)-ATPase (274–280 kDa), both known to be activated by Tl, whereas in *Perca flavescens* the HMM-associated Tl fraction was minor (Caron et al. 2018). Although Tl binding to small biomolecules has been reported in aquatic organisms, no MMM, LMM, or VLMM peaks were observed in *D. truttae*. In fish liver, an additional VLMM Tl peak was sometimes visible in *S. trutta* and LMM Tl peaks predominated in *P. flavescens* (Caron et al. 2018), whereas Chaoborus larvae bound Tl exclusively to LMM thermostable ligands, likely amino or organic acids (malate, citrate, histidine, cysteine) (Rosabal et al. 2016). In *D. truttae*, increasing cytosolic Tl concentrations were accompanied by an increase in the height of the HMM peak, a trend similarly reported in fish liver and interpreted as evidence of incomplete Tl detoxification (Caron et al. 2018,

Dragun et al. 2018). These findings imply that *D. truttae* relies primarily on high-mass cytosolic proteins for Tl handling, which may be helpful in further studies on Acanthocephala metal-binding protens.

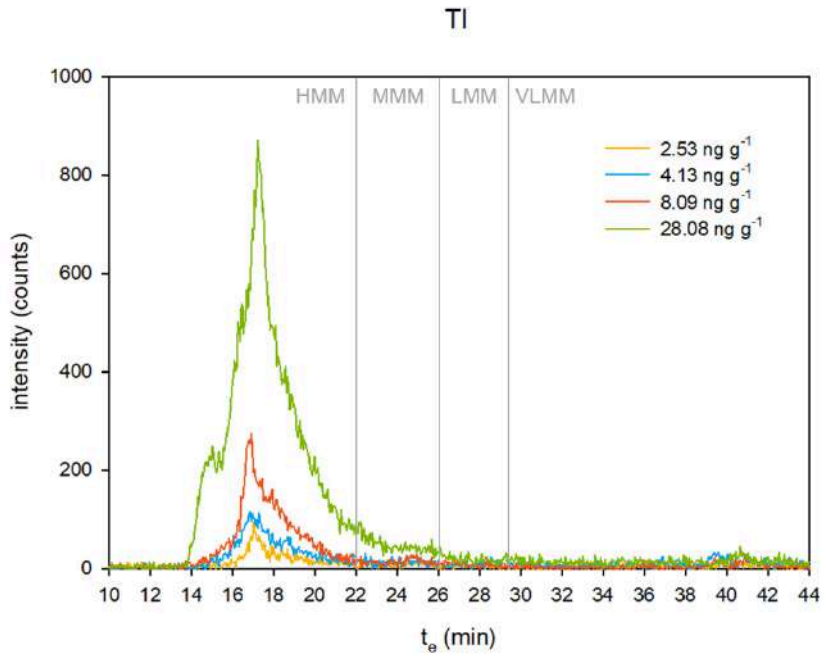

Figure 6. Representative Tl SEC-ICP-MS elution profiles showing the distribution of copper among cytosolic biomolecules of different molecular masses in the acanthocephalan *Dentitruncus truttae* collected from four individual fish

3. Literature

Ali, A., Tirloni, L., Isezaki, M., Seixas, A., Konnai, S., Ohashi, K., ... & Termignoni, C. (2014). Reprolysin metalloproteases from *Ixodes persulcatus*, *Rhipicephalus sanguineus* and *Rhipicephalus microplus* ticks. *Experimental and Applied Acarology*, *63*(4), 559-578.

Asmamaw, B. (2016). Transferrin in fishes. *Journal of Coastal Life Medicine*, *4*(3), 176-180.

Avendaño-Briseño, K. A., Escutia-Martínez, J., Pedraza-Chaverri, J., & Hernández-Cruz, E. Y. (2025). Thallium Toxicity: Mechanisms of Action, Available Therapies, and Experimental Models. *Future Pharmacology*, *5*(3), 49.

Bakke, A. M., Tashjian, D. H., Wang, C. F., Lee, S. H., Bai, S. C., & Hung, S. S. O. (2010). Competition between selenomethionine and methionine absorption in the intestinal tract of green sturgeon (*Acipenser medirostris*). *Aquatic Toxicology*, *96*(1), 62-69.

Bamberger, C. M., Schulte, H. M., & Chrousos, G. P. (1996). Molecular determinants of glucocorticoid receptor function and tissue sensitivity to glucocorticoids. *Endocrine reviews*, *17*(3), 245-261.

Beard, J. L., Dawson, H., & Piñero, D. J. (1996). Iron metabolism: a comprehensive review. *Nutrition Reviews*, *54*(10), 295-317.

Boivin, S., Aouffen, M. H., Fournier, A., & Mateescu, M. A. (2001). Molecular characterization of human and bovine ceruloplasmin using MALDI-TOF mass spectrometry. *Biochemical and biophysical research communications*, *288*(4), 1006-1010.

Bruschi, F., & Pinto, B. (2013). The significance of matrix metalloproteinases in parasitic infections involving the central nervous system. *Pathogens*, 2(1), 105-129.

Caron, A., Rosabal, M., Drevet, O., Couture, P., & Campbell, P. G. (2018). Binding of trace elements (Ag, Cd, Co, Cu, Ni, and Tl) to cytosolic biomolecules in livers of juvenile yellow perch (*Perca flavescens*) collected from lakes representing metal contamination gradients. *Environmental Toxicology and Chemistry*, *37*(2), 576-586.

Cilingir Yeltekin, A., & Saglamer, E. (2019). Toxic and trace element levels in *Salmo trutta* macrostigma and *Oncorhynchus mykiss* trout raised in different environments. *Polish Journal of Environmental Studies*, 28(3).

Coleman, J.E. (1974) Structure and Mechanism of Copper Oxidases in Advances in Chemistry, Food Related Enzymes, American Chemical Society, 11, 267-304, doi:10.1021/ba-1974-0136.ch011

Dragun, Z., Kiralj, Z., Ivanković, D., Bilić, B., Kazazić, S., & Kazazić, S. (2024). Iron-binding biomolecules in the soluble hepatic fraction of the northern pike (*Esox lucius*): two-dimensional chromatographic separation with mass spectrometry detection. *Analytical and Bioanalytical Chemistry*, *416*(23), 5097-5109.

Dragun, Z., Ivanković, D., Krasnići, N., Kiralj, Z., Cvitanović, M., Karamatić, I., Valić, D., Barac, F., Filipović Marijić, V., Mijošek, T., Gjurčević, E., Matanović, K., & Kužir, S. (2022). Metal-binding biomolecules in the liver of northern pike (*Esox lucius* Linnaeus,

1758): The first data for the family Esocidae. *Comparative Biochemistry and Physiology Part C: Toxicology & Pharmacology*, 257, 109327.

Dragun, Z., Krasnići, N., Ivanković, D., Marijić, V. F., Mijošek, T., Redžović, Z., & Erk, M. (2020). Comparison of intracellular trace element distributions in the liver and gills of the invasive freshwater fish species, Prussian carp (*Carassius gibelio* Bloch, 1782). *Science of the total environment*, *730*, 138923.

Dragun, Z., Krasnići, N., Kolar, N., Marijić, V. F., Ivanković, D., & Erk, M. (2018). Cytosolic distributions of highly toxic metals Cd and Tl and several essential elements in the liver of brown trout (*Salmo trutta* L.) analyzed by size exclusion chromatography and inductively coupled plasma mass spectrometry. *Chemosphere*, *207*, 162-173.

Ferrarello, C., Fernández de la Campa, M., & Sanz-Medel, A. (2002). Multielement trace-element speciation in metal-biomolecules by chromatography coupled with ICP–MS. *Analytical and bioanalytical chemistry*, *373*(6), 412-421.

Gasteiger, E., Hoogland, C., Gattiker, A., Duvaud, S. E., Wilkins, M. R., Appel, R. D., & Bairoch, A. (2005). Protein identification and analysis tools on the ExPASy server. In *The proteomics protocols handbook* (pp. 571-607). Totowa, NJ: Humana press.

Genchi, G., Sinicropi, M. S., Lauria, G., Carocci, A., & Catalano, A. (2020). The effects of cadmium toxicity. *International journal of environmental research and public health*, *17*(11), 3782.

Hare, D. J., Roberts, B. R., & McColl, G. (2016). Profiling changes to natively-bound metals during *Caenorhabditis elegans* development. *RSC advances*, *6*(114), 113689-113693.

Herr, C. Q., & Hausinger, R. P. (2018). Amazing diversity in biochemical roles of Fe (II)/2-oxoglutarate oxygenases. *Trends in Biochemical Sciences*, 43(7), 517-532.

Kalisińska, E., & Budis, H. (2019). Manganese, Mn. Mammals and birds as bioindicators of trace element contaminations in terrestrial environments: an ecotoxicological assessment of the Northern Hemisphere, 213-246.

Krasnići, N., Dragun, Z., Kazazić, S., Muharemović, H., Erk, M., Jordanova, M., ... & Kostov, V. (2019). Characterization and identification of selected metal-binding biomolecules from hepatic and gill cytosols of Vardar chub (*Squalius vardarensis* Karaman, 1928) using various techniques of liquid chromatography and mass spectrometry. *Metallomics*, *11*(6), 1060-1078.

Krasnići, N., Dragun, Z., Erk, M., Ramani, S., Jordanova, M., Rebok, K., & Kostov, V. (2018). Size-exclusion HPLC analysis of trace element distributions in hepatic and gill cytosol of Vardar chub (*Squalius vardarensis* Karaman) from mining impacted rivers in north-eastern Macedonia. *Science of the total environment*, *613*, 1055-1068.

Krasnići, N., Dragun, Z., Erk, M., & Raspor, B. (2014). Distribution of Co, Cu, Fe, Mn, Se, Zn, and Cd among cytosolic proteins of different molecular masses in gills of European chub (*Squalius cephalus* L.). *Environmental science and pollution research*, *21*(23), 13512-13521.

Krasnići, N., Dragun, Z., Erk, M., & Raspor, B. (2013). Distribution of selected essential (Co, Cu, Fe, Mn, Mo, Se, and Zn) and nonessential (Cd, Pb) trace elements among protein fractions from hepatic cytosol of European chub (*Squalius cephalus* L.). *Environmental science and pollution research*, *20*(4), 2340-2351.

Lopez Heras, I., Palomo, M., & Madrid, Y. (2011). Selenoproteins: the key factor in selenium essentiality. State of the art analytical techniques for selenoprotein studies. *Analytical and bioanalytical chemistry*, 400(6), 1717-1727.

Maret, W., & Li, Y. (2009). Coordination dynamics of zinc in proteins. *Chemical reviews*, 109(10), 4682-4707.

Martin-Antonio, B., Jimenez-Cantizano, R. M., Salas-Leiton, E., Infante, C., & Manchado, M. (2009). Genomic characterization and gene expression analysis of four hepcidin genes in the redbanded seabream (*Pagrus auriga*). *Fish & shellfish immunology*, *26*(3), 483-491.

Martín-Galiano, A. J., & Sotillo, J. (2022). Insights into the functional expansion of the astacin peptidase family in parasitic helminths. *International Journal for Parasitology*, *52*(4), 243-251.

Mijošek, T., Šariri, S., Kljaković-Gašpić, Z., Fiket, Ž., & Filipović Marijić, V. (2024). Interrelation between environmental conditions, acanthocephalan infection and metal (loid) accumulation in fish intestine: An in-depth study. *Environmental pollution*, *356*, 124358.

Mijošek, T., Filipović Marijić, V., Dragun, Z., Ivanković, D., Krasnići, N., & Erk, M. (2022). Efficiency of metal bioaccumulation in acanthocephalans, gammarids and fish in relation to metal exposure conditions in a karst freshwater ecosystem. *Journal of trace elements in medicine and biology*, *73*, 127037.

Mijošek, T., Filipović Marijić, V., Dragun, Z., Krasnići, N., Ivanković, D., Redžović, Z., & Erk, M. (2021). First insight in trace element distribution in the intestinal cytosol of two freshwater fish species challenged with moderate environmental contamination. *Science of the total environment*, *798*, 149274.

Mijošek, T., Filipović Marijić, V., Dragun, Z., Ivanković, D., Krasnići, N., Erk, M., Gottstein,

S., Lajtner, J., Sertić Perić, M., & Matoničkin Kepčija, R. (2019). Comparison of electrochemically determined metallothionein concentrations in wild freshwater salmon fish and gammarids and their relation to total and cytosolic metal levels. *Ecological indicators*, *105*, 188-198.

Nachev, M., Schertzinger, G., & Sures, B. (2013). Comparison of the metal accumulation capacity between the acanthocephalan *Pomphorhynchus laevis* and larval nematodes of the genus *Eustrongylides sp.* infecting barbel (*Barbus barbus*). *Parasites & Vectors*, *6*(1), 21.

Nachev, M., & Sures, B. (2016). Seasonal profile of metal accumulation in the acanthocephalan Pomphorhynchus laevis: a valuable tool to study infection dynamics and implications for metal monitoring. *Parasites & Vectors*, *9*(1), 300.

Rosabal, M., Mounicou, S., Hare, L., & Campbell, P. G. (2016). Metal (Ag, Cd, Cu, Ni, Tl, and Zn) binding to cytosolic biomolecules in field-collected larvae of the insect Chaoborus. *Environmental Science & Technology*, *50*(6), 3247-3255.

Shen, S., Li, X. F., Cullen, W. R., Weinfeld, M., & Le, X. C. (2013). Arsenic binding to proteins. *Chemical reviews*, *113*(10), 7769-7792.

Spuches, A. M., & Wilcox, D. E. (2008). Monomethylarsenite competes with Zn^{2+} for binding sites in the glucocorticoid receptor. *Journal of the American Chemical Society*, 130(26), 8148-8149.

Sures, B. (2001). The use of fish parasites as bioindicators of heavy metals in aquatic ecosystems: a review. *Aquatic Ecology*, *35*(2), 245-255.

Stancato, L. F., Hutchison, K. A., Krishna, P., & Pratt, W. B. (1996). Animal and plant cell lysates share a conserved chaperone system that assembles the glucocorticoid receptor into a functional heterocomplex with hsp90. *Biochemistry*, *35*(2), 554-561.

Strižak, Ž., Ivanković, D., Pröfrock, D., Helmholz, H., Cindrić, A. M., Erk, M., & Prange, A. (2014). Characterization of the cytosolic distribution of priority pollutant metals and

metalloids in the digestive gland cytosol of marine mussels: seasonal and spatial variability. *Science of the total environment*, *470*, 159-170.

Szpunar, J., & Lobinski, R. (1999). Species-selective analysis for metalbiomacromolecular complexes using hyphenated techniques. *Pure and applied chemistry*, *71*, 899-918.

Šariri, S., Valić, D., Kralj, T., Cvetković, Ž., Mijošek, T., Redžović, Z., Karamatić, I., & Filipović Marijić, V. (2024). Long-term and seasonal trends of water parameters in the karst riverine catchment and general literature overview based on CiteSpace. *Environmental science and pollution research*, 31(3), 3887-3901.

Šariri, S., Mijošek Pavin, T., Redžović, Z., Kiralj, Z., Ivanković, D., & Filipović Marijić, V. (2025a). Biomarker-based assessment of sublethal metal exposure in brown trout and parasites acanthocephalans from a protected karst river. *Environmental toxicology and pharmacology*, 104823.

Šariri, S., Vardić Smrzlić, I., Mijošek Pavin, T., & Filipović Marijić, V. (2025b). First insight into metal binding proteins from the de novo transcriptome of acanthocephalan parasite *Dentitruncus truttae*. Scientific reports, 15(1), 26152.Trokter, M., Mücke, N., & Surrey, T. (2012). Reconstitution of the human cytoplasmic dynein complex. *Proceedings of the National Academy of Sciences*, *109*(51), 20895-20900.

Tsang, T., Davis, C. I., & Brady, D. C. (2021). Copper biology. *Current Biology*, *31*(9), R421-R427

Urien, N., Jacob, S., Couture, P., & Campbell, P. G. (2018). Cytosolic distribution of metals (Cd, Cu) and metalloids (As, Se) in livers and gonads of field-collected fish exposed to an environmental contamination gradient: an SEC-ICP-MS analysis. *Environments*, 5(9), 102.

Van Campenhout, K., Infante, H. G., Hoff, P. T., Moens, L., Goemans, G., Belpaire, C., ... & Bervoets, L. (2010). Cytosolic distribution of Cd, Cu and Zn, and metallothionein levels in relation to physiological changes in gibel carp (*Carassius auratus gibelio*) from metal-impacted habitats. *Ecotoxicology and environmental safety*, *73*(3), 296-305.

Van Campenhout, K., Infante, H. G., Goemans, G., Belpaire, C., Adams, F., Blust, R., & Bervoets, L. (2008). A field survey of metal binding to metallothionein and other cytosolic ligands in liver of eels using an on-line isotope dilution method in combination with size exclusion (SE) high pressure liquid chromatography (HPLC) coupled to inductively coupled

plasma time-of-flight mass spectrometry (ICP-TOFMS). *Science of the total environment*, *394*(2-3), 379-389.

Vergara-Gerónimo, C. A., Del Río, A. L., Rodríguez-Dorantes, M., Ostrosky-Wegman, P., & Salazar, A. M. (2021). Arsenic-protein interactions as a mechanism of arsenic toxicity. *Toxicology and Applied Pharmacology*, *431*, 115738.

Viarengo, A., & Nott, J. A. (1993). Mechanisms of heavy metal cation homeostasis in marine invertebrates. *Comparative Biochemistry and Physiology Part C: Comparative Pharmacology*, *104*(3), 355-372.

Williams, J. B. (2015). Elucidating the Molecular Function of Reprolysin Metalloproteases in Tick-Host-Pathogen Interaction.

Wolf, C., Wenda, N., Richter, A., & Kyriakopoulos, A. (2007). Alteration of biological samples in speciation analysis of metalloproteins. *Analytical and bioanalytical chemistry*, *389*(3), 799-810.

Wrobel, J. K., Power, R., & Toborek, M. (2016). Biological activity of selenium: Revisited. *IUBMB life*, 68(2), 97-105.

APPENDIX D: Differential gene expression analysis

1. Materials and methods

1.1. Transcriptome Quantification, Differential Expression, and Functional Enrichment Analyses

The analyses were conducted on paired samples of fish intestinal tissue (*Salmo trutta*) and acanthocephalans (*Dentitruncus truttae*) isolated from the same hosts. In total, six fish from the polluted site (KRK) and six fish from the reference site (KRS) were analyzed. Following parasite removal, both parasite and intestinal tissue samples were washed in phosphate-buffered saline (PBS) to remove impurities.

Total RNA extraction from acanthocephalans, as well as library preparation, RNA sequencing, quality control, and *de novo* transcriptome assembly, were performed as described in Šariri et al. (2025). The procedure for fish intestinal tissue followed the same protocol, with minor modifications during the homogenization step. In fish, the anterior (esophagus and stomach), central (pyloric ceca and small intestine), and posterior (colon) sections of the intestine from each specimen were pooled into a single sample. In acanthocephalans, multiple individuals from the same host were pooled. Fish intestinal samples were homogenized using a Bead Ruptor 4 homogenizer (Omni International) for 90 s at speed level 5, whereas acanthocephalan samples were homogenized using an Ultra Turrax T8 homogenizer (IKA Werke). All subsequent steps were identical for both organisms. Total RNA was extracted using a Direct-zol™ RNA Miniprep Kit (Zymo Research) and subsequent library preparation, RNA sequencing, quality control, and de novo transcriptome assembly were carried out commercially by Novogene (UK) Company Limited (https://www.novogene.com/us-en/).

Gene expression levels were quantified by assessing the abundance of transcripts, which directly reflects gene expression. The filtered Trinity-reconstructed transcriptome, processed with Corset (Davidson and Oshlack 2014), served as the reference for the analysis. Alignment was performed using RSEM software (Li et al. 2011). To estimate gene expression levels, FPKM (Fragments Per Kilobase of transcript sequence per Million mapped reads) was employed. This method accounts for both sequencing depth and transcript length, ensuring an accurate representation of gene expression levels. Differential gene expression analysis (DEG analysis) was conducted using the DESeq2 software package (version 1.26.0) with criteria set at p-adjust < 0.05 and $|\log2FC| \geq 1$. This method ensured robust statistical control for multiple hypothesis testing while accounting for variability across replicates. The input data for this analysis consisted of read counts obtained from the gene expression quantification. Volcano plots were used to illustrate the overall distribution of differentially expressed genes (DEGs). Functional enrichment analysis of the differential expressed genes was performed to identify biological functions or pathways associated with DEG. Gene Ontology (GO) enrichment analysis was performed using GOSeq (version 1.32.0) and topGO (version 2.32.0). GOSeq was utilized to correct for potential gene length biases inherent to RNA-seq data, while topGO provided statistical analysis for enriched GO terms. GO terms were classified into three main categories: biological processes, molecular functions, and cellular components. Only GO terms with a corrected p-value < 0.05 (adjusted for multiple testing) were

considered significantly enriched. Kyoto Encyclopedia of Genes and Genomes (KEGG) pathway enrichment analysis was carried out using KOBAS (version 3.0). The software mapped DEGs to known KEGG pathways to identify biological pathways significantly associated with the dataset. Pathway enrichment significance was determined using a corrected p-value < 0.05.

1.2. Selection of genes for qPCR validation

To validate the transcriptomic results, we selected genes that showed significantly higher expression at the KRK sampling site compared to KRS. In quantitative polymerase chain reactions (qPCR) their expression was quantified relative to the reference gene with stable expression (no differences between samples or locations). From the list of differentially expressed genes (DEGs), for both acanthocephalans and fish we chose five upregulated genes with the highest fold-change values ($p < 0.05$).

For acanthocephalans, genes annotated as "unknown," those showing high similarity to host (fish) genes, and genes not expressed consistently across all samples (read count = 0 in any sample) were excluded to avoid ambiguous annotations and potential contamination. Reference genes (*Lr32, EIF*, and *Act1*) were selected based on literature from related taxa, as no qPCR studies have previously been performed on acanthocephalans. Similar criteria were used for gene selection in fish, but only one reference gene - *EIF1a*, was selected based on the literature, as it has previously been shown to be the most stably expressed in the intestinal tissue of *S. trutta* (Sun et al. 2022).

1.3. RNA isolation for qPCR analysis

Total RNA was isolated from pooled acanthocephalan samples (on average three specimens per sample), originating from the same fish hosts as those used for RNA sequencing and transcriptome assembly (Šariri et al. 2025). RNA extraction followed the procedure described by Šariri et al. (2025) and included: 1) homogenization in TRI Reagent (Zymo Research) using a TissueLyser homogenizer (Qiagen), 2) RNA isolation with the Direct-zol™ RNA MiniPrep Kit (Zymo Research) and 3) assessment of RNA quantity (BiospecNano, Shimadzu) and quality (1% agarose gel electrophoresis). Fish RNA for qPCR analysis was isolated from the same intestinal samples used for RNA sequencing and transcriptome assembly, as residual

material remained after those procedures. These samples were stored in TRI Reagent (Zymo Research) at – 80 °C and thawed prior to further processing. The lysate was transferred to a new tube containing beads and homogenized in 1 mL of TRI Reagent using a TissueLyser LT (Qiagen) for 3 min at the highest speed. Subsequent steps followed the same protocol as described above. All RNA samples from both fish and acanthocephalans were diluted to 50 ng μL^{-1} and reverse-transcribed to cDNA using SuperScript™ IV VILO™ Master Mix (Invitrogen), following the manufacturer's instructions.

1.4. Primer design and testing

Nucleotide sequences of selected reference and upregulated genes were used for primer design. For each gene, 10 primer pairs were generated using Primer3 (version 2.5.0) within NCBI Primer-BLAST (Ye et al. 2012). Of these, five primer pairs per gene were selected, synthesized commercially by Thermo Fisher Scientific and tested by conventional PCR. Polymerase chain reactions were performed in 50 µl volumes containing: 0.2 µM each primer, 25 µl EmeraldAmp® GT PCR Master Mix, 200 ng cDNA template and 21 µl ultrapure water. Polymerase chain reaction cycling conditions were as follows: denaturation at 98°C for 10 s, annealing for 30 s at 63°C for acanthocephalans and 60°C for fish, extension at 72°C for 1 min per kb. The best-performing primer pair for each gene was selected based on amplicon specificity visualized on agarose gels.

1.4. qPCR amplification

Quantitative PCR was performed on a QuantStudio 5 system (Applied Biosystems) using PowerTrack™ SYBR™ Green Master Mix (Applied Biosystems). Primer efficiency was evaluated across a dilution series of cDNA (0, 0.1, 1, 2.5, 5, and 10 ng per reaction), and 10 ng cDNA per reaction was selected for subsequent analyses. Each reaction (20 µL) contained: 2 µL cDNA (10 ng), 1 µL of each primer (300 nM), 10 µL SYBR Green Master Mix and 6 µL ultrapure water. Thermal cycling conditions were: 50 °C for 2 min, 95 °C for 10 min followed by 40 cycles of 95 °C for 15 s and 63°C for acanthocephalans and 60°C for fish for 1 min. Melt curve analysis was carried out from 60 °C to 95 °C (1.6 °C/s). All reactions were run in duplicate. No-template controls containing sterile water instead of cDNA were included for each primer pair.

1.5. Identification of reference genes in acanthocephalans

Expression stability of the three candidate reference genes (LR32, EIF, and Act1) was evaluated using BestKeeper and geNorm (Pfaffl et al. 2004, Vandesompele et al. 2002). The dataset included 12 biological samples per gene with mean cycle threshold (Ct) values calculated from technical duplicates. BestKeeper analysis was conducted using the original Excel-based BestKeeper macro tool (version available at https://www.gene-quantification.de). The software calculated mean Ct, standard deviation (SD), coefficient of variation (CV), and Pearson correlation (r) with the BestKeeper Index to assess expression consistency. GeNorm analysis was performed using relative quantities (RQ) calculated from mean Ct values, and gene stability (M-values) was determined from the pairwise variation of log-transformed expression ratios. Genes with lower M-values were considered more stably expressed.

1.6. Gene expression quantification and plotting

Quantitative gene expression levels for five target genes in both acanthocephalans and fish were analyzed using the $2^{-\Delta\Delta Ct}$ method across two sampling sites (KRK and KRS) with normalization to the reference gene EIF (Schmittgen and Livak 2008). Expression data were collected in tabular form and analyzed using Python 3.11 in Jupyter Notebook. The analysis was conducted using the following Python libraries: pandas for data manipulation, matplotlib and seaborn for boxplot visualization, and scipy.stats for statistical testing. Each dataset was first reshaped to long format using pandas.melt() to allow comparison between the two sites (KRK vs. KRS). Boxplots were generated with seaborn.boxplot() to visualize the distribution of relative gene expression levels. For statistical comparison between KRK and KRS groups, a Welch's two-sample t-test was performed using (scipy.stats.ttest_ind with unequal variance assumption). The resulting p-values were added to each figure above the boxes, and significance was annotated using the following convention: ns - not significant ($p \geq 0.05$) and * - $p < 0.05$.

2. Results and discussion

2.1. Acanthocephalans

2.1.1. Enrichment analysis of the differential expressed genes

The differential gene expression analysis revealed 594 DEGs between acanthocephalans from KRK and KRS, of which 347 were upregulated and 247 downregulated (Fig. 1). GO enrichment analysis identified no statistically significant (padj < 0.05) biological processes (BP), cellular components (CC), or molecular functions (MF). The highest-ranked (but not significant) upregulated BP was vesicle-mediated transport (p_{adj} = 0.374), while the highest-ranked downregulated BP was generation of precursor metabolites and energy (p_{adj} = 0.402). Among CCs, nucleolus (p_{adj} = 0.111), plasma membrane (p_{adj} = 0.203), and lipid droplet (p_{adj} = 0.434) showed the strongest upregulation trends, and no downregulated CCs were detected. Upregulated MF trends included nucleotidyltransferase activity (p_{adj} = 0.203), enzyme regulator activity (p_{adj} = 0.434), and ligase activity (p_{adj} = 0.556), with no downregulated MFs. Although parasites from KRK showed a substantial number of DEGs compared to KRS, which may be result of different environmental conditions, these patterns did not highlight any dominant biological process. This is consistent with the chemical data, as metal concentrations in water, sediment, fish intestine, gut content, and acanthocephalans showed variable and often non-significant spatial differences (Mijošek et al. 2023, 2024). Still, general trends of higher Ba, As, Co, Cu, Zn, K, and Ca at KRK and higher Cd at KRS were observed across all these five compartments. As, Fe, and Sr were consistently higher at KRK in all compartments except sediment. However, the gene expression patterns cannot be explained by pollution alone, and other factors likely contributed. Parasite infection intensity in the fish used for molecular analyses was approximately twice as high at KRS (36.9 parasites/fish) compared to KRK (17.8), and high intrapopulation densities can also impose stress due to competition for space, mates, and nutrients (Hassanine et al. 2008, Kennedy 1985).

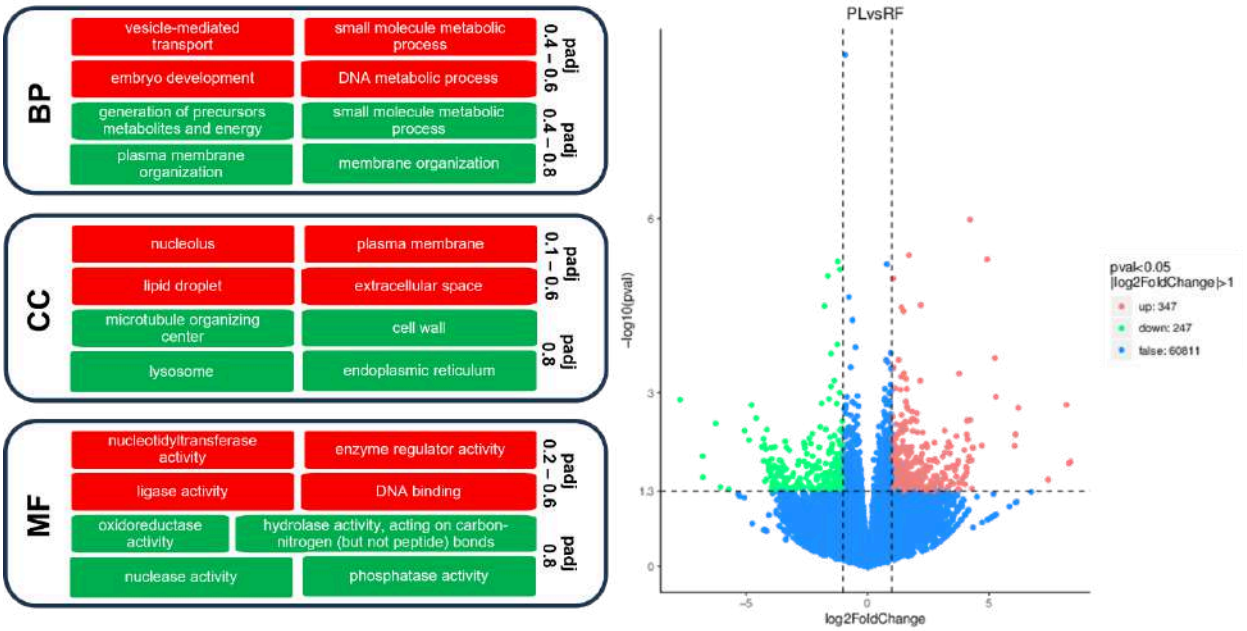

Figure 1. Volcano plot of differentially expressed genes (DEGs) and summary of their associated GO enrichment results. The x-axis shows the $\log_2$ fold change in gene expression between D. truttae from the polluted site (KRK) and the reference site (KRS) in the Krka River; the y-axis shows the statistical significance ($-log_{10}$ *p*-value). Red and green points indicate significantly up- and downregulated DEGs, respectively ($q < 0.005$ and $|log_2FC| > 1$), while blue points represent genes without significant change. GO enrichment results are categorized into Biological Process (BP), Cellular Component (CC), and Molecular Function (MF). Upregulated GO terms are shown in red and downregulated terms in green, with the range of adjusted p-values indicated by the scale on the right.

In cotrast, KEGG pathway enrichment analysis to comparing transcriptomic profiles of parasites from the polluted KRK versus reference KRS site, revealed several statistically enriched pathways (Fig. 2). African trypanosomiasis and Glycolysis/Glycogenesis were significantly more active at KRK. The KEGG pathway for African trypanosomiasis involves cellular processes relevant to immune response, oxidative stress, cell signalling, and other stress-related mechanisms. However, this pathway likely reflects the activation of universal cellular stress and survival mechanisms – such as energy metabolism, antioxidant defense, and cytoskeletal dynamics - that are conserved across diverse organisms (Rodgers et al. 2009). Compounds such as: calcium cation, L-Tryptophan, L-Kynurenine, diacylglycerol (DAG), nitric oxide, D-myo-Inositol 1,4,5-trisphosphate (IP3) are listed as main compounds within African trypanosomiasis pathway (Rodgers et al. 2009). Increased levels of IP3, DAG,

and calcium ions suggest that the parasite is activating calcium and lipid signaling pathways, which play key roles in cellular adaptation and defense (Docampo and Huang 2015, Docampo and Moreno 2021). These signals may help regulate cellular responses to environmental changes, allowing the parasite to survive in polluted conditions. The upregulation of tryptophan and kynurenine suggests that pollution is driving metabolic shifts (Jamshed et al. 2022). By channeling tryptophan metabolism into the kynurenine pathway, the parasite may be activating pathways that help mitigate damage and maintain cellular function under stress. The upregulation of glycolysis and gluconeogenesis in Acanthocephala from polluted sites is likely a multifaceted adaptation that allows the parasite to: adapt to potential hypoxic condition in the fish gut (Han and Hagiwara 2023, Martínez-González et al. 2022), cope with pollutants ingested indirectly through the fish host (Brulle et al. 2010, Hou et al. 2023, Lee et al. 2023), manage increased oxidative stress (Mullarky and Cantley 2015) and sustain energy production in a potentially nutrient-limited and toxic environment (Liu et al. 2024).

Statistically enriched KEGG pathways that are downregulated in parasites in KRK versus reference KRS sites were associated with Parkinson's, Alzheimer and Huntington disease, oxidative phosphorylation, thermogenesis, cardiac muscle contraction and non-alcoholic fatty liver disease (NAFLD). The same KEGG pathways were enriched in transcriptome of midgut of *Bombyx mori* exposed to Pb and *Enchytraeus crypticus* exposed to Ni, linking them with metal exposure response (Gomes et al. 2019, Ye et al. 2024). Enrichment of KEGG pathways associated with human neurodegenerative diseases, such as Parkinson's disease (PD), Alzheimer's disease (AD), and Huntington's disease (HD), is a common outcome in transcriptome studies of non-model invertebrates and should not be interpreted as evidence of disease-specific processes. KEGG "disease" pathways are constructed primarily from human molecular interaction networks, but they consist largely of deeply conserved mitochondrial, metabolic, proteostasis, and stress-response components that are shared across eukaryotes (Garcia-Reyero et al. 2011, Kanehisa et al. 2021). Thus, enrichment of these pathways in *D. truttae* reflects regulation of these underlying core biological processes, not the presence of disease phenotypes.

Pathways in the KEGG PD map are dominated by genes involved in oxidative phosphorylation, mitochondrial electron transport chain (ETC) complexes, and reactive oxygen species (ROS) management, all of which are highly conserved across animals including helminths (Chatterjee et al. 2017, Gaki and Papavassiliou 2014). Similarly, AD- and HD-associated pathways include gene modules related to protein quality control, chaperone

systems, ubiquitin-mediated degradation, and apoptosis, representing universal eukaryotic mechanisms of proteostasis and cellular stress (Balchin et al. 2018, Soto & Pritzkow 2018).

Similar enrichment of KEGG neurodegenerative disease pathways has been reported in multiple invertebrate transcriptomes, including cadmium-exposed crayfish (*Procambarus clarkii*) and Chinese mitten crab (*Eriocheir sinensis*), as well as stress-activated immune transcriptomes in insects such as *Tenebrio molitor*, reflecting conserved mitochondrial and oxidative phosphorylation modules rather than nervous system–specific pathology (Liu et al. 2021, Tang et al. 2019, Zhu et al. 2013). Related patterns have been reported in aquatic invertebrates and parasitic helminths exposed to environmental stressors, where conserved mitochondrial and proteostasis pathways dominate the transcriptional response (Martis et al. 2017).

Therefore, in *D. truttae*, enrichment of KEGG pathways labeled as Parkinson's, Alzheimer's, or Huntington's disease likely indicates altered mitochondrial activity, disrupted oxidative phosphorylation, or increased proteotoxic and oxidative stress, particularly in parasites from the polluted site. These findings should be interpreted as evidence of generalized cellular stress and metabolic perturbation, rather than as disease-specific signaling.

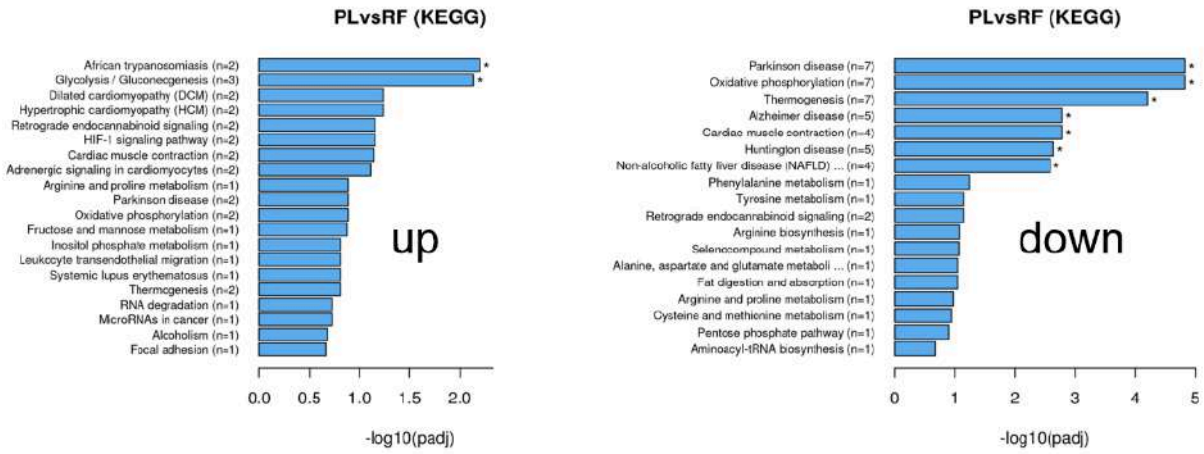

Figure 2. Enriched KEGG pathways in *D. truttae* from the polluted site. Bar charts display the top 20 enriched pathways among upregulated (top) and downregulated (bottom) differentially expressed genes (DEGs) at the polluted KRK (PL) site relative to the reference KRS (RF) site. Statistical significance is indicated by an asterisk ($p < 0.05$).

2.1.2. Identification of reference genes for qPCR

In the BestKeeper analysis, all candidate genes exhibited SD values below 1.0, meeting the stability threshold (Table 1). *EIF* emerged as the most stable reference gene, as it was displaying the lowest SD (0.30) and highest correlation with the BestKeeper Index (r = 0.940). *Lr32* displayed moderate stability, whereas *Act1* showed the greatest variability (Table 1). The geNorm analysis yielded consistent results, with all genes showing acceptable stability (M < 1.5) (Fig. 3). *EIF* was again the most stable (M = 0.444), followed by *Lr32* (M = 0.553) and *Act1* (M = 0.658). Together, these analyses identify *EIF* as the most reliable reference gene for qPCR normalization under the tested environmental conditions. In accordance with MIQE recommendations, the combination of *EIF* and *Lr32* provides the most robust normalization strategy for qPCR studies in this species. To our knowledge, this is the first validated set of reference genes for *D. truttae*, providing a solid foundation for future transcriptomic and ecotoxicological research.

Table 1. Results of gene stability analysis using BestKeeper

Gene	Mean Ct	SD [±Ct]	CV [%Ct]	Pearson r (vs. BestKeeper Index)	p-value
Lr32	19.28	**0.43**	2.21%	**0.823**	0.001
EIF	20.01	**0.30**	1.52%	**0.940**	0.001
Act1	24.32	**0.54**	2.21%	**0.725**	0.008

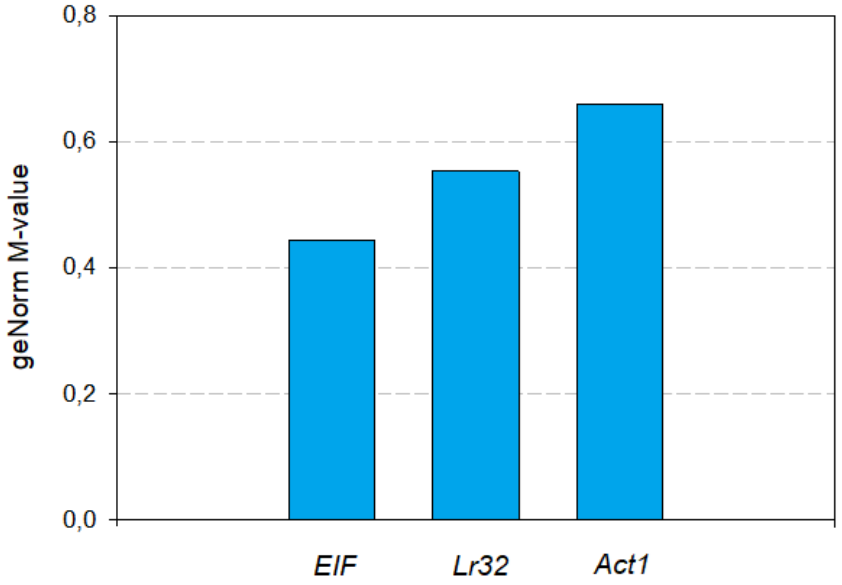

Figure 3. Results of gene stability analysis using geNorm

2.1.3. qPCR validation of transcriptomics

qPCR validation was performed on five genes identified as upregulated in the transcriptomic analysis: *Hyp*, *UNK*, *Cfdp2*, *Sbpi* and *Uptr* (Table 2). The *UNK* gene showed statistically significant upregulation ($p < 0.05$) in samples from the polluted KRK site compared to the reference KRS site (Fig. 4). The remaining four genes also exhibited higher expression in the samples from KRK, consistent with the transcriptomic results, though these differences were not statistically significant (Fig. 5). Notably, all five genes showed the same direction of regulation as observed in the transcriptome data.

The qPCR results provide partial validation of the transcriptomic findings. While only one gene reached statistical significance, all five genes displayed upregulation trends consistent with the RNA-seq results. This directional agreement supports the robustness of the transcriptomic analysis, although limited sample size in the qPCR assays likely reduced statistical power. Similar limitations are common in field-based environmental studies, where sample collection is often constrained. Future work with increased sample sizes could help confirm these gene expression patterns with greater statistical confidence.

Table 2. *Dentitruncus truttae* genes selected for qPCR analysis based on their identification as upregulated at the polluted site KRK compared with the reference site KRS in the transcriptomic analysis.

Gene abbreviation	Protein product description	Transcriptome Cluster
Hyp	hypothetical protein	Cluster 13705.4301
UNK	unknown protein	Cluster 12766.0
Cfdp2	craniofacial development protein 2–like	Cluster 12666.20791
Sbpi	serum basic protease inhibitor	Cluster 12666.19620
Uptr	unnamed protein product (*Trichobilharzia regent*)	Cluster 12666.32947

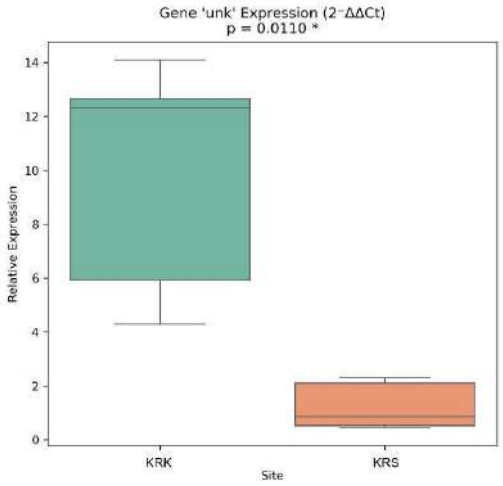

Figure 4. Relative expression of the *Unk* gene in *Dentitruncus truttae* collected from the polluted (KRK) and reference (KRS) sites in the Krka River. Expression levels are normalized to the reference gene *EIF*. A statistically significant difference between sites was detected using Welch's *t*-test and is indicated by an asterisk (*p*-value shown in the figure).

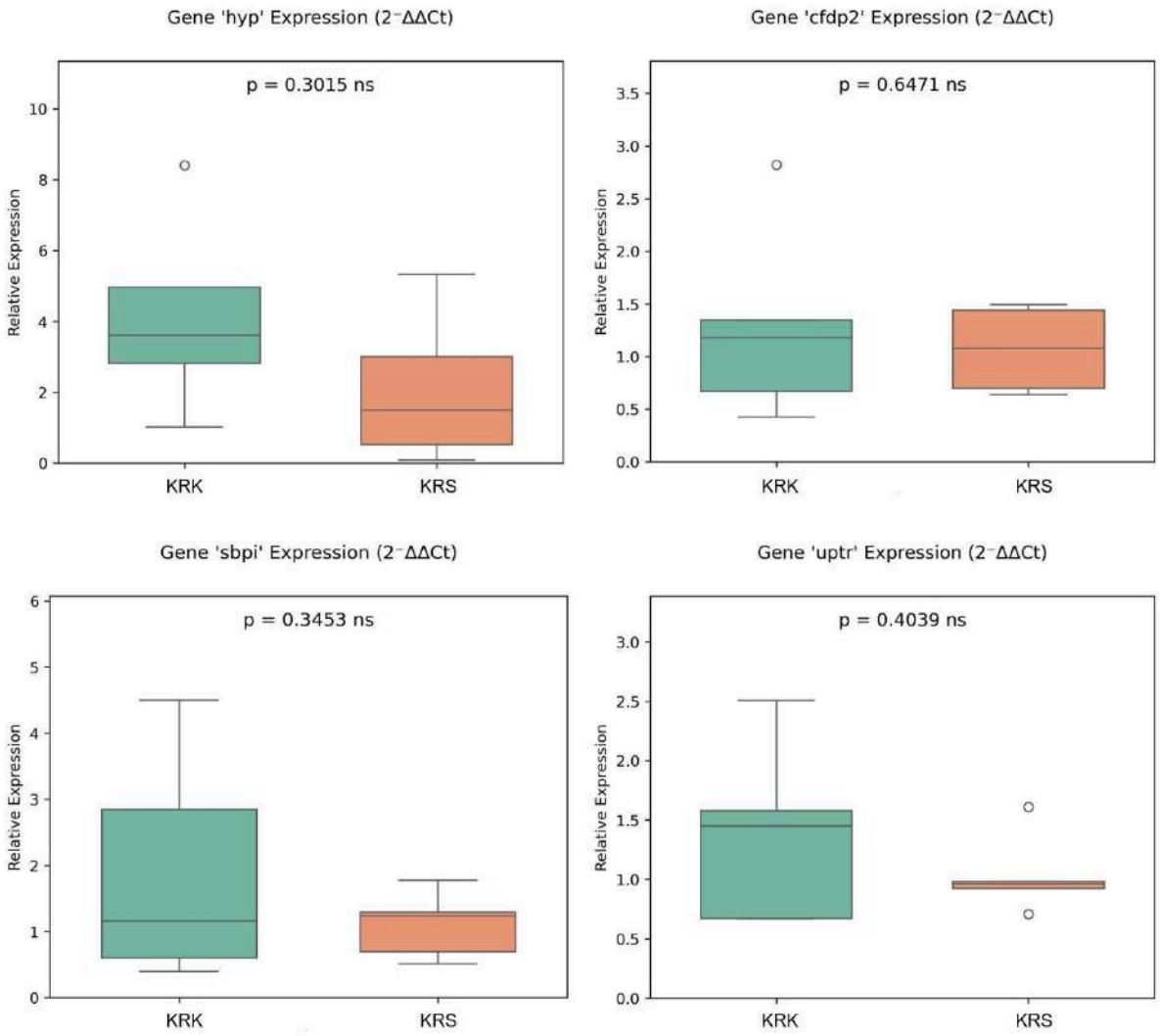

Figure 5. Relative expression of the genes *Hyp*, *Cfdp2*, *Sbpi* and *Uptr* in *Dentitruncus truttae* collected from fish at the polluted site (KRK) and the reference site (KRS) in the Krka River. Data are normalized to the reference gene *EIF*. No statistically significant differences between sites were detected using Welch's *t*-test (*p*-values shown in the figure; ns - not significant).

2.2. Fish intestine

2.2.1. *De novo* assembly and functional annotation of the *S. trutta* transcriptome

A total of 142.8 Gb of clean reads (98.82% of raw reads) were generated from 11 samples of *Salmo trutta* (Table 3), with an average of 43.2 million clean reads per sample. The Trinity assembler generated 432,258 transcripts with an average length of 1,077 bp and an N50 of 1,741 bp and a total of 217,771 unigenes with an average length of 793 bp and an N50 of 1,023 bp. The total assembly length was 465,614,207 bp when considering the transcripts,

whereas it was 172,601,340 bp when accounting for the unigenes. The majority of sequences fell whitin 300-500 bp range (40.1% of transcripts and 53.0% of unigenes), while 14.9% of transcripts and 7.5% of unigenes were larger than 2,000 bp. Sequence lengths ranged from a minimum of 301 bp to a maximum of 13,922 bp for both datasets. BUSCO assessment confirmed the high quality and completeness of the *S. trutta* transcriptome. The percentage of fragmented BUSCOs was low (1.5% for Trinity.fasta and 6.9% for unigene.fasta sequences), while the percentage of missing BUSCOs was negligible (0.0% for Trinity.fasta and 0.4% for unigene.fasta sequences).

Table 3. Statistical table of sequencing data of all *Salmo trutta* samples. Raw/clean bases – (number of raw/clean reads) * (sequence length); Gb – gigabases; Q20/30 - Phred values greater than 20/30 base number contain the percentage of total base

Sample	Raw reads	Raw bases (Gb)	Clean reads	Clean bases (Gb)	Error rate (%)	Q20 (%)	Q30 (%)	GC content (%)
KRK1	47,689,709	14.3	46,916,247	14.1	0.03	97.44	92.78	45.92
KRK2	44,161,062	13.2	43,633,232	13.1	0.03	97.63	93.26	48.21
KRK3	41,474,555	12.4	40,983,178	12.3	0.03	97.75	93.72	48.1
KRK4	38,697,841	11.6	38,222,507	11.5	0.03	97.59	93.25	46.71
KRK5	38,814,947	11.6	38,273,783	11.5	0.03	97.36	92.86	46.06
KRS1	44,819,262	13.4	44,068,888	13.2	0.03	97.57	93.44	46.34
KRS2	37,434,840	11.2	36,942,203	11.1	0.03	97.6	93.35	46.77
KRS3	46,398,299	13.9	45,678,553	13.7	0.03	97.38	92.7	46.58
KRS4	44,378,319	13.3	43,591,414	13.1	0.03	97.66	93.68	46.54
KRS5	48,059,901	14.4	47,463,404	14.2	0.03	97.45	92.71	47.39
KRS6	50,603,500	15.2	49,920,309	15	0.03	97.46	92.68	47.28

Annotation statistics for genes successfully identified by each database are presented in Table 4. A substantially higher proportion of unigenes (82.8%) was annotated in at least one database in *Salmo trutta* compared with acanthocephalans (40.6%) (Šariri et al. 2025). This difference was expected, as *S. trutta* is a well-characterized organism with a published reference genome (Hansen et al. 2021). The high annotation coverage for *S. trutta* enabled more robust functional characterization of differentially expressed genes and facilitated downstream enrichment analyses.

Table 4. Proportion of genes successfully annotated in the *S. trutta* transcriptome across different databases with percentages calculated relative to the total unigene count

	Number of unigenes	Percentage (%)
annotated in NR	93,729	43.04
annotated in NT	163,320	74.99
annotated in KO	47,148	21.65
annotated in SwissProt	50,386	23.13
annotated in PFAM	55,435	25.45
annotated in GO	54,361	24.96
annotated in KOG	20,839	9.56
annotated in all databases	10,696	4.91
annotated in at least one database	180,319	82.8
total unigenes	217,771	100

2.2.2. Enrichment analysis of the differentially expressed genes

A total of 14,280 DEGs were identified between fish from KRK and KRS, with 7,572 genes upregulated and 6,708 downregulated (Fig. 6). The number of DEGs detected in the present

study was substantially higher than that reported for intestinal tissue of *Danio rerio* following acute $HgCl_2$ exposure (30 μg/L) and for gill tissue of *Rita rita* collected from polluted versus pristine sites in the Ganga River, exceeding those values by approximately six- and seven-fold, respectively (Mitra et al. 2020, Zhang et al. 2020). Upregulated genes accounted for 53% of all DEGs, a proportion intermediate relative to previous studies, including experimentally Hg-exposed *D. rerio* intestine (79%), gills of *R. rita* from polluted sites (47%), and intestine of *Salmo trutta* chronically exposed to metal pollution (26%) (Mitra et al. 2020, Uren Webster et al. 2013, Zhang et al. 2020). Such variation in DEG magnitude and direction likely reflects differences in species, tissue type, exposure duration, types of pollutants, and environmental and biological context.

Transcriptomic differences between *S. trutta* from KRK and KRS were predominantly characterized by gene upregulation at the polluted site. GO enrichment analysis revealed several significantly enriched Biological Processes (BP; $p_{adj} < 0.05$) among upregulated genes, including ribosome biogenesis, protein catabolic process, nucleobase-containing small molecule metabolic process, and chromatin organization; conversely, no significantly enriched BPs were detected among downregulated genes. Overall, these enrichment patterns differed from those reported in previous studies, although some overlap was observed. In a study examining intestinal gene expression in *S. trutta* from a metal-polluted river, over-represented BPs included proteolysis, platelet activation, cell activation, coagulation, and hemostasis (Uren Webster et al. 2013). Nevertheless, enrichment of ribosome biogenesis and protein catabolic processes has been reported in fish tissues affected by pollution, suggesting increased protein turnover and cellular activity under pollutant stress (Mitra et al. 2020, Oleksiak 2008). In contrast, GO enrichment analysis of Hg-exposed *D. rerio* intestine highlighted BPs related to xenobiotic responses, metabolism, development, and immune function (Zhang et al. 2020), patterns not observed in the present study, further emphasizing the context dependence of transcriptomic responses to environmental stressors.

Significantly enriched Cellular Components (CCs) among upregulated genes included ribosome, organelle, mitochondrion, and chromosome, with no enriched CCs observed among downregulated genes, consistent with findings reported for gills of fish from polluted environments (Mitra et al. 2020). However, in the intestine of *S. trutta* from a metal-polluted river in England, enriched CCs included extracellular space, extracellular region, extracellular region part, and fibrinogen complex (Uren Webster et al. 2013). In addition, in gills of *S. trutta* from metal-impacted rivers in the United Kingdom, protein catabolic process (BP) and

chromosome (CC) were significantly underrepresented, contrasting with the results observed in our study (Paris et al. 2024).

Among MFs, upregulated genes were significantly associated with RNA binding, isomerase, GTPase, hydrolase, and structural molecule activities, while oxidoreductase activity was the only significantly enriched downregulated MF. In a previous study of *S. trutta* intestine, over-represented MFs at a metal-polluted site included serine hydrolase activity, serine-type peptidase activity, serine-type endopeptidase activity, peptidase activity, and endopeptidase activity (Uren Webster et al. 2013). RNA binding has previously been identified as a pollution-sensitive MF in fish gills (Mitra et al. 2020). In contrast, oxidoreductase activity (MF) was enriched in *S. trutta* gills from metal-impacted rivers, again differing from the pattern observed in the present study (Paris et al. 2024).

Together, these enrichment patterns indicate increased cellular, transcriptional, and metabolic activity in the intestinal tissue of fish from KRK compared to KRS, likely reflecting increased energetic and biosynthetic demands associated with coping with chronic environmental stress. The selective downregulation of oxidoreductase activity suggests targeted modulation of redox-related pathways rather than a general suppression of metabolic function.

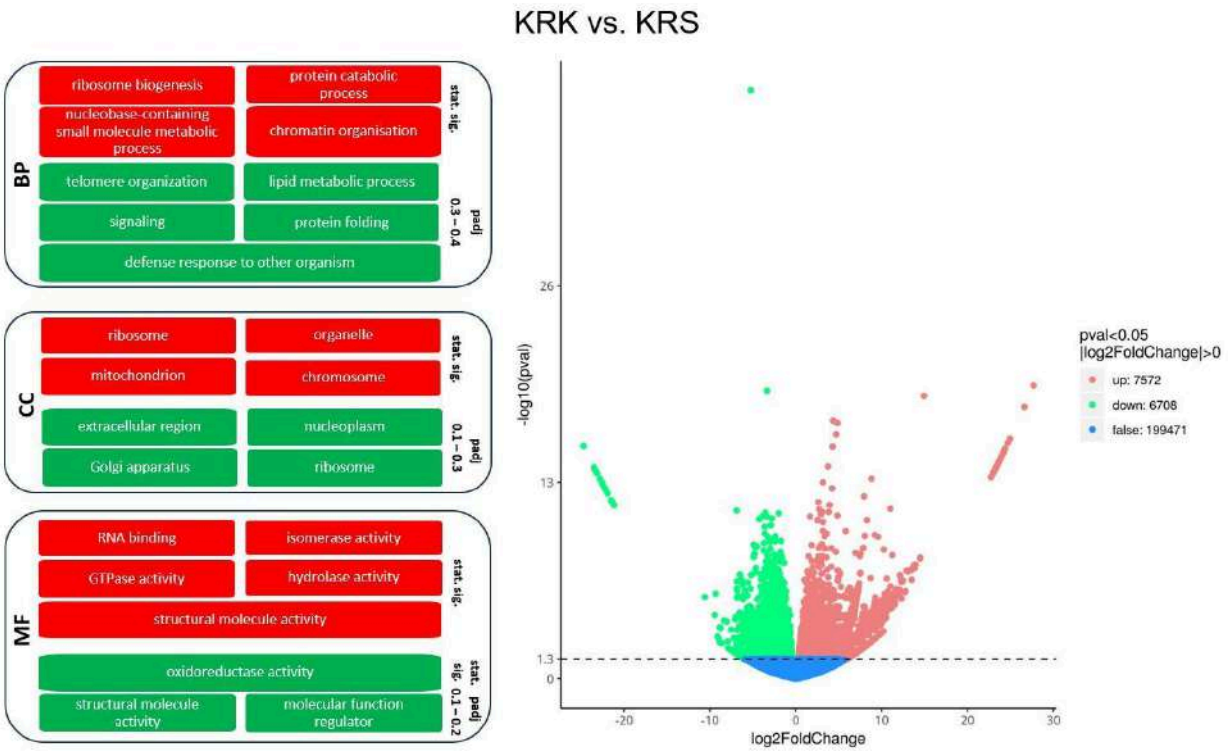

Figure 6. Volcano plot of differentially expressed genes (DEGs) and summary of their associated GO enrichment results. The x-axis shows the $\log_2$ fold change in gene expression between *S. trutta* from the polluted site (KRK) and the reference site (KRS) in the Krka River; the y-axis represents statistical significance ($-log_{10}$pvalue). Red and green points indicate significantly up- and downregulated DEGs, respectively ($q < 0.005$ and $|log_2FC| > 1$), while blue points represent genes without significant change. GO enrichment results are grouped into Biological Process (BP), Cellular Component (CC), and Molecular Function (MF) categories. Upregulated GO terms are shown in red and downregulated terms in green, with the corresponding range of adjusted p-values displayed on the right.

KEGG enrichment analysis identified 41 significantly upregulated pathways in fish from KRK relative to KRS (Fig. 7). Based on adjusted p value and number of involved genes, the most prominent upregulated pathways included Proteasome, Primary immunodeficiency, Phagosome, and Thermogenesis. Several disease-associated pathways (e.g. Systemic lupus erythematosus, Parkinson disease, Huntington disease, Epstein–Barr virus infection, and Alzheimer disease) were also significantly enriched. However, rather than representing disease states, these pathways reflect conserved gene sets involved in proteostasis, mitochondrial function, cellular stress responses, and immune signaling. Collectively, the

enriched upregulated KEGG pathways were associated with protein turnover, energy metabolism, immune activation, and host defense mechanisms, closely aligning with the functional patterns identified in the GO enrichment analysis.

Our findings are consistent with most fish transcriptomic studies conducted *in situ,* which have consistently identified lipid and xenobiotic metabolism pathways, cell death, immune and inflammatory response, oxidative stress and hormonal signaling as central components of fish responses to environmental pollution (Cardenas-Camacho et al. 2025). In contrast, enrichment of metal- and ion-homeostasis pathways observed in wild *S. trutta* from a long-term metal-polluted river (Urien Webster et al. 2013) was not a dominant feature in the present study. Despite differences in species and tissue, similar functional categories have been reported in the gills of *R. rita* exposed to pollution, where KEGG enrichment highlighted altered energy metabolism, immune responses, translational and transcriptional regulation, and protein folding and degradation pathways (Mitra et al. 2020). In both studies, innate immune–related pathways, including phagocytosis and antimicrobial defenses, showed higher expression in fish from polluted river stretches, supporting the interpretation that activation of phagosome-related pathways and immune-associated genes reflects enhanced cellular defense and stress-mitigation processes in polluted environments.

In contrast, 12 KEGG pathways were significantly downregulated in fish from KRK, most notably Chemical carcinogenesis, Retinol metabolism, Steroid hormone biosynthesis, Metabolism of xenobiotics by cytochrome P450, Pancreatic secretion, Bile secretion, and Cholesterol metabolism. Together, these pathways indicate a reduced intestinal capacity for xenobiotic biotransformation, lipid and vitamin metabolism, steroid synthesis, and digestive and secretory functions at the polluted site. Cytochrome P450–mediated xenobiotic metabolism is a well-established detoxification pathway in fish and is commonly reported as responsive to metal exposure and other environmental pollutants (Zhang et al. 2019). However, suppression rather than activation of these pathways under chronic exposure conditions suggests a trade-off between energy-demanding detoxification processes and other stress-response mechanisms.

Downregulation of bile and pancreatic secretion pathways further indicates compromised digestive and absorptive capacity, with potential consequences for lipid handling, uptake of fat-soluble vitamins, cholesterol homeostasis, and elimination of metabolic waste products. Similar shifts in metabolic and energy-related pathways have been reported in *F. heteroclitus*,

where modulation of oxidative phosphorylation and lipid metabolism was interpreted as altered energy allocation in polluted environments (Oleksiak 2008). Taken together, the KEGG enrichment patterns observed in the present study suggest a coordinated response characterized by enhanced cellular maintenance, immune activation, and energy demand, alongside reduced digestive, metabolic, endocrine, and detoxification functions.

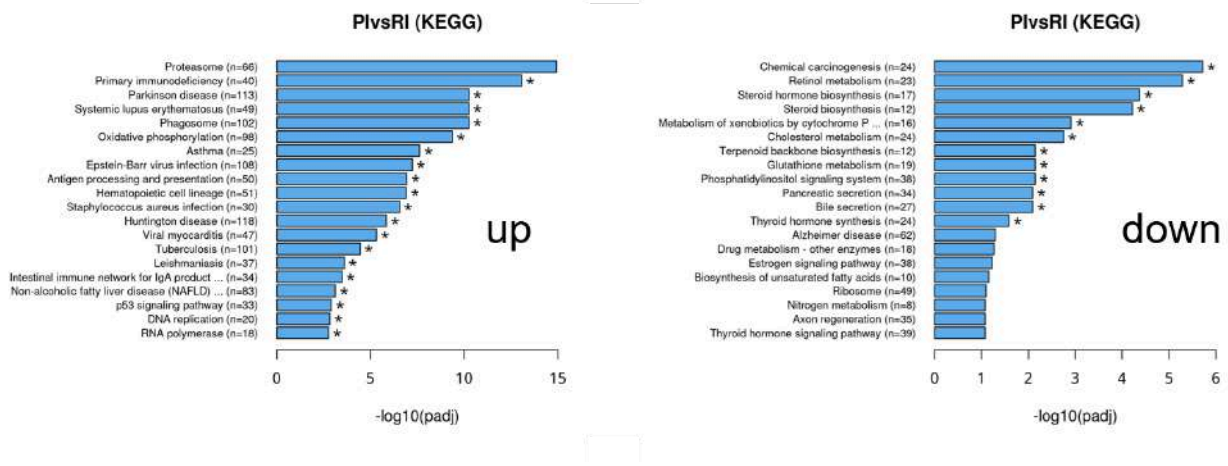

Figure 7. Enriched KEGG pathways in the intestine of *S. trutta*. Bar charts display the top 20 KEGG pathways enriched among upregulated (top) and downregulated (bottom) differentially expressed genes (DEGs) in *S. trutta* at polluted KRK (Pl) site relative to the reference KRS (Rf) site. Significantly enriched pathways are indicated by an asterisk (corrected *p*-value < 0.05).

2.2.3. qPCR validation of transcriptomics

qPCR validation was performed on five genes identified as upregulated in the transcriptomic analysis: *28S* (28S ribosomal protein S16, mitochondrial-like), *39S* (39S ribosomal protein L14, mitochondrial precursor), *C8* (uncharacterized protein C8orf59 homolog), *rho* (rho GTPase-activating protein 20-like), and *Mx* (interferon-induced GTP-binding protein Mx2-like).

Genes *28S*, *39S*, and *C8* showed statistically significant ($p < 0.05$) upregulation in samples from the polluted KRK site compared to the reference KRS site (Fig. 8), while *rho* and *Mx* also exhibited higher expression in samples from KRK, although these differences were not statistically significant (Fig. 9). Importantly, all five genes displayed the same direction of

regulation as observed in the transcriptomic data, supporting the overall reliability and consistency of the RNA-seq results.

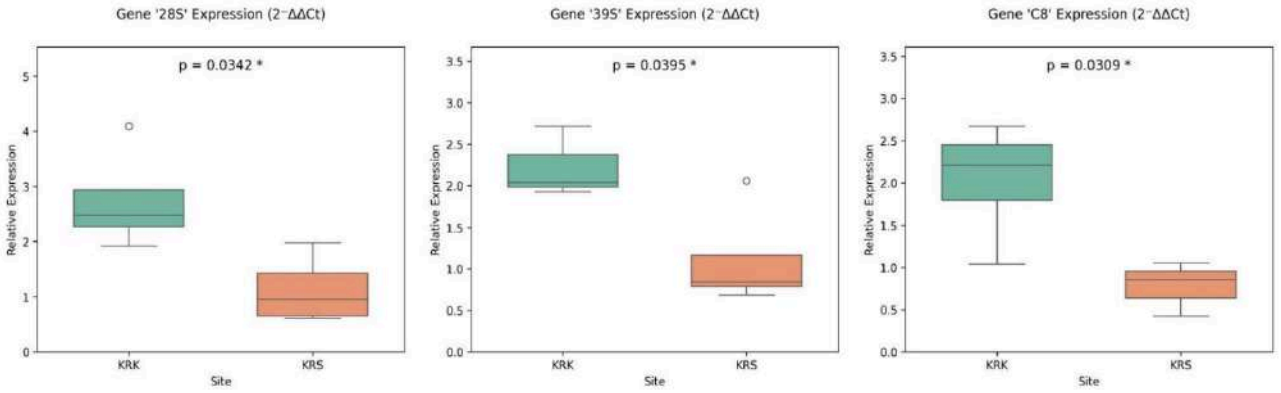

Figure 8. Relative expression of the genes *28S*, *39S* and *C8* genes in the intestine of *Salmo trutta* from the polluted site KRK and the reference site KRS in the Krka River. Data are normalized to the reference gene *EIF1a*. Statistical significance determined by Welch's *t*-test and is indicated by an asterisk (*p*-value shown in the figure).

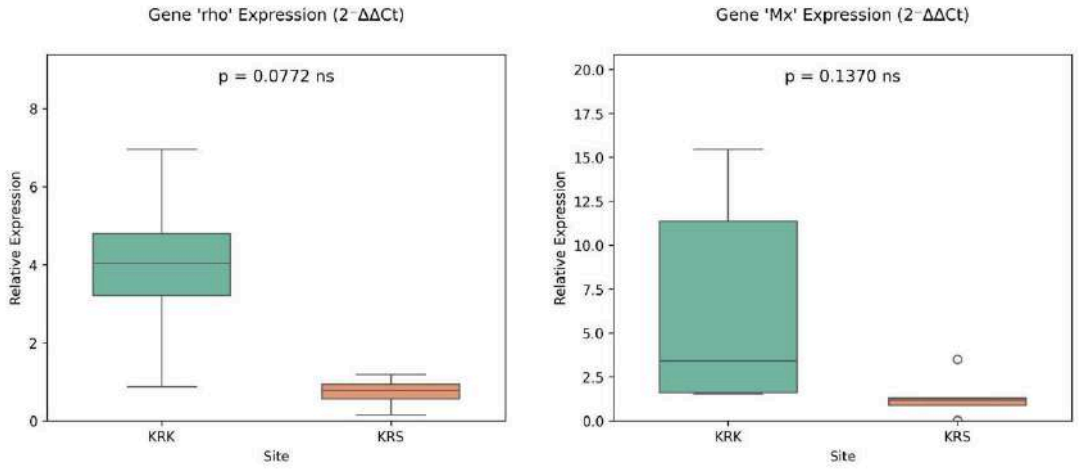

Figure 9. Relative expression of *rho* and *Mx* genes in the intestine of *Salmo trutta* from the polluted site (KRK) and the reference site (KRS) in the Krka River. Data are normalized to the reference gene *EIF1a*. No statistically significant differences between sites were detected (Welch's t-test; p-values indicated; ns - not significant).

3. Literature

Brulle, F., Morgan, A. J., Cocquerelle, C., & Vandenbulcke, F. (2010). Transcriptomic underpinning of toxicant-mediated physiological function alterations in three terrestrial invertebrate taxa: a review. *Environmental Pollution*, *158*(9), 2793-2808.

Canchi, S., Raao, B., Masliah, D., Rosenthal, S. B., Sasik, R., Fisch, K. M., ... & Rissman, R. A. (2019). Integrating gene and protein expression reveals perturbed functional networks in Alzheimer's disease. *Cell reports*, 28(4), 1103-1116.

Cardenas-Camacho, J., Calderón-Delgado, I., Corredor-Santamaría, W., & Velasco-Santamaría, Y. M. (2025). The use of transcriptomics in situ study through fish: a systematic review on pollution. *Neotropical Ichthyology*, *23*, e240133.

Chatterjee, P., Roy, D., Bhattacharyya, M., & Bandyopadhyay, S. (2017). Biological networks in Parkinson's disease: an insight into the epigenetic mechanisms associated with this disease. *BMC genomics*, *18*(1), 721.

Davidson, N. M., & Oshlack, A. (2014). Corset: enabling differential gene expression analysis for de novo assembled transcriptomes. *Genome biology*, *15*(7), 410.

Docampo, R., & Huang, G. (2015). Calcium signaling in trypanosomatid parasites. *Cell calcium*, *57*(3), 194-202.

Docampo, R., & Moreno, S. N. (2021). Calcium signaling in intracellular protist parasites. *Current opinion in microbiology*, *64*, 33-40.

Gaki, G. S., & Papavassiliou, A. G. (2014). Oxidative stress-induced signaling pathways implicated in the pathogenesis of Parkinson's disease. *Neuromolecular medicine*, *16*(2), 217-230.

Garcia-Reyero, N., Habib, T., Pirooznia, M., Gust, K. A., Gong, P., Warner, C., ... & Perkins, E. (2011). Conserved toxic responses across divergent phylogenetic lineages: a meta-analysis of the neurotoxic effects of RDX among multiple species using toxicogenomics. *Ecotoxicology*, 20(3), 580-594.

Gomes, S. I., Roca, C. P., Scott-Fordsmand, J. J., & Amorim, M. J. (2019). High-throughput transcriptomics: Insights into the pathways involved in (nano) nickel toxicity in a key invertebrate test species. *Environmental Pollution*, *245*, 131-140.

Han, C., & Hagiwara, A. (2023). Differing modes of growth performance induced by hypoxia and effects on oxidative defense and glycolysis metabolism in two marine Brachionus rotifer species. *Aquaculture*, 567, 739286.

Hansen, T., Fjelldal, P. G., Lien, S., Smith, M., Corton, C., Oliver, K., ... & Blaxter, M. (2021). The genome sequence of the brown trout, *Salmo trutta* Linnaeus 1758. *Wellcome Open Research*, *6*, 108.

Hassanine, R. M. E. S., & Al-Jahdali, M. O. (2008). Intraspecific density-dependent effects on growth and fecundity of *Diplosentis nudus* (Harada, 1938) Pichelin et Cribb, 2001 (Acanthocephala, Cavisomidae). *Acta Parasitologica*, 53(3), 289-295.

Hausen, J., Otte, J. C., Legradi, J., Yang, L., Strähle, U., Fenske, M., ... & Ottermanns, R. (2018). Fishing for contaminants: identification of three mechanism specific transcriptome signatures using *Danio rerio* embryos. *Environmental Science and Pollution Research*, *25*(5), 4023-4036.

Hou, Z., Mo, F., & Zhou, Q. (2023). Elucidating response mechanisms at the metabolic scale of Eisenia fetida in typical oil pollution sites: A native driver in influencing carbon flow. *Environmental Pollution*, *337*, 122545.

Jamshed, L., Debnath, A., Jamshed, S., Wish, J. V., Raine, J. C., Tomy, G. T., ... & Holloway, A. C. (2022). An emerging cross-species marker for organismal health: tryptophan-kynurenine pathway. *International Journal of Molecular Sciences*, *23*(11), 6300.

Kanehisa, M., Furumichi, M., Sato, Y., Kawashima, M., & Ishiguro-Watanabe, M. (2021). KEGG: integrating viruses and cellular organisms. *Nucleic Acids Research, 49*(D1), D545–D551. https://doi.org/10.1093/nar/gkaa970

Kennedy, C. R. (1985). Regulation and dynamics of acanthocephalan populations. *Biology of the Acanthocephala*, 385-416.

Lee, J., Giordano, S., & Zhang, J. (2012). Autophagy, mitochondria and oxidative stress: cross-talk and redox signalling. *Biochemical Journal*, *441*(2), 523-540.

Lee, J., Jeon, M. J., Won, E. J., Yoo, J. W., & Lee, Y. M. (2023). Effect of heavy metals on the energy metabolism in the brackish water flea *Diaphanosoma celebensis*. *Ecotoxicology and Environmental Safety*, 262, 115189.

Li, B., & Dewey, C. N. (2011). RSEM: accurate transcript quantification from RNA-Seq data with or without a reference genome. *BMC bioinformatics*, *12*(1), 323.

Liu, X., Jiang, H., Ye, B. *et al.* Comparative transcriptome analysis of the gills and hepatopancreas from *Macrobrachium rosenbergii* exposed to the heavy metal Cadmium (Cd^{2+}). *Scientific Reports* **11**, 16140 (2021). https://doi.org/10.1038/s41598-021-95709-w

Liu, J., Jin, P., Li, M., Yi, X., Tian, Y., Zhang, Z., ... & Shi, L. (2024). The energy metabolism of the freshwater leech Whitmania pigra in response to fasting. *Comparative Biochemistry and Physiology Part B: Biochemistry and Molecular Biology*, 274, 110999.

Martínez-González, J. D. J., Guevara-Flores, A., & del Arenal Mena, I. P. (2022). Evolutionary adaptations of parasitic flatworms to different oxygen tensions. *Antioxidants*, *11*(6), 1102.

Martis, M. M., Tarbiat, B., Tyden, E., Jansson, D. S., & Höglund, J. (2017). RNA-Seq de novo assembly and differential transcriptome analysis of the nematode Ascaridia galli in relation to in vivo exposure to flubendazole. *PLoS One*, *12*(11), e0185182.

Mitra, T., Mahanty, A., Ganguly, S., & Mohanty, B. P. (2020). Transcriptomic responses to pollution in natural riverine environment in Rita rita. *Environmental Research*, *186*, 109508.

Mullarky, E., & Cantley, L. C. (2015). Diverting glycolysis to combat oxidative stress. *Innovative medicine: basic research and development*, 3-23.

Oleksiak, M. F. (2008). Changes in gene expression due to chronic exposure to environmental pollutants. *Aquatic Toxicology*, *90*(3), 161-171.

Pfaffl, M. W., Tichopad, A., Prgomet, C., & Neuvians, T. P. (2004). Determination of stable housekeeping genes, differentially regulated target genes and sample integrity: BestKeeper–Excel-based tool using pair-wise correlations. *Biotechnology letters*, *26*(6), 509-515.

Rodgers, J., Stone, T. W., Barrett, M. P., Bradley, B., & Kennedy, P. G. (2009). Kynurenine pathway inhibition reduces central nervous system inflammation in a model of human African trypanosomiasis. *Brain*, *132*(5), 1259-1267.

Schmittgen, T. D., & Livak, K. J. (2008). Analyzing real-time PCR data by the comparative CT method. *Nature protocols*, *3*(6), 1101-1108.

Soto, C., & Pritzkow, S. (2018). Protein misfolding, aggregation, and conformational strains in neurodegenerative diseases. *Nature neuroscience*, 21(10), 1332-1340.

Sun, S., Wang, Z., Yuan, D., Ni, M., Xu, H., Wang, W., ... & Li, M. (2022). Selection of stable reference genes for RT–qPCR in *Salmo trutta*. *Aquaculture Reports*, 26, 101290.

Tang, D., Guo, H., Shi, X., & Wang, Z. (2019). Comparative transcriptome analysis of the gills from the Chinese mitten crab (*Eriocheir japonica sinensis*) exposed to the heavy metal cadmium. *Turkish Journal of Fisheries and Aquatic Sciences*, 20, 467–479.

Uren Webster, T. M., Bury, N., van Aerle, R., & Santos, E. M. (2013). Global transcriptome profiling reveals molecular mechanisms of metal tolerance in a chronically exposed wild population of brown trout. *Environmental science & technology*, *47*(15), 8869-8877.

Vandesompele, J., De Preter, K., Pattyn, F., Poppe, B., Van Roy, N., De Paepe, A., & Speleman, F. (2002). Accurate normalization of real-time quantitative RT-PCR data by geometric averaging of multiple internal control genes. *Genome biology*, *3*(7), research0034-1.

Wieder, C., Bundy, J. G., Frainay, C., Poupin, N., Rodríguez-Mier, P., Vinson, F., ... & Ebbels, T. M. (2022). Avoiding the misuse of pathway analysis tools in environmental metabolomics. *Environmental Science & Technology*, 56(20), 14219-14222.

Ye, J., Coulouris, G., Zaretskaya, I., Cutcutache, I., Rozen, S., & Madden, T. L. (2012). Primer-BLAST: a tool to design target-specific primers for polymerase chain reaction. *BMC bioinformatics*, *13*(1), 134.

Ye, Y., Shi, Y. X., Jiang, Q., Jin, Y., Chen, F. X., Tang, W. H., ... & Wang, J. L. (2024). Transcriptome analysis reveals antioxidant defense mechanisms in the silkworm *Bombyx mori* after exposure to lead. *Animals*, *14*(12), 1822

Zhang, Q. L., Dong, Z. X., Luo, Z. W., Zhang, M., Deng, X. Y., Guo, J., ... & Lin, L. B. (2020). The impact of mercury on the genome-wide transcription profile of zebrafish intestine. *Journal of hazardous materials*, *389*, 121842.

Zheng, Y., Liu, C., Luo, J., Zou, D., Tang, Z., He, J., & Bai, J. (2024). Integrated transcriptomic and biochemical characterization of the mechanisms governing stress responses in soil-dwelling invertebrate (Folsomia candida) upon exposure to dibutyl phthalate. *Journal of Hazardous Materials*, 462, 132644.

Zhu J-Y, Yang P, Zhang Z, Wu G-X, Yang B (2013) Transcriptomic Immune Response of Tenebrio molitor Pupae to Parasitization by Scleroderma guani. *PLoS O*ne, 8(1):e54411.doi:10.1371/journal.pone.0054411

Biography

Sara Šariri was born in Osijek in 1996. In 2015, she moved to Zagreb to study Environmental Sciences at the Faculty of Science, University of Zagreb, where she completed her master's degree in 2021. During her studies, she completed an internship at the freshwater aquarium Aquatika in Karlovac, laboratory skills training at the Division of Zoology of the Faculty of Science, and an IAESTE internship at the Marine and Environmental Sciences Centre in Lisbon. In 2020, she received the Scholarship for Excellence of the University of Zagreb. In 2021, she was employed as a Research Assistant at the Ruđer Bošković Institute in the Laboratory for Biological Effects of Metals, Division for Marine and Environmental Research, on the Croatian Science Foundation project "Integrated evaluation of aquatic organism responses to metal exposure: gene expression, bioavailability, toxicity and biomarker responses (BIOTOXMET)". In the same year, she enrolled in the doctoral study program in Biology at the Faculty of Science. Her scientific interests include ecotoxicology and environmental parasitology, particularly the effects of metals and microplastics on aquatic organisms. During her doctoral studies, she participated in several international research mobilities and training programs, including mobility at BOKU University in Vienna, training school "Recent trends in microplastic research" in Jena, summer school "Environmental History and Historical Ecology of the Dinaric Karst" in Ljubljana, and research mobilities at the University of Duisburg-Essen and the University of Ljubljana. She has presented her research at 21 scientific conferences, contributed to the organization of five, completed the Laboratory Animal Science Course and participated in numerous science popularization activities between 2017 and 2025. In 2023, she received an award from THE CIVICS Innovation Hub within the Erasmus+ Young Climate Professionals program for her project idea "Understanding microplastics in our water," which was implemented in 2024. She is the first author of four scientific papers.

List of author's publications:

Redžović, Z., Erk, M., Gottstein, S., Sokolova, I. M., Sokolov, E. P., Mijošek Pavin, T., Šariri, S., Sertić Perić, M., Dautović, J., Fiket, Ž., Filipović Marijić, V., Ivanković, D., & Cindrić, M. (2025). Oxidative stress and metabolic adaptation in *Synurella ambulans*: Assessing pollution impact in the hyporheic zone. *Environmental Pollution*, 127234.

Šariri, S., Mijošek Pavin, T., Redžović, Z., Kiralj, Z., Ivanković, D., & Filipović Marijić, V. (2025). Biomarker-based assessment of sublethal metal exposure in brown trout and parasites acanthocephalans from a protected karst river. *Environmental toxicology and pharmacology*, 104823.

Šariri, S., Vardić Smrzlić, I., Mijošek Pavin, T., & Filipović Marijić, V. (2025). First insight into metal binding proteins from the de novo transcriptome of acanthocephalan parasite *Dentitruncus truttae*. *Scientific reports*, *15*(1), 26152.

Šariri, S., Cvetković, Ž., Mijošek Pavin, T., Kljaković-Gašpić, Z., Valić, D., Kralj, T., Brkić, A., Redžović, Z., & Filipović Marijić, V. (2025). Association of toxic effects and the quality of surface water and wastewater: Application under environmental conditions and literature overview by CiteSpace. *Journal of contaminant hydrology*, 274, 104667.

Filipović Marijić, V., Šariri, S., & Miošek, T. (2024). Osvrti: Integrirana procjena odgovora akvatičkih organizama na izloženost metalima: ekspresija gena, bioraspoloživost, toksičnost i biomarkerski odgovori (BIOTOXMET). *Kemija u industriji: Časopis kemičara i kemijskih inženjera Hrvatske*, *73*(11-12), 499-501.

Dragun, Z., Ivanković, D., Tepić, N., Filipović Marijić, V., Šariri, S., Mijošek Pavin, T., Drk, S., Gjurčević, E., Matanović, K., Kužir, S., Barac, F., Kiralj, Z., Kralj, T., & Valić, D. (2024). Metal bioaccumulation in the muscle of the northern pike (*Esox lucius*) from historically contaminated river and the estimation of the human health risk. *Fishes*, *9*(9), 364.

Mijošek, T., Šariri, S., Kljaković-Gašpić, Z., Fiket, Ž., & Filipović Marijić, V. (2024). Interrelation between environmental conditions, acanthocephalan infection and metal (loid) accumulation in fish intestine: An in-depth study. *Environmental pollution*, *356*, 124358.

Šariri, S., Valić, D., Kralj, T., Cvetković, Ž., Mijošek, T., Redžović, Z., Karamatić, I., & Filipović Marijić, V. (2024). Long-term and seasonal trends of water parameters in the karst riverine catchment and general literature overview based on CiteSpace. *Environmental science and pollution research*, 31(3), 3887-3901.

Vardić Smrzlić, I., Čolić, B., Kapetanović, D., Šariri, S., Mijošek, T., & Filipović Marijić, V. (2024). Phylogeny and genetic variability of Rotifer's closest relatives Acanthocephala: an example from Croatia. *Hydrobiologia*, 851(12), 2845-2860.

Perrot-Minnot, M. J., Cozzarolo, C. S., Amin, O., Barčák, D., Bauer, A., Filipović Marijić, V., García-Varela, M., Hernández-Orts, J. S., Yen Le, T. T., Nachev, M., Orosová, M., Rigaud, T., Šariri, S., Wattier, R., Reyda, F., & Sures, B. (2023). Hooking the scientific community on thorny-headed worms: interesting and exciting facts, knowledge gaps and perspectives for research directions on Acanthocephala. *Parasite*, *30*, 23.

Mijošek, T., Kljaković-Gašpić, Z., Kralj, T., Valić, D., Redžović, Z., Šariri, S., Karamatić, I., & Filipović Marijić, V. (2023). Spatial and temporal variability of dissolved metal (loid) s in water of the karst ecosystem: consequences of long-term exposure to wastewaters. *Environmental technology & innovation*, 32, 103254.

Bjedov, D., Velki, M., Toth, L., Filipović Marijić, V., Mikuška, T., Jurinović, L., Ečimović, S., Turić, N., Lončarić, Z., Šariri, S., Al Marsoomi, Y., & Mikuška, A. (2023). Heavy metal (loid) effect on multi-biomarker responses in apex predator: Novel assays in the monitoring of white stork nestlings. *Environmental pollution*, *324*, 121398.